# Enhancing cardiomyocyte survival from myocardial infarction with cardiac stromal cell-secreted factors

**Chrystalla Constantinou**

A thesis submitted for the degree of Doctor of Philosophy and the Diploma of Imperial College

National Heart and Lung Institute

Faculty of Medicine

Imperial College London

## Declaration of originality

I certify that this thesis, and the research to which it refers, are the product of my own work, conducted over the past four years as part of my PhD degree at Imperial College London. Any ideas or quotations from the work of other people published or otherwise, or from my own previous work are fully acknowledged in accordance with the standard referencing practices of the discipline.

## Acknowledgments

First, I would like to express my sincere gratitude to National Heart and Lung foundation for my stipend throughout this project as well as my supervisors, Prof Michael Schneider and Dr Michela Noseda for their continuous support and excellent guidance. I would also like to thank the British Heart Foundation and the Wellcome Trust Foundation for supporting work of my lab, including this project. Besides my supervisors and sponsors, I would also like to thank the two examiners that have read my thesis and provided invaluable feedback; Dr Nicola Smart and Dr Graeme Birdsey. Many thanks to the wider Imperial College community and all collaborators, internal and external, that have contributed to this work.

I would also like to extend my gratitude to all members of Schneider and Noseda labs, past and present, for all the useful discussions, lunch breaks, coffee breaks and mind-opening chats; special thanks to Patricia, Pelin, Antonio, Riccardo, Sam, Sara, Kevin and Liliana for not only being my colleagues but also my friends.

Special thanks to all my friends in London and Cyprus – especially Myria, Eleftheria, Elena, Christina, Gianna, Ioanna, Nicoletta, Nandia, Irene and Chara, thanks for being the highlight of my days and being there for me throughout this journey.

Last but not least, to Marcos, there are obviously no words to contain the amount of help and motivation I have received from you, the countless times you made me smile, please know that I will be forever grateful. To my family back home, mama, papa, Nicola and Marie, thanks for being there to distract me when I needed it the most; I would not have made it without your constant support. And finally, my one and only Andrés, thank you for being my beam of light and reminding me what really matters in life.

## Copyright Declaration

The copyright of this thesis rests with the author. Unless otherwise indicated, its contents are licensed under a Creative Commons Attribution-Non Commercial 4.0 International Licence (CC BY-NC).

Under this licence, you may copy and redistribute the material in any medium or format. You may also create and distribute modified versions of the work. This is on the condition that: you credit the author and do not use it, or any derivative works, for a commercial purpose.

When reusing or sharing this work, ensure you make the licence terms clear to others by naming the licence and linking to the licence text. Where a work has been adapted, you should indicate that the work has been changed and describe those changes. Please seek permission from the copyright holder for uses of this work that are not included in this licence or permitted under UK Copyright Law.

## Abstract

Myocardial infarction is the leading cause of death globally, and progression to heart failure is directly proportional to infarct size. Targeting cardiomyocyte loss is vital to stop cardiac damage. Previous data from our group show that intramyocardial injection of cardiac stromal cells (CSC) at time of infarct results in scar size reduction and improvement in ejection fraction. However, injected CSC are poorly retained, hence early paracrine signals might explain the observed improvement of cardiac function. Here we showed that injecting CSC-conditioned media into the mouse infarct border zone reduced apoptotic cardiomyocytes >70% locally. Subsequently, the paracrine effects of CSC were investigated, using human pluripotent stem cell-derived cardiomyocytes (hPSC-CM) as a target more relevant to translation. In co-culture and conditioned medium studies, the CSC secretome markedly inhibited human myocyte death, induced by three different cardiotoxic molecules; menadione, doxorubicin and imatinib. Follow-on studies were chiefly performed with menadione, showing preserved mitochondrial membrane depolarization and inhibited ROS generation in the presence of CSC-conditioned media. Functional assays revealed that calcium cycling and action potential generation were also preserved following CSC-conditioned medium treatment of menadione-stressed cells. Characterization studies on the protective secretome pointed to exosome-independent molecules, which were thermolabile and > 3 kDa in size. RNA-sequencing revealed that the CSC-secretome downregulated pro-apoptotic genes and preserved cardiac function and contractility markers in stressed hPSC-CM. A novel bioinformatic tool was used to predict the potential ligand-receptor interactions under conditions of cardiomyocyte stress. In terms of proteomics, cytokine arrays highlighted protein factors enriched in conditioned media from protective versus non-protective populations. Human CSC were also characterized and found to resemble mouse CSC in molecular signature, as well as in their paracrine protective ability. Thus, hPSC-CM provide an auspicious, relevant human platform to investigate extracellular signals for cardiac muscle survival, corroborating human cardioprotection by the CSC-secretome and supporting the further investigation of CSC-conditioned medium as a potential cell-free therapeutic product.

## Table of Contents

Declaration of originality ..... 2
Copyright Declaration ..... 4
Abstract ..... 5
Table of Contents ..... 6
List of Figures ..... 11
List of Tables ..... 13
List of abbreviations ..... 14
1. Introduction ..... 20
1.1. The burden of cardiovascular disease ..... 20
1.2. Myocardial infarction and progression to heart failure ..... 21
1.3. Oxidative stress in myocardial infarction ..... 22
1.3.1. Menadione as an inducer of oxidative stress ..... 24
1.4. Cardiotoxic anti-cancer agents as sources of oxidative stress in the heart . 26
1.4.1. Anthracyclines like doxorubicin ..... 26
1.4.2. Tyrosine Kinase Inhibitors ..... 28
1.5. Mechanisms of cell death and implications for heart disease ..... 30
1.5.1. A historical perspective of regulated cell death ..... 31
1.5.2. Death receptor pathway ..... 40
1.5.3. Mitochondrial pathway ..... 44
1.5.4. Cell death during myocardial infarction and heart failure ..... 50
1.6. The regenerative capacity of the adult human heart ..... 53
1.6.1. The promise of regenerative medicine in the heart ..... 54
1.6.2. First-generation cell therapy for heart regeneration ..... 55
1.6.3. Second-generation cell therapy for heart regeneration ..... 59
1.7. Cardiac stem/progenitor cells ..... 60
1.7.1. The c-kit$^+$ cardiac progenitor ..... 60
1.7.2. The Sca-1$^+$ cardiac progenitor ..... 62
1.7.3. PDGFRα$^+$ Cardiac Stromal Cells (CSC) ..... 65
1.8. Cell enhancement and cell-free approaches: the next generation? ..... 69
1.8.1. Growth factors ..... 71
1.8.2. Cytokines and chemokines ..... 82
1.8.3. Antioxidants ..... 90

1.8.4. Paracrine-secreted hormones with newly discovered cardioprotective activities ..... 92
1.8.5. Mitochondrial transfer ..... 94
1.8.6. Other factors and small molecules ..... 95
1.8.7. microRNAs ..... 98
1.8.8. The role of exosomes in cardiac repair ..... 99
1.9. Preclinical models of cardiac disease and paracrine protection ..... 102
1.9.1. In vitro: myocyte cell culture ..... 103
1.9.2. Ex vivo: isolated perfused hearts ..... 107
1.9.3. In vivo: permanent and transient coronary artery occlusion ..... 108
1.9.4. The issue of translation: toward human trial design ..... 109
1.10. Human pluripotent stem cell-derived cardiomyocytes as a platform for cardiomyocyte toxicity and protection ..... 110
1.11. Our model system ..... 113
1.12. Hypothesis, aim and objectives ..... 117
2. Materials and Methods ..... 120
2.1. Mouse cardiac stromal cell isolation ..... 120
2.2. Cell culture ..... 120
2.3. Conditioned media production and modification ..... 122
2.4. Myocardial Infarction ..... 122
2.5. Immunohistochemistry and confocal imaging ..... 123
2.6. TUNEL staining in tissue sections and fixed cells ..... 125
2.7. Co-culture ..... 125
2.8. Cell staining and high-throughput imaging ..... 126
2.9. Calcium cycling and action potential assays ..... 127
2.10. Human cardiac troponin I immunoassay ..... 128
2.11. Adenylate kinase release cytotoxicity detection assay ..... 129
2.12. $H_2O_2$ detection in cell culture supernatants ..... 129
2.13. JC-10 assay for detection of mitochondrial depolarization ..... 130
2.14. Exosome isolation and characterization ..... 130
2.15. Flow cytometry and sorting ..... 131
2.16. Human cardiac stromal cell isolation ..... 132
2.17. Single cell qRT-PCR ..... 132
2.18. Recombinant factor supplementation ..... 133

2.19. Bulk RNA-Seq on CSC and IMR90 cardiomyocytes ..... 133
2.20. CellPhone Database analysis ..... 135
2.21. Cytokine arrays ..... 136
2.22. Statistics ..... 137
3. Results ..... 145
3.1. Protection of cardiomyocytes by Sca1$^+$ SP CSC-secreted factor(s) ..... 146
3.1.1. Sca1$^+$ SP CSC population and rationale ..... 146
3.1.2. CSC-conditioned media protect mouse myocardium after myocardial infarction ..... 148
3.1.3. CSC inhibit the death of neonatal mouse and adult human cardiomyocytes in trans-well co-culture ..... 151
3.1.4. Human cardiomyocyte co-culture with Sca1$^+$ PDGFRα$^+$ CD31$^-$ cells .. 155
3.1.5. CSC- but not TTF-conditioned media protect hPSC-CM from menadione-induced death ..... 158
3.1.6. Cardiomyocyte protection with CSC-conditioned media administered one hr after menadione stress induction ..... 161
3.1.7. CSC-conditioned media prevent the release of cardiac troponin I from human cardiomyocytes ..... 162
3.1.8. CSC-conditioned media do not induce DNA synthesis in hPSC-CM .. 165
3.1.9. CSC-conditioned media prevent DNA fragmentation in hPSC-CM after menadione stress ..... 168
3.1.10. ROS generation before mitochondrial membrane depolarisation in menadione-stressed cardiomyocytes ..... 171
3.1.11. CSC-conditioned media inhibit mitochondrial depolarisation in hPSC-CM after menadione stress. ..... 175
3.1.12. CSC-conditioned media inhibit ROS in hPSC-CM after menadione. .. 176
3.1.13. CSC-conditioned media inhibit mitochondrial superoxide in hPSC-CM after menadione ..... 180
3.1.14. CSC-conditioned media inhibit death of hPSC-CM induced by doxorubicin ..... 182
3.1.15. Detection of mitochondrial depolarisation in hPSC-CM by doxorubicin and possible protection by CSC-conditioned medium ..... 185
3.1.16. CSC-conditioned media fail to reduce ROS levels in hPSC-CM after doxorubicin stress ..... 188
3.1.17. CSC-conditioned media fail to reduce superoxide levels in mitochondria of hPSC-CM after doxorubicin stress ..... 189

3.1.18. CSC-conditioned media inhibit mitochondrial depolarisation and cardiomyocyte death following imatinib stress ..... 191
3.1.19. CSC-conditioned media preserve $Ca^{2+}$ cycling in hPSC-CM at sublethal concentrations of menadione ..... 193
3.1.20. CSC-conditioned media preserve action potential in hPSC-CM at sublethal concentrations of menadione ..... 196
3.1.21. Summary and conclusions ..... 199
3.2. Characterisation of the cardioprotective CSC secretome ..... 200
3.2.1. Protection by CSC-conditioned media is mediated by the >3kDa molecular fraction ..... 200
3.2.2. Protection by CSC-conditioned media depends on thermo-labile molecules ..... 201
3.2.3. Protection by CSC-conditioned media is exosome-independent ..... 203
3.2.4. Paracrine candidate identification in CSC by single cell qPCR and bulk RNA-Seq ..... 210
3.2.5. Neither single-factor titrations nor a six-factor cocktail protects human cardiomyocytes from menadione ..... 213
3.2.6. RNA-Seq of menadione treated IMR90 cardiomyocytes with and without CSC-conditioned medium ..... 216
3.2.7. Cytokine Array screen reveals secreted factors enriched in CSC ..... 228
3.2.8. Summary and conclusions ..... 232
3.3. Human cardiac stromal cell characterisation and function ..... 233
3.3.1. Molecular signature of human CSC resembles mouse CSC ..... 233
3.3.2. Human CSC protect hPSC-CM from menadione-induced stress ..... 236
3.3.3. Cytokine array screen reveals potential candidates for protection secreted by human CSC ..... 239
3.3.4. Summary and conclusions ..... 242
4. Discussion ..... 243
4.1. Human cardiomyocyte protection from cell death by CSC-secreted factors 243
4.2. Is CSC-conditioned medium sufficient to protect cardiomyocytes from acute oxidative stress? ..... 244
4.2.1. The unmet need in cardiac drug discovery ..... 244
4.2.2. Early human cardiomyocyte sources ..... 246
4.2.3. Human pluripotent stem cell-derived cardiomyocytes: a step closer to the patient phenotype ..... 248

4.2.4. Human PSC-CM: mitigating their limitations ..... 249
4.2.5. Engineered heart tissue and 3D cultures ..... 251
4.3. CSC-responsive mechanisms for human cardiomyocyte death ..... 253
4.3.1. Sensitivity of hPSC-CM to menadione stress ..... 253
4.3.2. Menadione-induced downstream signalling and implications in hPSC-CM 255
4.3.3. ROS-independent protection of human cardiomyocytes from doxorubicin by CSC-conditioned media ..... 258
4.3.4. Other players in doxorubicin-induced cardiotoxicity ..... 261
4.4. CSC-mediated cardioprotection is exosome-independent ..... 262
4.5. Characterisation of CSC-conditioned medium by genomic and proteomic approaches ..... 266
4.5.1. Transcriptomic profiling of the secretor cells and preliminary candidate testing 267
4.5.2. Transcriptomic profiling of the target cells and identification of potential protective mediators ..... 268
4.5.3. Identification of potential cardio-protective ligand-receptor pairs using bioinformatic tools ..... 269
4.5.4. Proteomic profiling of the protective medium ..... 274
4.6. Study limitations and future directions ..... 276
4.6.1. Model system ..... 276
4.6.2. Identification of the protective molecule(s) ..... 278
4.7. Implications of this study ..... 279
4.7.1. Human PSC-CM established as a platform for paracrine protection studies 279
4.7.2. Using menadione to model MI stress in cardiomyocytes ..... 280
4.7.3. Identification of the CSC-conditioned medium as an inhibitor of cardiomyocyte death at the time of MI ..... 281
5. References ..... 284
6. Supplementary Material ..... 383
Supplement 6.1. ..... 383
Supplement 6.2. ..... 389
Supplement 6.3. ..... 395
Supplement 6.4. ..... 401
Supplement 6.5. ..... 405

## List of Figures

Figure 1.1: Toxic effects of anthracycline agent doxorubicin in cardiomyocytes. ..... 28
Figure 1.2: Toxic effects of anti-cancer agent Imatinib in cancer cells and cardiomyocytes. ..... 30
Figure 1.3: Pathways of death receptor apoptosis and necroptosis. ..... 44
Figure 1.4: Pathway of mitochondrial apoptosis and overlap with death-receptor pathway via caspase-8 activity. ..... 47
Figure 1.5: Cell therapy for heart regeneration. ..... 55
Figure 1.6: The paracrine hypothesis. ..... 70
Figure 1.7: Intercellular mitochondrial transfer via tunnelling nanotubes. ..... 95
Figure 1.8: $Sca1^{+}$ SP CSC, the major cell population to be used in this work, are enriched in $PDGFR\alpha^{+}$ after culture expansion. ..... 116
Figure 1.9: Experimental design overview. ..... 119
Figure 3.1: CSC-conditioned media protect mouse myocardium after myocardial infarction. ..... 151
Figure 3.2: CSC inhibit the death of neonatal mouse and adult human cardiomyocytes in trans-well co-culture. ..... 154
Figure 3.3: Human cardiomyocyte co-culture with Sca1+ PDGFRα+ CD31- cells. 157
Figure 3.4: CSC- but not TTF-conditioned media protect hPSC-CM from menadione-induced death. ..... 161
Figure 3.6: CSC-conditioned media prevent the release of cardiac troponin I from human cardiomyocytes. ..... 165
Figure 3.7: CSC-conditioned media do not induce DNA synthesis in hPSC-CM. ... 167
Figure 3.8: CSC-conditioned media prevent DNA fragmentation in hPSC-CM after menadione stress. ..... 170
Figure 3.9: ROS generation before mitochondrial membrane depolarisation in menadione-stressed cardiomyocytes. ..... 175
Figure 3.10: CSC-conditioned media inhibit mitochondrial depolarisation in hPSC-CM after menadione stress. ..... 176
Figure 3.11: CSC-conditioned media inhibit ROS in hPSC-CM after menadione... 180
Figure 3.13: CSC-conditioned media inhibit death of hPSC-CM by doxorubicin. ... 184

Figure 3.14: Detection of mitochondrial depolarisation in hPSC-CM by doxorubicin and possible protection by CSC-conditioned medium. ..... 187
Figure 3.15: CSC-conditioned media fail to reduce ROS levels in hPSC-CM after doxorubicin stress. ..... 189
Figure 3.16: CSC-conditioned media fail to reduce superoxide levels in mitochondria of hPSC-CM after doxorubicin stress. ..... 190
Figure 3.17: CSC-conditioned media inhibit mitochondrial depolarisation and cardiomyocyte death following imatinib stress. ..... 193
Figure 18: CSC-conditioned media preserve Ca2+ cycling in hPSC-CM at sublethal concentrations of menadione. ..... 195
Figure 3.19: CSC-conditioned media preserve action potential in hPSC-CM at sublethal concentrations of menadione. ..... 198
Figure 3.20: Protection effect by CSC-conditioned media is mediated by the >3kDa molecular fraction. ..... 201
Figure 3.21: Protection by CSC-conditioned media depends on thermo-labile molecules. ..... 203
Figure 3.22: Exosome depletion and identification from CSC-conditioned media by ultracentrifugation and flow cytometry. ..... 206
Figure 3.23: Protection by CSC-conditioned media is exosome-independent. ..... 209
Figure 3.24: Paracrine candidate identification by single cell qPCR. ..... 211
Figure 3.25: Paracrine candidate identification by bulk RNA-Seq. ..... 212
Figure 3.26: Single factor titrations of candidates are insufficient to protect hPSC-CM from menadione stress. ..... 214
Figure 3.28: IMR90-cardiomyocyte characterisation. ..... 220
Figure 3.29: Conditioned medium down-regulates apoptosis-related genes and preserves cardiac structural genes in lethally stressed human cardiomyocytes. ..... 223
Figure 3.30: Receptor-ligand interaction screen by CellPhone DB to predict protective candidates. ..... 227
Figure 3.31: Cytokine array screen reveals candidate factors enriched in CSC. ..... 232
Figure 3.32: Molecular signature of human CSC resembles mouse CSC. ..... 236
Figure 3.33: Human CSC protect hPSC-CM from menadione-induced stress. ..... 238
Figure 3.34: Cytokine array screen reveals candidate factors enriched in CSC. ..... 241
Figure 4.1: Study summary. ..... 283

## List of Tables

Table 1.1: Representative mouse genetic models implicating cell-death regulator genes in cardiomyocytes. ..... 33
Table 1.2. Summary of studies demonstrating improved cardiac function in the heart after cell therapy, accompanied by poor cell retention/engraftment and attributed, at least in part, to paracrine effects. ..... 66
Table 2.1. Reagents and resources ..... 138

## List of abbreviations

| Abbreviation | Name | Abbreviation | Name |
|---|---|---|---|
| **ACTC1** | Actin alpha cardiac muscle 1 | **BCL2** | B-cell lymphoma 2 |
| **ADAM** | ADAM metallopeptidase domain 17 | **BH** | BCL homology |
| **ADSC** | Adipose derived stem cells | **BID** | BH3 interacting domain death agonist |
| **AK** | Adenylate kinase | **BMMNC** | Bone marrow mononuclear cells |
| **AKT** | Protein kinase B | **BMP** | Bone morphogenetic protein |
| **ALK7/ACVR1C** | Activin A receptor type 1C | **BMPER** | BMP binding endothelial regulator |
| **AMP** | Adenoside monophosphate | **BNIP3** | Bcl-2 intercting protein 3 |
| **AMPK** | AMP kinase | **CACNA1C** | L-type calcium channel |
| **ANGPT** | Angiopoietin | **CACNA1T** | T-type calcium channel |
| **ANXA5** | Annexin 5 | **CAD** | Coronary artery disease |
| **APAF** | Apoptotic protease activating factor | **CASP** | Caspase |
| **APOA1** | Apolipoprotein A1 | **CAT** | Catalase |
| **ASK1** | Apoptosis-signal-regulating-kinase 1 | **cCFU** | Cardiac colony forming units |
| **ATF** | Activating transcription factor | **CCL** | C-C motif chemokine ligand |
| **ATG** | Autophagy related | **CCN** | Cyclin |
| **ATP** | Adenoside tri-phosphate | **CDC** | Cardiosphere derived cells |
| **ATP1A2** | ATPase $Na^+/K^+$ transporting subunit alpha 2 | **CDK** | Cyclin dependent kinase |
| **BAD** | Bcl-2 associated death promoter | **CED** | C. elegans death |
| **BAK** | Bcl-2 homologous antagonist killer | **CFLAR** | CASP8 and FADD like apoptosis regulator |
| **BAX** | Bcl-associated X protein | **CLU** | Clusterin |
| **BCL10** | BCL10 immune signalling adaptor | **CondM** | Conditioned media |

| | | | |
|---|---|---|---|
| **CPC** | Cardiac progenitor cells | **ECG** | Electrocardiogram |
| **CM** | Cardiomyocyte | **EGF** | Epidermal growth factor |
| **CRISPR** | Clustered regularly interspaced short palindromic repeats | **eIF2a** | Translation initiation factor 2 |
| **CsA** | Cyclosporin A | **EOMES** | Eomesodermin |
| **CSC** | Cardiac stromal cells | **EPC** | Endothelial progenitor cells |
| **CT1** | Cardiotrophin-1 | **EPDC** | Epicardial progenitor cells |
| **CVD** | Cardiovascular disease | **EPO** | Erythropoietin |
| **CXCL** | C-X-C chemokine ligand | **EREG** | Epiregulin |
| **CYLD** | Cylindomatosis | **ERK** | Extracellular signal regulated kinase |
| **CYP1B1** | Cytochrome P450 family 1 subfamily B member 1 | **ETS1** | ETS proto-oncogene 1 |
| **CYPD** | Cyclophilin D | **FADD** | Fas associated death domain protein |
| **CytC** | Cytochrome c | **FCCP** | Carbonyl cyanide-4-(trifluoromethoxy) phenylhydrazone |
| **DIABLO** | Direct inhibitor of apoptosis binding protein with low PI | **FGF2** | Fibroblast growth factor |
| **DCN** | Decorin | **FNDC5** | Fibronectin type III domain containing 5 |
| **DDR2** | Discoidin domain receptor tyrosine kinase 2 | **FOS** | Fos proto-oncogene AP-1 trascription factor subunit |
| **DKK1** | Dickkopf Wnt signalling pathway inhibitor 1 | **FOXL2** | Forkhead box L2 |
| **DNA** | Deoxyribonucleic acid | **FTC** | Fumitremorgin C |
| **DOX** | Doxorubicin | **GADD45** | Growth arrest and DNA damage inducible |
| **DPP4** | Dipeptidyl peptidase 4 | **GATA4** | GATA binding protein 4 |
| **DR** | Death receptor | **G-CSF** | Growth colony stimulating factor |
| **DTK/TYRO3** | TYRO3 protein tyrosine kinase | **GDF** | Growth differentiation factor |

| | | | |
|---|---|---|---|
| **GO** | Gene Ontology | **KDR** | Kinase insert domain receptor |
| **GPX** | Glutathione peroxidase | **LA** | Left atrium |
| **$H_2O_2$** | Hydrogen peroxide | **LAD** | Left anterior descending |
| **HAND2** | Heart and neural crest derivatives expressed 2 | **LIF** | LIF interleukin 6 family cytokine |
| **hCSC** | Human cardiac stromal cells | **LIN** | Lineage |
| **HDF** | Human dermal fibroblasts | **LUBAC** | Linear ubiquitin chain assembly complex |
| **HDL** | High density lipoprotein | **LV** | Left ventricle |
| **hERG/KCNH2** | Potassium voltage gated channel subfamily H member 2 | **LVEF** | Left ventricular ejection fraction |
| **HGF** | Hepatocyte growth factor | **MAPK** | Mitogen-activated protein kinase |
| **hPSC-CM** | Human pluripotent stem cell-derived cardiomyocytes | **MCP1** | Monocyte chemoattractant protein |
| **HRP** | Hydroperoxidase | **MEF2A** | Myocyte enhancer factor 2A |
| **HTRA2** | High temperature requirement protein A2 | **MEKK** | MAPK/extracellular signal regulated kinase kinase 1 |
| **I/R** | Ischemia/reperfusion | **MESP1** | Mesoderm posterior BHLH transcription factor 1 |
| **IGF1** | Insulin like growth factor 1 | **MI** | Myocardial infarction |
| **IGFBP** | IGF binding factor | **MIF** | Macrophage migration inhibitor |
| **IL** | Interleukin | **miRNA** | MicroRNA |
| **INHBA** | Inhibin subunit beta A | **MIP2/CXCL2** | C-X-C motif chemokine ligand 2 |
| **IRF1** | Interferon regulatory factor 1 | **MLC** | Myosin light chain |
| **IVS** | Intraventricular septum | **MLKL** | Mixed lineage kinase domain like pseudo-kinase |
| **JAK** | Janus kinase | **MMP** | Metalloproteinase |
| **KCNJ5** | Potassium Inwardly Rectifying Channel Subfamily J Member 5 | **mPGES** | Microsomal enzyme prostaglandin E synthase |

| | | | |
|---|---|---|---|
| **mPTP** | Mitochondrial membrane transition pore | **PGRN** | Progesterin |
| **MSC** | Mesenchymal stromal cells | **PHLDA** | Pleckstrin homology like domain family A member 1 |
| **MYH** | Myosin heacy chain | **PKC** | Protein kinase C |
| **NANOG** | Nanog homeobox | **PLEKHN1** | Pleckstrin homology domain containing N1 |
| **NEC-1** | Necrostatin-1 | **PLN** | Phospholamban |
| **NGF** | Neural Growth factor | **PMAIP1** | Phorbol-12-myristate-13-acetate-induced protein 1 |
| **NHANES** | National health and nutrition examination survey | **POU5F1** | POU class 5 homeobox 1 |
| **NKX2-5** | NK2 homeobox 5 | **PP1** | Protein phosphatase 1 |
| **NLRP3** | NLR family pyrin domain containing 3 | **PPIF** | Peptidylprolyl Isomerase F |
| **NOL3** | Nucleolar protein 3 | **PTC** | Patched receptor |
| **NOX** | NADPH oxidase | **PUMA** | P53 upregulated modulator of apoptosis |
| **NPPA** | Natriuretic peptide A | **RA** | Right atrium |
| **NRG1** | Neuregulin-1 | **RB** | RB transcriptional corepressor 1 |
| **NTCC** | L-type $Ca^{2+}$ channel | **RIP** | Remote ischemic preconditioning |
| **OMM or MOMP** | Outer mitochondrial membrane permeabilisation | **RIPK** | Receptor interacting serine/threonine kinase |
| **OPN** | Osteopontin | **RLU** | Relative luminescence units |
| **PARP1** | Poly-ADP ribose polymerase-1 | **RNA** | Ribonucleic acid |
| **PBMNC** | Peripheral blood mononuclear cells | **RNAi** | RNA interference |
| **PBS** | Phosphate buffered saline | **RNS** | Reactive nitrogen species |
| **PDGFR** | Platelet derived growth factor receptor | **ROS** | Reactive oxygen species |
| **PEG** | Poly-ethelene glycol | **RV** | Right ventricle |

| | | | |
|---|---|---|---|
| **SCA1** | Stem cell antigen 1 | **TdT** | Terminal deoxynucleotidyl transferase |
| **SCN5A** | Sodium Voltage-Gated Channel Alpha Subunit 5 | **THBS** | Thrombospondin1 |
| **SDF1** | Stem cell derived factor 1 | **TNF** | Tumour necrosis factor |
| **SEM** | Standard error of the mean | **THY1** | Thy-1 cell surface antigen |
| **SFRP2** | Secreted frizzled related protein | **TGF** | Transforming growth factor |
| **SHED** | Human exfoliated desiduous teeth | **TIMP** | TIMP metallopeptidase inhibitor 1 |
| **SHH** | Sonic hedgehog receptor | **TKI** | Tyrosine kinase inhibitors |
| **siRNA** | Silencing RNA | **TNFRSF** | TNF receptor superfamily |
| **SMAC** | Second mitochondria derived activator of caspase | **TLR** | Toll-like receptor |
| **SOD** | Superoxide dismutase | **TMRM** | Tetramethylrhodamine |
| **SOX2** | SRY-Box transcription factor 2 | **TNNC1** | Troponin C1 |
| **SP** | Side population | **TNNI** | Troponin I |
| **STAT** | Signal transducer and activator of transcription | **TNNT2** | Troponin T2 |
| **SRB1** | Scavenger receptor class B1 | **TRADD** | TNFRSF1A associated via death domain |
| **STEMI** | ST-elevation MI | **TRAF** | TNF receptor associated factor |
| **Tβ4** | Thymosin β 4 | **TRAIL** | TNF superfamily member 1 |
| **TAB** | Activated kinase binding proteins | **TRDN** | triadin |
| **TAK** | Activated kinase | **TRIF** | Toll-like adaptor molecule |
| **TBM** | 3,3’,5,5’-tetramethylbenzidine | **TTF** | Tail tip fibroblasts |
| **TBX** | T-box transcription factor | **TUNEL** | Terminal deoxynucleotidyl transferase dUTP nick end labelling |

| | | | |
|---|---|---|---|
| **SLN** | Sarcolipin | **VEGF** | Vascular endothelial growth factor |
| **TOP2β** | Topoisomerase 2 β | **XIAP** | X-linked inhibitor of apoptosis |
| **VDAC** | Voltage-dependent anion channel | **ZBP1** | Z-DNA binding protein |
| **Ub** | Ubiquitin | | |

# 1. Introduction

## 1.1. The burden of cardiovascular disease

Cardiovascular disease (CVD) is the number one leading cause of death and poses an undoubtedly immense health and economic burden globally (Benjamin et al., 2019). Every year 3.9 million deaths are attributed to CVD, which accounts for 45% of total deaths in Europe alone (Wilkins et al., 2017). Based on data from the National Health and Nutrition Examination Survey (NHANES) of the United States, in 2016 CVD prevalence was 48% in adults > 20 years old and is increasing with age in both males and females (Benjamin et al., 2019). In terms of the economic burden, CVD is estimated to cost the European Union economy €210 billion per year, out of which 53% would be accounted to health care costs; 26% to productivity losses and 21% to after-care of people with CVD (Wilkins et al., 2017). Similarly, in the US, the average annual direct and indirect cost of CVD and stroke was an estimated $318 billion in 2015 and is projected increase to more than $749 billion by 2035 (Benjamin et al., 2019). Over the past 15 years there has been a 14.5% decrease in age-adjusted deaths accounted to CVD globally; however, CVD currently claims more lives each year than cancer and lung disease combined and is expected to account for more than 23.6 million deaths by 2030 (Benjamin et al., 2019). The most recent data indicate that CVD prevalence and costs are projected to increase substantially over the near future, due to the increasing age of the population and urbanization. Hence, intensive efforts in the scientific field focus on reducing the incidence and severity of CVD worldwide.

## 1.2. Myocardial infarction and progression to heart failure

One of the most common manifestations of CVD is myocardial infarction (MI). MI happens when the blood flow and oxygen supply to the heart muscle are interrupted by a narrowing or blockage of a coronary artery, typically due to rupture of the atherosclerotic plaque, leading to severe myocardial ischemia and eventual necrosis (Saleh and Ambrose, 2018). MI is one of the major causes of heart failure; the inadequacy of the heart to pump blood to support the requirements of the body (Anderson and Morrow, 2017; Saleh and Ambrose, 2018).

Heart failure is a global disease challenge affecting 38 million people worldwide (Braunwald, 2015). The associated prognosis upon a diagnosis of heart failure is worse than that of most cancers, with a 50% survival rate at 5 years (Cahill et al., 2017). Heart failure-related health care costs are projected to increase to $70 billion by 2030 (Heidenreich et al., 2013), the condition being a principal cause of hospitalisation, adverse quality of life, and death.

Current treatments of MI focus on protecting the heart from progressing to heart failure acting mainly through the recanalization of the occluded artery, to restore blood flow and minimise myocardial necrosis (Sacks et al., 2014). Commonly used methods of mechanical revascularisation include thrombolytic therapy, percutaneous coronary intervention (angioplasty, stents), and coronary artery bypass graft surgery (Er et al., 2016; Eyuboglu, 2015; González-Cambeiro et al., 2016). Several pharmacotherapy approaches are also widely used to target the maladaptive counter-regulatory mechanisms that lead to left ventricular remodelling after an infarct (Cahill et al., 2017). Although these strategies reduce patient mortality, neither revascularisation nor

pharmacotherapeutic agents address the underlying issue of cardiomyocyte and vasculature loss, rendering MI fundamentally incurable.

The reperfusion strategy of choice in the developed world is primary percutaneous coronary intervention, which has decreased inpatient mortality following acute MI from 20% to 5-7% since the 1980s (Jernberg et al., 2011; Smilowitz and Feit, 2016). Nevertheless, the ensuing cardiomyocyte death can promote left ventricular dysfunction, which – in many patients – culminates with heart failure (Cahill and Kharbanda, 2017). Importantly, for every 5% increase in infarct size, there is an associated 20% increase in the risk of heart failure and one year all-cause mortality (Mozaffarian et al., 2016). Despite significant progress in the management of acute myocardial infarction, heart failure prevalence remains high and its increasing incidence, rather than being paradoxical, is specifically attributed to improved early survival after primary percutaneous coronary intervention (Ezekowitz et al., 2009; Velagaleti et al., 2008). The opening of the occluded coronary artery by primary percutaneous coronary intervention reduces the ultimate extent of dying myocardium, but in the short-term, leads to a burst of oxidative stress that itself sparks additional cardiomyocyte death (Juránek and Bezek, 2005; Rodrigo et al., 2013). Thus, current treatments might restore blood flow and oxygen supply to the injured heart, however they fail to repair the damage that has already occurred in the myocardium and, moreover, contribute to myocyte loss via the so-called reperfusion injury.

## 1.3. Oxidative stress in myocardial infarction

Upon restoration of blood flow following ischemia, there is a burst of reactive oxygen species (ROS) generation, which is the major cause of myocardial damage by reperfusion injury (Rodrigo et al., 2013). Oxidative stress in the heart takes place when

oxidant products of metabolism become toxic either due to their increased production levels, or due to reduced availability of antioxidant or protective mechanisms (Ferrari et al., 1998; Juránek and Bezek, 2005). Increased ROS in the myocardium is mediated by activation of xanthine oxidase in endothelial cells, NADPH oxidase (NOX) in inflammatory cells and mitochondrial electron transport chain reactions in cardiomyocytes (Chamiec et al., 1996). Due to their contractile function, cardiomyocytes have an exceptionally high demand for ATP and as a result they might be particularly susceptible to agents that disturb mitochondrial function, either as a primary or a secondary effect.

Extensive work has been performed describing the sources of oxidative stress in cardiomyocytes. One notion was that the functional uncoupling of the respiratory chain was a result of complex I inactivation (Ide et al., 1999). Alternatively, increased ROS in the myocardium might be a result of defective antioxidant activity (Dhalla and Singal, 1994) or stimulation of NOX enzymes, which are a major source of superoxide species production through the transfer of electrons across the membrane to molecular oxygen (Bedard and Krause, 2007). An example is Nox4, the role of which has not been fully clarified yet in the heart, with available evidence demonstrating both a deleterious and a cardio-protective function of the enzyme (Morawietz, 2018). Early work demonstrated that Nox4 has an important role in induction of oxidative stress, mediating mitochondrial and cardiac dysfunction during pressure overload in mice (Kuroda et al., 2010). More recent studies by other groups revealed the specifics of a cardio-protective redox signalling pathway involving activation of Nox4 and subsequent binding to inhibit protein phosphatase (PP1) activity, increasing translation initiation factor 2 (eIF2a) phosphorylation and levels of activating transcription factor 4

(ATF4), ultimately enhancing cell survival and protecting tissues under stress (Santos et al., 2016).

Mitochondria are the major organelles involved in ATP production and thus any damage would cause defects in cellular energy production that could lead to different consequences including apoptosis (González-Montero et al., 2018). At the time of ischemia followed by reperfusion injury, due to the absence of oxygen in the former and sudden hyperoxic stress in the latter, the electron transport chain malfunctions, leading to the release of high levels of ROS. Meanwhile, ROS cause oxidative damage on mitochondrial DNA, introducing defects in mitochondrial function, and creating a vicious feedback loop. Oxidative damage also affects the mitochondrial membrane, leading to depolarisation and uncoupling of oxidative phosphorylation resulting in defects in cellular respiration and ultimately, induction of apoptosis (Nathan and Singer, 1999). Hence, induction of oxidative stress in cultured myocytes is not only an efficient tool to simulate reperfusion injury, but also a platform to test and predict protective interventions.

### 1.3.1. Menadione as an inducer of oxidative stress

Menadione is one of the major oxidative stress inducers used in the work presented here. Oxidative stress can be induced either using cell-independent ROS producers or cell-dependent, endogenous ROS inducers. Certain compounds like polyphenolic and other food-derived antioxidants undergo redox cycling that produces hydrogen peroxide ($H_2O_2$) when added to culture medium, independent of cells, due to the presence of pyruvate or catalase (Babich et al., 2009; Kelts et al., 2015; Long and Halliwell, 2009). In contrast, menadione-induced ROS production, depends on a

cellular mechanism; redox cycling to a semiquinone, which is then re-oxidised to a quinone by oxygen, forming superoxide (Criddle et al., 2006; Thor et al., 1982).

Menadione, or vitamin K, is a naphthoquinone that generally maintains healthy blood clotting and prevents excessive bleeding (Hassan, 2013). In the body, it also functions in the maintenance of healthy bone structure and carbohydrate storage (Hassan, 2013). Vitamin K derivatives have been found to be potent electron carriers between electron-donating and electron-accepting enzyme complexes of the mitochondrial respiratory chain and thus, an efficient source of endogenous ROS generation (Shneyvays et al., 2005; Yue et al., 2001).

In cultured cardiomyocytes, menadione induces rapid oxidation both in the cytosol and in the mitochondrial matrix (Loor et al., 2010). Subsequently, mitochondrial potential is reduced and cytochrome c release is triggered (Loor et al., 2010). The same study showed that other well-defined apoptosis-triggering molecules are all dispensable for menadione-induced death. These include components of the mitochondrial permeabilization pathway Bax/Bak and cyclophilin D (CypD), as well as members of the apoptosome complex cytochrome c and caspase 9 (all discussed in detail in section 1.5 below). In contrast, poly-ADP ribose polymerase-1 (PARP-1), seems to play an essential role in mediating menadione-activated cell death pathways (Loor et al., 2010). PARP activation has been linked to mitochondrial dysfunction, release of cytochrome c and bioenergetic deficiency-mediated death (Gagné et al., 2006; Yu et al., 2002). Genetic deletion of PARP-1 leads to significant protection from menadione, suggesting that it might be a common element of the pathways activated following menadione stress (Loor et al., 2010).

The cytotoxic effect of menadione has been reported in neonatal and adult rat cardiomyocytes (Loor et al., 2010; Tzeng et al., 1994), however there is a gap in the understanding of menadione toxicity mechanisms in physiologically relevant human models, as the one predominantly used in the present thesis. Nevertheless, rigorous prior work affirms the use of menadione as a cell culture surrogate of MI in the state-of-the-art human pluripotent stem cell derived cardiomyocytes (hPSC-CM), demonstrating the predictive power of the model, at least at the level of translation to whole-animal studies (Fiedler et al., 2019; Grimm et al., 2015).

## 1.4. Cardiotoxic anti-cancer agents as sources of oxidative stress in the heart

With the emergence of improved cancer treatments and strategies for early diagnosis, the major alternative cause of death in cancer survivors is now cardiovascular disease (Bloom et al., 2016; Yeh and Chang, 2016). For decades, traditional chemotherapeutics such as anthracyclines and radiation therapy have been coupled with cardiotoxic side effects (Moslehi, 2016; Rosa et al., 2016). More recently, targeted chemotherapeutics such as tyrosine kinase inhibitors (TKI) are more precise in affecting malignant cells (Ky et al., 2013; Moslehi, 2016). Nevertheless, cardiovascular side effects have not ceased even with the new-generation cancer therapies.

### 1.4.1. Anthracyclines like doxorubicin

Currently one of the most cardiotoxic drugs in clinical use is doxorubicin; a very efficacious anthracycline agent used routinely in anti-cancer chemotherapy (Ewer and Ewer, 2015). Doxorubicin-induced cardiotoxicity has been ascribed primarily to ROS generation (Singal and Iliskovic, 1998), however, ROS-scavengers like coenzyme

Q10, L-carnitive, NAC or vitamins E and C have failed to protect against the anthracycline drug in the clinic, suggesting additional involvement of alternative mechanisms (van Dalen et al., 2008; Martin et al., 2009; Myers et al., 1983). Despite the several pioneering studies investigating doxorubicin-induced cardiotoxicity, the basic underlying molecular mechanisms are only partly understood (Figure 1.1).

Recent emerging explanations for anthracycline-induced cardiac side effects implicate modulation of signalling networks that control DNA damage, cardiomyocyte survival, cardiac inflammation, mitophagy, energetic stress and modulation of gene expression (Ghigo et al., 2016). A landmark study by Zhang et al identified topoisomerase 2 (Top2) as an essential contributor to doxorubicin-mediated DNA damage (Zhang et al., 2012). While Top2α, the primary target isoform of anthracyclines in cancer cells, is absent from adult mammalian cardiomyocytes, Top2β is highly expressed in the myocardium. In the presence of doxorubicin, interaction with Top2β introduces DNA double strand breaks and a p53-dependent alteration in the transcriptome, which is implicated in oxidative phosphorylation and defective mitochondrial biogenesis in cardiomyocytes (Ghigo et al., 2016; Sahin et al., 2011; Zhang et al., 2012). Therefore, among others, targeting DNA damage and mitochondrial dysfunction in cardiomyocytes could provide useful strategies in the quest to reduce the cardiovascular burden of anti-cancer therapies.

### 1.4.2. Tyrosine Kinase Inhibitors

Apart from anthracyclines like doxorubicin, tyrosine kinase inhibitors (TKI) like imatinib are a different class of anti-cancer agents, also implicated in cardiotoxic side effects. TKI have been reported to mediate their toxicity through both on-target and off-target effects (Chen et al., 2008). For instance, sunitinib and sorafenib directly inhibit tyrosine kinase receptors such as vascular endothelial growth factor receptor (VEGFR) (Robinson et al., 2010; Schmidinger et al., 2008) whilst sunitinib has also been reported to induce cardiomyocyte apoptosis through inhibition of AMP-activated protein kinase phosphorylation (Kerkela et al., 2009). Thus, TKIs are a common cause of human cardiac muscle cell death, for which therapeutic interventions are not presently available.

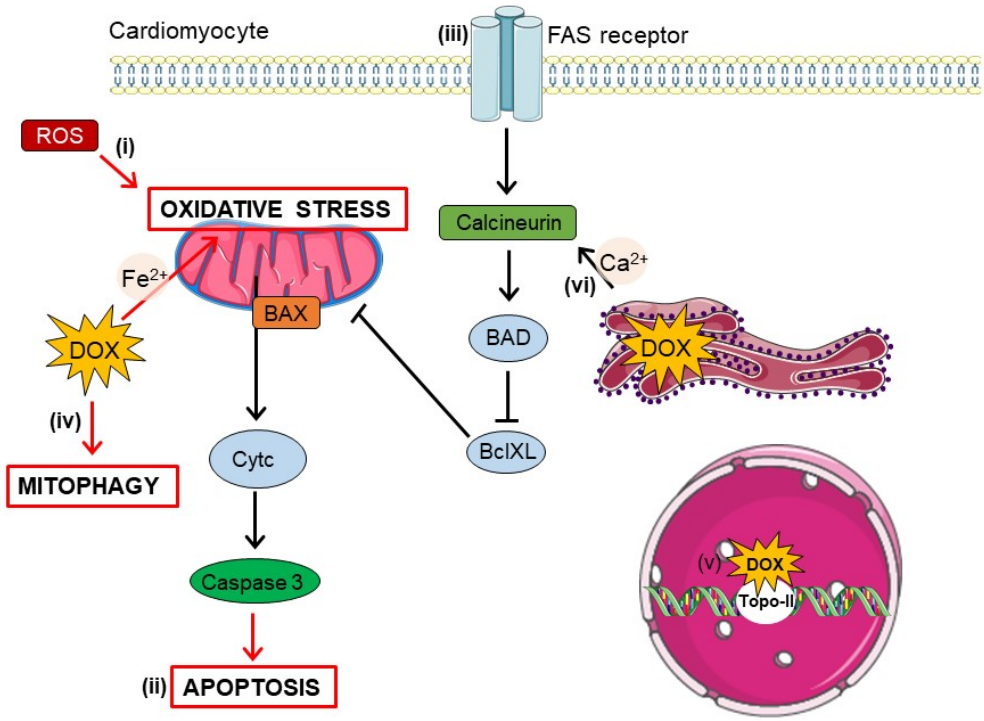



**Figure 1.1: Toxic effects of anthracycline agent doxorubicin in cardiomyocytes.** Molecular mechanisms of doxorubicin-induced cardiotoxicity include **(i)** ROS generation, **(ii)** mitochondrial apoptosis pathway, **(iii)** FAS-mediated apoptosis, **(iv)** mitophagy, **(v)** DNA damage and **(vi)** alteration of calcium homeostasis in sarcoplasmic reticulum. Schematic diagrams modified from the Servier Medical Art image database (https://smart.servier.com/).

Imatinib is one of the first-generation TKI approved in 2001 for the treatment of Chronic Myeloid Leukaemia and can be an alternative trigger of human cardiomyocyte toxicity (O'Brien et al., 2003). Inhibition of tyrosine kinase ABL in cardiomyocytes results in the downregulation of normal cardiac function in patients (Figure 1.2) (Force et al., 2007a; Kerkelä et al., 2006). Studies in cultured cardiomyocytes demonstrate imatinib-induced mitochondrial membrane dissipation, cytochrome c release and severely impaired ATP generation, associated with a type of cell death that exhibits a combination of apoptotic and necrotic features i.e. DNA fragmentation as a hallmark of apoptosis but also cytosolic vacuolisation; loss of membrane integrity and negligible activation of caspase-3, which point to necrosis (Force et al., 2007a). The detection of both necrotic and apoptotic features is consistent with the notion that apoptosis is an energy-requiring process. Hence, if energy generation is impaired, cells yield to necrotic death (Ankarcrona et al., 1995; Yuan et al., 2003). Thus, TKIs likewise induce cardiotoxicity, but through mechanisms complementary to those of anthracyclines, and counter-measures to inhibit human cardiac muscle cell death might fruitfully examine both.

As in the case of menadione- and doxorubicin-induced stress, mitochondrial dysfunction has the key role in the manifestation of the cardiotoxic response to imatinib. However here, the underlying mechanism seems to be the induction of endoplasmic reticulum (ER) stress, which has been observed both in cultured myocytes and in mouse hearts (Force et al., 2007a; Zhang and Kaufman, 2006). TKI-induced cardiovascular toxicities include myocardial ischemia, heart failure, QT prolongation and hypertension, thus early cardiotoxicity awareness, diagnosis and appropriate management are essential to achieve the benefits of TKI therapy.

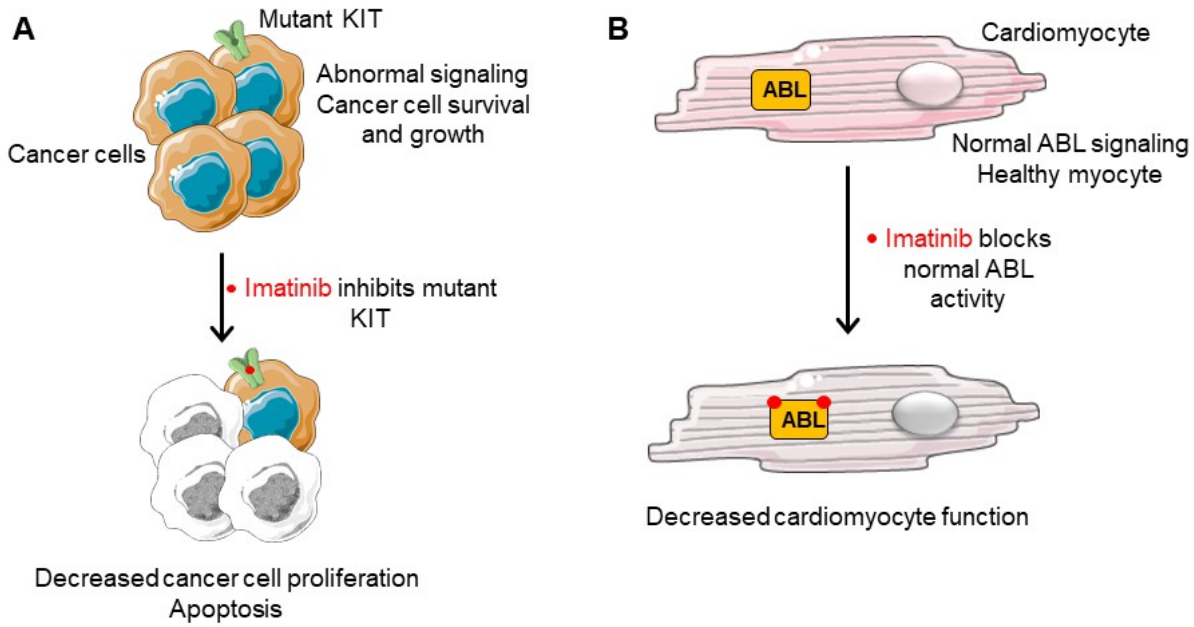



**Figure 1.2: Toxic effects of anti-cancer agent Imatinib in cancer cells and cardiomyocytes. A,** Imatinib binds to the ATP-binding pocket of tyrosine kinases blocking the mutant KIT receptor activity in tumour cells, leading to inhibition of intracellular signalling, decreased cell proliferation, and apoptosis of the cancer cells. **B,** Imatinib also inhibits the ABL kinase necessary for normal cardiac signalling, resulting in decreased cardiac myocyte function (via induction of ER stress, mitochondrial depolarisation and eventually cell death). Schematic diagrams modified from the Servier Medical Art image database (https://smart.servier.com/).

## 1.5. Mechanisms of cell death and implications for heart disease

Cardiomyocyte loss is an important component in the pathogenesis of heart failure and has been shown to occur within a spectrum of both apoptosis and necrosis via death receptor or mitochondrial signalling (Del Re et al., 2019). Given that regulated cell death is actively mediated through molecular pathways, strategies to inhibit parts of this signalling can be used to reduce cardiac damage and dysfunction. In the context of this thesis, a solid understanding of the molecular mechanisms involved in cardiomyocyte death could provide insights in the prediction of possible cardio-protective effectors present in the cardiac stromal cell conditioned media.

### 1.5.1. A historical perspective of regulated cell death

More than 30 years ago, cell death was considered passive and unregulated occurring as a result of direct damage to cellular components. Apoptosis was first described in 1972 (Kerr et al., 1972) as a morphologically different form of death than necrosis, however the idea that it was a regulated process had not yet surfaced. Programmed cell death was initially used to describe the elimination of specific cells at specific times during development in certain vertebrate and invertebrate organisms (Glucksmann, 1951; Hamburger and Levi-Montalcini, 1949; Lockshin and Williams, 1965; Saunders et al., 1962). In the 1980-90s, a network of genes that mediate these developmental cell deaths was identified in C. elegans and named ced-9, ced-4, ced-3 (Malin and Shaham, 2015). This discovery established the notion of a regulated and actively mediated suicide process in cells that occurred in a cell-autonomous manner (Yuan and Horvitz, 1990).

The ced-mediated genetic pathway has been conserved over millions of years of evolution to humans, where it regulates not only developmental but also cell death in embryonic and adult life. The orthologs of *ced-9*, *ced-4* and *ced-3* in mammals are the Bcl-2 family (Hengartner and Horvitz, 1994), Apaf-1 (Zou et al., 1997) and the caspase family (Yuan et al., 1993), respectively, all of which are essential mediators of the mitochondrial apoptosis pathway. Extensive research during the ’90s characterised the biochemical events taking place during the mitochondrial pathway of cell death, as well as a second pathway involving plasma membrane “death receptors” resembling the receptor for tumour necrosis factor-α (Amgalan et al., 2017a; Ashkenazi and Dixit, 1998; Galluzzi et al., 2018).

By the beginning of 2000, the assumption that apoptosis was the only regulated and active form of death was doubted, as necrosis was also shown to be actively mediated through regulated pathways; despite notable differences to apoptotic signalling, necrotic regulation also involves the mitochondria (Baines et al., 2005) or death receptor pathway, which denotes a specific mode of death, referred to as necroptosis (Holler et al., 2000; Micheau and Tschopp, 2003; Vercammen et al., 1998).

In addition to apoptosis and necrosis, several other death programs have been described since, including ferroptosis (Dixon et al., 2012), pyroptosis (Fink and Cookson, 2006), parthanatos (Fatokun et al., 2014), entotic cell death (Krishna and Overholtzer, 2016), NETotic cell death (Fuchs et al., 2007), lysosome-dependent cell death (Serrano-Puebla and Boya, 2016), autophagy-dependent cell death (Anding and Baehrecke, 2015), anoikis (Gilmore, 2005) and immunogenic cell death (Galluzzi et al., 2017). While each of these modes of death are differentiated by morphological and mechanistic features, further investigation is required to establish their true independence or whether they are functioning in an intercalated manner (Del Re et al., 2019). In addition, their respective contributions to cardiac pathobiology are uncertain. So far, entotic and lysosome-dependent cell death have not been demonstrated in cardiac cells, whereas NETotic cell death has been indirectly implicated via effects on neutrophils (Bonaventura et al., 2019). Table 1.1. below provides a concise summary of genetic models of cell death regulator genes in cardiomyocytes. The following section will expand on the mechanisms for which relevance to the heart is best established, namely, death receptor and mitochondrial pathways of cell death, with a focus on the overlap among apoptosis, necrosis and necroptosis, in the context of MI and heart failure.

**Table 1.1: Representative mouse genetic models implicating cell-death regulator genes in cardiomyocytes.** Modified and updated from (Chiong et al., 2011; Fiedler et al., 2014; Del Re et al., 2019). Genes were ordered alphabetically.

| Gene | Model | Phenotype | Reference |
|---|---|---|---|
| **AMPK** | AMPK-kinase dead | Attenuated autophagic response to ischemia, increased infarct size, poorer cardiac function | (Russell et al., 2004) |
| **ATF6** | ATF6-MER and caATF6 overexpression in cardiomyocytes | Better functional recovery, reduced cell death | (Martindale et al., 2006; Toko et al., 2010) |
| | dnATF6 overexpression in cardiomyocytes | LV dilatation, reduced fractional shortening, heart failure | (Toko et al., 2010) |
| **ATG5** | $Atg5^{-/-}$ | Hypertrophy and cardiac dysfunction with pressure overload | (Nakai et al., 2007) |
| **BCL2** | Bcl2 overexpression in cardiomyocytes | Increased functional recovery, decreased LDH release post-I/R, decreased infarct size and apoptosis | (Chen et al., 2001a, 2001b; Imahashi et al., 2004) |
| **BAX** | $Bax^{-/-}$ | Decreased creatine kinase release, casp3 activity and infarct size post I/R | (Hochhauser et al., 2007; Hoehhauser et al., 2003) |
| | $Bax^{-/-}$/$Bak^{-/-}$ in cardiomyocytes | Reduced infarct size, apoptosis and necrosis post I/R | (Whelan et al., 2012) |
| **BECLIN1** | $Beclin1^{+/-}$ | Decreased hypertrophy to pressure overload | (Zhu et al., 2007) |
| | | Reduced autophagy and infarct size after I/R | (Matsui et al., 2007) |
| | | Accelerated heart failure and early mortality at baseline | (Zhu et al., 2007) |

| | | | |
|---|---|---|---|
| | Beclin1 overexpression in cardiomyocytes | Exacerbated hypertrophy to pressure overload | (Chen et al., 2001b) |
| **BNIP3** | $Bnip3^{-/-}$ | Abrogated apoptosis in I/R, preserved LV systolic performance, reduced LV dilatation | (Diwan et al., 2007) |
| | | Reduced mitochondrial abnormalities and mortality after doxorubicin | (Dhingra et al., 2014) |
| | Bnip3 overexpression in cardiomyocytes | Increased apoptosis leading to progressive LV dilatation, conditional overexpression exacerbated apoptosis and infarct size | (Martindale et al., 2006; Toko et al., 2010) |
| **CASP1** | $Casp1^{-/-}$ | Decreased hypertrophy, improved survival, enhanced left ventricular function post -MI | (Merkle et al., 2007) |
| | | Reduced infarct size post-I/R | (Kawaguchi et al., 2011) |
| | YVAD inhibitor | Decreased ischemia-induced dysfunction of myocardium, improved contractility | (Pomerantz et al., 2001) |
| | Casp1 overexpression in cardiomyocytes | Heart failure at baseline | (Merkle et al., 2007) |
| | | Increased infarct size post-I/R | (Syed et al., 2005) |
| **CASP3** | Casp3 overexpression in cardiomyocytes | Nuclear and myofibrillar damage, increased infarct size, decreased survival post-MI | (Condorelli et al., 2001) |
| | $Procaspase\text{-}3^{-/-}$ in cardiomyocytes | | (Inserte et al., 2016) |

| | | | |
|---|---|---|---|
| **CASP7** | Procaspase-7$^{-/-}$ in cardiomyocytes | No reduction in infarct size post-I/R or post-MI dysfunction | |
| **CASP8** | Casp8$^{-/-}$ | Embryonic lethality, impaired cardiac muscle development, MEFs resistant to death-receptor induced apoptosis | (Varfolomeev et al., 1998) |
| | FKBP-Casp8 overexpression in cardiomyocytes | Extensive cardiomyocyte apoptosis and death, low levels of Casp8 led to low apoptosis and lethal DCM; abolished by pan-caspase inhibitor | (Wencker et al., 2003) |
| **cFLAR/CASPER** | Casper$^{-/-}$ | Embryonic lethality, impaired heart development, increased FasL and TNF-induced apoptosis | (Yeh et al., 2000) |
| **cIAP2** | IAP-2 overexpression in cardiomyocytes | Reduced infarct size, apoptosis, necrosis and TUNEL$^{+}$ cells post-I/R | (Chen et al., 2001b; Chua et al., 2007) |
| **CrmA** | CrmA overexpression in cardiomyocytes | Induction of apoptosis following doxorubicin treatment via caspase-independent pathways, likely AIF | (Bae et al., 2010) |
| **FADD** | Fadd$^{-/-}$ | Embryonic lethality, impaired cardiomyogenesis, abdominal haemorrhage | (Yeh et al., 1998) |
| | miR-103/107 antagomir | Reduced infarct size and necrosis post I/R | (Wang et al., 2015) |
| **FAS** | Fas$^{-/-}$ | Inhibited apoptosis following doxorubicin treatment, reduced infarct size post-I/R | (Lee et al., 2003b; Nakamura et al., 2000a) |

| | | | |
|---|---|---|---|
| **FAS/CD95/ TNFRSF6** | $Fas^{lpr}$ | Reduced apoptosis and infarct size post -MI | (Lee et al., 2003a) |
| **$Fe^{2+}$** | Perfusion of deferoxamine (iron chelator) or glutaminolysis inhibitor | Reduced infarct size post I/R | (Gao et al., 2015) |
| | Ferrostatin-1 | Reduced infarct size post I/R, reduced cardiac dysfunction post-doxorubicin | (Fang et al., 2019) |
| | | Cardiac dysfunction and pathological remodelling post-I/R, reduced cardiac cell death after transplantation | (Li et al., 2019a) |
| **Gαq** | Gαq overexpression in cardiomyocytes | Hypertrophy, modest apoptosis and cardiac drop-out following pressure overload, cardiac contractile failure<br><br>Reduced heart failure during pregnancy after capsase inhibition | (Adams et al., 1998; D'Angelo et al., 1997; Hayakawa et al., 2002) |
| | Tet-off ER-targeted Nix | Hearts protected against cell death, Bax/Bak-independent and mPTP-dependent cell death | (Yussman et al., 2002) |
| | Ter-off mitochondrial-targeted Nix | Hearts not protected against cell death, Bax/Bak- and caspase-dependent apoptosis | |
| **GPX4** | GPX4 overexpression in mitochondria | Reduced creatine kinase release post I/R | (Dabkowski et al., 2008) |
| **LTCC** | siRNA | Cardiac hypertrophy, interstitial fibrosis, | (Nakayama et al., 2007) |

| | | | |
|---|---|---|---|
| **LTCC** | | increased cardiomyocyte death after $Ca^{2+}$ overload | |
| | LTCC inhibitor | Prevented $Ca^{2+}$ influx-induced cell death and cardiomyopathy | (Nakai et al., 2007) |
| | LTCC overexpression in cardiomyocytes | $Ca^{2+}$ overload, necrosis, heart failure and premature death | (Nakayama et al., 2007) |
| **MIF** | $Mif^{-/-}$ | Increased infarct size post-I/R | (Miller et al., 2008; Qi et al., 2009) |
| **NIX/BNIP3L** | sNix overexpression in cardiomyocytes | Protection against peripartum cardiomyopathy in $G_{aq}$ transgenic females | (Chen et al., 2010b; Yussman et al., 2002) |
| **NLRP3/IκB** | miR-223-3p | Reduced infarct size and I/R-induced cardiac necroptosis | (Qin et al., 2016) |
| **TNFR1/DR6** | miR-223-5p | | |
| **NOL3/ARC** | $Nol3^{-/-}$ | Increased infarct size post-I/R, DCM development | (Foo et al., 2007) |
| | ARC overexpression in cardiomyocytes | Reduced infarct size post I/R | (Pyo et al., 2008) |
| **OMI/HTRA2** | Small molecule inhibitor | Reduced infarct size and cardiac dysfunction post-I/R, reduced IAP loss, decreased casp9 and casp3 activity | (Bhuiyan and Fukunaga, 2007; Liu et al., 2005b) |
| **PARP1** | $Parp1^{-/-}$ | Reduced cardiac contractile dysfunction post I/R | (Docherty et al., 1999; Grupp et al., 1999; Pieper et al., 2000; Zhou et al., 2006a) |
| | | Reduced infarct size and myocardial enzyme release | (Yang et al., 2000a; Zingarelli et al., 1997) |

| | | | |
|---|---|---|---|
| | | Reduced pathological remodelling after pressure overload | (Pillai et al., 2005) |
| **PPIF/CypD** | CsA or SfA | Inhibited cell death, improved left ventricular developed pressure (LVDP), reduced infarct size, CK and TnTI release | (Clarke et al., 2002; Piot et al., 2008) |
| | $Ppif^{-/-}$ | Isolated mitochondria resistant to mPTP opening in response to $Ca^{2+}$ and oxidative stress, mice resistant to I/R injury but sensitive to apoptotic stimuli | (Baines, 2007; Baines et al., 2005; Nakayama et al., 2007) |
| | $Ppif^{-/-}$; $Bax^{-/-}$ (cardiomyocytes only); $Bak^{-/-}$ | No further reduction in infarct size post-I/R, beyond the effect of Bax/Bak alone | (Whelan et al., 2012) |
| | $Ppif^{-/-}$ | Mortality in 5 days after swimming, increased hypertrophy and pulmonary edema | (Elrod et al., 2010) |
| | | Dilated cardiomyopathy and heart failure after pressure overload. Shift from fatty acid to glucose use | |
| **PUMA** | $Puma^{-/-}$ | Inhibited pressure overload-induced apoptosis and fibrosis; preserved pump function, rescued DCM in Mdm4 cardiac CKO, reduced infarct size in ex-vivo Langendorff model | (Mandl et al., 2011; Toth et al., 2006) |
| **RIPK1** | Small molecule inhibitor Nec-1 | Reduced infarct size post-I/R | (Lim et al., 2007) (Smith et al., 2007) |

| | | | |
|---|---|---|---|
| **RIPK3** | $Ripk3^{-/-}$ | Reduced infarct size post-I/R | (Newton et al., 2004; Zhang et al., 2016a) |
| | | Reduced cardiac remodelling and heart failure post-MI | |
| **RIPK1/RIPK33** | miR-873 | Reduced infarct size and necrosis post I/R | (Wang et al., 2016) |
| **STAT1** | STAT1 KO | Enhanced autophagy, protected from reperfusion | (Mccormick et al., 2012) |
| **TAK1** | $Tak1^{-/-}$ in cardiomyocytes | Dilated cardiomyopathy and heart failure at baseline | (Li et al., 2014a) |
| | $Tak1^{-/-}$ in cardiomyocytes; $Tnfr1^{-/-}$ | Inhibited pathological phenotype of $Tak1^{-/-}$ | |
| **TNF** | Tnf overexpression in cardiomyocytes | Spontaneous death of weaning mice, cardiac inflammation, interstitial edema | (Kubota et al., 1997) |
| **TNFR1/DR6** | Tnf overexpression in cardiomyocytes | Increased heart weight to body weight ratio, reduced ejection fraction, dilatation, inflammation, cardiomyocyte death | (Kuhota et al., 1997; Sivasubramanian et al., 2001) |
| **TNFRSF1a/b** | $Tnfrsf1a^{-/-}$<br>$Tnfrsf1b^{-/-}$<br>Double KO | Increased infarct size in double KO post-MI and accelerated apoptosis | (Kurrelmeyer et al., 2000) |
| **TRAF2** | $Traf^{-/-}$ in cardiomyocytes | Dilated cardiomyopathy and heart failure at baseline | (Guo et al., 2017) |
| | $Traf^{+/-}$ in cardiomyocytes | Dilated cardiomyopathy and heart failure post-MI | |

| | | | |
|---|---|---|---|
| | $Traf2^{-/-}$ in cardiomyocytes; $Tnfr1^{-/-}$ | Inhibited pathological phenotype of $Traf2^{-/-}$ | |
| | $Traf2^{-/-}$ in cardiomyocytes; $RIPK3^{-/-}$ | | |
| **VDAC1/3** | $Vdac1^{-/-}$; $Vdac3^{-/-}$; Double KO | Isolated mitochondria show $Ca^{2+}$ swelling, no effect on cyt c release or caspase cleavage in response to Bax and Bid | (Baines et al., 2007) |
| **XIAP** | $Xiap^{-/-}$ | Reduced infarct size post I/R | (Brocheriou et al., 2000; Chen et al., 2001b) |
| | | Increased cardiomyocyte sensitivity to cyt-c induced apoptosis | (Potts et al., 2003) |

### 1.5.2. Death receptor pathway

As its name suggests, the death receptor pathway is regulated by the binding of specific death-promoting ligands to their receptors on the cell surface. The outcome of this signalling is not only apoptosis as originally thought, but also necroptosis, cell survival, proliferation and inflammation (Galluzzi and Kroemer, 2008; Hitomi et al., 2008; Shan et al., 2018a; Vercammen et al., 1998; Weinlich et al., 2017). Death receptors have been classified in two groups; the tumour necrosis factor superfamily (Ashkenazi and Dixit, 1998) and a more disputable set of 'dependency receptors', a heterogeneous family which includes among others the prototypical netrin-1 receptor (DCC) and the 12-transmembrane Sonic hedgehog (Shh) receptor Patched (Ptc) (Goldschneider and Mehlen, 2010; Mehlen et al., 1998; Mille et al., 2009; Thibert et al., 2003). Dependency receptors are thought to not only transduce 'positive' survival

signals when their ligands are present, but also ‘negative’ death signals when they are ligand-free (Mehlen, 2010).

Death receptor signalling is initiated following binding of the death receptor ligand (e.g. tumour necrosis factor α (TNFα)) to its receptor on the plasma membrane (e.g. TNF receptor 1 (TNFR1)) and formation of Complex I on the receptor’s cytoplasmic tail, which transduces signaling cascades for survival, death receptor apoptosis or necroptosis (Figure 1.3) (Aggarwal, 2003; Berghe et al., 2014). For Complex I formation, TNFR1-associated death domain (TRADD) is recruited, which then binds receptor interacting protein kinase 1 (RIPK1). The adaptor proteins TNFR-associated factor 2 and 5 (TRAF2/5) and cellular inhibitor of apoptosis proteins 1 and 2 (cIAP1/2) bind to TRADD. The linear ubiquitin chain assembly complex (LUBAC) is then recruited to the assembled structure catalyzing ubiquitylation of RIPK1. In its ubiquitylated form, RIPK1 transduces signals for survival which involve interaction of activated kinase 1 (TAK1) with TAK1 binding proteins 2 and 3 (TAB2/3), activation of mitogen-activated protein kinases (MAPK) and nuclear factor κB (NFκB) (Figure 1.3) (Brenner et al., 2015; Shan et al., 2018a). Decreases in RIPK1 ubiquitination catalysed by cylindromatosis (CYLD) and A20 result in different cytosolic complexes derived from Complex I, which trigger apoptosis and necroptosis (Draber et al., 2015; Wartz et al., 2004).

Death receptor mediated apoptosis can be RIPK1-dependent and RIPK1-independent (Shan et al., 2018a), however it requires activation of caspase-8 and formation of a complex with Fas-associated death domain protein (FADD) and phosphorylated RIPK1 - if available - or TNFR1-associated death domain protein (TRADD), in the absence of RIPK1 (Figure 1.3). The resulting molecular group, termed ‘Complex IIa’

catalyses the activation of caspases-3 and -7 which execute cell death processes via the extrinsic pathway of apoptosis. Ubiquitination and phosphorylation of RIPK1 are the critical steps prompting the selection between RIPK1-dependent and RIPK1-independent pathways; however the underlying mechanisms are incompletely understood (Dondelinger et al., 2015; Geng et al., 2017).

In the absence of caspase-8 the necrosome (complex IIb) is formed which facilitates necroptosis. Absence of caspase-8 might result from a range of apoptosis-inhibitory mechanisms such as viral protein dependent caspase-8 inhibition, which enables viral persistence and amplification (Ray and Pickup, 1996). Another factor regulating the occurrence of necroptosis is the abundance of cellular FLIP (c-FLIP), a recently identified homologue of caspase-8, which is enriched in the heart and might be responsible for inhibiting apoptosis via the Fas pathway in cardiomyocytes (Imanishi et al., 2000; Irmler et al., 1997). The proposed c-FLIP-dependent apoptosis-inhibitory mechanism relies on procaspase-8-c-FLIP heterodimerisation (Oberst et al., 2011), markedly inhibiting caspase-8 activation and ultimately blocking apoptosis and pushing the cell down the necroptotic pathway (Feoktistova et al., 2011).

Necroptosis refers to a regulated form of necrosis that depends on mixed lineage kinase domain like pseudo-kinase (MLKL), serine-threonine kinase interacting protein 3 (RIPK3) and in some instances on (RIPK1) (Degterev et al., 2005; Festjens et al., 2006; Galluzzi et al., 2018; Kroemer et al., 2009) (Figure 1.3). At the molecular level, upon necroptosis initiation by TNFR1, RIPK1 catalyses the activation of RIPK3 through phosphorylation. Necrostatin-1 (Nec-1) and its derivatives (Nec-1s) are allosteric RIPK1 inhibitors used in several studies to demonstrate the role of necroptosis in a range of cell death pathologies including brain ischemic injury,

myocardial infarction and chemotherapy-induced death (Vandenabeele et al., 2008). Importantly, RIPK3 can be activated independently of RIPK1, through its interaction with Toll-like receptor adaptor molecule 1 (TRIF) (Kaiser et al., 2013) or Z-DNA binding protein (ZBP1) (Maelfait et al., 2017). Subsequently, activated RIPK3 phosphorylates MLKL catalysing its oligomerisation and translocation to the plasma membrane to bind phosphatidylinositol species which are translocated to the outer leaflet of the plasma membrane, ultimately triggering membrane permeabilization via an incompletely understood mechanism which might involve $Na^{+}/Ca^{2+}$ influx, osmotic changes and activation of endosomal sorting complexes (Cai et al., 2014; Gong et al., 2017; Murphy et al., 2013).

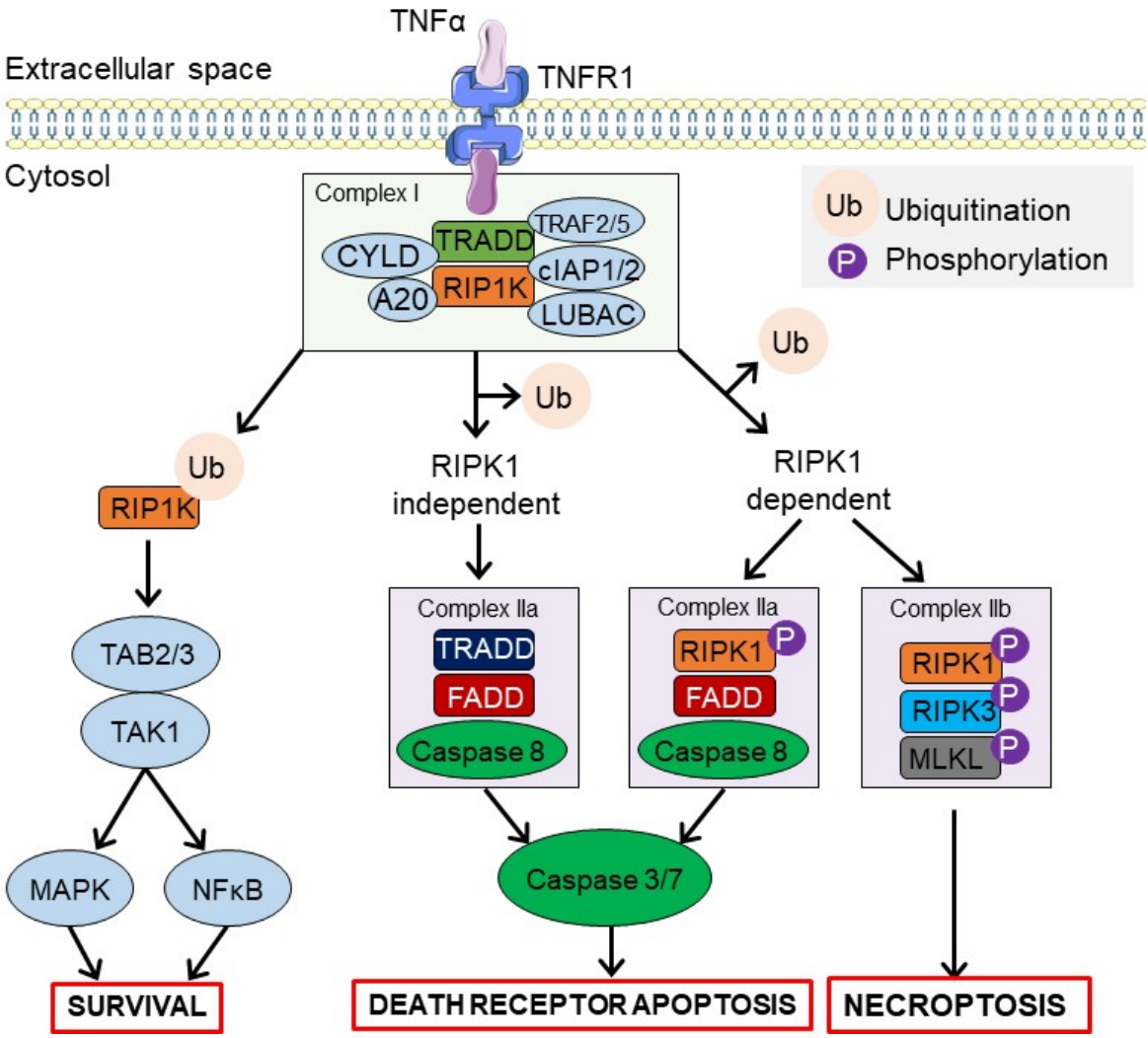


**Figure 1.3: Pathways of death receptor apoptosis and necroptosis.** The death receptor ligand (e.g. tumour necrosis factor α (TNFα)) binds to its receptor on the plasma membrane (e.g. TNF receptor 1 (TNFR1)), triggering Complex I assembly on the receptor's cytoplasmic tail and activating cascades that lead to cell survival, apoptosis and necroptosis. Complex I is formed following the recruitment of TNFR1-associated death domain (TRADD) which then binds receptor interacting protein kinase 1 (RIPK1). The adaptor proteins TNFR-associated factor 2 and 5 (TRAF2/5) and cellular inhibitor of apoptosis proteins 1 and 2 (cIAP1/2) bind to TRADD. The linear ubiquitin chain assembly complex (LUBAC) is the recruited to the assembled structure catalysing ubiquitylation of RIPK1. Subsequent interaction of activated kinase 1 (TAK1) with TAK1 binding proteins 2 and 3 (TAB2/3) leads to activation of mitogen-activated protein kinases (MAPK) and nuclear factor κB (NFκB) which promote cell survival. Transition from Complex I to Complex II initiates cell death responses. Decreases in RIPK1 ubiquitination catalysed by cylindromatosis (CYLD) and A20 result in death receptor apoptosis or necroptosis through formation of Complex IIa or IIb, respectively. Complex IIa can form with or without RIPK1; binding of TRADD-FADD-pro-caspase-8 leads to RIPK1-independent apoptosis via activation of caspases-3 and -7. Alternatively, binding of activated RIPK1-FADD-pro-caspase-8 leads to RIPK1-dependent apoptosis. Upon inhibition of capsase-8, RIPK1 and RIPK3 form Complex IIb that phosphorylates and activates mixed lineage kinase like domain (MLKL), which translocates to and permeabilises the plasma membrane resulting in necroptosis. Modified from (Del Re et al., 2019). Schematic diagrams modified from the Servier Medical Art image database (https://smart.servier.com/).

### 1.5.3. Mitochondrial pathway

The mitochondria have a central role in both apoptosis and necrosis and can be activated by several stimuli including but not limited to: survival factors; hypoxia/reoxygenation; ischemia/reperfusion; oxidative stress; DNA damage; increases in $Ca^{2+}$ concentrations and multiple toxins or drugs (Danial and Korsmeyer, 2004). Mitochondrial-mediated apoptosis largely depends on mitochondrial outer membrane (OMM) permeabilization, or MOMP (Figure 1.4).

The regulation of MOMP depends on the family of B-cell lymphoma 2 (BCL-2) proteins, which consists of three subfamilies, grouped according to which BCL-2 homology (BH) domains they carry and their apoptosis-promoting or -inhibitory functions: the pro-

survival BH1-4; the pro-death BH1-3 and the pro-death BH3-only containing proteins (Chipuk et al., 2010). The three subfamilies engage in complex interactions in order to regulate MOMP (Figure 1.4). Briefly, BH-3 only proteins transduce signals to activate BCL-2 associated X protein (BAX) and BCL-2 antagonist/killer 1 (BAK) and inactivate the pro-survival BCL-2. In contrast, the anti-apoptotic BCL-2 proteins inactivate BAX and BAK (Del Re et al., 2019).

Once activated, BAX and BAK oligomerise on the mitochondrial membrane inducing MOMP, which allows the release of so-called apoptogens into the cytosol, such as cytochrome c, second mitochondria-derived activator of caspase (SMAC) / direct inhibitor of apoptosis (IAP) binding protein with low PI (DIABLO) and OMI/high temperature requirement protein A2 (HtrA2) (Faccio et al., 2000; Suzuki et al., 2001). Once in the cytosol, cytochrome c facilitates the assembly of the apoptosome, a multi-protein complex made up of Apaf1, dATP and procaspase-9 (Acehan et al., 2002). The complex binds in a way that triggers activation of initiator caspase-9, which in turn cleaves and activates downstream effectors including caspases-3 and -7 leading to apoptosis.

Interestingly, an interconnecting cascade between the death receptor and mitochondrial apoptosis pathways has been reported (Figure 1.4). Caspase-8, which is activated during death receptor-mediated apoptosis, can cleave BH3-interacting domain death agonist (BID), producing truncated BID (tBID), which then binds and activates BAX and BAK (Gross et al., 1999; Li et al., 1998). This mechanism provides not only a bridge between the mitochondrial and death receptor pathways of apoptosis but also a critical amplification loop required by death receptor ligands to enhance caspase activation in a number of cell types.

Apart from the central role in apoptotic death, mitochondria are essential players in death by necrosis, as ATP depletion is a hallmark of this state; however, molecular details of the pathway for necrosis are not yet well-defined (Del Re et al., 2019). One suggested mechanism proposes that the intra-mitochondrial elevation of $Ca^{2+}$ concentration triggers the opening of the mitochondrial membrane transition pore (mPTP) in the inner mitochondrial membrane (IMM). $Ca^{2+}$-induced mPTP can be triggered by several stimuli, some of which are relevant to reperfusion, including oxidative stress, increased phosphate, and reduced adenine nucleotides (ATP and ADP). Moreover, CypD has been reported as a strong positive regulator of $Ca^{2+}$-mediated pore-opening: its genetic deletion effectively inhibits $Ca^{2+}$-mediated mPTP and thus, mitochondrial-dependent necrosis (Baines et al., 2005). Additional supporting studies have reported that cyclosporin A, a CypD inhibitor, attenuates $Ca^{2+}$-induced mPTP, while blocking I/R injury at least in preclinical models (Crompton et al., 1988; Lim et al., 2012; Ong et al., 2015).

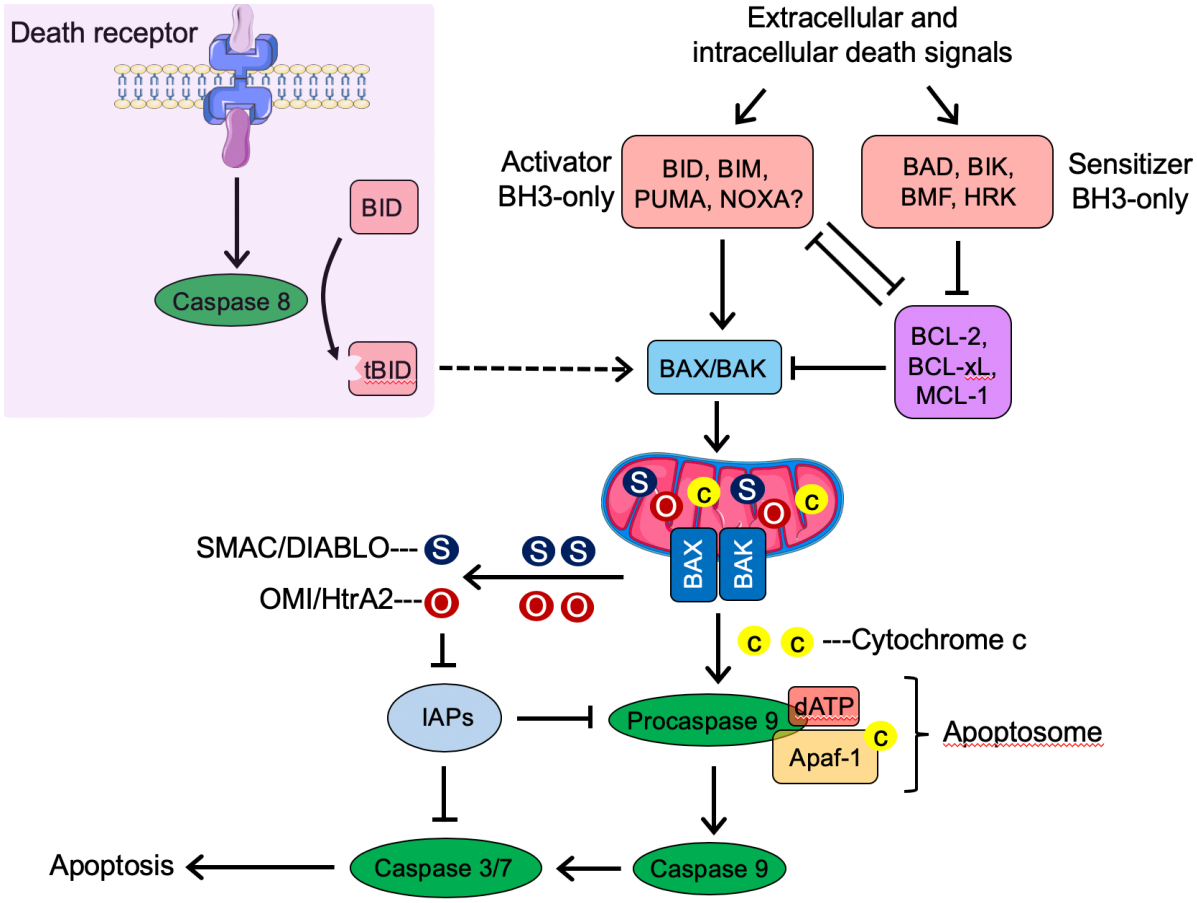



**Figure 1.4: Pathway of mitochondrial apoptosis and overlap with death-receptor pathway via caspase-8 activity.** Various extracellular and intracellular stress stimuli could trigger the mitochondrial apoptosis pathway. The major event is outer mitochondrial membrane permeabilization (OMM), a tightly regulated process by B cell lymphoma-2 (BCL-2) family proteins. Activator BH3-only proteins [which include BCL-2 interacting domain death agonist (BID), BCL2-interacting mediator of cell death (BIM), p53 upregulated modulator of apoptosis (PUMA) and possibly phorpbol-12-myristate-13-acetate-induced protein 1 (NOXA)] directly bind and activate BCL2-associated X-protein (BAX) and BCL-2 antagonist/killer-1 (BAK). Alternatively, the pro-survival proteins, [which include BCL-2, BCL2-like1 long form (BCL-xL), and myeloid cell leukemia 1 (MCL-1)] sequester the activator BH3-only proteins and inhibit BAX/BAK. In turn, the pro-survival proteins are inactivated by sensitizer BH3-only proteins [which include BCL-2 antagonist of cell death (BAD), BCL-2 interacting killer (BIK), BCL-2 modifying factor (BMF) and Harakiri (HRK)], effectively preventing inhibition of BAX/BAK. Once BAX/BAK are activated, they oligomerize within the OMM initiating membrane permeabilization and release of apoptogens such as cytochrome c, second mitochondrial-derived activator of caspase (SMAC)/direct inhibitor of apoptosis (IAP) binding protein with low PI (DIABLO) and OMI/high temperature requirement protein A2 (HtrA2). Release of cytochrome c contributes to the formation of the apoptosome which consists of dATP and Apaf-1 and activates pro-caspase-9

into its effector caspase-9 form, which subsequently activates downstream caspases-3 and -7. IAPs bind and inhibit procaspase-caspases-3 and -7. Conversely, SMAC/DIABLO and OMI/HtrA2 bind and inhibit IAPs resulting in activation of caspases. Caspase-8 is the link between the death receptor and the mitochondrial pathway by cleaving and activating BID (into tBID) which in turn activates BAX. Modified from (Del Re et al., 2019). Schematic diagrams modified from the Servier Medical Art image database (https://smart.servier.com/).

An important challenge among researchers has been the elucidation of how $Ca^{2+}$ levels increase in the mitochondrial matrix, according to different pathologies. In the case of I/R injury, a suggested pathway proposes that during ischemia, the production of lactic acid due to anaerobic metabolism increases the intracellular proton ($H^+$) content (Murphy et al., 1991). This can be reversed in part by the plasma membrane $Na^+/H^+$ exchanger (Griffith et al., 1995). However, with the ensuing $Na^+$ overload, the plasma membrane $Na^+/Ca^{2+}$ exchanger responds by importing large amounts of $Ca^{2+}$ (Bolli et al., 2004; Imahashi et al., 2005). Meanwhile, the sarcoplasmic reticulum contributes to additional release of $Ca^{2+}$, which unavoidably reaches the mitochondrial matrix. As previously suggested, mPTP opening occurs during the reperfusion phase, after being stimulated by ROS and changes in acidosis. The aforementioned pathway was the basis for the use of $Na^+/H^+$ exchange inhibitors in I/R, which showed promising results in preclinical models, but failed in clinical trials for reasons that were not fully understood (Karmazyn, 1988; Murphy et al., 1991; Théroux et al., 2000).

Recent work has revealed that despite their established role in MOMP and apoptosis, BAX and BAK are also involved in necrosis via the mitochondrial pathway by sensitising cells to $Ca^{2+}$-induced mPTP opening (Karch et al., 2013; Whelan et al., 2012). Cardiomyocyte-specific deletion of *Bax* and global deletion of *Bak* in a mouse model of I/R reduced infarct size as well as morphological features of necrosis such

as mitochondrial fragmentation and sarcomeric structure disorganisation (Whelan et al., 2012). Furthermore, triple knockout mice lacking BAX/BAK and CypD fail to show any additional reduction in infarct size over the ones lacking BAX/BAK. These data not only provide genetic evidence that BAX/BAK and CypD pathways overlap, but also introduce a plausible role of BAX/BAK in necrotic death.

The mechanisms underlying mPTP-mediated necrosis are partly understood. The field agrees on two major consequences resulting from mPTP opening: first, the immediate dissipation of the $H^+$ gradient across the IMM, resulting in a halt of ATP synthesis, and, second, rapid water flow down its osmotic gradient into the matrix, leading to mitochondrial swelling (Del Re et al., 2019). Thus, a hallmark of necrosis is the depletion in ATP levels brought about not only by the cessation in ATP synthesis, but also, its uncontrollable expenditure often described as “energetic crisis” (Leist et al., 1997; Saelens et al., 2005; Soldani and Scovassi, 2002; Sun et al., 2004). ATP depletion, leading to defects in plasma membrane pump activity, might be the explanation for the loss of plasma membrane integrity, a second hallmark of necrosis (Esmann et al., 2008). In stark contrast, apoptotic cells utilise caspase-mediated cleavage of effectors to arrest several energy-requiring processes including DNA repair, protein translation and proteasomal function (Del Re et al., 2019).

Despite the aforementioned differences between necrosis and apoptosis, the two modes of cell death share a number of interconnections. As described above, the death receptor pathway can shift between apoptosis and necrosis via the differential activation of complex IIa or IIb (Figure 1.3). Furthermore, there is a plausible interconnection at the level of the mitochondrial pathway, although less well defined (Amgalan et al., 2017b). One study demonstrated that the osmotic effects following

mPTP opening, promote OMM rupture, leading to cytochrome c release and subsequent caspase activation (Baines et al., 2005). The extent to which this caspase activation amplifies necrotic cell death is a subject for further research. An alternative route of interconnection between the two modes of cell death, was revealed by caspase-mediated cleavage of NADH dehydrogenase Fe-S protein 1 (NDUFS1), which was found to lead to necrotic features like oxidative stress, mitochondrial depolarisation and swelling (Ricci et al., 2004). Hence, the overlapping nature of the pathways is clear from currently available data, however future work needs to focus on establishing the details of the bidirectional connection between apoptosis and necrosis within the mitochondrial pathway.

### 1.5.4. Cell death during myocardial infarction and heart failure

MI is most commonly caused by ischemia, which occurs when there is an occlusion in the supply of oxygen and nutrients to portion of the heart, resulting in several structural and functional consequences, the most irreversible being myocardial cell death. Cardiomyocytes and non-myocytes are equally affected, however the former have been better studied (Hayakawa et al., 2002; Scarabelli et al., 2001; Takemura et al., 1998). Over the last years, there has been ample documentation of genetic and pharmacological manipulations of cell death pathways and their positive effects on infarct size and improvement of cardiac function in preclinical models of MI (Fiedler et al., 2014; Del Re et al., 2019). Despite the overall trend of beneficial effects following cardiomyocyte salvation, the critical balance between different cell death programmes at the time of MI remains to be elucidated.

When apoptosis was still the major regulated pathway of cell death to be known, several genetic manipulation studies were performed that inhibited apoptosis

signalling by perturbations in both the death receptor and the mitochondrial pathway. These studies demonstrated successful reduction in apoptotic markers such as terminal deoxynucleotidyl transferase dUTP nick end labeling (TUNEL) in cardiomyocytes as well as in infarct size in mice (Chen et al., 2001b; Fujio et al., 2000; Gottlieb et al., 1994; Jeremias et al., 2000; Lee et al., 2003a; Matsui et al., 2001; Miao et al., 2000), concluding that cardiomyocyte apoptosis is a critical event in the pathogenesis of MI. Later studies disputed the suggested role of apoptosis in cardiomyocyte death during MI, demonstrating negligible contribution of caspases-3 and -7 to cardiomyocyte death induced in a mouse model of coronary occlusion (Inserte et al., 2016). Genetic inhibition of pathways mediating mitochondria-dependent necrosis (Baines et al., 2005; Inserte et al., 2016), necroptosis (Lee et al., 2003a; Nakagawa et al., 2005; Newton et al., 2016; Zhang et al., 2016b), ferroptosis (Baba et al., 2018; Dabkowski et al., 2008; Dixon et al., 2012; Gao et al., 2015), pyroptosis (Kawaguchi et al., 2011), parthanatos (Yang et al., 2000b) and autophagy (Liu et al., 2013b; Matsui et al., 2007) have also demonstrated convincing reductions in death of cardiomyocytes and size of infarct during MI. Whether cardiomyocyte death in the context of MI is occurring through multiple cell death programmes, or whether the analyses have been confounded due to the high overlap and interconnections between the different death mechanisms are subjects of further study.

In contrast to MI, where the dominant event is cardiomyocyte death, in heart failure myocyte death coexists with other processes, as one contributor among several to the overall pathogenesis, including fibrosis, inflammation, and vascular remodelling (Metra and Teerlink, 2017). Methods of quantifying cardiomyocyte numbers *in vivo* are highly controversial and technically limiting and in order to be addressed, markers of cell death programmes such as DNA laddering and TUNEL, have been used. In failing

human hearts, the rate of TUNEL-positive cardiomyocytes has been estimated to be 0.08-0.25%, compared to 0.001-0.002% in non-failing hearts (Guerra et al., 1999; Narula et al., 1996; Olivetti et al., 1997; Saraste et al., 1999). These miniscule numbers have raised the question of whether cardiomyocyte death is important in the pathogenesis of the failing heart. A strong response to this question comes from the large number of studies – a few of which are described below – manipulating cell death pathways and demonstrating the significant role of dying cardiomyocytes in the progression of heart failure.

Specifically, genetic manipulation of critical components of the death receptor pathway have been shown to counter-act the pathogenesis of heart failure. In a study by Luedde et al., global RIPK3 knockout did not change infarct size, but rather reduced adverse cardiac remodelling and dysfunction after 1 month (Luedde et al., 2014). However, the study did not assess additional necroptosis markers. In a complementary study, lack of RIPK3 was found to attenuate doxorubicin-induced cardiac dysfunction (Zhang et al., 2016b). In the context of the mitochondrial pathway of cell death, deletion of CypD, attenuated fibrosis, cardiac dysfunction and facilitated a rescue from heart failure in doxorubicin-treated mice (Nakayama et al., 2007). In complementary studies, CypD deletion in cells led to normal levels of death following apoptotic triggers but rescued necrotic death induced by ROS and $Ca^{2+}$ overload, while CypD-deficient mice were resistant to I/R injury (Baines et al., 2005; Nakagawa et al., 2005). Similarly, the overexpression of anti-apoptotic BCL-2 reduced I/R injury but only partially attenuated cardiomyocyte apoptosis, implicating multiple cell death pathways in the pathogenesis of heart failure (Haudek et al., 2007; Imahashi et al., 2005; Nakayama et al., 2007).

In summary, the studies described in this section conclude that regulated forms of cell death are significant contributors to the pathogenesis of MI and heart failure. However, the primary limitation of this notion is that most genetic and pharmacological studies to date have been performed in animal models and proceeding clinical trials failed to provide fruitful results. Nevertheless, heart samples from patients with cardiac dysfunction pathologies show various markers confirming the existence of multiple cell death programmes. For instance, explanted hearts from patients with idiopathic dilated cardiomyopathy not only showed caspase-3 activation and TUNEL detection in myocytes but also presence of autophagic vacuoles and complement 9, a marker of oncotic death (Kostin et al., 2003). As emphasised above, acute cardiomyocyte loss both is the central event in the pathogenesis of MI and also drives subsequent adverse remodelling, leading to heart failure. Hence, inhibition of regulated cell death programmes after MI is a plausible and cogent route for future therapeutic strategies to delay, minimise, or prevent progression to heart failure.

## 1.6. The regenerative capacity of the adult human heart

One of the major reasons for the severe effects of cardiomyocyte loss is that the adult human heart has meagre capacity to regenerate (Bergmann et al., 2009; Cui et al., 2018; Hashimoto et al., 2018). The lack of cardiomyocyte regeneration leads to the formation of a fibrotic scar to replace the lost cells (Volders et al., 1993). Apart from myocyte loss, the presence of scar tissue itself leads to loss of pump function and deficiencies in circulation capacity (Sabbah and Goldstein, 1993). Subsequently, the injured heart follows a remodelling process that manifests through further fibrosis, myocardium loss, cardiac dysfunction and dilatation, all of which result in fatal heart failure (Cohn et al., 2000). After a patient has developed end-stage heart failure,

limited therapies are available to salvage the advanced remodelled heart: left ventricular assist devices (Rose et al., 2001) and cardiac resynchronisation therapy (Bristow et al., 2004) have shown beneficial outcomes, but the only intervention that can restore the impaired heart is a transplantation. Pragmatically, heart transplantation is not a realistic course of therapy on the scale required by the scope of disease, due to the surgical complexities involved, as well as the lack of available donors worldwide (Yacoub, 2015). To restore the failing heart, therefore, scientific interest has been recently directed towards cardiac regenerative medicine.

### 1.6.1. The promise of regenerative medicine in the heart

Regenerative medicine for heart disease aims to overcome the challenges encountered by current treatments for MI by employing three objectives; encouraging cardiac regeneration; activating self-repair and preventing cardiomyocyte loss. To date, scientific efforts towards the regeneration of the heart have developed within two major routes of investigation: 1) cardioprotective therapy in acute MI and 2) cardiorestorative therapy in failing or chronically ischemic hearts (Behfar et al., 2014). Cardioprotective therapy aims to limit the extent of damage from ischemia and prevent heart failure by altering the innate injury response (Gerczuk and Kloner, 2012). Alternatively, cardiorestorative therapy intends to recover normal cardiac function through cell-mediated and/or paracrine mediated mechanisms of repair (Behfar et al., 2014). Cell therapy for cardiac regeneration has been evolving for the past decades and its major milestones are summarised in this section (Figure 1.5).

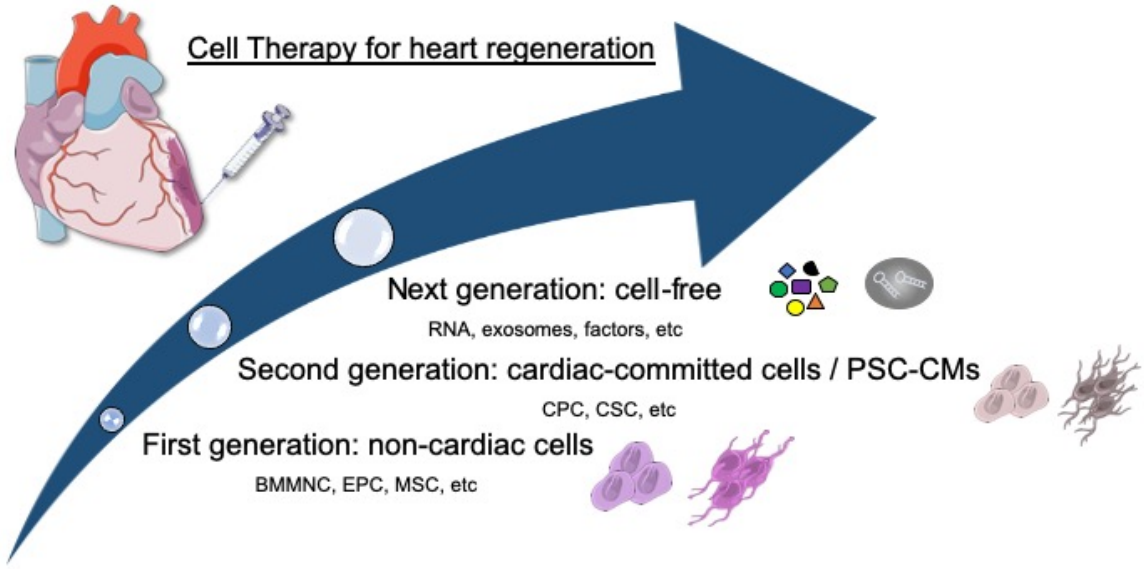



**Figure 1.5: Cell therapy for heart regeneration.** Translational cardiac regenerative therapies have evolved over the past two decades. First-generation cell types such as bone marrow mononuclear cells (BMMNC), endothelial progenitor cells (EPC) and mesenchymal stromal cells (MSC) demonstrated safety and feasibility with limited efficacy in the clinic. Second-generation cell therapies were developed with the objective to better match the target organ and they included cardiac progenitor cells (CPC) and cardiac stem cells (CSC). Next generation therapies are targeted towards cell-free concepts such as growth factors, non-coding RNAs and extracellular vesicles. Schematic diagrams modified from the Servier Medical Art image database (https://smart.servier.com/).

### 1.6.2. First-generation cell therapy for heart regeneration

First-generation cell therapies involved non cardiac stem/progenitor cells, the most widely tested among them being bone marrow mononuclear cells (BMMNC). Preclinical studies demonstrated that these cells could undergo cardiac engraftment following transplantation after MI induced by coronary artery occlusion (Deb et al., 2003; Jackson et al., 2001; Orlic et al., 2001). Reportedly, the cells could also differentiate into cardiomyocytes and endothelial cells in the border-zone (area in close proximity to the infarct) (Jackson et al., 2001) and contributed to the generation of new functional tissues within the infarct site (Fernández-Avilés et al., 2004; Meyer et al., 2006; Orlic et al., 2001; Strauer et al., 2002). Later studies however demonstrated that

bone-marrow-derived cells adopted mature haematopoietic fates in the ischemic myocardium and were incapable of transdifferentiating into cardiac myocytes to regenerate heart tissue (Balsam et al., 2004; Murry et al., 2004). These studies did not doubt the beneficial effects of BMMNC in the heart but argued that they are likely conferred via mechanisms other than myocyte replacement. At the time of these discoveries, access to bone marrow and BMMNC was well established in haematology, enabling the introduction of this 'first-generation cell-based therapy approach' in the clinical field of cardiology between 2002 and 2006. Initial studies assessing the safety and efficacy of BMMNC in MI demonstrated consistent, but modest improvements in cardiac contractility, tissue remodelling and scar formation (Assmus et al., 2002; Fernández-Avilés et al., 2004; Meyer et al., 2006; Strauer et al., 2002).

A more refined first-generation cell type derived from bone marrow is the autologous purified $CD34^+$ population of endothelial progenitor cells (EPC), which aspired to have a beneficial effect in the injured heart through neovascularisation (Ruifrok et al., 2009). Early clinical studies using BMMNC and EPC demonstrated benefits after implantation in patients with angina (Losordo et al., 2007, 2011; Mangi et al., 2003; van Ramshorst et al., 2009). EPC have also been used to treat dilated cardiomyopathy, with strong efficacy claimed (Vrtovec et al., 2013a).

Notably however, a series of meta-analyses conducted over the following years revealed a number of concerns and discrepancies in the literature of BM-derived cell therapy (Francis et al., 2013; Nowbar et al., 2014). The meta-analysis by Nowbar et al., identified a significant association between the number of discrepancies in trials and the reported improvement in ejection fraction using BM-cell therapy (Nowbar et

al., 2014). The efficacy of BM-derived cell therapy was further thrown into question following an additional negative meta-analysis of randomised controlled trials, that showed a lack of beneficial effect of BM-derived cell therapy on adverse cardiac and cerebrovascular event rates (De Jong et al., 2014). Further doubt was cast by the ACCRUE meta-analysis, based on tracking individual patient data (Gyöngyösi et al., 2015; Kovacic and Fuster, 2015).

Mesenchymal stem cells (MSC) are an additional first-generation cell type which displayed encouraging preclinical results in terms of plasticity and multilineage differentiation (Jiang et al., 2002; Ross et al., 2006; Schwartz et al., 2002). Furthermore, they demonstrated significant therapeutic efficacy following transplantation in animal models, if engineered with persistent activation of Akt signalling (Mangi et al., 2003). Usually, MSC are isolated from the bone marrow, adipose tissue or peripheral blood in the adult and parts of the placenta or umbilical cord in the neonate (Hass et al., 2011). Due to their high expansion rate and immunomodulatory characteristics, MSCs have been employed as both allogeneic and autologous therapies. Although this point is controversial, MSC were considered immunoprivileged due to their cytokine secretion and antigen presentation properties (Kinkaid et al., 2010; Williams and Hare, 2011). Allogenic MSC have been found to lose their immune privilege upon differentiation (Lohan et al., 2014) leading to earlier clearance compared to autologous MSC (Huang et al., 2010). Following a series of successful preclinical trials ranging from small animals to pigs, MSC were tested in humans in the POSEIDON trial (NCT01087996), which showed that allogeneic MSC were as effective as autologous MSC in terms of benefits in functional capacity, quality of life and ventricular remodelling, with equally low rates of severe adverse events in both cell types (Hare et al., 2012). Furthermore, this trial provoked discussion around

the right cell dosing for cell therapy in general, as it reported a negative correlation between functional improvement and cell dosage used (Hare et al., 2012; Marbán and Malliaras, 2012). Furthermore, a consistent finding in stem cell studies is the poor cardiac retention and engraftment of the transplanted stem cells, introducing the notion of paracrine and endocrine mechanisms as the drivers of the observed benefits (Hare et al., 2012; Losordo et al., 2011). Work published by Preda et al shows that when MSC were subcutaneously injected in a way that they could not migrate, LV function was still detectably improved in a murine model of MI; the remote benefit was ascribed to circulating pentraxin 3 (Preda et al., 2014).

A number of issues could be associated with the modest outcomes of the first-generation cell-based therapy clinical trials (Chien et al., 2019; Mercola et al., 2011). Firstly, the therapeutic application of stem cells is complicated by sources of variability including differential handling, phenotypic characterisation, and delivery (Behfar et al., 2014). A second potential confounding factor is patient selection for the trials; most trials involving BMMNC relied on an inclusion criterion based on a left ventricular ejection fraction (LVEF) obtained immediately after MI. However, early post-MI LVEF has limited prognostic power in determining cardiac health in the long-term, due to a large percentage of hearts spontaneously recovering some degree of function early on. Therefore, the probability of documenting incremental therapeutic benefit is significantly reduced. The therapeutic utility of stem cell-based therapy could be better informed by developing more robust prognostic assays to identify vulnerable patients to chronic heart failure at the time of MI (Behfar et al., 2014).

The third challenge to be addressed is the particular nature of cell-based therapy, which involves delivery of a live and functional entity to achieve a clinical effect; unlike

conventional small molecule drugs or other biologic agents, cell-based therapy is by nature very complex and more closely mimics transplantation paradigms, rather than conventional pharmacological therapies. To ensure efficacy, biological potency and functionality need to be demonstrated for every 'dose' tested (Dimmeler et al., 2008). Therefore, the current standard of practice of reporting cell-surface markers or colony-forming units is not a sufficient quality control step to confirm uniform biological activity. The inconsistent benefits and lack of convincing transdifferentiation capacity associated with first-generation cell types have driven a shift towards the use of other cell types, thus cardiac-derived cell populations gained popularity due to their potential to better resemble differentiated cells of the target organ.

### 1.6.3. Second-generation cell therapy for heart regeneration

Second-generation therapies for heart repair involve delivery of cells either derived from the heart or lineage-specified cells (non-resident stem cells oriented towards cardiac differentiation) (Behfar et al., 2014; Cambria et al., 2017). Cardiac progenitor cells (CPC), thought to be multipotent and clonogenic, express stem cell markers such as Sca1 and c-Kit (Beltrami et al., 2003; Messina et al., 2004; Oh et al., 2003), or other features detailed below. A few published studies compare first- and second-generation cell types and they report that cardiac-committed cells display an improved therapeutic effect demonstrated by improved engraftment, cardiac function, angiogenesis and scar size (Citro et al., 2014; Li et al., 2012; Oskouei et al., 2012; Rossini et al., 2011; Zheng et al., 2013).

## 1.7. Cardiac stem/progenitor cells

Analogous to the satellite cell in the regeneration of skeletal muscle (Evano and Tajbakhsh, 2018), the concept of resident cardiac stem cells poses an attractive area of research because the isolation and exploitation of such cells could, in theory, generate new, autologous cells to regenerate the heart after damage. Every patient could thus be their own cardiomyocyte donor. However, the challenge for cardiovascular scientists was initially the identification of cardiac stem cells, in the absence of a known surface marker; it was like looking for a needle in a haystack, without even knowing what the needle looked like. As a priori candidates, investigators naturally turned first to the already characterised cell surface molecules of the hematopoietic system, such as c-kit and Sca-1. However, cardiac stem cell research has had a contentious history, which is briefly summarised in this section.

### 1.7.1. The c-kit$^+$ cardiac progenitor

Several prominent laboratories have reported that their isolated adult stem/progenitor cells can transdifferentiate and repopulate large infarcted or chemically injured areas of the heart, with the emergence of new cardiomyocytes that restore ventricular function fully. An example of a stem/progenitor cell population highly promoted as the true regenerative cardiac cell type was the c-kit$^+$ population. Publications in the early 2000s demonstrated that bone marrow- or cardiac-derived c-kit$^+$ cell injections regenerated up to ~70% of the infarcted myocardium in mice (Beltrami et al., 2003; Orlic et al., 2001). This was striking at the time since the consensus was that the heart is an organ with meagre capacity for regeneration following an infarct. However, several laboratories made unsuccessful attempts to replicate these findings and could not observe the ability of c-kit$^+$ CPC to generate new cardiomyocytes after injection,

nor could they detect cardiomyocyte generation from endogenous stem cell sources (Balsam et al., 2004; Fisher et al., 2016; Murry et al., 2004). Despite these negative results, the concept of endogenous cardiac stem cells remained a tantalizing mainstream idea and collective evidence from supportive studies (Hong et al., 2014; Li et al., 2012; Malliaras et al., 2014; Matsuura et al., 2009; Noseda et al., 2015a) moved the field into human clinical trials (SCIPIO, CADUCEUS, TICAP, ALCADIA and others) (Noseda et al., 2015b). Like the prior trials of BMMNC and MSC from different sources, the trials of heart-derived cells concluded that 'adult stem cell' injection is safe in patients, but efficacy remains unclear (Fisher et al., 2016). Over the past few years, the field has turned into a combat zone, with essentially two diametrically opposed camps that continue publishing data supportive of their original observations. In October 2018 this saga reached a turning point after the retraction of 31 papers from Harvard researcher Piero Anversa, who was studying c-Kit$^{+}$ cells and published data that formed the basis of clinical trials employing cardiac stem cell injections to overcome heart disease. This led to the halt not only of SCIPIO, but also of the CONCERT-HF clinical trial initiated in 2015, seeking to determine whether c-kit$^{+}$ cardiac stem cells alone or in combination to MSCs from bone marrow are safe and beneficial for people suffering from chronic heart failure (NHLBI, 2018).

In the meantime, a study by Molkentin's group, reported that c-kit+ cells in the adult mouse heart were unable to produce new cardiomyocytes (Hsieh et al., 2007). Molkentin's approach utilised a lineage-tracing technique that tagged c-Kit-expressing cells and their progeny with a fluorescent marker, which was accused of compromising the gene for c-kit and therefore impairing the progenitors' ability to regenerate (Vicinanza et al., 2018). Around the same time Li et al., published a report which to some presented 'undeniable evidence' against the ability of resident stem cells giving

rise to new cardiomyocytes (Li et al., 2018; Maliken and Molkentin, 2018). In this study, Li and colleagues used a sophisticated genetic experimental design; instead of tagging c-kit cells, they used the dual Cre-Dre lineage tracing genetic approach, which fluorescently labels nonmyocytes and newly generated muscle cells a different colour from existing myocytes. This way, the team could investigate any suggested stem cell population, and even stem cells yet to be identified, rather than specifically c-kit$^+$ cells. The experiments concluded that nonmyocytes could generate new cardiomyocytes in mouse embryo, but not in the adult mouse heart. However, the study used the native Rosa26 locus, which is remarkably less potent compared to later generation Rosa26-based methods incorporating the strong synthetic CAG promoter and woodchuck hepatitis virus posttranscriptional regulatory element (WPRE) (Madisen et al., 2010). Furthermore, none of the lineage-tracing studies post-MI included a previously reported co-stimulus such as Thymosin β4 or prostaglandin-E2 (Hsueh et al., 2014; Smart et al., 2012). Nonetheless, c-Kit was not the only disputed cardiac progenitor population.

### 1.7.2. The Sca-1$^+$ cardiac progenitor

Over the past two decades several endogenous cardiac progenitor/stem cell populations have been described by different groups worldwide, the majority of which are overlapping and heterogeneous. For instance, Sca1 is co-expressed by c-kit$^+$ cells (Bailey et al., 2012; Ellison et al., 2013; Linke et al., 2005) and by a subset of cardiosphere-derived cells (CDC), which have also demonstrated heart-repair potential (Messina et al., 2004). Both Sca1$^+$ and cardiosphere-derived populations as well the PDGFRα$^+$ cardiac colony forming units (cCFU) express characteristic MSC markers (Cheng et al., 2014a; Chong et al., 2011; Matsuura et al., 2009; Noseda et al., 2015a; Pelekanos et al., 2012).

In 2003, Professor Michael Schneider's group reported the isolation of Sca-1$^+$ mesenchymal stromal cells from mouse myocardium (Oh et al., 2003). This population has been shown to differentiate *in vitro* in response to 5'-azacytidine, partly depending on  signalling. These cells could be cultured and directed towards the cardiomyocyte lineage in the dish as well as differentiate into cardiomyocytes following injection into injured mouse hearts (Oh et al., 2003). However, transplantation of cultured cells, alone, cannot demonstrate the endogenous role of these cells during normal development or in disease. A study by Uchida and colleagues used a variation of lineage mapping to demonstrate that Sca-1$^+$ derived cells generate cardiomyocytes throughout their life, at a high rate (Uchida et al., 2013). Five years later, 2 research articles and 3 research letters were published in the same issue of Circulation, all of which employed modern mouse genetic engineering technology to address the concept of Sca-1 as an adult cardiac stem cell (Lee, 2018):

- Neidig et al introduced a tamoxifen-inducible recombinase into the mouse genome, at the Sca-1 locus. By turning on the recombinase with tamoxifen and marking the population of interest, they were able to detect very few Sca1$^+$ cell-derived cardiomyocytes but high numbers of Sca1$^+$ cell-derived endothelial cells (Neidig et al., 2018).
- Vagnozzi and colleagues used both inducible and constitutive recombinase at the Sca1 locus, reporting that Sca1$^+$ cells generated cardiac vasculature throughout development, during aging and following injury, however with miniscule contribution to the numbers of cardiomyocytes (Vagnozzi et al., 2012).

- Zhang et al generated a series of genetically modified mice to pinpoint and trace $Sca1^+$ cells in the heart, concluding that $Sca\text{-}1^+$ cells contribute to the endothelial lineage (Zhang et al., 2018).
- In a different approach, a mouse model was engineered by Tang et al with a self-cleaving peptide sequence between the inducible Cre recombinase protein and the endogenous Sca1 protein. This precaution ensures that the endogenous production of $Sca1^+$ is not disrupted. Nevertheless, these researchers found that $Sca1^+$ cells generated endothelial cells and fibroblasts, but did not produce any cardiomyocytes (Tang et al., 2018).
- The fifth study isolated mouse $Sca1^+$ cells that expressed a fluorescent reporter protein plus a second reporter that marked cardiomyocyte nuclei allowing their visualisation after transplantation into injured hearts. The investigators identified no cardiomyocytes arising from the transplanted $Sca1^+$ cells (Soonpaa et al., 2018).

Thus, using state-of-the-art techniques, 5 different laboratories showed that $Sca1^+$ cells in the heart rarely generate cardiomyocytes and their dominant fate is towards the endothelial lineage. However, all the 5 studies described above share the same three limitations. First, their mapping approaches underestimate or fail to label the cardiogenic subpopulation of $Sca1^+$ $PDGFR\alpha^+$ $CD31^-$ cells characterised by Noseda and colleagues (Noseda et al., 2015a). Second, even though the studies described raise doubts regarding the generation of cardiomyocytes from endogenous $Sca1^+$ cells, they do not eliminate the possibility of culture expansion and productive manipulation of the $Sca1^+$ cells in the laboratory. Third, as true for c-kit, the Sca1 fate-mapping studies of infarction all omitted the use of a therapeutic stimulus, as is needed, e.g., for cardiomyocyte formation by the activated epicardium (Smart et al.,

2012). In addition, stem cells may not need to become new myocytes to aid heart regeneration and repair. Currently, as discussed below, there is consensus towards the idea that stem cells are not replacing damaged cardiomyocytes, but rather secrete paracrine factors that mediate the beneficial effects.

### 1.7.3. PDGFRα$^+$ Cardiac Stromal Cells (CSC)

The large and heterogeneous Sca1$^+$ population has been better refined in a study by Noseda et al., where it was divided into two mutually exclusive subpopulations; the CD31$^+$ and the cardiogenic PDGFRα$^+$ cells (Noseda et al., 2015a). The latter population of cardiac stromal cells was subsequently shown to benefit cardiac function after intramyocardial injection following ischemic injury (Noseda et al., 2015a). This population is Sca1$^+$, PDGFRα$^+$ and exhibits the side population (SP) dye efflux phenotype. Hence, it has been shown to be 1000x more clonogenic than the unfractionated starting Sca1$^+$ population, establishing it as one of the most clonogenic populations found in the adult mammalian heart to date (Noseda et al., 2015a). As shown in recently published reports, these cells reduce infarct size after grafting, demonstrate cardiogenic potential and strongly resemble the cardiac colony forming unit-fibroblast and other cardiac mesenchymal cells in terms of molecular signature (Chong et al., 2011; Noseda et al., 2015a, 2015b). As mentioned above, the potential of these endogenous cells to contribute to new cardiomyocyte formation as a native population has been disputed by recent fate-mapping studies (Lee, 2018; Li et al., 2018; Neidig et al., 2018; Soonpaa et al., 2018; Tang et al., 2018; Vagnozzi et al., 2012), but those conclusions are limited by several serious issues of design. From here on in this thesis, acknowledging the controversy, we refer to this specific subpopulation and its ostensible human equivalent as cardiac stromal cells (CSC). The mechanisms underlying the long-term benefits of CSCs after experimental MI are

still unclear, but the most immediately plausible explanation is a paracrine effect, given the cells' poor long-term retention in the myocardium, analogous to most similar approaches involving direct cell injections, regardless of the donor cell type (Chimenti et al., 2010; Gallet et al., 2016; Hong et al., 2014; Ibrahim et al., 2014; Li et al., 2012; Noseda et al., 2015a; Wysoczynski et al., 2017; Zhang et al., 2015a). A summary of studies that have suggested potential paracrine effects mediating the observed cardioprotection is displayed in Table 1.2.

**Table 1.2. Summary of studies demonstrating improved cardiac function in the heart after cell therapy, accompanied by poor cell retention/engraftment and attributed, at least in part, to paracrine effects.**

| Therapeutic intervention | Disease Model | Delivery method | Cardiac function recovery | Cell retention | Reference |
|---|---|---|---|---|---|
| **Skeletal myoblasts** | MI, dog | Intramyocardial | Improved LVEF after 10 weeks | No detection after 10 weeks | (He et al., 2005) |
| | MI, rat | Intramyocardial or Intracoronary | Improved LVEF after 84 days | ~0.04% after 7-days, >0.01% after 28- and 84-days | (Fukushima et al., 2008) |
| **Rat BM-MSC** | MI, mouse | Intramyocardial | Improved LVEF after 21-days | No detection after 21-days | (Shan et al., 2018b) |
| **Sheep BMMNC** | MI, sheep | Intramyocardial | Preserved LVEF | None detected after 2-months | (Bel et al., 2003) |
| **Human BMMNC** | HF, human | Intracoronary | Improved LVEF after 4-months | Not quantified, but 'Improved when applying shock wave treatment' | (Assmus et al., 2013) |
| | MI, human | Intracoronary | Not reported, study investigated labelled BMMNC homing | 2% after 3-4 days | (Schächinger et al., 2008) |

| | | | | | |
|---|---|---|---|---|---|
| **CD34⁺ BMMNC** | DCM, human | Intracoronary | Improved LVEF after 1-year and 3-years | 7.1% after 2-hours, 5.3% after 18-hours | (Vrtovec et al., 2013b) |
| **BMMNC** | MI, human | Intracoronary | Not reported here | 1.3-2.6% after 50-75 minutes | (Hofmann et al., 2005) |
| | | Intravenous | | No cells detected after 60-70 minutes | |
| **CD34⁺ enriched BMNNC** | | Intracoronary | | 14-39% after 60-75 minutes | |
| **PBMNC** | MI, pig | Intramyocardial | Not reported here | 11% after 60-minutes | (Hou et al., 2005) |
| | | Intracoronary | | 2.6% after 60-minutes | |
| | | Intravenous | | 3.2% after 60-minutes | |
| **BMMNC** | MI, rat | Intramyocardial | Improved LVEF | 1.88% after 1-week, 1.33% after 2-weeks, none after 1- and 3-months | (Mazo et al., 2010) |
| | MI, rat | Intramyocardial | Improved LVEF after 3 months | 0.1% after 1-week, none at 4-weeks | (Mazo et al., 2008) |
| **Adipose-derived stem cells (ADSC)** | | | | 0.25% after 1-week, none at 4-weeks | |
| **ADSC** | MI, mouse | Intramyocardial | Improved LVEF after 4-weeks | 3% after 1 day, <1% after 3 days | (Yan et al., 2017) |
| **Sca1⁺ SP** | MI, mouse | Intramyocardial | Preserved LVEF up to 12-weeks post-MI | 1-8% after 1 day, 0.1-0.5% after 2-weeks | (Noseda et al., 2015a) |
| **Sca1⁺** | MI, mouse | Intramyocardial | Improved LVEF after 8-weeks | <0.5% after 8-weeks | (Li et al., 2009) |
| **c-kit⁺** | MI, mouse | Intracoronary infusion | Improved LV function after 35-days | 12.7% after 24-hours, 0.01% after 35 days | (Hong et al., 2014) |

| | | | | | |
|---|---|---|---|---|---|
| | MI, mouse | Intramyocardial | Increased left ventricular end diastolic and systolic volume after 28-days | No cells 28-days after | (Wysoczynski et al., 2017) |
| **Cardiospheres** | MI, mini pig | Intracoronary | Improved LVEF | ~8% after 24-hours | (Lee et al., 2011a) |
| **Human cardiosphere-derived cells, CDC** | MI, mouse | Intramyocardial | Improved LVEF after 3-weeks | 30% luciferase signal after 1-week, not detactable after 3-weeks | (Chimenti et al., 2010) |
| **Rat cardiac-derived stem cells, rCDC** | MI, rat | Intramyocardial | Not reported, this was a study to investigate a reporter gene, NIS, to track injected cells | 13.2% after 1-day, 2.8% after 2-days | (Terrovitis et al., 2008) |
| **Rat-cardiosphere derived cells** | MI, rat | Intramyocardial | Higher EF after 3-weeks | 2.5% after 24-hours,<br><1% after 3-weeks | (Cheng et al., 2012) |
| **Cell mimicking microparticle (CMMP)** | MI, mouse | Intramyocardial | Improved LVEF after 3-days | ~12% after 3-days | (Tang et al., 2017a) |
| **Human cardiopoietic stem cells** | MI, pig | Intramyocardial | Improved LVEF after 30-days | Only few cells detected 30-days after | (Emmert et al., 2017) |
| **Human MSC** | MI, mouse | Intravenous | Improved LVEF after 3-weeks | None after 3-weeks | (Iso et al., 2007) |
| **Porcine MSC** | Mouse, Pig | Intramuscular, Intracoronary | Not reported, study investigating cell tracking methods | ~2% after 2-weeks | (Leiker et al., 2008) |
| **Human CPC** | MI, mouse | Intramyocardial | Improved LVEF after 2-weeks | ~0.1% after 2-weeks, ~0.05% after 4-weeks | (Liu et al., 2012) |
| **Human W8B2$^{+}$** | MI, rat | Intramyocardial | Improved LV function | 'poor retention', no quantification | (Zhang et al., 2015a) |

| | | | | | |
|---|---|---|---|---|---|
| **Mesp1$^{+}$** | MI, mouse | Intramyocardial | Improved LVEF after 12-weeks | ~10% after 12-weeks | (Liu et al., 2016b) |
| **Foetal Cdx2$^{+}$ from mouse placenta** | MI, mouse | Intravenous | Improved LVEF after 1- and 3-months | 1.1% after 3-months | (Vadakke-Madathil et al., 2019) |
| **hPSC-CM** | MI, monkey | Intramyocardial | Improved LVEF after 28 days | ~0.4% after 3 days, 0.06% after 28 days | (Zhu et al., 2018) |
| **hESC** | MI, mouse | Intramyocardial | No significant effect | Little or no signal after 2-weeks | (Tachibana et al., 2017) |
| **hiPSC** | | | | | |
| **hESC-CM** | | | Improved LVEF after 4 weeks | 0.04% after 2-weeks, 0.02% after 4-weeks | |
| **hiPSC-CM** | | | | 0.04% after 2-weeks, 0.03% after 4-weeks | |
| **hiPSC-CM** | MI, pig | Intramyocardial | Improved LVEF after 4-weeks | 4.2% after 4-weeks, 8.97% after 4-weeks when administered with patch | (Ye et al., 2014) |
| **hiPSC-EC** | | | | | |
| **hiPSC-SMC** | | | | | |

## 1.8. Cell enhancement and cell-free approaches: the next generation?

Strategies aiming to overcome the poor performance demonstrated by transplanted cells focus on improving cell retention, survival, coupling, and maturity. For the amelioration of cell retention, scaffold-based approaches can be used, which include decellularized matrices, injectable biomaterials and cardiac patches made of synthetic or natural hydrogels (Georgiadis et al., 2014; Hastings et al., 2015). Scaffold-free constructs include cell sheets and microtissues (Emmert et al., 2013b, 2013a; Günter et al., 2016). Cell-free approaches are largely based on the hypothesis that cell

therapy functions through paracrine mechanisms. These strategies focus on the identification and subsequent administration of growth factors, other secreted proteins, and non-coding RNAs (Cambria et al., 2017). According to the paracrine theory, transplanted cells might act as *in situ* vessels of cytokines and growth factors, providing sustained release of these effectors and hence gradually influence the myocardial microenvironment driving a beneficial cardio-protective response (Figure 1.6) (Beohar et al., 2010; Ellison et al., 2011; Gyöngyösi et al., 2005; Henry et al., 2003; Linke et al., 2005; Ranganath et al., 2012; Ripa et al., 2006). Specific secreted signals relevant to heart repair are discussed below.

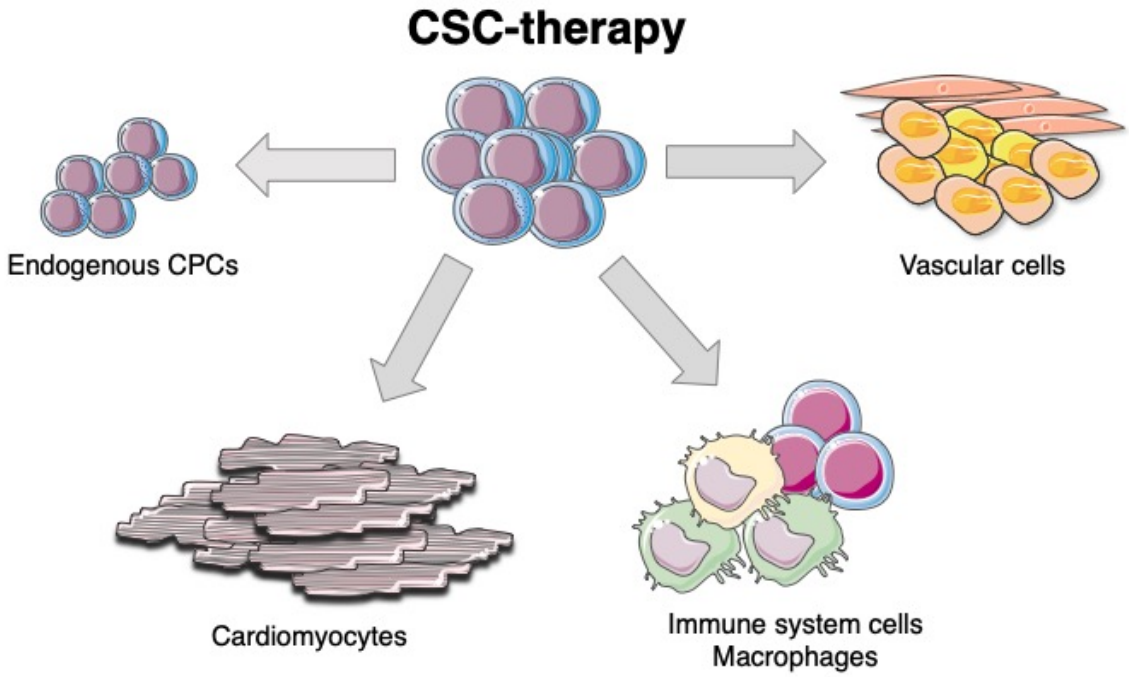



**Figure 1.6: The paracrine hypothesis.** Following injection in the infarcted myocardium, the cardiac stromal cells (CSC) release a number of soluble mediators (paracrine factors) which might include growth factors, cytokines, chemokines, antioxidants, humoral factors, small molecules, miRNAs and extracellular vesicles (EV). The secreted molecules interact with the different cell types in the infarct niche and mediate the cardioprotective effects observed some of which are induction of angiogenesis, proliferation, inflammation, stem cell recruitment and differentiation, reduction of apoptosis and reduction of fibrosis. Schematic diagrams modified from the Servier Medical Art image database (https://smart.servier.com/).

### 1.8.1. Growth factors

Research into the mechanistic pathways of cardiac development, growth and differentiation has led to the identification of several key growth factors, which might also have intriguing roles in cardio-protection and cardiac regeneration. Some of these growth factors were found to be released by cardiomyocytes during ischemia, pointing to a potential role in cardiac repair, angiogenesis or response to cardiac remodelling (Hausenloy and Yellon, 2009). The exogenous administration of such factors has been shown to protect the myocardium from the devastating effects of ischemia-reperfusion injury via activation of intracellular pathways linked to cardioprotection. At the time of myocardial reperfusion, previously identified growth factors with roles in cardiac development, were implicated in the activation of the signalling components of the reperfusion injury salvage kinase (RISK) pathway, which includes pro-survival kinases such as PI3K-AKT and MEK1/2-ERK1/2 (Hausenloy and Yellon, 2007).

Several pre-clinical studies have utilised growth factors with reported *in vitro* bioactivity on resident cardiac stem cell populations, suggesting their regenerative potential (Ellison et al., 2011; Ranganath et al., 2012). Examples of well-studied growth factors include vascular endothelial growth factor (VEGF) (Stewart et al., 2009), fibroblast growth factor 2 (FGF2) (House et al., 2003), granulocyte-colony stimulating growth factor (G-CSF) (Engelmann et al., 2006), erythropoietin (EPO) (Zafiriou et al., 2014), hepatocyte growth factor (HGF) (Gallo et al., 2014), Neuregulin-1 (NRG1) (Rupert and Coulombe, 2015), growth and differentiation factor 15 (GDF15) (Ago and Sadoshima, 2006) and insulin-like growth factor-1 (IGF-1) (Li et al., 1997). Despite the promising preclinical data using neonatal and adult cultured myocytes, as well as small and large mammal infarction models, these factors achieved minimal benefits when administered alone or in certain combinations in human clinical trials to date, whilst

results from later phase 2/3 clinical trials were even less impressive (Kieserman et al., 2019; Rebouças et al., 2016; Ylä-Herttuala and Baker, 2017).

#### 1.8.1.1. VEGF

Within the myocardium, the VEGF protein family has been shown to be involved in numerous paracrine and autocrine reparative responses, including recruitment and homing of stem cells (Shen et al., 2011), decreased apoptosis of endothelial cells and cardiomyocytes (Gerber et al., 1998; Xu et al., 2011) and increased vasodilation (Fukumura et al., 2001). Reduced levels of VEGF have been reported in models of advanced heart failure, making this factor a potential therapeutic target for disease management (Taimeh et al., 2013). Specifically, cardiac-specific reduction of VEGF expression in a conditional knockout mouse model translated into a defective microvascular density and a suppressed cardiac function, suggesting that VEGF is important in the maintenance of normal vasculature and healthy heart function (Giordano et al., 2001).

Initial successful attempts to demonstrate the benefits of VEGF were performed in animal models, using recombinant VEGF protein, administered via the intracoronary (Hariawala et al., 1996; Lopez et al., 1998) or intramyocardial routes (Radke et al., 2004). For instance, VEGF administration in a pig model of myocardial infarction demonstrated improved regional coronary flow and restored cardiac function (Harada et al., 1996). Moreover, adenoviral-mediated overexpression experiments of VEGF in rat cardiomyocyte cultures, induced a protective effect against doxorubicin toxicity by inhibiting death receptor mediated apoptosis (Chen et al., 2010a).

VEGF gene transfer has also been investigated in animal models showing ameliorated collateral flow and overall cardiac function (Tio et al., 1999). These positive results

failed to translate into benefits in humans; neither in the NORTHERN nor in the VIVA trials did VEGF protein or gene therapy, respectively, show a beneficial effect on perfusion of ischemic myocardium (Henry et al., 2003; Stewart et al., 2009). The disappointing results were attributed partly to the short half-life of VEGF protein (Giacca and Zacchigna, 2012) and secondly to the high dose of VEGF required for successful protein therapy, leading to blood pressure instability and a leaky, immature vascular plexus following nitric oxide release (Henry et al., 2003). In order to overcome these issues, VEGF modified RNA constructs were developed, which envision a better paracrine factor titration and temporal profile than gene therapy (Zangi et al., 2013).

Overall, despite the small amount of short-term safety data using VEGF available, caution should be applied, clinical end-points should be better-defined so that efficacy can be critically assessed and more studies are required to reach confidence and proceed with therapeutic applications of VEGF (Taimeh et al., 2013).

#### 1.8.1.2. FGF2

Another factor implicated in angiogenic responses as well as induction of heart regeneration and sustained structural and functional benefits is FGF2 (Kardami et al., 2007). Exogenously administered FGF-2 has been extensively shown to achieve protection from cardiac injury (Detillieux et al., 2003, 2004).

FGF-2 was reported to protect neonatal cultured cardiomyocytes from $H_2O_2$ stress (Padua et al., 1996). Furthermore, isolated adult rat and mouse hearts were found to protect the heart from subsequent ischemia-reperfusion induced contractile dysfunction and myocardial tissue loss (Padua et al., 1995). Chronic overexpression of FGF2 in transgenic mouse myocardium reduced the infarct size and improved cardiac function post-MI (House et al., 2003). The same group has also developed

FGF2 deficient mice and showed that endogenous FGF2 is essential for resistance to ischemic injury (House et al., 2003). In support of this notion, overexpression of human FGF2 in the FGF2-deficient mice restored the levels of cardiac function (House et al., 2003).

Despite the promising results using pre-clinical models, FGF2 treatment provided minimal cardioprotective effects in human patients with ischemic heart disease in a phase I trial (Simons et al., 2002). More specifically, a single intracoronary infusion of FGF2 did not improve myocardial perfusion but showed a promising trend toward symptomatic improvement at 90 days.

#### 1.8.1.3. G-CSF

Initial experimental data suggested that G-CSF induces the mobilisation and recruitment of bone marrow stem cells which then differentiate into cardiomyocytes. Later studies indicated that the G-CSF beneficial effects could be instead attributed to direct actions of the cytokine on injured myocardium by inhibition of apoptosis (Ince et al., 2006). Orlic et al., reported that administration of G-CSF in mouse models of MI inhibited LV remodelling, improved cardiac function and increased survival rate through significant reduction of apoptosis and induction of neovascularisation (Ohtsuka et al., 2004).

Subsequent studies in different pre-clinical models of ischemia-reperfusion injury, in rat (Harada et al., 2005) and rabbit (Sugano et al., 2005) also reported a reduction in infarct size in the presence of G-CSF. In a swine model of MI, G-CSF exhibited improved cardiac function and reduced LV remodelling, benefits which were attributed to decreased apoptosis, upregulation of VEGF expression as well as activation of the pro-survival and pro-angiogenic kinase Akt (Iwanaga et al., 2004). Despite the

numerous positive pre-clinical results, human clinical trials failed to show significant functional improvement of the myocardium compared to placebo controls (Engelmann et al., 2006; Kang et al., 2007; Ripa et al., 2006). REVIVAL-2 study showed a reduction in infarct size in the presence of G-CSF compared the control, as well as an improvement of LVEF, however none was statistically significant (Zohlnhöfer et al., 2006). Overall, G-CSF after reperfusion of infarcted myocardium is thought to be feasible, safe and promising but further adequately powered studies are necessary to confirm findings (Ince et al., 2006).

#### 1.8.1.4. EPO

Similar to G-CSF, EPO has been suggested to limit myocardial damage via reduction of apoptosis post-MI. EPO is a major regulator of erythropoiesis and haematopoiesis in humans and increases the levels of haemoglobin. Decreased haemoglobin levels are common in HF patients and despite their plasma EPO levels being higher, they are not sufficient to overcome the haemoglobin deficiency (Volpe et al., 1994). Recombinant EPO therapy has thus been found to significantly improve cardiac function and quality of life in chronic HF patients (Silverberg et al., 2001). Exogenous recombinant human EPO administration in different preclinical models was shown to protect myocardium from ischemic damage (Ohtsuka et al., 2004). Numerous studies employing rat or rabbit models of permanent MI report that EPO administration significantly reduced $TUNEL^{+}$ nuclei within the area at risk (Moon et al., 2006; Parsa et al., 2003; Tramontano et al., 2003). Furthermore, histologically measured infarct size was found to be 4-times smaller in the presence of EPO (Van Der Meer et al., 2005; Moon et al., 2003).

In contrast to the aforementioned positive results, Hale et al., reported no significant effects of EPO on MI size or LV volume and function in a rat model (Hale et al., 2005). However, the study noted that EF was higher in the EPO-treated animals. More recent studies in mini-pig models of MI demonstrated that EPO administration reduces apoptosis in the peri-infarct area, as well as infarct size and EF (Chua et al., 2011). In terms of larger animal studies, EPO was tested in pig models of ischemia-reperfusion injury and despite been shown to decrease interstitial fibrosis, increase capillary area and mediate functional improvement, the factor did not reduce infarct size or improve LV thickening (Toma et al., 2007). Similar results were obtained in a sheep model of reperfused MI, where high doses of EPO increased LVEF but failed to reduce infarct size (Olea et al., 2006).

Overall, preclinical studies on small rodents agree that EPO is effective in reducing infarct size and improving LVEF, although studies in larger animals were less promising, indicating a lack of effect. Nevertheless, due to its long-standing utility in the treatment of anaemia in end-stage renal failure (Bommer et al., 1988), EPO has been broadly investigated in clinical trials and its pharmacodynamics and pharmacokinetics in healthy individuals have been well established (Cheung et al., 1998).

Patients with acute MI have also been administered EPO in studies which conclude that the factor is ‘mostly’ safe (Talan and Latini, 2013). Similar to the factors mentioned above, human clinical studies failed to show improvement in LVEF or infarct size compared to placebo (Najjar et al., 2011; Ott et al., 2010; Prunier et al., 2012).

One common trait of all the human trials involving EPO is that the timing of administration was not the same as the one used in the preclinical studies.

Experimental data clearly show that effectiveness of the factor is reversely proportional to the elapsed time after the occlusion and the large number of animal studies indicated a very narrow and dose-dependent therapeutic window (Talan and Latini, 2013). Hence, the critical therapeutic window for EPO to show significant benefit might have not been achieved yet in human studies. Whether this timing is feasible given the clinical emergency of the patient, or the clinicians' lack of confidence in data coming from animal studies is subject to further investigation in the field, not only for EPO but for recombinant factors discussed here in general.

#### 1.8.1.5. HGF

HGF and its signalling plays important roles in physiological cardiac development as well as pathological myocardial function (Gallo et al., 2014). Anti-cancer therapies targeted to Met, the tyrosine kinase receptor of HGF, are cardio-toxic, emphasising the importance of this pathway in heart function. Under settings of I/R injury, HGF accumulates in the myocardium both in rodents and humans (Matsumori et al., 1996; Ono et al., 1997). Experiments in mice demonstrated that HGF counteracts oxidative stress (Nakamura et al., 2000b) and protects cardiomyocytes from apoptosis via activation of MEK/Erk1,2 (Kitta et al., 2001), p38MAPK (Arechederra et al., 2013) and PI3K/Akt (Wang et al., 2004). HGF has also been shown to inhibit caspase activation and protect against signals of apoptosis (Pietronave et al., 2010). Adenoviral-mediated HGF overexpression in MSC used to treat rat hearts post-MI, enhanced systolic and diastolic LV function, induced proliferation and reduced apoptosis in endothelial cells via induction of calcineurin expression (Guo et al., 2008). Furthermore, Liu et al showed that adenoviral delivery of HGF in rat hearts after MI preserved heart function and reduced scar size via inhibition of apoptosis (Liu et al., 2016a).

An interesting recent study using stem cells from human exfoliated deciduous teeth (SHED) showed that HGF in SHED-conditioned medium is indispensable for its cardio-protective functions (Yamaguchi et al., 2015). The authors first demonstrated that SHED release high concentrations of HGF, while its neutralisation inhibits the protective function of SHED-conditioned medium on cardiomyocyte apoptosis. When HGF-depleted SHED-conditioned medium was pre-administered in a mouse model of MI the beneficial effects of the medium on infarct size and apoptosis were significantly attenuated (Yamaguchi et al., 2015).

Despite the promising pre-clinical results of HGF as a paracrine factor in small animal models, not enough studies have been published in large animals or human models of cardiovascular disease. Hence, the role of HGF in cardiac regeneration is yet to be further explored.

#### 1.8.1.6. NRG1

Several studies of NRG1 and its receptor ErbB signalling have been carried out in the settings of heart development and disease. Results have indicated the importance of this pathway, despite the specifics of developmental and cardio-protective mechanisms being generally scattered and sometimes contradictory (Rupert and Coulombe, 2015). Experimental data using adult rat ventricular myocytes showed NRG1-mediated protection from apoptosis after $H_2O_2$ treatment (Kuramochi et al., 2004). Furthermore, intravenous administration of NRG1 in a rat model of MI reduced myocyte apoptosis, mitochondrial dysfunction and LV remodelling (Guo et al., 2012). Upon introduction of human NRG1 in a similar rat MI model, an increase in microvasculature followed by upregulation of VEFG occurred (Xiao et al., 2012). NRG1 encapsulation in microparticles for sustained release in rat heart, improved

overall cardiac function and more specifically, increased LVEF and LV mass and attenuated apoptosis and fibrotic remodelling (Formiga et al., 2014).

Recombinant human NRG1 has been used in two clinical trials with published results and is currently in a number of on-going ones (Mendes-Ferreira et al., 2013). The first completed Phase II study in chronic heart failure patients confirmed a tolerable and safe dose of human NRG1, capable of enhancing heart function and LV remodelling (Gao et al., 2010b). The second study, completed soon after, demonstrated significant cardiac output, stroke volume and mean arterial pressure (Jabbour et al., 2011). One of the on-going clinical studies is currently aiming to evaluate the functional efficacy of different NRG1 doses in reducing death rates of heart failure (NCT03388593). Hence, NRG1 effects in the clinical setting are yet to be fully revealed and cardioprotective functions of the NRG1/ErbB axis will be further untangled in the future.

#### 1.8.1.7. GDF15

GDF15 is a BMP-like growth factor and a member of the TGFβ superfamily (Blankenberg and Zeller, 2018). GDF15 is thought to be associated with oxidative stress, inflammation and biomechanical stretching-induced stress in the heart (Kempf et al., 2006). GDF15 has been shown to prevent apoptosis in rat ventricular cardiomyocytes, offering protection against different agents (Heger et al., 2010). Kempf et al., used a mouse model to show that endogenous GDF15 is indispensable for protection against I/R injury in the heart (Kempf et al., 2006).

Expression of GDF15 is negligible in normal adult heart and found to be induced upon hypertrophic and dilated cardiomyopathy conditions (Xu et al., 2006). Transgenic mice with cardiac specific overexpression of GDF15 showed partial resistance to pressure overload-induced hypertrophy, while overexpression of GDF15 in neonatal

cardiomyocyte cultures antagonised induction of hypertrophic phenotypes (Xu et al., 2006). The same study showed that transient expression of GDF15 outside the heart via intravenous delivery, prevented ventricular dilatation and subsequent heart failure via an endocrine effect (Xu et al., 2006).

Recent work by Zhang et al., showed high enrichment of GDF15 in cardio-protective human iPSC-derived MSC-conditioned medium, which protects mice against doxorubicin induced stress, via inhibition of apoptosis and reduction of ROS generation (Zhang et al., 2015b). Subsequent GDF15 immunodepletion of the conditioned medium had a diminishing effect on the observed beneficial effects, which could be then partially reversed by GDF15 injection (Zhang et al., 2015b).

Overall, experimental work on GDF15 paints the picture of yet another promising candidate for cardio-protection, which requires further exploration in larger animal and human preclinical models.

#### 1.8.1.8. IGF1

Last but not least, IGF1 is one of the best-studied growth factors in the setting of cardiac development and pathology. It has been robustly shown to enhance cardiomyocyte function, proliferation and prevent apoptosis both in preclinical cell culture and animal models (Fabbi et al., 2015; Li et al., 1997; Rupert and Coulombe, 2017; Troncoso et al., 2014). Transgenic mice overexpressing IGF1 in the heart, showed increased myocyte proliferation leading to an increased number of cells in the heart (Reiss et al., 1996).

Kawaguchi et al., has reported high levels of IGF1 in the secretome of c-kit$^{+}$ progenitor cells, which improved cardiomyocyte survival and contractility in a co-culture (Kawaguchi et al., 2010). IGF1-mediated suppression of cardiomyocyte apoptosis has

been also demonstrated in a mouse model of MI (Li et al., 1999), in a rat model of I/R injury (Buerke et al., 1995) as well as in cultured rat myocytes (Wang et al., 1998). Later experiments in cultured cells, showed that the anti-apoptotic effects are mediated by activation of the PI3K/Akt/mTOR and Ras/Raf/MEK/ERK signalling cascades (Opgaard and Wang, 2005).

Apart from its anti-apoptotic role, IGF1 has also been suggested to promote the regeneration of adult myocytes. Studies in adult rat cardiomyocytes reported that IGF1 activates DNA synthesis (Reiss et al., 1997), whilst experiments in transgenic mice showed that IGF1 receptor induces cardiac stem cell division, followed by enhanced telomerase activity, delayed senescence and preservation of stem cell potency (Torella et al., 2004).

Clinical studies have shown that low levels of IGF1 correlated with the severity of ventricular dysfunction in patients with heart failure (Anker et al., 2001; Niebauer et al., 1998). Nevertheless, in a similar scenario to the aforementioned factors, the pilot clinical study RESUS-AMI, in which low doses of IGF1 were given after reperfusion in STEMI indicated safety but were not found to improve LVEF (Caplice et al., 2018).

An alternative strategy attempting to enhance cardiac regeneration is administration of combinations of cardio-protective factors. Ellison et al., co-administered IGF1 and HGF in pigs undergoing MI and showed a dose-dependent improvement in cardiomyocyte survival, reduction in infarct size and fibrosis and improvement of LVEF (Ellison et al., 2011). A later study by Gomez et al., combined IGF1 and HGF in a pig model of MI and demonstrated that while the factor combination was safe and reduced inflammation, cardiac functional parameters were not significantly improved via a synergistic effect (Gómez-Mauricio et al., 2016).

Reasons for the poor efficacy of growth factor-based strategies include inappropriate doses or lack of organ selectivity. Furthermore, whereas injecting single factors might facilitate the analysis of the therapeutic potential of each effector, cardiovascular repair might well require synergistic activation of multiple pathways and combinations of factors (Behfar et al., 2010; Gnecchi et al., 2006), a limitation that has not yet been fully explored (Titmarsh et al., 2016).

### 1.8.2. Cytokines and chemokines

Cytokine production is a key aspect of the inflammatory response after MI and has a critical role in cardiac remodelling and host outcome. Cytokine release at the site of infarct can be triggered by mechanical deformation, ischemic stimulus, ROS and cytokine self-amplification pathways. Chemokines make up a family of around 50 cytokines that target G-protein coupled receptors and were first described for their role in facilitating cell migration to sites of infection or inflammation (Baggiolini, 2001). To date, hundreds of cytokines and chemokines have been reported with a range of context-dependent roles in the heart including inflammation, repair, responses to injury, contributions to cardiomyocyte death, and biomarker potential. The translation of experimental data into clinical practice is hampered by the widespread ambivalence in cytokine function, variability in study design, treatment regimens and selected end-points.

Increasing consensus suggests that stem cell transplantation might result in decreased levels of circulating inflammatory cytokines such as Tumour Necrosis Factor α (TNFα), Interleukin-6 (IL-6) and Interleukin-1β (IL-1β) in response to injury (Li et al., 2014b). The major candidates considered to be positive regulators of cardiomyocyte differentiation are Transforming Growth Factor β (TGFβ), IL-6 and

certain chemokine family members. A few of the major cytokines implicated in heart disease and discussed further below include Stem Cell Derived Factor 1 (SDF1/CXCL12) (Bromage et al., 2014; Takahashi, 2010), CC chemokine Monocyte Chemoattractant protein (MCP1/CCL2) (Becker, 2005), Interleukin-6 (IL6) (Fontes et al., 2015) and TGFβ (Liu et al., 2017).

#### 1.8.2.1. SDF1

Although a number of cytokines, growth factors and chemotherapeutic agents can mobilise stem cells, it is suggested that the SDF1/CXCR4 axis is one of the most paramount (Cottler-Fox et al., 2003). For example, the mechanism by which G-CSF functions is by disrupting the association of SDF1 on stem cells with CXCR4 on the bone marrow, inducing their mobilisation to the site of injury (Zaruba and Franz, 2010). A similar mechanism is employed by AMD3100, a selective CXCR4 antagonist functioning to increase circulating progenitor cells (Liles et al., 2003).

SDF1 has been shown to recruit bone marrow-derived stem cells to aid in the re-vascularisation process, prevent cell death and reduce scar size, as demonstrated in a rat model of MI (Sundararaman et al., 2011). Furthermore, overexpression of SDF1 in human cardiac stem cells has been shown by Tilokee et al., to enhance cardiac repair and new myocyte/vessel formation after MI in mouse (Tilokee et al., 2016). Further supporting evidence reported that adenovirus-mediated overexpression of SDF1 in the infarcted area of a mouse heart enhanced $cKit^+$ retention at the site, induced proliferation and reduced the infarct size via the CXCR4/PI3K pathway (Wang et al., 2012). Likewise, a study by Malik et al., showed protection of isolated human atrial trabeculae subjected to I/R injury by exogenous administration of SDF1 (Malik et al., 2015).

Recently, plasmid SDF1 has been used in the STOP-HF clinical trial for humans, to study its safety and efficacy (Penn et al., 2013). SDF1 administration to ischemic heart patients caused an increase in LVEF compared to placebo, 4 and 12 months after administration, while giving no adverse effects (Penn et al., 2013). While the improvement observed was not statistically significant, the investigators support that this would not be the case if enrolment was limited to high risk patients, as they are the ones that experienced the most significant remodelling effects (Penn et al., 2013).

Despite the promising results in culture settings, SDF1 is highly susceptible to proteolytic degradation *in vivo* by dipeptidyl peptidase 4 (DPP4). Following cleavage by DPP4, SDF1 is inactivated and the truncated product is antagonising the intact protein (Zhong and Rajagopalan, 2015). Strategies to overcome this include co-administration of parathyroid hormone, a potent DPP4 inhibitor, shown to enhance SDF1 content in the myocardium and increase the mobilisation of $CXCR4^{+}$ bone marrow cells (Burridge et al., 2014).

Last year, an exciting study by Huang and colleagues presented a novel way to improve targeting of SDF1 to the myocardium *in vivo* and more specifically to dead cells. The group developed a fusion protein of SDF1 with Annexin V (AnxA5), which can precisely detect and bind to dead cells *in vivo* (Huang et al., 2019). SDF1-AnxA5 administered by intravenous delivery in mouse model of MI, accumulated in the ischaemic myocardium and subsequently inhibited apoptosis, enhanced angiogenesis, reduced infarct size and improved overall cardiac function (Huang et al., 2019).

#### 1.8.2.2. MCP1

MCP1 is a chemokine that primarily recruits circulating monocytes to sites of inflammation, but has been found to play critical roles in the pathophysiology of MI, hence an interesting therapeutic target (Morimoto and Takahashi, 2007). Published studies describing the effects of MCP1 in the infarcted heart are in wide dispute. In cultured cells, MCP1 seems to mediate protection of mouse myocytes from hypoxic and I/R-induced death by inhibiting apoptosis (Morimoto et al., 2008; Tarzami et al., 2002, 2005). Other studies employing siRNA approaches for the degradation of MCP1 receptor (CCR2) in monocytes demonstrated reduced infarct size in mice (Leuschner et al., 2011).

Dewald and colleagues concluded that MCP1 plays an important role in the healing of necrotic areas of the murine myocardium after I/R injury (Dewald et al., 2005). Their $MCP1^{-/-}$ mice showed a delayed macrophage infiltration at the infarct site and a slower replacement of injured myocytes with granulation tissue (Dewald et al., 2005). Furthermore MCP1 neutralisation using an antibody showed attenuated LV remodelling but no changes in infarct size compared to wild type mice (Dewald et al., 2005). Supporting studies employing a targeted deletion of CCR in a mouse model of MI, found beneficial effects on LV remodelling after 7 and 28 days (Kaikita et al., 2004). While some of the observations above would suggest a beneficial role for MCP1 in promoting infarct healing, inhibition of LV remodelling and the unchanged size of infarct, point to a dual effect of the cytokine on the injured myocardium. In human patients, a recent 2-year survival analysis of 803 MI patients highlighted an association of low serum MCP1 levels with MI death or a higher risk of a future non-fatal MI (Leocádio et al., 2019). Hence, while MCP1 effect is beneficial in cultured myocytes, its role *in vivo* is still unclear.

#### 1.8.2.3. IL-6

Like MCP1, IL-6 is a pleiotropic cytokine with dual reported roles in cardioprotection and inflammation. It is released in response to perturbations in homeostasis, especially in the heart and signals through the homodimerization of the membrane bound receptor glycoprotein 130 (gp130) (Fontes et al., 2015). In the acute response to injury, IL-6 was shown to activate PI3K and NO-dependent signalling pathways in neonatal rat cardiomyocyte protection, by regulating $Ca^{2+}$ concentration in mitochondria, inhibiting mitochondrial membrane depolarisation, loss of structural integrity and swelling (Smart et al., 2006). Furthermore, IL6-family cytokines such as Cardiotrophin 1 (CT1) protect adult rat myocyte cultures and intact heart, against acute oxidative stress triggering the activation of a downstream anti-apoptotic program (Liao et al., 2002; López et al., 2005).

On the other side, IL-6 family signalling has been reported to repress myocyte contractility as well as their response to β-adrenergic receptors, leading to decreased function (Prabhu, 2004; Sugishita et al., 1999). Induction of pathological hypertrophy has also been shown, in response to IL-6 induced gene expression changes in neonatal rat cardiomyocytes (Wollert et al., 1996). Chronically exposed myocytes to IL-6, show defects in contractility associated with JAK/STAT signalling but not the ERK pathway, indicating that the differential regulation of downstream signalling could be exploited in fine-tuning the response to IL-6 (Yu et al., 2003). Hence, while acute exposure to IL-6 seems to be beneficial due to attenuation of apoptosis limiting the infarct size, chronically elevated levels of the cytokine become deleterious, reducing contractility and inducing a hypertrophy genetic program, contributing to cardiovascular disease (Fontes et al., 2015).

Recently published results from the BIOSTAT-CHF clinical study concluded that in a large heterogeneous cohort of 2,329 HF patients, elevated IL-6 levels were found in more than 50% of the patients and were associated with reduced LVEF, atrial fibrillation, iron deficiency and overall poorer clinical outcomes (Markousis-Mavrogenis et al., 2019). Future investigation of IL-6 as a potential therapeutic target or approaches to fine-tune its signalling are thus required before clinical translation studies.

Approaches to silence the pathogenic effects of IL-6 include utilisation of the primary inhibitor of IL-6 family, SOCS3 (Babon et al., 2014). In cultured rat myocytes, SOCS3 overexpression attenuated induction of hypertrophy, but also reduced anti-apoptotic effects of IL-6 (Yasukawa et al., 2001). A reduced SOCS3 protein expression was also obtained in LV myocardia from human DCM patients (Podewski et al., 2003). Studies digging into the IL-6 associated downstream signalling, showed that STAT3 activation plays a major role in the pathway. Mice overexpressing STAT3 in the heart developed hypertrophy without additional stimuli, demonstrating that uncontrolled STAT3 signalling is sufficient to induce the pathogenic changes even in the absence of IL-6 (Kunisada et al., 2000).

The development of a method to block only the pathological effects of IL-6 is an exciting avenue for further research. Investigators are now focusing on the design of more specific inhibitors such as soluble gp130 decoys (sgp130) in order to block only the unwanted activity of IL-6 (Morieri et al., 2017).

#### 1.8.2.4. TGFβ

Similar to the IL-6 family above, the TGFβ superfamily in the infarcted heart modulates survival and hypertrophy, regulates immune cell function, activates fibroblasts and

stimulates matrix-preservation, earning the title of ‘Master of all trades’ (Liu et al., 2017). Several members of the TGFβ superfamily have been implicated in myocardial infarction, including TGFβ1, TGFβ2, TGFβ3, bone morphogenetic protein (BMP)2, BMP4, BMP10, GDF8, GDF11 and activin A (Frangogiannis, 2017; Hanna and Frangogiannis, 2019).

The relative contribution of different myocardial cell types to TGFβ production remains poorly defined. A pig model of MI found cardiomyocytes to be the major source of TGFβ1 (Wünsch et al., 1991), whereas mouse models of MI, pointed to macrophages as the key contributors to the cytokine response (Van Amerongen et al., 2007). Platelets have also been suggested as an important contributor of TGFβ under conditions of pressure-overload (Meyer et al., 2012). Activated fibroblasts, vascular cells and mast cells are also found in abundance in the infarcted heart and have been shown to produce and release TGFβ (Dobaczewski et al., 2010; Frangogiannis et al., 1998; Saxena et al., 2014; Weirather et al., 2014), however, whether their contributions are significant remains unknown.

Overexpression of TGFβ in mice has been associated with hypertrophic and fibrotic phenotypes (Rosenkranz et al., 2002). On the other hand, cardiac-specific overexpression was associated with atrial, but not ventricular fibrosis, suggesting a higher sensitivity of the atrial myocardium to TGFβ fibrogenic activity (Nakajima et al., 2000). Heterozygous $TGF\beta^{+/-}$ mice were protected from the development of aging-related fibrosis of the myocardium and diastolic dysfunction (Brooks and Conrad, 2000). Furthermore, TGFβ-receptor neutralisation inhibited myocardial fibrosis in an inflammatory cardiomyopathy mouse model (Sakata et al., 2008).

TGFβ administration inhibited oxidative stress and reduced pro-inflammatory cytokines in isolated perfused rat hearts undergoing I/R injury in an early study (Lefer et al., 1990). Later *in vitro* and *ex vivo* experiments produced conflicting results on the effect of TGFβ on cardiomyocyte survival. A reduction in cardiomyocyte death was observed in a feline model of MI after TGFβ administration (Lefer et al., 1993). Also, in isolated hearts TGFβ infusion protected cardiomyocytes from apoptosis through MAPK signalling (Baxter et al., 2001a).

In contrast, TGFβ signalling was found to mediate the pro-apoptotic effects of angiotensin II in cultured rat myocytes (Schröder et al., 2006), indicating that the effects of the cytokine are likely dependent on dose, time and context. In an alternative mouse model of TGFβ-receptor knockdown during MI, blocking of TGFβ signalling protected cardiomyocytes from death due to cardiac rupture, but induced a significant infiltration of neutrophils (Rainer et al., 2014). While the mechanism of protection is yet to be determined, TGFβ signalling in cardiomyocytes might suppress synthesis of cardioprotective genes such as Interleukin-33 (IL-33), GDF15 and Thrombospondin 4 (TSP4) (Rainer et al., 2014).

Apart from TGFβ isoforms, other members of the TGFβ superfamily have been implicated in cardiomyocyte survival effects. BMP2 was found to inhibit apoptosis in serum-deprived cardiomyocytes *in vitro* (Izumi et al., 2001), whereas its intravenous injection in mice undergoing MI reduced infarct size and the number of apoptotic cardiomyocytes in the infarct border zone (Ebelt et al., 2013). GDF15 (discussed in more detail in section 1.10.1.7 above) also exerted pro-survival actions on cardiomyocytes reducing the infarct size in a mouse model of MI (Kempf et al., 2006).

Another interesting member of the TGFβ superfamily is activin A, which has been overexpressed *in vitro* and *in vivo* and shown to protect ischaemic mouse cardiomyocytes from apoptosis, an action found to be antagonised by follistatin-like 3 (Fstl3) extracellular protein (Oshima et al., 2009).

Given the critical roles of all the aforementioned cytokine and chemokine families in heart repair and regeneration, they are thought to be obvious and attractive therapeutic targets for patients with MI (Leask, 2010). However, the pleiotropic and context-dependent actions of these cytokines, as well as the complex signalling cascades involved, pose significant challenges for their therapeutic translation.

### 1.8.3. Antioxidants

As previously mentioned, cellular redox levels play a key role in the pathogenesis of MI and heart failure. Whilst low levels of ROS are essential for homeostasis, differentiation and cell signalling, ischemia and reperfusion result in excessively high levels of oxygen radical production, accelerating myocardial damage (Hamilton, 2007).

The most well-studied group of antioxidants is the free radical scavengers, molecules or compounds that effectively neutralise ROS, preventing oxidative damage. Several effective scavengers have been synthesised and demonstrated to prevent oxidant-mediated cell damage, improving cell survival. A well-studied example is MCI-186, or edaravone, a strong free radical scavenger shown to protect endothelial cells against ROS via induction of prostacyclin production, inhibition of lipoxygenase metabolism of arachidonic acid, inhibition of alloxan-induced lipid peroxidation and quenching of active oxygen (Higashi et al., 2006; Nimata et al., 2005). The effects of edavarone in myocardial injury have been widely investigated in models ranging from I/R injury *in*

*vivo* and *in vitro* to heart failure, pressure-overload and autoimmune myocarditis (Higashi et al., 2006; Nimata et al., 2005). Edavarone was found to protect isolated rat and rabbit hearts from I/R injury through the reduction of myocyte damage and inhibition of lipid peroxidation (Minhaz et al., 1996; Wu et al., 2002; Yagi et al., 2005). Furthermore the scavenger was found to inhibit mPTP opening, preventing necrosis and cytochrome c release, as well as DNA fragmentation in a rat model of I/R injury (Rajesh et al., 2003).

A second class of scavengers, nitronyl nitroxides, are known for their high affinity for nitric oxide radicals, however they were later found to trap additional ROS such as hydroxyl, superoxide and hydrogen peroxide species (Blasig et al., 2002). A modified version of nitronyl nitroxide scavengers has been synthesised by Wu and colleagues, to increase their potency and reduce cytotoxic effects (Wu et al., 2006). Likewise, Toth and colleagues investigated a hexa-membered ring, HO-3073, for its scavenging activity and found that it exerts cardioprotection in rat hearts following I/R injury, through the inhibition of lipid peroxidation, protein oxidation and activation of PI3K/Akt cardioprotective pathway (Toth et al., 2003). These data suggest that radical-scavenging compounds mediate cardioprotective effects, not only via attenuation of oxidative-induced damage in lipids, proteins and DNA, but also by inducing pro-survival signalling pathways like PI3K/Akt.

An alternative approach to target oxidant stress is to use agents that mimic or enhance the activity of endogenous antioxidants; superoxide dismutase (SOD), glutathione, catalase, etc. Several SOD mimetics have been reported, all showing efficient attenuation of oxidant stress after myocardial I/R in animal models (Muscoli et al., 2003). An example is M40403, a stable, low molecular weight SOD analogue, which

has been found to significantly decrease myocardial damage and ventricular arrhythmias (Di Filippo et al., 2004; Masini et al., 2002). Although different SOD mimetics are being studied in the context of Parkinson's disease and cancer, not many studies have looked at their effects in cardiovascular pathology, to date (Filograna et al., 2016; Murphy et al., 2008).

Plant extract supplements have also been shown to preserve and increase the endogenous activity of antioxidants and have shown positive effects in acute MI rat models (Karthikeyan et al., 2003; Sun et al., 2005). Nevertheless, there is a lack for translatable preclinical data before these molecules can be tested in humans (Hamilton, 2007).

After an anti-oxidant exerts its scavenging activity, it is converted into an oxidant product. Thus, it is possible that some of the observed effects result from pro-oxidant activity of these molecules. Furthermore, despite the benefits of antioxidant mediated cardioprotection, data from human models in the context of cardiovascular disease are sparse, calling for further investigations before definite conclusions can be made (Hamilton, 2007).

### 1.8.4. Paracrine-secreted hormones with newly discovered cardioprotective activities

In the recent years, cardiomyocyte receptor and intracellular signalling activation studies have identified known hormones that were not previously considered to be cardioprotective. Two examples of such hormones are reviewed here, ghrelin and irisin.

Ghrelin is a growth hormone-releasing peptide first discovered in the rat gastro-intestine and later seen to circulate in healthy human blood plasma (Shiiya et al.,

2002). The cardiovascular tissue has been found, surprisingly, to be rich in ghrelin receptors and its mRNA is abundant in cardiac tissue including human and rat myocardial cells (Gnanapavan et al., 2002). Being an important autocrine/paracrine factor, ghrelin is anti-inflammatory and increases myocardial contractility and vasodilation (Jeffery et al., 2003; Papotti et al., 2016). Ghrelin has been shown to inhibit apoptosis of primary adult and H9C2 cardiomyocytes via ERK1/2 and Akt (Baldanzi et al., 2002). Furthermore, the des-acetylated form of the hormone (des-acyl ghrelin) prevented doxorubicin-induced myocardial fibrosis and apoptosis in adult mice (Pei et al., 2014). Ghrelin administration in rat models of MI showed improved left ventricular remodelling and restored cardiac contraction with limited inflammation, lipid peroxidation and improved antioxidant activity (Eid et al., 2018). Ghrelin-mediated effects in the cardiovascular system are recent discoveries, so more work is needed to elucidate the implicated underlying mechanisms (Tokudome et al., 2019).

Irisin is a recently identified myokine, secreted by skeletal muscle and myocardium during exercise, as a cleavage product of type I membrane protein fibronectin type III domain containing 5 (FNDC5), which was shown to reduce oxidative stress and apoptosis in different contexts (Boström et al., 2012; Park et al., 2015; Zhu et al., 2015). Irisin treatment suppressed myocardial apoptosis and oxidative stress in mouse ischemic heart and protected H9C2 cardiomyocytes from cell death by improving mitochondrial function (Wang et al., 2017a). In a subsequent study by the same group, irisin was shown to protect rat heart against I/R injury through a mitochondrial mechanism that involves SOD2 (Wang et al., 2018b). These current studies demonstrate a promising role for irisin in protection against ischemic injury, holding promise for the development of novel therapeutic strategies.

### 1.8.5. Mitochondrial transfer

A different discovery from recent studies is the role of mitochondrial transfer between cells that confers protection from different modes of stress (Islam et al., 2012; Liu et al., 2014). Membrane nanotubes are long, thin, membrane-based distant connections that allow cell-exchange of a range of cargoes (Figure 1.7) (Rustom et al., 2004; Torralba et al., 2016). These 'tunnelling nanotubes' have a diameter of 50-200 nm and a length of up to several cell diameters (Rustom et al., 2004). Cardiomyocytes have been found to employ these structures in the long-distance intercellular transfer of mitochondria and $Ca^{2+}$ (He et al., 2011). In 2018, Shen et al demonstrated that mitochondrial transfer through membrane nanotubes between intact myofibroblasts and stressed cardiomyocytes upon hypoxia/reoxygenation injury, can rescue the myocytes from apoptosis (Shen et al., 2018). However, unlike the other examples discussed, this mechanism requires cell proximity and is not recapitulated using just the cells' conditioned medium.

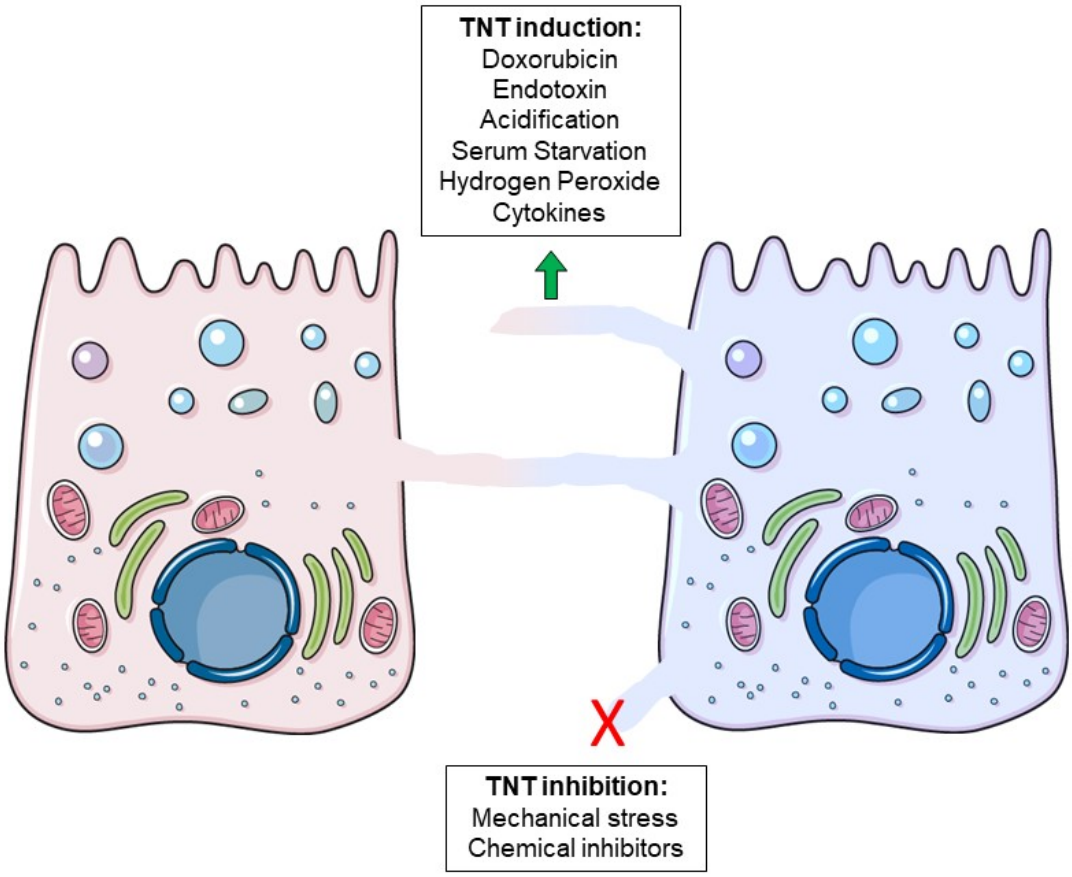



**Figure 1.7: Intercellular mitochondrial transfer via tunnelling nanotubes.** Tunnelling nanotubes (TNT) are long, thin structures of 50-200nm diameter which facilitate organelle transfer between different cells. Depending on the cell type TNT can contain cytoskeletal elements (such as actin and microtubules), mitochondria and lysosomes. Formation of TNTs can be inhibited by mechanical stress and chemical inhibitors and induced by doxorubicin, endotoxin, acidification, serum starvation, hydrogen peroxide and cytokines. Schematic diagrams modified from the Servier Medical Art image database (https://smart.servier.com/).

### 1.8.6. Other factors and small molecules

Within the cocktail of cytokines and growth factors secreted by stem cells a broad range of additional factors and small molecules has been identified and shown to be cardioprotective. Among others these include small peptides like thymosin β4 (Tβ4), opioids, heat shock proteins, adenosine, endovanilloids, cannabinoids and apolipoproteins (Dubé and Smart, 2018; Tsibulnikov et al., 2019).

One of the most abundantly secreted factors by cardioprotective BM-MSC and the highly angiogenic embryonic endothelial progenitor cells (eEPC) was found to be Tβ4 (Gnecchi et al., 2006; Kupatt et al., 2005). Further studies revealed that Tβ4 mediates beneficial effects in the ischemic heart via enhancement of cardiomyocyte survival through activation of AKT (Bock-Marquette et al., 2004), modulation of the inflammatory environment as a response to TNFα stimulation (Sosne et al., 2007), induction of neovascularisation and contribution to vessel stability (Rossdeutsch et al., 2012). Furthermore, Tβ4 has been found to act as a co-stimulant, to restore the cardiovascular potential in a subset of quiescent cardiac progenitor cells, the epicardial progenitor cells (EPDC) (Smart et al., 2007). Notably, Tβ4-activated EPDC have been shown to contribute to paracrine signalling, increasing vessel intensity and improving cardiac function in a mouse model of MI (Zhou et al., 2011). Given the promising effects of Tβ4 a number of approaches have been tested for its robust and durable delivery in the infarcted myocardium. Despite the remarkable improvement in cardiac function obtained after intracardiac and intraperitoneal injection shortly after MI in mice (Bock-Marquette et al., 2004) and pigs (Hinkel et al., 2008), Tβ4 delivery and dosing was further optimised in both acute and chronic phases after injury (Bollini et al., 2015). Composite hydrogels such as collagen-chitosan have been tested for Tβ4 controlled release which enhanced the beneficial activity of the factor in rat models *in vitro* and *in vivo* (Chiu and Radisic, 2011). The first human pilot study of Tβ4 in MI patients was conducted by RegeneRx Biopharmaceuticals and demonstrated potential clinical benefits of the factor in the regeneration and repair of damaged tissue and the improvement of cardiac function (Zhu et al., 2016). Larger clinical trials are currently under-way to validate the promising findings.

Humoral factors produced by the myocardium following remote ischemic pre-conditioning (RIP) have also been shown to exhibit an anti-necrotic effect on the myocardium itself as well as other organs. This protective effect is abolished by blockade of $K_{ATP}$ channels or naloxone, a non-selective opioid inhibitor, implicating opioid peptides in cardioprotection (Dickson et al., 2002). Furthermore, occlusion/reperfusion of the femoral artery in pigs mediates a cardioprotective effect that has also been associated with activation of opioid receptors (Xie et al., 2006).

A study by Shimizu et al showed that hydrophobic, low molecular weight factors both in rabbit plasma and dialysed plasma (filtered through a 15 kDa cut-off dialysis membrane) could protect Langendorff-perfused hearts from ischaemia/reperfusion and isolated cardiomyocytes from necrosis, an effect which could be blocked by naloxone (Shimizu et al., 2009). Further characterisation studies on the protective factor pointed to heat shock protein 10 (HSP-10) which mediates PKC activation and $K_{ATP}$ channel opening (Maciel et al., 2017; Yang et al., 2010).

The notion of adenosine-mediated cardiac benefits has been introduced in the mid-1980s (Lasley, 2018). A number of reports demonstrated implication of adenosine receptors in cardioprotection from I/R showing significant infarct size reduction (Headrick and Lasley, 2009; McIntosh and Lasley, 2012). Despite the numerous reports in preclinical models, there have been minimal clinical trials of adenosine receptor cardioprotection in humans, partly due to the lack of clinically relevant animal models with relevant morbidities; almost all experimental studies have been performed in healthy, adult animals, which are vastly imprecise mimetics of human MI in terms of aging and lack of co-morbidities such as diabetes and hyper-tension (Lasley, 2018).

Endogenous agonists of cannabinoid receptors were used to demonstrate the involvement of cannabinoids in cardioprotective RIP in a rat model (Hajrasouliha et al., 2008). Similarly, endovanilloids, the agonists of the mechanosensitive vanilloid channels found on cardiomyocyte sarcolemma are involved in the anti-necrotic, reparative effects of RIP in isolated rat heart (Randhawa and Jaggi, 2017). Despite the few promising results in animal models, overall there is paucity of supporting data in human models for the role of cannabinoid and vanilloid receptors in cardioprotection (Tsibulnikov et al., 2019). More specifically, there are indications of a detrimental effect of cannabinoid receptor 1 in the cardiovascular system, ranging from drop in blood pressure (Gorelick et al., 2013), tachycardia, increased heart rate (Schmid et al., 2010), higher incidence of heart attack, all of which were side effects reported in cannabis users (Pratap and Korniyenko, 2012).

Lipid-like molecules that have been involved in cardioprotection include apolipoprotein A-1 (ApoA-1) and high-density lipoprotein (HDL). ApoA-1 and HDL-C levels are strongly correlated, as ApoA-1 is a cofactor, involved in the removal of excess cholesterol from tissues and incorporating it onto HDL for transfer to the liver (Imahashi et al., 2005; Srivastava and Srivastava, 2000). Injection of ApoA-1 reduced infarct size in a rat model of MI by almost 20%, while HDL protected against mouse neonatal and immortalised human ventricular cardiomyocyte necrosis via activation of Akt and PI3K, through its high affinity receptor, Scavenger Receptor class B1 (SRB1) (Durham et al., 2018; Hibert et al., 2013).

### 1.8.7. microRNAs

Increasing evidence points to circulating microRNAs (miRNAs), a group of endogenous, stable, single-stranded, short non-coding RNA sequences as diagnostic

biomarkers of cardiovascular disease, as well as potential therapeutic targets (Zhou et al., 2018a). Their unique ability to silence gene expression, allows miRNAs to participate in a number of regulatory processes in cardiomyocytes including growth, proliferation, metabolism and apoptosis (Chang and Mendell, 2007).

In recent years, numerous miRNAs have been identified as potential therapeutic targets for cardiac pathology. For example, overexpression of miR-99a in a mouse model of MI improved LV function and survival 4 weeks post-injury, through reduction of hypoxia-mediated apoptosis (Li et al., 2014c). Similarly, adenovirus delivered miR-214pr miR-21 decreased myocyte apoptosis and improved LV remodelling in rat models of MI or I/R injury (Qin et al., 2012; Yang et al., 2016). Furthermore, administration of miR-320 anti-miRs reduced apoptosis and myocardial fibrosis responses in LV remodelling (Song et al., 2014). Generally, it is thought that the majority of miRNAs migrate to their target cells through circulation, enclosed in exosomes or extracellular vesicles, which are discussed in more detail in the next section (Barile et al., 2017).

### 1.8.8. The role of exosomes in cardiac repair

Exosomes have been implicated in paracrine signalling and they provide a plausible therapeutic approach for cardiac repair. Exosomes are produced and released from cells by fusion of intracellular vesicular bodies with the cell membrane (Colombo et al., 2014). They are 30-100nm in diameter and characterised by the presence of specific surface markers such as CD9, CD63 and CD81 (Colombo et al., 2014). Exosomes can contain a range of cargos including proteins, lipids and RNAs. They are an important component of intracellular communication and accumulating evidence

highlights their role in cell-cell communication between cardiac cells (Sluijter et al., 2014; Valadi et al., 2007).

CDC are a unique type of cardiac progenitor population expanded from patient biopsies *ex vivo* and were originally described by Messina and colleagues (Messina et al., 2004). Studies utilising CDC in culture and preclinical models suggested that the cardiac benefits were mediated through paracrine mechanisms including angiogenesis, survival (of both cardiomyocytes and stem cells), proliferation, stem cell migration, inflammation, improvements of cardiac metabolism and contractility (Cheng et al., 2014b; Kanazawa et al., 2015, 2016; White et al., 2013). Nevertheless ALLSTAR, the phase I trial using CDC in patients with MI was recently terminated due to a low probability of attaining its primary endpoint (Chakravarty et al., 2017; Reuters, 2017). Despite the inadequate efficacy demonstrated by the trial, great interest remains in the potential of CDC to repair heart damage, via their released exosomes (Davidson and Yellon, 2018). Human explant-derived exosomes were found to reduce cardiomyocyte apoptosis and scar formation, increase blood vessel density and prevent ventricular impairment in a rat model of MI (Barile et al., 2014). In the same study, exosomes isolated from dermal fibroblasts failed to show beneficial effects, suggesting a cardiosphere-specific effect. Furthermore, human CDC-derived exosomes have been administered in acute and chronic models of cardiac ischaemia in pigs and demonstrated reduction in infarct size and preservation of systolic function after intramyocardial delivery (de Couto et al., 2017; Gallet et al., 2017). Notably, the exosome-treated hearts were found to be richer in antibodies against the allogeneic CDC-derived exosomes, a sign of a mild immune response (Gallet et al., 2017), moreover this study used polyethelene-glycol (PEG)-precipitated exosomes, which

results in less pure preparations and has been shown to have a questionable effect on cardiac function (Paolini et al., 2016).

CDC are not the only cardiac cell product reported to act through exosomes. Mouse cardiac progenitor cell-derived exosomes inhibited cardiomyocyte apoptosis both in cultured rat cardiomyocytes and a mouse model of MI (Chen et al., 2013). In a number of additional preclinical studies of animal models of MI, human cardiac stem cell-derived exosomes improved heart function and attenuated cardiac remodelling (Gallet et al., 2016; Ibrahim et al., 2014).

MSC-derived exosomes have also been extensively studied. For instance, delivery of MSC-derived exosomes in a mouse model of ischaemia-reperfusion injury reduced oxidative stress and enhanced cardiomyocyte survival via the PI3K/Akt signalling pathway (Arslan et al., 2013). An alternative study by Liang et al used bone marrow-derived MSC-exosomes to pre-condition c-Kit+ cardiac stem cells before transplantation (Liang et al., 2016). The pre-conditioned stem cells demonstrated enhanced proliferation, migration and angiotube formation *in vitro*. Furthermore, when injected in a rat model of MI, the pre-conditioned stem cells exhibited better survival, with enhanced effects on capillary density, cardiac fibrosis and cardiac function (Liang et al., 2016). However, the isolated particle size was 10-80 nm, raising concern of possible contamination by serum-derived lipoprotein particles, which themselves can be cardioprotective, as discussed (Davidson and Yellon, 2018; Liang et al., 2016). Overall, the data published in support of exosome-mediated cardioprotection are promising. However, for methodological reasons, the results need to be interpreted with caution.

As of today, 130 clinical trials involving exosomes are listed in www.clinicaltrials.gov. Most of these studies investigate the use of body fluid-derived exosomes as early diagnostic markers to predict various treatment outcomes. Just four of the trials evaluate MSC-derived exosomes in four different conditions, none of them involving heart disease (ischemic stroke, macular hole, type I diabetes and pancreatic cancer). Despite the number of preclinical studies demonstrating the safety and scalability of exosomes to large clinically relevant doses for heart disease, their clinical use is still limited, even at the level of investigational studies (Bagno et al., 2018; Mendt et al., 2019). Several critical issues need to be resolved prior to the translation of exosome-based therapies from preclinical models to clinical trials and these include optimisation of the culture conditions and protocols for exosome production, isolation and storage. Also, batch uniformity is essential as well as investigations to establish optimal dosing, schedule of administration and potency assays to enable evaluation of efficacy (Börger et al., 2017; Lou et al., 2017; Squillaro et al., 2016). A few studies have recently investigated the effects of exosomes on human pluripotent stem cell derived cardiomyocytes, a promising model that has opened the door to mechanistic studies using renewable sources of human cells (Gartz et al., 2018).

## 1.9. Preclinical models of cardiac disease and paracrine protection

Myocardial ischemia comes in many forms: it can be of large calibre or result of microvascular disease; can range in extent from low flow to total occlusion; can vary in extent, number and location of narrowings; can be of short to long duration; can involve superimposed plaque rupture or not; can be effectively reversed by re-oxygenation rapidly or not at all; can induce injury or even provide cardioprotection. Hence, there is a wide range of preclinical models to address each type of ischemia

and provide conclusive derivations for better-informed translation of therapies to the clinic. In this section, we discuss the strengths and limitations of some of the most popular preclinical models for myocardial ischemia, providing a rationale for the necessity for more translationally relevant models for the purposes of better clinical trial design.

### 1.9.1. In vitro: myocyte cell culture

The most widely used *in vitro* model for I/R is isolated fresh or cultured cardiomyocytes. Ischemia is usually simulated by hypoxia with or without starvation medium and reperfusion by re-oxygenation and restoration of nutrients (Lindsey et al., 2018). The most important advantage of this system is the ability of the investigator to precisely control the cellular and extracellular environment and investigate I/R effects on purified cardiomyocyte populations, without the confounding effects of unwanted cell types or circulating factors. Cardiomyocytes in culture have also been extensively used to model the oxidative stress aspect of MI, using various extracellular triggers such as $H_2O_2$ (Janero et al., 1991), menadione (Loor et al., 2010) or doxorubicin (Hanf et al., 2019).

Cardiomyocyte sources can greatly vary from freshly isolated neonatal and adult cardiomyocytes to immortalised cell lines and human induced pluripotent stem cell-derived cardiomyocytes. Neonatal rodent cardiomyocytes are the most commonly used model, due to their relatively simple isolation procedure and low cost. Neonatal mouse cardiomyocytes undergo a rapid dedifferentiation-redifferentiation cycle once cultured, that typically gives spontaneously beating cells after 20 hours, while adult cardiomyocytes tend to require pacing to achieve contraction (Ehler et al., 2013). Furthermore, neonatal myocytes are more transfectable with simple liposomal

transfection methods, whereas adult myocytes require viral vectors for successful delivery of transgenic DNA (Ehler et al., 2013). However, along with many other issues of molecular and functional maturity, these have been found to be considerably more resistant to hypoxia than adult cardiomyocytes, via mechanisms that are still under investigation (Ostadalova et al., 1998; Riva and Hearse, 1993). This might lead to inconclusive results when designing translational studies (Ostádal et al., 2009).

Therefore, some researchers turn to freshly isolated adult myocytes, as they are a more relevant model for ischemic heart disease. Adult myocyte isolation is more complicated and their adaptation in culture is a concern; overtime the rod-shaped cells flatten, loose sarcomere organisation and re-acquire some of their primitive properties. Nevertheless, this adaptive flexibility has proved useful in studies of human cardiomyopathies (Eppenberger et al., 1994), as well as early experiments investigating myofibrillar degradation and re-establishment of the contractile mechanisms (Eppenberger et al., 1988; Piper et al., 1982). While adult cardiomyocytes are durable enough for short-term I/R studies, their long-term instability becomes a concern for overexpression and knock-down experiments which require more days for protein expression and subsequent read-outs to be achieved (Lindsey et al., 2018). Furthermore, adult myocytes are unable to form monolayers in culture, as seen by neonatal cells, restricting their utility for electrophysiology or gap junction studies.

To overcome some of these drawbacks, many groups prefer immortalised cardiomyocyte cell lines that can proliferate in culture such as AT-1 cells established from a mouse atrial tumour (Steinhelper et al., 1990), cell lines established from transgenic mice that express SV40 T-tag (Brunskill et al., 2001; Katz et al., 1992;

Negishi et al., 2000) or transformation of foetal cardiomyocytes with the SV40 oncogene (Li et al., 1996; Wang et al., 1991). These provide a better option for genetic modification studies or as a complement to adult cardiomyocyte studies. However, transformed cell lines suffer a number of disadvantages such as the lack of a typical structural cardiomyocyte phenotype, a limited or sustained capacity to be passaged, de-differentiation in the case of prolonged culture, and confounding effects of the transforming genes, including inactivation of p53. Claycomb et al., described the HL-1 cell line, a mouse atrial line derived from AT-1 cells, that could be serially passaged, differentiated and maintained typical characteristics of adult mouse cardiomyocytes such as their morphological, biochemical, electrophysiological properties and their ability to contract. Nevertheless, at the ultrastructural level, the investigators reported cytoplasmic organisation and myofibrillogenesis typical of embryonic, mitotic, cardiomyocytes. The authors admit that the HL-1 line is a hybrid between an embryonic and an adult myocyte. Their ability to divide, gives them a less differentiated and less organised structure similar to an embryonic myocyte. However, they transcriptomic analysis showed that HL-1 cells express genes typical of mature cardiomyocytes such as α-cardiac myosin heavy chain, α-cardiac actin, and connexin43 (Claycomb et al., 1998). Despite the overall resemblance to adult myocytes, this line is a limiting model for human ventricular cardiomyocyte biology and pathobiology, given its murine, atrial origin (Claycomb et al., 1998).

Early attempts for stable transformation of SV40 oncogene into primary adult human cardiomyocytes were difficult due to unsuccessful gene delivery and the post-mitotic nature of the cells (Miller et al., 1994). In 2005, Davidson et al. described a method to immortalise human primary adult ventricular myocytes using fusion with a SV40 transformed fibroblast cell line lacking mitochondrial DNA (Davidson et al., 2005).

Using this method the researchers obtained stable cell lines, that could be passaged for over 120 generations and recovered from freezing while maintaining their characteristic phenotype (Davidson et al., 2005). Stable human cardiac cell lines, allowing manipulation of their proliferation and differentiation properties through alterations in their culture environment as well as genome, are a useful tool to study cardiac gene expression and function during development and disease. As one exemplar, a recent paper by Lin et al., uses this technology to demonstrate protection of human cardiomyocytes by mesenchymal stromal cell-secreted factors from amyloid fibril-induced damage (Lin et al., 2017). Use of immortalized human CMs might overcome some of the mentioned limitations of primary cells, however their response to I/R has not been fully characterised and might be subject to their respective stage of maturation (Robertson et al., 2013). Human induced pluripotent stem cell derived cardiomyocytes (hiPSC-CM) as a potentially better preclinical model will be discussed in more detail in section 1.12 below.

Despite the ease of isolation and culture, as well as the precise manipulation of experimental parameters, *in vitro* conditions cannot fully recapitulate the full spectrum of I/R injury *in vivo*. Although *in vitro* models are mechanistically informative and can be used to identify targets, results need to be further validated in whole animal models (Lindsey et al., 2018). There have been cases of discrepancy between *in vitro* and *in vivo* models, emphasising the requirement for parallel studies. For instance, angiopoietin-like protein 4 did not prevent cardiomyocyte death *in vitro* but reduced infarct size *in vivo*, suggesting that other cell types in the infarct milieu are essential for the cardioprotective effect of this specific factor (Galaup et al., 2012). Conversely, factors found to prevent cardiomyocyte death *in vitro* might not confer the same effect *in vivo*, where the effect might be outweighed by other confounding factors. The most

relevant discrepancies include direct and indirect interactions with surrounding cell types and their secretome, the presence of a constant flow of blood washing away the factors and introducing new ones or the presence of an inflammatory response to the treatment which might involve cell recruitment or antagonising factor release.

### 1.9.2. Ex vivo: isolated perfused hearts

A convenient and robust model to study mechanisms of myocardial injury and cardioprotection is the *ex vivo* perfused heart, which involves heart removal from the animal and its subsequent perfusion with blood or with physiological saline solution (Bell et al., 2011; Liao et al., 2012). This model is mainly used for potential cardio-protective drug testing due to the exclusion of confounding circulating factors with retention of overall heart functionality, composition and architecture. However, this does not mean it fully represents *in vivo* conditions, as it lacks the presence of neurohumoral factors leading to a typically lower heart rate than in the animal itself. In the Langendorff procedure, perfusion happens through the coronary arteries and the heart keeps beating for several hours (Sutherland and Hearse, 2000).

One of the advantages of perfused heart models is the ability to accommodate either global or regional ischemic injuries: in a global ischemic model perfusate flow to the entire heart is stopped, whereas for regional ischemia a suture is used to occlude a coronary artery. Following an ischemic period, perfusion is re-started and the heart keeps beating, but showing signs of post-ischemic dysfunction known as stunning (Lindsey et al., 2018). Nevertheless, the perfused heart model preparation requires some degree of skill to avoid potential contusion injuries. At high pressures, the perfusate flow in the aorta might lead to defects in the aortic valve, resulting in a lower volume of perfusate passing through the coronary circulation (Skrzypiec-Spring et al.,

2007). The coronary flow rate and rheological properties of the perfusion buffer are generally different than physiological blood flow and this might introduce additional discrepancies such as sheer stress along the endothelium or the coronary arteries (Skrzypiec-Spring et al., 2007). The lack of blood-derived antioxidants and gluococorticosteroids makes the model susceptible to immune stimuli such as bacterial endotoxin which is frequently found in perfusion and surgical equipment and would result in stimulation of endogenous NO synthase, peroxynitrite generation and faster deterioration of heart function (Doring et al., 1987).

### 1.9.3. In vivo: permanent and transient coronary artery occlusion

*In vivo* MI preclinical mammalian models can be generally divided into the coronary artery permanent occlusion with or without reperfusion. Permanent coronary occlusion without reperfusion is a representative model of ~15—25% of all patients, who do not receive timely or successful reperfusion (Cohen et al., 2010; Gharacholou et al., 2010). Unlike in the reperfused MI model, typically, permanent occlusion results in exacerbated dysfunction and a more robust remodelling response (LV wall thinning and dilatation), reflecting induction of a more extensive infarct and a less effective repair response. While reperfusion injury comes closer to the clinical scenario, it might expand the area of damage and requires a more technically challenging and longer surgery procedure (Lindsey et al., 2018). However, despite this barrier to its adoption, surgical ischemia with reperfusion is widely employed to model acute myocardial infarction (Becerra et al., 2016; Heusch, 2013).

Major species variability in response to MI depends on temporal and spatial kinetics and differences coming down to the size of the myocardium, heart rate, diffusion distance and the presence or absence of coronary collateral vessels. In mice, coronary

occlusions longer than 60-90 minutes are considered irreversible and show signs of accelerated inflammation and wound healing responses (Dewald et al., 2004; Frantz et al., 2009; Michael et al., 1995, 1999). In contrast, studies in larger animals have shown that ischemic myocardium can be occluded for up to 6 hours, after which reperfusion is no longer effective (Reimer et al., 1983). In mice and rats, reperfused infarcts typically affect the mid-myocardium with sub-epicardial and sub-endocardial regions being frequently spared (Christia et al., 2013; Du et al., 2017; Yoshihara et al., 2015). A study in sheep showed a similar spatial response to small animals (Sakamoto et al., 2007). Undoubtedly, the pig model of coronary occlusion with reperfusion shows the closest temporal and spatial outcomes to a human STEMI (Heusch et al., 2011). Non-human primate models have significant physiological, metabolic, biochemical and genetic similarity to humans (Camacho et al., 2016). However, non-human primate models have been sparsely used in the study of cardiac diseases due to the high morbidity and mortality associated with induction of MI due to high susceptibility to arrythmias, cardiac arrest, infections and open-chest induced lung damage (Airaksinen, 1999; Contamin et al., 2012).

### 1.9.4. The issue of translation: toward human trial design

Aside from timely reperfusion, there is no other established intervention known to limit heart damage and improve the clinical outcome in patients experiencing myocardial ischemia. The failure to find a cardioprotective therapy despite more than 30 years of research, has been mainly ascribed to the insufficiency of simplified animal models to represent the complex clinical reality of a reperfused STEMI patient (Hausenloy et al., 2017). A number of missing parameters from preclinical studies of infarct size reduction have been identified and include underpowered studies, absence of sufficient blinding, and insufficient methodological detail (Heusch, 2017; Kloner, 2013).

These elements might partly explain the current failure to translate preclinical results into effecting treatments in human patients (Hausenloy et al., 2017). Among several recommendations for the improvement of future cardioprotection studies, a position paper of the 'European Society of Cardiology Working Group of Cellular Biology of the Heart', advises researchers to always consider human heart tissue models of acute ischemia reperfusion injury (including human atrial tissue, cell-based heart tissue models or human stem cell derived cardiomyocytes), before moving their therapeutic approach to the clinical setting (Hausenloy et al., 2017).

## 1.10. Human pluripotent stem cell-derived cardiomyocytes as a platform for cardiomyocyte toxicity and protection

Most of the protection strategies in ischemic heart disease demonstrate modest efficacy between phases I and III (Hausenloy and Yellon, 2015; Heusch, 2013). Therapeutic progress has been hampered, partly due to the failure of animal models to predict success in clinical cardioprotection. This limitation has been orchestrated by the lack of workable systems for pre-clinical human validation in the cardiovascular field.

The development of human induced pluripotent stem cells (hPSC) marks the beginning of a new era of research and development of disease models. They count a number of advantages over traditional animal models including the possibility of indefinite passaging *in vitro* and exponential scale-up. More importantly, hPSC technology enables the personalised study of individual patients and potential therapeutic testing (Stack et al., 2019).

In the cardiovascular field, traditional routes of obtaining human cardiac tissue from biopsies are too invasive, explanted hearts are too infrequent, and the samples cannot be maintained in prolonged culture. Hence, the introduction of human induced pluripotent stem cell-derived cardiomyocytes (hPSC-CM) is viewed as an important turning point in the field. Apart from expressing most cardiac-specific ion channels and currents, hPSC-CM recapitulate the physiology of cardiomyocytes and possess the mechanisms required for excitation-contraction coupling and relaxation. Patch-clamp analysis has been used in the characterisation of hPSC-CM action potential morphologies, identifying the existence of atrial, nodal and ventricular subtypes (Burridge et al., 2016; Lee et al., 2017a), even though the validity of such analysis has been disputed by some in the electrophysiology field (Du et al., 2015; Kane and Terracciano, 2017).

The utmost limitation of hPSC-CM is their immaturity, correlating them more to foetal than adult cardiomyocytes in terms of structure, electrophysiology, gene programs and metabolism (Cao et al., 2008; Lundy et al., 2013). It is extremely difficult for these cells to naturally acquire mature cardiomyocyte characteristics due to the differences between the *in vivo* environment and *in vitro* culture conditions. As a result, the extrapolation of a translational impact on mature cells needs to be approached with caution until factors or cellular programmes that lead to phenotypic maturity are developed.

Approaches to encourage hPSC-CM maturation include 3D culture and organ-on-a-chip technologies, which produce more physiological experimental conditions (Amano et al., 2016; Eder et al., 2016). These setups allow the integration of cardiac fibroblasts and endothelial cells creating capillary-like networks within the model (Eder et al.,

2016). In a recent study by Amano et al., doxorubicin cardiotoxicity was tested on a 3D model and revealed reduced sensitivity to the drug than the 2D culture, accompanied by physiological responses such as defects in beating rate (Amano et al., 2016). Another avenue of inducing hPSC-CM maturation is the addition of small molecules in the culture medium such as Tri-iodo-L-thyronine (T3) which has been found to increase sarcomere length and cell size, improve calcium handling properties and reduce the proliferative activity of these cells (Yang et al., 2010). Metabolic maturation of hPS-CM has also gained considerable interest, and one approach is to use glucose-free medium to force the cells to switch to fatty acid metabolism. This method was shown to increase sarcomere length, improve electrophysiological characteristics and increased expression of maturation genes (Correia et al., 2017; Drawnel et al., 2014). Despite the increase in maturation reported by the approaches mentioned, no study to date has demonstrated complete maturation of hPSC-CM using only these methods. Hence, consensus in the field is now moving into combinations of more than one maturation tactic, to achieve a more consistent phenotype to adult human cardiomyocytes (Machiraju and Greenway, 2019). Notably, despite their the immaturity downside, even routine 2D culture of hPSC-CM has proved to be a strong predictor of pro-arrhythmic effects (Blinova et al., 2018) and potential cardiotoxicity of oncological agents (Gintant et al., 2017; Sharma et al., 2018).

The application of hPSC-CM has been recently expanded to model chemotherapy-mediated cardiotoxicity. Burridge et al, report that hPSC-CM derived from doxorubicin-induced cardiotoxicity patients were more sensitive to the anthracycline drug *in vitro* when compared to hPSC-CM from patients who did not experience cardiotoxicity (Burridge et al., 2016). This work demonstrates the applicability of hPSC-CM in the

modelling of disease and study of treatment options on individual patients (Stack et al., 2019).

Despite the increasing usage of hPSC-CM in disease modelling, regeneration strategies and drug testing (Fiedler et al., 2019), this human model has not been used in paracrine protection studies, most of which still rely on traditional non-human preclinical evidence. Here, we demonstrate that hPSC-CM can be used as a workable platform for paracrine protection, to complement available data from animal models, contributing to a better-informed transition to the clinical trial phase.

## 1.11. Our model system

In this work we establish a platform to test the plausible paracrine protective effects of $Sca1^+$ SP CSC on two independent hPSC-CM lines; commercially available vCor.4U human ventricular myocytes (Ncardia) and IMR-90-derived human cardiomyocytes produced in-house (Harding lab).

The vCor.4U cardiomyocytes are commercialised as hPSC-CM primary-like ventricular cells, by the manufacturer. Studies using key cardiac channel modulators are available online (https://ncardia.com/product/vc.or.4u-cardiomyocyte-kit-discontinued.html#product_data), demonstrating no response to Carbachol, used to determine if the atrial current $I_{KACh}$ is present. The cells' lack of response to the drug, in addition to manual patch-clamp analysis and action potential measurements are the basis for Ncardia to classify them as ventricular. Notably, vCor.4U are a suitable model for a number of applications since they display a high degree of structural sarcomere organisation with binucleated cells, a low resting membrane potential, and a robust action potential amplitude. Short tandem repeat (STR) testing has determined that this

cell product was derived from the human embryonic stem cell line RUES2 (Steven Dublin, Ncardia, personal communication).

The second hPSC-CM line we use is IMR-90, which was differentiated from induced pluripotent stem cell clones of foetal origin, originally described by Yu et al. (Burridge et al., 2011; Yu et al., 2007; Zhang et al., 2009). They have been effectively used as a 2D platform to study cardiac contractility, relaxation and calcium handling properties (Lee et al., 2011b; Rodriguez et al., 2014). Investigations of IMR-90 calcium homeostasis revealed spontaneous rhythmic calcium transients with immature calcium handling properties, associated with smaller amplitudes, slower upstroke and slower decay velocity when compared to human embryonic stem cell derived cardiomyocytes (Lee et al., 2011b). IMR-90 cardiomyocytes have also been used in the formation of engineered heart tissue constructs, 3D models of cardiac muscle valuable for cardiac biology and disease modelling studies (Abilez et al., 2018). To our knowledge, neither of the two aforementioned hPSC-CM lines has been used as a platform for paracrine protection studies.

The $Sca1^+$ SP cardiac stromal cells (from here on, CSC) used in this work have been originally isolated from adult male mice as highly propagatable $Sca1^+$ cells (Figure 1.8). After culture expansion, our cells were found to also be enriched for PDGFRα, thus strongly associate with a cardiogenic molecular signature (Messina et al., 2004; Noseda et al., 2015a), natively expressing the majority of heart-forming factors used in reprogramming of various non-myocytes to a cardiomyocyte identity (Chen et al., 2017; Tani et al., 2018). Following intra-myocardial injections into infarcted mice, the CSC demonstrated improved ejection fraction and reduced infarct size 12-weeks post-injury (Figure 1.8), despite the negligible cell retention rates, as frequently observed in

similar studies involving direct cell injections in the myocardium (Chimenti et al., 2010; Hong et al., 2014; Ibrahim et al., 2014; Li et al., 2012; Noseda et al., 2015a; Wysoczynski et al., 2017; Zhang et al., 2015a). Hence, the beneficial results could be attributed to the paracrine effect which speculates that the injected cells secrete soluble factors which mediate cardioprotection. The present thesis tests the plausible paracrine effect of mouse CSC and their human equivalent, using human cardiomyocytes as the target in a model of lethal oxidative stress.

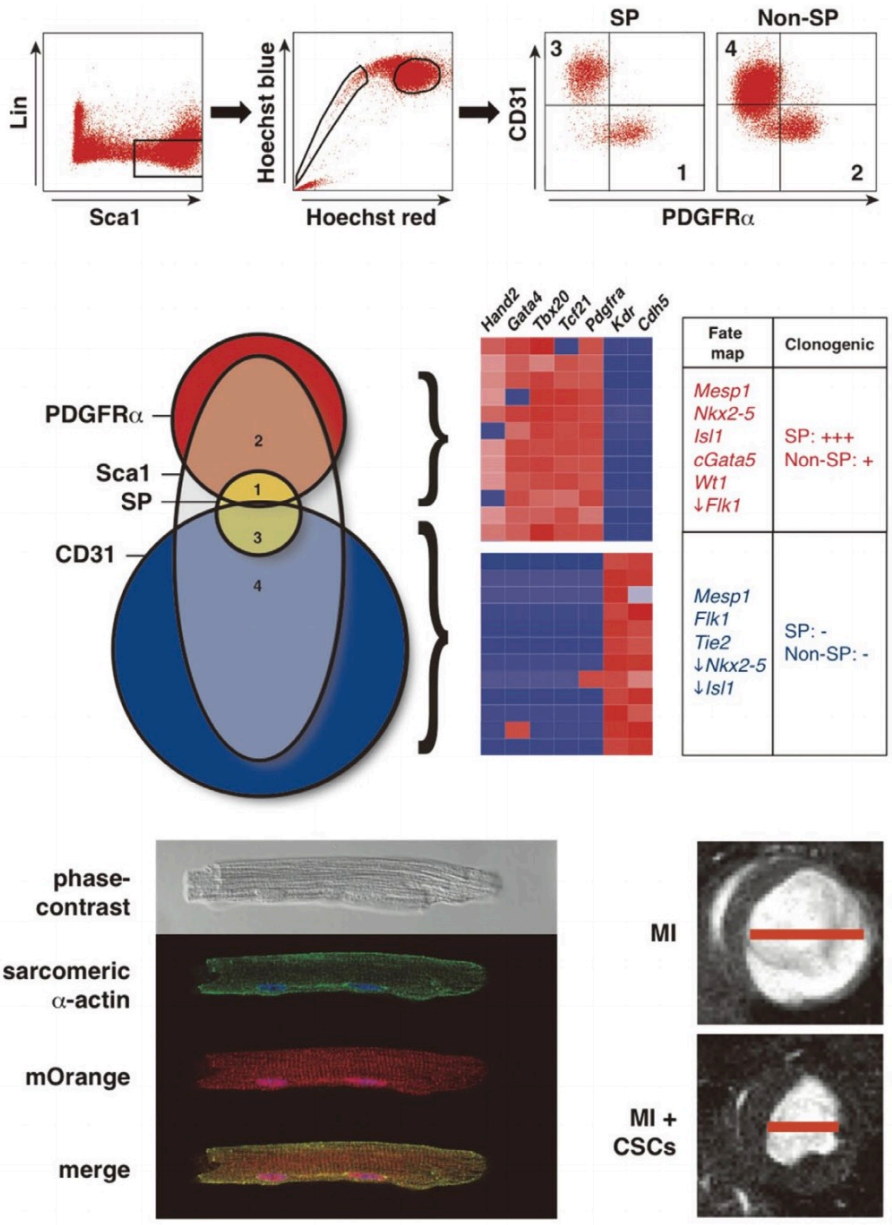



**Figure 1.8: Sca1⁺ SP CSC, the major cell population to be used in this work, are enriched in PDGFRα⁺ after culture expansion. Top panel** shows flow sorting based on lineage (Lin) negative, Sca1⁺ expression used to isolate mouse stromal cells from dissociated myocardium. These cells demonstrate Hoechst dye efflux i.e. side population (SP) phenotype and mutually exclusive expression of CD31 and PDGFRα markers. **Middle panel** shows that regardless of their SP classification, PDGFRα⁺ cells map to a cardiogenic molecular signature which encompasses cardiac transcription factors and is highly clonogenic. Each region of the Venn diagram maps to its corresponding population in the flow cytometry dot plots. **Lower left panel** shows an example of grafted CSC-derived cardiomyocyte 12-weeks after injection. **Lower right panel** shows CSC-mediated reduction of adverse cardiac remodelling and reduction of infarct size by 9.4 Tesla magnetic resonance tomography (MRI). Taken from (Noseda et al., 2015b).

## 1.12. Hypothesis, aim and objectives

Based on the reduction of infarct size despite a lack of durable engraftment, we hypothesise that CSC secrete factors sufficient to protect cardiomyocytes from oxidative stress, as one mechanism for the observed benefit (potentially, among others). We test this hypothesis using both trans-well co-cultures and conditioned media setups, where we stress mouse and human cardiomyocytes with different types of cardiotoxic compounds. High-throughput imaging assays to characterise cell death and its relevant components, as well as cardiomyocyte function, are employed to study the mechanisms underlying the protection. Upon proving paracrine protection of human cardiomyocytes, the further aim of this project is to identify potential paracrine factors for subsequent testing on human cardiomyocyte models of ischemic injury. In order to address these issues, the questions we asked and our corresponding objectives were:

1. Is CSC-conditioned medium sufficient to protect cardiomyocytes from acute oxidative stress?
    - Demonstrate that CSC-conditioned medium is sufficient to protect cardiomyocytes *in vivo*, in a mouse model of acute ischemic injury, simulating the conditions used previously for CSC themselves.
    - Establish a platform for paracrine protection studies using human pluripotent stem cell-derived cardiomyocytes in lieu of rodent cells.
    - Investigate the mechanisms underlying human cardiomyocyte cell death by complementary stress molecules in the absence or presence of CSC-mediated protection.

2. Which factor(s) secreted by the CSC is sufficient to confer human cardiomyocyte protection?
    - Characterise CSC and hPSC-CM responses using transcriptomic approaches including bulk RNA-Sequencing, to predict enriched candidate paracrine factors and potential ligand-receptor pairs.
    - Identify highly secreted protein factors in the CSC-conditioned medium empirically, using cytokine arrays.
3. Do human cardiac stromal cells exhibit similar cardioprotective effects?
    - Determine if human cardiac stromal cells exhibit similar molecular signature as the mouse CSC.
    - Validate the protective capacity of a more translatable human CSC to human cardiomyocyte model of protection from oxidative stress.
    - Identify enriched protein factors in the human CSC-secretome using cytokine arrays.

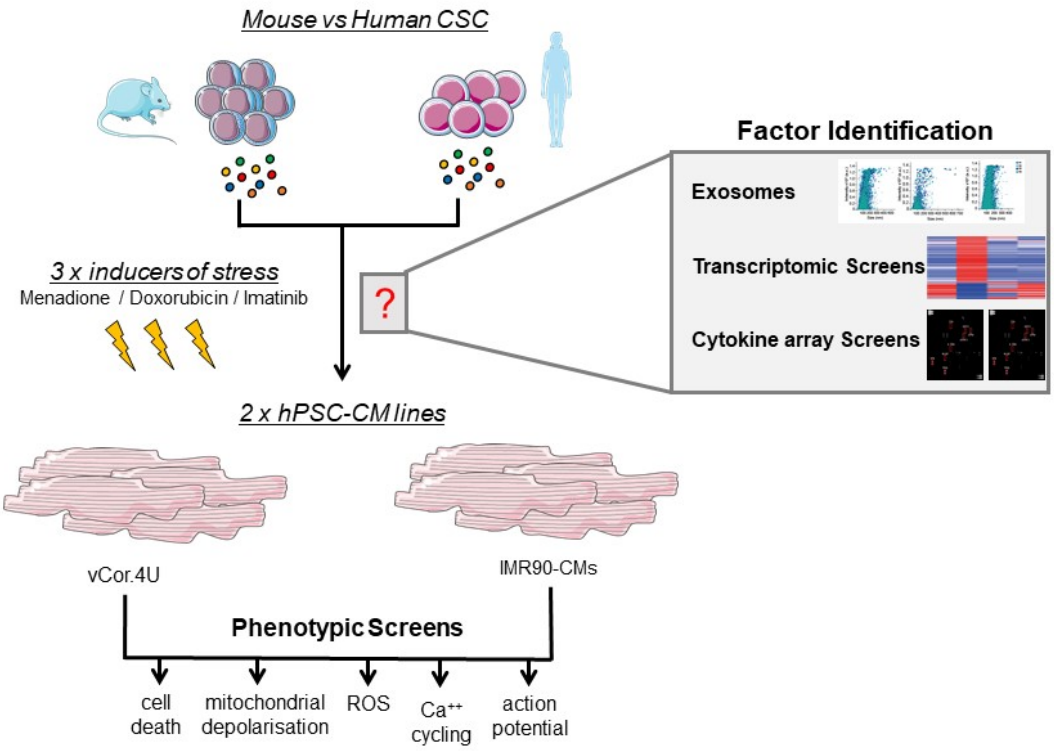


**Figure 1.9: Experimental design overview.** In this work the secretome from mouse and human CSC was used to treat two independent human pluripotent stem cell-derived cardiomyocyte lines (vCor.4U and IMR90), stressed with 3 different cardiotoxic molecules (menadione, doxorubicin or imatinib). Phenotypic screens included assays for protection from cell death, preservation of mitochondrial membrane depolarisation, inhibition of ROS generation, $Ca^{2+}$ cycling and action potential mitigation. An insight into the protective factors was achieved using CSC-conditioned medium exosome-depletion assays, transcriptomic profiles of the CSC and the target hPSC-CM and cytokine array screens of protective and non-protective secretomes.

# 2. Materials and Methods

## 2.1. Mouse cardiac stromal cell isolation

UK Home Office approval (PL 70/6806, 70/7880) was obtained for all animal procedures which also conformed to the UK Animals (Scientific Procedures) Act, 1986, incorporating Directive 2010/63/EU of the European Parliament. Hearts from C57Bl/6 adult male mice (8-13 weeks old; Charles River) were dissociated using 100 μg/ml Liberase and 50 μg/ml DNAse I (Roche) (Noseda et al., 2015a). The preparation was filtered through a 70 μm mesh for cardiomyocyte depletion (BD Falcon). Subsequently, hematopoietic lineage (Lin) depletion was performed using an AutoMACS Pro Separator (Miltenyi Biotec). To distinguish between SP and non-SP cells, staining with 5 μg/ml Hoechst 33342 (Sigma-Aldrich) was performed (Noseda et al., 2015a).

## 2.2. Cell culture

Adult mouse cardiac $Lin^-/Sca1^+$/SP cells and $Lin^-/Sca1^+/PDGFR\alpha^+/CD31^-$ cells were selected by magnetic sorting ($Lin^-$) followed by FACS (for SP, Sca1, PDGFRα and CD31) (Noseda et al., 2015a) and cultured in CSC-maintenance medium (35% Iscove's modified Dulbecco's medium (IMDM, Invitrogen), 32.5% Dulbecco's modified Eagle's medium (DMEM, Invitrogen), 32.5% Ham's F12 (Invitrogen), 1.3% B27 supplement (Invitrogen), 2 mM L-glutamine (Invitrogen), 1x Antibiotic-Antimycotic (Invitrogen), 0.14 mM 2-mercaptoethanol (Sigma-Aldrich), 3.5% bovine growth serum (Hyclone), 6.5 ng/ml recombinant human epidermal growth factor (Peprotech), 13 ng/ml recombinant human fibroblast growth factor-basic (Peprotech), 0.0005 U $ml^{-1}$ thrombin (Roche), 0.65 ng/ml cardiotrophin-1 (Cell Sciences) (Messina et al., 2004; Noseda et al., 2015a). Culture plates were coated with 50 μg/ml collagen type I (BD

Bioscience). Cells were detached using Trypsin-0.25% EDTA (Gibco) and counted using a Vi-CELL XR (Beckman Coulter). CSC were used for experiments at passages 16-30. Human CSC were propagated the same way and used at passages 2-8.

Tails from 30 adult C57BL/6 mice (Charles River) were mechanically and enzymatically dissociated to obtain tail tip fibroblasts (TTF). Tails were minced into 1-3 mm pieces in pre-warmed 0.25% Trypsin-EDTA (Gibco) and incubated for 1 hour at 37°C. Tissue fragments were transferred into 0.1% gelatin- (Sigma-Aldrich) coated 10 cm dishes with 12 mL of DMEM containing 15% fetal bovine serum (Gibco) and 2 mM L-glutamine, where they were incubated for a week at 37°C in 2% $O_2$ to allow fibroblast outgrowth and attachment. At 30-50% confluency, the cells were passaged using 0.25% Trypsin-EDTA (Gibco) and maintained passage 8-10.

Human dermal fibroblasts (HDF, Promocell) were maintained in Fibroblast Basal Medium 2 (PromoCell) plus Fibroblast Growth Medium 2 Supplemental Pack (PromoCell), containing fetal calf serum, recombinant human basic fibroblast growth factor and recombinant human insulin. Cells were passaged as above with 0.25% Trypsin-EDTA.

Human ventricular pluripotent stem cell derived cardiomyocytes (hPS-CMs) (vCor.4U; Ncardia) were obtained from Axiogenesis AG/ Ncardia AG (Cologne, Germany). STR testing has determined that the cell product was derived from the human embryonic stem cell line RUES2. Cardiomyocytes were plated at 100,000 cells/$cm^2$ in fibronectin- (Sigma) coated half-area 96-well microclear black-bottom plates (Greiner) and maintained in Cor.4U Complete Culture Medium (Ncardia).

IMR-90-derived cardiomyocytes (iPS(IMR90)-4, WiCell) were differentiated as previously described (Lian et al., 2012; Matsa et al., 2014) by Sian Harding's laboratory under the BHF Centre for Cardiovascular Regenerative Medicine. IMR90-

CMs were obtained on day 16-17 of the differentiation protocol and maintained in RPMI (Sigma-Aldrich) supplemented with B27 and antibiotic-antimycotic (Thermo Fisher). The cells were re-plated on day 23 after dissociating in cell dissociation solution (Thermo Fisher) mixed with 0.05% Trypsin-EDTA (Gibco) and RPMI and treated according to the assay at ~ day 30. All cells were cultured at 37ºC in 21% $O_2$ and 5% $CO_2$. For hypoxic treatments cells were kept in a chamber at 2% $O_2$.

### 2.3. Conditioned media production and modification

CSC, TTF or HDF were seeded in their respective maintenance media (described above) onto collagen-coated 6-well plates at 20,000-100,000 cells/$cm^2$. After 24 hours, the medium was replaced with Cor.4U Complete Culture Medium, following two washes. Conditioned media were obtained 20-24 hours later, after filtering through a 0.2 µm syringe (GE Healthcare). Conditioned media were either injected at the time of coronary artery ligation *in vivo* or added to hPS-CMs at the time of stress induction, unless otherwise indicated. Pierce PES columns with a cutoff of 3 kDa (Thermo Fisher) were used to concentrate the media for *in vivo* experiments and to discriminate between low and higher molecular weight fractions. Thermostability testing was carried out by heating the media at 90°C for 10 min on a heat-block.

### 2.4. Myocardial Infarction

All animal work follows the UK Animals (Scientific Procedures) Act, 1986, incorporating Directive 2010/63/EU of the European Parliament. For induction of myocardial infarction (MI) C57/Bl6 male mice aged 12-15 weeks were used. Prior to surgery general anaesthesia was induced with 4% isoflurane (Baxter), then maintained at 2% in complete $O_2$. Mice received 0.024 mg buprenorphine (Alstoe

Animal Health) subcutaneously (i.e. average dose, 1.1 mg $kg^{-1}$) and were intubated and ventilated with a tidal volume of 250 µl and respiratory rate of 150 breaths $min^{-1}$ (Hugo-Sachs MiniVent type 845; Harvard Apparatus Ltd). Heart rate, electrocardiogram (ECG) and core body temperature were monitored throughout the surgery. For MI, a left thoracotomy was performed in the fourth intercostal space to allow the removal of the pericardium. A 6-0 polypropylene suture was used to permanently occlude the left anterior descending (LAD). Ischemia was confirmed by blanching of the myocardium downstream of the suture and a clear ST-segment elevation on ECG tracings. Concentrated CSC-conditioned media or vehicle (x50) were immediately injected into the infarct border zone (2 injections of 10 µl each). After surgery, mice recovered in a heated chamber for 20 min, then moved to a normal holding cage with supplemental heat. Hearts were collected for immunohistochemistry 24 hours post-MI. For collection, general anaesthesia was induced with 5% isofluorane and maintained at 2.5% with 100% $O_2$. Animals were subsequently perfused via intracardiac injection with PBS for 30 seconds and 4% Pierce Formaldehyde (PFA; Thermo Fisher) in PBS for 60 seconds. The heart was then extracted, washed briefly in PBS and placed in 4% PFA. Myocardial infarction and heart PFA perfusion were performed by Dr Mohamed Bellahcene.

### 2.5. Immunohistochemistry and confocal imaging

Extracted hearts were fixed for 2 hours in 4% PFA. Subsequently, the organs were incubated in cryoprotective solutions containing gradually increasing concentrations of sucrose (Sigma) in distilled $H_2O$ for the following time periods: 10% sucrose (~16 h), 20% sucrose (8 h) and 30% sucrose (~16 h). Hearts were then frozen in OCT (Tissue-Tek) and stored in -80°C until sectioning.

For tissue staining, 10 μm sections were washed and permeabilized using 0.5% Tween-20 (Sigma) in PBS. Apoptosis staining was performed using the Click-iT TUNEL Alexa Fluor 594 Imaging Assay (Invitrogen). After TUNEL staining, sections were blocked in 5% donkey serum (Sigma) and 1% bovine serum albumin (BSA, Sigma) in PBS for 30 min, washed twice in PBS for 3 min and incubated with a-actinin (Abcam) primary antibody overnight at 4˚C. The following day, sections were washed twice in PBS for 3 min and incubated with donkey anti-rabbit 647 secondary antibody (Invitrogen) for 2 h at 4°C. Sections were then washed twice in PBS for 3 min, mounted in Vectashield antifade mounting medium with DAPI (Vector Laboratories), and kept at 4°C until scanned. Slides were equilibrated for 15 min at room temperature prior to image acquisition.

Confocal imaging acquisition was performed with a Zeiss LSM-780 inverted microscope, using the EC Plan Neofluor 40x/1.3 oil objective. Images were acquired as a Z-stack, ranging from 17-21 optical sections at 1.5 μm intervals, with a pinhole aperture of 1.3 μm. Images encompassed three regions per heart with ~10% overlap (infarct area, border zone and remote area / interventricular septum (IVS)) and quantification was performed in 2 sections per region, encompassing 18-24 fields each. Higher resolution images were acquired as representative images of the TUNEL staining by acquiring Z-stacks of 50 optical sections at a 0.36 μm interval, with a pinhole aperture of 1.3 μm and zoom of 2X. Confocal image acquisition was performed by Dr Antonio MA Miranda. Post-acquisition processing was performed using FiJi (ImageJ2 (Rueden et al., 2017)). TUNEL staining in cardiomyocytes (an average of ~3400 cardiomyocytes were counted per heart) was scored manually following blinding of conditions.

## 2.6. TUNEL staining in tissue sections and fixed cells

The Click-iT Plus TUNEL Alexa Fluor imaging assay kit (ThermoFisher, Invitrogen) was used to detect DNA fragmentation in fixed cells and tissue sections 24-hours following menadione treatment or myocardial infarction respectively, in the presence and absence of CSC-conditioned media. The kit uses a fluorescein-modified nucleotide (dUTP), modified with an alkyne bio-orthogonal functional group that enables the nucleotide to be readily incorporated at the 3'-OH ends of fragmented DNA by terminal deoxynucleotidyl transferase (TdT) enzyme. Detection is based on a click reaction, between an azide and an alkyne, catalysed by copper (I). Fixed tissue sections are briefly washed in PBS and permeabilized in 0.25% Tween-20 in PBS before starting the reaction. For the reaction, TdT reaction buffer is first added to sections or wells and incubated for 10 min at 37 °C. To proceed, TdT reaction mixture is freshly prepared by mixing EdUTP nucleotide mixture and TdT enzyme in reaction buffer and added to sections or wells for 1 hour at 37 °C. At the end of the incubation, slides are rinsed in $dH_2O$ and washed in 3% BSA / 0.1% Triton X-100 in PBS. Cells are only washed with 3% BSA in PBS. The Click-iT Plus TUNEL reaction cocktail is then prepared fresh and added to each well or slide for 30 min at 37 °C. Finally, samples are washed with 3% BSA in PBS and antibody staining follows if necessary.

## 2.7. Co-culture

HTS Transwell 96-well permeable supports with polyethylene terephthalate membranes and 1.0 µm pores were used (Corning). Cardiomyocytes were seeded onto the bottom well at a density of 100,000 cells/$cm^2$ in Cor.4U Complete Culture Medium. One day before starting co-cultures, CSCs were seeded at a density of 100,000 cells/$cm^2$ on the apical side of inserts coated with 50 µg/ml collagen in CSC-

maintenance medium. Seven days after cardiomyocytes' seeding, CSC-seeded inserts were placed above the cardiomyocytes and menadione (CorV4U: 18 µM – 88 µM; IMR90: 8 µM – 41.6 µM) or doxorubicin (0.1 µM – 100 µM) (both Sigma-Aldrich) treatment performed. As a control the stressor was always added to cardiomyocytes in the absence of CSC.

### 2.8. Cell staining and high-throughput imaging

To measure cardiomyocyte death, hPSC-CMs were stained with DRAQ7 (Biolegend) at a final concentration of 3 µM and counter-stained with 8 µM Hoechst 33342 (Sigma-Aldrich). Mitochondrial depolarisation was visualized following incubation with 20 nM TMRM (ThermoFisher) for 30 min at 37°C. As a positive control to induce mitochondrial depolarization, 10 µM carbonyl cyanide-4-(trifluoromethoxy) phenylhydrazone (FCCP; Abcam), 1 µM oligomycin (Abcam) and 1 µM rotenone (Abcam), were added 15 min before the end of the incubation period. CellROX Green and MitoSOX Red (Invitrogen) were used to detect cytosolic reactive oxygen species (ROS) and mitochondrial superoxide, after incubation with 5 µM dye at 37°C for 30 or 10 min, respectively. Nuclei were counterstained with Hoechst 33342 as above.

Live-cell images were acquired at 37°C with 5% $CO_2$ on a Cellomics ArrayScan VTI platform (ThermoFisher), using the HCS Studio with Cellomics Scan Version 6.4.4 software (ThermoFisher). The automated Zeiss Observer Z1 epifluorescence microscope was used to acquire 6-20 fields per well (wells with ≤ 100 objects were then excluded from the analysis) with suitable filter sets at 20x magnification (for TMRM and MitoSOX) or 10x magnification (all others). Fluorescence intensity was recorded in channels 1-4, using the filter sets XF93 Hoechst (DAPI), XF93 FITC (GFP), XF32-TRITC sensitive (dsRed) and XF93Cy5 (Alexa-647), respectively. All

experiments consisted of technical triplicates or quadruplicates, and independently performed at least three times, except where noted. Images were analyzed using the HCS Studio BioApplication Cell Health Profiling V4 (ThermoFisher). Some of the analyses were performed by Dr Michela Noseda.

After live-cell image acquisition, cells were fixed in 3.7% formaldehyde in PBS for 15 min at room temperature and stored at 4°C. DNA fragmentation was detected as described, using the Click-iT Plus TUNEL Alexa Fluor 594 assay for apoptosis detection (Invitrogen) and Cellomics ArrayScan VTI.

### 2.9. Calcium cycling and action potential assays

Calcium cycling was studied using the high affinity, intracellular calcium indicator Fura-4F, AM (ThermoFischer). The acetoxymethyl (AM) ester form of this ratiometric indicator, is useful for non-invasive intracellular loading. At the end of the incubation period after menadione treatment +/- CSC-conditioned media, hPS-CMs were loaded with 8 μM Fura-4F in serum-free medium, which consisted of phenol-red serum free media (Gibco), supplemented with 10 mM galactose (Sigma), 10 mM sodium pyruvate (Gibco) and 2 mM L-glutamine. After 30 min incubation and a wash, the calcium indicator was allowed 20-30 min to de-esterify prior to recording calcium transients on the CellOptiq® platform (Clyde Biosciences). Ratiometric imaging was performed using fast switching between light-emitting diode (LED) excitation wavelengths of 335 nm and 380 nm. Emitted light was collected by a photo-multiplier (PMT) at 510-560 nm. The two fluorescent signals were digitized at 10,000 Hz and the fluorescent ratio (long wavelength / short wavelength) was used to identify the occurrence of calcium transients.

Action potential transients were recorded in two ways. First, using the potentiometric probe Di-4-ANNEPPS (Invitrogen) which allows detection of transient (millisecond) membrane potential changes. Twenty-four hours following menadione treatment +/- CSC-conditioned media, hPS-CMs were loaded with 8μM Di-4-ANNEPPS in serum free media (as above). After ~1 min, cells were washed and allowed to de-esterify 20-30 min prior to recording of voltage transients on the CellOptiq® platform.

For each well, Fura-4F and di-4-ANNEPPS signals were recorded from three independent, randomly selected areas (0.2 mm x 0.2 mm), using a 40x (NA 0.6) objective lens for 30 seconds. Offline analysis was performed using proprietary software (CellOPTIQ).

### 2.10. Human cardiac troponin I immunoassay

The Human cardiac troponin I SimpleStep ELISA® Kit (Abcam) was used to measure cardiac troponin I in cell culture supernatants of dying cardiomyocytes. Cardiac troponin I is immunocaptured in solution by an affinity tag labelled capture antibody and a reporter conjugated receptor antibody, forming a complex. The whole complex is then immobilized via immunoaffinity of an anti-tag coating the well plate supplied with the kit. Supernatants were collected following incubation of hPS-CMs with the stress signal, and frozen at -80°C. For the assay, 50μl of standards and samples (diluted 1:4) were added to the ELISA plate and incubated for 1 hour with 50μl of the antibody mix. The wells were then washed to remove any unbound material and 100 μl 3,3',5,5'- tetramethylbenzidine (TMB) development solution was added and catalysed by horseradish peroxidase (HRP) present in the bound complex, generating a blue colour. The reaction is stopped by addition of 100 μl stop solution completing

any colour change from blue to yellow. Signal intensity is measured at 450 nm using a plate reader (Paradigm, Beckman).

### 2.11. Adenylate kinase release cytotoxicity detection assay

The ToxiLight™ BioAssay Kit (Lonza) was used to measure the release of adenylate kinase (AK) enzyme from dying cells. AK actively phosphorylates ADP into ATP, which is in turn measured using the bioluminescent firefly luciferase reaction. As the levels of cell death increase, the amount of AK in the supernatant also increases, resulting in emission of higher light intensity by the ToxiLight™ reagent. Supernatants are collected prior to DRAQ7 and Hoechst staining described above, and frozen at -80°C. for the assay, supernatants are defrosted, and 20 µl is transferred into an empty 96-well plate. Following reconstitution of the AK detection reagent in assay buffer, 100 µl per well are added for 5 min. Luminescence is measured immediately using the luminometer (PHERAstar, BMG Labtech).

### 2.12. $H_2O_2$ detection in cell culture supernatants

The ROS-Glo™ $H_2O_2$ Assay (Promega) was used to determine the levels of hydrogen peroxide induction in cardiomyocyte cultures upon induction of oxidative stress in the presence or absence of CSC-conditioned media. The cardiomyocytes were treated with the oxidative stress signal as normal, and for the last 6 hours of the treatment, the $H_2O_2$ substrate was added, which reacts directly with $H_2O_2$ in culture to create the luciferin precursor, which is converted to luciferin after 20 min incubation with the ROS-Glo™ Substrate Detection solution. The light signal produced by luciferin is proportional to the amount of $H_2O_2$ in the well and was detected using the luminescence settings of a plate reader (Paradigm, Beckman).

### 2.13. JC-10 assay for detection of mitochondrial depolarization

JC-10 Mitochondrial Membrane potential assay kit (Abcam) was used to determine mitochondrial depolarization in human cardiomyocytes with and without oxidative stress. The protocol depends on detection of mitochondrial membrane depolarization by the JC-10 dye, a cationic, lipophilic probe which concentrates in the mitochondrial matrix of healthy cells forming red fluorescent aggregates. In apoptotic and necrotic cells, JC-10 leaks out of the mitochondria, changing to its monomeric form and emitting green fluorescence. At the end of the incubation with the oxidative stress signal the JC-10 dye loading solution was added to the wells and the plate was incubated for 45 min at 37°C. Assay buffer B was then added to stop the reaction, prior to monitoring fluorescence using the plate reader FL-cartridge (Beckman; excitation at 485 nm and emission at 535 nm and 595 nm). The results were plotted as the ratio of 535 nm : 595 nm emission.

### 2.14. Exosome isolation and characterization

Conditioned medium was fractionated by ultracentrifugation (Mincheva-Nilsson et al., 2016). More specifically, medium was first centrifuged at 4°C for 30 min at 2,500 x g (ThermoFisher, Heraeus Multifuge 3SR+). The supernatant was then centrifuged at 4°C for 35 min at 4,565 x g, passed through a 0.2 μm filter, and re-centrifuged at 4°C for 2 hours at 110,000 x g in an Optima XPN ultracentrifuge with a SW32 Ti rotor (Beckman Coulter). The cleared supernatant was the exosome-depleted fraction, whereas the pellets were resuspended in Cor.4U medium as the exosome-enriched fraction. For exosome identification by flow cytometry, (Lässer et al., 2012) 75,000 4 μm aldehyde/sulphate latex beads (ThermoFisher) were resuspended in 25 mM MES buffer (2-(N-Morpholino)ethanesulfonic acid; Sigma-Aldrich). Beads were then coated

with 8 µg CD63 (Biolegend) or rat IgG2α (Biolegend) by incubating on a rotator for 20 min in a final volume of 50 µl PBS. Bead-antibody complexes were then incubated for 30 min with 100 mM glycine (Sigma-Aldrich) to occupy any unreacted sites. The different media fractions were incubated with the antibody-coated beads in a final volume of 250 µl for 15 min allowing for any exosomes present in the samples to bind to the labelled beads. Exosome-bead complexes were stained with 10 µg/ml FITC conjugated anti-CD9 (Biolegend), with gentle agitation for 30 min in the dark. Results were visualized using an LSRII flow cytometer (Becton Dickinson) equipped with five lasers (Noseda et al., 2015a), and were analysed using FlowJo (v10, FlowJo).

For exosome isolation using the ExoSpin columns (Cell Guidance Systems) CSC-conditioned medium was prepared and centrifuged as described above to remove cells or debris and 50 ml were mixed with the ExoSpin buffer and allowed to precipitate for 1 hour at 4°C. The resulting mixture was centrifuged, and the supernatant was discarded. The exosome-containing pellet was resuspended in 100 µl PBS and loaded onto an equilibrated ExoSpin purification column for elution. Following the manufacturer recommendations, the columns were centrifuged and washed prior to elution of a final volume of 200 µl purified exosomes.

### 2.15. Flow cytometry and sorting

Flow cytometry and sorting were performed using a FACS AriaII (Becton Dickinson) equipped with 355 nm ultraviolet, 405 nm violet, 488 nm blue, 561 nm yellow–green and 640 nm red lasers and analysed using FlowJo v10. Antibodies and dyes are detailed in Table 2.1. Flow cytometry and sorting were performed by Dr Patricia Chaves.

### 2.16. Human cardiac stromal cell isolation

Adult human heart samples were obtained from the NIH-funded National Disease Research Interchange (NDRI), with protocols reviewed and approved annually by the University of Pennsylvania Institutional Review Board. Human CSC were obtained after 4 rounds of 7 min enzymatic digestion with 90 μg/ml Liberase (Roche) and 50 μg/ml DNase I (Roche), followed by filtering through a 70 μm sterile mesh. The cells were then purified by Percoll gradient centrifugation, to remove debris and red blood cells. Isolation of human cardiac stromal cells was performed by Dr Noseda and Anita M Chandler.

### 2.17. Single cell qRT-PCR

CellDirect One-Step qRT–PCR kits (Invitrogen) were used for pre-amplification by adding 10 μl of the reaction mixture directly into 96-well plates (Noseda et al., 2015a). Pre-amplification was performed for 22 cycles (Veriti Thermal Cycler). Non-template samples were included in each run at the pre-amplification stage as negative controls. Quantitative amplification was performed using Dynamic Array chips for 96 assays x 96 samples on the BioMark HD system (Fluidigm). For TaqMan primer/probe sets (ABI, ThermoFisher) see Table 2.1. Cycle threshold (Ct) values were calculated and exported using Fluidigm software (v4; Fluidigm). Fluidigm chips were run by Dr Patricia Chaves.

Data analysis was performed based on Ct values obtained by the Fluidigm software, using an R pipeline developed in-house. Outliers were identified from quantile-quantile plots of Ct values for an internal control gene (Ubc), using a quality control step based on robust standardized expression fractions and expression levels (Vandesompele et al., 2002). Ct values were normalised on a per-sample basis, expressing all Ct values

as their difference to the Ubc value for the same sample ($\Delta Ct_{sample,\ gene} = Ct_{sample,\ gene} - Ct_{sample,\ Ubc}$); ΔCt values were subsequently centered on the sample mean ($\Delta Ct_{centered} = \Delta Ct_{sample,\ gene} - Ct_{sample\ mean}$). Opposite values ($-\Delta Ct_{centered}$) were used for visualisation and further analyses. Euclidean distances among samples and among genes were used to compute hierarchical clustering, using the complete linkage method. Differential expression was determined using ANOVA with Tukey's test, using a significance level of $P < 0.05$. Dimensionality reduction was performed by principal component analysis using FactoMineR. All plotting was performed using R base graphics and ggplot2. All scripts were written by Dr Andrea Massaia and analysis was performed by Dr Patricia Chaves and Dr Michela Noseda.

### 2.18. Recombinant factor supplementation

For titration studies, human recombinant proteins were reconstituted and diluted to final concentrations according to manufacturer's instructions. Briefly, vials were centrifuged at 13,000 rpm for 30-60 seconds, followed by reconstitution in distilled $H_2O$ to a stock concentration of 1 mg/ml. Further dilution to the final concentration denoted in the figure for each factor, was performed in 0.1% BSA in PBS solution. Factors were stored at -20°C in aliquots. Recombinant factors were used to treat human cardiomyocytes in the presence and absence of menadione for 24 hours, following detection of cell death by DRAQ7 analysis and high-content imaging as described above.

### 2.19. Bulk RNA-Seq on CSC and IMR90 cardiomyocytes

For RNA-Seq CSC and TTF were seeded at 20,000/$cm^2$ in three 10 $cm^2$ dishes per cell type, allowed to attach for 24 h followed by media change to vCor.4U medium for

the next 48 h. Cells were detached as described above using 0.25% Trypsin-EDTA centrifuged to form a pellet. The cell pellet was resuspended in 700 µl TRI reagent (Sigma) for 5 minutes and RNA extraction was then performed using the RNeasy mini kit (Qiagen). Samples were submitted to the Imperial BRC Genomics facility for sequencing. For IMR90-cardiomyocytes' RNA-Seq cells were cultured at 100,000 cells/cm$^2$ in 6-well plates, including four conditions: 1) untreated cells; 2) cells treated with 20 µM menadione for 24 hours; 3) cells maintained in CSC-conditioned media for 24 hours and 4) cells treated with menadione and CSC-conditioned media. At the end of the incubation period media were collected from all the wells and centrifuged. Cells were washed in PBS and dissociated using cell dissociation solution containing 0.05% Trypsin-EDTA for 8 minutes. Trypsin was inactivated on ice using a trypsin blocking solution containing 10% FBS and cells were centrifuged at 4°C for 4 min at 200*g*. Cell pellets from the same conditions were pooled and resuspended in 900 µl cold PBS which were then divided into three equal replicates per condition. Samples were centrifuged at 4,000 RPM for 5 min at 4°C and pellets were resuspended in 300 µl TRI Reagent (Sigma) for 5 min. Samples were stored at -80°C until further processing. RNA extraction was performed using DirectZol RNA Miniprep kit (Zymo Research). Library preparation and sequencing were performed by Genewiz, UK as described below.

Each RNA sample was quantified using Qubit and ran on a Tapestation to assess sample integrity. mRNA was isolated from total RNA using oligo dT beads. After fragmentation, the sample was converted to double stranded DNA and ligated to Illumina adapters. The second strand (cDNA) was then degraded by the UNG enzyme providing directional information to the library. PCR was used for indexing each sample and for each pool of libraries, Tapestation was used to assess fragment

distribution and presence of artefacts. Prior to sequencing, each submitted library was quantified by Qubit and qPCR. For the mouse samples, sequencing was performed using a HiSeq4000. One lane was run as 75 bases paired-end and the total expected output was 45 million reads per sample. For the human samples processing involved RNA with polyA selection followed by sequencing using Illumina HiSeq 4000 using the 2 x 150 bp configuration. The total expected output was 350 million raw pair-ended reads per lane i.e. 20 – 30 million reads per sample.

The data was then downloaded for review of the QC results and downstream analysis. Trim Galore (Babraham Bioinformatics) was used to trim the adapter sequences from the raw sequences and reads were aligned to the mouse genome (mm10) or the human genome (GFCh38) using STAR (Dobin et al., 2013). Data was then imported to SeqMonk (Babraham Bioinformatics) to quantify, explore and generate heatmaps. Quantitation was performed using the SeqMonk RNA-Seq pipeline, correcting for genomic DNA contamination and merging transcripts isoforms. The DESeq2 R pipeline within SeqMonk was used to identify differentially expressed transcripts between the samples, using a $P<0.05$ to denote statistical significance. Dr Antonio MA Miranda downloaded the raw data, performed trimming, alignment and quantification in SeqMonk.

### 2.20. CellPhone Database analysis

The CellPhone DB bioinformatic analysis tool was used to predict possible receptor-ligand interactions in our RNA-Seq data-sets from mouse CSC and hPSC-CM (Efremova et al., 2019). Prior to uploading our data onto the CellPhone DB, and in order to detect interactions between our mouse and human data, the mouse genes were converted to their human orthologues and any duplicates removed to achieve

good alignment. For construction of the matrix, only the genes encoding for receptors and ligands were used, taken from a list provided by CellPhone DB. Raw data were uploaded as normalised counts (per million reads). After processing, the data were downloaded as .txt files of 'mean', 'p-value' and 'significant mean' for the different interaction partners. The 'mean' was the average expression value of the individual partner in the corresponding interacting pair of cell types. The 'p-value' represented the enrichment of the interacting ligand-receptor pair in each of the interacting pairs of cell types. The 'significant mean' displayed the mean for all the pairs for which the p-value was < 0.05. Dr Antonio MA Miranda prepared the RNA-Seq raw data counts and matrix to be uploaded to the CellPhone DB tool.

### 2.21. Cytokine arrays

High density array membranes (RayBiotech) with 308 mouse or 507 human proteins were used in a semi-quantitative approach to screen mouse and human CSC-, mouse TTF- and human HDF-conditioned media for the presence of secreted factors. Complete IMR90 medium (RPMI supplemented with B27 and antibiotics) was also tested as a control. Following collection of conditioned media from cells seeded at 20,000/cm$^2$ as described above, samples were dialysed overnight in PBS to remove small molecular weight molecules including salts and ions. Protein concentration was determined using the 660 nm assay (ThermoFisher) before and after dialysis and used to calculate the amount of biotin-labelling reagent to add per sample (7.2µl reagent per 1mg of total protein as per manufacturer's protocol). Solutions were incubated at room temperature for 30 min with gentle shaking prior to addition of 5 µl stop solution to halt biotin-labelling. Spin columns and centrifugation were then used to remove unbound biotin and elute the samples. Membranes were first blocked using the

provided blocking buffer for 2 hours at room temperature with gentle shaking. Each sample was then diluted 5-fold and 8 ml per sample were added onto the blocked membranes and incubated overnight at 4°C with gentle shaking. Subsequently, the membranes were washed in wash buffers 1 and 2 and incubated with HRP-conjugated streptavidin for 2 hours at room temperature with gentle shaking. Membranes were washed as before incubation with detection buffer for 2 min. Signal was detected by exposing the arrays to an X-ray film (Amersham) followed by subsequent development for 1.5- and 5- min for human and mouse membranes, respectively (Supplement 6.3).

Java scripts in Fiji were used for automated quantification of the dots' intensity in ImageJ. Numerical results were analysed using Microsoft Excel. Scripts were written by Stephen Rothery (Imperial FILM facility), edited by Dr Antonio MA Miranda and Chrystalla Constantinou and they are provided in their final forms in Supplement 6.2.

### 2.22. Statistics

GraphPad Prism (versions 6 and 7) was used to perform statistical analyses. Results are shown as the mean ± SEM ($P < 0.05$). Unless otherwise stated in the figure legend, all experiments have been performed at least 3 times independently, with technical triplicates per experiment. Data were analyzed by two-way ANOVA, using the Bonferroni correction for multiple comparisons and Welch's t-test for pairwise comparisons. The immunohistochemistry data were analysed using an unpaired non-parametric one-tail Mann-Whitney test. The cytokine array data were analysed using an unpaired Student's t test.

**Table 2.1. Reagents and resources**

| REAGENT or RESOURCE | SOURCE | IDENTIFIER |
|---|---|---|
| Antibodies | | |
| Anti-human Lineage cocktail, biotin-conjugated | Miltenyi Biotec | 130092211 |
| Anti-mouse Lineage cocktail, biotin-conjugated | Miltenyi Biotec | 130090858 |
| Anti-rabbit α-actinin | Abcam | AB18051 |
| Goat anti-rabbit IgG, PE-conjugated | Cell Signaling | 14705 |
| Donkey Serum | Sigma | D9663 |
| Mouse anti-human CD105, BV421-conjugated, clone 43A3 | BioLegend | 323219 |
| Mouse anti-human CD29, AF700 conjugated, clone TS2/16 | BioLegend | 303020 |
| Mouse anti-human CD31 (PECAM-1), AF488-conjugated, clone WM59 | BioLegend | 303110 |
| Mouse anti-human CD73, PerCP/Cy5.5-conjugated, clone IM7 | BioLegend | 344014 |
| Mouse anti-human CD90, BV510-conjugated, clone 5E10 | BioLegend | 328125 |
| Rabbit anti-human CD140 (PDGFRα), clone D13C6 | Cell Signalling | 5241 |
| Rat anti-mouse CD140 (PDGFRα), APC-conjugated, clone APA5 | BioLegend | 135908 |
| Rat anti-mouse CD63, clone NVG-2 | BioLegend | 143901 |
| Rat anti-mouse CD9, FITC-conjugated, clone MZ3 | BioLegend | 124807 |
| Rat anti-mouse Ly6A/E (Sca-1), PE-conjugated, clone D7 | BioLegend | 108108 |
| Rat anti-mouse/human CD44, AF647-conjugated, clone IM7 | BioLegend | 103018 |
| Rat IgG2a, κ isotype control antibody, | BioLegend | 400505 |

| | | |
|---|---|---|
| FITC-conjugated, clone RTK2758 | | |
| Rat IgG2a, κ isotype control antibody, clone RTK2758 | BioLegend | 400501 |
| Streptavidin, PE/Cy7-conjugated | BioLegend | 405206 |
| Vectashield Mounting medium with DAPI | Vector | H-1200 |
| Biological Samples | | |
| Human heart tissue | NDRI | N/A |
| Chemicals, Peptides, and Recombinant Proteins | | |
| Aldehyde/sulphate latex beads | ThermoFisher | A37304 |
| Antibiotic-Antimycotic | Invitrogen | 15240-096 |
| Bovine growth serum | Hyclone | SH30541 |
| B27 | Invitrogen | 17504-044 |
| Buprenorphine | Alstoe Animal Health | - |
| Cardiotrophin-1 | Cell Sciences | CRC700B |
| CellBrite Green cytoplasmic membrane dye | Cambridge Bioscience | BT30021 |
| Cell Dissociation buffer, enzyme-free PBS | ThermoFisher | 13151014 |
| Collagen type I | BD Bioscience | 354236 |
| Cor.4U Culture Medium | Ncardia (Axiogenesis) | Ax-M-HC250 |
| Di-4-ANNEPPS | Invitrogen | D1199 |
| DMEM, no glucose, no glutamine, no phenol red | Gibco | A14430-01 |
| DNAse I | Roche | 11284932001 |
| DRAQ7 | Biolegend | 424001 |
| Dulbecco's Modified Eagle's Medium (DMEM) | Invitrogen | 11965-092 |
| FCCP (carbonyl cyanide-4-phenylhydrazone) | Abcam | CAS 370-86-5 |
| Fetal bovine serum | Gibco | 10270 |

| | | |
|---|---|---|
| Fibroblast basal medium 2 | PromoCell | C-23220 |
| Fibroblast growth medium 2 supplemental pack | PromoCell | C-39320 |
| Fibronectin, bovine plasma | Sigma-Aldrich | F1141 |
| Formaldehyde solution, neutral buffered, 10% | Sigma | 111M4387 |
| Fura-4F, AM | Invitrogen | F14175 |
| Galactose | Sigma | G0750-100G |
| Gelatin solution | Sigma | G1393-100ML |
| Glycine | Sigma | 50046-50 |
| Ham's F12 | Invitrogen | 11765-054 |
| Hoescht 33342 | Molecular Probes | CAS 23491-52-3 |
| Human recombinant Crossveinless-2 (BMPER) | R&D systems | 1956-CV |
| Human recombinant DKK-3 | Peprotech | 120-46 |
| Human recombinant ENA-78 (CXCL5) | Peprotech | 300-22B |
| Human recombinant Epiregulin | Peprotech | 100-04 |
| Human epidermal growth factor | Peprotech | AF-100-15 |
| Human fibroblast growth factor-basic | Peprotech | 100-18B |
| Human recombinant GROα/MGSA (CXCL1) | Peprotech | 300-11 |
| Human recombinant IGF1 | Peprotech | 100-11 |
| Human recombinant IL-6 | Peprotech | 200-06 |
| Human recombinant M-CSF | Peprotech | 300-25 |
| Human recombinant MCP-1 (CCL2) | Peprotech | 300-04 |
| Human recombinant SDF1α (CXCL12) | Peprotech | 300-28A |
| Human recombinant sFRP-2 | R&D systems | 6838-FR |
| Iscove's modified Dulbecco's medium | Invitrogen | 12440-046 |
| Isofluorane | Baxter | FDG9623 |
| L-Glutamine (200 mM) | ThermoFisher | 25030-081 |
| Liberase | Roche | 05401151001 |
| Menadione | SigmaAldrich | M5750 |

| | | |
|---|---|---|
| MES buffer (2-(N-Morpholino) ethanesulfonic acid | Sigma | M3671-50 |
| Oligomycin A | Abcam | CAS 1404-19-9 |
| Pierce Formaldehyde 16% (w/v), methanol-free | ThermoFisher | 28906 |
| Rotenone | Abcam | CAS 83-79-4 |
| RPMI | SigmaAldrich | R8758 |
| Sodium Pyruvate (100 mM) | Gibco | 11360070 |
| Thrombin | Roche | 10602400001 |
| TMRM (tetramethylehodamine methyl ester perchlorate | ThermoFisher | T668 |
| Triton X-100 | Sigma | 9002-93-1 |
| Trypsin-0.25% EDTA | Gibco | 25200-056 |
| Trypsin-0.05% EDTA | Gibco | 25300054 |
| Tween-20 | Sigma | P9416 |
| Vectashield antifade mounting medium with DAPI | Vector Laboratories | H-1200 |
| 2-mercaptoethanol | Sigma-Aldrich | M7522 |
| Critical Commercial Assays | | |
| CellDirect One-Step qRT–PCR kits | Invitrogen | 11753500 |
| CellROX Green | Invitrogen | C10444 |
| Click-iT Plus Terminal deoxynucleotidyl transferase (TdT) dUTP Nick-End Labeling (TUNEL) assay | Invitrogen | C10618 / C10246 |
| ExoSpin Columns | Cell Guidance Systems | EX01-8 |
| Human Cardiac Troponin 1 SimpleStep ELISA® Kit | Abcam | ab200016 |
| Human L507 Array, Membrane | RayBiotech | AAH-BLM-1A-4 |
| JC-10 Mitochondrial Membrane Potential Assay Kit (Microplate) | Abcam | ab112134 |
| MitoSOX Red | Invitrogen | M36008 |
| Mouse L308 Array, Membrane | RayBiotech | AAM-BLM-1A-4 |

| | | |
|---|---|---|
| ROS-Glo™ $H_2O_2$ Assay | Promega | G8820 |
| ToxiLight™ BioAssay Kit | Lonza | LT17-217 |
| Pierce 660nm protein assay reagent | ThermoFisher | 22660 |
| Experimental Models: Cell Lines | | |
| Human dermal fibroblasts | Promocell | C-12302 |
| Human PSC-derived cardiomyocytes; IMR-90 | Sian Harding | https://www.ncbi.nlm.nih.gov/pubmed/29086457 |
| Human PSC-derived cardiomyocytes: vCor.4U | Ncardia (Axiogenesis) | Ax-B-HC03-1M |
| Experimental Models: Organisms/Strains | | |
| C57BL/6 mice | Charles River | C57BL/6NCrl |
| Oligonucleotides | | |
| TaqMan Probe *CD29_ITGB1* | ThermoFisher | Hs00559595_m1 |
| TaqMan Probe *CD44* | ThermoFisher | Hs01075861_m1 |
| TaqMan Probe *CD73_NT5E* | ThermoFisher | Hs00159686_m1 |
| TaqMan Probe *CD90_THY1* | ThermoFisher | Hs00174816_m1 |
| TaqMan Probe *CD105* | ThermoFisher | Hs00923996_m1 |
| TaqMan Probe *Gata4* | ThermoFisher | Hs00171403_m1 |
| TaqMan Probe *Gata6* | ThermoFisher | Hs00232018_m1 |
| TaqMan Probe *Hand1* | ThermoFisher | Hs02330376_s1 |
| TaqMan Probe *Hand2* | ThermoFisher | Hs00232769_m1 |
| TaqMan Probe *Isl1* | ThermoFisher | Hs00158126_m1 |
| TaqMan Probe *Mb* | ThermoFisher | Hs00193520_m1 |
| TaqMan Probe *Mef2a* | ThermoFisher | Hs01050409_m1 |
| TaqMan Probe *Mef2c* | ThermoFisher | Hs00231149_m1 |
| TaqMan Probe *Myh6* | ThermoFisher | Hs01101425_m1 |
| TaqMan Probe *Myh7* | ThermoFisher | Hs01110632_m1 |
| TaqMan Probe *Myh11* | ThermoFisher | Hs00224610_m1 |
| TaqMan Probe *Myl2* | ThermoFisher | Hs00166405_m1 |
| TaqMan Probe *Myl3* | ThermoFisher | Hs00193520_m1 |
| TaqMan Probe *Myl7/Myl2a* | ThermoFisher | Hs00221909_m1 |
| TaqMan Probe *Nppa* | ThermoFisher | Hs00383230_g1 |

| | | |
|---|---|---|
| TaqMan Probe *Nkx2.5* | ThermoFisher | Hs00231763_m1 |
| TaqMan Probe *PDGFRa* | ThermoFisher | Hs00998018_m1 |
| TaqMan Probe *Ptprc/CD45* | ThermoFisher | Hs04189704_m1 |
| TaqMan Probe *Tbx5* | ThermoFisher | Hs00361155_m1 |
| TaqMan Probe *Tbx20* | ThermoFisher | Hs00396596_m1 |
| Software and Algorithms | | |
| Bioconductor package collection | Bioconductor project | https://www.bioconductor.org |
| CellOPTIQ | Clyde Biosciences | N/A |
| Fiji | ImageJ | https://imagej.net/Welcome |
| FlowJo Version 10 | FlowJo | N/A |
| Fluidigm software Version 4 | Fluidigm | N/A |
| HCS Studio BioApplication Cell Health Profiling V4 | ThermoFisher | N/A |
| Prism Versions 6 and 7 | GraphPad Software Inc | http://www.graphpad.com/scientific-software/prism/ |
| SeqMonk | Babraham Bioinformatics | http://www.bioinformatics.babraham.ac.uk/projects/seqmonk/ |
| TrimGalore | Babraham Bioinformatics | http://www.bioinformatics.babraham.ac.uk/projects/trim_galore/ |
| R software environment | The R Foundation | https://cran.r-project.org |
| Other | | |
| Amersham Hyperfilm ECL (18 x 24 cm) | GE Life Sciences | 28906836 |
| Array chips for 96 assays x 96 samples | Fluidigm | BMK-M10-96.96 |
| ArrayScan VTI High Content Screening platform | Cellomics | N/A |
| BioMark HD system | Fluidigm | N/A |
| CellOPTIQ | Clyde Biosciences | N/A |
| Cell strainer mesh 70 µm | BD Falcon | 352350 |
| Direct-zol RNA Miniprep kit | Zymo Research | T2051 |

| | | |
|---|---|---|
| Half-area 96-well microclear black-bottom plates | Greiner | 675096 |
| HTS Transwell 96-well permeable supports with polyethylene terephthalate membranes and 1.0 micron pores | Corning | 3392 |
| RNeasy Mini kit | Qiagen | 74104 |
| 0.2 μm filter units FP30/0.2 CA-S | GE Healthcare | 10462200 |
| 96-MicroWell™ plate, flat bottomed wells, with lid | Nunclon, VWR | 734-2097 |
| Veriti Thermal Cycler | ABI, ThermoFisher | N/A |

# 3. Results

This thesis systematically addresses the critical gaps in the existing information as denoted at the end of the Introduction section. Chapter One studies the sufficiency of the CSC-conditioned medium to protect cardiomyocytes from acute oxidative stress by first testing the *in vivo* efficacy as a proof-of-principle and then investigating in-cell efficacy in human pluripotent stem cell-derived cardiomyocytes (hPSC-CM). The first chapter then moves into the pathways mitigating cell death from three different cardiotoxic molecules and phenotypic screens encompassing assays of cell death, mitochondrial membrane depolarisation, ROS generation, calcium cycling and action potential. Chapter Two proceeds into the identification of the potential CSC-released protective components using transcriptomic studies of the CSC and the target hPSC-CM, as well as prediction of the implicated receptor-ligand interactions using one of the latest bioinformatic tools available. Highly secreted protein factors in the mouse CSC-conditioned medium identified by cytokine arrays are also reported. Chapter Three then focuses on the characterisation of human cardiac stromal cells and their ability to also protect hPSC-CM from oxidative stress. The chapter ends with a cytokine array screen of protective and non-protective conditioned media derived from human cells.

## 3.1. Protection of cardiomyocytes by Sca1$^+$ SP CSC-secreted factor(s)

### 3.1.1. Sca1$^+$ SP CSC population and rationale

Most of the experiments described in this thesis have been performed using the well-characterized population of Sca1$^+$ SP cardiac stromal cells (CSC). This population is a rare subset of immature stem-like stromal/fibroblast cells found in the interstitial compartment of the adult mouse heart (Oh et al., 2003). The clonogenic and cardiogenic subpopulation of Sca1$^+$ stromal cells exhibits the SP phenotype and expresses the mesodermal marker PDGFRα, but not the mutually exclusive vascular and endothelial marker CD31 (Noseda et al., 2015a). Our CSC population shows an overlap with cardiac fibroblasts and a strong resemblance to the population of cardiac colony forming unit-fibroblasts (cCFU) (Chong et al., 2011).

Clonal progeny of single Sca1$^+$ SP cells show tri-lineage cardiovascular potential following cardiac grafting and improve cardiac function following injury, even though durable engraftment is rare (Noseda et al., 2015a). In agreement with other similar studies, cell retention one day after injection varied from 1-8% and declined to 0.1-0.5% after two weeks (Li et al., 2009; Noseda et al., 2015a). Hence, on the basis of this paradoxical improvement, we hypothesise that early paracrine factors mediate the beneficial, cardioprotective effects of Sca1$^+$ SP cells. This central hypothesis was tested here using three well-established models in the field; an adult mouse model of myocardial infarction, neonatal mouse cardiomyocytes in culture, and the current state-of-the-art for relevance to human biology, human pluripotent stem cell-derived cardiomyocytes (hPSC-CM) (Blinova et al., 2017; Gintant et al., 2017; Golforoush and Schneider, 2020). Most of our findings are substantiated in two independent hPSC-

CM lines; commercially available vCor.4U cardiomyocytes (Ncardia) and in-house-derived IMR-90 cardiomyocytes (BHF Centre for Cardiovascular Regenerative Medicine).

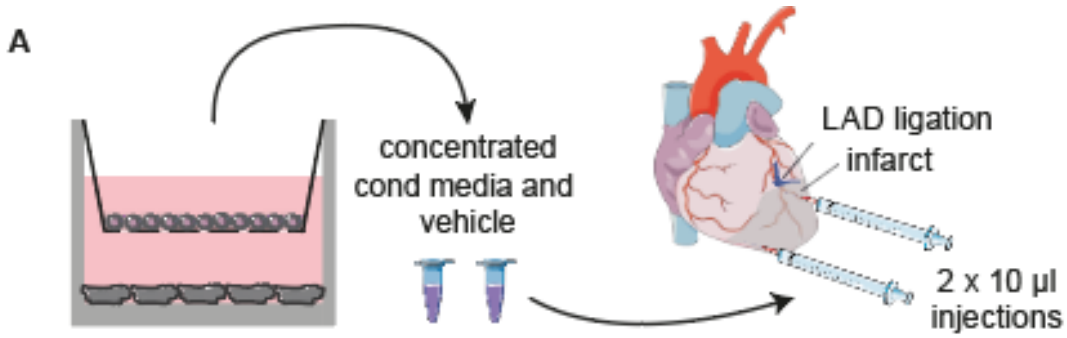
Here, we present a series of experiments demonstrating that CSC-secreted molecules protect mouse and human cardiomyocytes, both in terms of survival and preservation of function, against different forms of cardiotoxic stressors. Briefly, we started by performing an *in vivo* proof of concept experiment, in which conditioned media from CSC were injected in mouse models of myocardial infarction, showing a local reduction in apoptotic cardiomyocytes 24 hr later. In order to investigate the direct effects of CSC on target cardiomyocytes, we moved on to trans-well co-culture experiments employing neonatal mouse and human cardiomyocytes, which were protected in the presence of CSC from oxidative stress conditions. Apart from the $Sca1^+$ SP cells, which co-express PDGFRα after culture expansion, the freshly isolated, prospectively purified $Sca1^+$ SP $PDGFR\alpha^+$ subpopulation was also found to be protective. Co-culture experiments were superseded with CSC-conditioned medium experiments, which increase the translatability of the model towards cell-free approaches. CSC-conditioned media protected hPSC-CM from different forms of cardiotoxic molecules including oxidative stress generators in culture, DNA-damaging entities, and tyrosine kinase inhibitors. Finally, CSC-conditioned media successfully counter-act the mentioned forms of stress, not only by maintaining human cardiomyocyte survival but also preserving the key essential functions of calcium cycling and action potential generation. In summary, our CSC population protects mouse cardiomyocytes *in vivo* and mouse and human cardiomyocytes *in vitro,* and the responsible mechanisms of cell death and protection are investigated here.

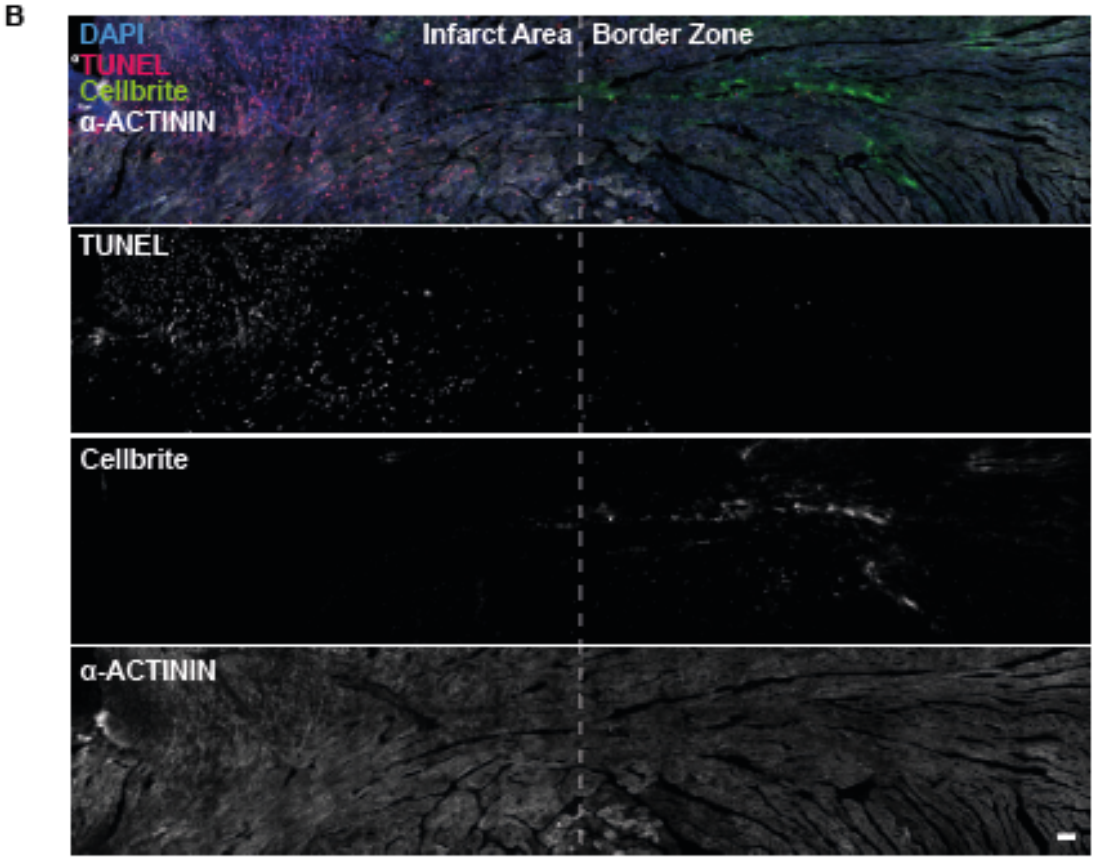
### 3.1.2. CSC-conditioned media protect mouse myocardium after myocardial infarction

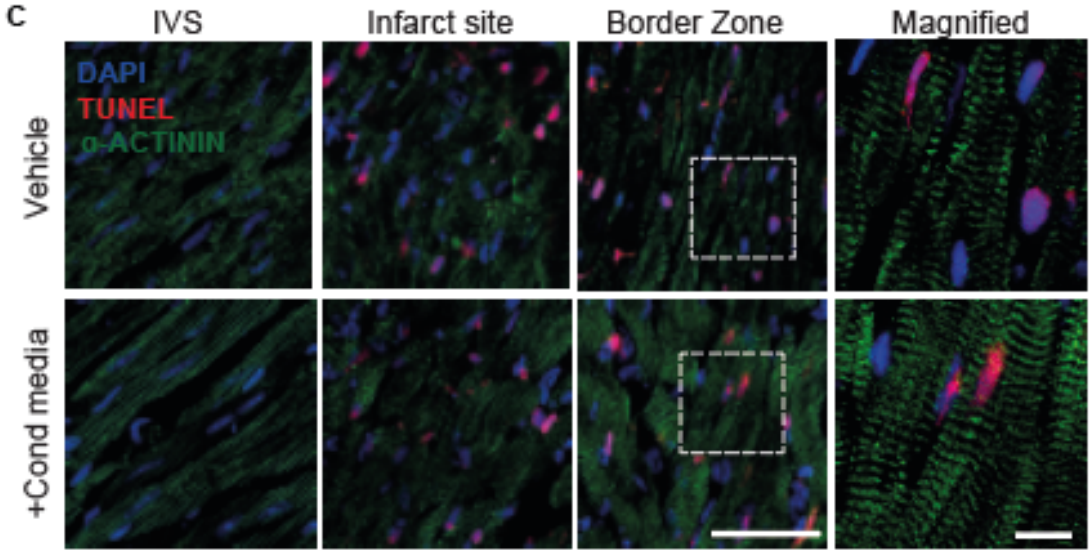
In order to test the postulated paracrine effect, we collected conditioned media from the CSC population and injected it into mouse myocardium at the time of infarct. Permanent ligation of the descending coronary artery was performed to induce myocardial infarction in C57/Bl6 mice, as done previously (Noseda et al., 2015a). We then performed two 10µl injections of 20x concentrated CSC-conditioned media or the unconditioned vehicle control into the border zone at the time of injury, in 3 mice per condition (Figure 3.1A). To confirm intramyocardial delivery and spatial distribution, the media were co-injected with a lipophilic, fluorescent carbocyanine dye (Figure 3.1B). Hearts were collected and fixed 24 hr after MI, and cardiac apoptosis was measured through quantification of cells co-stained with a cardiomyocyte marker, α-actinin, and the TUNEL stain for DNA fragmentation (Figure 3.1C). The TUNEL assay marks the 3' ends of fragmented DNA with the incorporation of a labelled nucleotide (dUTP-alkyne) in a reaction catalysed by the enzyme terminal deoxynucleotide transferase. The marked DNA fragments can be then bound with a fluorescently conjugated probe (alexa fluor-azide) by click chemistry, allowing their detection. Quantification was performed for the intra-ventricular septum (IVS) and the right ventricle (not shown) as negative control areas of remote myocardium, where a low occurrence of $TUNEL^+$ cardiomyocytes was expected. The thinned area closest to the coronary artery suture (infarct site) was the positive control area, where the highest proportion of $TUNEL^+$ cardiomyocytes was expected. The border zone region was defined as the area immediately close to the infarct site overlapping with the co-injected CellBrite tracker. Cardiomyocyte nuclei were quantified in a blinded fashion, covering a total of two cross-sectional slices per area investigated (IVS, border zone,

infarct site), separated by a distance of at least 120μm from each other and encompassing at least 2,500 cardiomyocyte nuclei per heart.

In the negative control region, 1.58±0.7% $TUNEL^+$ myocytes were counted in the presence of vehicle and 1.46±0.9% in the presence of CSC-conditioned media. Thus, the baseline prevalence was minuscule, as expected. In contrast, the central region of infarction, remote from the local injection, contained 45.1±9.0% $TUNEL^+$ myocytes (P=0.0022 versus vehicle-treated at IVS), which was reduced to 32.9±2.8% by the CSC-conditioned media (P=0.0626 versus vehicle-treated at infarct site). $TUNEL^+$ cells were likewise increased in the border zone of vehicle-treated mice (36.5±7.8%; P=0.0022 versus vehicle-treated at IVS); however, apoptosis was significantly reduced to 9.8±3.5% by CSC-conditioned media (P<0.01; Figure 3.1D). Thus, in agreement with our hypothesis, these data demonstrate suppression of apoptosis, by >70%, in the myocardium close to the injection site. The significant reduction of apoptotic myocytes by CSC-conditioned media delivered to the border zone demonstrates clearly that the studied CSC emit paracrine signals, which promote cardiomyocyte survival following ischemic injury *in vivo*. In a permanent occlusion model like this one, the absence of significant protective effect in the infarct site is expected, as access of the injected factors to the central area of the infarct is unlikely and passive diffusion enables spread of the medium only in a limited area around the injection site.


A
concentrated
cond media and
vehicle
LAD ligation
infarct
2 x 10 µl
injections


B
DAPI
TUNEL
Cellbrite
α-ACTININ
Infarct Area
Border Zone
TUNEL
Cellbrite
α-ACTININ


C
IVS
Infarct site
Border Zone
Magnified
DAPI
TUNEL
α-ACTININ
Vehicle
+Cond media

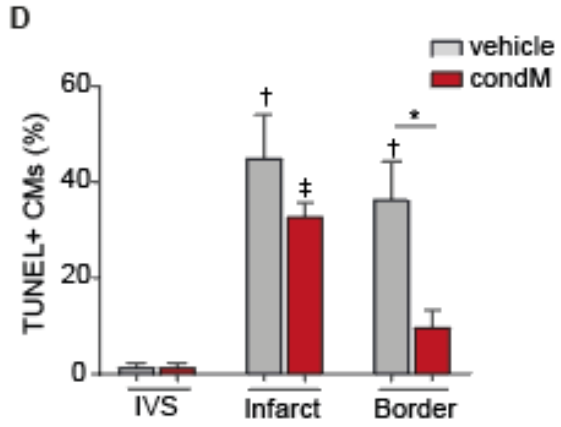



**Figure 3.1: CSC-conditioned media protect mouse myocardium after myocardial infarction. A,** Schematic representation of CSC-conditioned medium production, concentration, and intramyocardial injection following ligation of the LAD. Two injections of 10µl concentrated CSC-conditioned media or concentrated standard media, supplemented with Cellbrite green fluorescent dye, were performed into the infarct border zone. **B,** Representative montage of 48 fields including the infarct area and adjacent border zone of a heart injected with conditioned medium, supplemented with Cellbrite to mark the site of injection. Nuclei were counter-stained with DAPI, apoptotic cells were identified by TUNEL, and cardiomyocytes were identified by sarcomeric α-actinin. Scale bar, 100µm. **C,** Representative immunohistochemistry images of TUNEL staining, 24 hr after myocardial infarction. Scale bar, 50µm and 10µm ("Magnified"). **D,** Bar graph of TUNEL staining in cardiomyocytes in remote myocardium (intraventricular septum, IVS), the infarct site, and the border zone. Data are shown as the mean ± SEM. n = 3 mice per condition; *, $P < 0.05$, vehicle versus CSC-conditioned media; †, $P<0.001$, vehicle versus IVS; ‡, $P<0.01$, CSC-conditioned medium versus IVS. Confocal images and montages produced by Dr Antonio MA Miranda. *These data are part of a publication currently in press by Scientific Reports.*

### 3.1.3. CSC inhibit the death of neonatal mouse and adult human cardiomyocytes in trans-well co-culture

To test a putative paracrine protective effect of CSC *in vitro*, we used cultured cardiomyocytes as the target for experimental injury in the absence or presence of secretor cells. We started with neonatal mouse cardiomyocytes, given the species for which protection was proven after myocardial infarction itself. Subsequently, we progressed to hPSC-CM, which, as discussed (Introduction, section 1.13), have more immediate translational relevance. CSC and cardiomyocytes were seeded in trans-

well co-culture dishes, across an impermeable membrane perforated with 1µm pores that allows soluble factors through, but no direct cell contact (Figure 3.2A). CSC were seeded above the membrane and cardiomyocytes below. Cardiomyocytes were seeded on the receiver plate on day 0 at a density of 100,000/$cm^2$, whilst CSC were seeded on the insert at the same density on day 7 and treatment with the pro-death trigger was started on day 8. Both the CSC and cardiomyocyte chambers were challenged using an oxidative stress inducer, hydrogen peroxide in the case of neonatal mouse cardiomyocytes and menadione in human cardiomyocytes, both of which introduce reactive oxygen species (ROS) in culture (Loor and Schumacker, 2008). Twenty-four hours later, the membrane impermeant dye, DRAQ7, was added to the cardiomyocytes and allowed 10 min to penetrate dead cells. Cells were then counter-stained with Hoechst 33342, for an additional 10 min at 37°C. Between 9 and 12 images were acquired per well using the Cellomics high content platform and any well containing less than 100 objects was excluded from the analysis as a measure of quality control. Wells stained with just Hoechst in addition to untreated wells without a stressor were our negative controls for DRAQ7. Analysis to obtain the percentage of $DRAQ7^+$ cells per well was performed automatically using the Array Scan software (ThermoFisher).

Under these settings, CSC conferred protection, not only to mouse neonatal cardiomyocytes (Figure 3.2B), but also to human vCor.4U PSC-CM (Figure 3.2D). In the presence of CSC, cell death was completely abolished in neonatal mouse cardiomyocytes at 100µM $H_2O_2$, from 58.3±18.3% to 0.66±0.45% ($P<0.001$). The concentration of menadione to use was titrated using human vCor.4U cardiomyocytes and 62.5µM was selected as the concentration that achieves around 50% cell death (Figure 3.2C). A trend like neonatal mouse cardiomyocytes was observed in human

vCor.4U cardiomyocytes, where at 62.5μM menadione, cell death was reduced from 32.8±4.3% to 14.3±4.3% ($P<0.001$) in the presence of CSC-conditioned media (Figure 3.2D).

A noteworthy difference in the amplitude of CSC protection was observed between the neonatal mouse cardiomyocytes (~100% protected) and the adult hPSC-CM (~50% protection). This might reflect inherent species-specific differences or alternative mouse-mouse and mouse-human signalling of the murine progenitors towards the respective target cells. Alternatively, the gap in protection might be a result of maturational differences between the neonatal mouse and the pluripotent cell-derived human cardiomyocytes or might simply be accounted for by the differences in the antecedent media of the two cardiomyocyte types. Nevertheless, our results demonstrate the translatability of the CSC protective effect, since both mouse and human cardiomyocytes were effectively targeted.

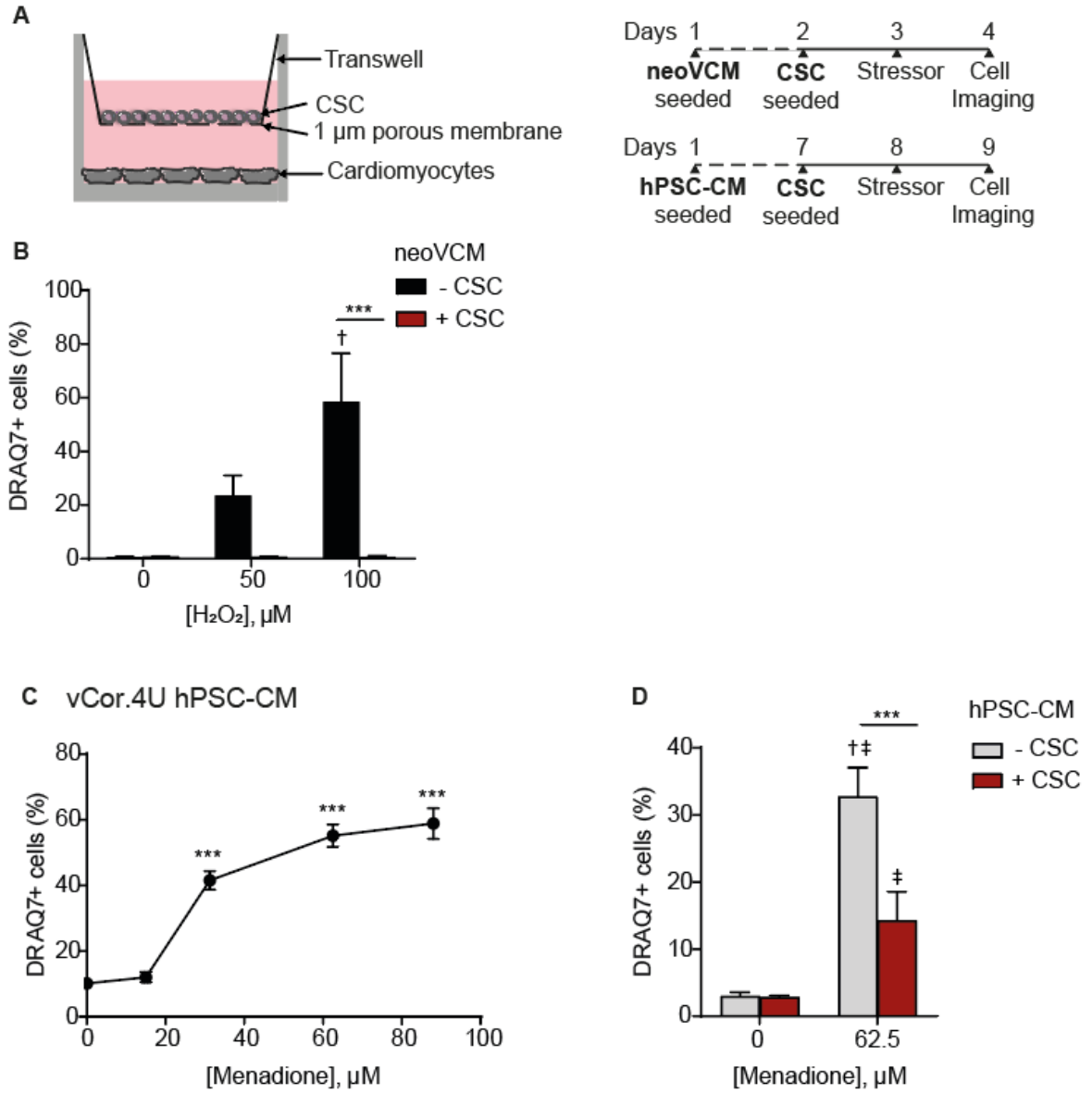



**Figure 3.2: CSC inhibit the death of neonatal mouse and adult human cardiomyocytes in trans-well co-culture. A, Left,** Schematic representation of trans-well co-culture setup of cardiomyocytes with CSC. **Right,** Timelines of the experiments for neonatal mouse cardiomyocytes (neoVCM) and hPSC-CM from cell seeding to imaging. **B,** Bar graph of DRAQ7 uptake of mouse neonatal ventricular cardiomyocytes (neoVCM) in the presence and absence of CSC-conditioned media following $H_2O_2$ stress. **C,** Line graph of DRAQ7 uptake in vCor.4U hPSC-CM following a titration of menadione treatment after 24 hr. Data are shown as the mean ± SEM. n = 3; ***, P < 0.001 versus no menadione. **D,** Bar graph of DRAQ7 uptake of hPSC-CM in the presence and absence of CSC-conditioned media following 24 hr of menadione stress. Data are shown as the mean ± SEM. n = 6; ***, P < 0.001; †, P<0.0001, versus no menadione; ‡, P<0.01, versus no menadione plus CSC-conditioned media.

### 3.1.4. Human cardiomyocyte co-culture with Sca1$^+$ PDGFRα$^+$ CD31$^-$ cells

The heterogenous Sca1$^+$ population was extensively characterised in our lab. Two main subpopulations, the Sca1$^+$ CD31$^+$ and Sca1$^+$ PDGFRα$^+$, are largely mutually exclusive with only the latter encompassing the cardiogenic molecular signature (Noseda et al., 2015a). We have also shown that the SP status and PDGFRα synergize in determining clonogenicity (Noseda et al., 2015a). To verify PDGFRα expression in Sca1$^+$ SP cells (passage 16-30) used here, we performed flow cytometry. The scattergram shows that the Sca1$^+$ SP population after culture expansion was highly enriched in PDGFRα expression (81.8% of the total population was Sca1$^+$ PDGFRα$^+$; Figure 3.3A). Given that the Hoechst 33342 used for SP staining is a potential mutagen (Durand and Olive, 1982), we sought to exclude any hypothetical artefactual effect on the cardiac cells' phenotype and consequently their paracrine effects. We tested short-term cultured Sca1$^+$ PDGFRα$^+$ CD31$^-$ CSC (passage 5-10) that were not selected for SP and therefore never exposed to Hoechst 33342. Given the co-expression of SP and PDGFRα in freshly isolated cells and the enrichment of PDGFRα expression in Sca1$^+$ SP cells expanded in culture, we expected an enrichment of SP in Sca1$^+$ PDGFRα CD31$^-$. Thus the SP status was subsequently tested in Sca1$^+$ PDGFRα$^+$ CD31$^-$ cells by staining with Hoechst 33342 in the absence and presence of fumitremorgin C (FTC), a selective inhibitor of the ABCG2 transporter that is chiefly responsible for the dye-extrusion activity and analysed by flow cytometry (Golebiewska et al., 2011; Noseda et al., 2015a). Sca1$^+$ PDGFRα$^+$ CD31$^-$ cardiac cells were highly enriched for the SP phenotype, with 65.3% of the cells displaying SP status, which was reduced to 1.68% in the presence of FTC (Figure 3.3B).

To test the protective effect of this subpopulation, we co-cultured vCor.4U hPSC-CM with Sca1$^+$ PDGFRα$^+$ CD31$^-$ CSC. Due to previous work reporting the effects of hypoxia on the secretion of various paracrine factors (Chanyshev et al., 2012; Fidelis-De-Oliveira et al., 2012), we were intrigued to investigate whether the oxygen concentration of our culture conditions would affect the CSCs' protective properties. After isolation, Sca1$^+$ PDGFRα$^+$ were expanded at either hypoxic (2%) or normoxic (21%) conditions for 5-10 passages before use. Flow cytometry analysis was used to confirm that these populations were also exhibiting the SP phenotype (Figure 3.3C). Our results showed no change in the proportion of SP cells at 2% $O_2$ (62.6%) or 21% $O_2$ (65.3%). We then performed co-cultures, as described above, using the populations grown at the two different oxygen concentrations. Flow cytometry and sorting were performed by Dr Patricia Chaves.

The co-cultures were incubated for 24 hr with and without menadione stress. At 88 μM menadione, hPSC-CM exhibit 44±2.3% cell death, which is reduced by co-culture with hypoxic Sca1$^+$ PDGFRα$^+$ cells to 20.5±7.5% ($P<0.0001$) and by co-culture with normoxic Sca1$^+$ PDGFRα$^+$ cells to 11.1±2.2% ($P<0.0001$). Our results showed that the highly purified Sca1$^+$ PDGFRα$^+$ CD31$^-$ population is capable of conferring ~2-3-fold cardiomyocyte protection from oxidative stress, an effect achieved at similar magnitude by our Sca1$^+$ SP population. Thus, following culture expansion the Sca1$^+$ SP population is (1) enriched in PDGFRα and (2) functionally protective as the highly purified population. Expansion of the subpopulation in hypoxia or normoxia did not show any significant difference in terms of hPSC-CM protection (Figure 3.3D). Even though direct measurements to confirm the hypoxic response, such as increased levels of HIF-1a, have not been taken in this study, our results suggest that under normal culture conditions the CSC are maximally protective.

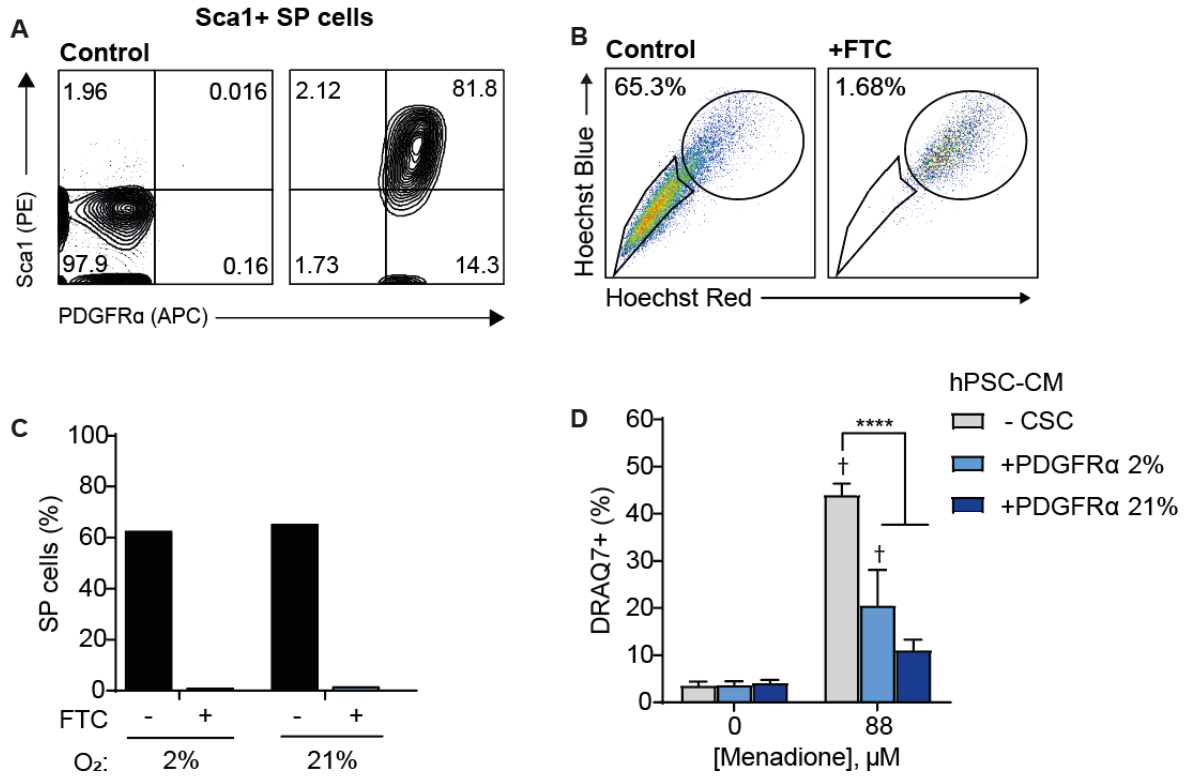



**Figure 3.3: Human cardiomyocyte co-culture with Sca1+ PDGFRα+ CD31- cells.** **A,** Hematopoietic lineage marker-negative ($Lin^-$) $Sca1^+$ cardiac cells encompass PDGFRα and SP cells, with a partial overlap between the latter two. CSC routinely used in this thesis were prospectively sorted as $Lin^-$ $Sca1^+$ SP. The flow cytometry 2D contour plot confirmed the co-expression and enrichment of $Sca1^+$ and PDGFRα after *in vitro* expansion of SP-sorted cardiac cells. Quadrants were drawn based on the unstained control (left panel). **B,** $Lin^-$ $Sca1^+$ $PDGFR\alpha^+$ $CD31^-$ cardiac cells (passage 8), enrich for the SP phenotype as shown by flow cytometry. Fumitremorgin C (FTC) was used as a negative control for SP. **C,** Bar graph showing marked enrichment for the SP phenotype in $PDGFR\alpha^+$ $Sca1^+$ cells expanded at either 2% or 21% $O_2$. Roughly 65% of cells displayed the SP dye-efflux, regardless of the culture condition. Data shown are single measurements for the 4 conditions tested (at least 10,000 events acquired per sample). **D,** Enhanced survival of vCor.4U myocytes treated with conditioned media from the PDGFRα-sorted cells shown in B and C. Bar graph of DRAQ7 uptake 24 hr after oxidative stress. Data are shown as the mean ± SEM. n = 6; ****, $P < 0.0001$; †, $P<0.05$, versus no menadione. Flow cytometry staining and data analysis was performed by Dr Patricia Chaves. These data are part of a publication currently in press by Scientific Reports.

### 3.1.5. CSC- but not TTF-conditioned media protect hPSC-CM from menadione-induced death

A mechanistically more relevant and translational configuration for paracrine studies is the conditioned medium approach. In our case, and in contrast to the co-cultures where both CSC and cardiomyocytes were exposed to stress, the conditioned medium setup allows for CSC to remain unstimulated. This would enable us to investigate whether cardioprotection is mediated by CSC even when they are grown under unstressed, basal conditions. CSC were seeded at increasing cell densities (20,000 cells/cm$^2$, 50,000 cells/cm$^2$ and 100,000 cells/cm$^2$) and allowed 24 hr to attach, before changing the media to cardiomyocyte-specific medium for another 24 hr (Figure 3.4A). CSC-conditioned media were then collected and used at three dilutions (33%, 50% and 100%) to treat menadione-stressed vCor.4U cardiomyocytes. Our results show that the CSC secretome was sufficient to protect vCor.4U hPSC-CM from cell death, significantly blocking DRAQ7 penetration regardless of the CSC density or conditioned medium dilution used. At the CSC density of 20,000 cells/cm$^2$, there is gradual but statistically significant protection from cell death with increasing conditioned media concentration; DRAQ7$^+$ cells' prevalence was reduced from 47.2±2.4% to 22.2±3.8% at 33% CSC conditioned media ($P<0.0001$), 19.1±3.6% at 50% CSC-conditioned media ($P<0.0001$), and 9.2±3.7% at 100% CSC-conditioned media ($P<0.0001$). At the highest CSC densities (100,000 cells/cm$^2$), the protective effect was maximised, with complete elimination of DRAQ7 uptake, back to the levels of unstressed cardiomyocytes, from 47.2±2.9%, to 2.4±0.32% even at the lowest concentration of conditioned media ($P<0.0001$; Figure 3.4B). Therefore, this experiment demonstrates that CSC-conditioned media are capable of protecting hPSC-CM under basal conditions, without requiring a stress trigger.

In order to establish whether the CSC protective effect is generalisable, we repeated the experiment using a second independent hPSC-CM line, IMR-90 cardiomyocytes, at the maximal CSC seeding density (100,000 cells/cm$^2$) and conditioned media concentration (100%). Under the conditions tested, IMR-90 were more sensitive to oxidative stress, reaching ~50% death at 18.5μM menadione (Figure 3.4C). Despite this, at 41.6μM menadione, CSC-conditioned media successfully reduced cell death from 62.9±3.7% to basal levels (7.1±1.3%, P<0.0001; Figure 3.4D). Our results demonstrate that the CSC-mediated protective effect is not idiosyncratic in the vCor.4U population and could thus be applied to independent hPSC-CM lines, highlighting its potential translational value.

In order to assess the relative potency of CSC in protecting cardiomyocytes, we performed a side by side comparison of CSC-conditioned media against mouse tail tip fibroblast (TTF) conditioned media, which was predicted to act as a negative control. For this experiment, the two cell types were seeded at non-saturating densities of 20,000 cells/cm$^2$ and the respective conditioned media were used undiluted to treat menadione-stressed vCor.4U hPSC-CMs. Unlike the medium from CSC, TTF-conditioned media were unable to confer cardiomyocyte protection, maintaining the DRAQ7 uptake levels at 38.3±3.2%, i.e., indistinguishable from cardiomyocytes treated with menadione alone, 38.5±2.6% (Figure 3.4E). We have therefore shown that an extraneous mouse cell population under identical conditions fails to reduce hPSC-CM death, demonstrating that the protective effect is neither dependent on factors present in the culture medium itself, nor inherent to all cultured cell populations from the mouse.

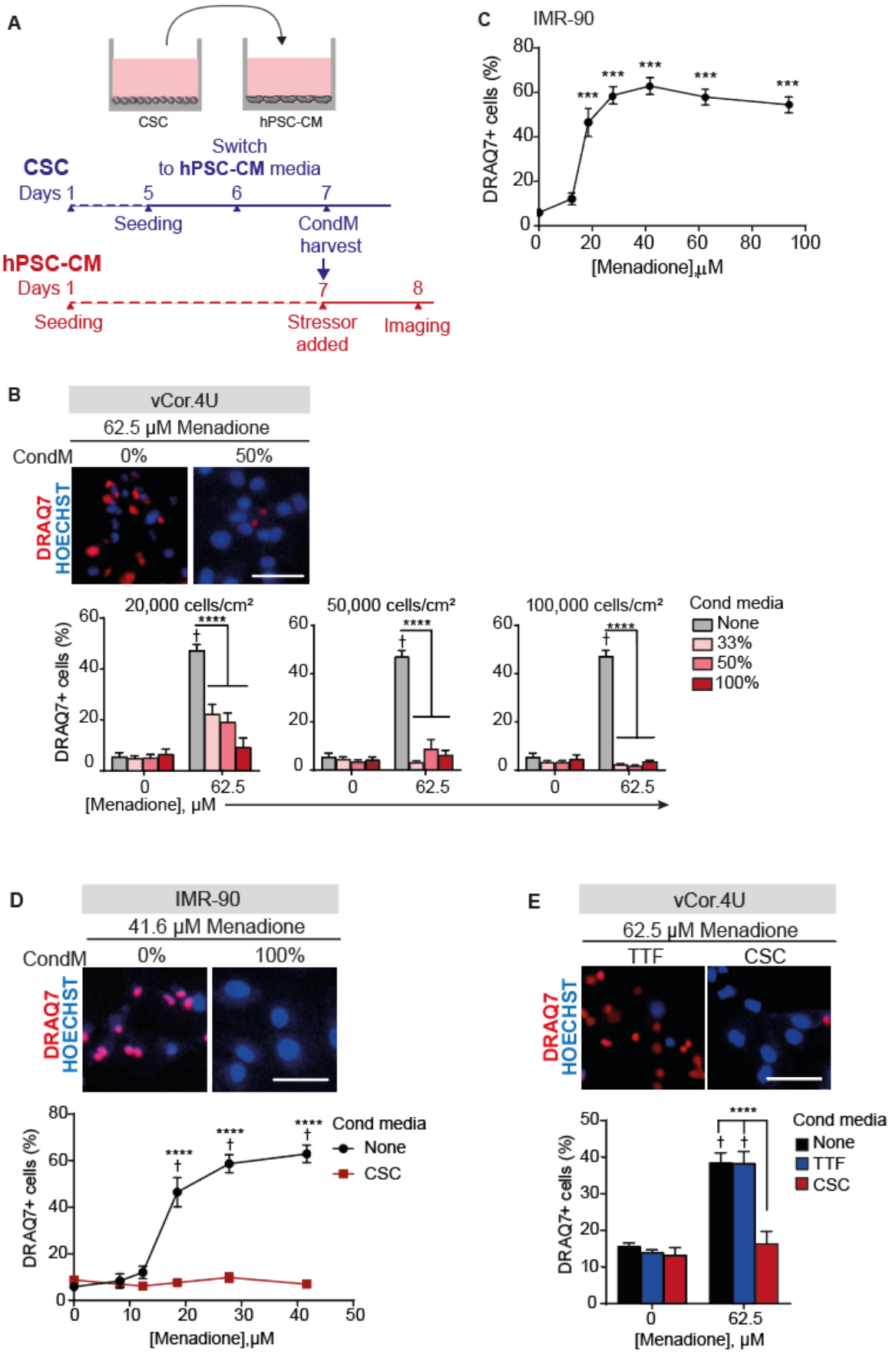

A
CSC
hPSC-CM
Switch
to hPSC-CM media
CSC
Days 1
5
6
7
Seeding
CondM
harvest
hPSC-CM
Days 1
7
8
Seeding
Stressor
added
Imaging
C
IMR-90
DRAQ7+ cells (%)
[Menadione],μM
B
vCor.4U
62.5 μM Menadione
CondM
0%
50%
DRAQ7
HOECHST
20,000 cells/cm²
50,000 cells/cm²
100,000 cells/cm²
DRAQ7+ cells (%)
[Menadione], μM
Cond media
None
33%
50%
100%
D
IMR-90
41.6 μM Menadione
CondM
0%
100%
DRAQ7
HOECHST
DRAQ7+ cells (%)
[Menadione],μM
Cond media
None
CSC
E
vCor.4U
62.5 μM Menadione
TTF
CSC
DRAQ7
HOECHST
DRAQ7+ cells (%)
[Menadione], μM
Cond media
None
TTF
CSC

**Figure 3.4: CSC- but not TTF-conditioned media protect hPSC-CM from menadione-induced death. A, Left,** Schematic representation of CSC-conditioned medium treatment of cardiomyocytes. **Right,** Timeline of the experiment from cell seeding to imaging for CSC (blue) and hPSC-CM (red). **B, Above,** Representative images of nuclear DRAQ7 staining following menadione in the presence and absence of CSC-conditioned media produced following CSC culture at 100,000 cells/cm$^2$ and used at a dilution of 50%. **Below,** Representative bar graphs of DRAQ7 uptake at the indicated CSC seeding densities and media concentrations; n=9. **C,** Line graph of DRAQ7 uptake in hPSC-CM following a titration of menadione after 24 hr. Data are shown as the mean ± SEM. n = 12; ***, P < 0.001 versus no menadione. **D,** CSC-conditioned media protective effect was tested on IMR-90 hPSC-CM, an independent human cardiomyocyte line. Representative images and line graph of DRAQ7 uptake after 24 hr of menadione stress; n=12. **E,** Conditioned media from mouse tail tip fibroblasts were used as an extraneous negative control for vCor.4U cardiomyocyte protection. Representative images and bar graph of DRAQ7 uptake after 24 hr of menadione stress; n=12. Scale bars, 50μm; data are shown as the mean ± SEM. ****, P < 0.0001; †, P<0.05, versus no menadione. These data are part of a publication currently in press by Scientific Reports.

### 3.1.6. Cardiomyocyte protection with CSC-conditioned media administered one hr after menadione stress induction

In terms of translational relevance as a potential therapy for myocardial infarction, CSC-conditioned media treatment given after the induction of oxidative stress rather than at the same time, would be superior. To investigate whether CSC-conditioned media is still protective, even when given after the menadione stress, we performed a post-treatment experiment in IMR-90 cardiomyocytes. Cardiomyocytes were stressed for one hr, prior to addition of the CSC-conditioned media. As expected, CSC-conditioned media given one hr later, inhibited DRAQ7 uptake significantly, but to a lesser extent than when given simultaneously: at 41.7μM menadione, DRAQ7 uptake was reduced from 70.3±3.9% to 22.9±3.2% (P<0.0001) if conditioned medium is given concurrently, as opposed to 51.7±3.5% when conditioned medium is given one hr later (P<0.0001; both for CSC-conditioned media versus control and for post-treatment

versus concurrent treatment) (Figure 3.5). Thus, the protective ability of CSC-conditioned medium declines with delayed administration, consistent with the time-dependent window for administration of other cardio-protective agents such as the beta-adrenergic blocker metoprolol and novel MAP4K4 inhibitors (Fiedler et al., 2014; García-Ruiz et al., 2016).

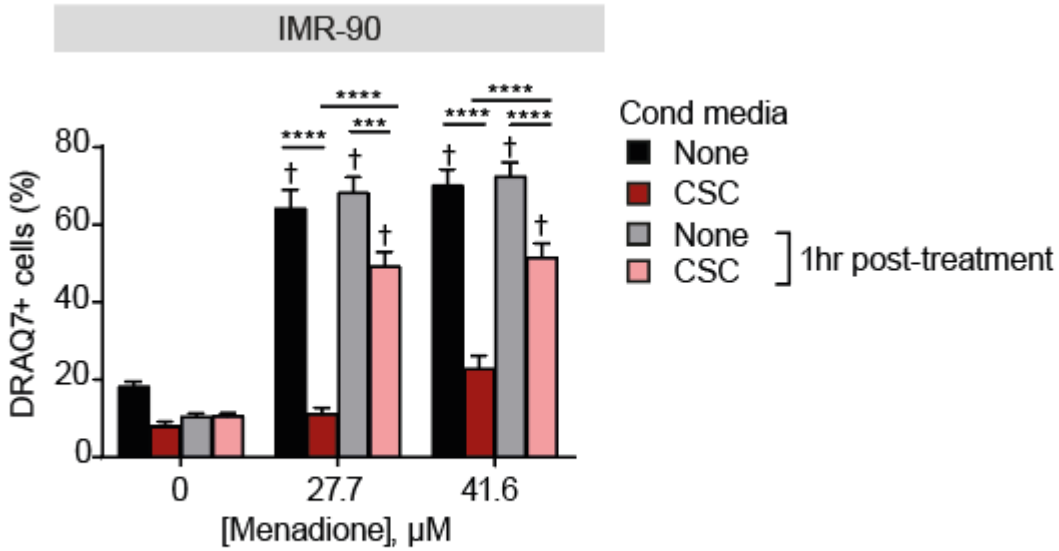



**Figure 3.5: CSC-conditioned media protect cardiomyocytes even when administered one hr after menadione stress induction.** Bar graph of DRAQ7 uptake in IMR-90 cardiomyocytes 24 hr after induction of menadione stress. CSC-conditioned media were added either at the same time as menadione, or 1 hr later for the post-treatment condition. Data are shown as the mean ± SEM. n = 11; ***, P < 0.001; ****, P < 0.0001; †, P < 0.05, versus no menadione. These data are part of a publication currently in press by Scientific Reports.

### 3.1.7. CSC-conditioned media prevent the release of cardiac troponin I from human cardiomyocytes

Apart from measuring the level of cell death by imaging DRAQ7 uptake into the cardiomyocytes, we confirmed our results using assays that define levels of cell damage from biomarkers released into the supernatants. Human cardiac troponin I (cTnI) is a well-known biomarker of cardiac muscle injury with essential prognostic

value as a measure of infarct size and hence future clinical outcome (Latini et al., 2007; Nagarajan et al., 2012; Peacock et al., 2008). Additionally, high sensitivity troponin assays are well-established diagnostic tests for acute myocardial infarction (Segraves and Frishman, 2015). Hence, to confirm the cardioprotective effect of CSC-conditioned media, we measured cTnI levels in supernatants collected from our cultures of treated hPSC-CM using each of two independent cTnI immunoassays; the cardiac troponin I ALPHAlisa assay (Perkin Emler; Figure 3.6A) and the human cardiac troponin 1 SimpleStep ELISA kit (Abcam; Figure 3.6B). Our results by each of the two assay methods, show dramatic reduction in cTnI release compared to the controls receiving menadione alone. More specifically, the ALPHAlisa assay indicates an average of 15.1±2.5 ng/ml released cTnI upon treatment with 62.5μM menadione, which is reduced to 1.98±0.6 ng/ml by CSC-conditioned media. Under the same conditions, the SimpleStep ELISA kit, gives an average of 846±193 pg/ml released cTnI, reduced to 118±27.9 pg/ml by CSC-conditioned media.

In comparison, the ALPHAlisa reading is 17-fold higher than the SimpleStep ELISA reading, which can be attributed to the different technology and detection range employed by the assays. According to information obtained from the manufacturers, despite both assay sensitivities being very similar (4.7pg/ml for the ALPHAlisa and 4.4pg/ml for the SimpleStep ELISA), the dynamic detection range differs, with the ALPHAlisa being able to detect a broader range of concentrations (4.7 – 100,000 pg/ml for the ALPHAlisa and 31.3 – 4000 pg/ml for the SimpleStep ELISA). Therefore, the maximum level of cTnI detected by the ALPHAlisa in the menadione-stressed condition is 4-fold the maximum detection limit of the SimpleStep assay. In fact, unlike the standard curve from the ALPHAlisa (Figure 3.6C), the standard curve from the

SimpleStep assay (Figure 3.6D) showed evidence of signal saturation after the concentration of 1 ng/ml (Figure 3.6C, D).

Overall, the results given by the cTnI assays are in agreement with the data obtained from cardiomyocyte imaging using the DRAQ7 marker. An advantage of the cTnI assay is its specificity in detecting cardiomyocyte death, however in our cultures of hPSC-CM, purity is not a confounding factor, according to patch-clamp analysis provided by the manufacturer online (https://www.ncardia.com/product/vc..or.4u-sup-sup-cardiomyocyte-kit.html), as well as immunohistochemistry markers previously reported by our group (Fiedler et al., 2019). We therefore decided to use DRAQ7 imaging as our primary assay of cell death detection for logistical reasons (cheaper and faster).

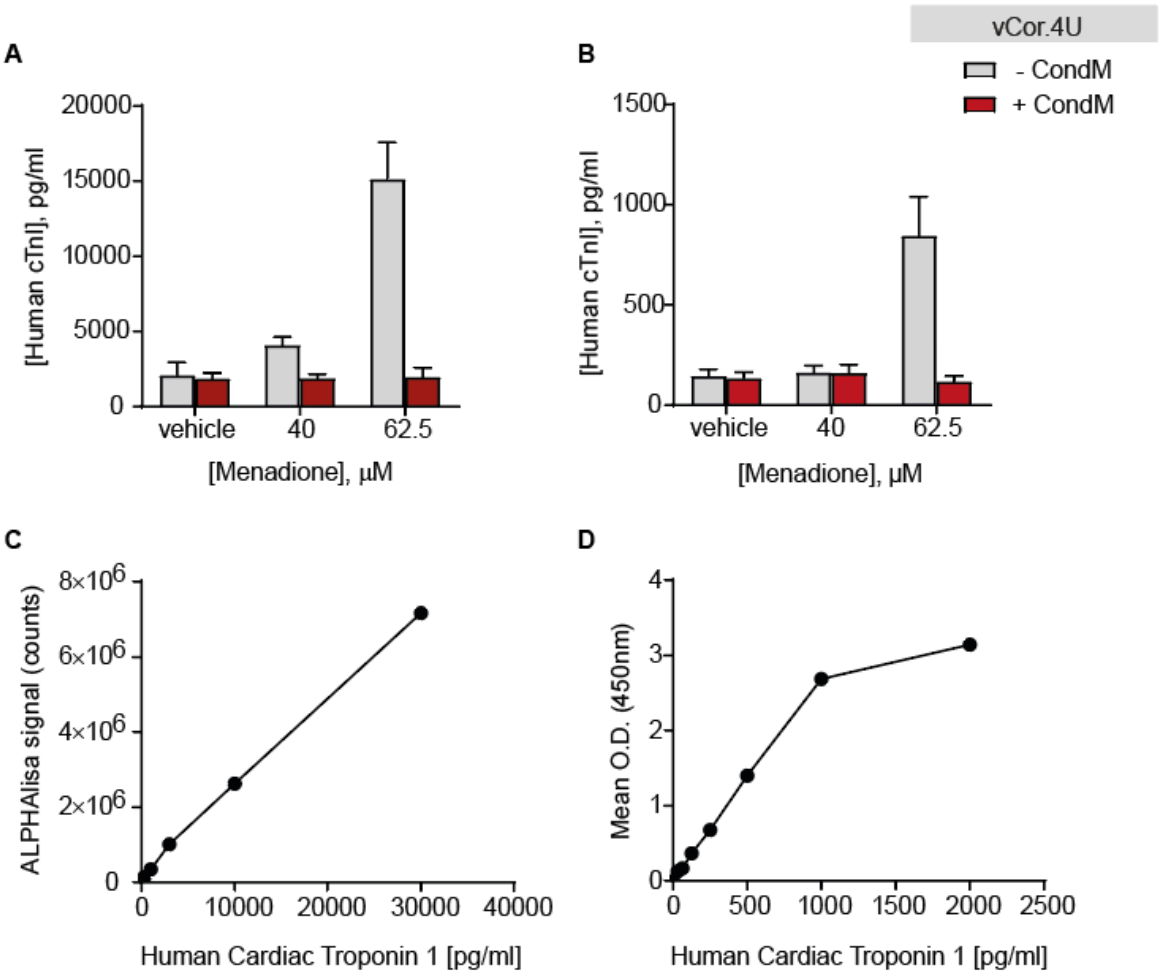



**Figure 3.6: CSC-conditioned media prevent the release of cardiac troponin I from human cardiomyocytes.** Bar graphs of human troponin I release by vCor.4U cardiomyocytes, in the presence and absence of CSC-conditioned media following 24 hr of menadione stress using **A,** the AlphaLISA assay kit (Perkin Emler); n=3 (two independent experiments) or **B,** the SimpleStep ELISA kit (Abcam); n=6 (two independent experiments). Data are shown as the mean ± SEM. **C, D,** Standard curves for the ALPHAlisa assay **(C)** and for the SimpleStep ELISA assay **(D)**, which shows saturation of the signal by the latter assay on cTnI concentrations > 1000pg/ml. Both standard curves are displaying the average of two wells per standard concentration point.

### 3.1.8. CSC-conditioned media do not induce DNA synthesis in hPSC-CM

Despite the post-mitotic nature of adult human cardiomyocytes, and their meagre capacity to enter the cell cycle and regenerate, cardiac progenitor populations have

previously been reported to induce proliferation responses in cardiomyocytes (Wei et al., 2015). Prior to looking for proliferation per se, we first wanted to test whether in addition to the pro-survival effects on hPSC-CM, CSC-conditioned media could also induce myocyte DNA synthesis, a necessary pre-requisite for a proliferative response. Human vCor.4U cells were treated with CSC-conditioned media for a total of 48 hr and for the last 24 hr supplemented with the thymidine analogue EdU, which is efficiently incorporated into newly synthesised DNA. Subsequently cells were fixed with 3.7% paraformaldehyde in PBS and stained using the Click-iT EdU Alexa Fluor 647 HCS Assay kit (Invitrogen), which fluorescently labels the incorporated EdU with a specific and bright Alexa Fluor dye, followed by Hoechst 33342 for nuclei identification (Figure 3.7A). Wells were scanned using the Cellomics high content imaging platform.

Our results showed that CSC-conditioned media are unable to induce DNA synthesis in hPSC-CM, at least after 48 hr of culture (Figure 3.7B). The proportion of DNA replicating cells remains constant from 2.88±0.27% at baseline to 2.99±0.15% after incubation with CSC-conditioned media and 2.44±0.42% even after stimulation with 20% FBS. Thus, despite their origination from pluripotent cells, the hPSC-CM are effectively non-responsive to conventional mitogenic stimulation. This was confirmed in additional studies with increasing concentrations of foetal bovine serum (FBS) from 1-20% FBS (Figure 3.7C). Our results indicate that under these conditions of culture, the cells have progressed to a mature, mitogen-resistant state of cell cycle exit, consistent with the reported post-mitotic phenotype in other studies employing 2D human cardiomyocyte cultures (Mohamed et al., 2018).

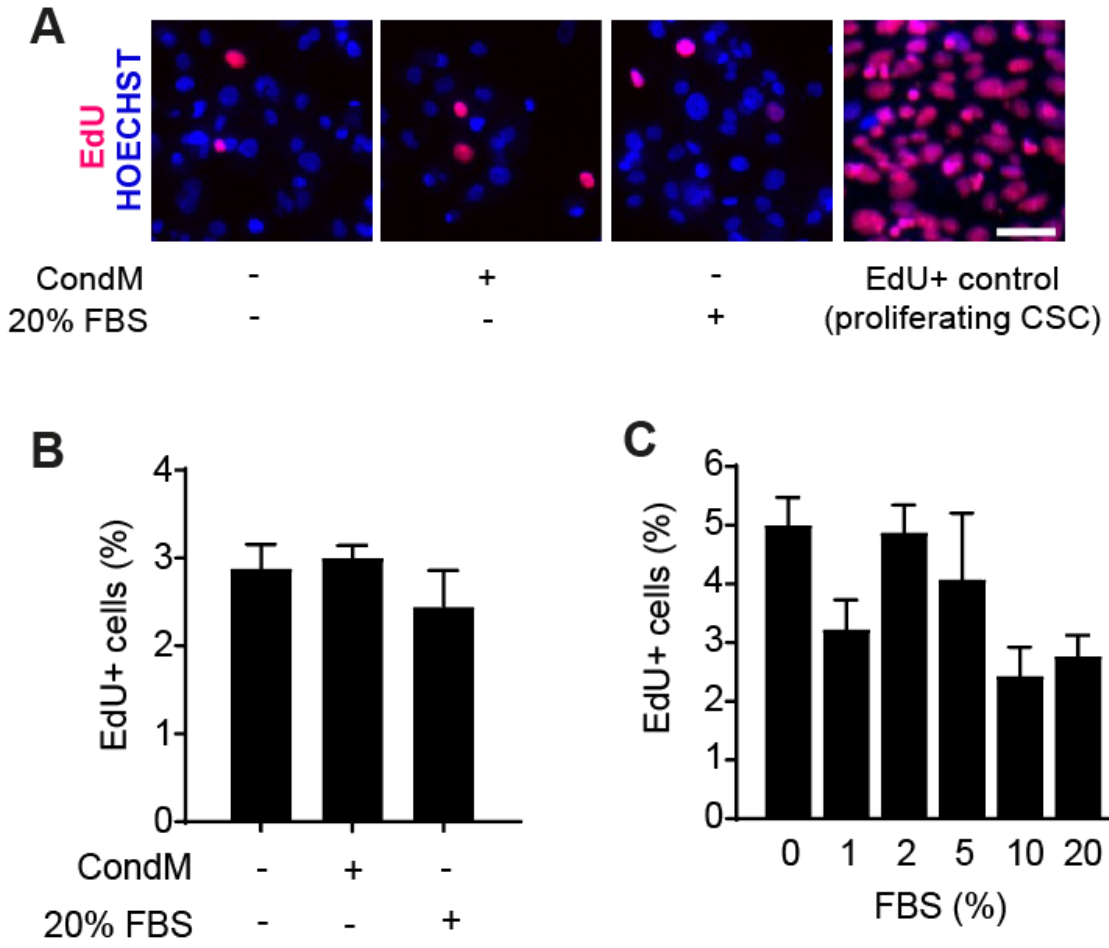



**Figure 3.7: CSC-conditioned media do not induce DNA synthesis in hPSC-CM.** **A,** Representative images of EdU incorporation in vCor4.4U cardiomyocytes at baseline and in addition of CSC-conditioned medium or 20% FBS. Proliferating CSC are shown as the positive control after 24 h of $EdU^{+}$ incorporation. **B,** Bar graph of EdU incorporation in vCor.4U cardiomyocytes at baseline and 48 hr after treatment with CSC-conditioned medium or stimulation with 20% FBS. **C,** Bar graph of EdU incorporation in vCor.4U cardiomyocytes following supplementation with increasing concentrations FBS in the culture medium. Scale bar, 50 μm; data are shown as the mean ± SEM; **B,** n = 8 and **C,** n = 3. These data are part of a publication currently in press by Scientific Reports.

### 3.1.9. CSC-conditioned media prevent DNA fragmentation in hPSC-CM after menadione stress

An important aspect in the pathogenesis of the heart is cardiomyocyte loss through apoptosis and necrosis, which can be mediated by distinct, but significantly overlapping signalling cascades (Galluzzi et al., 2018; Kung et al., 2011; Del Re et al., 2019). The next set of experiments was performed aiming to explore the mechanisms underlying hPSC-CM death and gain insight into the pathways through which CSC-conditioned media prevent it. One of the well-established apoptosis hallmarks is DNA fragmentation, which can be stimulated through a number of different pathways as discussed in section 1.4.

TUNEL staining was performed on fixed plates from the CSC-conditioned media titration experiment in vCor.4U cardiomyocytes, described in section 3.1.5 above (Figure 3.8A). The thorough titration of CSC densities and conditioned media dilutions show an induction of DNA fragmentation in over 50% of hPSC-CM, at 62.5μM menadione ($P<0.0001$; Figure 3.8B).

Protection is clearly seen already from conditioned media generated with 20,000 cells/cm$^2$ at the highest concentration and complete at 50,000 cells/cm$^2$ at the lowest concentration. A discrepancy between the DRAQ7 and TUNEL assays appears when using the lowest concentration of CSC-conditioned media (derived from the 20,000 cells/cm$^2$), with TUNEL staining showing a trend for inhibition of DNA fragmentation (53.8±4.2% in the untreated was reduced to 40.7±2.8% and 37.7±6.8% at 33% and 50% conditioned media dilutions respectively), which is not statistically significant (unlike in DRAQ7 results, Figure 3.4B). The possible difference between the two assays can be ascribed to the timing of the processes, as endonuclease activation

and subsequent degradation of chromosomal DNA ($TUNEL^+$ fragments) take place prior to cytomorphological changes such as chromatin and cytoplasmic condensation and plasma membrane disintegration, allowing entry of DRAQ7. Thus, the DRAQ7 assay might be prone to underestimating cells that are committed to a death programme but have not reached the plasma membrane permeabilization stage.

Nevertheless, overall the TUNEL assay results are in agreement with the DRAQ7 data, showing that menadione-induced DNA fragmentation in hPSC-CM was significantly inhibited by CSC-conditioned media; even diluted conditioned media derived from a CSC density of 50,000 cells/$cm^2$ reduced DNA fragmentation in cardiomyocytes from 53.2±5.1% to 12.6±2.5% i.e. to baseline levels ($P<0.0001$; Figure 3.8B). Thus, CSC-conditioned media facilitate cardiomyocyte protection under these conditions, acting upstream of the DNA fragmentation and inhibiting the induction of apoptosis.

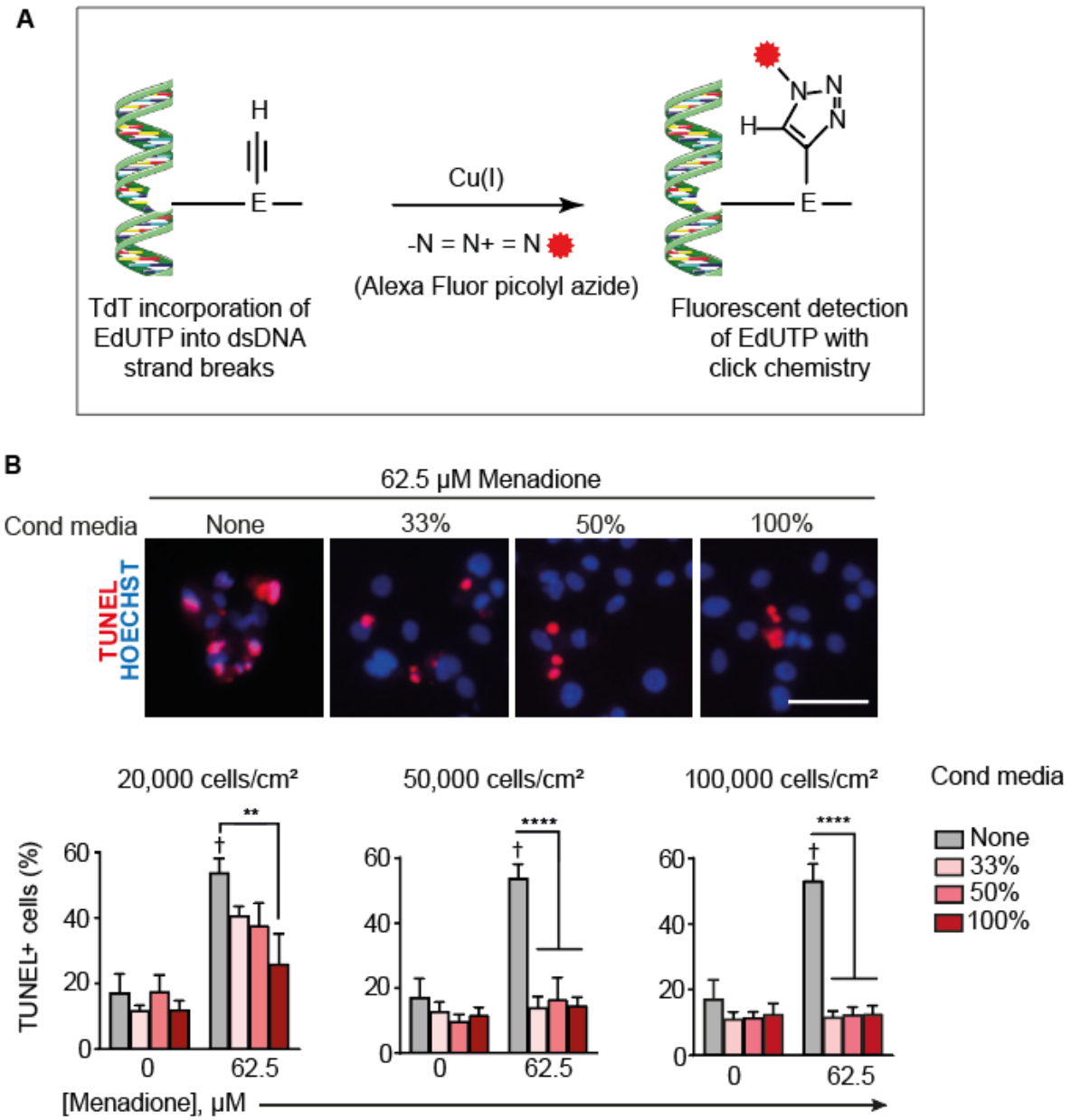



**Figure 3.8: CSC-conditioned media prevent DNA fragmentation in hPSC-CM after menadione stress. A,** Apoptosis detection with Click-iT Plus TUNEL assay involves incubation with the enzyme TdT which catalyses the addition of EdUTP nucleotides onto the 3' end of fragmented DNA molecules. Subsequently, a copper-catalysed click reaction step incorporates the fluorescently tagged picolyl azide which is then detected using high-content imaging. Some components of this diagram were obtained from Servier Medical Art, free image database (http://smart.servier.com). **B,** Representative images and bar graphs of TUNEL⁺ vCor.4U cardiomyocytes, 24 hr after menadione with and without titrated CSC-conditioned media derived from a range of CSC seeding densities. Scale bar, 50 μm; data are shown as the mean ± SEM; **, $P < 0.01$; ****, $P < 0.0001$; †, $P < 0.05$, versus no menadione. These data are part of a publication currently in press by Scientific Reports.

### 3.1.10. ROS generation before mitochondrial membrane depolarisation in menadione-stressed cardiomyocytes

In addition to DNA fragmentation, a second hallmark of regulated cell death is mitochondrial membrane depolarisation, which is central to both apoptosis and necrosis, but manifests in spatially and mechanistically distinct forms. For instance, the primary event in apoptosis is outer mitochondrial membrane (OMM) permeabilization, which results in the release of apoptogens. In the case of necrosis, the defining primary event is early opening of the mitochondrial permeability transition pore (mPTP) in the inner mitochondrial membrane (IMM) (Konstantinidis et al., 2012). In order to look at the mitochondrial membrane potential changes, we used tetramethylrhodamine, methyl ester (TMRM), which is a lipophilic dye that accumulates in the matrix of healthy, polarised mitochondria and emits red-orange fluorescent signal. Upon mitochondrial membrane depolarisation, the dye leaks out into the cytoplasm, where it is no longer fluorescent. We first performed a time-course in IMR-90 hPSC-CM, looking at the levels of TMRM 2, 4, 8 and 24 hr following menadione treatment. Our results show that mitochondrial membrane depolarisation is significantly induced 4 to 24 hr following treatment with 18.5μM and 27.7μM menadione (Figure 3.9A). After 24 hr of 27.7μM menadione, the TMRM signal in IMR-90 cardiomyocytes diminishes from 70.1±7.1% to 1.69±0.67% ($P<0.0001$). Despite the catastrophic effect on mitochondrial depolarisation at even shorter durations of menadione treatment, we chose to test the protective ability of CSC-conditioned media on cardiomyocytes at 24 hr.

Given the known role of menadione in redox cycling and production of reactive oxygen species (ROS) in the cytosol (Loor et al., 2010), we next tested whether CSC-

conditioned media attenuate oxidative stress, using a direct fluorescence detection assay, CellROX Green. This cell-permeant probe is weakly fluorescent while in a reduced state and exhibits bright fluorescence upon oxidation by ROS and subsequent binding to DNA. We performed a time-course experiment in IMR-90 determining the prevalence of CellROX signal at 2, 4, 8 and 24 hr following increasing menadione stress (Figure 3.9B). Our results demonstrate that at 18.5μM menadione, ROS prevalence rises to ~10-15% after 2 and 4 hr and to ~30-40% after 8 and 24 hr respectively.

Apart from inducing cytosolic ROS, menadione is also known to generate high levels of oxidative stress in the mitochondria, which undergo feedback loops further amplifying ROS production (Damm et al., 2001). We decided to test the effects of menadione on mitochondrial ROS production using MitoSOX, a fluorogenic detector of superoxide in live cells. This cell-permeant probe consists of a derivative of hydroxyethidium that selectively targets mitochondria and is rapidly oxidised by superoxide, but not other ROS or RNS (Robinson et al., 2006, 2008; Zielonka et al., 2008). The oxidised product is highly fluorescent upon binding to nucleic acid. In order to detect the appropriate time-point of MitoSOX induction under our stress conditions we performed a time-course in IMR-90 cardiomyocytes (Figure 3.9C). In comparison to the intracellular ROS levels seen above, our results demonstrate an earlier induction of mitochondrial superoxide, with $MitoSOX^{+}$ signal reaching a prevalence of ~50% just 2 hr after menadione treatment (Figure 3.9C). The induction of MitoSOX signal was not affected by the duration of menadione treatment, however it slightly increased with increasing concentrations of the stressor. Our results suggest that mitochondrial superoxide may be induced at an even earlier time-point than the ones tested here.

Given the very early induction of mitochondrial superoxide following menadione stress, we decided to test the CSC-conditioned media effect at 2 and 4 hr following treatment.

From the three time-course experiments described here we can conclude, after menadione stress, that human cardiomyocytes undergo rapid induction of mitochondrial superoxide (MitoSOX) and cytosolic ROS (CellROX) in the first 2 hr of treatment, with subsequent loss of mitochondrial membrane potential (TMRM), first detected at 4 hr under the conditions tested.

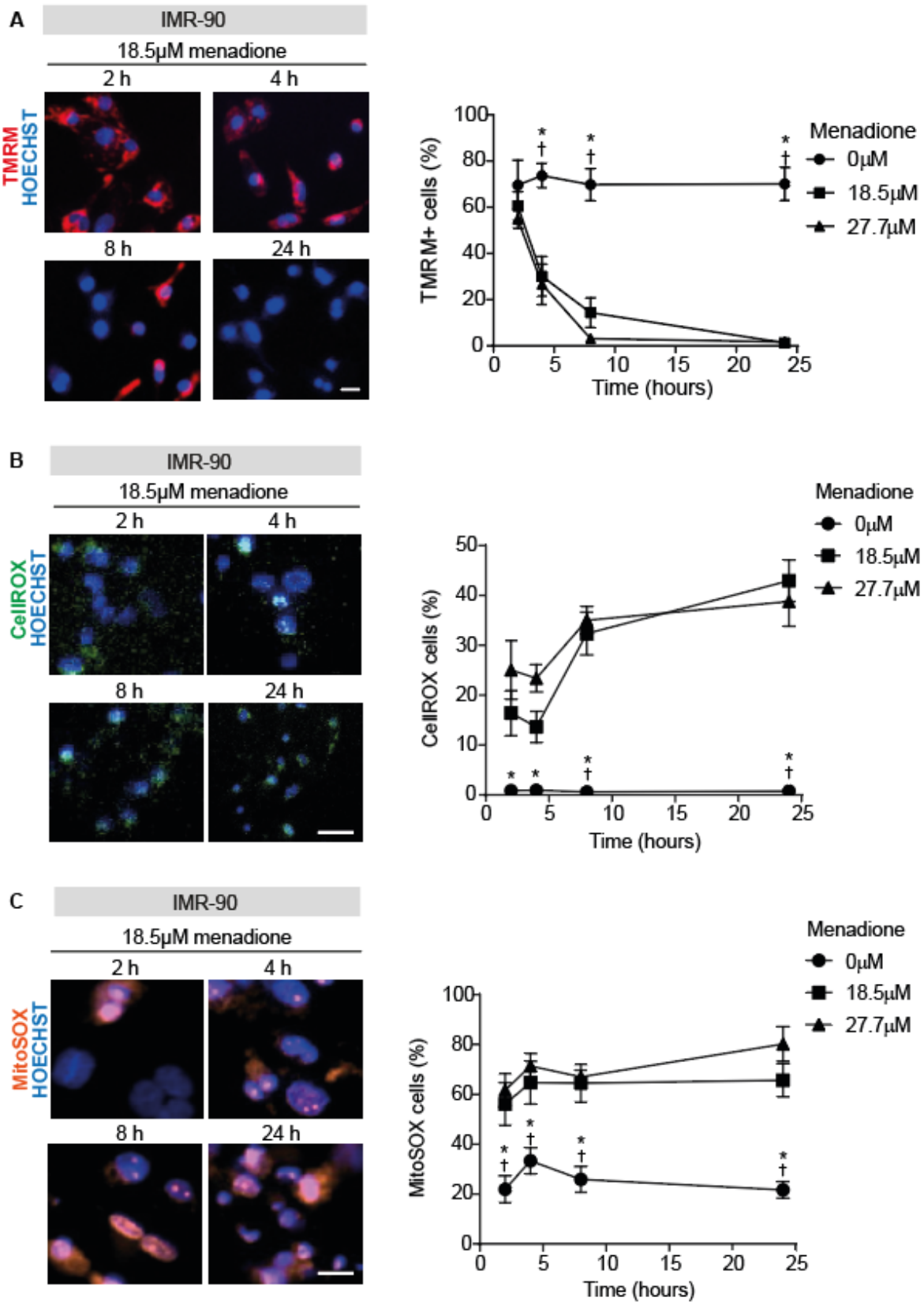

A
IMR-90
18.5μM menadione
2 h
4 h
8 h
24 h
TMRM
HOECHST
TMRM+ cells (%)
Time (hours)
Menadione
0μM
18.5μM
27.7μM
B
IMR-90
18.5μM menadione
2 h
4 h
8 h
24 h
CellROX
HOECHST
CellROX cells (%)
Time (hours)
Menadione
0μM
18.5μM
27.7μM
C
IMR-90
18.5μM menadione
2 h
4 h
8 h
24 h
MitoSOX
HOECHST
MitoSOX cells (%)
Time (hours)
Menadione
0μM
18.5μM
27.7μM

**Figure 3.9: ROS generation before mitochondrial membrane depolarisation in menadione-stressed cardiomyocytes.** Representative images and line graph of **A,** TMRM loss; n=11 **B,** CellROX uptake; n=12 and **C,** MitoSOX uptake; n=12, in IMR-90 myocytes overtime following menadione stress. Scale bar, 50 μm; data are shown as the mean ± SEM; *, P < 0.05, versus 18.5μM menadione; †, P < 0.05, versus 27.7μM menadione.

### 3.1.11. CSC-conditioned media inhibit mitochondrial depolarisation in hPSC-CM after menadione stress.

As the role of menadione on mitochondrial membrane depolarisation is not yet well-established in human cardiomyocytes, we next used a mix of electron transport chain uncouplers (FCCP, rotenone and oligomycin) as positive controls for membrane depolarisation. CSC-conditioned media treatment significantly reduced mitochondrial membrane depolarisation as denoted by TMRM loss, both in the vCor.4U (Figure 3.10A) and IMR-90 (Figure 3.10B) hPSC-CM lines. Specifically, the proportion of $TMRM^+$ IMR-90 increased more than 5-fold from 10.9±4.2% to 62.9±8.5% at 41.7μM menadione (P<0.0001). In the case of vCor.4U cardiomyocytes, mitochondrial depolarisation was inhibited 2-fold by CSC-conditioned media; at 62.5μM menadione, the TMRM signal was increased from 38.1±7.5% in the cells treated with menadione alone to 81.5±1.1% in the conditioned media-treated cells (P<0.0001). Given the overlapping nature of the mechanisms of cell death, TMRM loss by itself cannot distinguish between the intrinsic or extrinsic pathways and is a marker of both apoptosis and necrosis.

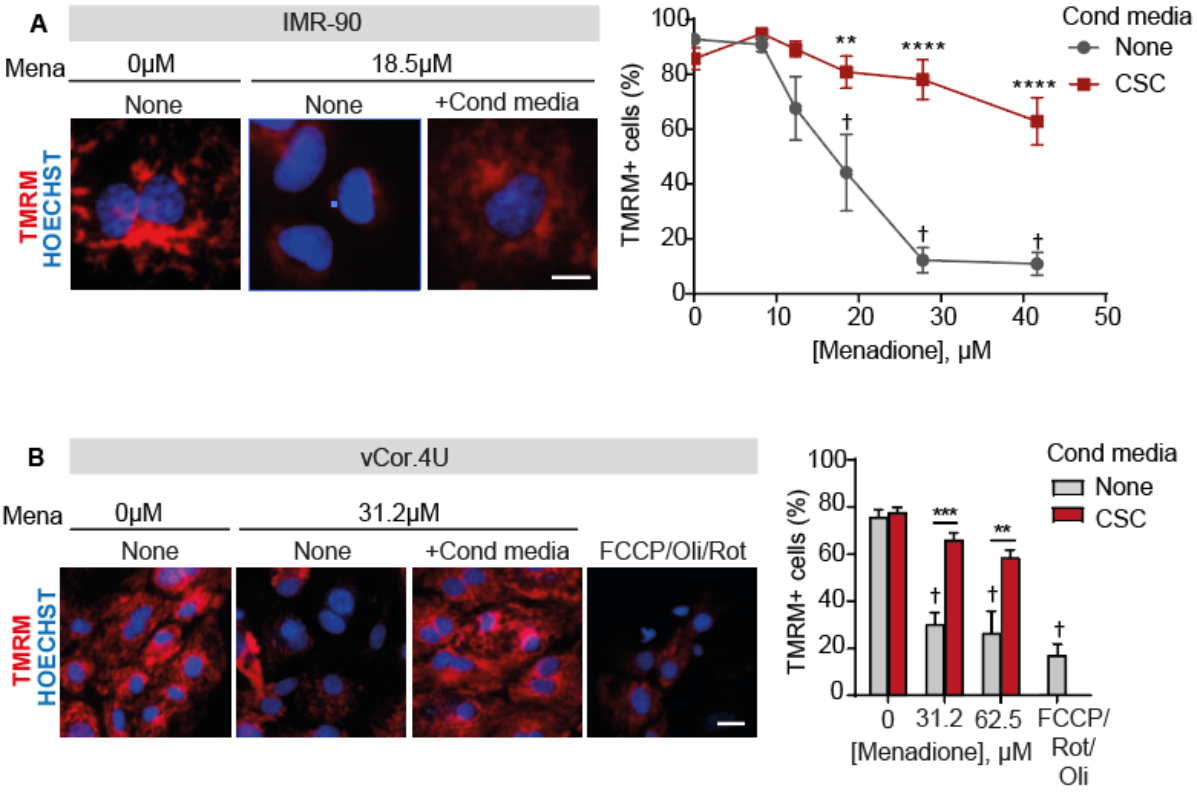



**Figure 3.10: CSC-conditioned media inhibit mitochondrial depolarisation in hPSC-CM after menadione stress.** Representative images and graphs of TMRM loss in **(A)** IMR-90; n=9 and **(B)** vCor.4U; n=7 cardiomyocytes in the presence and absence of CSC-conditioned media following 24 hr of menadione stress. Carbonyl cyanide 4-(trifluoromethoxy) phenylhydrazone (FCCP), oligomycin (Oli) and rotenone (Rot), uncouplers of oxidative phosphorylation, were used as controls for TMRM loss. Scale bar, 50 μm; data are shown as the mean ± SEM; **, P < 0.01; ***, P < 0.001; ****, P < 0.0001; †, P < 0.05, versus no menadione. These data are part of a publication currently in press by Scientific Reports.

### 3.1.12. CSC-conditioned media inhibit ROS in hPSC-CM after menadione.

In order to investigate in more detail, the mechanisms by which CSC-conditioned media inhibit mitochondrial membrane depolarisation, we used CellROX to detect ROS levels in the menadione-stressed human cardiomyocytes with and without conditioned media. We chose to perform the protection assay at 8- and 24 hr after menadione treatment, when significantly higher induction of CellROX signal is

obtained (Figure 3.11B). During the optimisation steps of this assay, dead, floating cardiomyocytes exhibited auto-fluorescence in the FITC channel, the one acquiring CellROX$^+$ cells, but not in other wavelengths. To eliminate any false positive CellROX signal, DRAQ7 was included in the staining and at the time of analysis, DRAQ7$^-$ CellROX$^+$ objects were scored and used to plot the graphs below. Our results showed that after 8 hr of menadione treatment, there was a consistently significant reduction in the proportion of CellROX$^+$ cells from 38.3±6.5% to 7.9±2.4% ($P<0.0001$) and 55±6.4% to 12.6±2.1% ($P<0.0001$) in IMR-90 and vCor.4U respectively (Figure 3.11A, B). The 24-hr time-point is not shown because results were compromised due to the high number of auto-fluorescent, floating dead cells.

In order to overcome the auto-fluorescence drawback of the live imaging assay above and detect ROS levels in menadione-stressed cells after the 24-hr treatment, we then used a different assay, ROS-Glo $H_2O_2$, which instead measures an increase or decrease in ROS generated in the culture medium of cells using relative luminescence. Menadione treatment for 24 hr resulted in a concentration-dependent increase in ROS levels which was significant at stressor concentrations higher than 18.5μM (prevalence increased from 3193±321 RLU to 22413±3610 RLU, $P<0.001$; Figure 3.11C). In the presence of CSC-conditioned media, there was a significant reduction in the levels of ROS at concentrations above 18.5μM menadione; at 27.8μM menadione, there was an induction of 37163±5794 RLU, which was significantly reduced by CSC-conditioned media to 14447±1432 RLU ($P<0.0001$). Thus, we show using two independent ROS-detection assays that the CSC-conditioned media protective mechanism against menadione acts through reduction of intracellular ROS in cardiomyocytes.

Our data up to this point raise the mechanistic question of how exactly CSC-conditioned media reduce ROS. To investigate whether CSC-conditioned media act merely as a ROS scavenger, we used the ROS-Glo $H_2O_2$ assay to study the effect of CSC-conditioned media in the reduction of $H_2O_2$, in the complete absence of cells. Solutions of 1mM $H_2O_2$ were prepared in either standard cardiomyocyte medium (RPMI) or CSC-conditioned medium. Catalase was used as a positive control for $H_2O_2$ scavenging activity, at a final concentration of 2U for 10 min (Figure 3.11D). Our results show significant induction of $H_2O_2$ luminescence in the presence of 1mM $H_2O_2$ from 72,602±1600 RLU in RPMI and 147,917±10,705 RLU in CSC-conditioned media to 2,000,000 RLU, which is the maximum detection range for the assay ($P<0.0001$). Therefore, CSC-conditioned medium did not exhibit any $H_2O_2$ scavenging activity. In contrast, catalase significantly reduced the $H_2O_2$ levels down to 141,800±5922 RLU in RPMI and 135,313±538 RLU in CSC-conditioned media ($P<0.0001$). Apart from the saturation of the signal in the assay, another limitation of our approach is that the concentration of 1mM $H_2O_2$ used could be too high for the CSC-conditioned medium to scavenge. If time permitted the repetition of this experiment, we would first measure the levels of $H_2O_2$ in the menadione-stressed cardiomyocyte cultures, and then use that same concentration range to test the scavenging activity of CSC-conditioned medium.

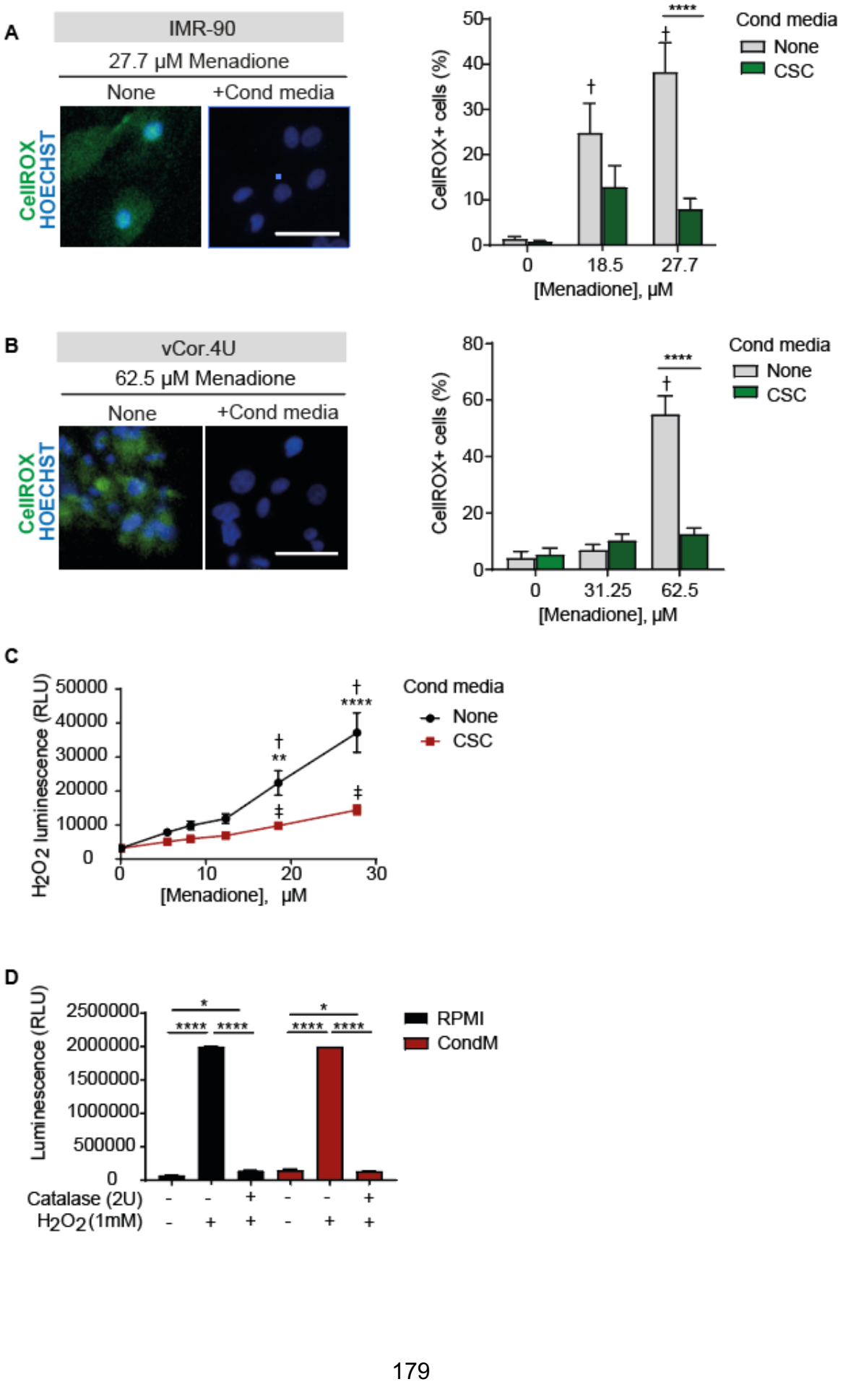

A
IMR-90
27.7 μM Menadione
None
+Cond media
CellROX
HOECHST
CellROX+ cells (%)
Cond media
None
CSC
[Menadione], μM
B
vCor.4U
62.5 μM Menadione
C
H2O2 luminescence (RLU)
[Menadione], μM
D
Luminescence (RLU)
RPMI
CondM
Catalase (2U)
H2O2 (1mM)

**Figure 3.11: CSC-conditioned media inhibit ROS in hPSC-CM after menadione.** Representative images and bar graphs of CellROX uptake in **(A)** IMR-90; n=12 and **(B)** vCor.4U; n=12 cardiomyocytes in the presence and absence of CSC-conditioned media following 8 hr of menadione stress. **C,** Line graph of $H_2O_2$ relative luminescence signal in IMR-90 cardiomyocytes after menadione stress, with and without CSC-conditioned media. Scale bar, 50 μm; data are shown as the mean ± SEM; ****, P < 0.0001; †, P < 0.05, versus no menadione in standard medium; ‡, P<0.05, versus no menadione in CSC-conditioned medium. **D,** Bar graph of $H_2O_2$ relative luminescence signal in standard medium (RPMI) or CSC-conditioned medium (CondM) with and without catalase to detect ROS scavenging activity of the conditioned medium. Data are shown as the mean ± SEM; *, P < 0.05; ****, P < 0.0001. These data are part of a publication currently in press by Scientific Reports.

### 3.1.13. CSC-conditioned media inhibit mitochondrial superoxide in hPSC-CM after menadione

Given that CellROX cannot distinguish between cytosolic and mitochondrial ROS, in order to study whether CSC-conditioned media fight oxidative stress by acting specifically on mitochondria we used the MitoSOX probe for the detection of mitochondrial superoxide. In the presence of CSC-conditioned media, the levels of mitochondrial superoxide were reduced, both in IMR-90 (Figure 3.12A) vCor4.U (Figure 3.12B) hPSC-CM lines, 2 and 4 hr following menadione treatment, respectively. More specifically there was a reduction of 65.8±5.1% to 17.3±3.8% and 65.7±6.8% to 29.7±7.6% (P<0.0001) in the proportion of $MitoSOX^+$ cells at the highest concentration of menadione treatment, in IMR-90 and vCor.4U, respectively. Thus, CSC-conditioned media protect cardiomyocytes from oxidative stress-induced death, by inhibiting mitochondrial levels of ROS.

In summary, Fig. 3.8-3.12 give an insight into the series of events taking place following induction of menadione stress in cardiomyocytes and the points where CSC-conditioned media interfere to stop the death process. We demonstrate that upon

menadione stress, there is induction of superoxide and cytosolic ROS levels in hPSC-CM, which might lead to mitochondrial depolarisation and presumably activate downstream cascades that result in DNA fragmentation and cell death. Whether mitochondrial depolarisation is a result of ROS generation or other induced changes in the mitochondrial compartment is subject to further analysis. Although not investigated further in this project, the intermediate steps known to couple mitochondrial depolarisation to cell death include release of cytochrome c, formation of the apoptosome, and activation of executioner caspases (Galluzzi et al., 2018; Del Re et al., 2019).

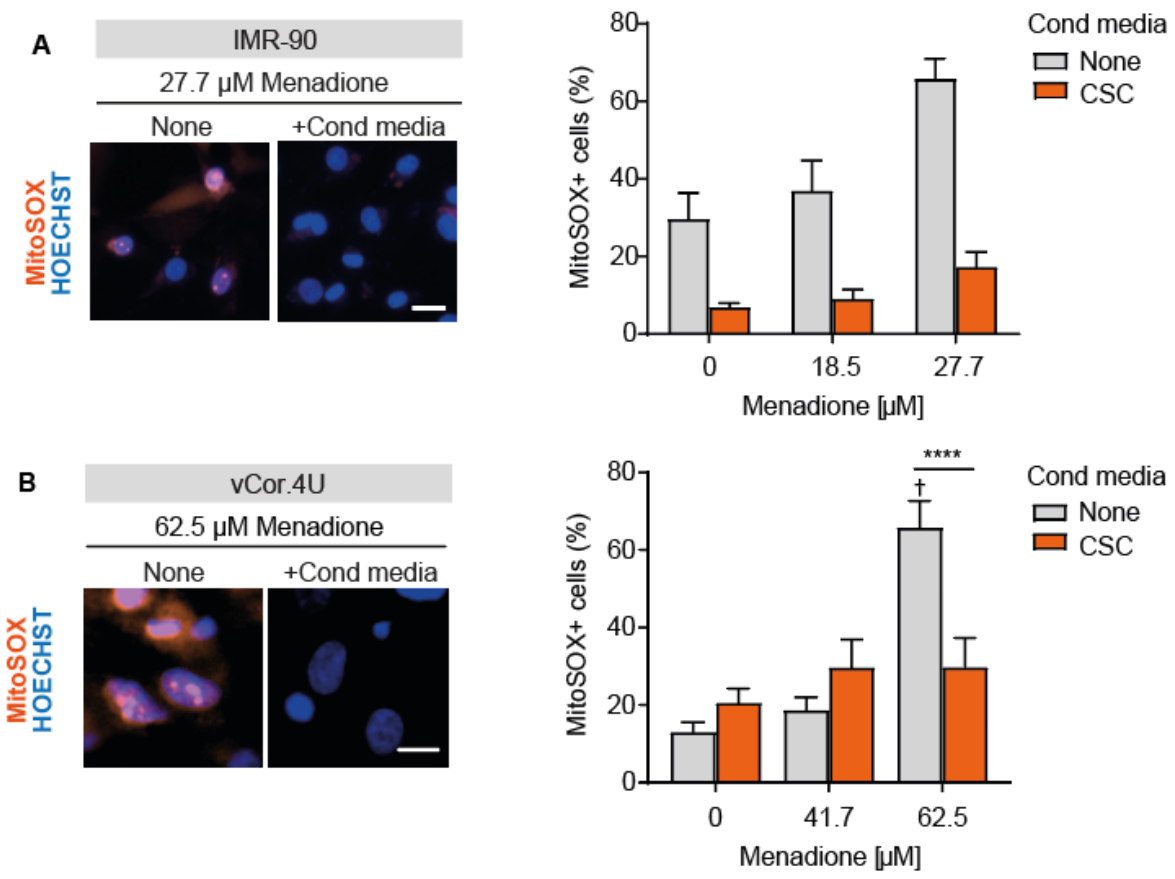



**Figure 3.12: CSC-conditioned media inhibit mitochondrial superoxide in hPSC-CM after menadione.** Representative images and bar graphs of MitoSOX uptake in **(A)** IMR-90 cardiomyocytes 2 hr after induction of stress; n=8 (two independent experiments) and **(B)** vCor.4U cardiomyocytes 4 hr after induction of stress; n=10 in the presence and absence of CSC-conditioned media following menadione. Scale bar,

50 μm; data are shown as the mean ± SEM; **, P < 0.01; ***, P<0.001; ****, P < 0.0001; †, P < 0.05, versus no menadione.

### 3.1.14. CSC-conditioned media inhibit death of hPSC-CM induced by doxorubicin

Apart from menadione, we were interested in testing complementary stress molecules to investigate whether the protective effect of CSC-conditioned media is more generalisable. We investigated doxorubicin, an anthracycline chemotherapeutic agent which causes dose-related cardiotoxicity that can lead to heart failure (Burridge et al., 2016; Zhao and Zhang, 2017). Doxorubicin damages cardiomyocytes not only by inducing oxidative stress and mitochondrial damage, but also inhibiting topoisomerase IIβ and mitochondrial topoisomerase I, in addition to DNA double strand-break damage (Deavall et al., 2012; Hanna et al., 2014; Higo et al., 2017; Khiati et al., 2014; Zhang et al., 2012). Hence, by comparison with the impact of menadione, the death effector pathways engaged by doxorubicin are not only distinct, but also wider ranging.

In order to investigate the effect of CSC-conditioned media on doxorubicin-stressed cardiomyocytes, we treated vCor.4U and IMR-90 cells with increasing doses of the drug for 24 hr. We then stained the cardiomyocytes with DRAQ7 and measured cell death on the Cellomics platform. Supernatants from these experiments were collected for confirmatory cell death assays. CSC-conditioned media was capable of significantly inhibiting DRAQ7 uptake by roughly half from 51.9±4.9% to 24.2±3.1% (P<0.0001) and 49.2±6.5% to 25.7±4.0% (P<0.0001) at the highest concentrations of doxorubicin used in vCor4.U (Figure 3.13A) and IMR-90 (Figure 3.13B) cardiomyocytes, respectively.

As a confirmatory assay to use alongside the DRAQ7 uptake, we employed ToxiLight, a low-cost orthogonal bioassay, that investigates the released adenylate kinase levels in the culture supernatants. Adenylate kinase is an abundant protein in all eukaryotic cells, released into the culture medium upon death. It can thus be used in a bioluminescence assay to quantitate the levels of cell death under different conditions (Daniels et al., 2006). Adenylate kinase activity was inhibited almost 6-fold by conditioned media, at the highest drug concentration (Figure 3.13C). More specifically, CSC-conditioned media treatment reduced the adenylate kinase levels from 11.6±1.8 fold to 1.8±0.4 fold ($P<0.0001$) in vCor.4U human cardiomyocyte supernatants. Thus, CSC-conditioned media are cardio-protective against this alternative form of stress, demonstrating that their effect could be applicable to a wider range of clinically relevant cardiac death signals than just ischemic injury and its cell culture surrogate.

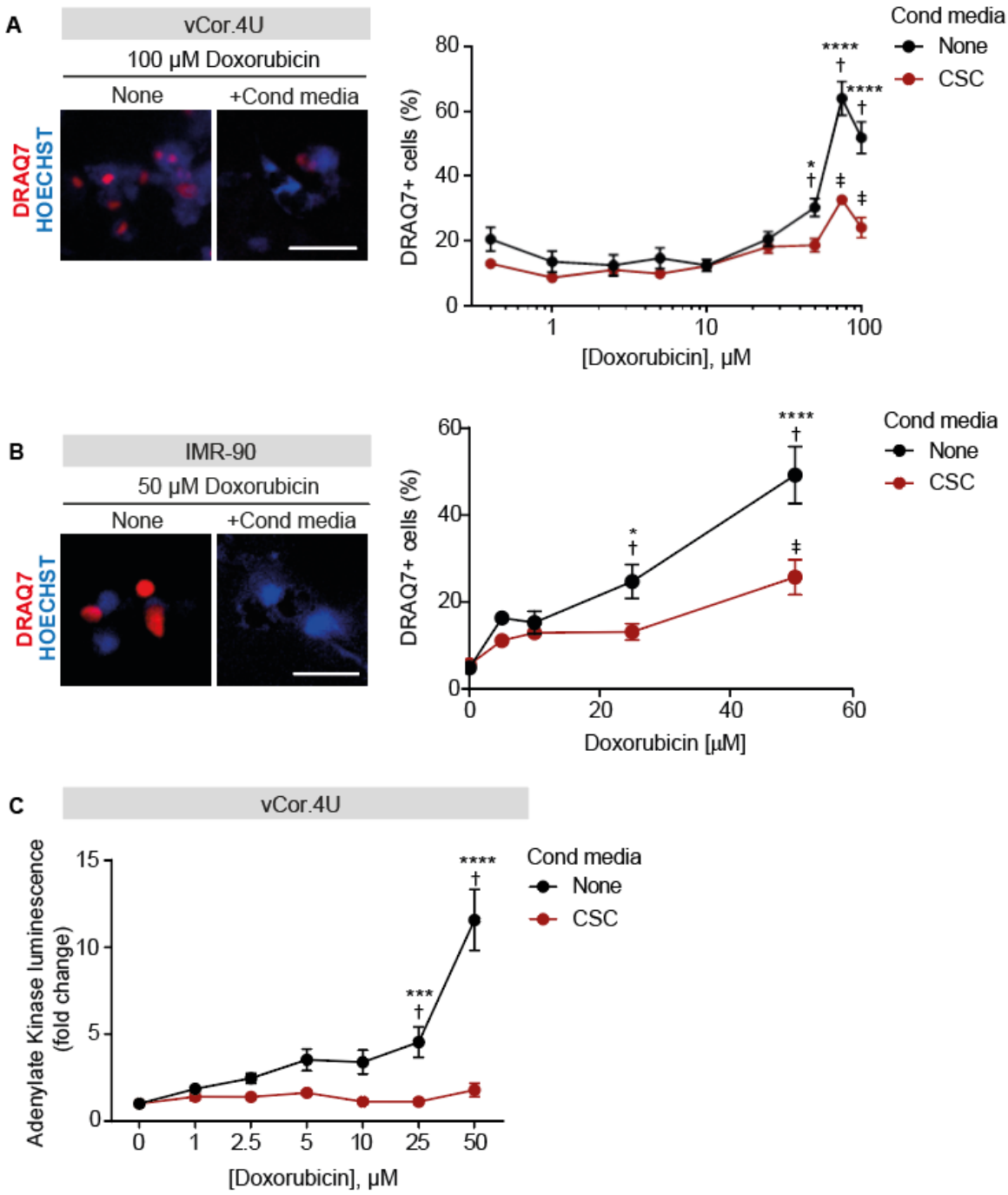



**Figure 3.13: CSC-conditioned media inhibit death of hPSC-CM by doxorubicin.** Representative images and line graphs of DRAQ7 uptake in **A,** vCor.4U and **B,** IMR-90 cardiomyocytes following doxorubicin for 24 hr, in the presence and absence of CSC-conditioned media. **C,** Line graph of relative luminescence of adenylate kinase plotted as a fold change from the untreated control. Human vCor4U cardiomyocytes were stressed with doxorubicin in the presence and absence of CSC-conditioned media for 24 hr prior to the assay. Scale bar, 50 µm; data are shown as the mean ± SEM; n=9; *, P < 0.05; ****, P<0.0001; †, P < 0.05, versus no menadione in standard medium; ‡, P<0.05, versus no menadione in CSC-conditioned medium.

### 3.1.15. Detection of mitochondrial depolarisation in hPSC-CM by doxorubicin and possible protection by CSC-conditioned medium

A hallmark of apoptotic death is mitochondrial depolarisation, which we previously showed to be significantly inhibited after menadione stress by CSC-conditioned media (Figure 3.10). In order to investigate whether the mechanisms of cardiomyocyte protection from doxorubicin stress are similar, we used the TMRM assay to detect mitochondrial depolarisation in IMR-90 human cardiomyocytes and monitor how it changes in the presence of doxorubicin plus CSC-conditioned media. Increasing doxorubicin stress did not affect IMR-90 mitochondrial depolarisation (Figure 3.14A). In fact, TMRM levels fluctuated around 60-80% at 24 hr of doxorubicin treatment regardless of the drug concentration. In the presence of CSC-conditioned media there was no change in the prevalence of $TMRM^+$ cells, which were maintained at 70-80%. In contrast, cardiomyocytes treated with a mix of mitochondrial membrane uncouplers (FCCP, Oliogomycin and Rotenone), showed increased TMRM loss, down to 21.8%±13.9 ($P<0.0001$). From these results, it seems that, under the conditions tested, doxorubicin does not affect mitochondrial depolarisation and is likely thus killing cardiomyocytes solely by activating other pathways. As a counter-interpretation, the TMRM assay might be hampered by technical issues such as the bright red colour of doxorubicin, which might be interfering with the TMRM signal, giving false positive events at higher doxorubicin concentrations and obscuring the extent of mitochondrial depolarization in the cultures.

In order to explore this possible technical limitation, we attempted to detect the levels of mitochondrial depolarisation using the alternative colorimetric JC-10 assay, as done by others using IMR-90 cells (Burridge et al., 2016). Furthermore, we used a

concentration of 1 μM doxorubicin, dilute enough to avoid the overt change in medium colour in the assayed wells. JC-10 dye is a cationic, lipophilic, better soluble alternative to the earlier JC-1 probe, that accumulates in the mitochondrial matrix, forming red fluorescent aggregates (emission at 590 nm). In apoptotic and necrotic cells, JC-10 leaks out of mitochondria, where it changes to the monomeric form labelling cells with green fluorescence (emission at 520 nm). IMR-90 cells were treated with 1 μM doxorubicin in the presence and absence of CSC-conditioned media for 24 hr, were then stained with JC-10 and fluorescence was measured using a microplate reader at the two available wavelengths of our instrument, 535 nm and 595 nm (Figure 3.14B). The ratio of 535:595 nm shows an induction of mitochondrial membrane depolarisation with increasing concentrations of doxorubicin; 0.4±0.03 at 0 μM doxorubicin was increased to 0.7±0.03 at 1 μM. In the presence of CSC-conditioned media there was statistically significant reduction in the ratio of 535 nm to 595 nm; the ratio was reduced to 0.56±0.03. Thus, our results suggest that the microplate reader assay is a bit more sensitive in terms of membrane depolarisation detection compared to the fluorescence imaging assay, in the case of doxorubicin. Cardiomyocytes treated with a mix of mitochondrial membrane uncouplers (FCCP, Oligomycin and Rotenone), showed increased 535:595 ratio, to 2.06±0.15. In both aforementioned assays, mitochondrial depolarisation was clearly detected in the uncoupler-treated wells, demonstrating that the assays were technically robust. However, the associated media colour change resulting from the properties of the drug, at least for the TMRM assay, might still skew the data, which need to be interpreted with caution. With additional time available, alternative relevant assays of mitochondrial dissipation, not fraught by this issue, could include the release of mitochondrial apoptogens into the cytoplasm, such as cytochrome c, apoptosis-inducing factor, and Smac/Diablo (Xiao-Xu et al., 2017).

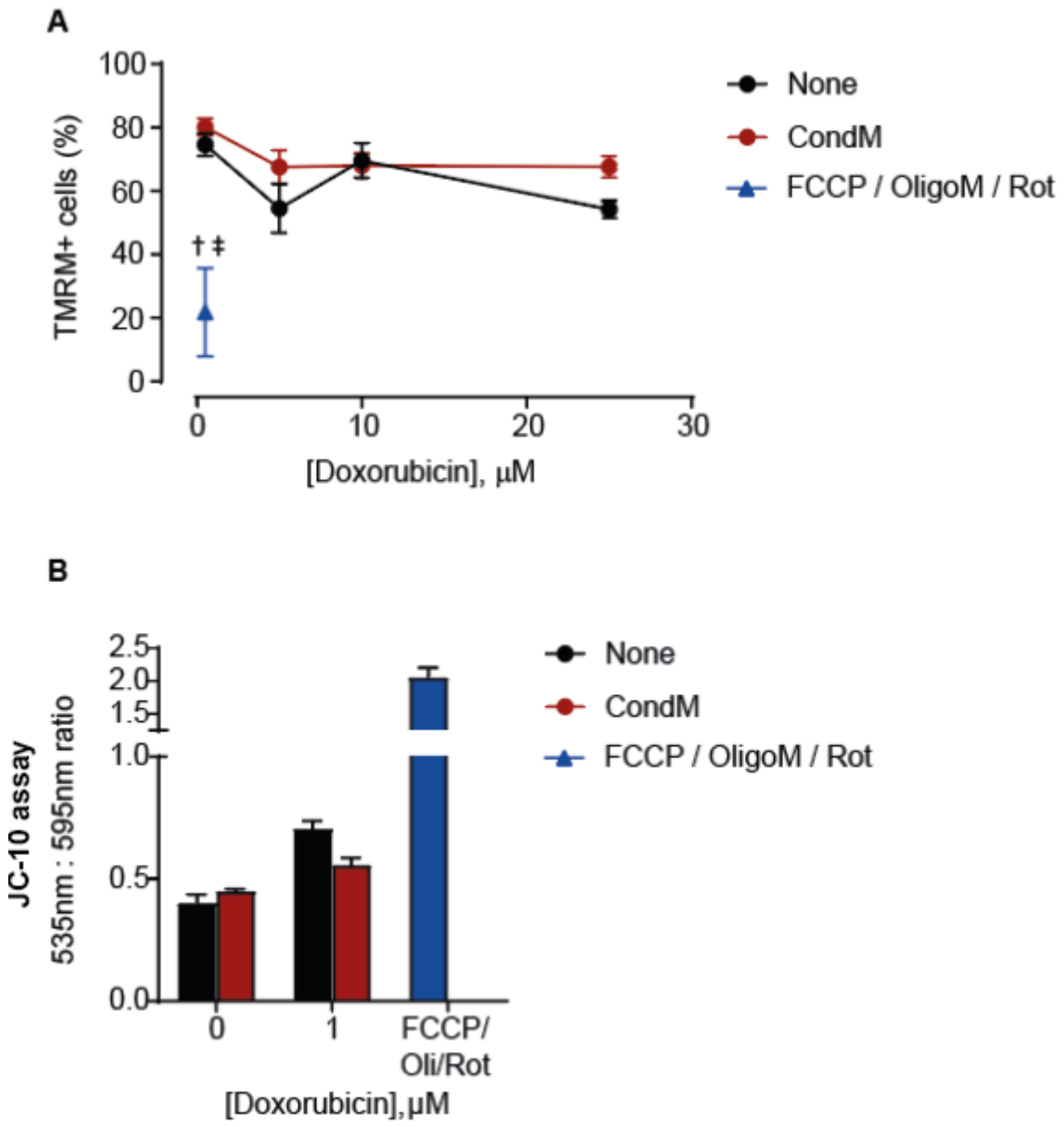



**Figure 3.14: Detection of mitochondrial depolarisation in hPSC-CM by doxorubicin and possible protection by CSC-conditioned medium. A,** Line graph for TMRM uptake in IMR-90 cardiomyocytes 24 hr following induction of doxorubicin stress, in the presence and absence of CSC-conditioned media. †, $P < 0.05$, versus no menadione in standard medium; ‡, $P<0.05$, versus no menadione in CSC-conditioned medium. **B,** Bar graph for JC-10 assay for mitochondrial membrane potential following a 24-hr treatment with doxorubicin in the presence and absence of CSC-conditioned media. The ratio of JC-10 in its monomeric form (emits at 535nm) to its aggregated form (emits at 595nm) was plotted. Data are shown as the mean ± SEM; n=6 (two independent experiments).

### 3.1.16. CSC-conditioned media fail to reduce ROS levels in hPSC-CM after doxorubicin stress

Given that one of the mechanisms of anthracycline-induced damage in cardiomyocytes is oxidative stress (Songbo et al., 2019), we used CellROX to confirm an increase in intracellular ROS levels, with increasing doxorubicin concentrations over a 24 hr treatment in IMR-90 cardiomyocytes. We were also intrigued to find out whether CSC-conditioned media reduce the levels of ROS and thus inhibit cardiomyocyte death using a similar mechanism as against menadione stress. Whilst the levels of CellROX signal increase at higher concentrations of doxorubicin stress, CSC-conditioned media were unable to avert this (Figure 3.15A). The proportion of $CellROX^+$ cardiomyocytes increased from 0.3±0.1% to 75.5±2.5% in the untreated and to 79.4±3.5% in the presence of CSC-conditioned media, at 50μM doxorubicin.

We used an independent cell-based assay, ROS-Glo $H_2O_2$ to confirm the lack of ROS inhibition in IMR-90 cells by CSC-conditioned media. In agreement to the CellROX results, $H_2O_2$ luminescence increased in a concentration-dependent manner in the presence of doxorubicin but was not significantly reduced by CSC-conditioned media (Figure 3.15B). At 50μM doxorubicin, where we previously saw significant protection from cell death, $H_2O_2$ luminescence was induced highly by doxorubicin regardless of conditioned medium: 12058±1283 RLU in the cells receiving doxorubicin alone and 10228±556 RLU ($P>0.05$) in the presence of CSC-conditioned media. Thus, unlike the menadione stress conditions, our data suggest that CSC-conditioned media prevent cell death in doxorubicin-stressed cardiomyocytes through a mechanism independent of inhibiting intracellular ROS, presumably via one or more effectors of ROS.

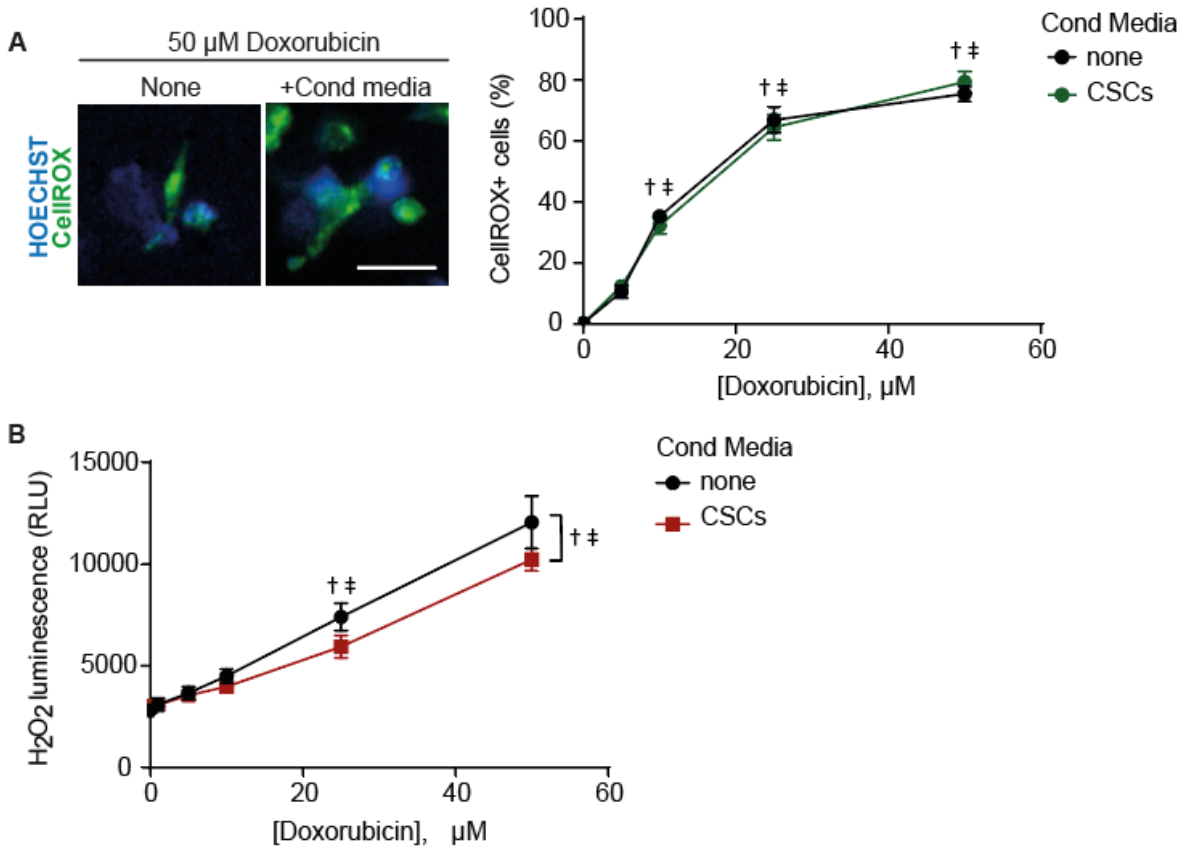



**Figure 3.15: CSC-conditioned media fail to reduce ROS levels in hPSC-CM after doxorubicin stress. A,** Representative images and line graph of CellROX uptake 24 hr following doxorubicin in the presence and absence of CSC-conditioned media; n=9. **B,** Line graph of $H_2O_2$ relative luminescence following 24 hr of doxorubicin with and without CSC-conditioned media; n=6. Data are shown as the mean ± SEM; †, P < 0.05, versus no doxorubicin in standard medium; ‡, P<0.05, versus no doxorubicin in CSC-conditioned medium.

### 3.1.17. CSC-conditioned media fail to reduce superoxide levels in mitochondria of hPSC-CM after doxorubicin stress

Given the finding that CSC-conditioned media do not reduce intracellular ROS levels following doxorubicin treatment, we were intrigued to investigate whether the protection is compartmentalised, e.g., by inhibition of mitochondrial superoxide instead. We thus employed the MitoSOX live cell assay to establish whether CSC-

conditioned media reduce the levels of mitochondrial superoxide following doxorubicin stress in IMR-90 cardiomyocytes. Superoxide induction was detected following treatment of cardiomyocytes with 25 μM doxorubicin for 30 min, as previously reported (Mukhopadhyay et al., 2007), in the presence and absence of conditioned media. Our results demonstrate that the level of MitoSOX$^{+}$ signal increased 1.6-fold in the untreated from 15.3±5.6% without doxorubicin to 25.5±10% at 25μM doxorubicin. However, in the presence of CSC-conditioned media there was no significant reduction in superoxide levels; 5.5±1.5% MitoSOX$^{+}$ cells in the untreated were increased to 25.6±7.5% following anthracycline-treatment (Figure 3.16). Thus, consistent with our results with CellROX and ROS-GLO above, these data show that CSC-conditioned media are likely to protect doxorubicin-stressed cardiomyocytes downstream and independent of mitochondrial ROS induction.

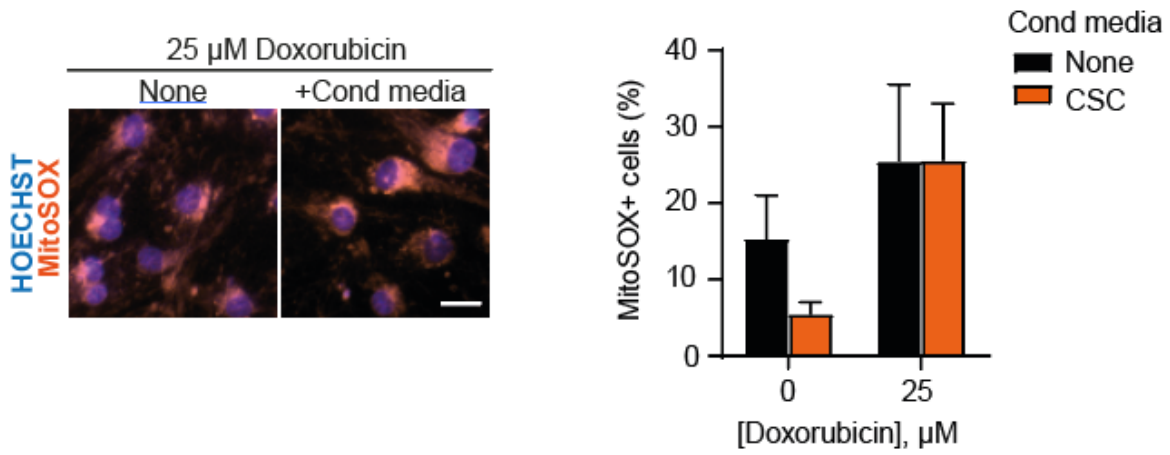



**Figure 3.16: CSC-conditioned media fail to reduce superoxide levels in mitochondria of hPSC-CM after doxorubicin stress.** Representative images and line graph of MitoSOX uptake in IMR-90 30-min following doxorubicin in the presence and absence of CSC-conditioned media. Data are shown as the mean ± SEM; n=12; P>0.05.

### 3.1.18. CSC-conditioned media inhibit mitochondrial depolarisation and cardiomyocyte death following imatinib stress

Given the capacity of our CSC-conditioned media to protect human cardiomyocytes from different types of stress molecules, and the dual effects we saw, alternatively upstream or downstream from ROS, we were intrigued to test an additional, wholly different stressor, that acts by interfering with an altogether distinct pathway in the cardiomyocytes. Imatinib is a small molecule kinase inhibitor used in cancer treatment and marketed by Novartis as Glivec. It acts by inhibiting specific tyrosine kinase enzymes in human cells, including but not limited to the SCF receptor, NGF receptor, PDGFα/β receptor, MCSF1 receptor and EDD1 receptor (Carroll et al., 1997; Druker et al., 1996). Interestingly, previous studies have shown that imatinib-induced cardiomyocyte death does not happen through the classical apoptotic programme mediated by capsase-3 cleavage, suggesting the occurrence of a necrotic death mechanism (Barr et al., 2014). Furthermore, this drug's cardiotoxicity involves lysosomal accumulation, disruption of autophagy and induction of ER-stress, independent of c-Abl inhibition (Hu et al., 2012). Lastly, a recent network-level analysis emphasizes other mechanistic differences in cardiomyocyte killing by doxorubicin versus tyrosine kinase inhibitors (Wang et al., 2019).

Hence, we were interested in the effect of imatinib on IMR-90 cardiomyocytes as well as the ability of CSC-conditioned media to block the drug's actions. We performed a dose response curve, in the presence and absence of CSC-conditioned media and measured DRAQ7 and TMRM signals. Imatinib induced IMR-90 death by increasing DRAQ7 uptake 2-fold from 14.3±2% in the cells without imatinib to 28.3±3% in cells treated with 26.7μM imatinib. CSC-conditioned media significantly protected IMR-90

from imatinib-induced death, at concentrations higher than 20 μM; for instance, there was a reduction of DRAQ7 signal 1.5- to 2-fold, from 28.3± 1.1% to 13.1± 1.3% at 26.7 μM and from 41.2±4.2% to 26.9±3.1% at 47.5 μM imatinib (Figure 3.17A).

Mitochondrial membrane dissipation was compromised by imatinib, with TMRM signal dropping 2- to 4-fold from 79.3±4.9% in the cells without imatinib to 40.9±2.9% at 26.7 μM and 11.8±4.9% by 35.6 μM (Figure 3.17B). In fact, mitochondrial dysfunction seems to have a central role in the cardiotoxic response to imatinib, but the mechanism is reported to arise as a response to ER stress, both in mouse hearts and cells in culture (Kerkelä et al., 2006) Furthermore, CSC-conditioned media exhibited inhibition of mitochondrial membrane dissipation under imatinib stress; at 26.7 μM imatinib TMRM signal was maintained by CSC-conditioned medium at 81.6±4.2% and at 35.6 μM imatinib TMRM signal was preserved at 46.4±6.3% (Figure 3.17A). Although both doxorubicin and imatinib are anthracycline drugs, their underlying mechanisms cardiotoxicity might differ (Force et al., 2007b; Ghigo et al., 2016) and so would the subsequent mechanism of CSC-mediated protection. Nevertheless, these results in combination to the previously established protection against menadione and doxorubicin, highlight the potential applicability of our CSC treatment against a wide range of cardiac stress triggers.

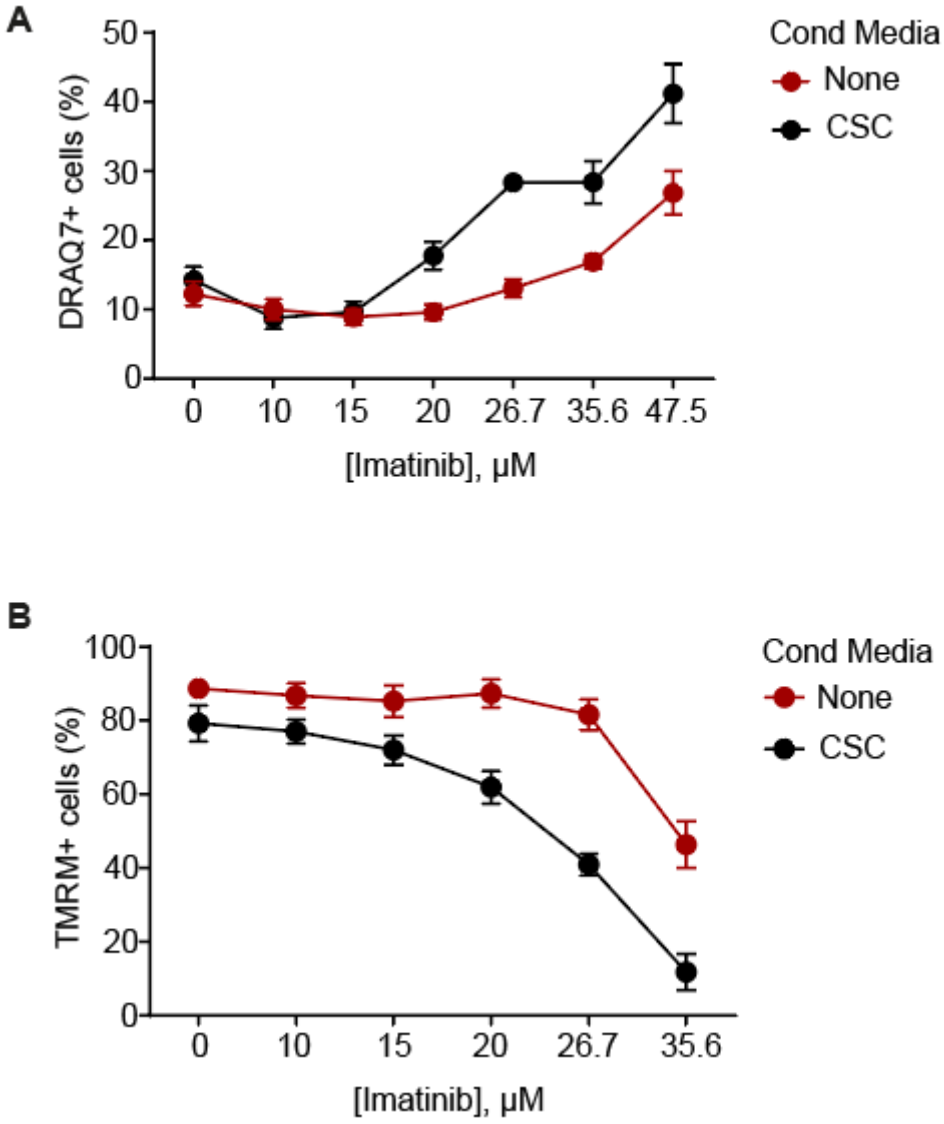



**Figure 3.17: CSC-conditioned media inhibit mitochondrial depolarisation and cardiomyocyte death following imatinib stress.** Line graphs of **A,** DRAQ7 uptake and **B,** TMRM loss, following 24 hr of imatinib stress in vCor.4U cardiomyocytes with and without CSC-conditioned media. Data are shown as the mean ± SEM; n=8 (two independent experiments). These data are part of a publication currently in press by Scientific Reports.

### 3.1.19. CSC-conditioned media preserve $Ca^{2+}$ cycling in hPSC-CM at sublethal concentrations of menadione

Given the previously demonstrated CSC-conditioned media protective effects on human cardiomyocyte survival, we wanted to test whether rescued cells maintain their

functional characteristics. We started by studying the signature biophysical property of cardiomyocytes, $Ca^{2+}$ cycling, which refers to the release and re-uptake of intracellular $Ca^{2+}$ that drives muscle contraction and relaxation. Calcium cycling is highly regulated in cardiomyocytes and is susceptible to redox- and phosphorylation-dependent aberrations (Meissner, 2017). Using the CellOptiq platform, we intended to test the effect of sublethal menadione stress on vCor.4U $Ca^{2+}$ signalling, as well as the ability of CSC-conditioned media to inhibit this effect. We used a ratiometric dye, Fura-4 AM which is a widely used intracellular $Ca^{2+}$ indicator (Figure 3.18). Although $Ca^{2+}$ cycling amplitude was not significantly changed in the presence of menadione, the overall cycle length was increased almost 2-fold (0.651±0.017 s in the absence of menadione to 1.127±0.096 s at 40 μM of menadione, $P<0.0001$), and the beating rate was significantly reduced (88.7±2.1 bpm in the absence of menadione to 55.5±3.1 bpm at 40 μM of menadione, $P<0.0001$). More specifically, even though the time to peak did not particularly change (105.1±13.8 ms in the absence of menadione to 142.7±13.8 ms at 40 μM menadione), time taken for re-uptake was prolonged 1.2-fold, with time to 75% decay being increased from 271.8±7.1 ms to 342.1±14.5 ms ($P<0.0001$) and time to 90% decay from 331.4±8.9 ms to 424.7±17.9 ms ($P<0.0001$). Even though menadione effects on particular $Ca^{2+}$ transport pathways have not been studied here, our results showing prolongation of the transient, as characteristic in diverse forms of heart disease, allow us to hypothesise induced defects in re-uptake involving the sarcoplasmic reticulum $Ca^{2+}$ ATPase (SERCA2) (Rossi and Dirksen, 2006). In the presence of CSC-conditioned media, the menadione-induced impairments were all prevented, maintaining a healthy $Ca^{2+}$ transient (with ADP75 reduced to 242.6±9.3 ms versus 342.1±14.5 ms in menadione alone, ADP90 reduced to 300.1±10.6 ms versus 424.7±17.9 ms in menadione alone, $P<0.0001$). Lastly,

normal beating rate was recovered to 78±1.4 bpm versus 55.5±3.1 bpm at 40 μM of menadione (P<0.0001; Figure 18). Thus, CSC-conditioned media not only protect human cardiomyocytes from oxidative stress-induced death, but also preserve normal $Ca^{2+}$ cycling and allow the maintenance of a healthy beating rate in the rescued cells.

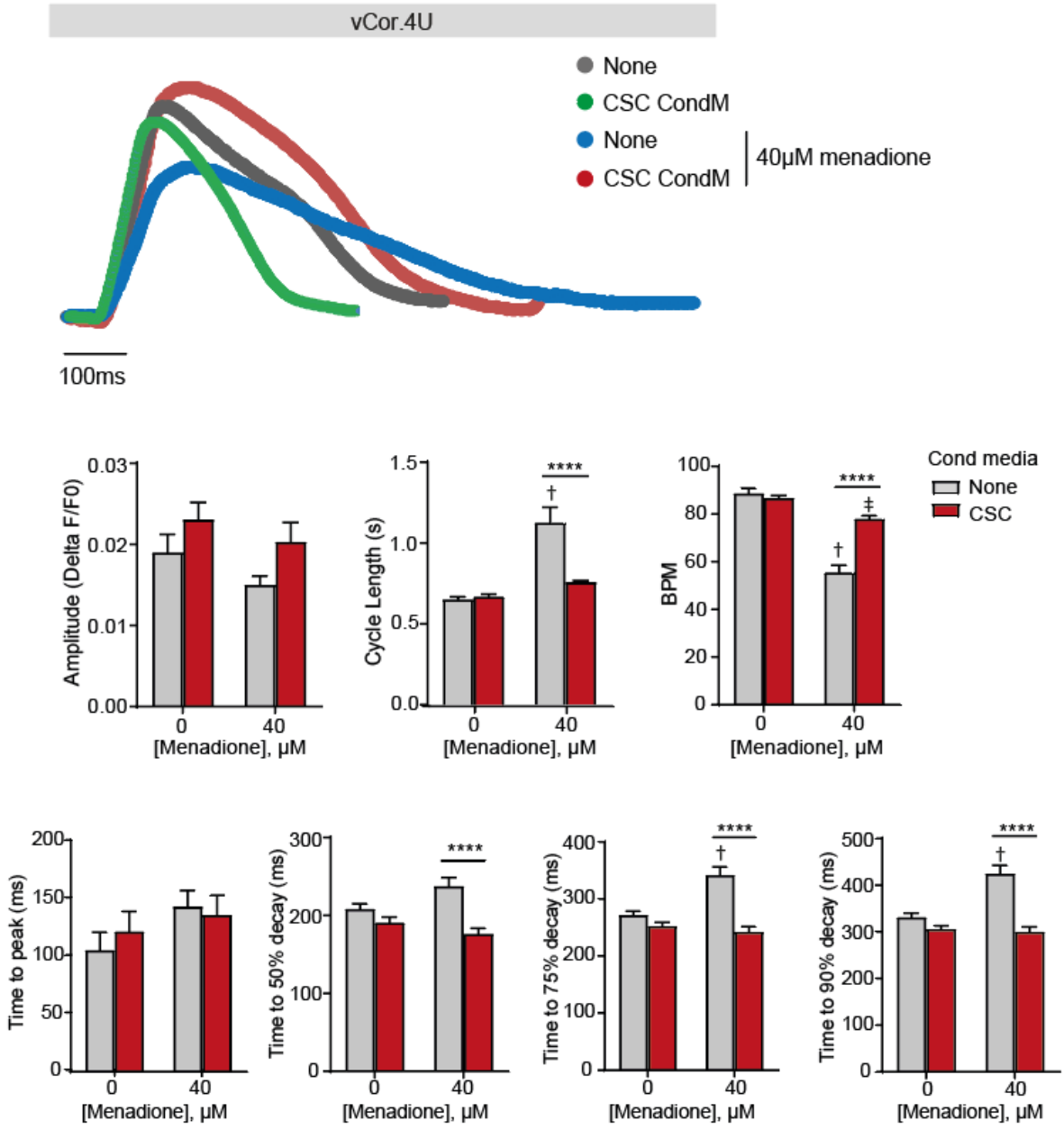



**Figure 18: CSC-conditioned media preserve Ca2+ cycling in hPSC-CM at sublethal concentrations of menadione.** Representative montage of calcium

cycling traces at baseline and following 24 hr of 40μM menadione, in the presence and absence of CSC-conditioned media. Bar graphs of calcium cycling parameters following staining with Fura4-AM. Data are shown as the mean ± SEM; n=15; ****, P<0.0001; †, P < 0.05, versus no menadione in standard medium; ‡, P<0.05, versus no menadione in CSC-conditioned medium.

### 3.1.20. CSC-conditioned media preserve action potential in hPSC-CM at sublethal concentrations of menadione

These abnormalities in calcium cycling do not distinguish between a direct effect versus consequences of changes in the action potential, the sequence of ion fluxes through specialized channels in the surface membrane, leading to cardiac contraction by triggering release of calcium from the sarcoplasmic reticulum. Abnormalities in action potential associated with oxidative stress may lead to defects in cardiac contraction, arrhythmias and sudden cardiac death (Ward and Giles, 1997). Here, we wanted to test whether menadione-induced oxidative stress leads to electrical dysfunction in human cardiomyocytes and subsequently, whether CSC-conditioned media ameliorate these effects. We treated vCor.4U cardiomyocytes at the sublethal concentration of 40μM menadione for 24 hr (Figure 3.6) in the presence and absence of CSC-conditioned media and used the ratiometric dye di-4-ANEPPS, a fast-response probe that changes fluorescent properties in response to a change in its surrounding electrical field (Hortigon-Vinagre et al., 2016; Ribeiro et al., 2015). We then acquired voltage measurements on the CellOptiq platform (Figure 3.19). In the presence of menadione, the voltage amplitude did not change (0.017±0.002 ms without menadione to 0.012±0.0003 ms at 40 μM). Cycle length showed a delay of 1.6-fold from 0.823±0.008 s without menadione to 1.321s±0.002 at 40 μM. Furthermore, menadione caused little or no effect on the time to peak from 40±0.685 ms without menadione to 47.3±1.9 ms at 40 μM menadione, but a marked delay in time to 75% or 90% decay from 240±14.7 ms and 273.2±10.4 ms in the absence of

menadione to 402.8±8.9 ms and 445.6±6.0 ms at 40 μM respectively (Figure 3.19). Thus, these data show action potential prolongation in menadione-treated cardiomyocytes, mainly a result of longer plateau and repolarisation phase (increased time taken for signal decay), rather than delays in depolarisation. Conversely, CSC-conditioned media inhibited the menadione-induced effects, maintaining a more normal action potential transient. More specifically, in the presence of CSC-conditioned media, action potential amplitude was recovered 1.6-fold from the menadione-treated condition to 0.018±0.001 ms in the presence of CSC-conditioned media, accompanied by a decrease of 1.4-fold in cycle length at 40 μM of menadione to 0.946±0.002 s in the presence of conditioned medium. In terms of action potential repolarisation, CSC-conditioned media promoted a recovery in time to peak of 38.4±0.692 ms from the menadione-treated myocytes and a 1.4-fold reduction in the time taken for 75% and 90% signal decay from the menadione-stressed condition to 277.3±4.0 ms and 319.6±7.2 ms, respectively (Figure 3.19). Membrane repolarisation depends on the correct function of $Ca^{2+}$ channels, which need to close and allow rectifier $K^{+}$ channels to return the transmembrane potential to baseline (typically -90 mV). Therefore, the effects in action potential prolongation that we observe here most likely relate to one or both essential mechanisms for repolarisation.

.

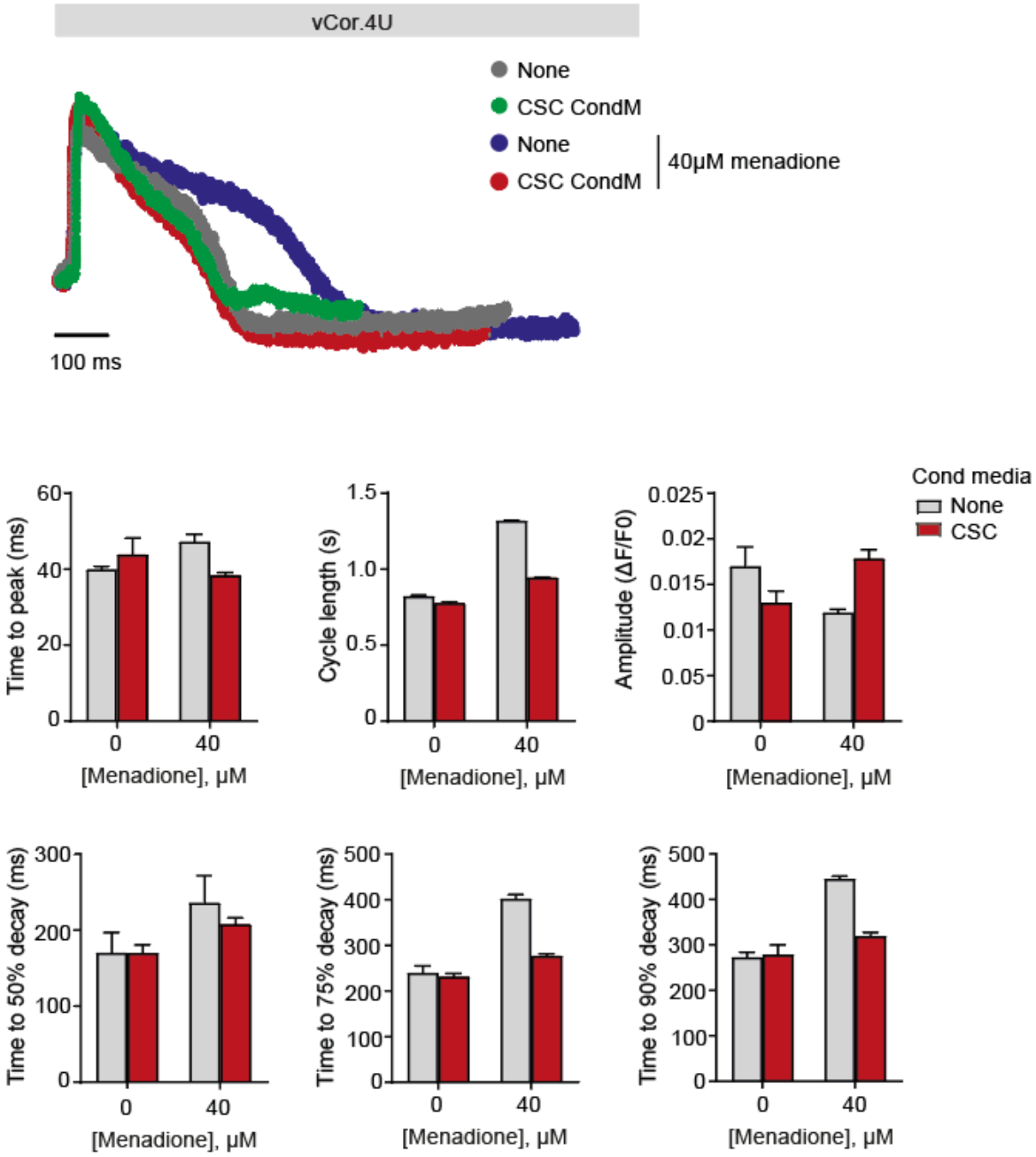



**Figure 3.19: CSC-conditioned media preserve action potential in hPSC-CM at sublethal concentrations of menadione.** Representative montage of voltage traces at baseline and following 24 hr of 40μM menadione, in the presence and absence of CSC-conditioned media. Bar graphs of voltage parameters following staining with di-4-ANEPPS. Data are shown as the mean ± SEM; n=6 (one independent experiment).

### 3.1.21. Summary and conclusions

Earlier work from our group showed that when injected in the mouse heart at the time of MI, Sca1$^+$ SP CSC significantly improve cardiac function, partly via a reduction in infarct size, despite the poor cell retention even one day after injury. Thus, we tested a putative paracrine protective effect on cardiomyocytes. As a first proof of concept, we injected cell-free CSC-derived conditioned medium at the time of MI and observed significant inhibition of cardiomyocyte apoptosis 24 hr later. Using a more translationally relevant target model, we showed that CSC-conditioned media confer significant protection of human cardiomyocytes (hPSC-CM) from oxidative stress-mediated death. Specifically, the CSC secretome protects two independent hPSC-CM lines (vCor.4U and IMR-90) from menadione-, doxorubicin- and imatinib-induced stress. Mechanisms of protection from menadione include inhibition of DNA fragmentation, preservation of mitochondrial polarisation and reduction of ROS. For doxorubicin, CSC-conditioned medium protection did not involve reduction of ROS and the results on mitochondrial depolarisation were inconclusive due to technical issues arising from the red colour of the drug and possibly interfering with the respective assays. In contrast, for imatinib, CSC-conditioned media inhibited hPSC-CM death through preservation of mitochondrial depolarisation. While CSC-conditioned media inhibit hPSC-CM death following both doxorubicin and imatinib stress, the underlying mechanisms might differ and need to be further investigated. Notably, following treatment with sublethal concentrations of menadione, surviving hPSC-CM were found to maintain their functionality, as demonstrated by calcium cycling and action potential experiments, suggesting that CSC-conditioned media protect myocytes not only from cell death, but also from functional defects.

## 3.2. Characterisation of the cardioprotective CSC secretome

In the previous chapter we demonstrated that CSC-conditioned media protect mouse and human cardiomyocytes against cell death mediated by different categories of stress molecules, including the oxidative stress inducer menadione and two unrelated cardiotoxic anti-cancer agents, doxorubicin and imatinib. Our next aim was to investigate what CSC-secreted signals might be mediating the described cardio-protective effect. This chapter focuses on the characterisation of the secretor CSC, the target hPSC-CM and the CSC-conditioned medium aiming to gain an insight into the specific paracrine factors mediating the protection.

### 3.2.1. Protection by CSC-conditioned media is mediated by the >3kDa molecular fraction

In our quest to gain an insight in the specific factors that achieve the previously described cardio-protective effects, we performed size fractionation of the CSC-conditioned medium using concentrator columns with a molecular weight cut-off of 3kDa. Following syringe-filtration and a 90-minute centrifugation at ~4600g, the fraction retained by the columns, i.e. >3kDa in size, had the ability to significantly protect both vCor4.U (Figure 3.20A) and IMR-90 (Figure 3.20B) hPSC-CM from menadione-induced death. More specifically, the proportion of $DRAQ7^+$ vCor.4U cardiomyocytes was reduced from 24.8±4.3% after menadione treatment, to 6.2±1.2% by unfractionated CSC-conditioned media and to 9.4±1.6% by the >3kDa fraction. With IMR-90 cells the prevalence of $DRAQ7^+$ myocytes provoked by menadione was reduced from 50.5±17% to 11.7±2.4% by the unfractionated CSC-conditioned media and to 8.99±2.7% by the >3kDa fraction. Thus, the CSC-induced effect is not mediated by small molecular weight metabolites (such as nitric oxide, adenoside, prostanoids,

endovanilloids, endocannabinoids, leukotrienes, serofendic acid, metabolites of the aminoacids phenylalanine, tryptophan and tyrosine, etc.), which have been reported to mediate cardioprotection in some models (Totzeck et al., 2017; Tsibulnikov et al., 2019).

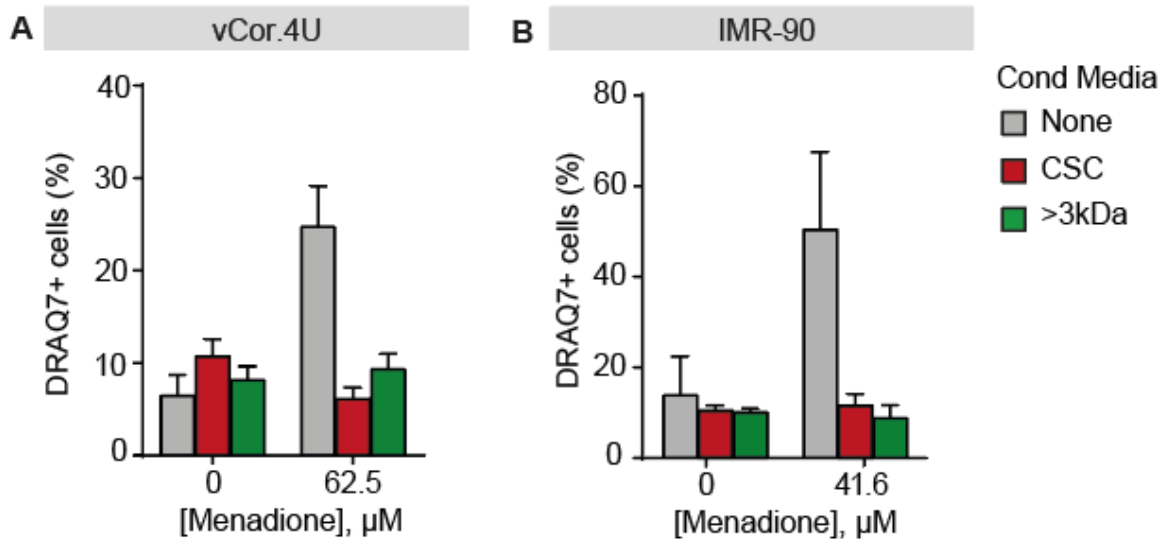



**Figure 3.20: Protection effect by CSC-conditioned media is mediated by the >3kDa molecular fraction.** CSC-conditioned media were fractionated using protein concentrator tubes with a molecular weight cut-off point of 3kDa. Bar graphs of DRAQ7 uptake in **A,** vCor.4U (n=6; two independent experiments) and **B,** IMR-90; n=3 (one independent experiment) 24 hr following menadione stress in the presence and absence of different size fractions of CSC-conditioned media. Data are shown as the mean ± SEM. These data are part of a publication currently in press by Scientific Reports.

### 3.2.2. Protection by CSC-conditioned media depends on thermo-labile molecules

The fraction of >3kDa encompasses several possible mediators including proteins, lipids and nucleotides. With the objective to narrow down these options, we performed a thermostability test, in which we heated CSC-conditioned media at 95°C for 10 min, a condition that would denature the protein component of the media, while keeping

most lipid and nucleotide components intact. Our results show that after heat-treatment, CSC-conditioned media lose their ability to protect both vCor4.U (Figure 3.21A) and IMR-90 (Figure 3.21B) cardiomyocytes from menadione-induced stress. In more detail, in vCor4U cells, the proportion of $DRAQ7^+$ cells without menadione was 6.4±1.8% and was increased 4-fold to 27.9±2.7% by 41.6μM menadione ($P<0.0001$). Unlike CSC-conditioned media, which reduced $DRAQ7^+$ prevalence back to 6.7±0.9% ($P<0.001$, versus menadione treated cells in standard medium), heated conditioned medium caused a further increase in death, reaching 55.6±6.8% $DRAQ7^+$ cardiomyocytes ($P<0.0001$, versus menadione-treated cells in standard medium). The latter increase is not surprising because heating might deplete the medium from essential growth factors and cytokines that help the response of the cells against menadione. Hence, potentially, the heat-denaturation of these proteins renders the cardiomyocytes even more susceptible to oxidative stress, resulting in higher death rates than with menadione alone.

In IMR-90 cardiomyocytes, menadione treatment induced a 4-fold increase in the prevalence of $DRAQ7^+$ cells, from 14.8±6.0% to 57.4±0.9% at 41.6μM menadione. CSC-conditioned media reduced the prevalence of $DRAQ7^+$ cells to 34.0±4.5%, whilst the heat-treated medium maintained a relatively high $DRAQ7^+$ signal at 61.0±5.1%. Therefore, heat-resistant lipids such as prostaglandins, whose role in cardio-protection has been extensively reported (Frias et al., 2008; Hsueh et al., 2014), as well as highly heat-resistant miRNAs (Mitchell et al., 2008) can be excluded from our list of likely effector molecules. Rather, our data point to a protective component having the nature of a secreted protein such as cytokine, chemokine or growth factor.

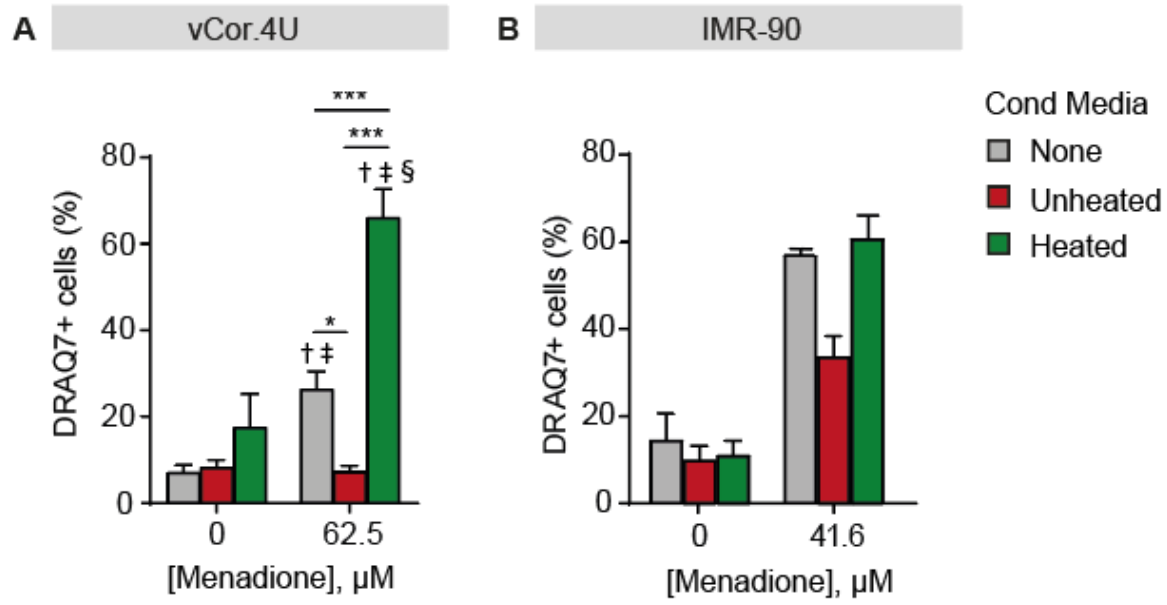



**Figure 3.21: Protection by CSC-conditioned media depends on thermo-labile molecules.** CSC-conditioned media were heated for 10 min at 90°C. Bar graphs of DRAQ7 uptake in **A,** vCor.4U (n=9) and **B,** IMR-90; n=6 (two independent experiments) 24 hr following menadione stress in the presence and absence of thermally treated CSC-conditioned media. Data are shown as the mean ± SEM; *, P<0.05; ***, P<0.001; †, P < 0.05, versus no menadione in standard medium; ‡, P<0.05, versus no menadione in CSC-conditioned medium; §, P<0.05, versus no menadione in heated conditioned medium. These data are part of a publication currently in press by Scientific Reports.

### 3.2.3. Protection by CSC-conditioned media is exosome-independent

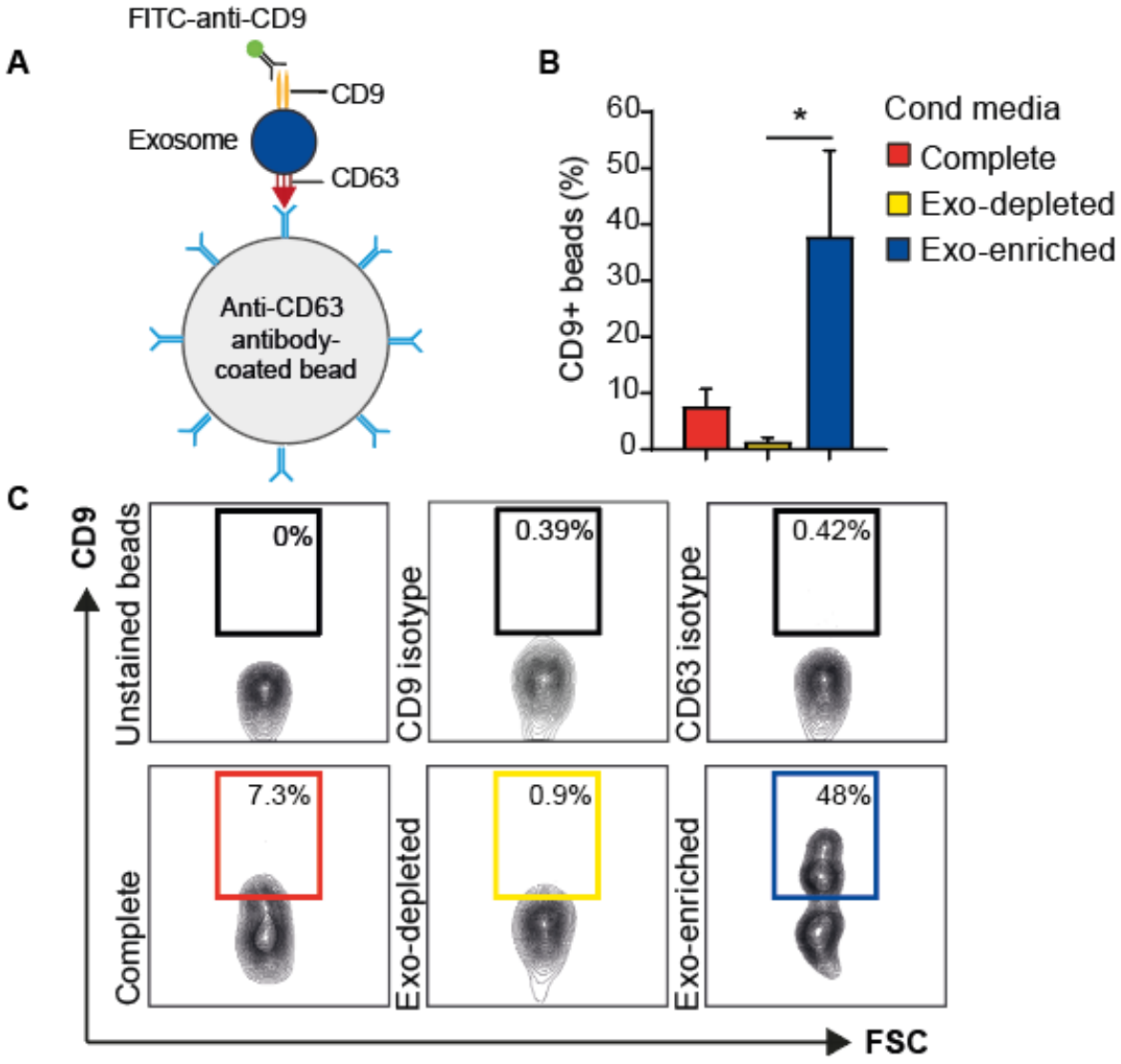
We hypothesise that our protective factor(s) is a secreted protein, but in several remarkable studies extracellular vesicles (exosomes) have been implicated in cardio-protection, suspected of carrying paracrine effectors into the site of infarction and its various component cells (Barile et al., 2014; Lai et al., 2010; Liang et al., 2016; Todorova et al., 2017; Zhao et al., 2015). Exosomes are nanosized extracellular vesicles of endosomal origin, secreted by a range of cells into the extracellular space, under normal and pathological conditions (Lawson et al., 2016; Sluijter et al., 2014; Valadi et al., 2007). Importantly, the paracrine benefits of several mouse and human

CSCs, cardiosphere-derived cells, mesenchymal stem cells (MSC) and pluripotent stem cell derived cardiomyocytes (PSC-CM) have been ascribed to cell-cell communication via exosomes (Davidson and Yellon, 2018; Ibrahim and Marbán, 2016).

Here, we used ultracentrifugation, the most commonly used method, for the isolation of exosomes from cell culture media. We then used a flow cytometry sandwich immunoassay approach to validate the exosome depletion from our media, employing exosome-surface proteins that bind to CD63-coated latex beads, forming a complex that then can be detected using a fluorescently labelled CD-9 antibody (Figure 22A). In the exosome-enriched fraction the prevalence of $CD9^+$ beads is 37.9±15.2%, which is a 5-fold enrichment over the unfractionated medium (7.67±3.1%; $P>0.05$) and 26-fold enrichment over the exosome-depleted fraction (1.45±0.6%; $P<0.05$; Figure 22B, C). These results confirm a successful fractionation of the exosome-enriched and -depleted conditioned media. Flow cytometry analysis was performed by Dr Patricia Chaves.

Particle size analysis in the different CSC-conditioned media fractions was performed using the NanoSight version NTA3.2DevBuild3.2.16 for nanoparticle tracking analysis (NTA) at the University of Bristol in a collaboration with Prof Costanza Emanueli. Samples isolated from the same experiment were run in quadruplicate with a detection threshold of 9 and a syringe pump speed of 50. As expected, our results confirm that the exosome-enriched fraction contains a higher proportion of nanoparticles with a concentration of $2.27±0.0366x10^{11}$ particles/ml as opposed to $8.18±0.165x10^{9}$ particles/ml in complete conditioned medium ($P<0.0001$) and $2.31±0.265x10^{9}$ particles/ml in the exosome-depleted fraction ($P<0.0001$ vs exosome-enriched and

P<0.05 vs complete; Figure 3.22D). Size distribution was similar between the different fractions: 114.3±1.49 nm, complete; 115.8±1.04, exosome-enriched; and 130.75±34.7, exosome-depleted. Despite the higher noise in the histogram obtained for the exosome-depleted fraction, the small number of residual particles seem to have the same size distribution as those in unfractionated or exosome-enriched media (Figure 3.22D).



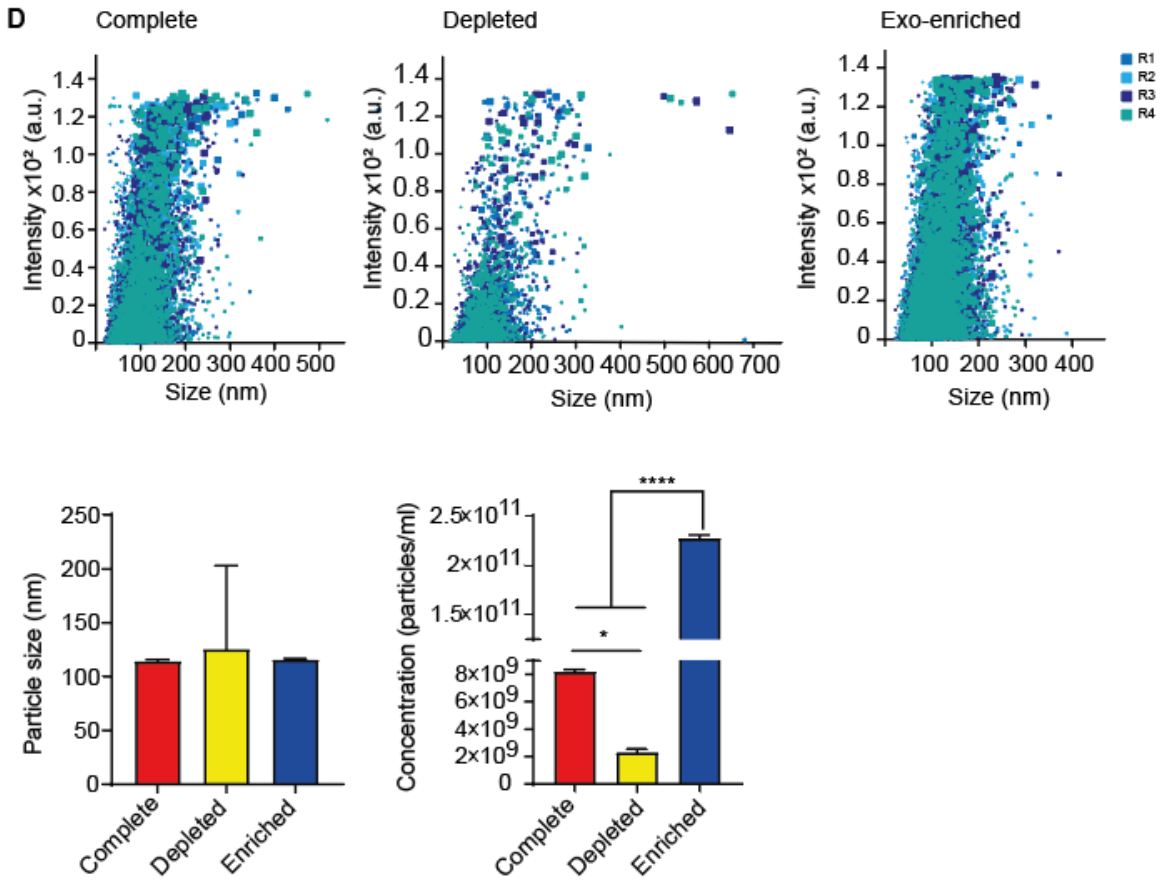



**Figure 3.22: Exosome depletion and identification from CSC-conditioned media by ultracentrifugation and flow cytometry. A,** Schematic of exosome detection assay using anti-CD63 coated latex beads to bind the exosomes and fluorescently-conjugated anti-CD9 for detection of bead-exosome complexes by flow cytometry. **B,** Bar graph showing the quantification of the contour plots in **(C)** indicating the proportion of $CD9^+$ bead-exosome complexes in the different CSC-conditioned media fractions. **C,** Contour plots depicting $CD9^+$ exosome-bead complexes in the exosome enriched fractions and negative controls (unstained beads, CD9 isotype and CD63 isotype). Data are shown as the mean ± SEM; *, $P<0.05$. Flow cytometry was performed by Dr Patricia Chaves. **D,** NTA analysis of the CSC-conditioned media fractions with histograms showing particle concentration and size distribution in the complete (left), depleted (centre) and exosome-enriched fraction (right). Summary bar graphs at the bottom show particle size and concentration measurements. Data are shown as the mean ± SD; n = 4; *, $P<0.05$; ****, $P<0.0001$. NTA analysis was performed by collaborator Prof Costanza Emanueli. These data are part of a publication currently in press by Scientific Reports.

The CSC-conditioned media fractions were then used in a protection assay to confirm their effect on menadione-stressed vCor.4U cardiomyocytes. A starting volume of 48ml CSC-conditioned medium was ultra-centrifuged to obtain the exosome-depleted and -enriched fractions. The exosome-enriched fraction was resuspended in 400µl PBS. In order to ensure that any lack of protection by the exosome-enriched fraction is not due to the loss or inactivation of essential nutrients or other factors during the ultracentrifugation step, we diluted the final fraction with fresh cardiomyocyte medium back to its original concentration (diluted x120). The exosome-depleted fraction maintained its ability to inhibit DRAQ7 uptake, whereas the exosome-enriched fraction did not (Figure 3.23). A 2-fold induction of cell death was obtained from 13.5±1.6% $DRAQ7^+$ myocytes in the absence of menadione, to 24.5±1.3% $DRAQ7^+$ myocytes at 62.5µM ($P>0.05$). The exosome-depleted medium reduced the prevalence of $DRAQ7^+$ signal to 8.0±1.3% ($P<0.0001$), i.e., around a third less than the reduction achieved by the unfractionated conditioned media control, 13.2±1.8% ($P<0.0001$). However, the exosome enriched fraction increased the levels of cell death to 32.9±0.9%, one-third higher than the menadione-treated cardiomyocytes ($P<0.001$; Figure 3.23). The higher level of $DRAQ7^+$ signal in the exosome-enriched fraction-treated cells than in the menadione-treated ones, could be explained by the ultracentrifugation-mediated unintended concentration of toxic bi-products of culture medium, such as ammonia which has been reported to appear from the spontaneous decomposition of L-glutamine (Heeneman et al., 1993). Other potential issues will be discussed later on, but might include toxicity of these particular cells' exosomes (Benjamins et al., 2019) or issues with the isolation strategy (Antounians et al., 2019). Nevertheless, under the conditions tested here, mechanisms alternative to exosomes likely mediate the observed protection of human cardiomyocytes from cell death.

While ultracentrifugation is currently the gold-standard method of choice in exosome isolation, it has some limitations as discussed above. Therefore, we confirmed our results using a different exosome isolation method, the ExoSpin columns (Cell Guidance Systems), that combine precipitation and size exclusion chromatography techniques to give highly pure exosome preparations. CSC-conditioned medium was prepared and centrifuged as described above to remove cells or debris and 50ml were mixed with the ExoSpin buffer and allowed to precipitate for 1 hr at 4°C. The resulting mixture was centrifuged and the supernatant was discarded. Note, that in this case, the exosome-depleted fraction could not be used for hPSC-CM treatment as it still contained the ExoSpin buffer, which could interfere with cell viability. The exosome-containing pellet was resuspended in 100µl PBS and loaded onto an equilibrated ExoSpin purification column for elution. Following the manufacturer recommendations, the columns were centrifuged and washed prior to elution of a final volume of 200µl purified exosomes. Similar to the ultracentrifugation-derived exosome fractions, our results showed that the exosome-enriched fraction was unable to protect hPSC-CM from menadione stress and indeed it seems to induce higher death than the menadione-only control (Figure 3.23B). In contrast, the unfractionated CSC-conditioned medium control significantly reduced DRAQ7 uptake in myocytes. In more detail, at 62.5µM menadione, DRAQ7 uptake was 35.2±6.4% in the menadione only condition and decreased to 10.1±1.7% in the presence of CSC-conditioned medium ($P<0.001$) whilst in the presence of the exosome-enriched fraction DRAQ7 uptake increased to 41.8±4.3% ($P<0.0001$ vs complete medium).

In summary, using two independent methods of exosome isolation and purification, we show here that CSC-conditioned medium-conferred protection on hPSC-CM from oxidative stress occurs independently of exosomes.

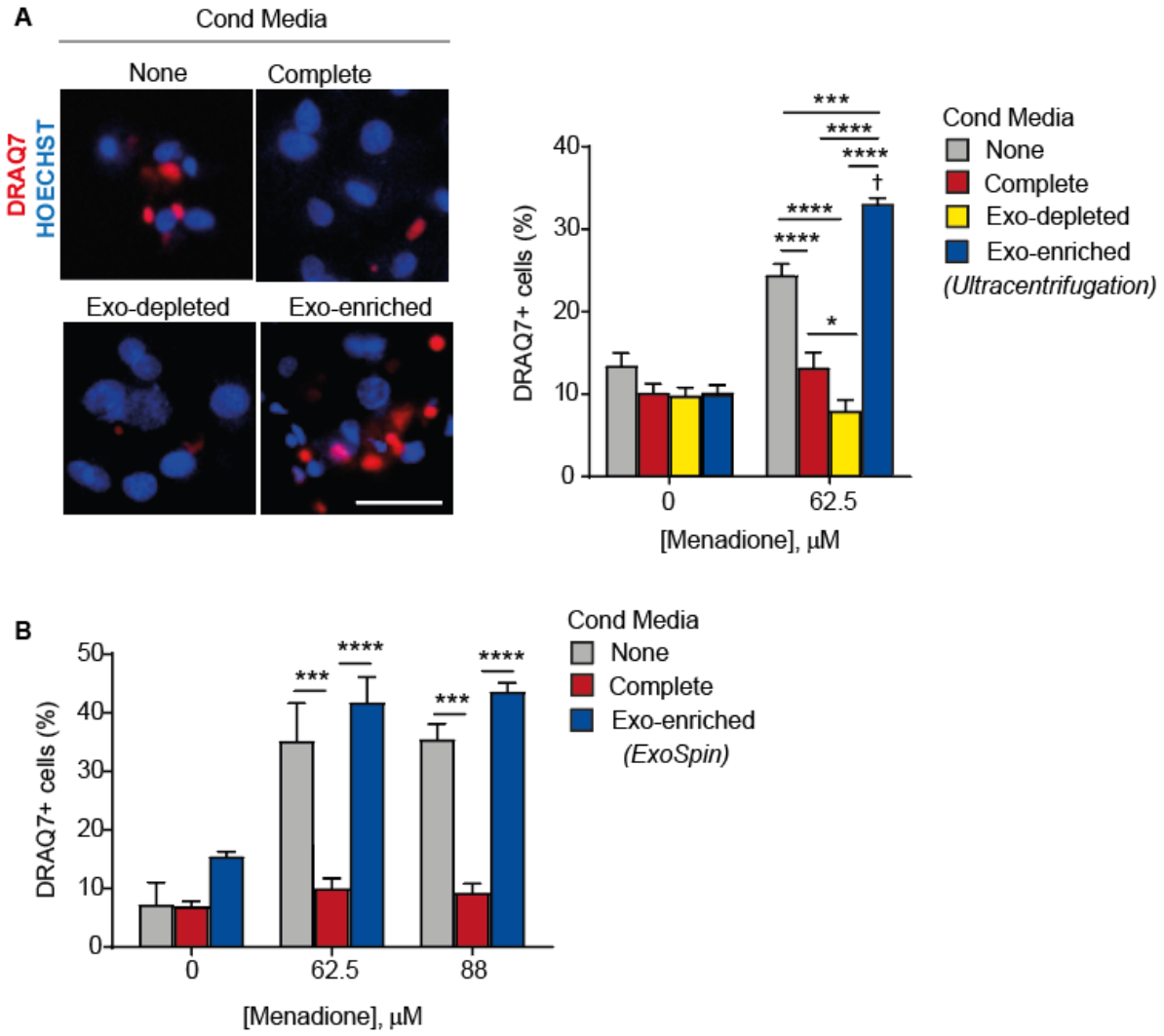



**Figure 3.23: Protection by CSC-conditioned media is exosome-independent.** Representative images and bar graph of DRAQ7 uptake in vCor.4U cells 24 hr following menadione stress, under treatment of exosome-fractionated CSC-conditioned media after **A,** ultracentrifugation or **B,** precipitation and purification using ExoSpin columns. Data are shown as the mean ± SEM; n=10 for **A** and n = 4 for **B**; *, P<0.05; ***, P<0.001; ****, P<0.0001; †, P < 0.05, versus no menadione in standard medium. These data are part of a publication currently in press by Scientific Reports.

### 3.2.4. Paracrine candidate identification in CSC by single cell qPCR and bulk RNA-Seq

To explore the cardio-protective paracrine potential of CSC, we aimed to define the genes encoding for secreted factors that enriched in protective CSC versus non-protective TTF populations. To compare the transcriptomes of the two populations we started with a candidate-driven single-cell qRT-PCR approach assaying 45 probes of known, previously studied cardioprotective paracrine factors taken from the literature (Figure 3.24). The heatmap shows unbiased 2D clustering with highly enriched genes depicted in red and low or negative gene expression in blue. The CSC population was enriched in cardiac transcription factor genes (*Tbx20, Tbx5, Hand2, Gata4*), which were absent from TTF. As expected, both populations showed no expression of late cardiac differentiation markers (*Hand1, Myh6, Myl2*), while paracrine factor expression was distinctly spread between the two populations. TTF were enriched in *Ereg, Sod3, Il11, Ccl7, Ccl2, Cxcl1, Angpt1, Il1rl1, Angpt4, mPGES1, Cxcl5* whereas CSC were enriched in *Il6, Bmp4* and *Igf1*. Both populations were equally enriched in *Angptl4, Ly6a, Sngptl2, Csf1, Cxcl12, Pdgfra, Bmper, Ngf* and *Ang* The relative enrichment of the non-protective TTF in so many paracrine factors, at least at the RNA level, was surprising, although, the relative protein levels remained to be validated. Microfluidic chips used for these qRT-PCR analyses were run by Chiara Beretta and analysed by Dr Michela Noseda.

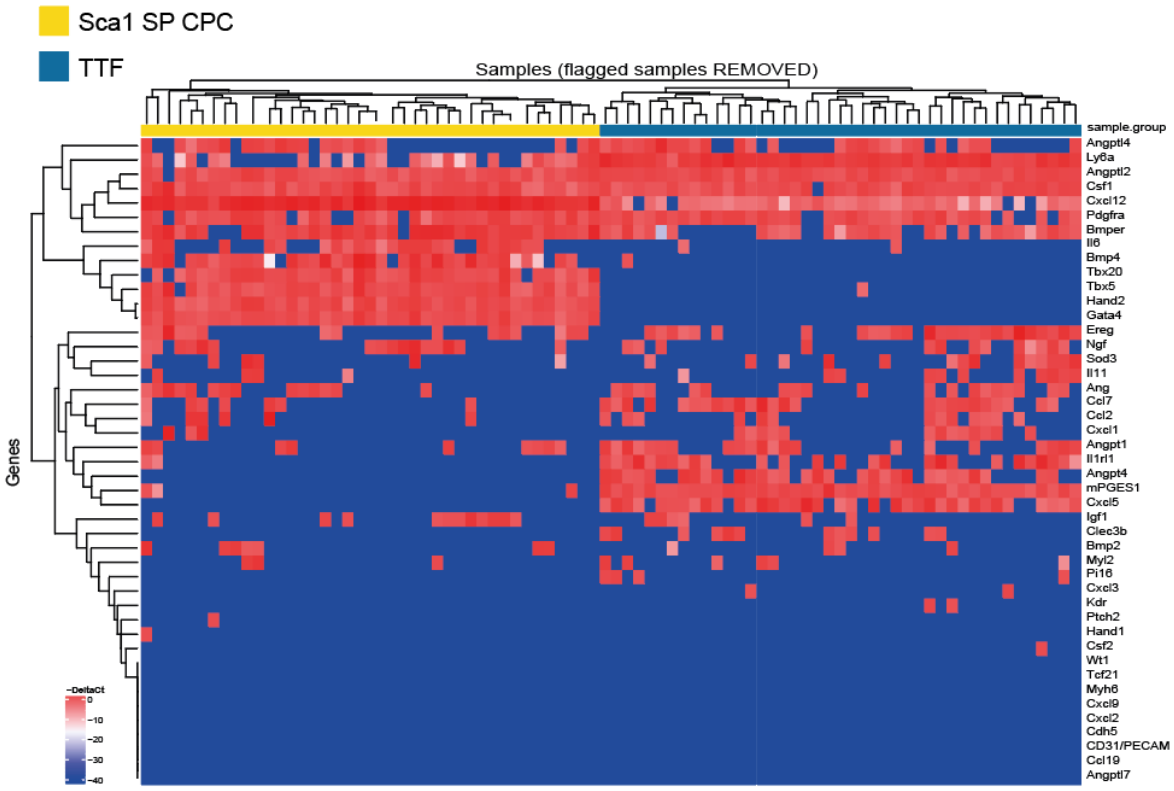



**Figure 3.24: Paracrine candidate identification by single cell qPCR.** Heat map of unbiased clustering with 85 single cells (41 CSC and 44 TTF cells) on the x-axis and 45 single genes on the y-axis. Expression is shown as $-\Delta_{Ct}$ values (red is high and blue is low or negative). Enrichment of paracrine genes was overlapping but distinguishable in the CSC and the TTF populations, which are resolved clearly from one another. Single cell qRT-PCR analysis was performed by Dr Michela Noseda.

Given the overlap in our selected paracrine candidates' expression between the protective CSC and non-protective TTF, we considered that an unbiased approach — bulk RNA-Seq — would benefit our investigation and provide previously overlooked transcripts to follow up. Using the DEseq2 tool in R, we identified 14,720 differentially expressed transcripts with a p-value < 0.05, out of which 4,328 were highly enriched in the CSC population with an average difference of > 3000 counts. Targets enriched in CSC versus TTF were mapped for relevant Gene Ontology categories, one of which was 'Negative Regulation of Cell Death', which gave us a total of 266 targets. Subsequently, MetazSecKB (Meinken et al., 2015) was used to identify more

specifically the curated transcripts that are secreted once translated, which gave us a total of 81 targets out of the 4,328 differentially expressed genes (Figure 3.25A). The overlapping 9 transcripts depicted in the heat map (Figure 3.25B) were identified - fulfilling the dual criteria of secreted proteins inhibiting cell death. Interestingly, two of the nine (Igf1, Bmp4) were among the three a priori candidates enriched in CSCs, as determined by previous single-cell PCR. The RNA-Seq data were analysed by Dr Antonio MA Miranda.

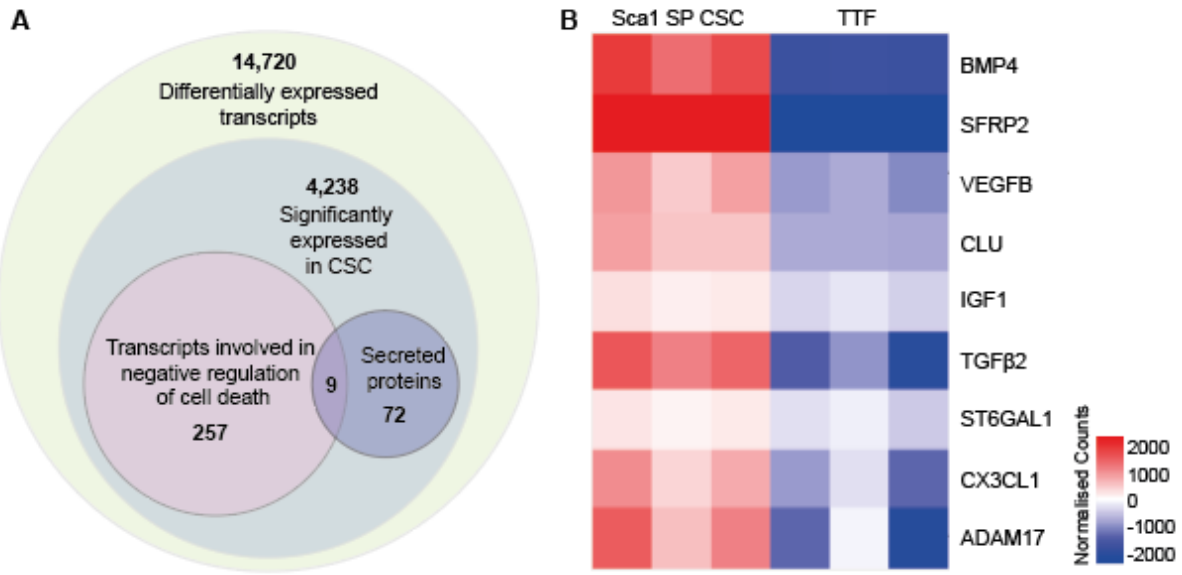



**Figure 3.25: Paracrine candidate identification by bulk RNA-Seq. A,** Venn diagram showing our data mining strategy. Out of 14,720 transcripts differentially expressed in the CSC versus the TTF and 4,238 transcripts significantly enriched in the CSC, a total of 266 were predicted to be involved in the negative regulation of cell death and 81 contained a sequence that predicted protein secretion. **B,** Heatmap of unbiased clustering of the 9 overlapping transcripts derived from the Venn diagram. The heatmap shows high gene expression in number of counts (high expression in red and low / negative expression in blue. Values represent read number change normalised to the average read number of each specific probe. RNA-Seq analysis was performed by Dr Antonio MA Miranda.

### 3.2.5. Neither single-factor titrations nor a six-factor cocktail protects human cardiomyocytes from menadione

With the objective to identify effective factor concentrations and as a pre-requisite for a combinatorial experiment, single factor titrations were performed on menadione-treated vCor.4U and IMR90 cells for 24 hr, with CSC-conditioned media-treated cardiomyocytes used as a positive control. At the end of the incubation period, cells were stained with the cell death marker DRAQ7 as before. Candidates tested using this screen included proteins encoded by the transcripts enriched in CSC versus TTF (*Il-6, Igf1*; Figure 3.25), as well as additional paracrine factors suspected to have a cardioprotective effect from the literature (*Ccl2, Cxcl1, Cxcl5, Cxcl12, Dkk3* and *Ereg*; Figure 3.26). In all the displayed experiments, there was induction of cardiomyocyte death at 62 μM or 18.5 μM menadione, depending on the target cardiomyocyte line used, and a reduction in the prevalence of $DRAQ7^+$ cells conferred by the CSC-conditioned medium. The results amongst all candidates screened were similar, in contrast, showing their insufficiency alone to protect hPSC-CM under the conditions tested.

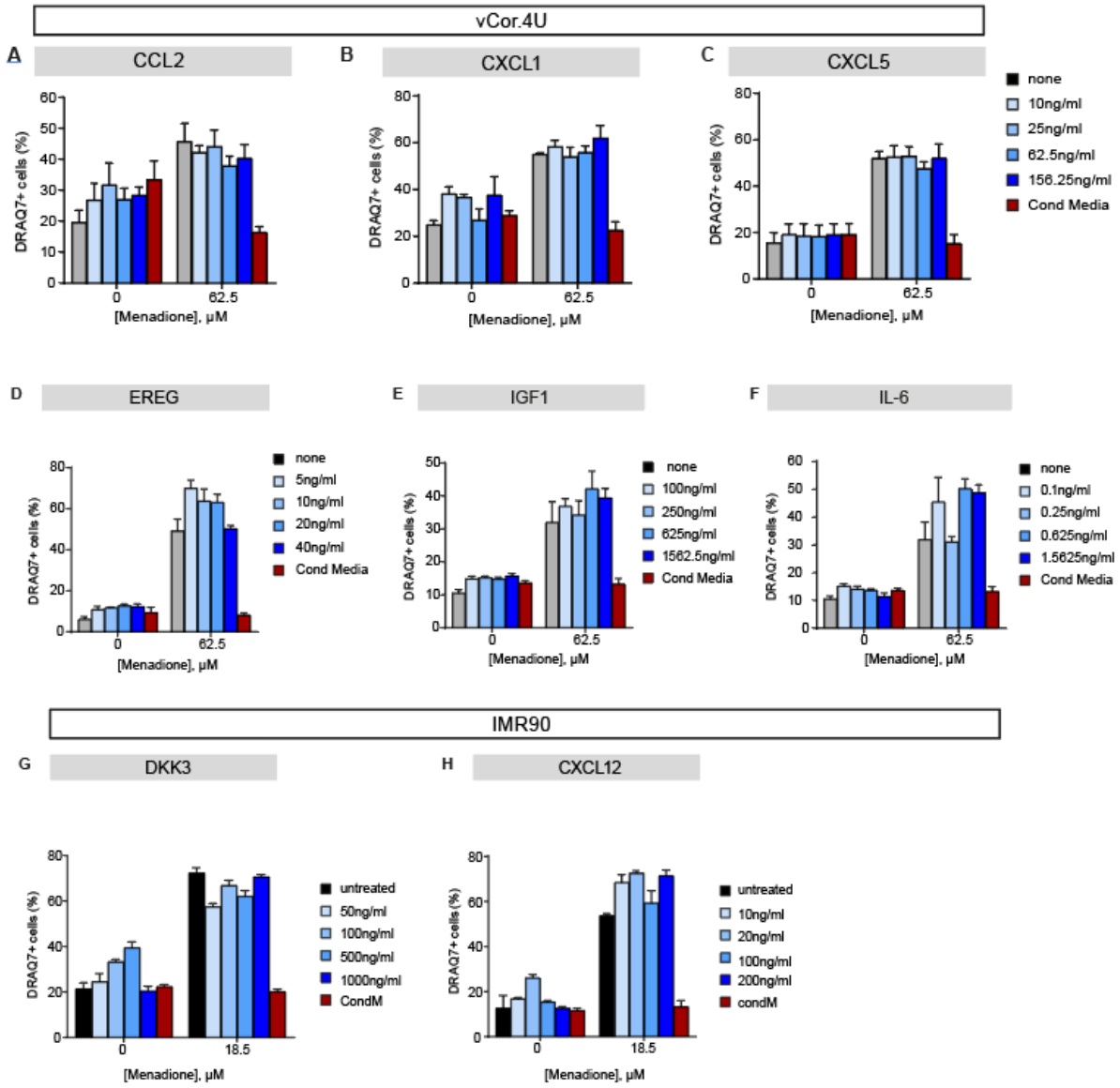



**Figure 3.26: Single factor titrations of candidates are insufficient to protect hPSC-CM from menadione stress.** Bar graphs of DRAQ7 uptake in vCor.4U or IMR90 cardiomyocytes (as labelled) 24 hr following 62.5µM or 18.5µM menadione stress in the presence of human recombinant **A,** CCL2; **B,** CXCL1; **C,** CXCL5; **D,** EREG; **E,** IGF1; **F,** IL-6; **G,** DKK3 and **H,** CXCL12. CSC-conditioned media shown in burgundy were used as the positive control. Data are shown as the mean ± SEM; n=3 (one independent experiment) for all factors except *Cxcl5*; n=6 (two independent experiments).

Since single factors were not sufficient to mimic the CSC-conditioned media protective effect, our next approach was to try a six-factor cocktail combining some of our

candidates that have been suggested to be cardioprotective in the literature. The concentrations used to make up the cocktail were selected based on the single-factor titrations, in combination with previously published specific activity data for each candidate (Figure 3.27A). The selected factors administered in a cocktail at the specific concentrations shown were insufficient to protect hPSC-CM from menadione-induced stress, unlike the CSC-conditioned media (Figure 3.27B). More specifically, cardiomyocyte cell death was significantly induced from 15.6±2.1% without menadione, to 33.7±3.7% at 62.5μM menadione. The prevalence of DRAQ7$^+$ cardiomyocytes was reduced 2-fold to 17.4±1.0% by CSC-conditioned media ($P<0.001$). The six-factor cocktail failed to reduce the prevalence of DRAQ7$^+$ cardiomyocytes, maintaining the signal at 33.3±3.3%. Thus, the protective effect might require a different set of factors or concentrations, and more thorough combinatorial studies are required to disentangle the paracrine molecules involved. Furthermore, at this point, we did not have any transcriptomic insight into the target cardiomyocytes and their responses e.g. how gene expression is changing or what receptors they express after menadione stress.

**A**

| Recombinant Factor | Final concentration (ng/ml) |
|---|---|
| BMPER | 600 |
| CCL2 | 60 |
| CXCL1 | 60 |
| CSF1 | 100 |
| EREG | 20 |
| IL-6 | 0.6 |

**B**

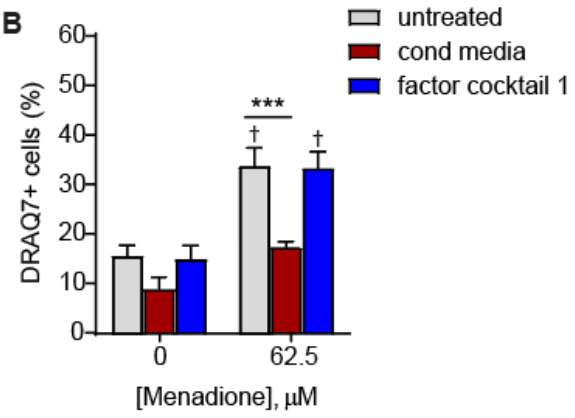



**Figure 3.27: A paracrine factor cocktail is insufficient to protect hPSC-CM from menadione stress. A,** Table of recombinant factor concentrations used and **B,** bar graph of DRAQ7 uptake in vCor.4U cardiomyocytes 24 hr following 62.5μM

menadione stress in the presence of a cocktail mix of human recombinant BMPER, CCL2, CXCL1, CSF1, EREG and IL6. CSC-conditioned media were used as the positive control. Data are shown as the mean ± SEM; n=11; ***, P<0.001; †, P < 0.05, versus no menadione.

### 3.2.6. RNA-Seq of menadione treated IMR90 cardiomyocytes with and without CSC-conditioned medium

To assess the transcriptional changes that occur in the human cardiomyocytes upon induction of oxidative stress and subsequent protection by CSC-conditioned media, we performed RNA-Seq on IMR90 cardiomyocytes (i) at baseline and following treatment with (ii) 20 μM menadione, (iii) CSC-conditioned medium, or (iv) 20 μM menadione plus CSC-conditioned medium for 24 hr.

#### 3.2.6.1. IMR90-cardiomyocyte quality and characterization

The availability of the wide transcriptomic information on the human IMR90-derived-cardiomyocytes, was an opportunity to perform some preliminary analysis on the genes demonstrating the quality and maturity of our stem cell-derived cardiomyocytes at baseline. Reads per million (RPM) are the number of sequenced oligonucleotides (read counts) divided first by the length of each gene and then by the scaling factor 1,000,000. RPM indicate the amplitude of expression of the specific gene within the data-set. In order to identify any residual expression of pluripotency genes the RPM for *NANOG* (0.5±0.03), *SOX2* (0.1±0.04) and *POU5F1* (0.008±0.001) were obtained, all of which seemed to be negligibly present in IMR90 cardiomyocytes (Figure 3.28A). Furthermore, there was no residual expression of genes specific to early cardiac or mesoderm progenitor cells such as *MESP1* (0.4±0.04), *EOMES* (0.002±0.001), *TBXT* (0), *KDR* (0.7±0.02) and *PDGFRα* (0.3±0.01; Figure 3.28A). In addition, fibroblast

markers like *DCN* (0.18±0.008) and *DDR2* (0.05±0.004) were absent (Figure 3.28 A). In contrast the cells showed highly robust expression of sarcomeric genes such as *MYH7* (544±26), which is the major myosin heavy chain gene in human ventricles, as well as *PLN* (2760±108), *ACTC1* (1396±5), *TNNC1* (926±28) and *TNNT2* (722±4; Figure 3.28A). Also, the cells showed little or no expression of the atrial-specific gene sarcolipin (*SLN*; 0.006±0.002) pointing to a ventricular signature, thus more relevant to our work. Amongst the limitations identified by this analysis was the high expression of *MYH6* (469±26), which was likely a reflection of immaturity rather than presence of atrial cells, given the lack of *SLN*. In addition, weak expression of genes for the ventricular protein triadin (*TRDN*; 1.19±0.07), cardiac troponin I (*TNNI3*; 49.6±1) and myosin light chain 2v (*MYL2*; 13.7±0.1) were further pointers to the immaturity of the cells (Figure 3.28A).

When looking at the RPM of genes encoding for cardiac-muscle specific channels, the major adult cardiac L-type calcium channel (*CACNA1C*; 0.5±0.03) had 7-fold higher counts than the fetal L-type calcium channel (*CACNA1D*; 0.07±0.004) and T-type calcium channel (*CACNA1H*; 0.09±0.007), which should be absent from the adult ventricle (Figure 3.28B) (Jiang et al., 2018; Napolitano and Antzelevitch, 2011). Furthermore, total counts were relatively high for hERG1 (*KCNH2*; 5.8±0.1), which is a major cardiac K channel, and *KCNJ5* (2.1±0.04), the inwardly rectifying K channel. The major cardiac Na channel *SCN5A* (1.7±0.1) was also highly expressed (Figure 3.28B). Furthermore, genes encoding for major cardiac transcription factors such as *NKX2-5* (99±6) and *MEF2A* (2.5±0.06) were robustly expressed (Figure 3.28C).

A more interesting gene-set to give an insight into the maturity of IMR90-derived cardiomyocytes was the cell cycle-specific genes. One of the most characteristic

properties of adult human heart compared to embryonic or neonatal heart is the loss of proliferation capacity and the acquisition of a post-mitotic, senescent phenotype. The studied cardiomyocytes showed 4-fold higher counts for *RB1* (0.3±0.006) versus *RBL1* (0.07±0.0004), encoding p107, confirming the developmental switch in tumour suppressor genes that underlies the post-mitotic phenotype (Figure 3.28D) (MacLellan et al., 2005; Sdek et al., 2011). Furthermore, high counts were observed for the genes encoding Cdk inhibitors p21 (*CDKN1A*; 33±1) and p27 (*CDKN1B*; 6±0.1) with lower counts for genes encoding cyclins A (*CCNA1, CCNA2*; 0.03±0.004, 2.7±0.114) and E (*CCNE1, CCNE2*; 0.9±0.02, 0.4±0.01; Figure 3.28D).

While the units of RPM provide a preliminary analysis and more solid conclusions can be obtained through direct comparisons of the IMR90 cells to published data-sets of human embryonic or adult heart, these data demonstrate an overall good quality of myocytes resembling mature human heart properties and provide a reasonable model for our work.

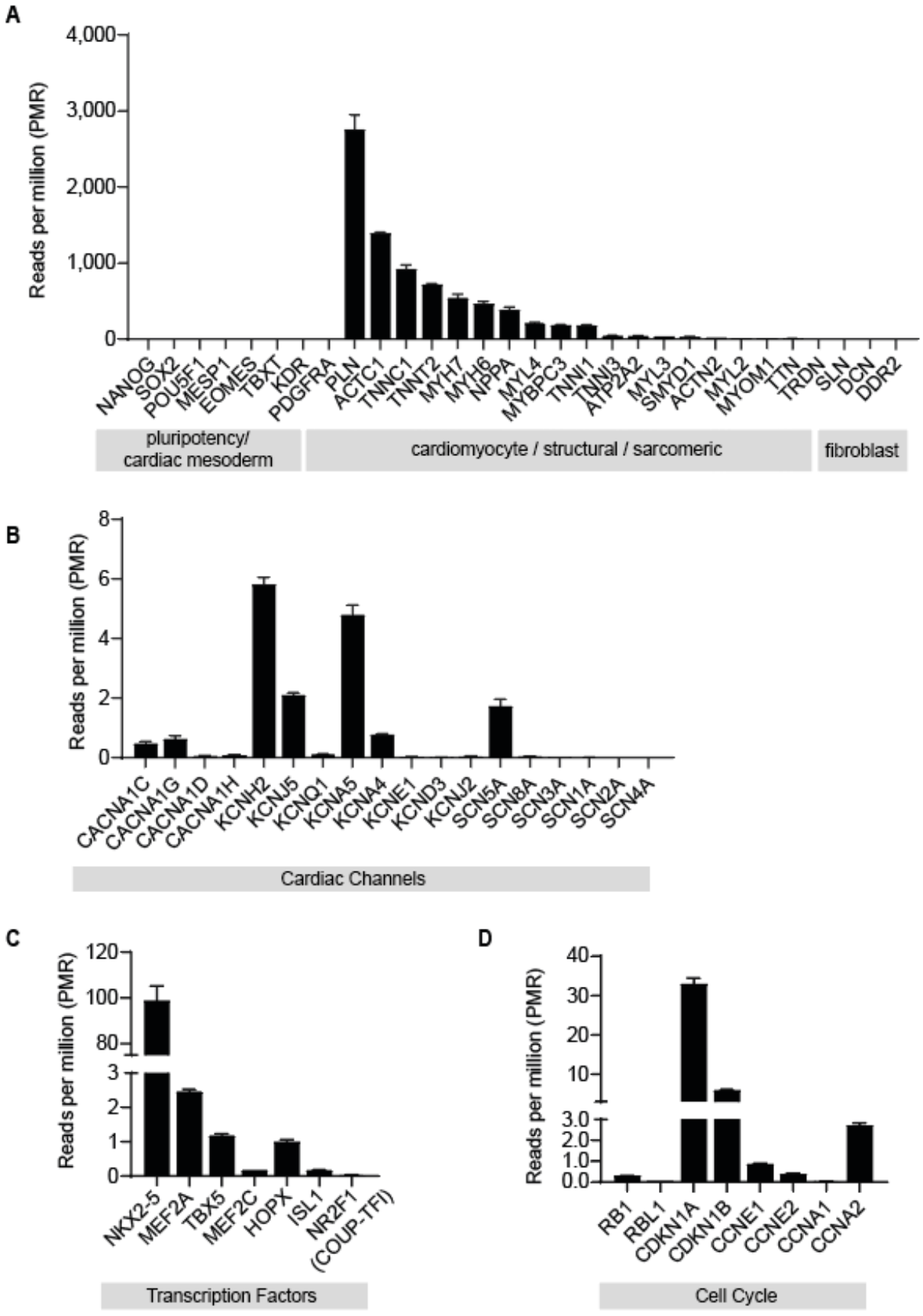

A
Reads per million (PMR)
4,000
3,000
2,000
1,000
0
NANOG
SOX2
POU5F1
MESP1
EOMES
TBXT
KDR
PDGFRA
PLN
ACTC1
TNNC1
TNNT2
MYH7
MYH6
NPPA
MYL4
MYBPC3
TNNI1
TNNI3
ATP2A2
MYL3
SMYD1
ACTN2
MYL2
MYOM1
TTN
TRDN
SLN
DCN
DDR2
pluripotency/
cardiac mesoderm
cardiomyocyte / structural / sarcomeric
fibroblast
B
Reads per million (PMR)
8
6
4
2
0
CACNA1C
CACNA1G
CACNA1D
CACNA1H
KCNH2
KCNJ5
KCNQ1
KCNA5
KCNA4
KCNE1
KCND3
KCNJ2
SCN5A
SCN8A
SCN3A
SCN1A
SCN2A
SCN4A
Cardiac Channels
C
Reads per million (PMR)
120
100
80
3
2
1
0
NKX2-5
MEF2A
TBX5
MEF2C
HOPX
ISL1
NR2F1
(COUP-TFI)
Transcription Factors
D
Reads per million (PMR)
40
30
20
10
3.0
2.0
1.0
0.0
RB1
RBL1
CDKN1A
CDKN1B
CCNE1
CCNE2
CCNA1
CCNA2
Cell Cycle

**Figure 3.28: IMR90-cardiomyocyte characterisation.** Bar graphs of reads per million (RPM) for the genes involved in **A,** Cardiac development and sarcomere identification; **B,** Cardiac channel expression and **C,** Cardiac transcription factors and **D,** Cell-cycle responses. Counts were obtained from RNA-Seq data-set on IMR90-cardiomyocytes at baseline. Data are mean ± SEM; n = 3. These data are part of a publication currently in press by Scientific Reports.

#### 3.2.6.2. Conditioned medium down-regulates apoptosis-related genes and preserves cardiac structural genes in lethally stressed human cardiomyocytes

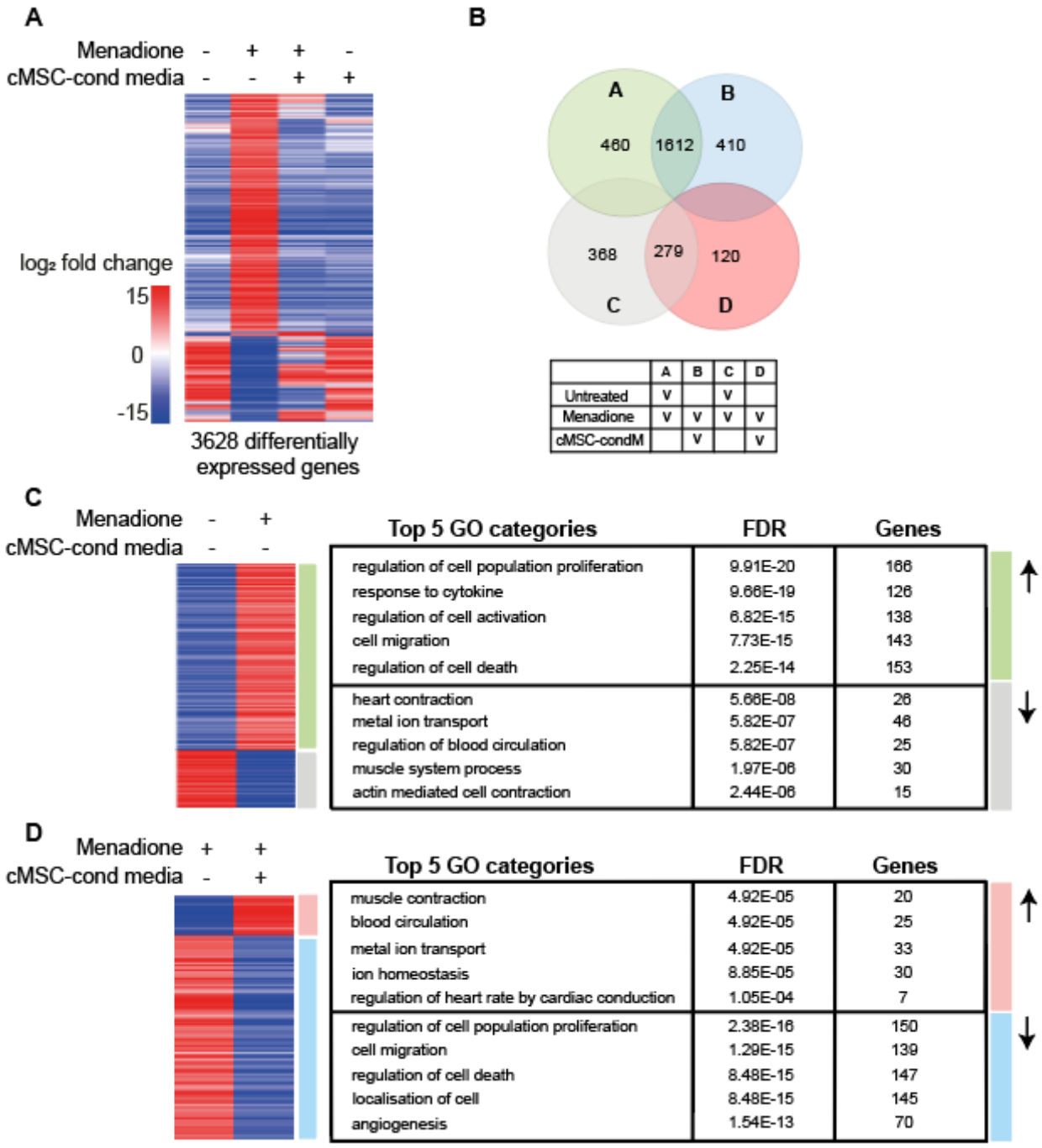
DESeq2 analysis identified 15,932 differentially expressed genes across the four conditions out of the total 60,639 (p-value < 0.05), which were further filtered using a more stringent threshold ($log_2$fold change > 2), resulting in a total of 3,628 differentially expressed genes (Figure 3.29A). Menadione treatment had a drastic change in the transcriptomic profile of human cardiomyocytes, driving the differential expression of 2,719 genes from the baseline i.e. ~75% of the transcripts (Figure 3.29A, B). In contrast, treatment of unstressed cells with CSC-conditioned media induced modest changes in the transcriptomic profile with none of the 15,932 genes being significantly affected from the baseline using the thresholds applied here. Notably, CSC-conditioned medium treatment of stressed cells, induced a differential expression of 2,421 transcripts compared to menadione-treated cells, thus effectively preserving ~90% of the differentially expressed transcriptome in IMR90 cardiomyocytes at levels represented in the baseline conditions, with only 72 genes remaining different to the unstressed cells (Figure 3.29A).

Data mining was performed using the ToppFun function in the ToppGene Suite tool to identify Gene Ontologies (GO, 'Biological Processes') for up- or down-regulated genes following menadione treatment. The top 50 GOs for each of the pairwise comparisons

can be found in Supplement 6.1. GO analysis of the transcripts induced in stressed myocytes identified categories directly relevant to the observed protection including ‘regulation of cell death’ (153 genes, FDR 7.56E-19), along with other GO categories relevant to paracrine circuits like ‘response to cytokine’ (126 genes, FDR 9.66E-19), ‘cell activation’ (138 genes, FDR 3.10E-17) and ‘regulation of cell population proliferation’ (166 genes, FDR 2.25E-14; Figure 3.29C and Supplement 6.1). Changes related to cell death included the induction of genes encoding proteins with proven adverse functions in cardiac muscle cell survival, such as death domain receptors (*TNFRSF8, TNFRSF10D, TNFRSF18*) (Zhao and Zhang, 2017) and DNA damage-inducible proteins and growth arrest mediators (*GADD45B, GADD45G*) (Kim et al., 2010b; Lucas et al., 2015; Salvador et al., 2013). Notable was the upregulation of *PMAIP1/NOXA*), whose product regulates mitochondrial membrane permeabilization and the release of apoptogens (Seo et al., 2003). Given that cardiomyocyte function is severely affected under conditions of oxidative stress, it was not surprising to detect downregulation of genes related to GOs of ‘heart contraction’ (FDR 5.66E-08) and ‘metal ion transport’ (FDR 5.82E-07), encompassing transcripts encoding major cardiac ion channels (*CACNA1G, KCNJ4, KCNJ5, SCN1A, SCN5A*), transporters (*ATP1A2*) and sarcomeric genes (*MYH7, TNNI2*; Figure 3.29C and Supplement 6.1) (van Duijvenboden et al., 2019; Harpster et al., 2006).

Treatment with CSC-conditioned media broadly interfered with menadione-dependent gene expression in the lethally stressed cardiomyocytes (Figure 3.29A, B). Conditioned medium prevents the expression of ~80% of the menadione-induced genes and it rescues >40% of the transcripts that were downregulated in the stressed cardiomyocytes (Figure 3.29B). Specifically, the CSC secretome prevented the expression of most genes associated with the GO cluster ‘regulation of cell death’

(FDR 8.48E-15), while preserving expression of genes in GOs related to cardiac function such as ‘muscle contraction’ (FDR 4.92E-05; Figure 3.29D and Supplement 6.1). Intriguingly, treating menadione-stressed myocytes with the CSC secretome inhibited the expression of transcripts for oxidative stress response factors (*ETS1, MMP3, FOS, CYP1B1, ANXA1*) (Ni et al., 2007; Venugopal and Jaiswal, 1996), pro-death signals (*TNFRSF8, TNFRSF10D, TNFRSF12A*) and Toll-like receptors (*TLR4, TLR6*) (Hoshino et al., 1999; Yu and Feng, 2018), which are part of the innate immunity circuit in cardiac muscle mediating some forms of cardiomyocyte death. Also, notable was interference with several transcripts encoding pro-apoptotic proteins known to affect cardiomyocytes (*ALK7, BCL10, GADD45B, PHLDA*) (Liu et al., 2013a; Wang et al., 2018a, 2017b) and others, not yet studied in the context of cardiac cell death, that are recognized mediators of apoptosis in other cell types (*FOXL2, INHBA, CASP4, IRF1, PMAIP1, PLEKHN1*) (Dogra et al., 2017; Galluzzi et al., 2018; Gao et al., 2010a; Kuriyama et al., 2018; Lee et al., 2005). In summary, transcriptomic analysis and, specifically, the downregulation of death- and apoptosis-related genes by CSC-conditioned medium suggests that the potent rescue of human cardiomyocyte survival depends on attenuation of one or more transcriptional circuits regulating apoptosis.




| | A | B | C | D |
|---|---|---|---|---|
| Untreated | V | | V | |
| Menadione | V | V | V | V |
| cMSC-condM | | V | | V |

| Top 5 GO categories | FDR | Genes |
|---|---|---|
| regulation of cell population proliferation | 9.91E-20 | 166 |
| response to cytokine | 9.66E-19 | 126 |
| regulation of cell activation | 6.82E-15 | 138 |
| cell migration | 7.73E-15 | 143 |
| regulation of cell death | 2.25E-14 | 153 |
| heart contraction | 5.66E-08 | 26 |
| metal ion transport | 5.82E-07 | 46 |
| regulation of blood circulation | 5.82E-07 | 25 |
| muscle system process | 1.97E-06 | 30 |
| actin mediated cell contraction | 2.44E-06 | 15 |

| Top 5 GO categories | FDR | Genes |
|---|---|---|
| muscle contraction | 4.92E-05 | 20 |
| blood circulation | 4.92E-05 | 25 |
| metal ion transport | 4.92E-05 | 33 |
| ion homeostasis | 8.85E-05 | 30 |
| regulation of heart rate by cardiac conduction | 1.05E-04 | 7 |
| regulation of cell population proliferation | 2.38E-16 | 150 |
| cell migration | 1.29E-15 | 139 |
| regulation of cell death | 8.48E-15 | 147 |
| localisation of cell | 8.48E-15 | 145 |
| angiogenesis | 1.54E-13 | 70 |

**Figure 3.29: Conditioned medium down-regulates apoptosis-related genes and preserves cardiac structural genes in lethally stressed human cardiomyocytes.** **A,** Heatmap of the 3,628 differentially expressed genes ($log_2$fold change > 2, p-value < 0.05) across the four IMR90-CM treatment groups (n = 3), shown by unsupervised cluster analysis. Oxidative stress was induced for 24hr with 20μM menadione with and without cMSC-conditioned medium treatment. The heatmap was created in SeqMonk using Pearson's Correlation clustering for the genes (y-axis). **B,** Venn diagram showing overlapping genes shared in the pairwise comparisons indicated. Green, up-regulated genes vs untreated; grey, down-regulated genes vs untreated; red, up-

regulated genes vs menadione-stressed; blue, down-regulated genes vs menadione-stressed. **C, D,** Curated heatmaps and tables of GOs for the changes induced by **(C)** menadione or **(D)** CSC-conditioned medium. Tables include top 5 non-redundant GOs, from the ToppGene 'Biological Process' database. For a full list of the generated GOs see Supplement 6.1. These data are part of a publication currently in press by Scientific Reports.

#### 3.2.6.3. Ligand-receptor interaction screen to predict protective candidates

Next, in order to identify potential pathways involved in cardiomyocyte protection by CSC-conditioned medium, we used a novel bioinformatics tool, CellPhoneDB (Efremova et al., 2019). This is a database of ligand-receptor interactions which can be used to interrogate large sequencing datasets and make computational inferences on protein interactions between the cell types analysed. Predicted receptor-ligand interactions between two cell types are calculated based on gene expression levels of a receptor by one cell type and the ligand by the second cell type. The interaction pairs included bi-directional pairwise comparisons between the following samples: CSC or TTF with IMR90-CM baseline (CMs), menadione-treated IMR90-CM (Mena-CMs), CSC-conditioned media treated CMs and menadione/CSC-conditioned media-treated CMs (Mena-CondM-CMs) (Figure 3.30A); The mean expression - which represents the average expression values of both partners in the corresponding interacting pair of cell types -was exported in a spreadsheet i.e. for each interaction pair *Mean Expression = Average (raw counts of Partner1+ raw counts of Partner2)*.

A selection approach was then undertaken to identify potentially interesting receptor-ligand interactions in our dataset (Figure 3.30B). Starting from a total of 1,084 interactions in all the pairs, 719 were excluded for not being present in any of the three biologically-relevant duos in our analysis, which were: (i) CSC → CMs; (ii) CSC → Mena-CMs (iii) CSC → Mena-CondM-CMs. Subsequently, 308 interactions were

excluded because they involved a ligand being expressed highly even by the non-protective TTF (TTF → CMs; TTF → Mena-CMs; TTF → Mena-CondM-CMs). In this case a 2-fold change threshold was used, i.e. a ligand was included only if it had a mean expression value in the CSC of at least 2-fold the mean expression value in the TTF. An additional 26 interactions were finally excluded due to ligands also being secreted by the hPSC-CM themselves even under non-protected conditions either at baseline or after menadione-treatment (CMs → CMs; Mena-CMs → Mena-CMs). Hence, following this series of exclusions, a total of 34 predicted 'interesting' interactions were flagged, out of the starting 1,084 (Figure 3.30D, Supplement 6.5).

Our results show that ~67% of the predicted interactions (23/34) between CSC ligands and receptors are present in cardiomyocytes that have been treated or not with menadione and conditioned medium (Figure 3.30C, D, Supplement 6.5). These ligand-receptor pairs included several Ephrin-Eph (mean expression (EFNA4-EPHA1) = 56.2) and TGFβ-TGFβR family interactions (mean expression (TGFβ1-TGFβR1) = 135), as well as IGF-IDE (mean expression = 616.7) and NRG-ERBB (mean expression = 122.8) interactions, all with previously reported roles in the regulation of cardiomyocyte apoptosis and survival (Bujak and Frangogiannis, 2007; O'Neal et al., 2013; Rupert and Coulombe, 2017; Zhao et al., 1998). Furthermore, CXCL10-DPP4 (mean expression = 3585.4) and IGF2-IDE (mean expression = 616.7; Figure 3.30D, Supplement 6.5) were the top two interactions specifically predicted in CSC-treated cardiomyocytes versus the ones treated with TTF-conditioned media. Both CXCL10 and IGF2 have been tested in published studies and shown to be beneficial for the heart during cardiovascular disease and development, respectively (Van Den Borne et al., 2001; Li et al., 2011). However, the localisation of the receptors and the precise cellular targets in these studies remain unexplored.

Notably, one of the flagged interactions involved a CSC-derived ligand binding to a myocyte receptor that was expressed only after menadione treatment (Figure 3.30C, D). This interaction pair was AVP-*AVPR1β* (mean expression = 77.7 in CSC vs 33.7 in TTF). The effect of AVP (vasopressin) has been previously studied in isolated adult rat cardiomyocytes which express AVPR1α receptors and was found to mediate inotropic effects through the IP3 pathway (Chandrashekhar et al., 2003). Furthermore, despite evidence that high concentrations of AVP are cytotoxic, AVPR1α blockade did not inhibit ventricular remodelling post-MI (Chandrashekhar et al., 2003). Interestingly, the AVPR1α receptor was reported to be downregulated in remodelled rat hearts post-MI, which agrees with our data showing downregulation of *AVPR1α* in menadione-treated CMs (Figure 3.30D, Supplement 6.5). In contrast, expression of the related family member *AVPR1β* -unidentified roles in the context of cardio-protection- is not affected by menadione-treatment (Figure 3.30D, Supplement 6.5).

Overall, downstream bioinformatic analysis of the transcriptomic data on the CSC and IMR90-CM has revealed a handful of putative ligand-receptor interactions that could mediate cardio-protection. Whether these interactions have a significant role in the observed protection is a subject for further study.

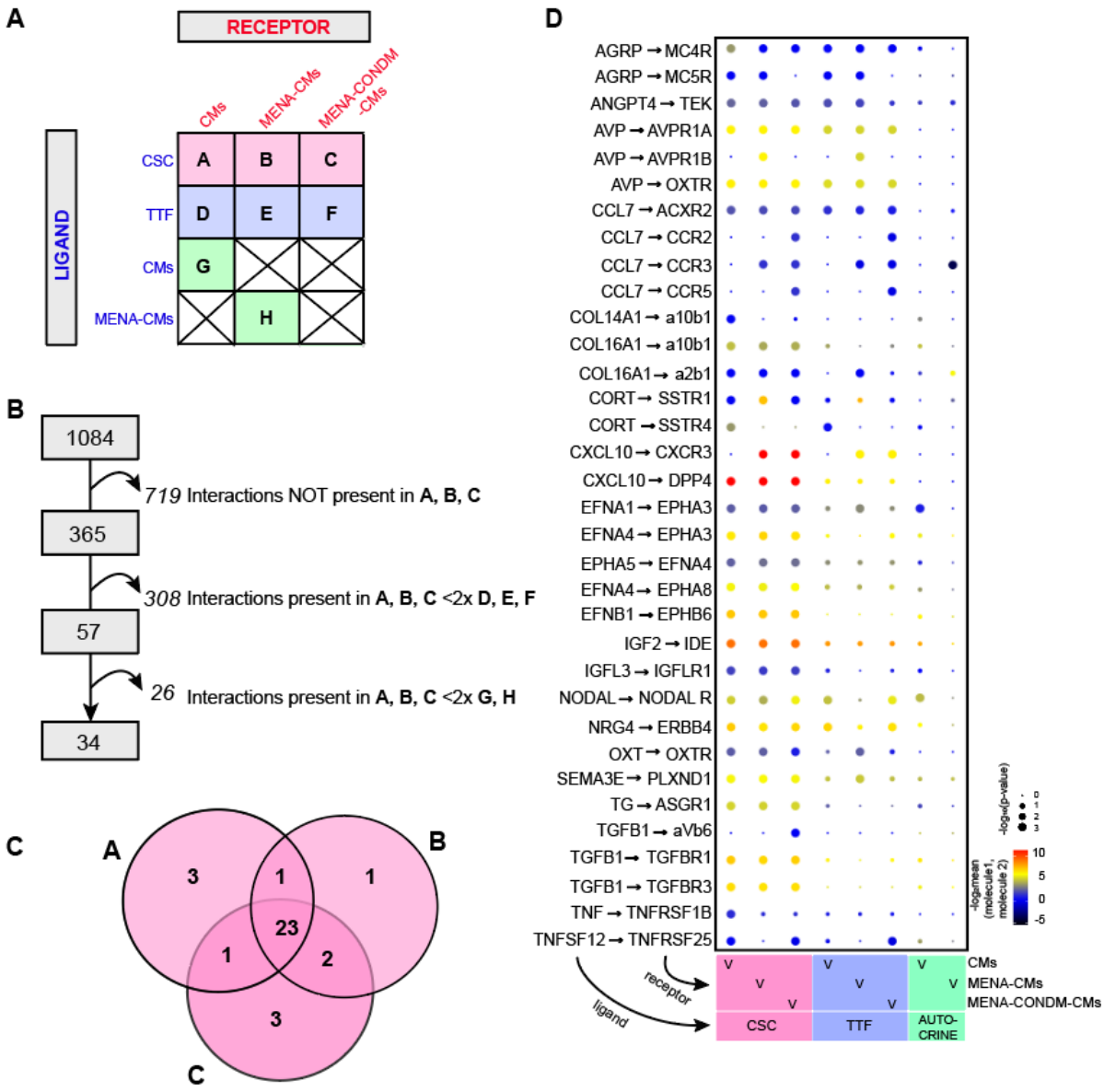



**Figure 3.30: Receptor-ligand interaction screen by CellPhone DB to predict protective candidates. A,** Table of pair-wise comparisons across the samples used in this analysis. CMs, IMR90-CMs at baseline; Mena-CMs, menadione-treated IMR90-CMs; Mena-CondM-CMs, menadione and CSC-conditioned media treated CMs. **B,** Step-wise exclusion strategy to narrow-down the list of interactions to the most relevant, based on our conditions. Steps 2 and 3 excluded interactions which involved ligands predicted to be expressed by TTF with means <2-fold the expression by the CSC. **C,** Venn diagram of receptor-ligand interactions resulting from the exclusion strategy, across the three most relevant pairwise comparisons involving CSC-predicted ligands. **D,** Dot plot of significant means (P<0.05) listing the ligand-receptor pairs in interactions resulting from the exclusion strategy. The first molecule in each pair denotes the ligand and the second molecule denotes the receptor. The size of each dot represents the -log$_{10}$(p-value) i.e. the larger a dot, the more significant the

interaction. The colour of each dot represents the -$log_2$mean(molecule1, molecule2) i.e. the more red a dot is, the higher the expression mean of the two molecules in the interaction pair. Significant mean expression values for the 34 interaction pairs in the different cell type combinations can be found in Supplement 6.5.

### 3.2.7. Cytokine Array screen reveals secreted factors enriched in CSC

As a complementary approach to identify potential protective candidates in the CSC-conditioned medium, we also used a semi-quantitative proteomic approach using cytokine array membranes (RayBiotech). Cytokine arrays were used for the analysis of three mouse samples: (i) IMR90 basal medium (RPMI+B27), (ii) TTF-conditioned medium and (iii) CSC-conditioned medium from cells seeded at 20,000/$cm^2$. Prior to their use in the cytokine screen, aliquots of the collected samples were tested for confirmation of their effect against menadione in IMR90 cardiomyocytes and as expected, CSC-conditioned medium was found to significantly protect IMR90 (Supplement 6.2), unlike the other two samples, in agreement to data shown in section 3.1.

Signal intensities were quantified by densitometry in ImageJ, using Java scripts for automation of the analysis (Supplement 6.2). Briefly, the scripts automated background subtraction based on the max integrated density from the 24 negative control spots which were spread across the membrane. Subsequently, a circular grid was applied which could be manually adjusted and aligned by the user to fit around the signal spots. Positive control signals included a total of 12 spots of anti-HRP (6 on top left of membrane) and anti-streptavidin (6 on bottom right of membrane), whose average integrated intensity signal was used by the script for normalisation of each spot in the corresponding membrane (= spot integrated density / average integrated density of positive controls). The normalised integrated density for each spot was

automatically calculated by the script and exported in a table which was copied into Microsoft Excel for downstream analysis. Microsoft Excel was used to obtain the average and standard deviation of integrated densities for each target protein from the duplicate spots. Target proteins that were visibly enriched in the CSC-conditioned medium compared to the basal medium and the TTF-conditioned medium were flagged and plotted (Figure 3.31A). Similarly, target proteins enriched in the TTF-conditioned medium were also plotted to identify any factors that could potentially decrease survival (Figure 3.31B).

Our results show enrichment of 7 proteins out of the 308 tested in the CSC-conditioned medium compared to the two controls; DTK, GDF-8, IGFBP-2, IL-15Rα, M-CSF, OPN and TRAIL (Figure 3.32A and Supplement 6.3). Of these, M-CSF, IL-15Ra and IGFBP2 have each been implicated in pro-survival signalling in the heart and specifically have been shown to inhibit cardiomyocyte apoptosis (Han et al., 2020; Okazaki et al., 2007; Yeghiazarians et al., 2014). GDF-8 (MYOSTATIN) best known as an inhibitor of skeletal muscle growth, regulates energy homeostasis in the mouse heart, prevents cardiac hypertrophy and inhibits cardiomyocyte proliferation in zebrafish, with no demonstrated impact on apoptosis (Biesemann et al., 2015; Dogra et al., 2017). The DTK receptor tyrosine kinase was recently shown to undergo a cleavage step and have an anti-apoptotic effect in cancer cells, though the role of the released extracellular domain is still unclear (Merilahti et al., 2017). Two pro-apoptotic mediators that commonly promote cell death but have highly variable consequences in cardiomyocytes, including induction of survival (OPN, TRAIL) were also enriched in the CSC secretome (Jiang et al., 2017; Singh et al., 2014; Toffoli et al., 2012; Zhao and Zhang, 2017).

Conditioned medium from TTF was found to be significantly enriched in 13 factors including; IGFBP-5, IGFBP-7, LIX, KC, MMP-2, MMP-3, TIMP-1, THBS-1, MCP-1, CCL-7, LIF, IL6-R, PGRN (Figure 3.31B and Supplement 6.3). Of these, THBS-1, MMP-2 and MMP-3 have been shown to induce apoptosis in cardiomyocytes through CD47 receptor signalling (for THBS-1) and β-adrenergic receptors or the TNFα pathway (for MMPs) (Chistiakov et al., 2017; Isenberg et al., 2007, 2008; Lee et al., 2008; Menon et al., 2005, 2006; Shen et al., 2006). Similarly, growth-suppressing IGF binding proteins -5 and -7 have been shown to alter IGF-1 signalling in mesenchymal stromal cells and kidney cells, but their effects on cardiomyocytes are still unknown (Imai et al., 2000; Kashani et al., 2013; Oh et al., 1996; Severino et al., 2013). Monocyte chemoattractant protein-1 (MCP-1) has a dual role inducing both survival and apoptosis in cardiomyocytes (Liu et al., 2015; Tarzami et al., 2005; Zhou et al., 2006b). Interestingly, tissue inhibitor of metalloproteinases (TIMP-1) is also enriched in TTF-conditioned medium and has been found to inhibit apoptosis in the ischemic myocardium via reducing the activity of MMP-2 (Uchinaka et al., 2014). Similarly, IL-6 family members (LIF, IL-6R) have been shown to have pleiotropic effects on cardiomyocytes, including protection from apoptosis (Kodama et al., 1997; Matsushita et al., 2005; Zou et al., 2003). Additional enriched factors such as LIX, KC, CCL-7 and PGRN have not been yet studied in the context of cardiomyocyte apoptosis, but the former two seem to be typically secreted in fibroblast conditioned media (LaFramboise et al., 2007).

Overall, the cytokine arrays point to possible candidates for cardiomyocyte protection from apoptosis, however whether these candidates act individually, in concert or in

conjunction to other molecules present in the infarct milieu is subject to further study.

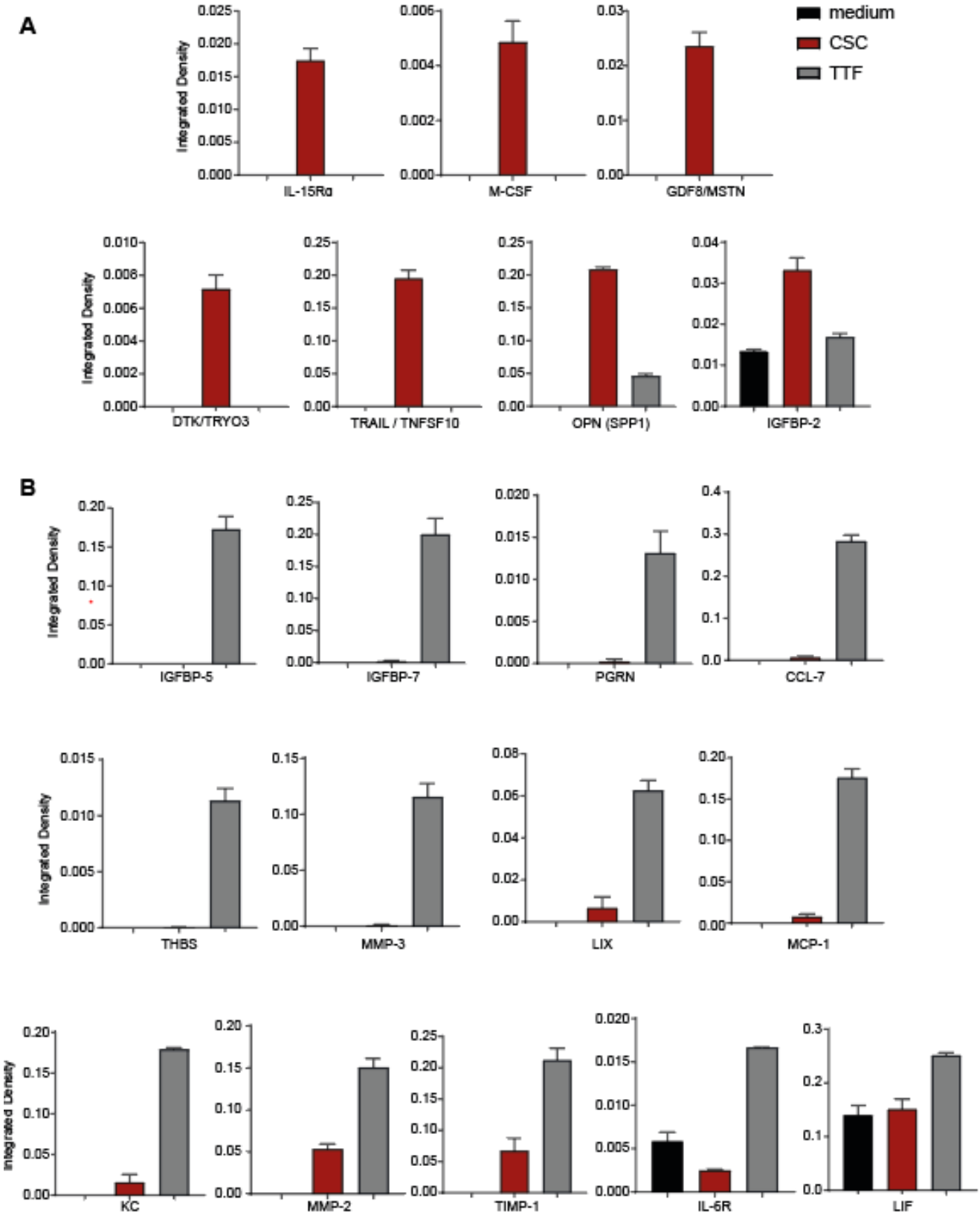


**Figure 3.31: Cytokine array screen reveals candidate factors enriched in CSC.** Bar graphs of cytokine levels, using low-density membrane arrays, for the factors enriched in **A,** CSC-conditioned medium and **B,** TTF-conditioned medium compared to the other two samples. Results are image analysis of integrated density, normalised to the average of anti-streptavidin and anti-HRP controls for each membrane. Enlarged versions of the arrays can be found in Supplement 6.3. Data are mean ± SEM; n=2. These data are part of a publication currently in press by Scientific Reports.

### 3.2.8. Summary and conclusions

Characterisation experiments showed that the CSC-derived protective factor(s) is likely to be a protein larger than 3kDa secreted via an exosome-independent mechanism. Hypothesis-driven gene expression analysis identified BMP4 and IGF1 as potential mediators of the protective effects but after being tested alone or in combinations, were found insufficient to protect hPSC-CM in culture. RNA-Seq on the target IMR-90 cardiomyocytes with and without menadione, in the presence and absence of CSC-conditioned medium showed dramatic recovery of transcriptomic changes induced by menadione stress upon treatment with CSC-conditioned media. Exploratory computational analysis of the transcriptomic results from the secretor cells (CSC) and receiving cardiomyocytes (hPSC-CM) by CellPhone DB highlighted candidate ligand-receptor pairs with putative cardioprotective functions including Ephrin-Eph, TGFβ-TGFβR and NRG-ERBB, which have been previously reported to regulate cardiomyocyte apoptosis and survival. Further, comparative experiments using cytokine arrays to analyse the secretome of the CSC-derived protective medium versus non-protective TTF conditioned media led to the identification of additional candidate secreted factors including M-CSF, IL-15Rα, IGFBP-2, GDF-8, DTK, TRAIL and OPN.

## 3.3. Human cardiac stromal cell characterisation and function

### 3.3.1. Molecular signature of human CSC resembles mouse CSC

As previously reported, PDGFRα$^{+}$ cells exist in the adult human cardiac interstitium, and albeit generally referred to as a subset of fibroblasts, their functional properties are largely unexplored (Chong et al., 2013). Here, we isolated and expanded human cardiac stromal cells (hCSC), from atria and ventricles of healthy human hearts, to test for paracrine protection in a wholly human model. Firstly, we hypothesised that the cells grown in culture could enrich for markers described for mouse CSC. Flow cytometry was used to test for the enrichment of SP cells in the hCSC populations, in the presence and absence of the ABCG2 transporter inhibitor (SP inhibitor), fumitremorgin C (Figure 3.32A). Furthermore, expression of PDGFRα and MSC markers (CD29, CD44, CD73, CD105) was confirmed by flow cytometry (Figure 3.32B) and by single cell qPCR (Fig. 3.32C). As shown in the heatmap, cardiac transcription factors are uniformly co-expressed (*GATA4, GATA6, HAND2, MEF2A, MEF2C, TBX20*) in the hCSC but not in the human dermal fibroblast used as control, which in turn was enriched in *CD90* (Figure 3.32D). Furthermore, the cells did not express mature cardiomyocyte markers (*MYH6, MYH7, MYL3, NKX2.5, NPPA, MYH11, MYL2*) (Figure 3.32C). Principal component analysis (PCA) of five cardiac stromal cell samples (three regions from two donors) are also displayed (Figure 3.32D). PC1 alone (30.52% variability) separates HDF from all five cardiac samples, whereas PC2 (18.8% variability) establishes a distinct separation between different sets of hCSC and a small subset of HDF. The gene loadings contributing to each variability indicate that *CD90/THY1* and cardiogenic transcription factors *GATA4, GATA6, HAND2, MEF2C, TBX20* explain the cross-group variability captured by PC1,

whereas *TBX5* contributes to the separation in PC2. These results suggest that the hCSC express a molecular signature that strongly resembles the previously characterised mouse CSC (Noseda et al., 2015a), as well as other human cardiac mesenchymal cells and closely related populations reported by others (Chong et al., 2011; Moore et al., 2016; Wysoczynski et al., 2017; Zhang et al., 2015b). For this experiment, microfluidic chips (Fluidigm) and single cell qRT-PCR analyses were run by Dr Patricia Chaves.

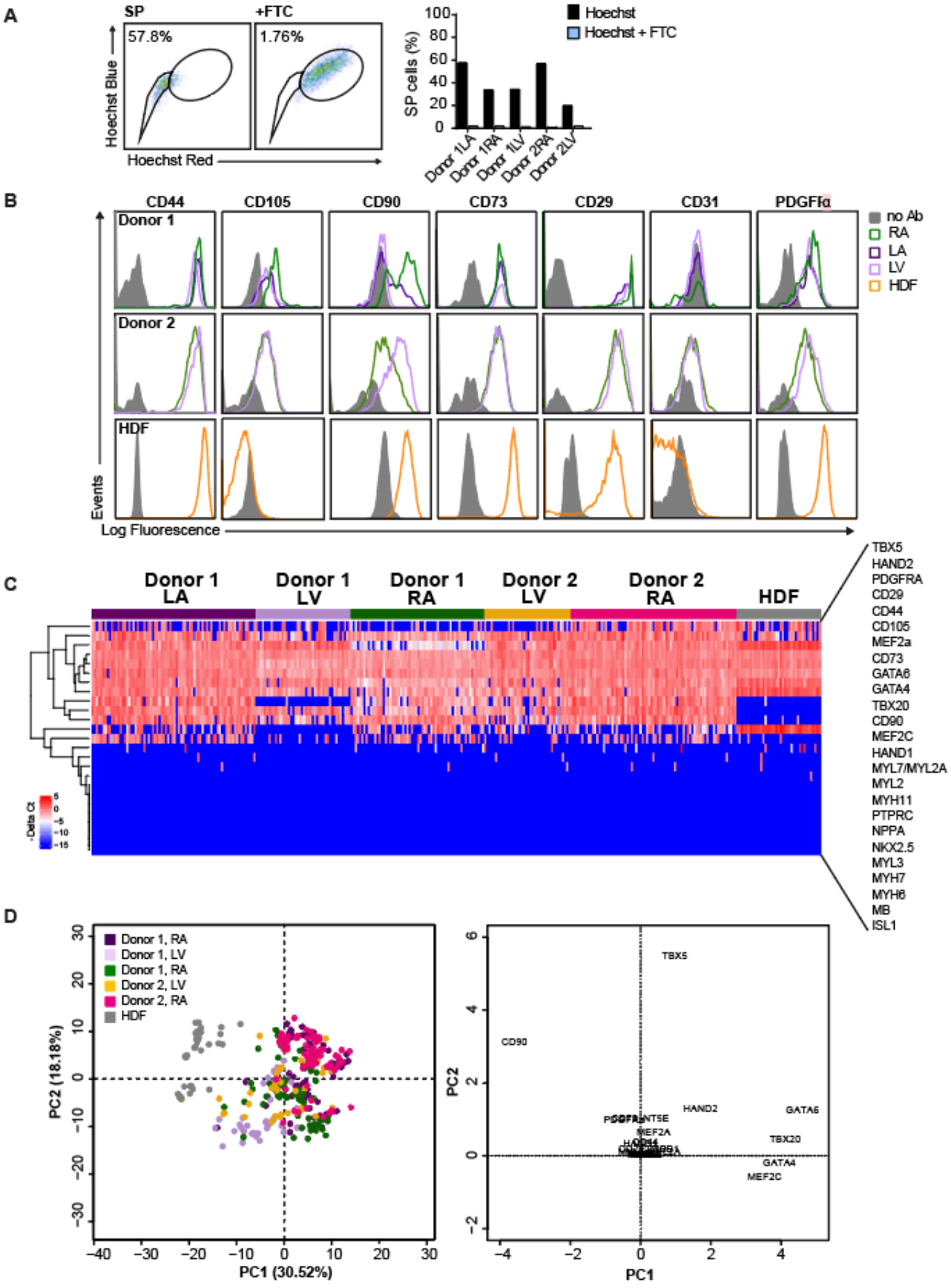

A
SP
+FTC
57.8%
1.76%
Hoechst Blue
Hoechst Red
SP cells (%)
Hoechst
Hoechst + FTC
Donor 1LA
Donor 1RA
Donor 1LV
Donor 2RA
Donor 2LV
B
CD44
CD105
CD90
CD73
CD29
CD31
PDGFRα
Donor 1
Donor 2
HDF
no Ab
RA
LA
LV
HDF
Events
Log Fluorescence
C
Donor 1 LA
Donor 1 LV
Donor 1 RA
Donor 2 LV
Donor 2 RA
HDF
TBX5
HAND2
PDGFRA
CD29
CD44
CD105
MEF2a
CD73
GATA6
GATA4
TBX20
CD90
MEF2C
HAND1
MYL7/MYL2A
MYL2
MYH11
PTPRC
NPPA
NKX2.5
MYL3
MYH7
MYH6
MB
ISL1
D
Donor 1, RA
Donor 1, LV
Donor 1, RA
Donor 2, LV
Donor 2, RA
HDF
PC2 (18.18%)
PC1 (30.52%)
TBX5
CD90
HAND2
GATA6
TBX20
GATA4
MEF2C
PC2
PC1

**Figure 3.32: Molecular signature of human CSC resembles mouse CSC. A,** Representative flow cytometry dot plot from the left atrium of Donor 1 and bar graph showing that all populations of hCSC from both donors are consistently enriched for the SP phenotype and their extrusion function is inhibited in the presence of Fumitremorgin C (FTC). **B,** Flow cytometry histograms comparing surface marker expression in the hCSC populations and human dermal fibroblasts (HDF). HDF can be differentiated by the absence of *CD105*. **C,** Single cell qRT-PCR comparing the co-expression of selected genes in hCSC and HDF. Expression is shown as $-\Delta_{Ct}$ values (blue, low; red, high). Genes were ordered based on hierarchical clustering. n=39-72 cells per sample. **D, Left,** Principal component analysis (PCA) of single-cell qRT-PCR profiles from five cardiac samples (two donors and three regions), versus HDF. **Right,** Gene loadings contributing to each variability displayed in the PCA plot. Right Atrium (RA); Left Atrium (LA), Right Ventricle (RV); Left Ventricle (LV). Flow cytometry and single cell qRT-PCR analysis was performed by Dr Patricia Chaves, using a script written by Dr Andrea Massaia. These data are part of a publication currently in press by Scientific Reports.

### 3.3.2. Human CSC protect hPSC-CM from menadione-induced stress

Given the strong resemblance of hCSC to the mouse CSC in terms of molecular signature, we were intrigued to investigate whether the human cells are capable of protecting cardiomyocytes from oxidative stress. Populations of hCSC from different heart regions of the two healthy donors were tested in a protection assay against menadione-induced stress. Following the 24 hr incubation, we stained the cardiomyocytes with the cell death marker DRAQ7. All cardiac stromal cell populations tested protect vCor.4U and IMR-90 cardiomyocytes from cell death (Figure 3.33). Different regions from the two donors conferred similar protective effect on human cardiomyocytes following menadione (Figure 3.33A, B). A representative example is the LV region from donor 1. In vCor.4U there was a 3-fold induction in cell death, from 12.9±2.1% in the absence of menadione to 38.5±2.7% DRAQ7 cardiomyocytes at 88μM menadione ($P<0.0001$). Prevalence of $DRAQ7^+$ cardiomyocytes was reduced

at least 2-fold by conditioned media from the LV-derived hCSC (17.4±1.5%, P<0.0001).

In the case of IMR-90 cardiomyocytes, DRAQ7$^+$ prevalence was 7.2±0.9% in healthy untreated cells and following menadione treatment (41.6μM) the proportion sharply raised to 59±2.2% (P<0.0001). Donor 1 LV-derived hCSC significantly decreased DRAQ7$^+$ signal to 8±1.5% (P<0.0001). Thus, the molecular signature of our mouse CSC and hCSC might predict cardio-protective cell populations, at least under the conditions tested here.

In order to test whether other fibroblast-like cells have protective effects, we used Human Dermal Fibroblasts (HDF). Conditioned media from these cells conferred no protection on vCor.4U cardiomyocytes: DRAQ7+ cells remained unchanged from 52.2%±2.2 in the menadione-treated cells to 51.8%±3.5 in the presence of HDF-conditioned media (Figure 3.33C). These data suggest that the protective effect of cardiomyocytes against oxidative stress is not a universal property of human cells, nor any fibroblasts. At least as ascertained under the stress conditions tested here, human CSC's secretome preferentially or uniquely contains factor(s) that, mediate cardio-protection.

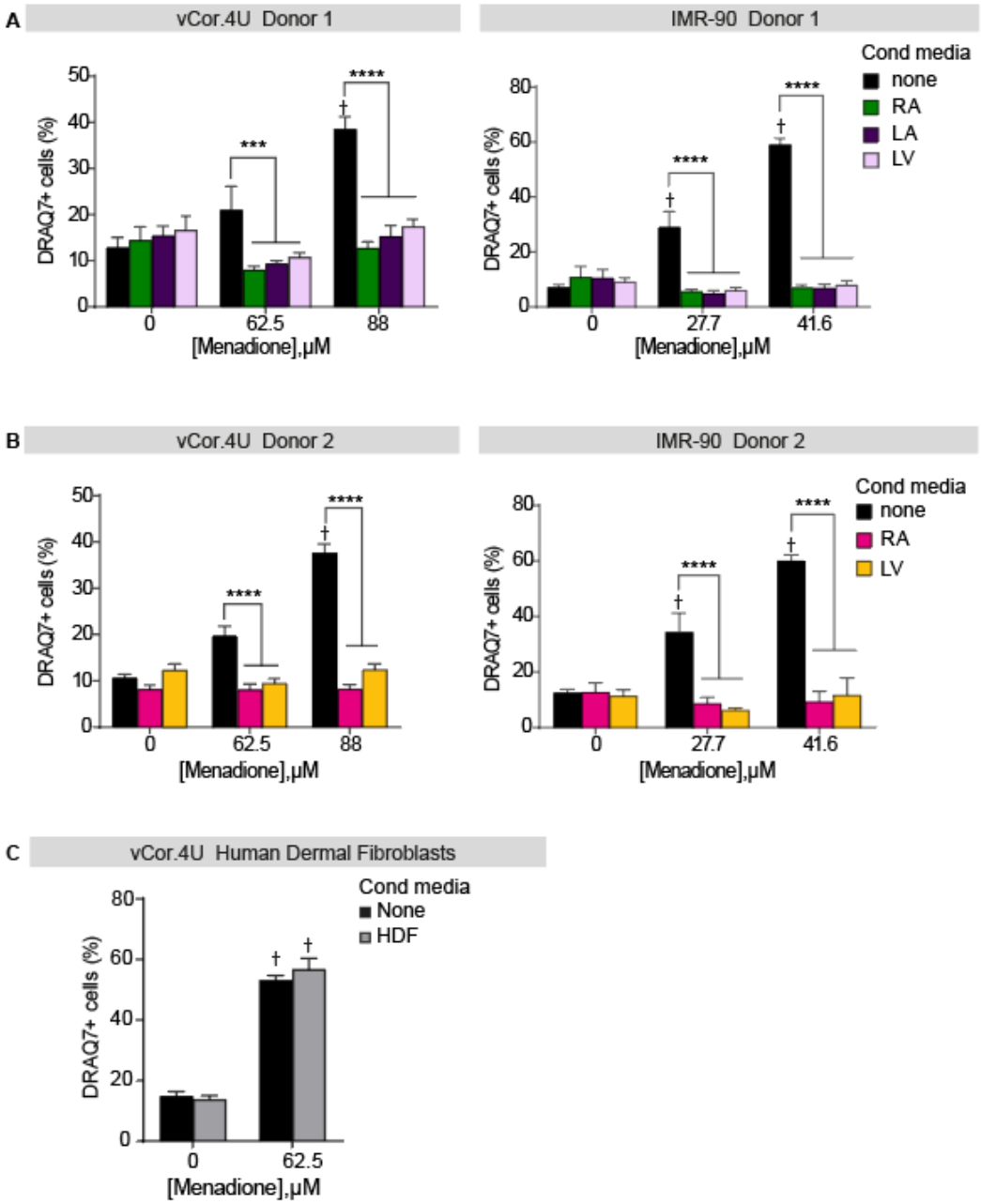



**Figure 3.33: Human CSC protect hPSC-CM from menadione-induced stress.** Bar graphs showing DRAQ7 uptake in vCor.4U and IMR-90 cardiomyocytes 24hr following menadione stress after treatment with conditioned media derived from different hCSC populations of **A,** Donor 1; **B,** Donor 2 and **C,** HDF which were used as a negative control for protection. Data is mean ± SEM; vCor,4U: n = 6; IMR-90: n = 9; HDF: n=9; ***, P < 0.001; ****, P < 0.0001; †, P < 0.05, versus no menadione. RA, Right Atrium; LA, Left Atrium; LV, Left Ventricle. These data are part of a publication currently in press by Scientific Reports.

### 3.3.3. Cytokine array screen reveals potential candidates for protection secreted by human CSC

Given that human CSC resemble the transcriptional signature of the mouse CSC as well the capacity to protect human cardiomyocytes from oxidative stress, we were intrigued if they also show similarities to the mouse CSC secretome. We thus performed a cytokine array screen on the hCSC-conditioned medium, using an equivalent human membrane (RayBiotech) pre-stained with 507 different antibody probes covering a wide range of cytokines, chemokines, adipokines, soluble receptors and other secreted proteins and small molecules. For this exploratory screen, we selected 'Donor 2 LV' as the representative hCSC population to test. Negative controls were unconditioned, basal cardiomyocyte medium and HDF-conditioned medium from cells seeded at 20,000/cm$^2$.

The protocol for the cytokine arrays was performed exactly as described for the mouse membranes (section 3.2.7), with the only difference being the exposure time of the film to the arrays, which in this case was 1.5 minute. The same scripts used for the mouse (Supplement 6.2) were slightly adjusted to match the human array size and negative control coordinates.

Our results showed enrichment of 6 proteins out of the 507 tested in the hCSC-conditioned medium compared to the two controls; CXCL1, IGFBP-7, MCP-1, MIP-2, MMP-1 and TIMP-1 (Figure 3.34 and Supplement 6.3, for enlarged membranes). While the role of IGFBP-7 has not been specifically determined in the heart, the rest of the enriched proteins have all been reported to exhibit pro-survival effects on cardiomyocytes or other cells (Bachmaier et al., 2014; Limb et al., 2005; Tarzami et al., 2005; Uchinaka et al., 2014; Wei et al., 2010). In contrast, conditioned media from

HDF were mostly enriched in pro-apoptotic factors (MMP-3, MMP-7, DECORIN) (Chiao et al., 2010; Lee et al., 2008; Neill et al., 2014), as well as several proteins with unknown effects on cardiomyocyte apoptosis (TIMP-2, TIMP-3, P-SELECTIN, UBIQUITIN+1, EDA-A2) (Fan et al., 2014).

Notably, none of the secreted factors identified by the human arrays overlap with those enriched in the mouse CSC. Hence, it might be more fruitful to focus future efforts on the delivery of the CSC-conditioned medium as a therapeutic product itself, rather than pursuing the identification of a single factor or group of factors to confer the protective effect, as it might be a result of a highly regulated network of numerous interactions between secreted factors themselves as well as other molecules found in the niche under conditions of stress.

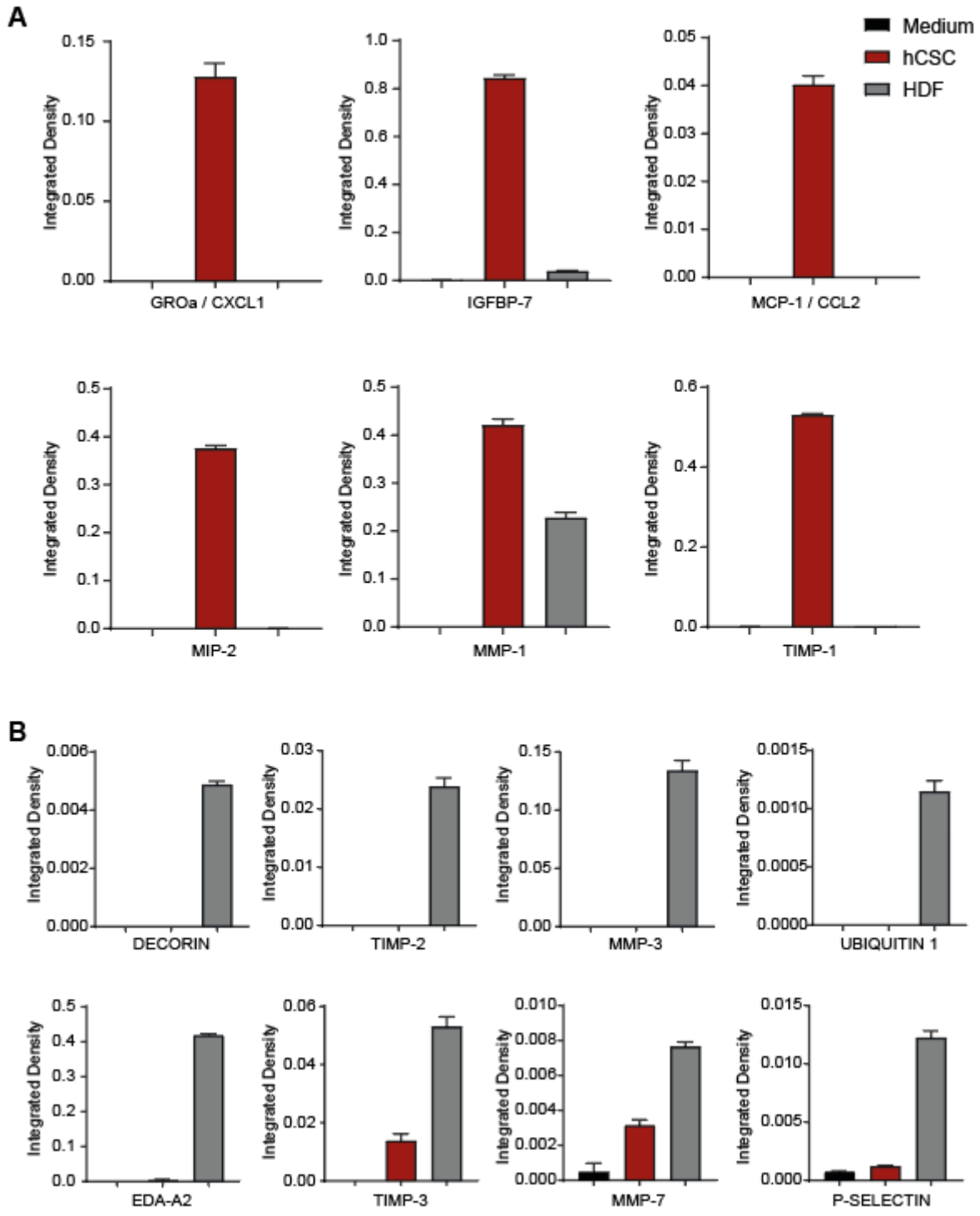



**Figure 3.34: Cytokine array screen reveals candidate factors enriched in CSC.** Bar graphs of cytokine levels, using low-density membrane arrays, for the factors enriched in **A,** human CSC-conditioned medium and **B,** HDF-conditioned medium compared to the other two samples. Results are image analysis of integrated density, normalised to the average of anti-streptavidin and anti-HRP controls for each membrane. Enlarged versions of the arrays can be found in Supplement 6.3. Data are mean ± SEM.

### 3.3.4. Summary and conclusions

Our results showed that human CSC isolated from atria and ventricles of healthy hearts resemble the mouse CSC's molecular signature, marker expression and were also found to significantly protect hPSC-CM from menadione-induced death. Cytokine array screening on the conditioned medium from one population of human CSC versus non-protective HDF-derived medium allowed to identify candidate factors that could play a role in the protective effect, including CXCL1, IGFBP-7, MCP-1, MIP-2, MMP-1 and TIMP-1.

# 4. Discussion

## 4.1. Human cardiomyocyte protection from cell death by CSC-secreted factors

This work tested the impact of paracrine signals on human cardiomyocytes using hPSC-CM as the target of mouse or human CSC with progenitor-like features. Our results showed that conditioned medium from mouse and human CSC can protect human cardiomyocytes from oxidative stress-induced death, while little or no protection was conferred by mouse tail tip or human dermal fibroblasts. Functional analyses showed that the CSC secretome suppressed apoptosis, inhibited induction of ROS, preserved mitochondrial membrane depolarisation, and maintained cyclical cardiomyocyte function. In agreement, transcriptomic profiling of the cardiomyocytes revealed a decline in cardiac function regulator genes provoked by menadione, with a reciprocal induction of oxidative stress response and pro-apoptotic genes, all of which responses were prevented by conditioned medium. Protection was exosome-independent and conferred by the >3kDa molecular weight fraction of the medium, which was sensitive to heat treatment, consistent with one or more proteins as the basis for protection. Cytokine array screens revealed candidate mediators of the protective effect in both mouse and human CSC-secretomes. The present discussion will attempt to use our data to answer the three research questions posed at the end of the introduction, declaring the novel findings originating from this work, tethering it to current literature, and pointing out potential limitations and exciting future directions.

## 4.2. Is CSC-conditioned medium sufficient to protect cardiomyocytes from acute oxidative stress?

Here we have tested whether the CSC's secretome is capable of protecting cardiac myocytes from heart disease-relevant stress inducers, employing more than one relevant preclinical model of the disease: first, an *in vivo* mouse model, then primary neonatal mouse cardiomyocytes in culture, and, lastly, two independent hPSC-CM lines. Following proof of principle preliminary studies in rodent myocytes *in vivo* and *in vitro*, a major aim of this project was to establish a platform for paracrine protection studies using hPSC-CM as the present state-of-the-art, in lieu of rodent cells. Despite the considerable limitations in terms of hPSC-CM maturity, it is undoubtedly one of the closest preclinical models to the human phenotype available, and its predictive power and utility as a model to test experimental therapeutics are now well-established in the field (Blinova et al., 2017; Gintant et al., 2017; Golforoush and Schneider, 2020).

### 4.2.1. The unmet need in cardiac drug discovery

Despite the reduction in the rate of age-adjusted deaths from ischemic heart disease between 2007 to 2017, the actual number of deaths during the same period have increased by 22.3% (Roth et al., 2018), suggesting that progress in alleviating ischemic heart disease is stunted. Hence the need for novel strategies to target heart muscle cell death and dysfunction remains paramount. However, statistics on the actual number of new cardiac drugs entering clinical practice are disappointing and reflect a number of underlying issues (Fordyce et al., 2015; Gromo et al., 2014). Strikingly from 2011 to 2019, the US Food and Drug Administration approved 90 novel drugs for cancer treatment, compared to only 4 that have direct effects on cardiac muscle (Golforoush and Schneider, 2020). Despite the numerous sources of credible

support from preclinical models of myocardial infarction involving whole-animal studies, proposed counter measures have failed to show efficacy in the clinic (Hausenloy and Yellon, 2015; Heusch, 2013; Lincoff et al., 2014; Newby et al., 2014; Ottani et al., 2016; Piot et al., 2008). Indeed, the likelihood of approval from Phase I as reported in the largest study of Clinical Development Success Rates 2006-2015 is amongst the lowest for cardiovascular drugs with just 6.6% (versus 26.6% for Hematology drugs) (David W. Thomas et al., 2016). Currently, there is even a paucity in new cardiac candidate applications coming forward to seek initiation of early phase trial studies (Fordyce et al., 2015).

Among the countless causes underlying the arrested progress, the most popular include: drug development costs; regulatory ambiguities; the difficulty in obtaining appealing biological targets; commercial viability; time, size and complexity of trial design; risk of reliance on back-up end-points; and poor return on investment, especially given the high costs of clinical failures (Fordyce et al., 2015; Pammolli et al., 2011). It is possible that one of the major reasons underlying this degree of failure in human cardiac trials, is the lack of systematic human preclinical data for target validation and drug development. Experimental validity of the therapeutic strategy on a human-based preclinical model would significantly de-risk the proposition before entering human trials. Small to large animal models are surely instructive and necessary, however to date they have failed to show sufficient predictive power for efficient target translation in humans (Sharma et al., 2010).

In contrast to the cardiac drug development process, in the apparently ‘faster-developing’ field of oncology, drugs enter human trials once having first been tested from an early stage using well-characterised human cancer cell lines widely available

in laboratories worldwide (Gazdar et al., 2016; Gillet et al., 2013; Sharma et al., 2010). Notably, human cell lines in cancer drug discovery are an essential and major field of rigorous work, as demonstrated by the National Cancer Institute's 60 human tumour cell line screen (Shoemaker, 2006) and by initiatives like the Cancer Cell Encyclopaedia (Ghandi et al., 2019; Rees et al., 2016). Human heart muscle on the other hand, does not have the same level of availability and can only be obtained sporadically from biopsies and explanted hearts. The lack of a routine, scalable and renewable resource for library screening, systematic testing and more relevant translational studies is a severe gap in the field. Furthermore, the post-mitotic nature of adult human cardiomyocytes prevents their sufficient and long-term expansion in culture to satisfy research requirements. Now, human cardiac muscle cells have become available in unlimited, expandable quantities from human pluripotent stem cell technologies, which provide access to 'heart-disease in a dish' and a potential to accelerate the stunted pace of cardiac drug discovery (Bellin et al., 2012; Burridge et al., 2016; Cameron et al., 2013; Gintant et al., 2017; Lee et al., 2017b; Liang et al., 2013; Matsa et al., 2014, 2016; Sharma et al., 2017).

### 4.2.2. Early human cardiomyocyte sources

Pluripotent stem cell reprogramming technologies over the last decades have enabled the non-invasive, detailed study of human cardiac function. The only way to access human cardiac tissue in living patients comes with a risk of perforation, and the obtained material is often insufficient for the needs of downstream molecular analysis. Furthermore, biopsies are usually available from the few patients with end-stage pathology, and the acquired cardiomyocytes are non-proliferative and difficult to maintain in culture. For these reasons, immortalised cell lines were widely used such

as rat H9C2 cells (Kuznetsov et al., 2015a; Watkins et al., 2011; Zhao et al., 2018; Zhou et al., 2018b) or the mouse HL-1 line (Claycomb et al., 1998; Kuznetsov et al., 2015b; White et al., 2004). While these cell lines undergo limitless proliferation, they also have their individual drawbacks i.e. their non-human origin, known biological disparities (e.g., lack of NCX in H9c2 cells), or tumour-like growth properties.

As one conceptual step beyond animal-derived primary cardiomyocytes and lines, the immortalised human ventricular AC16 cell line was developed through the fusion of primary human adult ventricular cardiomyocytes with an SV40-transformed fibroblast cell line (Davidson et al., 2005). This cell line has been used to date in more than 70 published studies of cardiac pharmacology, including investigations of cell death induced by oxidative stress and doxorubicin (Bell et al., 2019; Chen et al., 2019; Lee et al., 2018b; Manning et al., 2019; Pan et al., 2019; Wen et al., 2020; Yoon et al., 2019). While the transformed AC16 cells seem to resemble human cardiomyocytes in terms of cardiac-specific gene expression and contractility these studies were only performed after RNA interference to suppress the large T antigen and induce cell senescence and further differentiation into a more mature phenotype (Davidson et al., 2005). Furthermore, their proliferative capacity remains a limitation, as they are unable to maintain a stable myofibril morphology. The transforming gene might also interfere with the myocytes' responses to induction of death signals and survival pathways, for example via the inhibition of p53, an important transcription factor for the regulation of apoptosis (Sheppard et al., 1999). Hence, this line would not be a suitable model for our purpose as the rationale of the project is based on sensitivity to death signals and their inhibition.

### 4.2.3. Human pluripotent stem cell-derived cardiomyocytes: a step closer to the patient phenotype

Given the drawbacks of immortalised cardiomyocyte lines stated above, hPSC-CM were proposed as a more suitable model for predictive studies. A more systematic use of hPSC-CM in the field has been encouraged with in silico modelling and other prediction tools for safety pharmacology, encompassed within the Comprehensive *In Vitro* Proarrhythmia Assessment (CiPA) initiative (Blinova et al., 2018; Gintant et al., 2016, 2019). According to CiPA, hPSC-CM are now considered more complete biological integrators that not only detect complex drug effects on cardiac currents, but also modulatory effects on signalling pathways, channel-associated subunits, altered calcium handling, transporters and exchangers and potential changes in channel densities in myocytes (Gintant et al., 2017). The recent study by Blinova and colleagues, is a specifically informative exemplar to demonstrate the potential utility and predictive ability of hPSC-CM in drug-induced proarrhythmic effects (Blinova et al., 2018). This blinded, international, 10-site study of 28 drugs used two commercially available hPSC-CM lines and several electrophysiological platforms to test the prevalence of drug-induced repolarisation abnormalities and arrhythmia-like events. The data were used to construct a model of ventricular arrhythmia, Torsade de Pointes (TdP) risk and, regardless of the cell line used, hPSC-CM showed good predictive capabilities, allowing the investigators to pronounce the cells a highly reliable preclinical classifier of clinical TdP risk.

Alternative studies have demonstrated the utility of hPSC-CM as a robust preclinical model for profiling anti-cancer drug cardiotoxicity (Sharma et al., 2017, 2018; Zhang et al., 2012) and readily applicable experimental assays some of which have also been

applied in this work include biochemical read-outs (ATP production, cardiac troponin release), microscopy (loss of surface integrity, apoptosis) and biophysical studies (calcium handling, action potentials) (Golforoush and Schneider, 2020 in press). Here we employed various assays including the membrane integrity marker DRAQ7, the DNA fragmentation marker TUNEL, cardiac troponin I release, and adenylate kinase release, to measure cell death following induction of stress by three cardiotoxic molecules, menadione, doxorubicin and imatinib. Exploiting the model's predictive power, a recent report has used patient-derived hPSC-CM to study patients' vulnerability to cardiotoxic trastuzumab (Kitani et al., 2019) or pathways engaged in cardiotoxic responses by anthracyclines versus tyrosine kinase inhibitors (Wang et al., 2019). The latter study concluded that the different anti-cancer agents trigger vastly different transcriptomic signatures in hPSC-CM with doxorubicin primarily inducing DNA damage pathways and tyrosine kinase inhibitors mainly disrupting mitochondrial energetics, even at sublethal concentrations, leading to the reduction of oxidative phosphorylation and upregulation of glycolysis (Wang et al., 2019). In agreement, our results have shown hPSC-CM sensitivity both to doxorubicin and the tyrosine kinase inhibitor imatinib, which was rescued by treatment with CSC-conditioned media. This suggests that our countermeasure has a very broad protective capacity, despite many known differences in the underlying molecular and transcriptomic mediators of cardiomyocyte death.

### 4.2.4. Human PSC-CM: mitigating their limitations

Certainly, hPSC-CM do not come without their limitations. Despite their strong predictive power in culture, it is clear that hPSC-CM cannot model all possible phenotypes of interest and, indeed, in comparison to the native adult human heart they

show signs of immaturity. Shortcomings of this model include aspects of morphology (lack of sarcomere organisation, T-tubules, and mitochondrial density), molecular profile (weak expression of maturation-associated genes and splicing isoforms), metabolism (glycolysis, not fatty acid oxidation), contractility (lower contractile force), and electrophysiology (smaller upstroke velocity and amplitude) (Kodama et al., 2019; Patel et al., 2015; Sala et al., 2018; Ulmer et al., 2018).

As part of this work, we therefore analysed the transcriptome of one of the hPSC-CM lines used here by RNA-Seq and attempted to characterise these cells based on enrichment of cardiac-specificity and maturity markers. Furthermore, in order to compare IMR90-derived myocytes to respective hPSC-CM lines used by others, raw RNA-Seq data were downloaded from a study that derived cardiomyocytes from breast cancer patient fibroblasts and used them as a predictive model to recapitulate the susceptibility to doxorubicin induced cardiotoxicity (Burridge et al., 2014, 2016). We compared the top 100 highly expressed genes in IMR90-CMs versus Burridge's lines and generated a Venn diagram showing that almost 70% of the genes were overlapping in all 5 hPSC-CM lines (Supplement 6.4). Indeed, IMR90-CM even express 2 specific genes such as *NPPA* and *TNNI1* that were not enriched in the top 100 genes of the published lines we compared. In terms of maturity, RNA-Seq showed that IMR90-CMs highly expressed cardiomyocyte markers and essential ion channels, while they had little or no expression of pluripotency, mesodermal, and fibroblast markers. Nevertheless, their weak expression of ventricular genes such as *TRDN, TNNI3* and *MYL2* were acknowledged attributes of immaturity (Jiang et al., 2018).

Efforts to mitigate these limiting aspects and further enhance the predictive value of hPSC-CM have to date focused on the aspects of manipulating chamber and cell sub-

type specificity as well as improving structural and functional maturity (Golforoush and Schneider 2020, in press). Reported strategies demonstrating the best enhancement of hPSC-CM maturity thus far include 3D human engineered heart tissue, mechanical or electrical conditioning and heart-on-a-chip technologies (Feric and Radisic, 2016; Lemoine et al., 2017; Macqueen et al., 2018; Ronaldson-Bouchard et al., 2018; Tiburcy et al., 2017; Wang et al., 2014; Zhao et al., 2019), discussed in more detail below.

### 4.2.5. Engineered heart tissue and 3D cultures

In comparison to regular 2D culture, 3D engineered heart tissue has been reported to aid maturation of energy metabolism as demonstrated by an increase in mitochondrial mass, DNA content and protein abundance (Ulmer et al., 2018). Furthermore, hPSC-CM in 3D performed less anaerobic glycolysis and more oxidation of glucose, lactate and fatty acids (Ulmer et al., 2018). Notably, the incorporation of other cell types introduces essential cross-talk signalling, which promotes maturity or function as well as essential microvasculature characteristics required for oxygen delivery at a scale larger than what passive diffusion can allow. Remarkable work by Giacomelli and colleagues reported that 3D spheroids composed of hPSC-CM and hPDSC-derived endothelial cells display progressive changes in gene expression, more similar to post-natal development than monoculture of hPSC-CM alone (Giacomelli et al., 2017). Furthermore, hPSC-CM 3D culture within an engineered heart tissue construct including cardiac fibroblasts, along with long-term electrical stimulation, results in physiological responses that tend to be absent from routine 2D cultures (Feric et al., 2019; Zhao et al., 2019).

Several years after the publication of the first studies using 3D culture and despite the popularity and the numerous advantages over regular 2D models reported in recent literature, this technology is not widely used yet outside the field of regenerative medicine (Horvath et al., 2016). A major reason for this is that 2D culture is well established and widely accepted with ample support and guidance from existing literature. Furthermore, compared to 3D models, 2D culture is cheaper, less time-consuming, more standardised and easier to handle, especially for high-throughput studies. Thinking about the practical aspects of 3D culture, trivial tasks such as daily checks for growth and cell health become more complex because sometimes small tissues become opaque and single cells are not distinguishable unless stained or dispersed (Zuppinger, 2019). Nowadays, this is subject to change, as more and more tools are becoming available to facilitate 3D culturing, such as spheroid or engineered heart tissue production systems and suitable reagents, microfluidic technologies and optimised equipment, like adapted microscopes and specialised software for 3D live imaging. Indeed, the scientific community calls for standardisation of read-outs in efficacy and toxicity screening using 3D cultures, as a pre-requisite to integrate this model into the drug development pipeline (Kelm et al., 2019). Another important incentive in support of 3D technology is the gradual replacement of animal models by *in vitro* technologies and the use of human cells, an idea which has already shown significant impact in the field of cosmetic medicine where the use of animals has been banned at least in Europe (Hartung, 2013; Rimann and Graf-Hausner, 2012). Yet, it is debatable whether 3D cardiomyocyte models can provide sufficient predictive power to support the clinical outcome of a new drug as, for the moment, they still lack the complexity and proven physiological relevance of the animal or human heart.

## 4.3. CSC-responsive mechanisms for human cardiomyocyte death

In order to get an insight into the protective component of the CSC-conditioned medium we first attempted to understand the mechanisms underlying cardiomyocyte death after treatment with each cardiotoxic molecule. In agreement with the existing literature, our results show differences in the mechanisms of stress induction when comparing menadione to doxorubicin and, subsequently, differences in the processes blocked by the CSC-conditioned medium. At this point, it is certain that we lack the whole picture, i.e., whether the different responses we see result from quantitative or temporal differences in a single molecular pathway for cell death, or whether they instead result from different underlying pathways, will take years of investigation to untangle.

### 4.3.1. Sensitivity of hPSC-CM to menadione stress

Menadione induces intracellular ROS through quinone redox cycling and represents a valid and useful trigger for oxidative stress, as shown in recent translationally relevant studies (Badave et al., 2016; Fiedler et al., 2019; Grimm et al., 2015). The study by Grimm and colleagues concluded that a menadione concentration of 10 μM for 24 hr was sufficient to induce a steep decrease in the viability of iCell cardiomyocytes, another line of commercially available hPSC-CMs that was predictive in the CiPA safety pharmacology report (Blinova ref). Fiedler et al reported a 50% reduction of viability in vCor.4U cardiomyocytes at menadione concentrations of ~32μM for 24 hr, which is 2-fold less than our chosen concentration for the same cell line. The associated differences between our study and Grimm's can be attributed to the previously reported inherent differences between the two independent cardiomyocyte lines or a lower susceptibility of ventricular cardiomyocytes to

menadione stress (Fiedler et al., 2019). The small discrepancy between our study and Fiedler's might come down to the different types of assays used for cell death read-out: Fiedler et al. used the cytotoxicity assay CellTiter-Glo, which produces luminescence proportional to the number of viable cells that are metabolically active and produce ATP, whereas the assay used to titrate menadione conditions in our work was DRAQ7 penetration of compromised cells, followed by high-content image analysis. While high-content imaging can offer an advantageous measurement of cell death, as DRAQ7 can be multiplexed with additional cell-identifying or death markers, it could also be falsely excluding some events, due to cell detachment from the plate following death or loss of adherence (Suzanne and Steller, 2009).

The two human cardiomyocyte lines used here also show different susceptibilities to menadione stress, with IMR-90 being 3-4-fold more sensitive than vCor.4U myocytes. This variability in dose-dependence across different lines has been previously observed and might be inherent to the genetic background as well as small differences in the maturity and/or chamber specificity of the cardiomyocytes (Burridge et al., 2016; Doherty et al., 2015; Ebert et al., 2015). Variable sensitivities between different hPSC-CM lines have been observed and are widely reported and the need to achieve defined culture conditions and standardised protocols is imminent (Ebert et al., 2015). Reproducibility and standardisation throughout the scientific community is a major objective to ensure comparable data-sets and better applicability potential of hPSC-CM in disease modelling and drug development.

Our results show that CSC-conditioned media protect human cardiomyocytes from menadione-induced stress at least in part via downregulation of oxidative stress. Whether this happens through a ROS-scavenging activity or a feed-forward

mechanism that inhibits generation or amplification of ROS is a subject of further study.

### 4.3.2. Menadione-induced downstream signalling and implications in hPSC-CM

While the effects of doxorubicin on hPSC-CM have been quite extensively studied, the same cannot be said in the case of menadione. However, this vitamin K derivative has been used to treat other cell types in publications that we can use to make informed speculations and seek to explain our results.

Menadione-induced oxidative stress induces apoptosis in cultured myoblasts via caspase-3 and poly ADP ribose polymerase (PARP) (Lim et al., 2016). Chiou et al., used flow cytometry and Annexin V / Propidium iodide (PI) staining in menadione-treated C2C12 myoblasts and demonstrated that the mode of cell death changes according the concentration of the stress molecule; i.e., menadione treatment of up to 40 μM induced apoptosis (~40% $PI^-$/Annexin $V^+$), 80 μM induced both apoptosis and necrosis (40% $PI^+$/Annexin $V^+$), and 160 μM induced necrosis ( ~90% $PI^+$/Annexin $V^+$) (Chiou et al., 2003). Myoblast pre-treatment with antioxidant or iron-chelator molecules was found to inhibit menadione-induced levels of apoptosis and lipid peroxidation (Chiou et al., 2003). Hence, in our future work, it would be interesting to investigate whether different concentrations of menadione on hPSC-CM trigger alternative pathways of cell death and importantly, whether CSC-conditioned medium is sufficient to inhibit all of those that are engaged, or whether it can solely block mitochondrial-dependent apoptosis.

Several studies have linked cell responses to menadione stress with regulation of the downstream PI3K/Akt signalling pathway for cell survival (Lim et al., 2008, 2016). Notably, PI3K/Akt signalling amplitude seems to have a role in fine-tuning the differential susceptibility of different cell types to menadione stress: increased PI3K/Akt signalling makes the cells more resistant, whereas inhibition of PI3K or Akt renders the cell type more susceptible (Lim et al., 2008). Importantly, Akt has been implicated in the beneficial paracrine effects conferred by human MSC in adult rat cardiomyocytes and infarcted hearts (Gnecchi et al., 2006; Mangi et al., 2003). Therefore, the pro-survival pathway of PI3K/Akt might have a role, and any CSC-released cytokine or chemokine factors that activate this pathway are especially interesting candidates to look at.

A different kinase, activated in human monocytes following menadione treatment, is the energy sensor adenosine monophosphate-activated protein kinase (AMPK) (Davies et al., 2015). AMPK has been implicated in hPSC-CM survival and metabolism through inhibition of TGFβ signalling, and AMPK activators have been suggested to be beneficial in the treatment of fibrosis and hypertrophic cardiomyopathy (Travis Hinson et al., 2016). The role of AMPK in menadione-stressed hPSC-CM and their survival remains to be investigated.

A number of stress signals such as inflammatory cytokines tend to stimulate a range of protein kinases, some of which have contradicting effects, and thus result in a mix of death and survival signalling. Oxidative stress triggered by menadione has been shown to inhibit survival signalling by mitogen-activated-protein-kinase / extracellular-signal-regulated-kinase kinase 1 (MEKK1) and activate the apoptosis-signal-regulating-kinase 1 (ASK1) in a human adenocarcinoma cell line (Cross and

Templeton, 2004). In support of this mechanism, MEKK1 has been shown to suppress oxidative stress-induced apoptosis in mouse embryonic stem cell-derived cardiomyocytes via inhibition of TNFα (Minamino et al., 1999). On the other hand, ASK1 is an abundant kinase in the heart, known to mediate growth and death responses in cardiac myocytes in response to pathologic stimuli via both apoptosis and necrosis, depending on the stress conditions (Watanabe et al., 2005; Yamaguchi et al., 2003). Mechanistically, this kinase regulates cell death via other effectors including p38 and c-Jun N-terminal kinase (JNK). In support of this mechanism, menadione has also been shown to confer oxidant-induced damage in hepatocytes sustained JNK/c-Jun activation (Amir et al., 2012). Constitutive activation of ASK1 leads to the induction of apoptosis, whereas blocked expression of the kinase prevents cell death induced by TNFα, oxidative stress, anti-cancer agents and growth factor retraction (Chang et al., 1998; Hatai et al., 2000; Ichijo et al., 1997; Kanamoto et al., 2000; Saitoh et al., 1998). While the roles of ASK1 and MEKK1 have been generally investigated in the mouse heart, not many studies have looked at their regulation and effects in human cardiomyocytes. Given their implication in oxidative stress-affected survival and death pathways, these are interesting candidate pathways to keep in mind for future work.

Overall, further study into the kinases affected in our system could be vastly informative but extremely laborious given the hundreds of them implicated and the time required for pathway deconvolution for each. A powerful tool that has been broadly used in the study of cancer is phosphoproteomics-based kinase profiling, a mass spectrometry-based approach which allows the identification of thousands of phosphorylated peptides in a sample (Wirbel et al., 2018). Information on the activated kinases under menadione-stressed or CSC-conditioned media protected-conditions

could provide insights into the signalling mechanisms of stress and protection and could be extrapolated to predict the extracellular factors involved.

### 4.3.3. ROS-independent protection of human cardiomyocytes from doxorubicin by CSC-conditioned media

The second trigger of cardiotoxicity used here, doxorubicin, and its effects have been broadly studied in hPSC-CM (Burridge et al., 2016; Fang et al., 2019; Maillet et al., 2016). The study by Burridge et al demonstrated that hPSC-CM lines derived from different patients can have different sensitivities to doxorubicin, predictive of each individual's response to the anthracycline drug (Burridge et al., 2016). For instance, after 24 hr of 0.1-10 μM doxorubicin treatment, induction of ROS was 2-fold higher in myocytes derived from the susceptible individual compared to the healthy control and the patient that did not experience DOX cardiotoxicity. The same effect was seen when measuring the induction of endogenous $H_2O_2$ and the reduced levels of the antioxidant glutathione as a marker of the oxidative stress response. Further to that - like us - the Burridge study used MitoSOX and JC-10 to study the effect of doxorubicin in mitochondrial responses. All three of the tested hPSC-CM lines showed a consistent concentration-dependent increase in the levels of mitochondrial superoxide and a decrease in the mitochondrial membrane potential following doxorubicin treatment (Burridge et al., 2016). The fact that our CSC-conditioned medium does not counter-act the doxorubicin-induced increase in cellular ROS levels might point to a mechanism of protection that does not involve antioxidant activity or ROS scavenging responses; however, this conclusion differs from results for the protection from DOX by other agents (Babaei-Kouchaki et al., 2020; Russo et al., 2019; Yu et al., 2020) and is subject to further experimental testing. Indeed, several preclinical and clinical

studies using antioxidants to attenuate doxorubicin-mediated cardiotoxicity were not successful, pointing to deleterious mechanisms other than redox cycling (Ghigo et al., 2016; Maulik et al., 2018).

It is well-established from our data and published work that doxorubicin induces ROS generation within cardiomyocytes, which can then amplify several downstream pathways of cell dysregulation and death (Nebigil and Désaubry, 2018). For instance, once generated at high levels in the mitochondria, ROS forms a complex with a negatively charged phospholipid cardiolipin, which is implicated in oxidative phosphorylation and has a key role in mitochondrial-induced apoptosis. Cardiolipin peroxidation results in (i) respiratory complex uncoupling, (ii) formation of the mitochondrial transition pore (mPTP) and (iii) cytochrome c release from the mitochondrial matrix, facilitating caspase-mediated apoptosis signalling. Moreover, necrotic cell death can also be induced, via association of mPTP with Bcl2 family proteins, leading to the reduction of ATP, mitochondrial and cytoplasmic swelling and formation of sarcomeric lesions (Govender et al., 2014). At the transcriptomic level, DOX-generated ROS activate heat shock factor (HSF)-1 which increases the expression of heat shock protein (Hsp)-25 and activates the tumour suppressor p53 protein, thereby leading to altered levels of Bcl2 and Bax. The increased Bcl2 to Bax ratio stimulates mitochondrial-dependent apoptosis in the myocardium (Vedam et al., 2010).

Apart from the discussed role in inducing apoptotic and necrotic responses in cardiomyocytes, doxorubicin seems to have an even wider impact on cell death, as it has been also involved in induction of ferroptosis. Unlike apoptosis, ferroptosis is an iron-dependent and ROS-reliant form of death characterised by decreased

mitochondrial cristae, deformed outer mitochondrial membrane and loss of selective permeability of the plasma membrane, resulting from intense lipid peroxidation and oxidative stress (Cao and Dixon, 2016; Latunde-Dada, 2017; Yu et al., 2017). Ferroptosis has a noteworthy role in cancer cell killing and inhibition of cancer growth. Published work has shown that chemotherapeutic drugs, including doxorubicin, in combination with the ferroptosis inducer erastin exhibit a remarkable synergistic effect on fighting tumours, by triggering both necroptosis and ferroptosis pathways (Fang et al., 2019; Yu et al., 2017, 2015). Furthermore, doxorubicin-mediated iron accumulation in cardiomyocytes may be more deleterious than doxorubicin-induced ROS production; however, this aspect of anthracycline-mediated toxicity has not been explored experimentally here. Reportedly, iron accumulation following doxorubicin exposure activates oxidant-independent cell death pathways (Gammella et al., 2014).

More direct proof for the role of free iron in doxorubicin-induced cardiotoxicity comes from preclinical and clinical models of disease, where antioxidants failed to provide a therapeutic effect while iron chelators such as dexrazoxane (ICRF-187) were found to be more promising (Gammella et al., 2014; Ghigo et al., 2016). In rat cardiomyocytes, treatment with dexrazoxane was found to induce hypoxia-inducible factor (HIF) and prevented the activation of doxorubicin induced apoptosis. Further work showed that the iron chelator induced the synthesis of anti-apoptotic proteins and targets of HIF, such as survivin, Mcl1 and haeme oxygenase (Spagnuolo et al., 2011). In addition, dexrazoxane administration in murine (Bjelogrlic et al., 2007) and canine (Herman and Ferrans, 1981) models of doxorubicin-induced cardiomyopathy delayed the progression of heart failure phenotypes. Finally, two multicentre randomised controlled studies demonstrated the beneficial effects of dexrazoxane in breast cancer patients and has been approved as a cardioprotective strategy in the chemotherapy setting

(Swain et al., 1997; Venturini et al., 1996). In summary, protection against doxorubicin-induced cardiotoxicity can be ROS-independent as suggested both by a subset of the published findings and by our results for the ability of CSC-conditioned medium to prevent cardiomyocyte cell death without reducing the levels of cellular or mitochondrial ROS. Further investigation into the responsible secreted products of CSC or the effects of iron chelators and their inhibition in our model of human cardiomyocyte death are strategies that can provide more information.

### 4.3.4. Other players in doxorubicin-induced cardiotoxicity

A recent notion supports that doxorubicin induces apoptosis via upregulation of death receptors in cardiomyocytes. A study by Zhang's group revealed that anthracycline treatment causes a significant upregulation of death receptors including TNFR1, Fas, DR4 and DR5 in hPSC-CM, both at the mRNA and the protein level (Zhao and Zhang, 2017). Subsequently, human myocytes undergo spontaneous apoptosis, which can be further stimulated by death ligands such as TNF-related apoptosis inducing ligand (TRAIL) that binds DR4 and DR5 and triggers caspase activation (Kim et al.; Twomey et al., 2015; Wang et al., 2010; Wu et al., 2004). Therefore, under physiologically relevant conditions, TRAIL might be directly involved in doxorubicin-mediated cardiotoxicity via the extrinsic pathway of apoptosis and could be a potential therapeutic target.

Cytokine regulation has also been implicated in doxorubicin-induced cardiotoxicity and could be an alternative way through which CSC-conditioned medium counter-acts this form of stress. DOX was found to inhibit of one of the major pro-survival signalling cascades, the growth factor Neuregulin-1 (NRG) and its tyrosine kinase receptor ErbB. NRG-1 administration in doxorubicin-treated rat cardiomyocytes and mice has been

found to reduce release of cardiac troponins, maintain cardiac function, and improve survival (Bian et al., 2009). Furthermore, cardiomyocytes isolated from ErbB2-deleted hearts show an increased sensitivity to doxorubicin (Crone et al., 2002) and moreover, a heterozygous knock-out of NRG-1 upregulates doxorubicin-dependent systolic failure and mortality (Liu et al., 2005a).

The glycoprotein 130 (gp130) is an additional survival pathway in the heart, thought to be affected by doxorubicin signalling and could provide a potential therapeutic target via activation of the PI3K/Akt and STAT3 downstream cascades (Negoro et al., 2001).

Overall, the existence of several possible mechanistic explanations regarding doxorubicin-induced cardiotoxicity have emerged, revealing avenues towards numerous cardioprotective strategies that go beyond the traditional inhibition of oxidative stress scenario, into the roles of iron chelation, death receptor downregulation and cytokine/chemokine interactions in pro-survival pathways.

## 4.4. CSC-mediated cardioprotection is exosome-independent

Exosome biology has become very popular over the past decades and stem cell-derived exosomes have been shown to confer protective effects in the heart including decrease in infarct size, stimulation of angiogenesis, reduction of fibrosis and remodelling, regulation of immune cell function and enhancement of contractile function (Cheng et al., 2014b; Kanazawa et al., 2015, 2016; White et al., 2013). Despite the success of exosomes in animal studies, their clinical translation has proven challenging due to the heterogeneity of their isolation, low yield, long-term storage issues and presence of toxic contaminants in the preparations (Börger et al., 2017; Lou et al., 2017; Squillaro et al., 2016). Nevertheless, our results have shown

that CSC-derived exosomes do not contribute to the protection of human cardiomyocytes from cell death. A major reason for this discrepancy could be the type of cells used; as discussed earlier, the CSC populations used by different research groups consist of vastly heterogeneous and overlapping cell signatures. Our secretor CSC most closely resemble the population isolated and characterised by the group of Richard Harvey and named cardiac-resident colony forming unit-fibroblasts (cCFU-F). These cells have been shown to be cardio-protective (Le et al., 2019) but no study has looked at the implication of exosomes in their effects to date. Furthermore, to our knowledge, no study has demonstrated exosome-mediated protection of human cardiomyocytes from apoptotic death.

A study by Barile et al. showed that exosomes from human cardiac progenitor cells (CPC) inhibit cardiomyocyte apoptosis in mouse HL-1 cultured cells, as well as in mouse model of MI (Barile et al., 2014). Conditioned medium from the human CPC was filtered and exosomes were isolated using three different methods: (i) precipitation using the commercially available ExoQuick solution, (ii) ultracentrifugation at 100,000 g for 90 min and (iii) column precipitation using the commercially available Exo-spin kit. The presence of exosomes in their preparations was confirmed using nanoparticle tracking analysis and western blots to identify exosome marker expression (Barile et al., 2014). While their exosome isolation technique concurs with our work, their *in vitro* apoptosis assay was performed differently. Cell death was induced in mouse HL-1 culture by serum deprivation for 12 hr and followed by treatment with the different conditioned medium fractions for the next 36 hr. Cell death was measured using a live/dead staining kit and Caspase-3/7 activity assays. While the authors show insufficiency of the exosome-depleted medium to protect cardiomyocytes from death, the results do not show the effect of the exosome fraction on the cardiomyocytes

alone, a surprising omission, but rather the depleted medium reconstituted with the exosome fraction. Therefore, the study never demonstrates that the exosome fraction alone is able to confer the anti-apoptotic effect of the conditioned medium and cannot exclude a synergistic effect or even interdependence of the two complementary fractions.

A second study by Chen et al. used conditioned media from a population of $Sca1^+$ cardiac progenitor cells from adult mouse to isolate exosomes by precipitation in polyethylene glycol buffer overnight followed by centrifugation and identification using transmission electron microscopy (TEM) and Western blotting (Chen et al., 2013). Target cells for this study were rat H9C2 cardiomyoblasts, which were pre-treated with the medium, with or without exosomes, and then exposed to $H_2O_2$ for 4 hr. Cell death was then measured using the caspase-3/7 luminescence assay, claiming that, in the absence of exosomes, CPC-conditioned medium loses its ability to protect the cardiomyoblasts. However, the authors fail to show several necessary control conditions, i.e., the levels of caspase 3/7 activity in unstressed cells or stressed cells in the absence of CPC-conditioned medium. Hence, their results should be interpreted with caution.

Two additional studies demonstrating anti-apoptotic effects of mouse CPC- and human CDC- derived exosomes on neonatal rat cardiomyocyte cultures both used the ExoQuick kit for exosome precipitation (Ibrahim et al., 2014; Li et al., 2019b). Ibrahim et al. used Cobalt Chloride or $H_2O_2$ to stress the cardiomyocytes, followed by treatment with the conditioned medium fractions with and without exosomes, and measured viability using Calcein uptake (Ibrahim et al., 2014). On the other hand, Li et al., induced apoptosis in the cardiomyocytes by infecting them with the myocarditis virus

CVB3 and subsequently used flow cytometry to measure annexin V staining (Li et al., 2019b). In both cases, exosome-depleted fractions were unable to confer protection from cell death, unlike the complete conditioned media. However, as in the studies discussed before, neither used hPSC-CM as the target cell type nor menadione as the stressor molecule, so discrepancies in the results could be attributed to these large technical differences. Furthermore, the secretor cell populations used in these studies are more heterogeneous and possibly less expanded in culture, unlike our CSC population that is more pure and well-adapted to culture conditions.

Despite the drawbacks of the contradicting studies highlighted above, our technical approach is also not perfect. First, the exosome effect in our study could be hindered by the species difference; we are using mouse CSC-derived exosomes on human PSC-CM target cells. This might be unlikely, as every one of the studies mentioned above also employed species differences between their exosome-secreting cells and their protected target cells (Barile et al., 2014; Chen et al., 2013; Ibrahim et al., 2014; Li et al., 2019b). However, exosome depletion from the conditioned media of our human cardiac mesenchymal stromal cell populations and their subsequent effect on hPSC-CM protection is a straight-forward experiment that would tackle this issue.

A second limitation of our work comes down to the exosome characterisation and identification method. While our protocol has been developed based on the currently most widely used and established approaches on exosome isolation (El-Andaloussi et al., 2012; Tang et al., 2017b; Yakimchuk, 2015), and while our flow cytometry method of identifying $CD9^+/CD63^+$ exosomes gave comparable results to others (Lässer et al., 2012), we have not performed visualisation by TEM to confirm purity by this additional criterion. Furthermore, the cardiomyocyte medium used to derive the conditioned

medium is not serum-free; serum-derived exosomes and other small particles of similar diameter such as lipoproteins persist for up to 18 hr of ultracentrifugation and might thus interfere with the results (Davidson and Yellon, 2018; Liang et al., 2016; Shelke et al., 2014).

While ultracentrifugation is considered to be the gold standard and most frequently used method for exosome isolation, high-speed spinning might sometimes damage exosomes and impede their downstream analysis (Li et al., 2017). Likewise, it might be concentrating toxic products of the cell that could cause the increase in hPSC-CM death observed in our data, in the presence of the exosome fraction. It is conceivable that our CSC produce pro-apoptotic factors and toxic waste products, as they are seeded at very high densities for the derivation of the conditioned medium. Despite the limitations discussed for guaranteeing exosome purity in the enriched fraction, our major objectives were to ensure depletion of exosomes from the conditioned medium and subsequent protection of cardiomyocytes by this exosome-free fraction, both of which aspects were successful.

## 4.5. Characterisation of CSC-conditioned medium by genomic and proteomic approaches

The strategy used here for the identification of candidate paracrine mediators involved a range of transcriptomic approaches including candidate-driven single cell qRT-PCR and unbiased RNA-Seq comparisons of protective and non-protective secretor cell populations, as well as deep sequencing of the target hPSC-CM in the presence and absence of menadione, with and without rescue by CSC-conditioned medium. Despite the large amount of information obtained by genomic technologies, the validation of

enriched genes by proteomic approaches is vital. We thus used a mid-throughput cytokine array screen to identify protein mediators enriched in the protective media.

### 4.5.1. Transcriptomic profiling of the secretor cells and preliminary candidate testing

Both methods of sequencing used on the secretor cells flagged two potential candidates enriched in the CSC but not in the non-protective TTF: *Igf1* and *Bmp4*. Both genes encode for secreted proteins that have been generally associated with negative regulation of cell death based on their Gene Ontology categorisation. While IGF1 is an established anti-apoptotic factor in cardiomyocytes (Buerke et al., 1995; Kawaguchi et al., 2010; Li et al., 1997; Opgaard and Wang, 2005; Wang et al., 1998), BMP4 is better known for its use in cardiomyocyte differentiation protocols from progenitor cells (Cagavi et al., 2014; Hasani et al., 2020; Khaleghi et al., 2014). Furthermore, it has been shown that BMP signalling is essential for growth, viability and migratory potential of lung cancer cells (Mihajlović et al., 2019). However in cardiomyocytes, BMP4 has been associated with induction of hypertrophy, apoptosis, fibrosis and ion channel remodelling (Guo and Dong, 2014; Hu et al., 2014; Sun et al., 2013a, 2013b; Xing et al., 2015; Yuan et al., 2019). Hence, the effect of BMP4 on cardiomyocyte apoptosis was not further pursued in this work. Instead, a literature search was employed to prioritise other factors from the RNA-seq study, to be tested for their anti-apoptotic effects in our menadione-treated hPSC-CM culture model.

Recombinant protein titration experiments showed insufficiency of the tested factors to protect hPSC-CM from menadione-induced death. Several reasons could be underlying this negative result including: (i) the identification of correct dosing; (ii) the biological activity of the recombinant proteins; (iii) the presence of the receptors for

these ligands on the target hPSC-CM; (iv) the actual secretion of these factors by the CSC and (v) the sufficiency of each factor to confer protection on hPSC-CM alone. In an explorative attempt to address the latter point, we tested a combination of factors in a cocktail which was still incapable of protecting hPSC-CM from death. Further exploration of the counter-measures mentioned would require high amounts of resources and time and, fundamentally, might not be worth it, given uncertainty for even the existence of the relevant ligand/receptor interaction in our model system. Hence, as a revised RNA-seq approach, we decided to explore better the protective medium and its effects on the target cardiomyocytes, taking these datasets together for more solid candidate identification.

### 4.5.2. Transcriptomic profiling of the target cells and identification of potential protective mediators

Deep sequencing of menadione-treated IMR90-CM, in the presence and absence of CSC-conditioned medium, revealed striking transcriptomic changes upon induction of oxidative stress and a considerable rescue of the same magnitude in the presence of the protective medium. A recent study looking at the transcriptomic response in remote and infarct zones post-MI in the murine heart identified strong transcriptional changes in the border zone amongst which were the acute downregulation of mitochondrial oxidative phosphorylation, calcium handling, and sarcomere function (van Duijvenboden et al., 2019). An older study by Harpster et al. reported early changes in the transcriptome of the mouse left ventricle post-MI , also identifying decreases in transcripts encoding for essential sarcomeric proteins (Harpster et al., 2006). In agreement with these published data, menadione-induced oxidative stress caused significant downregulation of genes involved in physiological cardiac function and

contractility responses in IMR90-CM. Hence, these results validate the use of menadione on human cardiomyocytes in culture to model aspects of stress induction in the left ventricle after MI.

Our data showed that the treatment of lethally-stressed IMR90-CM with CSC-conditioned medium blocked the up-regulation of transcripts involved in oxidative stress and pro-apoptotic responses. Amongst these, *ETS1* encodes for the ETS transcription factor, a mediator of vascular remodelling and inflammation. As a response to different inflammatory mediators such as TNFα, ETS1 is responsible for the generation of ROS and more specifically $H_2O_2$ and superoxide anions ($O_2^-$) (Ni et al., 2007; Zhan et al., 2005). An alternative transcript up-regulated by menadione is *PHLDA,* which has been recently identified as a molecular marker for ischemic cardiomyopathy both in a rat model of permanent occlusion and in cardiomyocyte cell cultures (Wang et al., 2018a). Furthermore, *PHLDA* was reported to promote cardiomyocyte apoptosis via AKT phosphorylation and activation of the p53 pathway (Wang et al., 2018a). Treatment with CSC-conditioned medium prevents the up-regulation of *ETS1* and *PHLDA* expression, which could partly explain the inhibition of ROS and protection of IMR90-CM from apoptosis. However, additional validation experiments are necessary such as detection of the factor levels with and without CSC-conditioned medium by qRT-PCR and ELISA or forced expression by viral gene transfer to see if the protective effects of CSC-conditioned media are blocked.

### 4.5.3. Identification of potential cardio-protective ligand-receptor pairs using bioinformatic tools

Downstream bioinformatic analysis of the RNA-Seq data from the CSC and the IMR90-CMs using the CellPhone DB tool allowed the prediction of candidate ligand-

receptor pairs that could be responsible for the observed protective effect. The ligand with the highest significant mean expression was Cxcl10, either binding to CXCR3 or DPP4 receptors. Our data suggest that DPP4 is expressed by IMR90-CMs under all conditions (baseline, Mena-treated and Mena-CondM-treated), while CXCR3 is absent from the myocytes at baseline. Even though its direct effects on cardiomyocytes are unclear, CXCL10 is a pleiotropic cytokine which has been shown to induce migration, proliferation and survival of endothelial cells and vascular smooth muscle cells (Altara et al., 2016). Under conditions of MI CXCL10 exhibits angiostatic and anti-fibrotic roles, preventing premature neovascularisation and fibrosis until apoptotic cell clearance is complete in the damaged myocardium (Van Den Borne et al., 2001; Frangogiannis et al., 2001). A study by Bujak et al., used CXCL10-deficient mice to demonstrate that under MI conditions, CXCL10 promotes wound contraction and attenuates adverse remodelling (Bujak et al., 2009). DPP4 is a co-stimulatory receptor which truncates the N-terminus of CXCL10, resulting in an antagonistic form of the chemokine (Casrouge et al., 2011; Proost et al., 2001). Therefore, DPP4 inhibitors are attractive for experimental therapeutic approaches to preserve the bioactive form of the chemokine (Decalf et al., 2016). Our results thus predict that Cxcl10 signalling is inhibited at baseline due to the expression of DPP4. Upon menadione-treatment and in the presence of CSC-conditioned medium, the cardiomyocytes might induce expression of CXCR3 to balance the inhibition by DPP4 and allow some degree of CXCL10 signalling. This theory, as well as the reason why DPP4 is not down-regulated under stress can be tested experimentally.

Another set of interaction partners highlighted by CellPhone DB involves Ephrin-Eph signalling, the largest family of tyrosine kinase receptors with broad roles across differentiation, proliferation and migration of several cell types (Pasquale, 2008).

Ephrin ligands and their receptors have also been studied in the context of MI and shown to affect cardiomyocyte survival, regeneration and thus protection from MI-induced stress (Dries et al., 2011; O'Neal et al., 2013). More specifically, Ephrin A signalling has been reported to inhibit apoptosis via phosphorylation of AKT (Holen et al., 2008). Furthermore, synergistic effects of Ephrin A1 and growth factors such as FGF2 in cells that co-express EphA4 and FGFR receptors have been observed (Yokote et al., 2005). Furthermore, the predicted pair of NRG4 – ERBB4 has also been implicated in survival and growth of cardiomyocytes and ERBB4 receptor was found to be expressed in both neonatal and adult ventricular myocytes (Zhao et al., 1998).

Another pleiotropic ligand flagged in our 'interesting' interaction pairs is the TGFβ1 binding to aVb6 complex in the protected myocytes or to TGFβR receptors expressed by IMR90-CMs under all conditions tested. As described in the relevant section in the introduction (Section 1.7.6.4), TGFβ is a central mediator of cardiac healing after infarction and some of its protective effects might result from inhibition of cardiomyocyte apoptosis (Baxter et al., 2001b; Bujak and Frangogiannis, 2007). A potential mechanism contributing to myocyte protection by the CSC-conditioned medium might be the expression of aVb6 complex on the stressed IMR90-CMs, which is necessary for the cleavage of the pro-domain and the subsequent activation of latent TGFβ1 to its fully functioning form (Shi et al., 2011).

Additional predicted interactions that involved highly expressed ligand-receptor pairs in the tested cell types include NODAL – NODALR and OXT – OXTR, both of which have reported roles in cardiac development but their function in adult cardiomyocyte repair or apoptosis has not been investigated yet (Medeiros De Campos-Baptista et al., 2008; Paquin et al., 2002). Similarly, the predicted interaction between SEMA3E –

PLXND1 has not been studied in the context of cardiomyocyte apoptosis, however a recent study reports the role of the interaction in tumour cell survival and suppression of apoptosis via an intriguing mechanism (Sandireddy et al., 2019). When ligand-free, the dependency receptor PLXND1 (see introduction section 1.5.2) triggers apoptosis upon interaction with NR4A, an orphan nuclear receptor. Upon SEMA3E binding, the cytotoxic interaction is prevented, leading to apoptosis resistance and suggesting a therapeutic approach based on the activation of a dependency receptor pathway (Sandireddy et al., 2019).

Despite the supporting literature, CellPhone DB-derived interactions are just predictions and come with their limitations. According to the tool's website, interacting partners were considered as binary interactions annotated by IUPHAR (www.guidetopharmacology.org), innateDB (www.innatedb.com) and iMEX consortium (www.imexconsortium.org). While most of the ligand-receptor interactions were manually curated using UniProt and PubMed descriptions some of the predictions were only based on the online databases and textmining and might have not been validated extensively in experiments. One example of a disputable interaction that came up in our dataset is TNFSF12 – TNFRSF25 or more commonly called TWEAK – DR3. While TWEAK was originally identified as the only ligand for DR3, this could not be confirmed in follow-up studies which also demonstrated that TWEAK could signal in the absence of DR3 (Kaptein et al., 2000; Lynch et al., 1999; Marsters et al., 1998). Later, a more prominent receptor was identified for TWEAK and likewise, other more common ligands for DR3 (Bossen et al., 2006; Migone et al., 2002; Wiley et al., 2001). Further studies using flow cytometric binding assays and *in vivo* gene knock-out experiments confirmed that TWEAK is not a binding partner for DR3 (Bossen et al., 2006; Bull et al., 2008; Meylan et al., 2008; Wang, 2012). Hence, any

prediction given by the tool needs to be manually validated both using available literature and experimental work in our system.

Looking into our study more critically, it should be noted that the RNA samples of IMR90-CM were collected 24 hr after the induction of menadione stress or conditioned medium treatment, unavoidably limiting our predictions to the interactions that are still present at the end of the incubation period. Hence, the validity of our data is based on the assumption that 24 hr after menadione treatment, at least a proportion of the myocytes express protection-mediating receptors. Furthermore, additional cell pairs could have been used to obtain relevant interactions, such as the potentially interesting autocrine regulation in the protected IMR90-CMs. This sample has been treated with both menadione and CSC-conditioned medium for 24 hr and is thus also likely to express protection-mediating receptors. In terms of the self-released ligands, the CSC-conditioned medium might be inducing the cardiomyocytes to produce and release ligands to self-protect, contributing to the beneficial effect observed (Winegrad et al., 1999). Hence, our existing data could be re-visited using a different exclusion strategy to add to the potentially interesting interactions.

According to our results, the protected myocytes expressed four receptors specific to CCL7 chemokine; ACXR2, CCR2, CCR3, CCR5. These interactions were also present in the TTF → Mena-CondM-CMs pair but at a 4-fold lower expression level. Furthermore, our cytokine array experiment showed higher enrichment of CCL7 in the TTF- than in the CSC-secretome, hence it is unlikely that this chemokine confers myocyte protection alone. Nevertheless, these data serve as an additional reminder that the presence of a ligand in the non-protective conditioned medium should not

exclude it from being protective, when present in the right context, with the right interactors.

### 4.5.4. Proteomic profiling of the protective medium

Despite the usefulness of mapping the transcriptomic signature of the protective CSC and the target hPSC-CM, a more complete picture can only be obtained using proteomic approaches to identify the actual secreted factors enriched in the protective media. Our cytokine array screens identified enrichment of a mix of cytokines, chemokines and secreted receptor fragments in the protective media.

Soluble cytokine receptors have been previously identified in cell culture supernatants of both humans and mice and tend to keep their ligand binding capacities and regulate cytokine function (Mortier et al., 2004). Previous studies have shown that cleavage and release of IL-15Rα has beneficial functions *in vivo*, as it can be internalised, stored and used by cells for proliferation and survival (Tamzalit et al., 2014). Soluble IL15-Rα could also enhance IL-15 activity, reinforcing the ligand's binding potential on CD122/CD132 dimeric receptor (Mortier et al., 2004). While the role of the soluble receptor has not been studied in the context of cardiomyocytes, IL-15 signalling has been found to protect myocytes from hypoxia and oxidative stress through STAT3 and ERK1/2 pathways (Yeghiazarians et al., 2014). Another soluble receptor enriched in the CSC-conditioned medium is the Tyro-3 (DTK), which undergoes a cleavage step necessary for its functional role in the growth and proliferation of a mouse embryonic fibroblast cell line (Merilahti et al., 2017). While the exact role of the cleaved extracellular domain is still unclear in cardiomyocytes, DTK signalling has been shown to be anti-apoptotic in cancer cells via the Erk pathway (Kafri and Hafizi, 2019).

The presence of pro-apoptotic mediators in CSC-conditioned medium is not surprising and could be a result of autocrine loops in the high-density culture (Saeki et al., 1997). Osteopontin (OPN) has been found to promote left ventricular dysfunction in patients by decreasing mitochondrial 2-oxoglutarate dehydrogenase leading to increased oxidative stress and loss of mitochondrial integrity (Yousefi et al., 2019). However, OPN pro-survival roles have been reported in several cell types and tissues including tumour cells (Wai and Kuo, 2008), endothelial cells (Scatena et al., 1998), melanocytes (Geissinger et al., 2002), chondrocytes (Yumoto et al., 2002) and cardiac fibroblasts (Zohar et al., 2004). Furthermore, OPN has been identified in the secretome of protective $Sca1^+$ CPC (Matsuura et al., 2009). The anti-apoptotic actions of OPN have been attributed to interactions with the CD44 receptor and activation of the PI3K/Akt cascade (Lin and Yang-Yen, 2001). Similarly, despite the fact that TNF-related apoptosis-inducing ligand (TRAIL) has been widely used as a pro-apoptotic inducer in some tumours (Herbst et al., 2010; Secchiero et al., 2004; Soria et al., 2010), this ligand's failure to induce apoptosis has been reported in a number of cell types including vascular smooth muscle cells and cardiomyocytes (Pietro and Zauli, 2004; Secchiero et al., 2004; Toffoli et al., 2012). Hence, whether OPN and TRAIL have a pro-survival role in our model of hPSC-CM is subject to further study.

Despite the high resemblance between the mouse and human CSC at the transcriptomic level, protein factors enriched in the two protective media did not show any overlap. The cytokine array screen only included one human CSC population out of the 5 protective ones and more need to be analysed in order to determine if the heterogeneities are a result of species difference or a more general characteristic between the protective CSC populations. In fact, the human CSC-enriched MMP-1 and TIMP-1 were also enriched in the non-protective TTF-conditioned medium control.

Enrichment in the negative control media does not mean that the factors necessarily induce apoptosis, but they are probably not sufficient to confer protection by themselves. Overall, our results to date point to the existence of a combination of protective mediators which might be interacting with each other or with other factors in the milieu achieving a net effect of cardio-protection.

## 4.6. Study limitations and future directions

### 4.6.1. Model system

This study has used menadione as the principal reagent to model myocardial infarction-induced death in cardiomyocytes and while the generation of hyperoxic stress is a major contributor in cardiac muscle death, we agree that additional complementary models exist for cell culture, such as hypoxia/reoxygenation. A recent study by Hidalgo and colleagues reported a model of ischemia-reperfusion injury in hPSC-CM following metabolic maturation of the cells in order to increase their sensitivity to hypoxia and subsequent reoxygenation (Hidalgo et al., 2018). Apart from employing hypoxia/reoxygenation as a more translational model for the induction of stress, this study proposes an additional aspect that could improve our MI model, namely, hPSC-CM maturation. Our RNA-Seq data have shown that the IMR90-CMs used here express most of the cardiac-specific sarcomeric genes and ion transporters and are comparable to similar lines used previously for translational studies (Burridge et al., 2016). However, we also detected some signs of immaturity in our culture, which is expected from hPSC-CMs. Much work is been done in the field to develop protocols to induce metabolic maturity of these cells (Jiang et al., 2018). Currently available maturation strategies include: prolonged time in culture (Kamakura et al., 2013); three-dimensional cardiac tissue engineering approaches such as hydrogels for mechanical

support (DeForest and Anseth, 2012) or enrichment of extracellular substrates (Zhang et al., 2009); electrical or mechanical stimulation (Nunes et al., 2013); addition of miRNAs or hormones (Parikh et al., 2017) and co-culture with non-CMs (Kim et al., 2010a). Due to time limitations, further work on hPSC-CM maturation and a hypoxia/reoxygenation model is not reported in this thesis but is currently being considered through subsequent grant applications.

The most expedient approach to cardiomyocyte maturity in our institute is to use a more mature 3D model of hPSC-CM, i.e., engineered heart tissue (EHT) through existing collaborations with Sian Harding and Thomas Eschenhagen, to validate the protective effect of CSC-conditioned medium, as was done to corroborate protection by small-molecule inhibitors of MAP4K4 (Fiedler et al., 2019). Although small- and large-animal validation studies could follow, an improved delivery method should be optimised first, for retention and sustained release of the CSC-conditioned medium at the site of infarction.

Medium-loaded biomaterials for controlled local release are feasible and mostly involve direct intramyocardial injection. A recent study has employed a combination of gelatin and Laponite® in a hydrogel to carry human adipose derived stem cell-secretome to the infarcted myocardium and demonstrated biocompatibility, reduction of scar size, and increased capillary density (Waters et al., 2018). Earlier studies have shown the feasibility of fibrin glue (Mehanna et al., 2015) and a heparin-presenting nanofiber network (Webber et al., 2010) for conditioned medium delivery in the myocardium, all of which are feasible approaches in our setting.

### 4.6.2. Identification of the protective molecule(s)

Despite the extensive amount of work into the characterisation of both the target (hPSC-CM) and the secretor cells (CSC), this study has not reached the identification of a single or a definitive group of factors mediating the observed beneficial effects. Several previous studies using different secretor cells and cardiomyocyte targets than ours, as well as different inducers of stress, have identified single factors sufficient for rescuing infarct damage such as follistatin-like 1 (Wei et al., 2015), thymosin β-4 (Hinkel et al., 2008), insulin-like growth factor-1 (Kawaguchi et al., 2010), neuregulin-1 (Guo et al., 2012), hepatocyte-growth factor (Liu et al., 2016a) and others.

The presence of numerous interactions and cross-talk at the site of infarction is very likely and difficult to deconvolute. As our exploration of receptor-ligand interactions at the time of protection shows, CSC-conditioned medium might also have an indirect effect on the protection by priming the cardiomyocytes i.e. induce the hPSC-CM to release factors that subsequently transduce protective signals either within the cell or extracellularly, upon release. Alternatively, the protective factor might not be a protein but a heat-sensitive polynucleotide or a free radical scavenger which complicates its identification by thorough proteomic screens.

One way to complement the cytokine array screens and gain unbiased insight into the CSC-secreted components is by high-throughput Mass Spectrometry analysis of both mouse and human CSC-conditioned media as well as media from non-protective populations, an approach which was attempted in this project but could not be completed due to technical limitations. However, Mass Spectrometry on the CSC-conditioned medium would miss factors released by the primed hPSC-CM as part of self-regulation. A range of candidate factors and interaction partners have been

flagged by RNA-Seq and cytokine arrays performed here. A well-designed knock-down strategy could thus be the next step, to identify the most prominent mediators. Such an approach would involve silencing the secreted factors either by using sequestering antibodies in the medium or CRISPR technology to knock-down their expression at the gene level. Expression of the relevant receptors should be verified on the target cardiomyocytes, as well as the activation of downstream kinases implicated in each signalling pathway.

## 4.7. Implications of this study

### 4.7.1. Human PSC-CM established as a platform for paracrine protection studies

Considering the past failures of promising interventions for cardiomyocyte protection that were based on pre-clinical animal models alone, we recognised the necessity of a human model as a complementary platform to explore the mechanisms of protection and establish preclinical efficacy. Human cardiomyocytes are only sporadically available from biopsies or explanted hearts and, given their inability to expand adequately in culture, render the human cardiac phenotype inaccessible for routine and scalable experimental therapeutics. In recent years, the availability of hPSC-CM has solved most of the issues associated with routine accessibility to human cardiomyocytes, but thus far — apart from therapeutic grafting — has chiefly been applied in the fields of safety pharmacology (Gintant et al., 2017), drug-induced cardiomyopathies (Burridge et al., 2016) and hereditary disorders, not drug discovery for the most prevalent forms of acquired heart disease such as ischemic heart disease. Our study is largely exploiting hPSC-CM as a scalable, discovery platform which - to our knowledge - provides one of the first human models, to study paracrine benefits in

cardiac myocytes, enhancing the pull-through process to translation. An urgent therapeutic need to enhance cardiac function after MI is targeting myocyte survival to reduce infarct size, further preventing cell death as an adjunct to reperfusion (Lefer and Marbán, 2017). While paracrine protection studies *in vitro* give little or no information on the cellular landscape and intercellular interactions of the *in vivo* setting, they are an invaluable model to dissect the protective mechanisms specific to cardiomyocytes. Furthermore, our work provides preliminary evidence that the protective effect of CSC-conditioned medium on cardiomyocyte apoptosis can be reproduced in the infarcted mouse myocardium, adding to the evidence that supports the predictive capacity of 2D hPSC-CM models (Blinova et al., 2017; Fiedler et al., 2019; Gintant et al., 2017; Golforoush and Schneider, 2020; Kirby et al., 2018).

### 4.7.2. Using menadione to model MI stress in cardiomyocytes

In our experimental setting, sensitivity of both human cardiomyocyte lines to the stress molecule, as well as the paracrine protective effect was consistent with previous studies (Badave et al., 2016; Fiedler et al., 2019; Grimm et al., 2015). Phenotypic outcomes relevant to myocyte stress at the time of infarct including cell death, apoptotic DNA fragmentation, the dissipation of mitochondrial membrane potential, induction of cellular ROS and generation of mitochondrial superoxide were all significantly induced by menadione treatment and subsequently suppressed by CSC-conditioned medium. Furthermore, transcriptomic changes in menadione-treated hPSC-CM resemble the changes observed by others under conditions of ischemic cardiomyopathy (van Duijvenboden et al., 2019; Harpster et al., 2006). Hence, our work supports the use of menadione as an inducer of oxidative stress in cardiomyocytes, to model infarction-related damage in culture.

### 4.7.3. Identification of the CSC-conditioned medium as an inhibitor of cardiomyocyte death at the time of MI

Conditioned medium from CSC protects human cardiomyocytes from oxidative stress induced by menadione, but also two additional, clinically relevant, unrelated cardiotoxic drugs (doxorubicin and imatinib), suggesting the presence of multiple pro-survival mechanisms or even a shared mediator of protection. Our work validates a model to investigate extracellular signals that benefit human cardiac muscle survival, demonstrating that secretomes of both mouse and human CSC can suppress human cardiomyocyte death. We report not only an accessible, scalable, translationally relevant platform for future therapeutic cell-free strategies, based on the use of conditioned medium, but also the basis for more refined interventions through the validation of specific secreted mediators or their downstream effectors. The amplitude of protection conferred to hPSC-CM under these reductionist conditions - while just a first step - supports the hypothesis of human cardiomyocyte protection by cardiac-derived cells from lethal stress in clinical conditions (Lefer and Marbán, 2017).

A large portion of the assays used in this work involve high-throughput, high-content imaging well-suited for the limited numbers of hPSC-CM per well and adaptable to the large scale needed to deconvolute the conditioned medium in future loss- or gain-of-function experiments to validate protective mediators. Moreover, our data are consistent with the possibility that – if suitably optimised – the conditioned media can be used as a cell-free product to block myocyte death induced by ischemic injury, as a potential adjunct to the restoration of blood flow. The use of clinical-grade conditioned medium as a therapeutic product is advantageous over the use of cells in terms of translatability and importantly the prevention of histocompatibility issues.

Translational implementation will likely require a biomaterial-based delivery approach for controlled release and efficient local effect. Recent advances in the development of sophisticated scaffolds make the sustained release of conditioned medium or recombinant factors a tangible objective even in the setting of the heart (Lee et al., 2018a; Wei et al., 2015).

Finally, a potential niche application for the protective CSC-conditioned medium is its delivery as an adjuvant to hPSC-CM patches or sheets to preserve their survival and efficiency in the *in vivo* setting. Recent work has proposed a novel therapeutic treatment using hPSC-CM for cardiomyogenesis or derivation of cardiomyocytes *in vivo* (Hsiao et al., 2013; Kawamura et al., 2012, 2013). However, a persisting issue is the poor hPSC-CM survival under conditions of stress, which negatively influences therapeutic effects, limiting the efficacy of clinical applications (Kawamura et al., 2012, 2013; Yang et al., 2014). Hence, strategies to support the transplanted hPSC-CM by enhancing their survival must be identified. A recent study by Yoshida and colleagues reported that co-culture with human MSC enhanced hPSC-CM survival via suppression of ROS when the cells were transplanted (Yoshida et al., 2018). Similarly, CSC-conditioned medium could be used to prime hPSC-CM before delivery or even delivered together with the cells to enhance their therapeutic effect in the heart.

## 4.8. Conclusion

In conclusion, this work has demonstrated that hPSC-CM provide an auspicious, relevant human platform to investigate extracellular signals for cardiac muscle survival, corroborating human cardioprotection by the CSC-secretome (Figure 4.1). Mouse and human CSC have been shown to secrete a set of paracrine factors which have a protective, anti-apoptotic effect on human cardiomyocytes upon oxidative

stress. The underlying mechanisms involve inhibition of ROS and preservation of mitochondrial depolarization, while maintaining hPSC-CM functionality at least in terms of calcium cycling and action potential generation. The protective component is exosome-independent, thermo-labile and >3 kDa in size, while transcriptomic and proteomic candidate identification approaches have generated a list of candidate factors to be tested in the future.

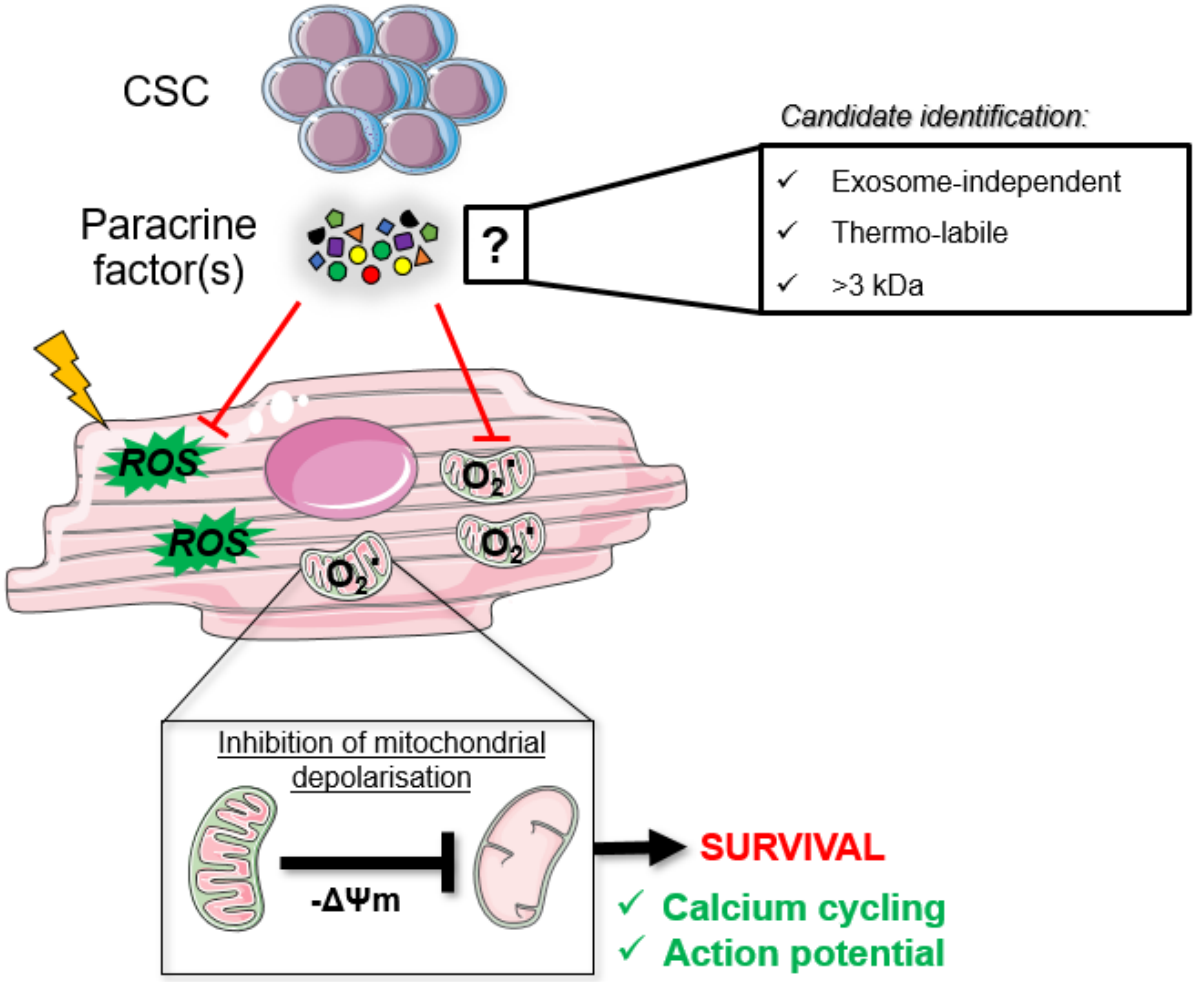



**Figure 4.1: Study summary.**

## 5. References


Abilez, O.J., Tzatzalos, E., Yang, H., Zhao, M.-T., Jung, G., Zöllner, A.M., Tiburcy, M., Riegler, J., Matsa, E., Shukla, P., et al. (2018). Passive stretch induces structural and functional maturation of engineered heart muscle as predicted by computational modeling. Stem Cells *36*, 265–277.

Acehan, D., Jiang, X., Morgan, D.G., Heuser, J.E., Wang, X., and Akey, C.W. (2002). Three-dimensional structure of the apoptosome: implications for assembly, procaspase-9 binding, and activation. Mol. Cell *9*, 423–432.

Adams, J.W., Sakata, Y., Davis, M.G., Sah, V.P., Wang, Y., Liggett, S.B., Chien, K.R., Brown, J.H., and Dorn, G.W. (1998). Enhanced Gαq signaling: A common pathway mediates cardiac hypertrophy and apoptotic heart failure. Proc. Natl. Acad. Sci. U. S. A. *95*, 10140–10145.

Aggarwal, B.B. (2003). Signalling pathways of the TNF superfamily: A double-edged sword. Nat. Rev. Immunol. *3*, 745–756.

Ago, T., and Sadoshima, J. (2006). GDF15, a cardioprotective TGF-beta superfamily protein. Circ. Res. *98*, 294–297.

Airaksinen, K.E.J. (1999). Autonomic mechanisms and sudden death after abrupt coronary occlusion. Ann. Med. *31*, 240–245.

Altara, R., Mallat, Z., Booz, G.W., and Zouein, F.A. (2016). The CXCL10/CXCR3 axis and cardiac inflammation: implications for immunotherapy to treat infectious and noninfectious diseases of the heart. J. Immunol. Res. *2016*, 1–12.

Amano, Y., Nishiguchi, A., Matsusaki, M., Iseoka, H., Miyagawa, S., Sawa, Y., Seo, M., Yamaguchi, T., and Akashi, M. (2016). Development of vascularized iPSC derived 3D-cardiomyocyte tissues by filtration Layer-by-Layer technique and their application for pharmaceutical assays. Acta Biomater. *33*, 110–121.

Van Amerongen, M.J., Harmsen, M.C., Van Rooijen, N., Petersen, A.H., and Van Luyn, M.J.A. (2007). Macrophage depletion impairs wound healing and increases left ventricular remodeling after myocardial injury in mice. Am. J. Pathol. *170*, 818–829.

Amgalan, D., Chen, Y., and Kitsis, R.N. (2017a). Death receptor signaling in the heart: cell survival, apoptosis, and necroptosis. Circulation *136*, 743–746.

Amgalan, D., Pekson, R., and Kitsis, R.N. (2017b). Troponin Release Following Brief Myocardial Ischemia: Apoptosis Versus Necrosis. JACC Basic to Transl. Sci. *2*, 118–121.

Amir, M., Liu, K., Zhao, E., and Czaja, M.J. (2012). Distinct functions of JNK and c-Jun in oxidant-induced hepatocyte death. J. Cell. Biochem. *113*, 3254–3265.

Anderson, J.L., and Morrow, D.A. (2017). Acute myocardial infarction. N. Engl. J. Med. *376*, 2053–2064.

Anding, A.L., and Baehrecke, E.H. (2015). Autophagy in cell life and cell death. Curr. Top. Dev. Biol. *114*, 67–91.

Ankarcrona, M., Dypbukt, J.M., Bonfoco, E., Zhivotovsky, B., Orrenius, S., Lipton, S.A., and Nicotera, P. (1995). Glutamate-induced neuronal death: A succession of necrosis or apoptosis depending on mitochondrial function. Neuron *15*, 961–973.

Anker, S.D., Volterrani, M., Pflaum, C.-D., Strasburger, C.J., Osterziel, K.J., Doehner, W., Ranke, M.B., Poole-Wilson, P.A., Giustina, A., Dietz, R., et al. (2001). Acquired growth hormone resistance in patients with chronic heart failure: implications for therapy with growth hormone. J. Am. Coll. Cardiol. *38*, 443–452.

Antounians, L., Tzanetakis, A., Pellerito, O., Catania, V.D., Sulistyo, A., Montalva, L., McVey, M.J., and Zani, A. (2019). The regenerative potential of amniotic fluid stem cell extracellular vesicles: lessons learned by comparing different isolation techniques. Sci. Rep. *9*, 1837.

Arechederra, M., Carmona, R., González-Nuñez, M., Gutiérrez-Uzquiza, Á., Bragado, P., Cruz-González, I., Cano, E., Guerrero, C., Sánchez, A., López-Novoa, J.M., et al. (2013). Met signaling in cardiomyocytes is required for normal cardiac function in adult mice. Biochim. Biophys. Acta - Mol. Basis Dis. *1832*, 2204–2215.

Arslan, F., Lai, R.C., Smeets, M.B., Akeroyd, L., Choo, A., Aguor, E.N.E., Timmers, L., van Rijen, H. V., Doevendans, P.A., Pasterkamp, G., et al. (2013). Mesenchymal stem cell-derived exosomes increase ATP levels, decrease oxidative stress and activate PI3K/Akt pathway to enhance myocardial viability and prevent adverse remodeling after myocardial ischemia/reperfusion injury. Stem Cell Res. *10*, 301–312.

Ashkenazi, A., and Dixit, V.M. (1998). Death receptors: signaling and modulation. Science *281*, 1305–1308.

Assmus, B., Schächinger, V., Teupe, C., Britten, M., Lehmann, R., Döbert, N.,

Grünwald, F., Aicher, A., Urbich, C., Martin, H., et al. (2002). Transplantation of progenitor cells and regeneration enhancement in acute myocardial infarction (TOPCARE-AMI). Circulation *106*, 3009–3017.

Assmus, B., Walter, D.H., Seeger, F.H., Leistner, D.M., Steiner, J., Ziegler, I., Lutz, A., Khaled, W., Klotsche, J., Tonn, T., et al. (2013). Effect of shock wave-facilitated intracoronary cell therapy on LVEF in patients with chronic heart failure: The CELLWAVE randomized clinical trial. JAMA - J. Am. Med. Assoc. *309*, 1622–1631.

Baba, Y., Higa, J.K., Shimada, B.K., Horiuchi, K.M., Suhara, T., Kobayashi, M., Woo, J.D., Aoyagi, H., Marh, K.S., Kitaoka, H., et al. (2018). Protective effects of the mechanistic target of rapamycin against excess iron and ferroptosis in cardiomyocytes. Am. J. Physiol. Circ. Physiol. *314*, H659–H668.

Babaei-Kouchaki, S., Babapour, V., Panahi, N., and Badalzadeh, R. (2020). Effect of troxerutin on oxidative stress and expression of genes regulating mitochondrial biogenesis in doxorubicin-induced myocardial injury in rats. Naunyn. Schmiedebergs. Arch. Pharmacol. *Online*.

Babich, H., Liebling, E.J., Burger, R.F., Zuckerbraun, H.L., and Schuck, A.G. (2009). Choice of DMEM, formulated with or without pyruvate, plays an important role in assessing the in vitro cytotoxicity of oxidants and prooxidant nutraceuticals. Vitr. Cell. Dev. Biol. - Anim. *45*, 226–233.

Babon, J.J., Varghese, L.N., and Nicola, N.A. (2014). Inhibition of IL-6 family cytokines by SOCS3. Semin. Immunol. *26*, 13–19.

Bachmaier, K., Toya, S., and Malik, A.B. (2014). Therapeutic administration of the chemokine CXCL1/KC abrogates autoimmune inflammatory heart disease. PLoS One *9*, 14–16.

Badave, K., Khan, A., and Rane, S. (2016). Anticancer Vitamin K3 Analogs: A Review. Anticancer. Agents Med. Chem. *16*, 1017–1030.

Bae, S., Siu, P.M., Choudhury, S., Ke, Q., Choi, J.H., Koh, Y.Y., and Kang, P.M. (2010). Delayed activation of caspase-independent apoptosis during heart failure in transgenic mice overexpressing caspase inhibitor CrmA. Am. J. Physiol. Circ. Physiol. *299*, H1374–H1381.

Baggiolini, M. (2001). Chemokines in pathology and medicine. J. Intern. Med. *250*, 91–104.

Bagno, L., Hatzistergos, K.E., Balkan, W., and Hare, J.M. (2018). Mesenchymal

stem cell-based therapy for cardiovascular disease: progress and challenges. Mol. Ther. *26*, 1610–1623.

Bailey, B., Fransioli, J., Gude, N.A., Alvarez, R., Zhan, X., Gustafsson, Å.B., and Sussman, M.A. (2012). Sca-1 Knockout Impairs Myocardial and Cardiac Progenitor Cell FunctionNovelty and Significance. Circ. Res. *111*.

Baines, C.P. (2007). The mitochondrial permeability transition pore as a target of cardioprotective signaling. Am. J. Physiol. - Hear. Circ. Physiol. *293*.

Baines, C.P., Kaiser, R.A., Purcell, N.H., Blair, N.S., Osinska, H., Hambleton, M.A., Brunskill, E.W., Sayen, M.R., Gottlieb, R.A., Dorn, G.W., et al. (2005). Loss of cyclophilin D reveals a critical role for mitochondrial permeability transition in cell death. Nature *434*, 658–662.

Baines, C.P., Kaiser, R.A., Sheiko, T., Craigen, W.J., and Molkentin, J.D. (2007). Voltage-dependent anion channels are dispensable for mitochondrial-dependent cell death. Nat. Cell Biol. *9*, 550–555.

Baldanzi, G., Filigheddu, N., Cutrupi, S., Catapano, F., Bonissoni, S., Fubini, A., Malan, D., Baj, G., Granata, R., Broglio, F., et al. (2002). Ghrelin and des-acyl ghrelin inhibit cell death in cardiomyocytes and endothelial cells through ERK1/2 and PI 3-kinase/AKT. J. Cell Biol. *159*, 1029–1037.

Balsam, L.B., Wagers, A.J., Christensen, J.L., Kofidis, T., Weissmann, I.L., Robbins, R.C., Weissman, I.L., and Robbins, R.C. (2004). Haematopoietic stem cells adopt mature haematopoietic fates in ischaemic myocardium. Nature *428*, 668–673.

Barile, L., Lionetti, V., Cervio, E., Matteucci, M., Gherghiceanu, M., Popescu, L.M., Torre, T., Siclari, F., Moccetti, T., and Vassalli, G. (2014). Extracellular vesicles from human cardiac progenitor cells inhibit cardiomyocyte apoptosis and improve cardiac function after myocardial infarction. Cardiovasc. Res. *103*, 530–541.

Barile, L., Moccetti, T., Marbán, E., and Vassalli, G. (2017). Roles of exosomes in cardioprotection. Eur. Heart J. *38*, 1372–1379.

Barr, L.A., Makarewich, C.A., Berretta, R.M., Gao, H., Troupes, C.D., Woitek, F., Recchia, F., Kubo, H., Force, T., and Houser, S.R. (2014). Imatinib activates pathological hypertrophy by altering myocyte calcium regulation. Clin. Transl. Sci. *7*, 360–367.

Baxter, G.F., Mocanu, M.M., Brar, B.K., Latchman, D.S., and Yellon, D.M. (2001a). Cardioprotective effects of transforming growth factor-beta1 during early

reoxygenation or reperfusion are mediated by p42/p44 MAPK. J. Cardiovasc. Pharmacol. *38*, 930–939.

Baxter, G.F., Mocanu, M.M., Brar, B.K., Latchman, D.S., and Yellon, D.M. (2001b). Cardioprotective effects of transforming growth factor-β1 during early reoxygenation or reperfusion are mediated by p42/p44 MAPK. J. Cardiovasc. Pharmacol. *38*, 930–939.

Becerra, R., Román, B., Di Carlo, M.N., Mariangelo, J.I., Salas, M., Sanchez, G., Donoso, P., Schinella, G.R., Vittone, L., Wehrens, X.H., et al. (2016). Reversible redox modifications of ryanodine receptor ameliorate ventricular arrhythmias in the ischemic-reperfused heart. Am. J. Physiol. Circ. Physiol. *311*, H713–H724.

Becker, L.C. (2005). Yin and yang of MCP-1. Circ. Res. *96*, 812–814.

Bedard, K., and Krause, K.H. (2007). The NOX family of ROS-generating NADPH oxidases: Physiology and pathophysiology. Physiol. Rev. *87*, 245–313.

Behfar, A., Yamada, S., Crespo-Diaz, R., Nesbitt, J.J., Rowe, L.A., Perez-Terzic, C., Gaussin, V., Homsy, C., Bartunek, J., and Terzic, A. (2010). Guided cardiopoiesis enhances therapeutic benefit of bone marrow human mesenchymal stem cells in chronic myocardial infarction. J. Am. Coll. Cardiol. *56*, 721–734.

Behfar, A., Crespo-Diaz, R., Terzic, A., and Gersh, B.J. (2014). Cell therapy for cardiac repair—lessons from clinical trials. Nat. Rev. Cardiol. *11*, 232–246.

Bel, A., Messas, E., Agbulut, O., Richard, P., Samuel, J.L., Bruneval, P., Hagège, A.A., and Menasché, P. (2003). Transplantation of autologous fresh bone marrow into infarcted myocardium: A word of caution. Circulation *108*, 247–252.

Bell, C.R., Jones, L.B., Crensha, B.J., Kumar, S., Rowe, G.C., Sims, B., Javan, G.T., and Matthews, Q.L. (2019). The role of lipopolysaccharide-induced extracellular vesicles in cardiac cell death. Biology (Basel). *8*.

Bell, R.M., Mocanu, M.M., and Yellon, D.M. (2011). Journal of Molecular and Cellular Cardiology Retrograde heart perfusion : The Langendorff technique of isolated heart perfusion. J. Mol. Cell. Cardiol. *50*, 940–950.

Bellin, M., Marchetto, M.C., Gage, F.H., and Mummery, C.L. (2012). Induced pluripotent stem cells: The new patient? Nat. Rev. Mol. Cell Biol. *13*, 713–726.

Beltrami, A.P., Barlucchi, L., Torella, D., Baker, M., Limana, F., Chimenti, S.,

Kasahara, H., Rota, M., Musso, E., Urbanek, K., et al. (2003). Adult cardiac stem cells are multipotent and support myocardial regeneration. Cell *114*, 763–776.

Benjamin, E.J., Muntner, P., Alonso, A., Bittencourt, M.S., Callaway, C.W., Carson, A.P., Chamberlain, A.M., Chang, A.R., Cheng, S., Das, S.R., et al. (2019). Heart disease and stroke statistics—2019 update: A report from the American Heart Association. Circulation *139*, 56–528.

Benjamins, J.A., Nedelkoska, L., Touil, H., Stemmer, P.M., Carruthers, N.J., Jena, B.P., Naik, A.R., Bar-Or, A., and Lisak, R.P. (2019). Exosome-enriched fractions from MS B cells induce oligodendrocyte death. Neurol. - Neuroimmunol. Neuroinflammation *6*, e550.

Beohar, N., Rapp, J., Pandya, S., and Losordo, D.W. (2010). Rebuilding the damaged heart. J. Am. Coll. Cardiol. *56*, 1287–1297.

Berghe, T. Vanden, Linkermann, A., Jouan-Lanhouet, S., Walczak, H., and Vandenabeele, P. (2014). Regulated necrosis: The expanding network of non-apoptotic cell death pathways. Nat. Rev. Mol. Cell Biol. *15*, 135–147.

Bergmann, O., Bhardwaj, R.D., Bernard, S., Zdunek, S., Barnabé-Heide, F., Walsh, S., Zupicich, J., Alkass, K., Buchholz, B.A., Druid, H., et al. (2009). Evidence for cardiomyocyte renewal in humans. Science (80-. ). *324*, 98–102.

Bhuiyan, M.S., and Fukunaga, K. (2007). Inhibition of HtrA2/Omi ameliorates heart dysfunction following ischemia/reperfusion injury in rat heart in vivo. Eur. J. Pharmacol. *557*, 168–177.

Bian, Y., Sun, M., Silver, M., Ho, K.K.L., Marchionni, M.A., Caggiano, A.O., Stone, J.R., Amende, I., Hampton, T.G., Morgan, J.P., et al. (2009). Neuregulin-1 attenuated doxorubicin-induced decrease in cardiac troponins. Am. J. Physiol. - Hear. Circ. Physiol. *297*.

Biesemann, N., Mendler, L., Kostin, S., Wietelmann, A., Borchardt, T., and Braun, T. (2015). Myostatin induces interstitial fibrosis in the heart via TAK1 and p38. Cell Tissue Res. *361*, 779–787.

Bjelogrlic, S.K., Radic, J., Radulovic, S., Jokanovic, M., and Jovic, V. (2007). Effects of Dexrazoxane and Amifostine on evolution of Doxorubicin cardiomyopathy in vivo. Exp Biol Med *232*, 1414–1424.

Blankenberg, S., and Zeller, T. (2018). Standard and novel biomarkers. In chronic coronary artery disease: A companion to Braunwald's heart disease (Elsevier).

Blasig, I.E., Mertsch, K., and Haseloff, R.F. (2002). Nitronyl nitroxides, a novel group of protective agents against oxidative stress in endothelial cells forming the blood-brain barrier. Neuropharmacology *43*, 1006–1014.

Blinova, K., Stohlman, J., Vicente, J., Chan, D., Johannesen, L., Hortigon-Vinagre, M.P., Zamora, V., Smith, G., Crumb, W.J., Pang, L., et al. (2017). Comprehensive translational assessment of human induced pluripotent stem cell derived cardiomyocytes for evaluating drug-induced arrhythmias. Toxicol. Sci. *155*, 237–247.

Blinova, K., Dang, Q., Millard, D., Smith, G., Pierson, J., Guo, L., Brock, M., Lu, H.R., Kraushaar, U., Zeng, H., et al. (2018). International multisite study of Human-induced pluripotent stem cell-derived cardiomyocytes for drug proarrhythmic potential assessment. Cell Rep. *24*, 3582–3592.

Bloom, M.W., Hamo, C.E., Cardinale, D., Ky, B., Nohria, A., Baer, L., Skopicki, H., Lenihan, D.J., Gheorghiade, M., Lyon, A.R., et al. (2016). Cancer therapy–related cardiac dysfunction and heart failure. Circ. Hear. Fail. *9*, e002661.

Bock-Marquette, I., Saxena, A., White, M.D., DiMaio, J.M., and Srivastava, D. (2004). Thymosin β4 activates integrin-linked kinase and promotes cardiac cell migration, survival and cardiac repair. Nature *432*, 466–472.

Bolli, R., Becker, L., Gross, G., Mentzer, R., Balshaw, D., Lathrop, D.A., and NHLBI (2004). Myocardial protection at a crossroads: the need for translation into clinical therapy. Circ. Res. *95*, 125–134.

Bollini, S., Riley, P.R., and Smart, N. (2015). Thymosin β4: Multiple functions in protection, repair andregeneration of the mammalian heart. Expert Opin. Biol. Ther. *15*, S163–S174.

Bommer, J., Kugel, M., Schoeppe, W., Brunkhorst, R., Samtleben, W., Bramsiepe, P., and Scigalla, P. (1988). Dose-related effects of recombinant human erythropoietin on erythropoiesis. Results of a multicenter trial in patients with end-stage renal disease. Contrib. Nephrol. *66*, 85–93.

Bonaventura, A., Montecucco, F., Dallegri, F., Carbone, F., Lüscher, T.F., Camici, G.G., and Liberale, L. (2019). Novel findings in neutrophil biology and their impact on cardiovascular disease. Cardiovasc. Res. *115*, 1266–1285.

Börger, V., Bremer, M., Ferrer-Tur, R., Gockeln, L., Stambouli, O., Becic, A., and Giebel, B. (2017). Mesenchymal stem/stromal cell-derived extracellular vesicles and their potential as novel immunomodulatory therapeutic agents. Int. J. Mol. Sci. *18*, 1450.

Van Den Borne, P., Quax, P.H.A., Hoefer, I.E., and Pasterkamp, G. (2001). The multifaceted functions of CXCL10 in cardiovascular disease. Biomed Res. Int. *2014*.

Bossen, C., Ingold, K., Tardivel, A., Bodmer, J.L., Gaide, O., Hertig, S., Ambrose, C., Tschopp, J., and Schneider, P. (2006). Interactions of tumor necrosis factor (TNF) and TNF receptor family members in the mouse and human. J. Biol. Chem. *281*, 13964–13971.

Boström, P., Wu, J., Jedrychowski, M.P., Korde, A., Ye, L., Lo, J.C., Rasbach, K. a, Boström, E.A., Choi, J.H., Long, J.Z., et al. (2012). A PGC1a dependent myokine that derives browning of white fat and thermogenesis. Nature *481*, 463–468.

Braunwald, E. (2015). The war against heart failure: the Lancet lecture. Lancet *385*, 812–824.

Brenner, D., Blaser, H., and Mak, T.W. (2015). Regulation of tumour necrosis factor signalling: Live or let die. Nat. Rev. Immunol. *15*, 362–374.

Bristow, M.R., Saxon, L.A., Boehmer, J., Krueger, S., Kass, D.A., De Marco, T., Carson, P., DiCarlo, L., DeMets, D., White, B.G., et al. (2004). Cardiac-resynchronization therapy with or without an Implantable defibrillator in advanced chronic heart failure. N. Engl. J. Med. *350*, 2140–2150.

Brocheriou, V., Hagège, A.A., Oubenaïssa, A., Lambert, M., Mallet, V.O., Duriez, M., Wassef, M., Kahn, A., Menasché, P., and Gilgenkrantz, H. (2000). Cardiac functional improvement by a human Bcl-2 transgene in a mouse model of ischemia/reperfusion injury. J. Gene Med. *2*, 326–333.

Bromage, D.I., Davidson, S.M., and Yellon, D.M. (2014). Stromal derived factor 1α: A chemokine that delivers a two-pronged defence of the myocardium. Pharmacol. Ther. *143*, 305–315.

Brooks, W.W., and Conrad, C.H. (2000). Myocardial fibrosis in transforming growth factor β1 heterozygous mice. J. Mol. Cell. Cardiol. *32*, 187–195.

Brunskill, E.W., Witte, D.P., Yutzey, K.E., and Potter, S.S. (2001). Novel cell lines promote the discovery of genes involved in early heart development. Dev. Biol. *235*, 507–520.

Buerke, M., Murohara, T., Skurk, C., Nuss, C., Tomaselli, K., and Lefer, A.M. (1995). Cardioprotective effect of insulin-like growth factor I in myocardial ischemia followed by reperfusion. Proc. Natl. Acad. Sci. U. S. A. *92*, 8031–8035.

Bujak, M., and Frangogiannis, N.G. (2007). The role of TGF-β signaling in myocardial infarction and cardiac remodeling. Cardiovasc. Res. *74*, 184–195.

Bujak, M., Dobaczewski, M., Gonzalez-Quesada, C., Xia, Y., Leucker, T., Zymek, P., Veeranna, V., Tager, A.M., Luster, A.D., and Frangogiannis, N.G. (2009). Induction of the CXC chemokine interferon-gamma-inducible protein 10 regulates the reparative response following myocardial infarction. Circ. Res. *105*, 973–983.

Bull, M.J., Williams, A.S., Mecklenburgh, Z., Calder, C.J., Twohig, J.P., Elford, C., Evans, B.A.J., Rowley, T.F., Slebioda, T.J., Taraban, V.Y., et al. (2008). The death receptor 3-TNF-like protein 1A pathway drives adverse bone pathology in inflammatory arthritis. J. Exp. Med. *205*, 2457–2464.

Burridge, P.W., Thompson, S., Millrod, M.A., Weinberg, S., Yuan, X., Peters, A., Mahairaki, V., Koliatsos, V.E., Tung, L., and Zambidis, E.T. (2011). A Universal System for Highly Efficient Cardiac Differentiation of Human Induced Pluripotent Stem Cells That Eliminates Interline Variability. PLoS One *6*, e18293.

Burridge, P.W., Matsa, E., Shukla, P., Lin, Z.C., Churko, J.M., Ebert, A.D., Lan, F., Diecke, S., Huber, B., Mordwinkin, N.M., et al. (2014). Chemically defined generation of human cardiomyocytes. Nat. Methods *11*, 855–860.

Burridge, P.W., Li, Y.F., Matsa, E., Wu, H., Ong, S.G., Sharma, A., Holmström, A., Chang, A.C., Coronado, M.J., Ebert, A.D., et al. (2016). Human induced pluripotent stem cell-derived cardiomyocytes recapitulate the predilection of breast cancer patients to doxorubicin-induced cardiotoxicity. Nat. Med. *22*, 547–556.

Cagavi, E., Bartulos, O., Suh, C.Y., Sun, B., Yue, Z., Jiang, Z., Yue, L., and Qyang, Y. (2014). Functional cardiomyocytes derived from Isl1 cardiac progenitors via Bmp4 stimulation. PLoS One *9*, e110752.

Cahill, T.J., and Kharbanda, R.K. (2017). Heart failure after myocardial infarction in the era of primary percutaneous coronary intervention: Mechanisms, incidence and identification of patients at risk. World J. Cardiol. *9*, 407–415.

Cahill, T.J., Choudhury, R.P., and Riley, P.R. (2017). Heart regeneration and repair after myocardial infarction: translational opportunities for novel therapeutics. Nat. Rev. Drug Discov. *16*, 699–717.

Cai, Z., Jitkaew, S., Zhao, J., Chiang, H.C., Choksi, S., Liu, J., Ward, Y., Wu, L.G., and Liu, Z.G. (2014). Plasma membrane translocation of trimerized MLKL protein is required for TNF-induced necroptosis. Nat. Cell Biol. *16*, 55–65.

Camacho, P., Fan, H., Liu, Z., and He, J.Q. (2016). Small mammalian animal models of heart disease. Am. J. Cardiovasc. Dis. *6*, 70–80.

Cambria, E., Pasqualini, F.S., Wolint, P., Günter, J., Steiger, J., Bopp, A., Hoerstrup, S.P., and Emmert, M.Y. (2017). Translational cardiac stem cell therapy: advancing from first-generation to next-generation cell types. Npj Regen. Med. *2*, 17.

Cameron, B.J., Gerry, A.B., Dukes, J., Harper, J. V., Kannan, V., Bianchi, F.C., Grand, F., Brewer, J.E., Gupta, M., Plesa, G., et al. (2013). Identification of a titin-derived HLA-A1-presented peptide as a cross-reactive target for engineered MAGE A3-directed T cells. Sci. Transl. Med. *5*.

Cao, J.Y., and Dixon, S.J. (2016). Mechanisms of ferroptosis. Cell. Mol. Life Sci. *73*, 2195–2209.

Cao, F., Wagner, R.A., Wilson, K.D., Xie, X., Fu, J.-D., Drukker, M., Lee, A., Li, R.A., Gambhir, S.S., Weissman, I.L., et al. (2008). Transcriptional and functional profiling of human embryonic stem cell-Dderived cardiomyocytes. PLoS One *3*, e3474.

Caplice, N.M., DeVoe, M.C., Choi, J., Dahly, D., Murphy, T., Spitzer, E., Van Geuns, R., Maher, M.M., Tuite, D., Kerins, D.M., et al. (2018). Randomized placebo controlled trial evaluating the safety and efficacy of single low-dose intracoronary insulin-like growth factor following percutaneous coronary intervention in acute myocardial infarction (RESUS-AMI). Am. Heart J. *200*, 110–117.

Carroll, M., Ohno-Jones, S., Tamura, S., Buchdunger, E., Zimmermann, J., Lydon, N.B., Gilliland, D.G., and Druker, B.J. (1997). CGP 57148, a tyrosine kinase inhibitor, inhibits the growth of cells expressing BCR-ABL, TEL-ABL, and TEL-PDGFR fusion proteins. Blood *90*, 4947–4952.

Casrouge, A., Decalf, J., Ahloulay, M., Lababidi, C., Mansour, H., Vallet-Pichard, A., Mallet, V., Mottez, E., Mapes, J., Fontanet, A., et al. (2011). Evidence for an antagonist form of the chemokine CXCL10 in patients chronically infected with HCV. J. Clin. Invest. *121*, 308–317.

Chakravarty, T., Makkar, R.R., Ascheim, D.D., Traverse, J.H., Schatz, R., Demaria, A., Francis, G.S., Povsic, T.J., Smith, R.R., Lima, J.A., et al. (2017). ALLogeneic Heart STem Cells to Achieve Myocardial Regeneration (ALLSTAR) Trial: Rationale and Design. Cell Transplant. *26*, 205–214.

Chamiec, T., Herbaczyńska-Cedro, K., and Ceremuzyński, L. (1996). Effects of antioxidant vitamins C and E on signal-averaged electrocardiogram in acute myocardial infarction. Am. J. Cardiol. *77*, 237–241.

Chandrashekhar, Y., Prahash, A.J., Sen, S., Gupta, S., Roy, S., and Anand, I.S. (2003). The role of arginine vasopressin and its receptors in the normal and failing rat heart. J. Mol. Cell. Cardiol. *35*, 495–504.

Chang, T.-C., and Mendell, J.T. (2007). microRNAs in vertebrate physiology and human disease. Annu. Rev. Genomics Hum. Genet. *8*, 215–239.

Chang, H.Y., Nishitoh, H., Yang, X., Ichijo, H., and Baltimore, D. (1998). Activation of Apoptosis signal-regulating kinase 1 (ASK1) by the adapter protein Daxx. Science (80-. ). *281*, 1860–1863.

Chanyshev, B., Shainberg, A., Isak, A., Chepurko, Y., Porat, E., and Hochhauser, E. (2012). Conditioned medium from hypoxic cells protects cardiomyocytes against ischemia. Mol. Cell. Biochem. *363*, 167–178.

Chen, J., Fujii, K., Zhang, L., Roberts, T., and Fu, H. (2001a). Raf-1 promotes cell survival by antagonizing apoptosis signal-regulating kinase 1 through a MEK-ERK independent mechanism. Proc. Natl. Acad. Sci. U. S. A. *98*, 7783–7788.

Chen, L., Wang, Y., Pan, Y., Zhang, L., Shen, C., Qin, G., Ashraf, M., Weintraub, N., Ma, G., and Tang, Y. (2013). Cardiac progenitor-derived exosomes protect ischemic myocardium from acute ischemia/reperfusion injury. Biochem. Biophys. Res. Commun. *431*, 566–571.

Chen, M.H., Kerkelä, R., and Force, T. (2008). Mechanisms of cardiac dysfunction associated with tyrosine kinase inhibitor cancer therapeutics. Circulation *118*, 84–95.

Chen, T., Zhou, G., Zhu, Q., Liu, X., Ha, T., Kelley, J.L., Kao, R.L., Williams, D.L., and Li, C. (2010a). Overexpression of vascular endothelial growth factor 165 (VEGF165) protects Cardiomyocytes against doxorubicin-induced apoptosis. J. Chemother. *22*, 402–406.

Chen, Y., Lewis, W., Diwan, A., Cheng, E.H.Y., Matkovich, S.J., and Dorn, G.W. (2010b). Dual autonomous mitochondrial cell death pathways are activated by Nix/BNip3L and induce cardiomyopathy. Proc. Natl. Acad. Sci. U. S. A. *107*, 9035–9042.

Chen, Y., Yang, Z., Zhao, Z.-A.A., and Shen, Z. (2017). Direct reprogramming of fibroblasts into cardiomyocytes. Stem Cell Res. Ther. *8*.

Chen, Y., Zhang, Z., Zhu, D., Zhao, W., and Li, F. (2019). Long non-coding RNA MEG3 serves as a ceRNA for microRNA-145 to induce apoptosis of AC16 cardiomyocytes under high glucose condition. Biosci. Rep. *39*.

Chen, Z., Chua, C.C., Ho, Y.-S.S., Hamdy, R.C., and Chua, B.H.L.L. (2001b). Overexpression of Bcl-2 attenuates apoptosis and protects against myocardial I/R injury in transgenic mice. *280*, H2313–H2320.

Cheng, K., Malliaras, K., Li, T.-S., Sun, B., Houde, C., Galang, G., Smith, J., Matsushita, N., and Marbán, E. (2012). Magnetic enhancement of cell retention, engraftment, and functional benefit after intracoronary delivery of cardiac-derived stem cells in a rat model of ischemia/reperfusion. Cell Transplant. *21*, 1121–1135.

Cheng, K., Ibrahim, A., Hensley, M.T., Shen, D., Sun, B., Middleton, R., Liu, W., Smith, R.R., and Marbán, E. (2014a). Relative roles of CD90 and c-kit to the regenerative efficacy of cardiosphere-derived cells in humans and in a mouse model of myocardial infarction. J. Am. Heart Assoc. *3*, e001260.

Cheng, K., Malliaras, K., Smith, R.R., Shen, D., Sun, B., Blusztajn, A., Xie, Y., Ibrahim, A., Aminzadeh, M.A., Liu, W., et al. (2014b). Human cardiosphere-derived cells from advanced heart failure patients exhibit augmented functional potency in myocardial repair. JACC Hear. Fail. *2*, 49–61.

Cheung, W.K., Goon, B.L., Guilfoyle, M.C., and Wacholtz, M.C. (1998). Pharmacokinetics and pharmacodynamics of recombinant human erythropoietin after single and multiple subcutaneous doses to healthy subjects. Clin. Pharmacol. Ther. *64*, 412–423.

Chiao, Y.A., Zamilpa, R., Lopez, E.F., Dai, Q., Escobar, G.P., Hakala, K., Weintraub, S.T., and Lindsey, M.L. (2010). In vivo matrix metalloproteinase-7 substrates identified in the left ventricle post-myocardial infarction using proteomics. J. Proteome Res. *9*, 2649–2657.

Chien, K.R., Frisén, J., Fritsche-Danielson, R., Melton, D.A., Murry, C.E., and Weissman, I.L. (2019). Regenerating the field of cardiovascular cell therapy. Nat. Biotechnol. *37*, 232–237.

Chimenti, I., Smith, R.R., Li, T.-S., Gerstenblith, G., Messina, E., Giacomello, A., and Marbán, E. (2010). Relative roles of direct regeneration versus paracrine effects of human cardiosphere-derived cells transplanted into infarcted mice. Circ. Res. *106*, 971–980.

Chiong, M., Wang, Z. V., Pedrozo, Z., Cao, D.J., Troncoso, R., Ibacache, M., Criollo, A., Nemchenko, A., Hill, J.A., and Lavandero, S. (2011). Cardiomyocyte death: Mechanisms and translational implications. Cell Death Dis. *2*.

Chiou, T.J., Chu, S.T., and Tzeng, W.F. (2003). Protection of cells from menadione-

induced apoptosis by inhibition of lipid peroxidation. Toxicology *191*, 77–88.

Chipuk, J.E., Moldoveanu, T., Llambi, F., Parsons, M.J., and Green, D.R. (2010). The BCL-2 Family Reunion. Mol. Cell *37*, 299–310.

Chistiakov, D.A., Melnichenko, A.A., Myasoedova, V.A., Grechko, A. V., and Orekhov, A.N. (2017). Thrombospondins: A role in cardiovascular disease. Int. J. Mol. Sci. *18*.

Chiu, L.L.Y., and Radisic, M. (2011). Controlled release of thymosin β4 using collagen-chitosan composite hydrogels promotes epicardial cell migration and angiogenesis. J. Control. Release *155*, 376–385.

Chong, J., Chandrakanthan, V., Xaymardan, M., Asli, N., Li, J., Ahmed, I., Heffernan, C., Menon, M., Scarlett, C., Rashidianfar, A., et al. (2011). Adult cardiac-resident MSC-like stem cells with a proepicardial origin. Cell Stem Cell *9*, 527–540.

Chong, J.J.H., Reinecke, H., Iwata, M., Torok-Storb, B., Stempien-Otero, A., and Murry, C.E. (2013). Progenitor cells identified by PDGFR-Alpha expression in the developing and diseased human heart. Stem Cells Dev. *22*, 1932.

Christia, P., Bujak, M., Gonzalez-Quesada, C., Chen, W., Dobaczewski, M., Reddy, A., and Frangogiannis, N.G. (2013). Systematic characterization of myocardial inflammation, repair, and remodeling in a mouse model of reperfused myocardial infarction. J. Histochem. Cytochem. *61*, 555–570.

Chua, C.C., Gao, J., Ho, Y.S., Xiong, Y., Xu, X., Chen, Z., Hamdy, R.C., and Chua, B.H.L. (2007). Overexpression of IAP-2 attenuates apoptosis and protects against myocardial ischemia/reperfusion injury in transgenic mice. Biochim. Biophys. Acta - Mol. Cell Res. *1773*, 577–583.

Chua, S., Leu, S., Lin, Y.C., Sheu, J.J., Sun, C.K., Chung, S.Y., Chai, H.T., Lee, F.Y., Kao, Y.H., Wu, C.J., et al. (2011). Early erythropoietin therapy attenuates remodeling and preserves function of left ventricle in porcine myocardial infarction. J. Investig. Med. *59*, 574–586.

Citro, L., Naidu, S., Hassan, F., Kuppusamy, M.L., Kuppusamy, P., Angelos, M.G., and Khan, M. (2014). Comparison of human induced pluripotent stem-cell derived cardiomyocytes with human mesenchymal stem cells following acute myocardial infarction. PLoS One *9*, e116281.

Clarke, S.J., McStay, G.P., and Halestrap, A.P. (2002). Sanglifehrin A acts as a potent inhibitor of the mitochondrial permeability transition and reperfusion injury of

the heart by binding to cyclophilin-D at a different site from cyclosporin A. J. Biol. Chem. *277*, 34793–34799.

Claycomb, W.C., Lanson, N.A., Stallworth, B.S., Egeland, D.B., Delcarpio, J.B., Bahinski, A., and Izzo, N.J. (1998). HL-1 cells: A cardiac muscle cell line that contracts and retains phenotypic characteristics of the adult cardiomyocyte. Proc. Natl. Acad. Sci. U. S. A. *95*, 2979–2984.

Cohen, M., Boiangiu, C., and Abidi, M. (2010). Therapy for ST-segment elevation myocardial infarction patients who present late or are ineligible for reperfusion therapy. J. Am. Coll. Cardiol. *55*, 1895–1906.

Cohn, J.N., Ferrari, R., Sharpe, N., and Remodeling, on B. of an I.F. on C. (2000). Cardiac remodeling—concepts and clinical implications: a consensus paper from an international forum on cardiac remodeling. J. Am. Coll. Cardiol. *35*, 569–582.

Colombo, M., Raposo, G., and Théry, C. (2014). Biogenesis, secretion, and intercellular interactions of exosomes and other extracellular vesicles. Annu. Rev. Cell Dev. Biol. *30*, 255–289.

Condorelli, G., Roncarati, R., Ross, J., Pisani, A., Stassi, G., Todaro, M., Trocha, S., Drusco, A., Gu, Y., Russo, M.A., et al. (2001). Heart-targeted overexpression of caspase3 in mice increases infarct size and depresses cardiac function. Proc. Natl. Acad. Sci. U. S. A. *98*, 9977–9982.

Contamin, H., Rioufol, G., Bettinger, T., Helbert, A., Portier, K.G., Lepage, O.M., Thomas, R., Broillet, A., Tranquart, F., and Schneider, M. (2012). A minimally-invasive closed chest myocardial occlusion-reperfusion model in rhesus monkeys (Macaca mulatta): Monitoring by contrast-enhanced ultrasound imaging. Int. J. Cardiovasc. Imaging *28*, 531–542.

Correia, C., Koshkin, A., Duarte, P., Hu, D., Teixeira, A., Domian, I., Serra, M., and Alves, P.M. (2017). Distinct carbon sources affect structural and functional maturation of cardiomyocytes derived from human pluripotent stem cells. Sci. Rep. *7*.

Cottler-Fox, M., Kollet, O., and Dipersio, J. (2003). Stem cell mobilization. Hematology *2003*, 419–137.

de Couto, G., Gallet, R., Cambier, L., Jaghatspanyan, E., Makkar, N., Dawkins, J.F., Berman, B.P., and Marbán, E. (2017). Exosomal microRNA iransfer into macrophages mediates cellular postconditioning. Circulation *136*, 200–214.

Criddle, D.N., Gillies, S., Baumgartner-Wilson, H.K., Jaffar, M., Chinje, E.C., Passmore, S., Chvanov, M., Barrow, S., Gerasimenko, O. V, Tepikin, A. V, et al. (2006). Menadione-induced reactive oxygen species generation via redox cycling promotes apoptosis of murine pancreatic acinar cells. J. Biol. Chem. *281*, 40485–40492.

Crompton, M., Ellinger, H., and Costi, A. (1988). Inhibition by cyclosporin A of a Ca2+-dependent pore in heart mitochondria activated by inorganic phosphate and oxidative stress. Biochem. J. *255*, 357–360.

Crone, S.A., Zhao, Y.Y., Fan, L., Gu, Y., Minamisawa, S., Liu, Y., Peterson, K.L., Chen, J., Kahn, R., Condorelli, G., et al. (2002). ErbB2 is essential in the prevention of dilated cardiomyopathy. Nat. Med. *8*, 459–465.

Cross, J. V., and Templeton, D.J. (2004). Oxidative stress inhibits MEKK1 by site-specific glutathionylation in the ATP-binding domain. Biochem. J. *381*, 675–683.

Cui, B., Zheng, Y., Sun, L., Shi, T., Shi, Z., Wang, L., Huang, G., and Sun, N. (2018). Heart regeneration in adult mammals after myocardial damage. Acta Cardiol. Sin. *34*, 115–123.

D'Angelo, D.D., Sakata, Y., Lorenz, J.N., Boivin, G.P., Walsh, R.A., Liggett, S.B., and Dorn, G.W. (1997). Transgenic Gαq overexpression induces cardiac contractile failure in mice. Proc. Natl. Acad. Sci. U. S. A. *94*, 8121–8126.

Dabkowski, E.R., Williamson, C.L., and Hollander, J.M. (2008). Mitochondria-specific transgenic overexpression of phospholipid hydroperoxide glutathione peroxidase (GPx4) attenuates ischemia/reperfusion-associated cardiac dysfunction. Free Radic. Biol. Med. *45*, 855–865.

van Dalen, E.C., Caron, H.N., Dickinson, H.O., and Kremer, L.C. (2008). Cardioprotective interventions for cancer patients receiving anthracyclines. Cochrane Database Syst. Rev. *2*, CD003917.

Damm, K., Hemmann, U., Garin-Chesa, P., Hauel, N., Kauffmann, I., Priepke, H., Niestroj, C., Daiber, C., Enenkel, B., Guilliard, B., et al. (2001). A highly selective telomerase inhibitor limiting human cancer cell proliferation. EMBO J. *20*, 6958–6968.

Danial, N.N., and Korsmeyer, S.J. (2004). Cell Death: Critical Control Points. Cell *116*, 205–219.

Daniels, I., Abulayha, A.M., Thomson, B.J., and Haynes, A.P. (2006). Caspase-

independent killing of Burkitt lymphoma cell lines by rituximab. Apoptosis *11*, 1013–1023.

David W. Thomas, Justin Burns, John Audette, Adam Carroll, Corey Dow-Hygelund, and Michael Hay (2016). Clinical development success rates. BioMedTracker *June*.

Davidson, S.M., and Yellon, D.M. (2018). Exosomes and cardioprotection – A critical analysis. Mol. Aspects Med. *60*, 104–114.

Davidson, M.M., Nesti, C., Palenzuela, L., Walker, W.F., Hernandez, E., Protas, L., Hirano, M., and Isaac, N.D. (2005). Novel cell lines derived from adult human ventricular cardiomyocytes. J. Mol. Cell. Cardiol. *39*, 133–147.

Davies, N.A., Watkeys, L., Butcher, L., Potter, S., Hughes, M.G., Moir, H., Morris, K., Thomas, A.W., and Webb, R. (2015). The contributions of oxidative stress, oxidised lipoproteins and AMPK towards exercise-associated PPARγ signalling within human monocytic cells. Free Radic. Res. *49*, 45–56.

Deavall, D.G., Martin, E.A., Horner, J.M., and Roberts, R. (2012). Drug-Induced Oxidative Stress and Toxicity. J. Toxicol. *2012*, 1–13.

Deb, A., Wang, S., Skelding, K.A., Miller, D., Simper, D., and Caplice, N.M. (2003). Bone marrow-derived cardiomyocytes are present in adult human heart: A study of gender-mismatched bone marrow transplantation patients. Circulation *107*, 1247–1249.

Decalf, J., Tarbell, K. V, Casrouge, A., Price, J.D., Linder, G., Mottez, E., Sultanik, P., Mallet, V., Pol, S., Duffy, D., et al. (2016). Inhibition of DPP 4 activity in humans establishes its in vivo role in CXCL 10 post-translational modification: prospective placebo-controlled clinical studies . EMBO Mol. Med. *8*, 679–683.

DeForest, C.A., and Anseth, K.S. (2012). Advances in bioactive hydrogels to probe and direct cell fate. Annu. Rev. Chem. Biomol. Eng. *3*, 421–444.

Degterev, A., Huang, Z., Boyce, M., Li, Y., Jagtap, P., Mizushima, N., Cuny, G.D., Mitchison, T.J., Moskowitz, M.A., and Yuan, J. (2005). Chemical inhibitor of nonapoptotic cell death with therapeutic potential for ischemic brain injury. Nat. Chem. Biol. *1*, 112–119.

Detillieux, K.A., Sheikh, F., Kardami, E., and Cattini, P.A. (2003). Biological activities of fibroblast growth factor-2 in the adult myocardium. Cardiovasc. Res. *57*, 8–19.

Detillieux, K.A., Cattini, P.A., and Kardami, E. (2004). Beyond angiogenesis: The cardioprotective potential of fibroblast growth factor-2. Can. J. Physiol. Pharmacol. *82*, 1044–1052.

Dewald, O., Ren, G., Duerr, G.D., Zoerlein, M., Klemm, C., Gersch, C., Tincey, S., Michael, L.H., Entman, M.L., and Frangogiannis, N.G. (2004). Of mice and dogs: species-specific differences in the inflammatory response following myocardial infarction. Am. J. Pathol. *164*, 665–677.

Dewald, O., Zymek, P., Winkelmann, K., Koerting, A., Ren, G., Abou-Khamis, T., Michael, L.H., Rollins, B.J., Entman, M.L., and Frangogiannis, N.G. (2005). CCL2/Monocyte Chemoattractant Protein-1 regulates inflammatory responses critical to healing myocardial infarcts. Circ. Res. *96*, 881–889.

Dhalla, A.K., and Singal, P.K. (1994). Antioxidant changes in hypertrophied and failing guinea pig hearts. Am. J. Physiol. - Hear. Circ. Physiol. *266*.

Dhingra, R., Margulets, V., Chowdhury, S.R., Thliveris, J., Jassal, D., Fernyhough, P., Dorn, G.W., and Kirshenbaum, L.A. (2014). Bnip3 mediates doxorubicin-induced cardiac myocyte necrosis and mortality through changes in mitochondrial signaling. Proc. Natl. Acad. Sci. U. S. A. *111*, E5537–E5544.

Dickson, E.W., Tubbs, R.J., Porcaro, W.A., Lee, W.J., Blehar, D.J., Carraway, R.E., Darling, C.E., and Przyklenk, K. (2002). Myocardial preconditioning factors evoke mesenteric ischemic tolerance via opioid receptors and K(ATP) channels. Am. J. Physiol. Heart Circ. Physiol. *283*, H22-8.

Dimmeler, S., Burchfield, J., and Zeiher, A.M. (2008). Cell-based therapy of myocardial infarction. Arterioscler. Thromb. Vasc. Biol. *28*, 208–216.

Diwan, A., Krenz, M., Syed, F.M., Wansapura, J., Ren, X., Koesters, A.G., Li, H., Kirshenbaum, L.A., Hahn, H.S., Robbins, J., et al. (2007). Inhibition of ischemic cardiomyocyte apoptosis through targeted ablation of Bnip3 restrains postinfarction remodeling in mice. J. Clin. Invest. *117*, 2825–2833.

Dixon, S.J., Lemberg, K.M., Lamprecht, M.R., Skouta, R., Zaitsev, E.M., Gleason, C.E., Patel, D.N., Bauer, A.J., Cantley, A.M., Yang, W.S., et al. (2012). Ferroptosis: an iron-dependent form of nonapoptotic cell death. Cell *149*, 1060–1072.

Dobaczewski, M., Xia, Y., Bujak, M., Gonzalez-Quesada, C., and Frangogiannis, N.G. (2010). CCR5 signaling suppresses inflammation and reduces adverse remodeling of the infarcted heart, mediating recruitment of regulatory T cells. Am. J. Pathol. *176*, 2177–2187.

Dobin, A., Davis, C.A., Schlesinger, F., Drenkow, J., Zaleski, C., Jha, S., Batut, P., Chaisson, M., and Gingeras, T.R. (2013). STAR: Ultrafast universal RNA-seq aligner. Bioinformatics *29*, 15–21.

Docherty, J.C., Kuzio, B., Silvester, J.A., Bowes, J., and Thiemermann, C. (1999). An inhibitor of poly (ADP-ribose) synthetase activity reduces contractile dysfunction and preserves high energy phosphate levels during reperfusion of the ischaemic rat heart. Br. J. Pharmacol. *127*, 1518–1524.

Dogra, D., Ahuja, S., Kim, H.-T.T., Rasouli, S.J., Stainier, D.Y.R.R., and Reischauer, S. (2017). Opposite effects of Activin type 2 receptor ligands on cardiomyocyte proliferation during development and repair. Nat. Commun. *8*, 1902.

Doherty, K.R., Talbert, D.R., Trusk, P.B., Moran, D.M., Shell, S.A., and Bacus, S. (2015). Structural and functional screening in human induced-pluripotent stem cell-derived cardiomyocytes accurately identifies cardiotoxicity of multiple drug types. Toxicol. Appl. Pharmacol. *285*, 51–60.

Dondelinger, Y., Jouan-Lanhouet, S., Divert, T., Theatre, E., Bertin, J., Gough, P.J., Giansanti, P., Heck, A.J.R., Dejardin, E., Vandenabeele, P., et al. (2015). NF-κB-independent role of IKKα/IKKβ in preventing RIPK1 kinase-dependent apoptotic and necroptotic cell death during TNF signaling. Mol. Cell *60*, 63–76.

Doring, H., Biomesstechnic, H.D.-B., Achern, U., and 1987, U. (1987). The isolated perfused heart according to Langendorff. Physiol Bohemoslov *39*, 481–504.

Draber, P., Kupka, S., Reichert, M., Draberova, H., Lafont, E., de Miguel, D., Spilgies, L., Surinova, S., Taraborrelli, L., Hartwig, T., et al. (2015). LUBAC-recruited CYLD and A20 regulate gene activation and cell death by exerting opposing effects on linear ubiquitin in signaling complexes. Cell Rep. *13*, 2258–2272.

Drawnel, F.M., Boccardo, S., Prummer, M., Delobel, F., Graff, A., Weber, M., Gérard, R., Badi, L., Kam-Thong, T., Bu, L., et al. (2014). Disease modeling and phenotypic drug screening for diabetic cardiomyopathy using human induced pluripotent stem cells. Cell Rep. *9*, 810–821.

Dries, J.L., Kent, S.D., and Virag, J.A.I. (2011). Intramyocardial administration of chimeric ephrinA1-Fc promotes tissue salvage following myocardial infarction in mice. J. Physiol. *589*, 1725–1740.

Druker, B.J., Tamura, S., Buchdunger, E., Ohno, S., Segal, G.M., Fanning, S., Zimmermann, J., and Lydon, N.B. (1996). Effects of a selective inhibitor of the Abl tyrosine kinase on the growth of Bcr–Abl positive cells. Nat. Med. *2*, 561–566.

Du, C.K., Zhan, D.Y., Akiyama, T., Inagaki, T., Shishido, T., Shirai, M., and Pearson, J.T. (2017). Myocardial interstitial levels of serotonin and its major metabolite 5-hydroxyindole acetic acid during ischemia-reperfusion. Am. J. Physiol. - Hear. Circ. Physiol. *312*, H60–H67.

Du, D.T.M., Hellen, N., Kane, C., and Terracciano, C.M.N. (2015). Action potential morphology of human induced pluripotent stem cell-derived cardiomyocytes does not predict cardiac chamber specificity and is dependent on cell density. Biophys. J. *108*, 1–4.

Dubé, K.N., and Smart, N. (2018). Thymosin β4 and the vasculature: multiple roles in development, repair and protection against disease. Expert Opin. Biol. Ther. *18*, 131–139.

van Duijvenboden, K., de Bakker, D.E.M., Man, J.C.K., Janssen, R., Günthel, M., Hill, M.C., Hooijkaas, I.B., van der Made, I., van der Kraak, P.H., Vink, A., et al. (2019). Conserved NPPB+ border zone switches from MEF2- to AP-1-driven gene program. Circulation *140*, 864–879.

Durand, R.E., and Olive, P.L. (1982). Cytotoxicity, Mutagenicity and DNA damage by Hoechst 33342. J. Histochem. Cytochem. *30*, 111–116.

Durham, K.K., Chathely, K.M., and Trigatti, B.L. (2018). High-density lipoprotein protects cardiomyocytes against necrosis induced by oxygen and glucose deprivation through SR-B1, PI3K, and AKT1 and 2. Biochem. J. *475*, 1253–1265.

Ebelt, H., Hillebrand, I., Arlt, S., Zhang, Y., Kostin, S., Neuhaus, H., Müller-Werdan, U., Schwarz, E., Werdan, K., and Braun, T. (2013). Treatment with bone morphogenetic protein 2 limits infarct size after myocardial infarction in mice. Shock *39*, 353–360.

Ebert, A.D., Diecke, S., Chen, I.Y., and Wu, J.C. (2015). Reprogramming and transdifferentiation for cardiovascular development and regenerative medicine: where do we stand? EMBO Mol. Med. *7*, 1090–1103.

Eder, A., Vollert, I., Hansen, A., and Eschenhagen, T. (2016). Human engineered heart tissue as a model system for drug testing. Adv. Drug Deliv. Rev. *96*, 214–224.

Efremova, M., Vento-Tormo, M., Teichmann, S.A., and Vento-Tormo, R. (2019). CellPhoneDB v2.0: Inferring cell-cell communication from combined expression of multi-subunit receptor-ligand complexes. BioRxiv 680926.

Ehler, E., Moore-Morris, T., and Lange, S. (2013). Isolation and culture of neonatal

mouse cardiomyocytes. J. Vis. Exp. e50154.

Eid, R.A., Alkhateeb, M.A., Eleawa, S., Al-Hashem, F.H., Al-Shraim, M., El-kott, A.F., Zaki, M.S.A., Dallak, M.A., and Aldera, H. (2018). Cardioprotective effect of ghrelin against myocardial infarction-induced left ventricular injury via inhibition of SOCS3 and activation of JAK2/STAT3 signaling. Basic Res. Cardiol. *113*.

El-Andaloussi, S., Lee, Y., Lakhal-Littleton, S., Li, J., Seow, Y., Gardiner, C., Alvarez-Erviti, L., Sargent, I.L., and Wood, M.J.A. (2012). Exosome-mediated delivery of siRNA in vitro and in vivo. Nat. Protoc. *7*, 2112–2126.

Ellison, G.M., Torella, D., Dellegrottaglie, S., Perez-Martinez, C., Perez de Prado, A., Vicinanza, C., Purushothaman, S., Galuppo, V., Iaconetti, C., Waring, C.D., et al. (2011). Endogenous cardiac stem cell activation by insulin-like growth factor-1/hepatocyte growth factor intracoronary injection fosters survival and regeneration of the infarcted pig heart. J. Am. Coll. Cardiol. *58*, 977–986.

Ellison, G.M., Vicinanza, C., Smith, A.J., Aquila, I., Leone, A., Waring, C.D., Henning, B.J., Stirparo, G.G., Papait, R., Scarfò, M., et al. (2013). Adult c-kit(pos) cardiac stem cells are necessary and sufficient for functional cardiac regeneration and repair. Cell *154*, 827–842.

Elrod, J.W., Wong, R., Mishra, S., Vagnozzi, R.J., Sakthievel, B., Goonasekera, S.A., Karch, J., Gabel, S., Farber, J., Force, T., et al. (2010). Cyclophilin D controls mitochondrial pore - Dependent Ca2+ exchange, metabolic flexibility, and propensity for heart failure in mice. J. Clin. Invest. *120*, 3680–3687.

Emmert, M.Y., Wolint, P., Winklhofer, S., Stolzmann, P., Cesarovic, N., Fleischmann, T., Nguyen, T.D.L., Frauenfelder, T., Böni, R., Scherman, J., et al. (2013a). Transcatheter based electromechanical mapping guided intramyocardial transplantation and in vivo tracking of human stem cell based three dimensional microtissues in the porcine heart. Biomaterials *34*, 2428–2441.

Emmert, M.Y., Wolint, P., Wickboldt, N., Gemayel, G., Weber, B., Brokopp, C.E., Boni, A., Falk, V., Bosman, A., Jaconi, M.E., et al. (2013b). Human stem cell-based three-dimensional microtissues for advanced cardiac cell therapies. Biomaterials *34*, 6339–6354.

Emmert, M.Y., Wolint, P., Jakab, A., Sheehy, S.P., Pasqualini, F.S., Nguyen, T.D.L., Hilbe, M., Seifert, B., Weber, B., Brokopp, C.E., et al. (2017). Safety and efficacy of cardiopoietic stem cells in the treatment of post-infarction left-ventricular dysfunction – From cardioprotection to functional repair in a translational pig infarction model. Biomaterials *122*, 48–62.

Engelmann, M.G., Theiss, H.D., Hennig-Theiss, C., Huber, A., Wintersperger, B.J., Werle-Ruedinger, A.-E., Schoenberg, S.O., Steinbeck, G., and Franz, W.-M. (2006). Autologous bone marrow stem cell mobilization induced by granulocyte colony-stimulating factor after subacute ST-segment elevation myocardial infarction undergoing late revascularization. J. Am. Coll. Cardiol. *48*, 1712–1721.

Eppenberger, H.M., Hertig, C., and Eppenberger-Eberhardt, M. (1994). Adult rat cardiomyocytes in culture. A model system to study the plasticity of the differentiated cardiac phenotype at the molecular and cellular levels. Trends Cardiovasc. Med. *4*, 187–193.

Eppenberger, M.E., Hauser, I., Baechi, T., Schaub, M.C., Brunner, U.T., Dechesne, C.A., and Eppenberger, H.M. (1988). Immunocytochemical analysis of the regeneration of myofibrils in long-term cultures of adult cardiomyocytes of the rat. Dev. Biol. *130*, 1–15.

Er, F., Dahlem, K.M., Nia, A.M., Erdmann, E., Waltenberger, J., Hellmich, M., Kuhr, K., Le, M.T., Herrfurth, T., Taghiyev, Z., et al. (2016). Randomized control of sympathetic drive with continuous intravenous Esmolol in patients with acute ST-Segment elevation myocardial infarction. JACC Cardiovasc. Interv. *9*, 231–240.

Esmann, M., Fedosova, N.U., and Marsh, D. (2008). Osmotic stress and viscous retardation of the Na,K-ATPase ion pump. Biophys. J. *94*, 2767–2776.

Evano, B., and Tajbakhsh, S. (2018). Skeletal muscle stem cells in comfort and stress. Npj Regen. Med. *3*.

Ewer, M.S., and Ewer, S.M. (2015). Cardiotoxicity of anticancer treatments. Nat. Rev. Cardiol. *12*, 547–558.

Eyuboglu, M. (2015). Effects of new antiplatelet agents and aldosterone receptor antagonists on mortality in patients with myocardial infarction. Cardiovasc. Drugs Ther. *29*, 495–495.

Ezekowitz, J.A., Kaul, P., Bakal, J.A., Armstrong, P.W., Welsh, R.C., and McAlister, F.A. (2009). Declining in-hospital mortality and increasing heart failure incidence in elderly patients with first myocardial infarction. J. Am. Coll. Cardiol. *53*, 13–20.

Fabbi, P., Spallarossa, P., Garibaldi, S., Barisione, C., Mura, M., Altieri, P., Rebesco, B., Monti, M.G., Canepa, M., Ghigliotti, G., et al. (2015). Doxorubicin impairs the insulin-like growth factor-1 system and causes insulin-like frowth factor-1 resistance in cardiomyocytes. PLoS One *10*, e0124643.

Faccio, L., Fusco, C., Chen, A., Martinotti, S., Bonventre, J. V, and Zervos, A.S. (2000). Characterization of a novel human serine protease that has extensive homology to bacterial heat shock endoprotease HtrA and is regulated by kidney ischemia. J. Biol. Chem. *275*, 2581–2588.

Fan, D., Takawale, A., Basu, R., Patel, V., Lee, J., Kandalam, V., Wang, X., Oudit, G.Y., and Kassiri, Z. (2014). Differential role of TIMP2 and TIMP3 in cardiac hypertrophy, fibrosis, and diastolic dysfunction. Cardiovasc. Res. *103*, 268–280.

Fang, X., Wang, H., Han, D., Xie, E., Yang, X., Wei, J., Gu, S., Gao, F., Zhu, N., Yin, X., et al. (2019). Ferroptosis as a target for protection against cardiomyopathy. Proc. Natl. Acad. Sci. U. S. A. *116*, 2672–2680.

Fatokun, A.A., Dawson, V.L., and Dawson, T.M. (2014). Parthanatos: mitochondrial-linked mechanisms and therapeutic opportunities. Br. J. Pharmacol. *171*, 2000–2016.

Feoktistova, M., Geserick, P., Kellert, B., Dimitrova, D.P., Langlais, C., Hupe, M., Cain, K., MacFarlane, M., Häcker, G., and Leverkus, M. (2011). cIAPs block ripoptosome formation, a RIP1/Caspase-8 containing intracellular cell death complex differentially regulated by cFLIP isoforms. Mol. Cell *43*, 449–463.

Feric, N.T., and Radisic, M. (2016). Maturing human pluripotent stem cell-derived cardiomyocytes in human engineered cardiac tissues. Adv. Drug Deliv. Rev. *96*, 110–134.

Feric, N.T., Pallotta, I., Singh, R., Bogdanowicz, D.R., Gustilo, M.M., Chaudhary, K.W., Willette, R.N., Chendrimada, T.P., Xu, X., Graziano, M.P., et al. (2019). Engineered cardiac tissues generated in the Biowire II: A platform for human-based drug discovery. Toxicol. Sci.

Fernández-Avilés, F., San Román, J.A., García-Frade, J., Fernández, M.E., Peñarrubia, M.J., de la Fuente, L., Gómez-Bueno, M., Cantalapiedra, A., Fernández, J., Gutierrez, O., et al. (2004). Experimental and clinical regenerative capability of human bone marrow cells after myocardial infarction. Circ. Res. *95*, 742–748.

Ferrari, R., Agnoletti, L., Comini, L., Gaia, G., Bachetti, T., Cargnoni, A., Ceconi, C., Curello, S., and Visioli, O. (1998). Oxidative stress during myocardial ischaemia and heart failure. Eur. Heart J. *19 Suppl B*, B2-11.

Festjens, N., Vanden Berghe, T., and Vandenabeele, P. (2006). Necrosis, a well-orchestrated form of cell demise: Signalling cascades, important mediators and concomitant immune response. Biochim. Biophys. Acta - Bioenerg. *1757*, 1371–

1387.

Fidelis-De-Oliveira, P., Werneck-De-Castro, J.P.S., Pinho-Ribeiro, V., Shalom, B.C.M., Nascimento-Silva, J.H., Souza, R.H.C. e, Cruz, I.S., Rangel, R.R., Goldenberg, R.C.S., and Campos-De-Carvalho, A.C. (2012). Soluble factors from mltipotent mesenchymal stromal cells have antinecrotic effect on cardiomyocytes in vitro and improve cardiac function in infarcted rat hearts. Cell Transplant. *21*, 1011–1021.

Fiedler, L.R., Maifoshie, E., and Schneider, M.D. (2014). Mouse models of heart failure: Cell signaling and cell survival. Curr. Top. Dev. Biol. *109*, 171–247.

Fiedler, L.R., Chapman, K., Xie, M., Maifoshie, E., Jenkins, M., Golforoush, P.A., Bellahcene, M., Noseda, M., Faust, D., Jarvis, A., et al. (2019). MAP4K4 inhibition promotes survival of human stem cell-derived cardiomyocytes and reduces infarct size in vivo. Cell Stem Cell *24*, 579-591.e12.

Di Filippo, C., Cuzzocrea, S., Marfella, R., Fabbroni, V., Scollo, G., Berrino, L., Giugliano, D., Rossi, F., and D'Amico, M. (2004). M40403 prevents myocardial injury induced by acute hyperglycaemia in perfused rat heart. Eur. J. Pharmacol. *497*, 65–74.

Filograna, R., Godena, V.K., Sanchez-Martinez, A., Ferrari, E., Casella, L., Beltramini, M., Bubacco, L., Whitworth, A.J., and Bisaglia, M. (2016). Superoxide Dismutase (SOD)-mimetic M40403 is protective in cell and fly models of paraquat toxicity: Implications for Parkinson disease. J. Biol. Chem. *291*, 9257–9267.

Fink, S.L., and Cookson, B.T. (2006). Caspase-1-dependent pore formation during pyroptosis leads to osmotic lysis of infected host macrophages. Cell. Microbiol. *8*, 1812–1825.

Fisher, S.A., Doree, C., Mathur, A., Taggart, D.P., and Martin-Rendon, E. (2016). Stem cell therapy for chronic ischaemic heart disease and congestive heart failure. Cochrane Database Syst. Rev. *12*, CD007888.

Fontes, J.A., Rose, N.R., and Čiháková, D. (2015). The varying faces of IL-6: From cardiac protection to cardiac failure. Cytokine *74*, 62–68.

Foo, R.S.Y., Chan, L.K.W., Kitsis, R.N., and Bennett, M.R. (2007). Ubiquitination and degradation of the anti-apoptotic protein ARC by MDM2. J. Biol. Chem. *282*, 5529–5535.

Force, T., Krause, D.S., and Van Etten, R.A. (2007a). Molecular mechanisms of

cardiotoxicity of tyrosine kinase inhibition. Nat. Rev. Cancer *7*, 332–344.

Force, T., Krause, D.S., and Van Etten, R.A. (2007b). Molecular mechanisms of cardiotoxicity of tyrosine kinase inhibition. Nat. Rev. Cancer *7*, 332–344.

Fordyce, C.B., Roe, M.T., Ahmad, T., Libby, P., Borer, J.S., Hiatt, W.R., Bristow, M.R., Packer, M., Wasserman, S.M., Braunstein, N., et al. (2015). Cardiovascular drug development: Is it dead or just hibernating? J. Am. Coll. Cardiol. *65*, 1567–1582.

Formiga, F.R., Pelacho, B., Garbayo, E., Imbuluzqueta, I., Díaz-Herráez, P., Abizanda, G., Gavira, J.J., Simón-Yarza, T., Albiasu, E., Tamayo, E., et al. (2014). Controlled delivery of fibroblast growth factor-1 and neuregulin-1 from biodegradable microparticles promotes cardiac repair in a rat myocardial infarction model through activation of endogenous regeneration. J. Control. Release *173*, 132–139.

Francis, D.P., Mielewczik, M., Zargaran, D., and Cole, G.D. (2013). Autologous bone marrow-derived stem cell therapy in heart disease: Discrepancies and contradictions. Int. J. Cardiol. *168*, 3381–3403.

Frangogiannis, N.G. (2017). The role of transforming growth factor (TGF)-β in the infarcted myocardium. J. Thorac. Dis. *9*, S52–S63.

Frangogiannis, N., Mendoza, L., … M.L.-T.F., and 2001, U. (2001). Induction and suppression of interferon-inducible protein 10 in reperfused myocardial infarcts may regulate angiogenesis. FASEB J. *15*, 1428–1430.

Frangogiannis, N.G., Perrard, J.L., Mendoza, L.H., Burns, A.R., Lindsey, M.L., Ballantyne, C.M., Michael, L.H., Smith, C.W., and Entman, M.L. (1998). Stem cell factor induction is associated with mast cell accumulation after canine myocardial ischemia and reperfusion. Circulation *98*, 687–698.

Frantz, S., Bauersachs, J., and Ertl, G. (2009). Post-infarct remodelling: contribution of wound healing and inflammation. Cardiovasc. Res. *81*, 474–481.

Frias, M.A., Somers, S., Gerber-Wicht, C., Opie, L.H., Lecour, S., and Lang, U. (2008). The PGE2-Stat3 interaction in doxorubicin-induced myocardial apoptosis. Cardiovasc. Res. *80*, 69–77.

Fuchs, T.A., Abed, U., Goosmann, C., Hurwitz, R., Schulze, I., Wahn, V., Weinrauch, Y., Brinkmann, V., and Zychlinsky, A. (2007). Novel cell death program leads to neutrophil extracellular traps. J. Cell Biol. *176*, 231–241.

Fujio, Y., Nguyen, T., Wencker, D., Kitsis, R.N., and Walsh, K. (2000). Akt promotes survival of cardiomyocytes in vitro and protects against ischemia-reperfusion injury in mouse heart. Circulation *101*, 660–667.

Fukumura, D., Gohongi, T., Kadambi, A., Izumi, Y., Ang, J., Yun, C.O., Buerk, D.G., Huang, P.L., and Jain, R.K. (2001). Predominant role of endothelial nitric oxide synthase in vascular endothelial growth factor-induced angiogenesis and vascular permeability. Proc. Natl. Acad. Sci. U. S. A. *98*, 2604–2609.

Fukushima, S., Coppen, S.R., Lee, J., Yamahara, K., Felkin, L.E., Terracciano, C.M.N., Barton, P.J.R., Yacoub, M.H., and Suzuki, K. (2008). Choice of cell-delivery route for skeletal myoblast transplantation for treating post-infarction chronic heart failure in rat. PLoS One *3*.

Gagné, J.P., Hendzel, M.J., Droit, A., and Poirier, G.G. (2006). The expanding role of poly(ADP-ribose) metabolism: Current challenges and new perspectives. Curr. Opin. Cell Biol. *18*, 145–151.

Galaup, A., Gomez, E., Souktani, R., Durand, M., Cazes, A., Monnot, C., Teillon, J., Le Jan, S., Bouleti, C., Briois, G., et al. (2012). Protection against myocardial infarction and no-reflow through preservation of vascular integrity by angiopoietin-like 4. Circulation *125*, 140–149.

Gallet, R., Dawkins, J., Valle, J., Simsolo, E., de Couto, G., Middleton, R., Tseliou, E., Luthringer, D., Kreke, M., Smith, R.R., et al. (2016). Exosomes secreted by cardiosphere-derived cells reduce scarring, attenuate adverse remodelling, and improve function in acute and chronic porcine myocardial infarction. Eur. Heart J. *38*, 201–211.

Gallet, R., Dawkins, J., Valle, J., Simsolo, E., de Couto, G., Middleton, R., Tseliou, E., Luthringer, D., Kreke, M., Smith, R.R., et al. (2017). Exosomes secreted by cardiosphere-derived cells reduce scarring, attenuate adverse remodelling, and improve function in acute and chronic porcine myocardial infarction. Eur. Heart J. *38*, 201–211.

Gallo, S., Sala, V., Gatti, S., and Crepaldi, T. (2014). HGF/Met axis in heart function and cardioprotection. Biomedicines *2*, 247–262.

Galluzzi, L., and Kroemer, G. (2008). Necroptosis: a specialized pathway of programmed necrosis. Cell *135*, 1161–1163.

Galluzzi, L., Buqué, A., Kepp, O., Zitvogel, L., and Kroemer, G. (2017). Immunogenic cell death in cancer and infectious disease. Nat. Rev. Immunol. *17*, 97–111.

Galluzzi, L., Vitale, I., Aaronson, S.A., Abrams, J.M., Adam, D., Agostinis, P., Alnemri, E.S., Altucci, L., Amelio, I., Andrews, D.W., et al. (2018). Molecular mechanisms of cell death: recommendations of the Nomenclature Committee on Cell Death 2018. Cell Death Differ. *25*, 486–541.

Gammella, E., Maccarinelli, F., Buratti, P., Recalcati, S., and Cairo, G. (2014). The role of iron in anthracycline cardiotoxicity. Front. Pharmacol. *5*.

Gao, J., Senthil, M., Ren, B., Yan, J., Xing, Q., Yu, J., Zhang, L., and Yim, J.H. (2010a). IRF-1 transcriptionally upregulates PUMA, which mediates the mitochondrial apoptotic pathway in IRF-1-induced apoptosis in cancer cells. Cell Death Differ. *17*, 699–709.

Gao, M., Monian, P., Quadri, N., Ramasamy, R., and Jiang, X. (2015). Glutaminolysis and transferrin regulate ferroptosis. Mol. Cell *59*, 298–308.

Gao, R., Zhang, J., Cheng, L., Wu, X., Dong, W., Yang, X., Li, T., Liu, X., Xu, Y., Li, X., et al. (2010b). A phase II, randomized, double-blind, multicenter, based on standard therapy, placebo-controlled study of the efficacy and safety of recombinant human neuregulin-1 in patients with chronic heart failure. J. Am. Coll. Cardiol. *55*, 1907–1914.

García-Ruiz, J.M., Fernández-Jiménez, R., García-Alvarez, A., Pizarro, G., Galán-Arriola, C., Fernández-Friera, L., Mateos, A., Nuno-Ayala, M., Aguero, J., Sánchez-González, J., et al. (2016). Impact of the timing of Metoprolol administration during STEMI on infarct size and ventricular function. J. Am. Coll. Cardiol. *67*, 2093–2104.

Gartz, M., Darlington, A., Afzal, M.Z., and Strande, J.L. (2018). Exosomes exert cardioprotection in dystrophin-deficient cardiomyocytes via ERK1/2-p38/MAPK signaling. Sci. Rep. *8*, 16519.

Gazdar, A.F., Hirsch, F.R., and Minna, J.D. (2016). From mice to men and back: An assessment of preclinical model systems for the study of lung cancers. J. Thorac. Oncol. *11*, 287–299.

Geissinger, E., Weisser, C., Fischer, P., Schartl, M., and Wellbrock, C. (2002). Autocrine stimulation by osteopontin contributes to antiapoptotic signalling of melanocytes in dermal collagen. Cancer Res. *62*, 4820–4828.

Geng, J., Ito, Y., Shi, L., Amin, P., Chu, J., Ouchida, A.T., Mookhtiar, A.K., Zhao, H., Xu, D., Shan, B., et al. (2017). Regulation of RIPK1 activation by TAK1-mediated phosphorylation dictates apoptosis and necroptosis. Nat. Commun. *8*, 359.

Georgiadis, V., Knight, R.A., Jayasinghe, S.N., and Stephanou, A. (2014). Cardiac tissue engineering: renewing the arsenal for the battle against heart disease. Integr. Biol. *6*, 111–126.

Gerber, H.P., Dixit, V., and Ferrara, N. (1998). Vascular endothelial growth factor induces expression of the antiapoptotic proteins Bcl-2 and A1 in vascular endothelial cells. J. Biol. Chem. *273*, 13313–13316.

Gerczuk, P.Z., and Kloner, R.A. (2012). An update on cardioprotection. J. Am. Coll. Cardiol. *59*, 969–978.

Ghandi, M., Huang, F.W., Jané-Valbuena, J., Kryukov, G. V., Lo, C.C., McDonald, E.R., Barretina, J., Gelfand, E.T., Bielski, C.M., Li, H., et al. (2019). Next-generation characterization of the Cancer Cell Line Encyclopedia. Nature.

Gharacholou, S.M., Alexander, K.P., Chen, A.Y., Wang, T.Y., Melloni, C., Gibler, W.B., Pollack, C. V, Ohman, E.M., Peterson, E.D., and Roe, M.T. (2010). Implications and reasons for the lack of use of reperfusion therapy in patients with ST-segment elevation myocardial infarction: findings from the CRUSADE initiative. Am. Heart J. *159*, 757–763.

Ghigo, A., Li, M., and Hirsch, E. (2016). New signal transduction paradigms in anthracycline-induced cardiotoxicity. Biochim. Biophys. Acta - Mol. Cell Res. *1863*, 1916–1925.

Giacca, M., and Zacchigna, S. (2012). VEGF gene therapy: Therapeutic angiogenesis in the clinic and beyond. Gene Ther. *19*, 622–629.

Giacomelli, E., Bellin, M., Sala, L., van Meer, B.J., Tertoolen, L.G.J., Orlova, V. V., and Mummery, C.L. (2017). Three-dimensional cardiac microtissues composed of cardiomyocytes and endothelial cells co-differentiated from human pluripotent stem cells. Dev. *144*, 1008–1017.

Gillet, J.P., Varma, S., and Gottesman, M.M. (2013). The clinical relevance of cancer cell lines. J. Natl. Cancer Inst. *105*, 452–458.

Gilmore, A.P. (2005). Anoikis. Cell Death Differ. *12*, 1473–1477.

Gintant, G., Sager, P.T., and Stockbridge, N. (2016). Evolution of strategies to improve preclinical cardiac safety testing. Nat. Rev. Drug Discov. *15*, 457–471.

Gintant, G., Fermini, B., Stockbridge, N., and Strauss, D. (2017). The evolving roles

of human iPSC-derived cardiomyocytes in drug safety and discovery. Cell Stem Cell *21*, 14–17.

Gintant, G., Burridge, P., Gepstein, L., Harding, S., Herron, T., Hong, C., Jalife, J., and Wu, J.C. (2019). Use of human induced pluripotent stem cell-derived cardiomyocytes in preclinical cancer drug cardiotoxicity testing: A scientific statement from the American Heart Association. Circ. Res. *125*, e75–e92.

Giordano, F.J., Gerber, H.P., Williams, S.P., Vanbruggen, N., Bunting, S., Ruiz-Lozano, P., Gu, Y., Nath, A.K., Huang, Y., Hickey, R., et al. (2001). A cardiac myocyte vascular endothelial growth factor paracrine pathway is required to maintain cardiac function. Proc. Natl. Acad. Sci. U. S. A. *98*, 5780–5785.

Glucksmann, A. (1951). Cell deaths in normal vertebrate ontology. Biol. Rev. *26*, 59–86.

Gnanapavan, S., Kola, B., Bustin, S.A., Morris, D.G., McGee, P., Fairclough, P., Bhattacharya, S., Carpenter, R., Grossman, A.B., and Korbonits, M. (2002). The tissue distribution of the mRNA of ghrelin and subtypes of its receptor, GHS-R, in humans. J. Clin. Endocrinol. Metab. *87*, 2988–2991.

Gnecchi, M., He, H., Noiseux, N., Liang, O.D., Zhang, L., Morello, F., Mu, H., Melo, L.G., Pratt, R.E., Ingwall, J.S., et al. (2006). Evidence supporting paracrine hypothesis for Akt-modified mesenchymal stem cell-mediated cardiac protection and functional improvement. *20*, 661–669.

Goldschneider, D., and Mehlen, P. (2010). Dependence receptors: A new paradigm in cell signaling and cancer therapy. Oncogene *29*, 1865–1882.

Golebiewska, A., Brons, N.H.C., Bjerkvig, R., and Niclou, S.P. (2011). Critical appraisal of the side population assay in stem cell and cancer stem cell research. Cell Stem Cell *8*, 136–147.

Golforoush, P.A., and Schneider, M.D. (2020). Intensive care for human hearts in pluripotent stem cell models. Npj Regen. Med. *in press*.

Gómez-Mauricio, G., Moscoso, I., Martín-Cancho, M.F., Crisóstomo, V., Prat-Vidal, C., Báez-Díaz, C., Sánchez-Margallo, F.M., and Bernad, A. (2016). Combined administration of mesenchymal stem cells overexpressing IGF-1 and HGF enhances neovascularization but moderately improves cardiac regeneration in a porcine model. Stem Cell Res. Ther. *7*.

Gong, Y.N., Guy, C., Olauson, H., Becker, J.U., Yang, M., Fitzgerald, P.,

Linkermann, A., and Green, D.R. (2017). ESCRT-III acts downstream of MLKL to regulate necroptotic cell death and its consequences. Cell *169*, 286-300.e16.

González-Cambeiro, M.C., López-López, A., Abu-Assi, E., Raposeiras-Roubín, S., Peña-Gil, C., García-Acuña, J., and González-Juanatey, R. (2016). Mortality benefit of long-term angiotensin-converting enzyme inhibitors or angiotensin receptor blockers after successful percutaneous coronary intervention in non-ST elevation acute myocardial infarction. Rev. Port. Cardiol. *35*, 645–653.

González-Montero, J., Brito, R., Gajardo, A.I., and Rodrigo, R. (2018). Myocardial reperfusion injury and oxidative stress: Therapeutic opportunities. World J. Cardiol. *10*, 74–86.

Gorelick, D.A., Goodwin, R.S., Schwilke, E., Schwope, D.M., Darwin, W.D., Kelly, D.L., McMahon, R.P., Liu, F., Ortemann-Renon, C., Bonnet, D., et al. (2013). Tolerance to effects of high-dose oral Δ9-tetrahydrocannabinol and plasma cannabinoid concentrations in male daily cannabis smokers. J. Anal. Toxicol. *37*, 11–16.

Gottlieb, R.A., Burleson, K.O., Kloner, R.A., Babior, B.M., and Engler, R.L. (1994). Reperfusion injury induces apoptosis in rabbit cardiomyocytes. J. Clin. Invest. *94*, 1621–1628.

Govender, J., Loos, B., Marais, E., and Engelbrecht, A.M. (2014). Mitochondrial catastrophe during doxorubicin-induced cardiotoxicity: A review of the protective role of melatonin. J. Pineal Res. *57*, 367–380.

Griffith, T.S., Brunner, T., Fletcher, S.M., Green, D.R., and Ferguson, T.A. (1995). Fas ligand-induced apoptosis as a mechanism of immune privilege. Science *270*, 1189–1192.

Grimm, F.A., Iwata, Y., Sirenko, O., Bittner, M., and Rusyn, I. (2015). High-content assay multiplexing for toxicity screening in induced pluripotent stem cell-derived cardiomyocytes and hepatocytes. Assay Drug Dev. Technol. *13*, 529–546.

Gromo, G., Mann, J., and Fitzgerald, J.D. (2014). Cardiovascular drug discovery: A perspective from a research-based pharmaceutical company. Cold Spring Harb. Perspect. Med. *4*.

Gross, A., Yin, X.M., Wang, K., Wei, M.C., Jockel, J., Milliman, C., Erdjument-Bromage, H., Tempst, P., and Korsmeyer, S.J. (1999). Caspase cleaved BID targets mitochondria and is required for cytochrome c release, while BCL-XL prevents this release but not tumor necrosis factor-R1/Fas death. J. Biol. Chem. *274*, 1156–1163.

Grupp, I.L., Jackson, T.M., Hake, P., Grupp, G., and Szabó, C. (1999). Protection against hypoxia-reoxygenation in the absence of poly (ADP ribose) synthetase in isolated working hearts. J. Mol. Cell. Cardiol. *31*, 297–303.

Guerra, S., Leri, A., Wang, X., Finato, N., Di Loreto, C., Beltrami, C.A., Kajstura, J., and Anversa, P. (1999). Myocyte death in thefailing human heart is gender dependent. Circ. Res. *85*, 856–866.

Günter, J., Wolint, P., Bopp, A., Steiger, J., Cambria, E., Hoerstrup, S.P., and Emmert, M.Y. (2016). Microtissues in cardiovascular medicine: regenerative potential based on a 3D microenvironment. Stem Cells Int. *2016*, 1–20.

Guo, W.T., and Dong, D.L. (2014). Bone morphogenetic protein-4: a novel therapeutic target for pathological cardiac hypertrophy/heart failure. Heart Fail. Rev. *19*, 781–788.

Guo, X., Yin, H., Li, L., Chen, Y., Li, J., Doan, J., Steinmetz, R., and Liu, Q. (2017). Cardioprotective role of tumor necrosis factor receptor-associated factor 2 by suppressing apoptosis and necroptosis. Circulation *136*, 729–742.

Guo, Y., He, J., Wu, J., Yang, L., Dai, S., Tan, X., and Liang, L. (2008). Locally overexpressing hepatocyte growth factor prevents post-ischemic heart failure by inhibition of apoptosis via calcineurin-mediated pathway and angiogenesis. Arch. Med. Res. *39*, 179–188.

Guo, Y.F., Zhang, X.X., Liu, Y., Duan, H.Y., Jie, B.Z., and Wu, X.S. (2012). Neuregulin-1 attenuates mitochondrial dysfunction in a rat model of heart failure. Chin. Med. J. (Engl). *125*, 807–814.

Gyöngyösi, M., Khorsand, A., Zamini, S., Sperker, W., Strehblow, C., Kastrup, J., Jorgensen, E., Hesse, B., Tägil, K., Bøtker, H.E., et al. (2005). NOGA-guided analysis of regional myocardial perfusion abnormalities treated with intramyocardial injections of plasmid encoding vascular endothelial growth factor A-165 in patients with chronic myocardial ischemia: subanalysis of the EUROINJECT-ONE multicenter double-blind randomized study. Circulation *112*, I157-65.

Gyöngyösi, M., Wojakowski, W., Lemarchand, P., Lunde, K., Tendera, M., Bartunek, J., Marban, E., Assmus, B., Henry, T.D., Traverse, J.H., et al. (2015). Meta-analysis of cell-based cardiac studies (ACCRUE) in patients with acute myocardial infarction based on individual patient data. Circ. Res. *116*, 1346–1360.

Hajrasouliha, A.R., Tavakoli, S., Ghasemi, M., Jabehdar-Maralani, P., Sadeghipour, H., Ebrahimi, F., and Dehpour, A.R. (2008). Endogenous cannabinoids contribute to

remote ischemic preconditioning via cannabinoid CB2 receptors in the rat heart. Eur. J. Pharmacol. *579*, 246–252.

Hale, S.L., Sesti, C., and Kloner, R.A. (2005). Administration of erythropoietin fails to improve long-term healing or cardiac function after myocardial infarction in the rat. J. Cardiovasc. Pharmacol. *46*, 211–215.

Hamburger, V., and Levi-Montalcini, R. (1949). Proliferation, differentiation and degeneration in the spinal ganglia of the chick embryo under normal and experimental conditions. J. Exp. Zool. *111*, 457–501.

Hamilton, K.L. (2007). Antioxidants and cardioprotection. In Medicine and Science in Sports and Exercise, pp. 1544–1553.

Han, N., Fang, H.-Y., Jiang, J.-X., and Xu, Q. (2020). Down-regulation of microRNA-873 attenuates insulin resistance and myocardial injury in rats with gestational diabetes mellitus by up-regulating IGFBP2. Am. J. Physiol. Metab. *online*.

Hanf, A., Oelze, M., Manea, A., Li, H., Münzel, T., and Daiber, A. (2019). The anti-cancer drug doxorubicin induces substantial epigenetic changes in cultured cardiomyocytes. Chem. Biol. Interact. *313*.

Hanna, A., and Frangogiannis, N.G. (2019). The role of the TGF-β superfamily in myocardial infarction. Front. Cardiovasc. Med. *6*.

Hanna, A.D., Lam, A., Tham, S., Dulhunty, A.F., and Beard, N.A. (2014). Adverse effects of doxorubicin and its metabolic product on cardiac RyR2 and SERCA2A. Mol. Pharmacol. *86*, 438–449.

Harada, K., Friedman, M., Lopez, J.J., Wang, S.Y., Li, J., Prasad, P. V, Pearlman, J.D., Edelman, E.R., Sellke, F.W., and Simons, M. (1996). Vascular endothelial growth factor administration in chronic myocardial ischemia. Am. J. Physiol. *270*, H1791-802.

Harada, M., Qin, Y., Takano, H., Minamino, T., Zou, Y., Toko, H., Ohtsuka, M., Matsuura, K., Sano, M., Nishi, J.I., et al. (2005). G-CSF prevents cardiac remodeling after myocardial infarction by activating the Jak-Stat pathway in cardiomyocytes. Nat. Med. *11*, 305–311.

Hare, J.M., Fishman, J.E., Gerstenblith, G., DiFede Velazquez, D.L., Zambrano, J.P., Suncion, V.Y., Tracy, M., Ghersin, E., Johnston, P. V., Brinker, J.A., et al. (2012). Comparison of allogeneic vs autologous bone marrow–derived mesenchymal stem cells delivered by transendocardial injection in patients with ischemic

cardiomyopathy. JAMA *308*, 2369.

Hariawala, M.D., Horowitz, J.R., Esakof, D., Sheriff, D.D., Walter, D.H., Keyt, B., Isner, J.M., and Symes, J.F. (1996). VEGF improves myocardial blood flow but produces EDRF-mediated hypotension in porcine hearts. In Journal of Surgical Research, (Academic Press Inc.), pp. 77–82.

Harpster, M.H., Bandyopadhyay, S., Thomas, D.P., Ivanov, P.S., Keele, J.A., Pineguina, N., Gao, B., Amarendran, V., Gomelsky, M., McCormick, R.J., et al. (2006). Earliest changes in the left ventricular transcriptome postmyocardial infarction. Mamm. Genome *17*, 701–715.

Hartung, T. (2013). Food for thought; Look back in anger - What clinical studies tell us about preclinical work. ALTEX *30*, 275–291.

Hasani, S., Javeri, A., Asadi, A., and Taha, M.F. (2020). Cardiac differentiation of adipose tissue-derived stem cells is driven by BMP4 and bFGF but counteracted by 5-azacytidine and valproic acid. Cell J. *22*, 273–282.

Hashimoto, H., Olson, E.N., and Bassel-Duby, R. (2018). Therapeutic approaches for cardiac regeneration and repair. Nat. Rev. Cardiol. *15*, 585–600.

Hass, R., Kasper, C., Böhm, S., and Jacobs, R. (2011). Different populations and sources of human mesenchymal stem cells (MSC): A comparison of adult and neonatal tissue-derived MSC. Cell Commun. Signal. *9*.

Hassan, G.S. (2013). Menadione. In Profiles of Drug Substances, Excipients, and Related Methodology, pp. 227–313.

Hastings, C.L., Roche, E.T., Ruiz-Hernandez, E., Schenke-Layland, K., Walsh, C.J., and Duffy, G.P. (2015). Drug and cell delivery for cardiac regeneration. Adv. Drug Deliv. Rev. *84*, 85–106.

Hatai, T., Matsuzawa, A., Inoshita, S., Mochida, Y., Kuroda, T., Sakamaki, K., Kuida, K., Yonehara, S., Ichijo, H., and Takeda, K. (2000). Execution of apoptosis signal-regulating kinase 1 (ASK1)-induced apoptosis by the mitochondria-dependent caspase activation. J. Biol. Chem. *275*, 26576–26581.

Haudek, S.B., Taffet, G.E., Schneider, M.D., and Mann, D.L. (2007). TNF provokes cardiomyocyte apoptosis and cardiac remodeling through activation of multiple cell death pathways. J. Clin. Invest. *117*, 2692–2701.

Hausenloy, D.J., and Yellon, D.M. (2007). Reperfusion injury salvage kinase signalling: Taking a RISK for cardioprotection. Heart Fail. Rev. *12*, 217–234.

Hausenloy, D.J., and Yellon, D.M. (2009). Cardioprotective growth factors. Cardiovasc. Res. *83*, 179–194.

Hausenloy, D.J., and Yellon, D.M. (2015). Targeting myocardial reperfusion injury — the search continues. N. Engl. J. Med. *373*, 1073–1075.

Hausenloy, D.J., Garcia-Dorado, D., Bøtker, H.E., Davidson, S.M., Downey, J., Engel, F.B., Jennings, R., Lecour, S., Leor, J., Madonna, R., et al. (2017). Novel targets and future strategies for acute cardioprotection: Position Paper of the European Society of Cardiology Working Group on Cellular Biology of the Heart. Cardiovasc. Res. *113*, 564–585.

Hayakawa, K., Takemura, G., Koda, M., Kawase, Y., Maruyama, R., Li, Y., Minatoguchi, S., Fujiwara, T., and Fujiwara, H. (2002). Sensitivity to apoptosis signal, clearance rate, and ultrastructure of Fas ligand-induced apoptosis in in vivo ddult cardiac cells. Circulation *105*, 3039–3045.

He, K., Shi, X., Zhang, X., Dang, S., Ma, X., Liu, F., Xu, M., Lv, Z., Han, D., Fang, X., et al. (2011). Long-distance intercellular connectivity between cardiomyocytes and cardiofibroblasts mediated by membrane nanotubes. Cardiovasc. Res. *92*, 39–47.

He, K.L., Yi, G.H., Sherman, W., Zhou, H., Zhang, G.P., Gu, A., Kao, R., Haimes, H.B., Harvey, J., Roos, E., et al. (2005). Autologous skeletal myoblast transplantation improved hemodynamics and left ventricular function in chronic heart failure dogs. J. Hear. Lung Transplant. *24*, 1940–1949.

Headrick, J.P., and Lasley, R.D. (2009). Adenosine receptors and reperfusion injury of the heart. Handb. Exp. Pharmacol. *193*, 189–214.

Heeneman, S., Deutz, N.E., and Buurman, W.A. (1993). The concentrations of glutamine and ammonia in commercially available cell culture media. J. Immunol. Methods *166*, 85–91.

Heger, J., Schiegnitz, E., Von Waldthausen, D., Anwar, M.M., Piper, H.M., and Euler, G. (2010). Growth differentiation factor 15 acts anti-apoptotic and pro-hypertrophic in adult cardiomyocytes. J. Cell. Physiol. *224*, 120–126.

Heidenreich, P.A., Albert, N.M., Allen, L.A., Bluemke, D.A., Butler, J., Fonarow, G.C., Ikonomidis, J.S., Khavjou, O., Konstam, M.A., Maddox, T.M., et al. (2013). Forecasting the impact of heart failure in the United States. Circ. Hear. Fail. *6*, 606–

619.

Hengartner, M.O., and Horvitz, H.R. (1994). C. elegans cell survival gene ced-9 encodes a functional homolog of the mammalian proto-oncogene bcl-2. Cell *76*, 665–676.

Henry, T.D., Annex, B.H., McKendall, G.R., Azrin, M.A., Lopez, J.J., Giordano, F.J., Shah, P.K., Willerson, J.T., Benza, R.L., Berman, D.S., et al. (2003). The VIVA trial: Vascular endothelial growth factor in ischemia for vascular angiogenesis. Circulation *107*, 1359–1365.

Herbst, R.S., Eckhardt, S.G., Kurzrock, R., Ebbinghaus, S., O'Dwyer, P.J., Gordon, M.S., Novotny, W., Goldwasser, M.A., Tohnya, T.M., Lum, B.L., et al. (2010). Phase I dose-escalation study of recombinant human Apo2L/TRAIL, a dual proapoptotic receptor agonist, in patients with advanced cancer. J. Clin. Oncol. *28*, 2839–2846.

Herman, E., and Ferrans, V.J. (1981). Reduction of chronic doxorubicin cardiotoxicity in dogs by pretreatment with (±)-1, 2-bis (3, 5-dioxopiperazinyl-1-yl) propane (ICRF-187). Cancer Res. *41*, 3436–3440.

Heusch, G. (2013). Cardioprotection: Chances and challenges of its translation to the clinic. Lancet *381*, 166–175.

Heusch, G. (2017). Critical issues for the translation of cardioprotection. Circ. Res. *120*, 1477–1486.

Heusch, G., Skyschally, A., and Schulz, R. (2011). The in-situ pig heart with regional ischemia/reperfusion - ready for translation. J. Mol. Cell. Cardiol. *50*, 951–963.

Hibert, P., Prunier-Mirebeau, D., Beseme, O., Chwastyniak, M., Tamareille, S., Lamon, D., Furber, A., Pinet, F., and Prunier, F. (2013). Apolipoprotein a-I is a potential mediator of remote ischemic preconditioning. PLoS One *8*, e77211.

Hidalgo, A., Glass, N., Ovchinnikov, D., Yang, S.-K., Zhang, X., Mazzone, S., Chen, C., Wolvetang, E., and Cooper-White, J. (2018). Modelling ischemia-reperfusion injury (IRI) in vitro using metabolically matured induced pluripotent stem cell-derived cardiomyocytes. Cit. APL Bioeng. *2*, 26102.

Higashi, Y., Jitsuiki, D., Chayama, K., and Yoshizumi, M. (2006). Edaravone (3-methyl-1-phenyl-2-pyrazolin-5-one), a novel free radical scavenger, for treatment of cardiovascular diseases. Recent Pat. Cardiovasc. Drug Discov. *1*, 85–93.

Higo, T., Naito, A.T., Sumida, T., Shibamoto, M., Okada, K., Nomura, S., Nakagawa, A., Yamaguchi, T., Sakai, T., Hashimoto, A., et al. (2017). DNA single-strand break-induced DNA damage response causes heart failure. Nat. Commun. *8*, 15104.

Hinkel, R., El-Aouni, C., Olson, T., Horstkotte, J., Mayer, S., Müller, S., Willhauck, M., Spitzweg, C., Gildehaus, F.J., Münzing, W., et al. (2008). Thymosin β4 is an essential paracrine factor of embryonic endothelial progenitor cell-mediated cardioprotection. Circulation *117*, 2232–2240.

Hitomi, J., Christofferson, D.E., Ng, A., Yao, J., Degterev, A., Xavier, R.J., and Yuan, J. (2008). Identification of a molecular signaling network that regulates a cellular necrotic cell death pathway. Cell *135*, 1311–1323.

Hochhauser, E., Cheporko, Y., Yasovich, N., Pinchas, L., Offen, D., Barhum, Y., Pannet, H., Tobar, A., Vidne, B.A., and Birk, E. (2007). Bax deficiency reduces infarct size and improves long-term function after myocardial infarction. Cell Biochem. Biophys. *47*, 11–20.

Hoehhauser, E., Kivity, S., Offen, D., Maulik, N., Otani, H., Barhum, Y., Pannet, H., Shneyvays, V., Shainberg, A., Goldshtaub, V., et al. (2003). Bax ablation protects against myocardial ischemiareperfusion injury in transgenic mice. Am. J. Physiol. - Hear. Circ. Physiol. *284*.

Hofmann, M., Wollert, K.C., Meyer, G.P., Menke, A., Arseniev, L., Hertenstein, B., Ganser, A., Knapp, W.H., and Drexler, H. (2005). Monitoring of bone marrow cell homing into the infarcted human myocardium. Circulation *111*, 2198–2202.

Holen, H.L., Shadidi, M., Narvhus, K., Kjøsnes, O., Tierens, A., and Aasheim, H.-C. (2008). Signaling through ephrin-A ligand leads to activation of Src-family kinases, Akt phosphorylation, and inhibition of antigen receptor-induced apoptosis. J. Leukoc. Biol. *84*, 1183–1191.

Holler, N., Zaru, R., Micheau, O., Thome, M., Attinger, A., Valitutti, S., Bodmer, J.-L., Schneider, P., Seed, B., and Tschopp, J. (2000). Fas triggers an alternative, caspase-8–independent cell death pathway using the kinase RIP as effector molecule. Nat. Immunol. *1*, 489–495.

Hong, K.U., Guo, Y., Li, Q.-H., Cao, P., Al-Maqtari, T., Vajravelu, B.N., Du, J., Book, M.J., Zhu, X., Nong, Y., et al. (2014). c-kit+ Cardiac stem cells alleviate post-myocardial infarction left ventricular dysfunction despite poor engraftment and negligible retention in the recipient heart. PLoS One *9*, e96725.

Hortigon-Vinagre, M.P., Zamora, V., Burton, F.L., Green, J., Gintant, G.A., and

Smith, G.L. (2016). The use of ratiometric fluorescence measurements of the voltage sensitive dye Di-4-ANEPPS to examine action potential characteristics and drug effects on human induced pluripotent stem cell-derived cardiomyocytes. Toxicol. Sci. *154*, 320–331.

Horvath, P., Aulner, N., Bickle, M., Davies, A.M., Nery, E. Del, Ebner, D., Montoya, M.C., Östling, P., Pietiäinen, V., Price, L.S., et al. (2016). Screening out irrelevant cell-based models of disease. Nat. Rev. Drug Discov. *15*, 751–769.

Hoshino, K., Takeuchi, O., Kawai, T., Sanjo, H., Ogawa, T., Takeda, Y., Takeda, K., and Akira, S. (1999). Cutting edge: Toll-like receptor 4 (TLR4)-deficient mice are hyporesponsive to lipopolysaccharide: evidence for TLR4 as the Lps gene product. J. Immunol. *162*, 3749–3752.

Hou, D., Youssef, E.A.S., Brinton, T.J., Zhang, P., Rogers, P., Price, E.T., Yeung, A.C., Johnstone, B.H., Yock, P.G., and March, K.L. (2005). Radiolabeled cell distribution after intramyocardial, intracoronary, and interstitial retrograde coronary venous delivery: Implications for current clinical trials. Circulation *112*, 150–156.

House, S.L., Bolte, C., Zhou, M., Doetschman, T., Klevitsky, R., Newman, G., and Schultz, J.E.J. (2003). Cardiac-specific overexpression of fibroblast growth factor-2 protects against myocardial dysfunction and infarction in a murine model of low-flow ischemia. Circulation *108*, 3140–3148.

Hsiao, L.C., Carr, C., Chang, K.C., Lin, S.Z., and Clarke, K. (2013). Stem cell-based therapy for ischemic heart disease. Cell Transplant. *22*, 663–675.

Hsieh, P.C.H., Segers, V.F.M., Davis, M.E., MacGillivray, C., Gannon, J., Molkentin, J.D., Robbins, J., and Lee, R.T. (2007). Evidence from a genetic fate-mapping study that stem cells refresh adult mammalian cardiomyocytes after injury. Nat. Med. *13*, 970–974.

Hsueh, Y.-C., Wu, J.M.F., Yu, C.-K., Wu, K.K., and Hsieh, P.C.H. (2014). Prostaglandin $E_2$ promotes post-infarction cardiomyocyte replenishment by endogenous stem cells. EMBO Mol. Med. *6*, 496–503.

Hu, C.W., Li, Q., Zhang, Y., Li, Y.H., Jiang, H.C., Liu, M.Y., Li, S.L., Han, W., and Dong, D.L. (2014). Bone morphogenetic protein-4 induces upregulation of Cav3.1 Ca 2+ channels in HL-1 atrial myocytes. Pflugers Arch. Eur. J. Physiol. *466*, 2049–2057.

Hu, W., Lu, S., McAlpine, I., Jamieson, J.D., Lee, D.U., D. Marroquin, L., Heyen, J.R., and Jessen, B.A. (2012). Mechanistic Investigation of Imatinib-Induced Cardiac Toxicity and the Involvement of c-Abl Kinase. Toxicol. Sci. *129*, 188–199.

Huang, F., Xia, T., Li, J., Li, C., Zhao, Z., Lei, W., Chen, L., Liao, Y., Xiao, D., Peng, Y., et al. (2019). The bifunctional SDF-1-AnxA5 fusion protein protects cardiac function after myocardial infarction. J. Cell. Mol. Med. *23*, 7673–7684.

Huang, X.-P., Sun, Z., Miyagi, Y., McDonald Kinkaid, H., Zhang, L., Weisel, R.D., and Li, R.-K. (2010). Differentiation of allogeneic mesenchymal stem cells induces immunogenicity and limits their long-term benefits for myocardial repair. Circulation *122*, 2419–2429.

Ibrahim, A., and Marbán, E. (2016). Exosomes: Fundamental biology and roles in cardiovascular physiology. Annu. Rev. Physiol. *78*, 67–83.

Ibrahim, A.G.-E.G.-E., Cheng, K., and Marbán, E. (2014). Exosomes as critical agents of cardiac regeneration triggered by cell therapy. Stem Cell Reports *2*, 606–619.

Ichijo, H., Nishida, E., Irie, K., Ten Dijke, P., Saitoh, M., Moriguchi, T., Takagi, M., Matsumoto, K., Miyazono, K., and Gotoh, Y. (1997). Induction of apoptosis by ASK1, a mammalian MAPKKK that activates SAPK/JNK and p38 signaling pathways. Science (80-. ). *275*, 90–94.

Ide, T., Tsutsui, H., Kinugawa, S., Utsumi, H., Kang, D., Hattori, N., Uchida, K., Arimura, K. i, Egashira, K., and Takeshita, A. (1999). Mitochondrial electron transport complex I is a potential source of oxygen free radicals in the failing myocardium. Circ. Res. *85*, 357–363.

Imahashi, K., Schneider, M.D., Steenbergen, C., and Murphy, E. (2004). Transgenic expression of Bcl-2 modulates energy metabolism, prevents cytosolic acidification during ischemia, and reduces ischemia/reperfusion injury. Circ. Res. *95*, 734–741.

Imahashi, K., Pott, C., Goldhaber, J.I., Steenbergen, C., Philipson, K.D., and Murphy, E. (2005). Cardiac-specific ablation of the Na+-Ca2+ exchanger confers protection against ischemia/reperfusion injury. Circ. Res. *97*, 916–921.

Imai, Y., Moralez, A., Andag, U., Clarke, J.B., Busby, W.H., and Clemmons, D.R. (2000). Substitutions for hydrophobic amino acids in the N-terminal domains of IGFBP-3 and -5 markedly reduce IGF-I binding and alter their biologic actions. J. Biol. Chem. *275*, 18188–18194.

Imanishi, T., Murry, C.E., Reinecke, H., Hano, T., Nishio, I., Liles, W.C., Hofsta, L., Kim, K., O'Brien, K.D., Schwartz, S.M., et al. (2000). Cellular FLIP is expressed in cardiomyocytes and down-regulated in TUNEL-positive grafted cardiac tissues. Cardiovasc. Res. *48*, 101–110.

Ince, H., Rehders, T.C., Kische, S., Drawert, S., Adolf, E., Kleinfeldt, T., Petzsch, M., and Nienaber, C.A. (2006). G-CSF in the setting of acute myocardial infarction. Eur. Hear. J. Suppl. H40–H45.

Inserte, J., Cardona, M., Poncelas-Nozal, M., Hernando, V., Vilardosa, Ú., Aluja, D., Parra, V.M., Sanchis, D., and Garcia-Dorado, D. (2016). Studies on the role of apoptosis after transient myocardial ischemia: genetic deletion of the executioner caspases-3 and -7 does not limit infarct size and ventricular remodeling. Basic Res. Cardiol. *111*, 18.

Irmler, M., Thome, M., Hahne, M., Schneider, P., Hofmann, K., Steiner, V., Bodmer, J.-L., Schröter, M., Burns, K., Mattmann, C., et al. (1997). Inhibition of death receptor signals by cellular FLIP. Nature *388*, 190–195.

Isenberg, J.S., Hyodo, F., Pappan, L.K., Abu-Asab, M., Tsokos, M., Krishna, M.C., Frazier, W.A., and Roberts, D.D. (2007). Blocking thrombospondin-1/CD47 signaling alleviates deleterious effects of aging on tissue responses to ischemia. Arterioscler. Thromb. Vasc. Biol. *27*, 2582–2588.

Isenberg, J.S., Roberts, D.D., and Frazier, W.A. (2008). CD47: A new target in cardiovascular therapy. Arterioscler. Thromb. Vasc. Biol. *28*, 615–621.

Islam, M.N., Das, S.R., Emin, M.T., Wei, M., Sun, L., Westphalen, K., Rowlands, D.J., Quadri, S.K., Bhattacharya, S., and Bhattacharya, J. (2012). Mitochondrial transfer from bone-marrow-derived stromal cells to pulmonary alveoli protects against acute lung injury. Nat. Med. *18*, 759–765.

Iso, Y., Spees, J.L., Serrano, C., Bakondi, B., Pochampally, R., Song, Y.H., Sobel, B.E., Delafontaine, P., and Prockop, D.J. (2007). Multipotent human stromal cells improve cardiac function after myocardial infarction in mice without long-term engraftment. Biochem. Biophys. Res. Commun. *354*, 700–706.

Iwanaga, K., Takano, H., Ohtsuka, M., Hasegawa, H., Zou, Y., Qin, Y., Odaka, K., Hiroshima, K., Tadokoro, H., and Komuro, I. (2004). Effects of G-CSF on cardiac remodeling after acute myocardial infarction in swine. Biochem. Biophys. Res. Commun. *325*, 1353–1359.

Izumi, M., Fujio, Y., Kunisada, K., Negoro, S., Tone, E., Funamoto, M., Osugi, T., Oshima, Y., Nakaoka, Y., Kishimoto, T., et al. (2001). Bone morphogenetic protein-2 inhibits serum deprivation-induced apoptosis of neonatal cardiac myocytes through activation of the Smad1 pathway. J. Biol. Chem. *276*, 31133–31141.

Jabbour, A., Hayward, C.S., Keogh, A.M., Kotlyar, E., McCrohon, J.A., England, J.F.,

Amor, R., Liu, X., Li, X.Y., Zhou, M.D., et al. (2011). Parenteral administration of recombinant human neuregulin-1 to patients with stable chronic heart failure produces favourable acute and chronic haemodynamic responses. Eur. J. Heart Fail. *13*, 83–92.

Jackson, K.A., Majka, S.M., Wang, H., Pocius, J., Hartley, C.J., Majesky, M.W., Entman, M.L., Michael, L.H., Hirschi, K.K., and Goodell, M.A. (2001). Regeneration of ischemic cardiac muscle and vascular endothelium by adult stem cells. J. Clin. Invest. *107*, 1395–1402.

Janero, D.R., Hreniuk, D., and Sharif, H.M. (1991). Hydrogen peroxide-induced oxidative stress to the mammalian heart-muscle cell (cardiomyocyte): Lethal peroxidative membrane injury. J. Cell. Physiol. *149*, 347–364.

Jeffery, P.L., Herington, A.C., and Chopin, L.K. (2003). The potential autocrine/paracrine roles of ghrelin and its receptor in hormone-dependent cancer. Cytokine Growth Factor Rev. *14*, 113–122.

Jeremias, I., Kupatt, C., Martin-Villalba, A., Habazettl, H., Schenkel, J., Boekstegers, P., and Debatin, K.M. (2000). Involvement of CD95/Apo1/Fas in cell death after myocardial ischemia. Circulation *102*, 915–920.

Jernberg, T., Johanson, P., Held, C., Svennblad, B., Lindbäck, J., Wallentin, L., and SWEDEHEART/RIKS-HIA (2011). Association between adoption of evidence-based treatment and survival for patients with ST-elevation myocardial infarction. JAMA *305*, 1677.

Jiang, P., Zhang, D., Qiu, H., Yi, X., Zhang, Y., Cao, Y., Zhao, B., Xia, Z., and Wang, C. (2017). Tiron ameliorates high glucose-induced cardiac myocyte apoptosis by PKCδ-dependent inhibition of osteopontin. Clin. Exp. Pharmacol. Physiol. *44*, 760–770.

Jiang, Y., Jahagirdar, B.N., Reinhardt, R.L., Schwartz, R.E., Keene, C.D., Ortiz-Gonzalez, X.R., Reyes, M., Lenvik, T., Lund, T., Blackstad, M., et al. (2002). Pluripotency of mesenchymal stem cells derived from adult marrow. Nature *418*, 41–49.

Jiang, Y., Park, P., Hong, S.M., and Ban, K. (2018). Maturation of cardiomyocytes derived from human pluripotent stem cells: Current strategies and limitations. Mol. Cells *41*, 613–621.

De Jong, R., Houtgraaf, J.H., Samiei, S., Boersma, E., and Duckers, H.J. (2014). Intracoronary stem cell infusion after acute myocardial infarction: A meta-analysis

and update on clinical trials. Circ. Cardiovasc. Interv. *7*, 156–167.

Juránek, I., and Bezek, S. (2005). Controversy of free radical hypothesis: reactive oxygen species--cause or consequence of tissue injury? Gen. Physiol. Biophys. *24*, 263–278.

Kafri, N. Al, and Hafizi, S. (2019). Tumour-Secreted Protein S ( ProS1 ) Activates a Tyro3-Erk Signalling Axis and Protects Cancer Cells from Apoptosis. Cancers (Basel). 1–17.

Kaikita, K., Hayasaki, T., Okuma, T., Kuziel, W.A., Ogawa, H., and Takeya, M. (2004). Targeted deletion of CC chemokine receptor 2 attenuates left ventricular remodeling after experimental myocardial infarction. Am. J. Pathol. *165*, 439–447.

Kaiser, W.J., Sridharan, H., Huang, C., Mandal, P., Upton, J.W., Gough, P.J., Sehon, C.A., Marquis, R.W., Bertin, J., and Mocarski, E.S. (2013). Toll-like Receptor 3-mediated Necrosis via TRIF, RIP3, and MLKL. J. Biol. Chem. *288*, 31268–31279.

Kamakura, T., Makiyama, T., Sasaki, K., Yoshida, Y., Wuriyanghai, Y., Chen, J., Hattori, T., Ohno, S., Kita, T., Horie, M., et al. (2013). Ultrastructural maturation of human-induced pluripotent stem cell-derived cardiomyocytes in a long-term culture. Circ. J. *77*, 1307–1314.

Kanamoto, T., Mota, M., Takeda, K., Rubin, L.L., Miyazono, K., Ichijo, H., and Bazenet, C.E. (2000). Role of apoptosis signal-regulating kinase in regulation of the c-Jun N-Terminal kinase pathway and apoptosis in sympathetic neurons. Mol. Cell. Biol. *20*, 196–204.

Kanazawa, H., Tseliou, E., Malliaras, K., Yee, K., Dawkins, J.F., De Couto, G., Smith, R.R., Kreke, M., Seinfeld, J., Middleton, R.C., et al. (2015). Cellular postconditioning: allogeneic cardiosphere-derived cells reduce infarct size and attenuate microvascular obstruction when administered after reperfusion in pigs with acute myocardial infarction. Circ. Heart Fail. *8*, 322–332.

Kanazawa, H., Tseliou, E., Dawkins, J.F., De Couto, G., Gallet, R., Malliaras, K., Yee, K., Kreke, M., Valle, I., Smith, R.R., et al. (2016). Durable benefits of cellular postconditioning: Long-term effects of allogeneic cardiosphere-derived cells infused after reperfusion in pigs with acute myocardial infarction. J. Am. Heart Assoc. *5*.

Kane, C., and Terracciano, C.M.N. (2017). Concise Review: Criteria for chamber-specific categorization of human cardiac myocytes derived from pluripotent stem cells. Stem Cells *35*, 1881–1897.

Kang, H.-J., Kim, H.-S., Koo, B.-K., Kim, Y.-J., Lee, D., Sohn, D.-W., Oh, B.-H., and Park, Y.-B. (2007). Intracoronary infusion of the mobilized peripheral blood stem cell by G-CSF is better than mobilization alone by G-CSF for improvement of cardiac function and remodeling: 2-Year follow-up results of the Myocardial Regeneration and Angiogenesis in Myocardial Infarction with G-CSF and Intra-Coronary Stem Cell Infusion (MAGIC Cell) 1 trial. Am. Heart J. *153*, 237.e1-237.e8.

Kaptein, A., Jansen, M., Dilaver, G., Kitson, J., Dash, L., Wang, E., Owen, M.J., Bodmer, J.L., Tschopp, J., and Farrow, S.N. (2000). Studies on the interaction between TWEAK and the death receptor WSL-1/TRAMP (DR3). FEBS Lett. *485*, 135–141.

Karch, J., Kwong, J.Q., Burr, A.R., Sargent, M.A., Elrod, J.W., Peixoto, P.M., Martinez-Caballero, S., Osinska, H., Cheng, E.H.-Y., Robbins, J., et al. (2013). Bax and Bak function as the outer membrane component of the mitochondrial permeability pore in regulating necrotic cell death in mice. Elife *2*, e00772.

Kardami, E., Detillieux, K., Ma, X., Jiang, Z., Santiago, J.J., Jimenez, S.K., and Cattini, P.A. (2007). Fibroblast growth factor-2 and cardioprotection. Heart Fail. Rev. *12*, 267–277.

Karmazyn, M. (1988). Amiloride enhances postischemic ventricular recovery: possible role of Na+-H+ exchange. Am. J. Physiol. *255*, H608-15.

Karthikeyan, K., Bai, B.R.S., Gauthaman, K., Sathish, K.S., and Devaraj, S.N. (2003). Cardioprotective effect of the alcoholic extract of Terminalia arjuna bark in an in vivo model of myocardial ischemic reperfusion injury. Life Sci. *73*, 2727–2739.

Kashani, K., Al-Khafaji, A., Ardiles, T., Artigas, A., Bagshaw, S.M., Bell, M., Bihorac, A., Birkhahn, R., Cely, C.M., Chawla, L.S., et al. (2013). Discovery and validation of cell cycle arrest biomarkers in human acute kidney injury. Crit. Care *17*.

Katz, E.B., Steinhelper, M.E., Delcarpio, J.B., Daud, A.I., Claycomb, W.C., and Field, L.J. (1992). Cardiomyocyte proliferation in mice expressing α-cardiac myosin heavy chain-SV40 T-antigen transgenes. Am. J. Physiol. - Hear. Circ. Physiol. *262*.

Kawaguchi, M., Takahashi, M., Hata, T., Kashima, Y., Usui, F., Morimoto, H., Izawa, A., Takahashi, Y., Masumoto, J., Koyama, J., et al. (2011). Inflammasome activation of cardiac fibroblasts is essential for myocardial ischemia/reperfusion injury. Circulation *123*, 594–604.

Kawaguchi, N., Smith, A.J., Waring, C.D., Hasan, M.K., Miyamoto, S., Matsuoka, R., and Ellison, G.M. (2010). c-kitpos GATA-4 high rat cardiac stem cells foster adult

cardiomyocyte survival through IGF-1 paracrine signalling. PLoS One *5*, e14297.

Kawamura, M., Miyagawa, S., Miki, K., Saito, A., Fukushima, S., Higuchi, T., Kawamura, T., Kuratani, T., Daimon, T., Shimizu, T., et al. (2012). Feasibility, safety, and therapeutic efficacy of human induced pluripotent stem cell-derived cardiomyocyte sheets in a porcine ischemic cardiomyopathy model. Circulation *126*.

Kawamura, M., Miyagawa, S., Fukushima, S., Saito, A., Miki, K., Ito, E., Sougawa, N., Kawamura, T., Daimon, T., Shimizu, T., et al. (2013). Enhanced survival of transplanted human induced pluripotent stem cell-derived cardiomyocytes by the combination of cell sheets with the pedicled omental flap technique in a porcine heart. Circulation *128*, S87-94.

Kelm, J.M., Lal-Nag, M., Sittampalam, G.S., and Ferrer, M. (2019). Translational in vitro research: integrating 3D drug discovery and development processes into the drug development pipeline. Drug Discov. Today *24*, 26–30.

Kelts, J.L., Cali, J.J., Duellman, S.J., and Shultz, J. (2015). Altered cytotoxicity of ROS-inducing compounds by sodium pyruvate in cell culture medium depends on the location of ROS generation. Springerplus *4*, 269.

Kempf, T., Eden, M., Strelau, J., Naguib, M., Willenbockel, C., Tongers, J., Heineke, J., Kotlarz, D., Xu, J., Molkentin, J.D., et al. (2006). The transforming growth factor-beta superfamily member growth-differentiation factor-15 protects the heart from ischemia/reperfusion injury. Circ. Res. *98*, 351–360.

Kerkela, R., Woulfe, K.C., Durand, J.-B., Vagnozzi, R., Kramer, D., Chu, T.F., Beahm, C., Chen, M.H., and Force, T. (2009). Sunitinib-induced cardiotoxicity is mediated by off-target inhibition of AMP-activated protein kinase. Clin. Transl. Sci. *2*, 15–25.

Kerkelä, R., Grazette, L., Yacobi, R., Iliescu, C., Patten, R., Beahm, C., Walters, B., Shevtsov, S., Pesant, S., Clubb, F.J., et al. (2006). Cardiotoxicity of the cancer therapeutic agent imatinib mesylate. Nat. Med. *12*, 908–916.

Kerr, J.F.R., Wyllie, A.H., and Currie, A.R. (1972). Apoptosis: A basic biological phenomenon with wideranging implications in tissue kinetics. Br. J. Cancer *26*, 239–257.

Khaleghi, M., Taha, M.F., Jafarzadeh, N., and Javeri, A. (2014). Atrial and ventricular specification of ADSCs is stimulated by different doses of BMP4. Biotechnol. Lett. *36*, 2581–2589.

Khiati, S., Dalla Rosa, I., Sourbier, C., Ma, X., Rao, V.A., Neckers, L.M., Zhang, H., and Pommier, Y. (2014). Mitochondrial topoisomerase I (Top1mt) is a novel limiting factor of Doxorubicin cardiotoxicity. Clin. Cancer Res. *20*, 4873–4881.

Kieserman, J.M., Myers, V.D., Dubey, P., Cheung, J.Y., and Feldman, A.M. (2019). Current Landscape of Heart Failure Gene Therapy. J. Am. Heart Assoc. *8*.

Kim, C., Majdi, M., Xia, P., Wei, K.A., Talantova, M., Spiering, S., Nelson, B., Mercola, M., and Chen, H.S.V. (2010a). Non-cardiomyocytes influence the electrophysiological maturation of human embryonic stem cell-derived cardiomyocytes during differentiation. Stem Cells Dev. *19*, 783–795.

Kim, M.-Y., Seo, E.J., Lee, D.H., Kim, E.J., Kim, H.S., Cho, H.-Y., Chung, E.Y., Lee, S.H., Baik, E.J., Moon, C.-H., et al. (2010b). Gadd45 is a novel mediator of cardiomyocyte apoptosis induced by ischaemia/hypoxia. Cardiovasc. Res. *87*, 119–126.

Kim, R., Tanabe, K., Emi, M., Uchida, Y., and Toge, T. Death receptor-dependent and -independent pathways in anticancer drug-induced apoptosis of breast cancer cells. Oncol. Rep. *10*, 1925–1930.

Kinkaid, H.Y.M., Huang, X.-P., Li, R.-K., and Weisel, R.D. (2010). What's new in cardiac cell therapy? Allogeneic bone marrow stromal cells as "Universal Donor Cells." J. Card. Surg. *25*, 359–366.

Kirby, R.J., Divlianska, D.B., Whig, K., Bryan, N., Morfa, C.J., Koo, A., Nguyen, K.H., Maloney, P., Peddibhotla, S., Sessions, E.H., et al. (2018). Discovery of novel small-molecule inducers of heme oxygenase-1 that protect human ipsc-derived cardiomyocytes from oxidative stress. J. Pharmacol. Exp. Ther. *364*, 87–96.

Kitani, T., Ong, S.G., Lam, C.K., Rhee, J.W., Zhang, J.Z., Oikonomopoulos, A., Ma, N., Tian, L., Lee, J., Telli, M.L., et al. (2019). Human-induced pluripotent stem cell model of Trastuzumab-induced cardiac dysfunction in patients with breast cancer. Circulation *139*, 2451–2465.

Kitta, K., Day, R.M., Ikeda, T., and Suzuki, Y.J. (2001). Hepatocyte growth factor protects cardiac myocytes against oxidative stress-induced apoptosis. Free Radic. Biol. Med. *31*, 902–910.

Kloner, R.A. (2013). Current state of clinical translation of cardioprotective agents for acute myocardial infarction. Circ. Res. *113*, 451–463.

Kodama, H., Fukuda, K., Pan, J., Makino, S., Baba, A., Hori, S., and Ogawa, S.

(1997). Leukemia inhibitory factor, a potent cardiac hypertrophic cytokine, activates the JAK/STAT pathway in rat cardiomyocytes. Circ. Res. *81*, 656–663.

Kodama, M., Furutani, K., Kimura, R., Ando, T., Sakamoto, K., Nagamori, S., Ashihara, T., Kurachi, Y., Sekino, Y., Furukawa, T., et al. (2019). Systematic expression analysis of genes related to generation of action potentials in human iPS cell-derived cardiomyocytes. J. Pharmacol. Sci. *140*, 325–330.

Konstantinidis, K., Whelan, R.S., and Kitsis, R.N. (2012). Mechanisms of cell death in heart disease. Arterioscler. Thromb. Vasc. Biol. *32*, 1552–1562.

Kostin, S., Pool, L., Elsässer, A., Hein, S., Drexler, H.C.A., Arnon, E., Hayakawa, Y., Zimmermann, R., Bauer, E., Klövekorn, W.P., et al. (2003). Myocytes die by multiple mechanisms in failing human hearts. Circ. Res. *92*, 715–724.

Kovacic, J.C., and Fuster, V. (2015). Cell therapy for patients with acute myocardial infarction: ACCRUEd evidence to date. Circ. Res. *116*, 1287–1290.

Krishna, S., and Overholtzer, M. (2016). Mechanisms and consequences of entosis. Cell. Mol. Life Sci. *73*, 2379–2386.

Kroemer, G., Galluzzi, L., Vandenabeele, P., Abrams, J., Alnemri, E.S., Baehrecke, E.H., Blagosklonny, M. V, El-Deiry, W.S., Golstein, P., Green, D.R., et al. (2009). Classification of cell death: recommendations of the Nomenclature Committee on Cell Death 2009. Cell Death Differ. *16*, 3–11.

Kubota, T., McTiernan, C.F., Frye, C.S., Demetris, A.J., and Feldman, A.M. (1997). Cardiac-specific overexpression of tumor necrosis factor-alpha causes lethal myocarditis in transgenic mice. J. Card. Fail. *3*, 117–124.

Kuhota, T., McTiernan, C.F., Frye, C.S., Slawson, S.E., Lemster, B.H., Koretsky, A.P., Demetris, A.J., and Feldman, A.M. (1997). Dilated cardiomyopathy in transgenic mice with cardiac-specific overexpression of tumor necrosis factor-α. Circ. Res. *81*, 627–635.

Kung, G., Konstantinidis, K., and Kitsis, R.N. (2011). Programmed necrosis, not apoptosis, in the heart. Circ. Res. *108*, 1017–1036.

Kunisada, K., Negoro, S., Tone, E., Funamoto, M., Osugi, T., Yamada, S., Okabe, M., Kishimoto, T., and Yamauchi-Takihara, K. (2000). Signal transducer and activator of transcription 3 in the heart transduces not only a hypertrophic signal but a protective signal against doxorubicin-induced cardiomyopathy. Proc. Natl. Acad. Sci. U. S. A. *97*, 315–319.

Kupatt, C., Horstkotte, J., Vlastos, G.A., Pfosser, A., Lebherz, C., Semisch, M., Thalgott, M., Büttner, K., Browarzyk, C., Mages, J., et al. (2005). Embryonic endothelial progenitor cells expressing a broad range of proangiogenic and remodeling factors enhance vascularization and tissue recovery in acute and chronic ischemia. FASEB J. *19*, 1576–1578.

Kuramochi, Y., Cote, G.M., Guo, X., Lebrasseur, N.K., Cui, L., Liao, R., and Sawyer, D.B. (2004). Cardiac endothelial cells regulate reactive oxygen species-induced cardiomyocyte apoptosis through neuregulin-1β/erbB4 signaling. J. Biol. Chem. *279*, 51141–51147.

Kuriyama, S., Tsuji, T., Sakuma, T., Yamamoto, T., and Tanaka, M. (2018). PLEKHN1 promotes apoptosis by enhancing Bax-Bak hetro-oligomerization through interaction with Bid in human colon cancer. Cell Death Discov. *4*, 11.

Kuroda, J., Ago, T., Matsushima, S., Zhai, P., Schneider, M.D., and Sadoshima, J. (2010). NADPH oxidase 4 (Nox4) is a major source of oxidative stress in the failing heart. Proc. Natl. Acad. Sci. U. S. A. *107*, 15565–15570.

Kurrelmeyer, K.M., Michael, L.H., Baumgarten, G., Taffet, G.E., Peschon, J.J., Sivasubramanian, N., Entman, M.L., and Mann, D.L. (2000). Endogenous tumor necrosis factor protects the adult cardiac myocyte against ischemic-induced apoptosis in a murine model of acute myocardial infarction. Proc. Natl. Acad. Sci. U. S. A. *97*, 5456–5461.

Kuznetsov, A. V., Javadov, S., Sickinger, S., Frotschnig, S., and Grimm, M. (2015a). H9c2 and HL-1 cells demonstrate distinct features of energy metabolism, mitochondrial function and sensitivity to hypoxia-reoxygenation. Biochim. Biophys. Acta - Mol. Cell Res. *1853*, 276–284.

Kuznetsov, A. V., Javadov, S., Sickinger, S., Frotschnig, S., and Grimm, M. (2015b). H9c2 and HL-1 cells demonstrate distinct features of energy metabolism, mitochondrial function and sensitivity to hypoxia-reoxygenation. Biochim. Biophys. Acta - Mol. Cell Res. *1853*, 276–284.

Ky, B., Vejpongsa, P., Yeh, E.T.H., Force, T., and Moslehi, J.J. (2013). Emerging paradigms in cardiomyopathies associated with cancer therapies. Circ. Res. *113*, 754–764.

LaFramboise, W.A., Scalise, D., Stoodley, P., Graner, S.R., Guthrie, R.D., Magovern, J.A., and Becich, M.J. (2007). Cardiac fibroblasts influence cardiomyocyte phenotype in vitro. Am. J. Physiol. - Cell Physiol. *292*.

Lai, R.C., Arslan, F., Lee, M.M., Sze, N.S.K., Choo, A., Chen, T.S., Salto-Tellez, M., Timmers, L., Lee, C.N., El Oakley, R.M., et al. (2010). Exosome secreted by MSC reduces myocardial ischemia/reperfusion injury. Stem Cell Res. *4*, 214–222.

Lasley, R.D. (2018). Adenosine receptor-mediated cardioprotection-current limitations and future directions. Front. Pharmacol. *9*, 310–317.

Lässer, C., Eldh, M., and Lötvall, J. (2012). Isolation and characterization of RNA-containing exosomes. J. Vis. Exp. e3037–e3037.

Latini, R., Masson, S., Anand, I.S., Missov, E., Carlson, M., Vago, T., Angelici, L., Barlera, S., Parrinello, G., Maggioni, A.P., et al. (2007). Prognostic value of very low plasma concentrations of Troponin T in patients with stable chronic heart failure. Circulation *116*, 1242–1249.

Latunde-Dada, G.O. (2017). Ferroptosis: Role of lipid peroxidation, iron and ferritinophagy. Biochim. Biophys. Acta - Gen. Subj. *1861*, 1893–1900.

Lawson, C., Vicencio, J.M., Yellon, D.M., and Davidson, S.M. (2016). Microvesicles and exosomes: new players in metabolic and cardiovascular disease. J. Endocrinol. *228*, R57–R71.

Le, T.Y.L., Pickett, H.A., Yang, A., Ho, J.W.K., Thavapalachandran, S., Igoor, S., Yang, S.F., Farraha, M., Voges, H.K., Hudson, J.E., et al. (2019). Enhanced cardiac repair by telomerase reverse transcriptase over-expression in human cardiac mesenchymal stromal cells. Sci. Rep. *9*, 10579.

Leask, A. (2010). Potential therapeutic targets for cardiac fibrosis: TGFβ, angiotensin, endothelin, CCN2, and PDGF, partners in fibroblast activation. Circ. Res. *106*, 1675–1680.

Lee, R.T. (2018). Adult cardiac stem cell concept and the process of science. Circulation *138*, 2940–2942.

Lee, A.S., Inayathullah, M., Lijkwan, M.A., Zhao, X., Sun, W., Park, S., Hong, W.X., Parekh, M.B., Malkovskiy, A. V., Lau, E., et al. (2018a). Prolonged survival of transplanted stem cells after ischaemic injury via the slow release of pro-survival peptides from a collagen matrix. Nat. Biomed. Eng. *2*, 104–113.

Lee, H.-Y., You, H.-J., Won, J.-Y., Youn, S.-W., Cho, H.-J., Park, K.-W., Park, W.-Y., Seo, J.-S., Park, Y.-B., Walsh, K., et al. (2008). Forkhead factor, FOXO3a, induces apoptosis of endothelial cells through activation of matrix metalloproteinases. Arterioscler. Thromb. Vasc. Biol. *28*, 302–308.

Lee, J.H., Protze, S.I., Laksman, Z., Backx, P.H., and Keller, G.M. (2017a). Human pluripotent stem cell-derived atrial and ventricular cardiomyocytes develop from distinct mesoderm populations. Cell Stem Cell *21*, 179-194.e4.

Lee, K., Pisarska, M.D., Ko, J.J., Kang, Y., Yoon, S., Ryou, S.M., Cha, K.Y., and Bae, J. (2005). Transcriptional factor FOXL2 interacts with DP103 and induces apoptosis. Biochem. Biophys. Res. Commun. *336*, 876–881.

Lee, P., Sata, M., Lefer, D.J., Factor, S.M., Walsh, K., and Kitsis, R.N. (2003a). Fas pathway is a critical mediator of cardiac myocyte death and MI during ischemia-reperfusion in vivo. *284*, H456–H463.

Lee, S.T., White, A.J., Matsushita, S., Malliaras, K., Steenbergen, C., Zhang, Y., Li, T.S., Terrovitis, J., Yee, K., Simsir, S., et al. (2011a). Intramyocardial injection of autologous cardiospheres or cardiosphere-derived cells preserves function and minimizes adverse ventricular remodeling in pigs with heart failure post-myocardial infarction. J. Am. Coll. Cardiol. *57*, 455–465.

Lee, S.Y., Maniak, P.J., Ingbar, D.H., and O'Grady, S.M. (2003b). Adult alveolar epithelial cells express multiple subtypes of voltage-gated $K^+$ channels that are located in apical membrane. Am. J. Physiol. Physiol. *284*, C1614–C1624.

Lee, W.H., Tsai, M.J., Chang, W.A., Wu, L.Y., Wang, H.Y., Chang, K.F., Su, H.M., and Kuo, P.L. (2018b). Deduction of novel genes potentially involved in hypoxic AC16 human cardiomyocytes using next-generation sequencing and bioinformatics approaches. Int. J. Mol. Med. *42*, 2489–2502.

Lee, Y.-K., Ng, K.-M., Lai, W.-H., Chan, Y.-C., Lau, Y.-M., Lian, Q., Tse, H.-F., and Siu, C.-W. (2011b). Calcium homeostasis in human induced pluripotent stem cell-derived cardiomyocytes. Stem Cell Rev. Reports *7*, 976–986.

Lee, Y.K., Lau, Y.M., Cai, Z.J., Lai, W.H., Wong, L.Y., Tse, H.F., Ng, K.M., and Siu, C.W. (2017b). Modeling treatment response for Lamin A/C related dilated cardiomyopathy in human induced pluripotent stem cells. J. Am. Heart Assoc. *6*.

Lefer, D.J., and Marbán, E. (2017). Is cardioprotection dead? Circulation *136*, 98–109.

Lefer, A.M., Tsao, P., Aoki, N., and Palladino, M.A. (1990). Mediation of cardioprotection by transforming growth factor-β. Science (80-. ). *249*, 61–64.

Lefer, A.M., Ma, X.L., Weyrich, A.S., and Scalia, R. (1993). Mechanism of the cardioprotective effect of transforming growth factor β1 in feline myocardial ischemia

and reperfusion. Proc. Natl. Acad. Sci. U. S. A. *90*, 1018–1022.

Leiker, M., Suzuki, G., Iyer, V.S., Canty, J.M., and Lee, T. (2008). Assessment of a nuclear affinity labeling method for tracking implanted mesenchymal stem cells. Cell Transplant. *17*, 911–922.

Leist, M., Single, B., Castoldi, A.F., Kühnle, S., and Nicotera, P. (1997). Intracellular adenosine triphosphate (ATP) concentration: a switch in the decision between apoptosis and necrosis. J. Exp. Med. *185*, 1481–1486.

Lemoine, M.D., Mannhardt, I., Breckwoldt, K., Prondzynski, M., Flenner, F., Ulmer, B., Hirt, M.N., Neuber, C., Horváth, A., Kloth, B., et al. (2017). Human iPSC-derived cardiomyocytes cultured in 3D engineered heart tissue show physiological upstroke velocity and sodium current density. Sci. Rep. *7*, 5464.

Leocádio, P.C.L., Menta, P.L. dos R., Dias, M.T.S., Fraga, J.R., Goulart, A.C., Santos, I.S., Lotufo, P.A., Bensenor, I.M., and Alvarez-Leite, J.I. (2019). Low serum levels of CCL2 are associated with worse prognosis in patients with Acute Coronary Syndrome: 2-year survival analysis. Biomed. Pharmacother. *109*, 1411–1416.

Leuschner, F., Dutta, P., Gorbatov, R., Novobrantseva, T.I., Donahoe, J.S., Courties, G., Lee, K.M., Kim, J.I., Markmann, J.F., Marinelli, B., et al. (2011). Therapeutic siRNA silencing in inflammatory monocytes in mice. Nat. Biotechnol. *29*, 1005–1010.

Li, B., Setoguchi, M., Wang, X., Andreoli, A.M., Leri, A., Malhotra, A., Kajstura, J., and Anversa, P. (1999). Insulin-like growth factor-1 attenuates the detrimental impact of nonocclusive coronary artery constriction on the heart. Circ. Res. *84*, 1007–1019.

Li, H., Zhu, H., Xu, C.J., and Yuan, J. (1998). Cleavage of BID by caspase 8 mediates the mitochondrial damage in the Fas pathway of apoptosis. Cell *94*, 491–501.

Li, L., Chen, Y., Doan, J., Murray, J., Molkentin, J.D., and Liu, Q. (2014a). Transforming growth factor β–activated kinase 1 signaling pathway critically regulates myocardial survival and remodeling. Circulation *130*, 2162–2172.

Li, N., Wang, C., Jia, L.X., and Du, J. (2014b). Heart regeneration, stem cells, and cytokines. Regen. Med. Res. *2*.

Li, P., Cavallero, S., Gu, Y., Chen, T.H.P., Hughes, J., Hassan, A.B., Brüning, J.C., Pashmforoush, M., and Sucov, H.M. (2011). IGF signaling directs ventricular cardiomyocyte proliferation during embryonic heart development. Development *138*, 1795–1805.

Li, P., Kaslan, M., Lee, S.H., Yao, J., and Gao, Z. (2017). Progress in exosome isolation techniques. Theranostics *7*, 789–804.

Li, Q., Li, B., Wang, X., Leri, A., Jana, K.P., Liu, Y., Kajstura, J., Baserga, R., and Anversa, P. (1997). Overexpression of insulin-like growth factor-1 in mice protects from myocyte death after infarction, attenuating ventricular dilation, wall stress, and cardiac hypertrophy. J. Clin. Invest. *100*, 1991–1999.

Li, Q., Xie, J., Li, R., Shi, J., Sun, J., Gu, R., Ding, L., Wang, L., and Xu, B. (2014c). Overexpression of microRNA-99a attenuates heart remodelling and improves cardiac performance after myocardial infarction. J. Cell. Mol. Med. *18*, 919–928.

Li, R.K., Mickle, D.A.G., Weisel, R.D., Carson, S., Omar, S.A., Tumiati, L.C., Wilson, G.J., and Williams, W.G. (1996). Human pediatric and adult ventricular cardiomyocytes in culture: Assessment of phenotypic changes with passaging. Cardiovasc. Res. *32*, 362–373.

Li, T.-S., Cheng, K., Malliaras, K., Smith, R.R., Zhang, Y., Sun, B., Matsushita, N., Blusztajn, A., Terrovitis, J., Kusuoka, H., et al. (2012). Direct comparison of different stem cell types and subpopulations reveals superior paracrine potency and myocardial repair efficacy with cardiosphere-derived cells. J. Am. Coll. Cardiol. *59*, 942–953.

Li, W., Feng, G., Gauthier, J.M., Lokshina, I., Higashikubo, R., Evans, S., Liu, X., Hassan, A., Tanaka, S., Cicka, M., et al. (2019a). Ferroptotic cell death and TLR4/Trif signaling initiate neutrophil recruitment after heart transplantation. J. Clin. Invest. *129*, 2293–2304.

Li, X., Yang, Z., Nie, W., Jiang, J., Li, S., Li, Z., Tian, L., and Ma, X. (2019b). Exosomes derived from cardiac progenitor cells attenuate CVB3-induced apoptosis via abrogating the proliferation of CVB3 and modulating the mTOR signaling pathways. Cell Death Dis. *10*, 691–707.

Li, Y., He, L., Huang, X., Issa Bhaloo, S., Zhao, H., Zhang, S., Pu, W., Tian, X., Li, Y., Liu, Q., et al. (2018). Genetic lineage tracing of non-myocyte population by dual recombinases. Circulation *138*, 793–805.

Li, Z., Lee, A., Huang, M., Chun, H., Chung, J., Chu, P., Hoyt, G., Yang, P., Rosenberg, J., Robbins, R.C., et al. (2009). Imaging survival and function of transplanted cardiac resident stem cells. J. Am. Coll. Cardiol. *53*, 1229–1240.

Lian, X., Zhang, J., Azarin, S.M., Zhu, K., Hazeltine, L.B., Bao, X., Hsiao, C., Kamp, T.J., and Palecek, S.P. (2012). Directed cardiomyocyte differentiation from human

pluripotent stem cells by modulating Wnt/β-catenin signaling under fully defined conditions. Nat. Protoc. *8*, 162–175.

Liang, P., Lan, F., Lee, A.S., Gong, T., Sanchez-Freire, V., Wang, Y., Diecke, S., Sallam, K., Knowles, J.W., Wang, P.J., et al. (2013). Drug screening using a library of human induced pluripotent stem cell-derived cardiomyocytes reveals disease-specific patterns of cardiotoxicity. Circulation *127*, 1677–1691.

Liang, X., Zhang, L., Wang, S., Han, Q., and Zhao, R.C. (2016). Exosomes secreted by mesenchymal stem cells promote endothelial cell angiogenesis by transferring miR-125a. J. Cell Sci. *129*, 2182–2189.

Liao, R., Podesser, B.K., and Lim, C.C. (2012). The continuing evolution of the Langendorff and ejecting murine heart: New advances in cardiac phenotyping. Am. J. Physiol. - Hear. Circ. Physiol. *303*, 156–167.

Liao, Z., Brar, B.K., Cai, Q., Stephanou, A., O'Leary, R.M., Pennica, D., Yellon, D.M., and Latchman, D.S. (2002). Cardiotrophin-1 (CT-1) can protect the adult heart from injury when added both prior to ischaemia and at reperfusion. Cardiovasc. Res. *53*, 902–910.

Liles, W.C., Broxmeyer, H.E., Rodger, E., Wood, B., Hü, K., Cooper, S., Hangoc, G., Bridger, G.J., Henson, G.W., Calandra, G., et al. (2003). Mobilization of hematopoietic progenitor cells in healthy volunteers by AMD3100, a CXCR4 antagonist.

Lim, J.A., Woo, J.H., and Kim, H.S. (2008). Phosphoinositide 3-kinase/Akt signalling is responsible for the differential susceptibility of myoblasts and myotubes to menadione-induced oxidative stress. Free Radic. Res. *42*, 798–806.

Lim, J.A., Choi, S.J., Moon, J.Y., and Kim, H.S. (2016). α-Syntrophin is involved in the survival signaling pathway in myoblasts under menadione-induced oxidative stress. Exp. Cell Res. *344*, 1–10.

Lim, S.Y., Davidson, S.M., Mocanu, M.M., Yellon, D.M., and Smith, C.C.T. (2007). The cardioprotective effect of necrostatin requires the cyclophilin-D component of the mitochondrial permeability transition pore. Cardiovasc. Drugs Ther. *21*, 467–469.

Lim, W., Messow, C., and Berry, C. (2012). Cyclosporin variably and inconsistently reduces infarct size in experimental models of reperfused myocardial infarction: a systematic review and meta-analysis. Br. J. Pharmacol. *165*, 2034–2043.

Limb, G.A., Matter, K., Murphy, G., Cambrey, A.D., Bishop, P.N., Morris, G.E., and

Khaw, P.T. (2005). Matrix metalloproteinase-1 associates with intracellular organelles and confers resistance to lamin A/C Degradation during apoptosis. Am. J. Pathol. *166*, 1555–1563.

Lin, Y.H., and Yang-Yen, H.F. (2001). The osteopontin-CD44 survival signal involves activation of the phosphatidylinositol 3-kinase/Akt signaling pathway. J. Biol. Chem. *276*, 46024–46030.

Lin, Y., Marin-Argany, M., Dick, C.J., Redhage, K.R., Blancas-Mejia, L.M., Bulur, P., Butler, G.W., Deeds, M.C., Madden, B.J., Williams, A., et al. (2017). Mesenchymal stromal cells protect human cardiomyocytes from amyloid fibril damage. Cytotherapy *19*, 1426–1437.

Lincoff, A.M., Roe, M., Aylward, P., Galla, J., Rynkiewicz, A., Guetta, V., Zelizko, M., Kleiman, N., White, H., McErlean, E., et al. (2014). Inhibition of delta-protein kinase C by delcasertib as an adjunct to primary percutaneous coronary intervention for acute anterior ST-segment elevation myocardial infarction: Results of the protection AMI randomized controlled trial. Eur. Heart J. *35*, 2516–2523.

Lindsey, M.L., Bolli, R., Canty, J.M., Du, X.J., Frangogiannis, N.G., Frantz, S., Gourdie, R.G., Holmes, J.W., Jones, S.P., Kloner, R.A., et al. (2018). Guidelines for experimental models of myocardial ischemia and infarction. Am. J. Physiol. - Hear. Circ. Physiol. *314*, H812–H838.

Linke, A., Muller, P., Nurzynska, D., Casarsa, C., Torella, D., Nascimbene, A., Castaldo, C., Cascapera, S., Bohm, M., Quaini, F., et al. (2005). Stem cells in the dog heart are self-renewing, clonogenic, and multipotent and regenerate infarcted myocardium, improving cardiac function. Proc. Natl. Acad. Sci. *102*, 8966–8971.

Liu, D., Zhang, X.L., Yan, C.H., Li, Y., Tian, X.X., Zhu, N., Rong, J.J., Peng, C.F., and Han, Y.L. (2015). MicroRNA-495 regulates the proliferation and apoptosis of human umbilical vein endothelial cells by targeting chemokine CCL2. Thromb. Res. *135*, 146–154.

Liu, F.-F., Stone, J.R., Schuldt, A.J.T., Okoshi, K., Okoshi, M.P., Nakayama, M., Ho, K.K.L., Manning, W.J., Marchionni, M.A., Lorell, B.H., et al. (2005a). Heterozygous knockout of neuregulin-1 gene in mice exacerbates doxorubicin-induced heart failure. Am. J. Physiol. Circ. Physiol. *289*, H660–H666.

Liu, G., Ma, C., Yang, H., and Zhang, P.Y. (2017). Transforming growth factor β and its role in heart disease. Exp. Ther. Med. *13*, 2123–2128.

Liu, H.R., Gao, E., Hu, A., Tao, L., Qu, Y., Most, P., Koch, W.J., Christopher, T.A.,

Lopez, B.L., Alnemri, E.S., et al. (2005b). Role of Omi/HtrA2 in apoptotic cell death after myocardial ischemia and reperfusion. Circulation *111*, 90–96.

Liu, J., Narsinh, K.H., Lan, F., Wang, L., Nguyen, P.K., Hu, S., Lee, A., Han, L., Gong, Y., Huang, M., et al. (2012). Early stem cell engraftment predicts late cardiac functional recovery preclinical insights from molecular imaging. Circ. Cardiovasc. Imaging *5*, 481–490.

Liu, J., Wu, P., Wang, Y., Du, Y., A, N., Liu, S., Zhang, Y., Zhou, N., Xu, Z., and Yang, Z. (2016a). Ad-HGF improves the cardiac remodeling of rat following myocardial infarction by upregulating autophagy and necroptosis and inhibiting apoptosis. Am. J. Transl. Res. *8*, 4605–4627.

Liu, K., Ji, K., Guo, L., Wu, W., Lu, H., Shan, P., and Yan, C. (2014). Mesenchymal stem cells rescue injured endothelial cells in an in vitro ischemia-reperfusion model via tunneling nanotube like structure-mediated mitochondrial transfer. Microvasc. Res. *92*, 10–18.

Liu, L., Ding, W.Y., Zhao, J., Wang, Z.H., Zhong, M., Zhang, W., Chen, Y.G., Zhang, Y., Li, L., and Tang, M.X. (2013a). Activin receptor-like kinase 7 mediates high glucose-induced H9c2 cardiomyoblast apoptosis through activation of Smad2/3. Int. J. Biochem. Cell Biol. *45*, 2027–2035.

Liu, Y., Shoji-Kawata, S., Sumpter, R.M., Wei, Y., Ginet, V., Zhang, L., Posner, B., Tran, K.A., Green, D.R., Xavier, R.J., et al. (2013b). Autosis is a Na+,K+-ATPase-regulated form of cell death triggered by autophagy-inducing peptides, starvation, and hypoxia-ischemia. Proc. Natl. Acad. Sci. U. S. A. *110*, 20364–20371.

Liu, Y., Chen, L., Diaz, A.D., Benham, A., Xu, X., Wijaya, C.S., Fa'Ak, F., Luo, W., Soibam, B., Azares, A., et al. (2016b). Mesp1 marked cardiac progenitor cells repair infarcted mouse hearts. Sci. Rep. *6*.

Lockshin, R.A., and Williams, C.M. (1965). Programmed cell death—I. Cytology of degeneration in the intersegmental muscles of the Pernyi silkmoth. J. Insect Physiol. *11*, 123–133.

Lohan, P., Coleman, C.M., Murphy, J., Griffin, M.D., Ritter, T., and Ryan, A.E. (2014). Changes in immunological profile of allogeneic mesenchymal stem cells after differentiation: should we be concerned? Stem Cell Res. Ther. *5*, 99–110.

Long, L.H., and Halliwell, B. (2009). Artefacts in cell culture: Pyruvate as a scavenger of hydrogen peroxide generated by ascorbate or epigallocatechin gallate in cell culture media. Biochem. Biophys. Res. Commun. *388*, 700–704.

Loor, G., and Schumacker, P.T. (2008). Role of hypoxia-inducible factor in cell survival during myocardial ischemia–reperfusion. Cell Death Differ. *15*, 686–690.

Loor, G., Kondapalli, J., Schriewer, J.M., Chandel, N.S., Vanden Hoek, T.L., and Schumacker, P.T. (2010). Menadione triggers cell death through ROS-dependent mechanisms involving PARP activation without requiring apoptosis. Free Radic. Biol. Med. *49*, 1925–1936.

Lopez, J.J., Laham, R.J., Stamler, A., Pearlman, J.D., Bunting, S., Kaplan, A., Carrozza, J.P., Sellke, F.W., and Simons, M. (1998). VEGF administration in chronic myocardial ischemia in pigs. Cardiovasc. Res. *40*, 272–281.

López, N., Díez, J., and Fortuño, M.A. (2005). Characterization of the protective effects of cardiotrophin-1 against non-ischemic death stimuli in adult cardiomyocytes. Cytokine *30*, 282–292.

Losordo, D.W., Schatz, R.A., White, C.J., Udelson, J.E., Veereshwarayya, V., Durgin, M., Poh, K.K., Weinstein, R., Kearney, M., Chaudhry, M., et al. (2007). Intramyocardial Transplantation of Autologous CD34 $^{+}$ Stem Cells for Intractable Angina. Circulation *115*, 3165–3172.

Losordo, D.W., Henry, T.D., Davidson, C., Sup Lee, J., Costa, M.A., Bass, T., Mendelsohn, F., Fortuin, F.D., Pepine, C.J., Traverse, J.H., et al. (2011). Intramyocardial, autologous CD34+ cell therapy for refractory angina. Circ. Res. *109*, 428–436.

Lou, G., Chen, Z., Zheng, M., and Liu, Y. (2017). Mesenchymal stem cell-derived exosomes as a new therapeutic strategy for liver diseases. Exp. Mol. Med. *49*, e346–e346.

Lucas, A., Mialet-Perez, J., Daviaud, D., Parini, A., Marber, M.S., and Sicard, P. (2015). Gadd45 *γ* regulates cardiomyocyte death and post-myocardial infarction left ventricular remodelling. Cardiovasc. Res. *108*, 254–267.

Luedde, M., Lutz, M., Carter, N., Sosna, J., Jacoby, C., Vucur, M., Gautheron, J., Roderburg, C., Borg, N., Reisinger, F., et al. (2014). RIP3, a kinase promoting necroptotic cell death, mediates adverse remodelling after myocardial infarction. Cardiovasc. Res. *103*, 206–216.

Lundy, S.D., Zhu, W.-Z., Regnier, M., and Laflamme, M.A. (2013). Structural and functional maturation of cardiomyocytes derived from human pluripotent stem cells. Stem Cells Dev. *22*, 1991–2002.

Lynch, C.N., Wang, Y.C., Lund, J.K., Chen, Y.W., Leal, J.A., and Wiley, S.R. (1999). TWEAK induces angiogenesis and proliferation of endothelial cells. J. Biol. Chem. *274*, 8455–8459.

Machiraju, P., and Greenway, S.C. (2019). Current methods for the maturation of induced pluripotent stem cellderived cardiomyocytes. World J. Stem Cells *11*, 33–43.

Maciel, L., de Oliveira, D.F., Verissimo da Costa, G.C., Bisch, P.M., and Nascimento, J.H.M. (2017). Cardioprotection by the transfer of coronary effluent from ischaemic preconditioned rat hearts: identification of cardioprotective humoral factors. Basic Res. Cardiol. *112*, 52.

MacLellan, W.R., Garcia, A., Oh, H., Frenkel, P., Jordan, M.C., Roos, K.P., and Schneider, M.D. (2005). Overlapping roles of pocket proteins in the myocardium are unmasked by germ line deletion of p130 plus heart-specific deletion of Rb. Mol. Cell. Biol. *25*, 2486–2497.

Macqueen, L.A., Sheehy, S.P., Chantre, C.O., Zimmerman, J.F., Pasqualini, F.S., Liu, X., Goss, J.A., Campbell, P.H., Gonzalez, G.M., Park, S.J., et al. (2018). A tissue-engineered scale model of the heart ventricle. Nat. Biomed. Eng. *2*, 930–941.

Madisen, L., Zwingman, T.A., Sunkin, S.M., Oh, S.W., Zariwala, H.A., Gu, H., Ng, L.L., Palmiter, R.D., Hawrylycz, M.J., Jones, A.R., et al. (2010). A robust and high-throughput Cre reporting and characterization system for the whole mouse brain. Nat. Neurosci. *13*, 133–140.

Maelfait, J., Liverpool, L., Bridgeman, A., Ragan, K.B., Upton, J.W., and Rehwinkel, J. (2017). Sensing of viral and endogenous RNA by ZBP 1/ DAI induces necroptosis. EMBO J. *36*, 2529–2543.

Maillet, A., Tan, K., Chai, X., Sadananda, S.N., Mehta, A., Ooi, J., Hayden, M.R., Pouladi, M.A., Ghosh, S., Shim, W., et al. (2016). Modeling Doxorubicin-induced cardiotoxicity in human pluripotent stem cell derived-cardiomyocytes. Sci. Rep. *6*, 25333.

Malik, A., Bromage, D.I., He, Z., Candilio, L., Hamarneh, A., Taferner, S., Davidson, S.M., and Yellon, D.M. (2015). Exogenous SDF-1α protects human myocardium from hypoxia-reoxygenation injury via CXCR4. Cardiovasc. Drugs Ther. *29*, 589–592.

Maliken, B.D., and Molkentin, J.D. (2018). Undeniable evidence that the adult mammalian heart lacks an endogenous regenerative stem cell. Circulation *138*, 806–808.

Malin, J.Z., and Shaham, S. (2015). Cell death in C. elegans development. Curr. Top. Dev. Biol. *114*, 1–42.

Malliaras, K., Ibrahim, A., Tseliou, E., Liu, W., Sun, B., Middleton, R.C., Seinfeld, J., Wang, L., Sharifi, B.G., and Marbán, E. (2014). Stimulation of endogenous cardioblasts by exogenous cell therapy after myocardial infarction. EMBO Mol. Med. *6*, 760–777.

Mandl, A., Pham, L.H., Toth, K., Zambetti, G., and Erhardt, P. (2011). Puma deletion delays cardiac dysfunction in murine heart failure models through attenuation of apoptosis. Circulation *124*, 31–39.

Mangi, A.A., Noiseux, N., Kong, D., He, H., Rezvani, M., Ingwall, J.S., and Dzau, V.J. (2003). Mesenchymal stem cells modified with Akt prevent remodeling and restore performance of infarcted hearts. Nat. Med. *9*, 1195–1201.

Manning, J.R., Thapa, D., Zhang, M., Stoner, M.W., Traba, J., Corey, C., Shiva, S., Sack, M.N., and Scott, I. (2019). Loss of GCN5L1 in cardiac cells disrupts glucose metabolism and promotes cell death via reduced Akt/mTORC2 signaling. Biochem. J. *476*, 1713–1724.

Marbán, E., and Malliaras, K. (2012). Mixed results for bone marrow–derived cell therapy for ischemic heart disease. JAMA *308*, 2405–2406.

Markousis-Mavrogenis, G., Tromp, J., Ouwerkerk, W., Devalaraja, M., Anker, S.D., Cleland, J.G., Dickstein, K., Filippatos, G.S., van der Harst, P., Lang, C.C., et al. (2019). The clinical significance of interleukin-6 in heart failure: results from the BIOSTAT-CHF study. Eur. J. Heart Fail. *21*, 965–973.

Marsters, S.A., Sheridan, J.P., Pitti, R.M., Brush, J., Goddard, A., and Ashkenazi, A. (1998). Identification of a ligand for the death-domain-containing receptor Apo3. Curr. Biol. *8*, 525–528.

Martin, E., Thougaard, A.V., Grauslund, M., Jensen, P.B., Bjorkling, F., Hasinoff, B.B., Tjørnelund, J., Sehested, M., and Jensen, L.H. (2009). Evaluation of the topoisomerase II-inactive bisdioxopiperazine ICRF-161 as a protectant against doxorubicin-induced cardiomyopathy. Toxicology *255*, 72–79.

Martindale, J.J., Fernandez, R., Thuerauf, D., Whittaker, R., Gude, N., Sussman, M.A., and Glembotski, C.C. (2006). Endoplasmic reticulum stress gene induction and protection from ischemia/reperfusion injury in the hearts of transgenic mice with a tamoxifen-regulated form of ATF6. Circ. Res. *98*, 1186–1193.

Masini, E., Cuzzocrea, S., Mazzon, E., Marzocca, C., Mannaioni, P.F., and Salvemini, D. (2002). Protective effects of M40403, a selective superoxide dismutase mimetic, in myocardial ischaemia and reperfusion injury in vivo. Br. J. Pharmacol. *136*, 905–917.

Matsa, E., Burridge, P.W., and Wu, J.C. (2014). Human stem cells for modeling heart disease and for drug discovery. Sci. Transl. Med. *6*, 239ps6-239ps6.

Matsa, E., Burridge, P.W., Yu, K.H., Ahrens, J.H., Termglinchan, V., Wu, H., Liu, C., Shukla, P., Sayed, N., Churko, J.M., et al. (2016). Transcriptome profiling of patient-specific human iPSC-cardiomyocytes predicts individual drug safety and efficacy responses in vitro. Cell Stem Cell *19*, 311–325.

Matsui, T., Tao, J., del Monte, F., Lee, K.-H., Li, L., Picard, M., Force, T.L., Franke, T.F., Hajjar, R.J., and Rosenzweig, A. (2001). Akt activation preserves cardiac function and prevents injury after transient cardiac ischemia in vivo. Circulation *104*, 330–335.

Matsui, Y., Takagi, H., Qu, X., Abdellatif, M., Sakoda, H., Asano, T., Levine, B., and Sadoshima, J. (2007). Distinct roles of autophagy in the heart during ischemia and reperfusion: roles of AMP-activated protein kinase and Beclin 1 in mediating autophagy. Circ. Res. *100*, 914–922.

Matsumori, A., Furukawa, Y., Hashimoto, T., Ono, K., Shioi, T., Okada, M., Iwasaki, A., Nishio, R., and Sasayama, S. (1996). Increased circulating hepatocyte growth factor in the early stage of acute myocardial infarction. Biochem. Biophys. Res. Commun. *221*, 391–395.

Matsushita, K., Iwanaga, S., Oda, T., Kimura, K., Shimada, M., Sano, M., Umezawa, A., Hata, J.I., and Ogawa, S. (2005). Interleukin-6/soluble interleukin-6 receptor complex reduces infarct size via inhibiting myocardial apoptosis. Lab. Investig. *85*, 1210–1223.

Matsuura, K., Honda, A., Nagai, T., Fukushima, N., Iwanaga, K., Tokunaga, M., Shimizu, T., Okano, T., Kasanuki, H., Hagiwara, N., et al. (2009). Transplantation of cardiac progenitor cells ameliorates cardiac dysfunction after myocardial infarction in mice. J. Clin. Invest. *119*, 2204–2017.

Maulik, A., Davidson, S.M., Piotrowska, I., Walker, M., and Yellon, D.M. (2018). Ischaemic preconditioning protects cardiomyocytes from anthracycline-induced toxicity via the PI3K pathway. Cardiovasc. Drugs Ther. *32*, 245–253.

Mazo, M., Planat-Bénard, V., Abizanda, G., Pelacho, B., Léobon, B., Gavira, J.J.,

Peñuelas, I., Cemborain, A., Pénicaud, L., Laharrague, P., et al. (2008). Transplantation of adipose derived stromal cells is associated with functional improvement in a rat model of chronic myocardial infarction. Eur. J. Heart Fail. *10*, 454–462.

Mazo, M., Gavira, J.J., Abizanda, G., Moreno, C., Ecay, M., Soriano, M., Aranda, P., Collantes, M., Alegría, E., Merino, J., et al. (2010). Transplantation of mesenchymal stem cells exerts a greater long-term effect than bone marrow mononuclear cells in a chronic myocardial infarction model in rat. Cell Transplant. *19*, 313–328.

Mccormick, J., Suleman, N., Scarabelli, T.M., Knight, R.A., Latchman, D.S., and Stephanou, A. (2012). STAT1 deficiency in the heart protects against myocardial infarction by enhancing autophagy. J. Cell. Mol. Med. *16*, 386–393.

McIntosh, V.J., and Lasley, R.D. (2012). Adenosine receptor-mediated cardioprotection: are all 4 subtypes required or redundant? J. Cardiovasc. Pharmacol. Ther. *17*, 21–33.

Medeiros De Campos-Baptista, M.I., Holtzman, N.G., Yelon, D., and Schier, A.F. (2008). Nodal signaling promotes the speed and directional movement of cardiomyocytes in zebrafish. Dev. Dyn. *237*, 3624–3633.

Van Der Meer, P., Lipsic, E., Henning, R.H., Boddeus, K., Van Der Velden, J., Voors, A.A., Van Veldhuisen, D.J., Van Gilst, W.H., and Schoemaker, R.G. (2005). Erythropoietin induces neovascularization and improves cardiac function in rats with heart failure after myocardial infarction. J. Am. Coll. Cardiol. *46*, 125–133.

Mehanna, R.A., Nabil, I., Attia, N., Bary, A.A., Razek, K.A., Ahmed, T.A.E., and Elsayed, F. (2015). The effect of bone marrow-derived mesenchymal stem cells and their conditioned media topically delivered in fibrin glue on chronic wound healing in rats. Biomed Res. Int. *2015*.

Mehlen, P. (2010). Dependence receptors: the trophic theory revisited. Sci. Signal. *3*, 47.

Mehlen, P., Rabizadeh, S., Snipas, S.J., Assa-Munt, N., Salvesen, G.S., and Bredesen, D.E. (1998). The DCC gene product induces apoptosis by a mechanism requiring receptor proteolysis. Nature *395*, 801–804.

Meinken, J., Walker, G., Cooper, C.R., and Min, X.J. (2015). MetazSecKB: the human and animal secretome and subcellular proteome knowledgebase. Database *2015*, bav077.

Meissner, G. (2017). The structural basis of ryanodine receptor ion channel function. J. Gen. Physiol. *149*, 1065–1089.

Mendes-Ferreira, P., De Keulenaer, G.W., Leite-Moreira, A.F., and Brás-Silva, C. (2013). Therapeutic potential of neuregulin-1 in cardiovascular disease. Drug Discov. Today *18*, 836–842.

Mendt, M., Rezvani, K., and Shpall, E. (2019). Mesenchymal stem cell-derived exosomes for clinical use. Bone Marrow Transplant. *54*, 789–792.

Menon, B., Singh, M., and Singh, K. (2005). Matrix metalloproteinases mediate β-adrenergic receptor-stimulated apoptosis in adult rat ventricular myocytes. Am. J. Physiol. - Cell Physiol. *289*, 168–176.

Menon, B., Singh, M., Ross, R.S., Johnson, J.N., and Singh, K. (2006). β-Adrenergic receptor-stimulated apoptosis in adult cardiac myocytes involves MMP-2-mediated disruption of β1 integrin signaling and mitochondrial pathway. Am. J. Physiol. - Cell Physiol. *290*, 179057.

Mercola, M., Ruiz-Lozano, P., and Schneider, M.D. (2011). Cardiac muscle regeneration: lessons from development. Genes Dev. *25*, 299–309.

Merilahti, J.A.M., Ojala, V.K., Knittle, A.M., Pulliainen, A.T., and Elenius, K. (2017). Genome-wide screen of gamma-secretase-mediated intramembrane cleavage of receptor tyrosine kinases. Mol. Biol. Cell *28*, 3123–3131.

Merkle, S., Frantz, S., Schön, M.P., Bauersachs, J., Buitrago, M., Frost, R.J.A., Schmitteckert, E.M., Lohse, M.J., and Engelhardt, S. (2007). A role for caspase-1 in heart failure. Circ. Res. *100*, 645–653.

Messina, E., De Angelis, L., Frati, G., Morrone, S., Chimenti, S., Fiordaliso, F., Salio, M., Battaglia, M., Latronico, M.V.G.G., Coletta, M., et al. (2004). Isolation and expansion of adult cardiac stem cells from human and murine heart. Circ. Res. *95*, 911–921.

Metra, M., and Teerlink, J.R. (2017). Heart failure. Lancet *390*, 1981–1995.

Meyer, A., Wang, W., Qu, J., Croft, L., Degen, J.L., Coller, B.S., and Ahamed, J. (2012). Platelet TGF-β1 contributions to plasma TGF-β1, cardiac fibrosis, and systolic dysfunction in a mouse model of pressure overload. Blood *119*, 1064–1074.

Meyer, G.P., Wollert, K.C., Lotz, J., Steffens, J., Lippolt, P., Fichtner, S., Hecker, H.,

Schaefer, A., Arseniev, L., Hertenstein, B., et al. (2006). Intracoronary bone marrow cell transfer after myocardial infarction. Circulation *113*, 1287–1294.

Meylan, F., Davidson, T.S., Kahle, E., Kinder, M., Acharya, K., Jankovic, D., Bundoc, V., Hodges, M., Shevach, E.M., Keane-Myers, A., et al. (2008). The TNF-family receptor DR3 is essential for diverse T cell-mediated inflammatory diseases. Immunity *29*, 79–89.

Miao, W., Luo, Z., Kitsis, R.N., and Walsh, K. (2000). Intracoronary, Adenovirus-mediated Akt Gene Transfer in Heart Limits Infarct Size Following Ischemia-reperfusion Injury in Vivo. J. Mol. Cell. Cardiol. *32*, 2397–2402.

Michael, L.H., Entman, M.L., Hartley, C.J., Youker, K.A., Zhu, J., Hall, S.R., Hawkins, H.K., Berens, K., and Ballantyne, C.M. (1995). Myocardial ischemia and reperfusion: A murine model. Am. J. Physiol. - Hear. Circ. Physiol. *269*, 2147–2154.

Michael, L.H., Ballantyne, C.M., Zachariah, J.P., Gould, K.E., Pocius, J.S., Taffet, G.E., Hartley, C.J., Pham, T.T., Daniel, S.L., Funk, E., et al. (1999). Myocardial infarction and remodeling in mice: Effect of reperfusion. Am. J. Physiol. - Hear. Circ. Physiol. *277*.

Micheau, O., and Tschopp, J. (2003). Induction of TNF receptor I-mediated apoptosis via two sequential signaling complexes. Cell *114*, 181–190.

Migone, T.S., Zhang, J., Luo, X., Zhuang, L., Chen, C., Hu, B., Hong, J.S., Perry, J.W., Chen, S.F., Zhou, J.X.H., et al. (2002). TL1A is a TNF-like ligand for DR3 and TR6/DcR3 and functions as a T cell costimulator. Immunity *16*, 479–492.

Mihajlović, J., Diehl, L.A.M., Hochhaus, A., and Clement, J.H. (2019). Inhibition of bone morphogenetic protein signaling reduces viability, growth and migratory potential of non-small cell lung carcinoma cells. J. Cancer Res. Clin. Oncol. *145*, 2675–2687.

Mille, F., Thibert, C., Fombonne, J., Rama, N., Guix, C., Hayashi, H., Corset, V., Reed, J.C., and Mehlen, P. (2009). The Patched dependence receptor triggers apoptosis through a DRAL-caspase-9 complex. Nat. Cell Biol. *11*, 739–746.

Miller, C., Rulfs, J., Jaspers, S.R., Buckholt, M., and Miller, T.B. (1994). Transformation of adult ventricular myocytes with the temperature sensitive A58 (tsA58) mutant of the SV40 large T antigen. Mol. Cell. Biochem. *136*, 29–34.

Miller, E.J., Li, J., Leng, L., McDonald, C., Atsumi, T., Bucala, R., and Young, L.H. (2008). Macrophage migration inhibitory factor stimulates AMP-activated protein

kinase in the ischaemic heart. Nature *451*, 578–582.

Minamino, T., Yujiri, T., Papst, P.J., Chan, E.D., Johnson, G.L., and Terada, N. (1999). MEKK1 suppresses oxidative stress-induced apoptosis of embryonic stem cell-derived cardiac myocytes. Proc. Natl. Acad. Sci. U. S. A. *96*, 15127–15132.

Mincheva-Nilsson, L., Baranov, V., Nagaeva, O., Dehlin, E., Mincheva-Nilsson, L., Baranov, V., Nagaeva, O., and Dehlin, E. (2016). Isolation and characterization of exosomes from cultures of tissue explants and cell lines. Curr. Protoc. Immunol. *115*, 1–21.

Minhaz, U., Tanaka, M., Tsukamoto, H., Watanabe, K., Koide, S., Shohtsu, A., and Nakazawa, H. (1996). Effect of MCI-186 on postischemic reperfusion injury in isolated rat heart. Free Radic. Res. *24*, 361–367.

Mitchell, P.S., Parkin, R.K., Kroh, E.M., Fritz, B.R., Wyman, S.K., Pogosova-Agadjanyan, E.L., Peterson, A., Noteboom, J., O'Briant, K.C., Allen, A., et al. (2008). Circulating microRNAs as stable blood-based markers for cancer detection. Proc. Natl. Acad. Sci. U. S. A. *105*, 10513–10518.

Mohamed, T.M.A., Ang, Y.S., Radzinsky, E., Zhou, P., Huang, Y., Elfenbein, A., Foley, A., Magnitsky, S., and Srivastava, D. (2018). Regulation of cell cycle to stimulate adult cardiomyocyte proliferation and cardiac regeneration. Cell *173*, 104-116.e12.

Moon, C., Krawczyk, M., Ahn, D., Ahmet, I., Paik, D., Lakatta, E.G., and Talan, M.I. (2003). Erythropoietin reduces myocardial infarction and left ventricular functional decline after coronary artery ligation in rats. Proc. Natl. Acad. Sci. U. S. A. *100*, 11612–1161.

Moon, C., Krawczyk, M., Lakatta, E.G., and Talan, M.I. (2006). Therapeutic effectiveness of a single vs multiple doses of erythropoietin after experimental myocardial infarction in rats. Cardiovasc. Drugs Ther. *20*, 245–251.

Moore, J.B., Zhao, J., Keith, M.C.L., Amraotkar, A.R., Wysoczynski, M., Hong, K.U., and Bolli, R. (2016). The epigenetic regulator HDAC1 modulates transcription of a core cardiogenic program in human cardiac mesenchymal stromal cells through a p53-dependent mechanism. Stem Cells *34*, 2916–2929.

Morawietz, H. (2018). Cardiovascular protection by Nox4 (Oxford University Press).

Morieri, M.L., Passaro, A., and Zuliani, G. (2017). Interleukin-6 "Trans-Signaling" and ischemic vascular disease: the important role of soluble gp130. Mediators Inflamm.

*2017*.

Morimoto, H., and Takahashi, M. (2007). Role of monocyte chemoattractant protein-1 in myocardial infarction. Int. J. Biomed. Sci. *3*, 159–167.

Morimoto, H., Hirose, M., Takahashi, M., Kawaguchi, M., Ise, H., Kolattukudy, P.E., Yamada, M., and Ikeda, U. (2008). MCP-1 induces cardioprotection against ischaemia/reperfusion injury: role of reactive oxygen species. Cardiovasc. Res. *78*, 554–562.

Mortier, E., Bernard, J., Plet, A., and Jacques, Y. (2004). Natural,proteolytic release of a soluble form of human IL-15 receptor α-Chain that behaves as a specific, high affinity IL-15 antagonist. J. Immunol. *173*, 1681–1688.

Moslehi, J.J. (2016). Cardiovascular toxic effects of targeted cancer therapies. N. Engl. J. Med. *375*, 1457–1467.

Mozaffarian, D., Benjamin, E.J., Go, A.S., Arnett, D.K., Blaha, M.J., Cushman, M., Das, S.R., de Ferranti, S., Després, J.-P., Fullerton, H.J., et al. (2016). Heart disease and stroke statistics—2016 update. Circulation *133*, e38–e360.

Mukhopadhyay, P., Rajesh, M., Yoshihiro, K., Haskó, G., and Pacher, P. (2007). Simple quantitative detection of mitochondrial superoxide production in live cells. Biochem. Biophys. Res. Commun. *358*, 203–208.

Murphy, C.K., Fey, E.G., Watkins, B.A., Wong, V., Rothstein, D., and Sonis, S.T. (2008). Efficacy of superoxide dismutase mimetic M40403 in attenuating radiation-induced oral mucositis in hamsters. Clin. Cancer Res. *14*, 4292–4297.

Murphy, E., Perlman, M., London, R.E., and Steenbergen, C. (1991). Amiloride delays the ischemia-induced rise in cytosolic free calcium. Circ. Res. *68*, 1250–1258.

Murphy, J.M., Czabotar, P.E., Hildebrand, J.M., Lucet, I.S., Zhang, J.-G., Alvarez-Diaz, S., Lewis, R., Lalaoui, N., Metcalf, D., Webb, A.I., et al. (2013). The pseudokinase MLKL mediates necroptosis via a molecular switch mechanism. Immunity *39*, 443–453.

Murry, C.E., Soonpaa, M.H., Reinecke, H., Nakajima, H.O.H., Nakajima, H.O.H., Rubart, M., Pasumarthi, K.B.S.S., Virag, J.I., Bartelmez, S.H., Poppa, V., et al. (2004). Haematopoietic stem cells do not transdifferentiate into cardiac myocytes in myocardial infarcts. Nature *428*, 664–668.

Muscoli, C., Cuzzocrea, S., Riley, D.P., Zweier, J.L., Thiemermann, C., Wang, Z.Q., and Salvemini, D. (2003). On the selectivity of superoxide dismutase mimetics and its importance in pharmacological studies. Br. J. Pharmacol. *140*, 445–460.

Myers, C., Bonow, R., Palmeri, S., Jenkins, J., Corden, B., Locker, G., Doroshow, J., and Epstein, S. (1983). A randomized controlled trial assessing the prevention of doxorubicin cardiomyopathy by N-acetylcysteine. Semin. Oncol. *10*, 53–55.

Nagarajan, V., Hernandez, A. V, and Tang, W.H.W. (2012). Prognostic value of cardiac troponin in chronic stable heart failure: a systematic review. Heart *98*, 1778–1786.

Najjar, S.S., Rao, S. V., Melloni, C., Raman, S. V., Povsic, T.J., Melton, L., Barsness, G.W., Prather, K., Heitner, J.F., Kilaru, R., et al. (2011). Intravenous erythropoietin in patients with ST-segment elevation myocardial infarction. JAMA *305*, 1863–1872.

Nakagawa, T., Shimizu, S., Watanabe, T., Yamaguchi, O., Otsu, K., Yamagata, H., Inohara, H., Kubo, T., and Tsujimoto, Y. (2005). Cyclophilin D-dependent mitochondrial permeability transition regulates some necrotic but not apoptotic cell death. Nature *434*, 652–658.

Nakai, A., Yamaguchi, O., Takeda, T., Higuchi, Y., Hikoso, S., Taniike, M., Omiya, S., Mizote, I., Matsumura, Y., Asahi, M., et al. (2007). The role of autophagy in cardiomyocytes in the basal state and in response to hemodynamic stress. Nat. Med. *13*, 619–624.

Nakajima, H., Nakajima, H.O., Salcher, O., Dittiè, A.S., Dembowsky, K., Jing, S., and Field, L.J. (2000). Atrial but not ventricular fibrosis in mice expressing a mutant transforming growth factor-β 1 transgene in the heart. Circ. Res. *86*, 571–579.

Nakamura, T., Ueda, Y., Juan, Y., Katsuda, S., Takahashi, H., and Koh, E. (2000a). Fas-mediated apoptosis in Adriamycin-induced cardiomyopathy in rats: In vivo study. Circulation *102*, 572–578.

Nakamura, T., Mizuno, S., Matsumoto, K., Sawa, Y., Matsuda, H., and Nakamura, T. (2000b). Myocardial protection from ischemia/reperfusion injury by endogenous and exogenous HGF. J. Clin. Invest. *106*, 1511–1519.

Nakayama, H., Chen, X., Baines, C.P., Klevitsky, R., Zhang, X., Zhang, H., Jaleel, N., Chua, B.H.L.L., Hewett, T.E., Robbins, J., et al. (2007). Ca2+- and mitochondrial-dependent cardiomyocyte necrosis as a primary mediator of heart failure. J. Clin. Invest. *117*, 2431–2444.

Napolitano, C., and Antzelevitch, C. (2011). Phenotypical manifestations of mutations in the genes encoding subunits of the cardiac voltage-dependent L-type calcium channel. Circ. Res. *108*, 607–618.

Narula, J., Haider, N., Virmani, R., DiSalvo, T.G., Kolodgie, F.D., Hajjar, R.J., Schmidt, U., Semigran, M.J., Dec, G.W., and Khaw, B.-A. (1996). Apoptosis in myocytes in end-stage heart failure. N. Engl. J. Med. *335*, 1182–1189.

Nathan, A.T., and Singer, M. (1999). The oxygen trail: tissue oxygenation. Br. Med. Bull. *55*, 96–108.

Nebigil, C.G., and Désaubry, L. (2018). Updates in anthracycline-mediated cardiotoxicity. Front. Pharmacol. *9*.

Negishi, Y., Kudo, A., Obinata, A., Kawashima, K., Hirano, H., Yanai, N., Obinata, M., and Endo, H. (2000). Multipotency of a bone marrow stromal cell line, TBR31-2, established from ts-SV40 T antigen gene transgenic mice. Biochem. Biophys. Res. Commun. *268*, 450–455.

Negoro, S., Oh, H., Tone, E., Kunisada, K., Fujio, Y., Walsh, K., Kishimoto, T., and Yamauchi-Takihara, K. (2001). Glycoprotein 130 regulates cardiac myocyte survival in doxorubicin-induced apoptosis through phosphatidylinositol 3-kinase/Akt phosphorylation and Bcl-xL/caspase-3 interaction. Circulation *103*, 555–561.

Neidig, L.E., Weinberger, F., Palpant, N.J., Mignone, J., Martinson, A.M., Sorensen, D.W., Bender, I., Nemoto, N., Reinecke, H., Pabon, L., et al. (2018). Evidence for minimal cardiogenic potential of stem cell antigen 1-positive cells in the adult mouse heart. Circulation *138*, 2960–2962.

Neill, T., Torres, A., Buraschi, S., Owens, R.T., Hoek, J.B., Baffa, R., and Iozzo, R. V. (2014). Decorin induces mitophagy in breast carcinoma cells via peroxisome proliferator-activated receptor γ coactivator-1α (PGC-1α) and mitostatin. J. Biol. Chem. *289*, 4952–4968.

Newby, L.K., Marber, M.S., Melloni, C., Sarov-Blat, L., Aberle, L.H., Aylward, P.E., Cai, G., De Winter, R.J., Hamm, C.W., Heitner, J.F., et al. (2014). Losmapimod, a novel p38 mitogen-activated protein kinase inhibitor, in non-ST-segment elevation myocardial infarction: A randomised phase 2 trial. Lancet *384*, 1187–1195.

Newton, K., Sun, X., and Dixit, V.M. (2004). Kinase RIP3 is dispensable for normal NF- Bs, signaling by the B-Cell and T-Cell receptors, tumor necrosis factor receptor 1, and toll-like receptors 2 and 4. Mol. Cell. Biol. *24*, 1464–1469.

Newton, K., Dugger, D.L., Maltzman, A., Greve, J.M., Hedehus, M., Martin-McNulty, B., Carano, R.A.D.D., Cao, T.C., Van Bruggen, N., Bernstein, L., et al. (2016). RIPK3 deficiency or catalytically inactive RIPK1 provides greater benefit than MLKL deficiency in mouse models of inflammation and tissue injury. *23*, 1565–1576.

NHLBI (2018). CONCERT-HF Study | National Heart, Lung, and Blood Institute (NHLBI).

Ni, W., Zhan, Y., He, H., Maynard, E., Balschi, J.A., and Oettgen, P. (2007). Ets-1 is a critical transcriptional regulator of reactive oxygen species and p47phox gene expression in response to angiotensin II. Circ. Res. *101*, 985–994.

Niebauer, J., Pflaum, C.-D., Clark, A.L., Strasburger, C.J., Hooper, J., Poole-Wilson, P.A., Coats, A.J.S., and Anker, S.D. (1998). Deficient insulin-like growth factor I in chronic heart failure predicts altered body composition, anabolic deficiency, cytokine and neurohormonal activation. J Am Coll Cardiol *32*, 393–397.

Nimata, M., Okabe, T.A., Hattori, M., Yuan, Z., Shioji, K., and Kishimoto, C. (2005). MCI-186 (edaravone), a novel free radical scavenger, protects against acute autoimmune myocarditis in rats. Am. J. Physiol. - Hear. Circ. Physiol. *289*.

Noseda, M., Harada, M., McSweeney, S., Leja, T., Belian, E., Stuckey, D.J., Abreu Paiva, M.S., Habib, J., Macaulay, I., de Smith, A.J., et al. (2015a). PDGFRα demarcates the cardiogenic clonogenic Sca1+ stem/progenitor cell in adult murine myocardium. Nat. Commun. *6*, 6930.

Noseda, M., Abreu-Paiva, M., and Schneider, M.D. (2015b). The Quest for the Adult Cardiac Stem Cell. Circ. J. *79*, 1422–1430.

Nowbar, A.N., Mielewczik, M., Karavassilis, M., Dehbi, H.-M., Shun-Shin, M.J., Jones, S., Howard, J.P., Cole, G.D., and Francis, D.P. (2014). Discrepancies in autologous bone marrow stem cell trials and enhancement of ejection fraction (DAMASCENE): weighted regression and meta-analysis. BMJ *348*, g2688–g2688.

Nunes, S.S., Miklas, J.W., Liu, J., Aschar-Sobbi, R., Xiao, Y., Zhang, B., Jiang, J., Massé, S., Gagliardi, M., Hsieh, A., et al. (2013). Biowire: A platform for maturation of human pluripotent stem cell-derived cardiomyocytes. Nat. Methods *10*, 781–787.

O'Brien, S.G., Guilhot, F., Larson, R.A., Gathmann, I., Baccarani, M., Cervantes, F., Cornelissen, J.J., Fischer, T., Hochhaus, A., Hughes, T., et al. (2003). Imatinib compared with interferon and low-dose cytarabine for newly diagnosed chronic-phase chronic myeloid leukemia. N. Engl. J. Med. *348*, 994–1004.

O'Neal, W.T., Griffin, W.F., Dries-Devlin, J.L., Kent, S.D., Chen, J., Willis, M.S., and Virag, J.A.I. (2013). Ephrin-Eph signaling as a potential therapeutic target for the treatment of myocardial infarction. Med. Hypotheses *80*, 738–744.

Oberst, A., Dillon, C.P., Weinlich, R., McCormick, L.L., Fitzgerald, P., Pop, C., Hakem, R., Salvesen, G.S., and Green, D.R. (2011). Catalytic activity of the caspase-8–FLIPL complex inhibits RIPK3-dependent necrosis. Nature *471*, 363–367.

Oh, H., Bradfute, S.B., Gallardo, T.D., Nakamura, T., Gaussin, V., Mishina, Y., Pocius, J., Michael, L.H., Behringer, R.R., Garry, D.J., et al. (2003). Cardiac progenitor cells from adult myocardium: homing, differentiation, and fusion after infarction. Proc. Natl. Acad. Sci. U. S. A. *100*, 12313–12318.

Oh, Y., Nagalla, S.R., Yamanaka, Y., Kim, H.S., Wilson, E., and Rosenfeld, R.G. (1996). Synthesis and characterization of insulin-like growth factor-binding protein (IGFBP)-7. Recombinant human mac25 protein specifically binds IGF-I and -II. J. Biol. Chem. *271*, 30322–30325.

Ohtsuka, M., Takano, H., Zou, Y., Toko, H., Akazawa, H., Qin, Y., Suzuki, M., Hasegawa, H., Nakaya, H., and Komuro, I. (2004). Cytokine therapy prevents left ventricular remodeling and dysfunction after myocardial infarction through neovascularization. FASEB J. *18*, 851–853.

Okazaki, T., Ebihara, S., Asada, M., Yamanda, S., Saijo, Y., Shiraishi, Y., Ebihara, T., Niu, K., Mei, H., Arai, H., et al. (2007). Macrophage colony-stimulating factor improves cardiac function after ischemic injury by inducing vascular endothelial growth factor production and survival of cardiomyocytes. Am. J. Pathol. *171*, 1093–1103.

Olea, F.D., Vera Janavel, G., De Lorenzi, A., Cuniberti, L., Yannarelli, G., Cabeza Meckert, P., Cearras, M., Laguens, R., and Crottogini, A. (2006). High-dose erythropoietin has no long-term protective effects in sheep with reperfused myocardial infarction. J. Cardiovasc. Pharmacol. *47*, 736–741.

Olivetti, G., Abbi, R., Quaini, F., Kajstura, J., Cheng, W., Nitahara, J.A., Quaini, E., Di Loreto, C., Beltrami, C.A., Krajewski, S., et al. (1997). Apoptosis in the failing human heart. N. Engl. J. Med. *336*, 1131–1141.

Ong, S.-B., Samangouei, P., Kalkhoran, S.B., and Hausenloy, D.J. (2015). The mitochondrial permeability transition pore and its role in myocardial ischemia reperfusion injury. J. Mol. Cell. Cardiol. *78*, 23–34.

Ono, K., Matsumori, A., Shioi, T., Furukawa, Y., and Sasayama, S. (1997). Enhanced expression of hepatocyte growth factor/c-Met by myocardial ischemia and reperfusion in a rat model. Circulation *95*, 2552–2558.

Opgaard, O.S., and Wang, P.H. (2005). IGF-I is a matter of heart. Growth Horm. IGF Res. *15*, 89–94.

Orlic, D., Kajstura, J., Chimenti, S., Jakoniuk, I., Anderson, S.M., Li, B., Pickel, J., McKay, R., Nadal-Ginard, B., Bodine, D.M., et al. (2001). Bone marrow cells regenerate infarcted myocardium. Nature *410*, 701–705.

Oshima, Y., Ouchi, N., Shimano, M., Pimentel, D.R., Papanicolaou, K.N., Panse, K.D., Tsuchida, K., Lara-Pezzi, E., Lee, S.J., and Walsh, K. (2009). Activin a and follistatin-like 3 determine the susceptibility of heart to ischemic injury. Circulation *120*, 1606–1615.

Oskouei, B.N., Lamirault, G., Joseph, C., Treuer, A. V, Landa, S., Da Silva, J., Hatzistergos, K., Dauer, M., Balkan, W., McNiece, I., et al. (2012). Increased potency of cardiac stem cells compared with bone marrow mesenchymal stem cells in cardiac repair. Stem Cells Transl. Med. *1*, 116–124.

Ostádal, B., Ostádalová, I., Kolár, F., Charvátová, Z., and Netuka, I. (2009). Ontogenetic development of cardiac tolerance to oxygen deprivation - possible mechanisms. Physiol. Res. *58 Suppl 2*, S1-12.

Ostadalova, I., Ostadal, B., Kolár, F., Parratt, J.R., and Wilson, S. (1998). Tolerance to ischaemia and ischaemic preconditioning in neonatal rat heart. J. Mol. Cell. Cardiol. *30*, 857–865.

Ott, I., Schulz, S., Mehilli, J., Fichtner, S., Hadamitzky, M., Hoppe, K., Ibrahim, T., Martinoff, S., Massberg, S., Laugwitz, K.-L., et al. (2010). Erythropoietin in patients with acute ST-segment elevation myocardial infarction undergoing primary percutaneous coronary intervention. Circ. Cardiovasc. Interv. *3*, 408–413.

Ottani, F., Latini, R., Staszewsky, L., La Vecchia, L., Locuratolo, N., Sicuro, M., Masson, S., Barlera, S., Milani, V., Lombardi, M., et al. (2016). Cyclosporine A in reperfused myocardial infarction the multicenter, controlled, open-label CYCLE trial. J. Am. Coll. Cardiol. *67*, 365–374.

Padua, R.R., Sethi, R., Dhalla, N.S., and Kardami, E. (1995). Basic fibroblast growth factor is cardioprotective in ischemia-reperfusion injury. Mol. Cell. Biochem. *143*, 129–135.

Padua, R.R., Liu, L., Sethi, R., Davey-Forgie, S.E., Dhalla, N.S., and Kardami, E. (1996). Cardioprotection and basic fibroblast growth factor. Pathophysiol. Hear. Fail. 501–518.

Pammolli, F., Magazzini, L., and Riccaboni, M. (2011). The productivity crisis in pharmaceutical R&D. Nat. Rev. Drug Discov. *10*, 428–438.

Pan, J.A., Tang, Y., Yu, J.Y., Zhang, H., Zhang, J.F., Wang, C.Q., and Gu, J. (2019). miR-146a attenuates apoptosis and modulates autophagy by targeting TAF9b/P53 pathway in doxorubicin-induced cardiotoxicity. Cell Death Dis. *10*.

Paolini, L., Zendrini, A., Di Noto, G., Busatto, S., Lottini, E., Radeghieri, A., Dossi, A., Caneschi, A., Ricotta, D., and Bergese, P. (2016). Residual matrix from different separation techniques impacts exosome biological activity. Sci. Rep. *6*, 23550.

Papotti, M., Ghe, C., Cassoni, P., Catapano, F., Deghenghi, R., Ghigo, E., Muccioli, G., Demling, R.H., Surgery, R., Lee, S.W., et al. (2016). Cardioprotective effects of growth hormone-releasing hormone agonist after myocardial infarction. Proc. Natl. Acad. Sci. *107*, 2604–2609.

Paquin, J., Danalache, B.A., Jankowski, M., McCann, S.M., and Gutkowska, J. (2002). Oxytocin induces differentiation of P19 embryonic stem cells to cardiomyocytes. Proc. Natl. Acad. Sci. U. S. A. *99*, 9550–9555.

Parikh, S.S., Blackwell, D.J., Gomez-Hurtado, N., Frisk, M., Wang, L., Kim, K., Dahl, C.P., Fiane, A., Tønnessen, T., Kryshtal, D.O., et al. (2017). Thyroid and glucocorticoid hormones promote functional T-tubule development in human-induced pluripotent stem cell-derived cardiomyocytes. Circ. Res. *121*, 1323–1330.

Park, M.-J., Kim, D.-I., Choi, J.-H., Heo, Y.-R., and Park, S.-H. (2015). New role of irisin in hepatocytes: The protective effect of hepatic steatosis in vitro. Cell. Signal. *27*, 1831–1839.

Parsa, C.J., Matsumoto, A., Kim, J., Riel, R.U., Pascal, L.S., Walton, G.B., Thompson, R.B., Petrofski, J.A., Annex, B.H., Stamler, J.S., et al. (2003). A novel protective effect of erythropoietin in the infarcted heart. J. Clin. Invest. *112*, 999–1007.

Pasquale, E.B. (2008). Eph-Ephrin Bidirectional Signaling in Physiology and Disease. Cell *133*, 38–52.

Patel, A.K., Celiz, A.D., Rajamohan, D., Anderson, D.G., Langer, R., Davies, M.C., Alexander, M.R., and Denning, C. (2015). A defined synthetic substrate for serum-

free culture of human stem cell derived cardiomyocytes with improved functional maturity identified using combinatorial materials microarrays. Biomaterials *61*, 257–265.

Peacock, W.F., De Marco, T., Fonarow, G.C., Diercks, D., Wynne, J., Apple, F.S., Wu, A.H.B., and ADHERE Investigators (2008). Cardiac troponin and outcome in acute heart failure. N. Engl. J. Med. *358*, 2117–2126.

Pei, X.M., Yung, B.Y., Yip, S.P., Ying, M., Benzie, I.F., and Siu, P.M. (2014). Desacyl ghrelin prevents doxorubicin-induced myocardial fibrosis and apoptosis via the GHSR-independent pathway. Am. J. Physiol. - Endocrinol. Metab. *306*.

Pelekanos, R.A., Li, J., Gongora, M., Chandrakanthan, V., Scown, J., Suhaimi, N., Brooke, G., Christensen, M.E., Doan, T., Rice, A.M., et al. (2012). Comprehensive transcriptome and immunophenotype analysis of renal and cardiac MSC-like populations supports strong congruence with bone marrow MSC despite maintenance of distinct identities. Stem Cell Res. *8*, 58–73.

Penn, M.S., Mendelsohn, F.O., Schaer, G.L., Sherman, W., Farr, M., Pastore, J., Rouy, D., Clemens, R., Aras, R., and Losordo, D.W. (2013). An open-label dose escalation study to evaluate the safety of administration of nonviral stromal cell-derived factor-1 plasmid to treat symptomatic ischemic heart failure. Circ. Res. *112*, 816–825.

Pieper, A.A., Walles, T., Wei, G., Clements, E.E., Verma, A., Snyder, S.H., and Zweier, J.L. (2000). Myocardial postischemic injury is reduced by polyADPripose polymerase-1 gene disruption. Mol. Med. *6*, 271–282.

Pietro, R. Di, and Zauli, G. (2004). Emerging non-apoptotic functions of tumor necrosis factor-related apoptosis-inducing ligand (TRAIL)/Apo2L. J. Cell. Physiol. *201*, 331–340.

Pietronave, S., Forte, G., Locarno, D., Merlin, S., Zamperone, A., Nicotra, G., Isidoro, C., Nardo, P. Di, and Prat, M. (2010). Agonist monoclonal antibodies against HGF receptor protect cardiac muscle cells from apoptosis. Am. J. Physiol. - Hear. Circ. Physiol. *298*.

Pillai, J.B., Russell, H.M., Raman, J., Jeevanandam, V., and Gupta, M.P. (2005). Increased expression of poly(ADP-ribose) polymerase-1 contributes to caspase-independent myocyte cell death during heart failure. Am. J. Physiol. - Hear. Circ. Physiol. *288*.

Piot, C., Croisille, P., Staat, P., Thibault, H., Rioufol, G., Mewton, N., Elbelghiti, R.,

Cung, T.T., Bonnefoy, E., Angoulvant, D., et al. (2008). Effect of Cyclosporine on reperfusion injury in acute myocardial infarction. N. Engl. J. Med. *359*, 473–481.

Piper, H.M., Probst, I., Schwartz, P., Hütter, F.J., and Spieckermann, P.G. (1982). Culturing of calcium stable adult cardiac myocytes. J. Mol. Cell. Cardiol. *14*, 397–412.

Podewski, E.K., Hilfiker-Kleiner, D., Hilfiker, A., Morawietz, H., Lichtenberg, A., Wollert, K.C., and Drexler, H. (2003). Alterations in Janus kinase (JAK)-signal transducers and activators of transcription (STAT) signaling in patients with end-stage dilated cardiomyopathy. Circulation *107*, 798–802.

Pomerantz, B.J., Reznikov, L.L., Harken, A.H., and Dinarello, C.A. (2001). Inhibition of caspase 1 reduces human myocardial ischemic dysfunction via inhibition of IL-18 and IL-1β. Proc. Natl. Acad. Sci. U. S. A. *98*, 2871–2876.

Potts, P.R., Singh, S., Knezek, M., Thompson, C.B., and Deshmukh, M. (2003). Critical function of endogenous XIAP in regulating caspase activation during sympathetic neuronal apoptosis. J. Cell Biol. *163*, 789–799.

Prabhu, S.D. (2004). Cytokine-induced modulation of cardiac function. Circ. Res. *95*, 1140–1153.

Pratap, B., and Korniyenko, A. (2012). Toxic effects of marijuana on the cardiovascular system. Cardiovasc. Toxicol. *12*, 143–148.

Preda, M.B., Rønningen, T., Burlacu, A., Simionescu, M., Moskaug, J.Ø., and Valen, G. (2014). Remote transplantation of mesenchymal stem cells protects the heart against ischemia-reperfusion injury. Stem Cells *32*, 2123–2134.

Proost, P., Schutyser, E., Menten, P., Struyf, S., Wuyts, A., Opdenakker, G., Detheux, M., Parmentier, M., Durinx, C., Lambeir, A.M., et al. (2001). Amino-terminal truncation of CXCR3 agonists impairs receptor signaling and lymphocyte chemotaxis, while preserving antiangiogenic properties. Blood *98*, 3554–3561.

Prunier, F., Bière, L., Gilard, M., Boschat, J., Mouquet, F., Bauchart, J.-J., Charbonnier, B., Genée, O., Guérin, P., Warin-Fresse, K., et al. (2012). Single high-dose erythropoietin administration immediately after reperfusion in patients with ST-segment elevation myocardial infarction: results of the Erythropoietin in Myocardial Infarction Trial. Am. Heart J. *163*, 200-207.e1.

Pyo, J.O., Nah, J., Kim, H.J., Chang, J.W., Song, Y.W., Yang, D.K., Jo, D.G., Kim, H.R., Chae, H.J., Chae, S.W., et al. (2008). Protection of cardiomyocytes from

ischemic/hypoxic cell death via Drbp1 and pMe2 GlyDH in cardio-specific ARC transgenic mice. J. Biol. Chem. *283*, 30707–30714.

Qi, D., Hu, X., Wu, X., Merk, M., Leng, L., Bucala, R., and Young, L.H. (2009). Cardiac macrophage migration inhibitory factor inhibits JNK pathway activation and injury during ischemia/reperfusion. J. Clin. Invest. *119*, 3807–3816.

Qin, D., Wang, X., Li, Y., Yang, L., Wang, R., Peng, J., Mu, K.E.X., Peng, T., Han, Q., Yu, K.J., et al. (2016). MicroRNA-223-5p and -3p Cooperatively suppress necroptosis in ischemic/reperfused hearts. J. Biol. Chem. *291*, 20247–20259.

Qin, Y., Yu, Y., Dong, H., Bian, X., Guo, X., and Dong, S. (2012). MicroRNA 21 inhibits left ventricular remodeling in the early phase of rat model with ischemia-reperfusion injury by suppressing cell apoptosis. Int. J. Med. Sci. *9*, 413–423.

Radke, P.W., Heinl-Green, A., Frass, O.M., Griesenbach, U., Ferrari, S., Geddes, D.M., and Alton, E.W.F.W. (2004). Effects of intramyocardial pVEGF165 delivery on regional myocardial blood flow: Evidence for a spatial “delivery-efficacy” mismatch. Gene Ther. *11*, 1249–1255.

Rainer, P.P., Hao, S., Vanhoutte, D., Lee, D.I., Koitabashi, N., Molkentin, J.D., and Kass, D.A. (2014). Cardiomyocyte-specific transforming growth factor β suppression blocks neutrophil infiltration, augments multiple cytoprotective cascades, and reduces early mortality after myocardial infarction. Circ. Res. *114*, 1246–1257.

Rajesh, K.G., Sasaguri, S., Suzuki, R., and Maeda, H. (2003). Antioxidant MCI-186 inhibits mitochondrial permeability transition pore and upregulates Bcl-2 expression. Am. J. Physiol. - Hear. Circ. Physiol. *285*.

van Ramshorst, J., Bax, J.J., Beeres, S.L.M.A., Dibbets-Schneider, P., Roes, S.D., Stokkel, M.P.M., de Roos, A., Fibbe, W.E., Zwaginga, J.J., Boersma, E., et al. (2009). Intramyocardial bone marrow cell injection for chronic myocardial ischemia. JAMA *301*, 1997–2004.

Randhawa, P.K., and Jaggi, A.S. (2017). Investigating the involvement of glycogen synthase kinase-3β and gap junction signaling in TRPV1 and remote hind preconditioning-induced cardioprotection. Eur. J. Pharmacol. *814*, 9–17.

Ranganath, S.H., Levy, O., Inamdar, M.S., and Karp, J.M. (2012). Harnessing the mesenchymal stem cell secretome for the treatment of cardiovascular disease. Cell Stem Cell *10*, 244–258.

Ray, C.A., and Pickup, D.J. (1996). The mode of death of pig kidney cells infected

with cowpox virus is governed by the expression of thecrmAGene. Virology *217*, 384–391.

Del Re, D.P., Amgalan, D., Linkermann, A., Liu, Q., and Kitsis, R.N. (2019). Fundamental Mechanisms of Regulated Cell Death and Implications for Heart Disease. Physiol. Rev. *99*, 1765–1817.

Rebouças, J. de S., Santos-Magalhães, N.S., and Formiga, F.R. (2016). Cardiac regeneration using growth factors: Advances and challenges. Arq. Bras. Cardiol. *107*, 271–275.

Rees, M.G., Seashore-Ludlow, B., Cheah, J.H., Adams, D.J., Price, E. V., Gill, S., Javaid, S., Coletti, M.E., Jones, V.L., Bodycombe, N.E., et al. (2016). Correlating chemical sensitivity and basal gene expression reveals mechanism of action. Nat. Chem. Biol. *12*, 109–116.

Reimer, K.A., Jennings, R.B., and Tatum, A.H. (1983). Pathobiology of acute myocardial ischemia: Metabolic, functional and ultrastructural studies. Am. J. Cardiol. *52*, 72–81.

Reiss, K., Cheng, W., Ferber, A., Kajstura, J., Li, P., Li, B., Olivetti, G., Homcy, C.J., Baserga, R., Anversa, P., et al. (1996). Overexpression of insulin-like growth factor-1 in the heart is coupled with myocyte proliferation in transgenic mice. Proc. Natl. Acad. Sci. U. S. A. *93*, 8630–8635.

Reiss, K., Cheng, W., Pierzchalski, P., Kodali, S., Li, B., Wang, S., Liu, Y., and Anversa, P. (1997). Insulin-like growth factor-1 receptor and its ligand regulate the reentry of adult ventricular myocytes into the cell cycle. Exp. Cell Res. *235*, 198–209.

Reuters (2017). BRIEF-Capricor Therapeutics provides update on ALLSTAR trial - Reuters.

Ribeiro, M.C., Tertoolen, L.G., Guadix, J.A., Bellin, M., Kosmidis, G., D'Aniello, C., Monshouwer-Kloots, J., Goumans, M.-J., Wang, Y., Feinberg, A.W., et al. (2015). Functional maturation of human pluripotent stem cell derived cardiomyocytes in vitro – Correlation between contraction force and electrophysiology. Biomaterials *51*, 138–150.

Ricci, J.-E., Muñoz-Pinedo, C., Fitzgerald, P., Bailly-Maitre, B., Perkins, G.A., Yadava, N., Scheffler, I.E., Ellisman, M.H., and Green, D.R. (2004). Disruption of mitochondrial function during apoptosis is mediated by caspase cleavage of the p75 subunit of complex I of the electron transport chain. Cell *117*, 773–786.

Rimann, M., and Graf-Hausner, U. (2012). Synthetic 3D multicellular systems for drug development. Curr. Opin. Biotechnol. *23*, 803–809.

Ripa, R.S., Jørgensen, E., Wang, Y., Thune, J.J., Nilsson, J.C., Søndergaard, L., Johnsen, H.E., Køber, L., Grande, P., and Kastrup, J. (2006). Stem cell mobilization induced by subcutaneous granulocyte-colony stimulating factor to improve cardiac regeneration after acute ST-Elevation myocardial infarction. Circulation *113*, 1983–1992.

Riva, E., and Hearse, D.J. (1993). Age-dependent changes in myocardial susceptibility to ischemic injury. Cardioscience *4*, 85–92.

Robertson, C., Tran, D.D., and George, S.C. (2013). Concise review: maturation phases of human pluripotent stem cell-derived cardiomyocytes. Stem Cells *31*, 829–837.

Robinson, E.S., Khankin, E. V., Karumanchi, S.A., and Humphreys, B.D. (2010). Hypertension induced by vascular endothelial growth factor signaling pathway inhibition: mechanisms and potential use as a biomarker. Semin. Nephrol. *30*, 591–601.

Robinson, K.M., Janes, M.S., Pehar, M., Monette, J.S., Ross, M.F., Hagen, T.M., Murphy, M.P., and Beckman, J.S. (2006). Selective fluorescent imaging of superoxide in vivo using ethidium-based probes. Proc. Natl. Acad. Sci. *103*, 15038–15043.

Robinson, K.M., Janes, M.S., and Beckman, J.S. (2008). The selective detection of mitochondrial superoxide by live cell imaging. Nat. Protoc. *3*, 941–947.

Rodrigo, R., Prieto, J.C., and Castillo, R. (2013). Cardioprotection against ischaemia/reperfusion by vitamins C and E plus *n* −3 fatty acids: molecular mechanisms and potential clinical applications. Clin. Sci. *124*, 1–15.

Rodriguez, M.L., Graham, B.T., Pabon, L.M., Han, S.J., Murry, C.E., and Sniadecki, N.J. (2014). Measuring the contractile forces of human induced pluripotent stem cell-derived cardiomyocytes with arrays of microposts. J. Biomech. Eng. *136*.

Ronaldson-Bouchard, K., Ma, S.P., Yeager, K., Chen, T., Song, L.J., Sirabella, D., Morikawa, K., Teles, D., Yazawa, M., and Vunjak-Novakovic, G. (2018). Advanced maturation of human cardiac tissue grown from pluripotent stem cells. Nature *556*, 239–243.

Rosa, G.M., Gigli, L., Tagliasacchi, M.I., Di Iorio, C., Carbone, F., Nencioni, A.,

Montecucco, F., and Brunelli, C. (2016). Update on cardiotoxicity of anti-cancer treatments. Eur. J. Clin. Invest. *46*, 264–284.

Rose, E.A., Gelijns, A.C., Moskowitz, A.J., Heitjan, D.F., Stevenson, L.W., Dembitsky, W., Long, J.W., Ascheim, D.D., Tierney, A.R., Levitan, R.G., et al. (2001). Long-term use of a left ventricular assist device for end-stage heart failure. N. Engl. J. Med. *345*, 1435–1443.

Rosenkranz, S., Flesch, M., Amann, K., Haeuseler, C., Kilter, H., Seeland, U., Schlüter, K.D., and Böhm, M. (2002). Alterations of β-adrenergic signaling and cardiac hypertrophy in transgenic mice overexpressing TGF-β1. Am. J. Physiol. - Hear. Circ. Physiol. *283*.

Ross, J.J., Hong, Z., Willenbring, B., Zeng, L., Isenberg, B., Lee, E.H., Reyes, M., Keirstead, S.A., Weir, E.K., Tranquillo, R.T., et al. (2006). Cytokine-induced differentiation of multipotent adult progenitor cells into functional smooth muscle cells. J. Clin. Invest. *116*, 3139–3149.

Rossdeutsch, A., Smart, N., Dubé, K.N., Turner, M., and Riley, P.R. (2012). Essential role for thymosin β4 in regulating vascular smooth muscle cell development and vessel wall stability. Circ. Res. *111*, e89-102.

Rossi, A.E., and Dirksen, R.T. (2006). Sarcoplasmic reticulum: The dynamic calcium governor of muscle. Muscle Nerve *33*, 715–731.

Rossini, A., Frati, C., Lagrasta, C., Graiani, G., Scopece, A., Cavalli, S., Musso, E., Baccarin, M., Di Segni, M., Fagnoni, F., et al. (2011). Human cardiac and bone marrow stromal cells exhibit distinctive properties related to their origin. Cardiovasc. Res. *89*, 650–660.

Roth, G.A., Abate, D., Abate, K.H., Abay, S.M., Abbafati, C., Abbasi, N., Abbastabar, H., Abd-Allah, F., Abdela, J., Abdelalim, A., et al. (2018). Global, regional, and national age-sex-specific mortality for 282 causes of death in 195 countries and territories, 1980–2017: a systematic analysis for the Global Burden of Disease Study 2017. Lancet *392*, 1736–1788.

Rueden, C.T., Schindelin, J., Hiner, M.C., DeZonia, B.E., Walter, A.E., Arena, E.T., and Eliceiri, K.W. (2017). ImageJ2: ImageJ for the next generation of scientific image data. BMC Bioinformatics *18*, 529.

Ruifrok, W.-P.T., de Boer, R.A., Iwakura, A., Silver, M., Kusano, K., Tio, R.A., and Losordo, D.W. (2009). Estradiol-induced, endothelial progenitor cell-mediated neovascularization in male mice with hind-limb ischemia. Vasc. Med. *14*, 29–36.

Rupert, C.E., and Coulombe, K.L.K. (2015). The roles of neuregulin-1 in cardiac development, homeostasis, and disease. Biomark. Insights *2015*, 1–9.

Rupert, C.E., and Coulombe, K.L.K. (2017). IGF1 and NRG1 enhance proliferation, metabolic maturity, and the force-frequency response in hESC-derived engineered cardiac tissues. Stem Cells Int. *2017*, 7648409.

Russell, R.R., Li, J., Coven, D.L., Pypaert, M., Zechner, C., Palmeri, M., Giordano, F.J., Mu, J., Birnbaum, M.J., and Young, L.H. (2004). AMP-activated protein kinase mediates ischemic glucose uptake and prevents postischemic cardiac dysfunction, apoptosis, and injury. J. Clin. Invest. *114*, 495–503.

Russo, M., Guida, F., Paparo, L., Trinchese, G., Aitoro, R., Avagliano, C., Fiordelisi, A., Napolitano, F., Mercurio, V., Sala, V., et al. (2019). The novel butyrate derivative phenylalanine-butyramide protects from doxorubicin-induced cardiotoxicity. Eur. J. Heart Fail. *21*, 519–528.

Rustom, A., Saffrich, R., Markovic, I., Walther, P., and Gerdes, H.-H. (2004). Nanotubular highways for intercellular organelle transport. Science (80-. ). *303*, 1007–1010.

Sabbah, H.N., and Goldstein, S. (1993). Ventricular remodelling: consequences and therapy. Eur. Heart J. *14 Suppl C*, 24–29.

Sacks, C.A., Jarcho, J.A., and Curfman, G.D. (2014). Paradigm shifts in heart-failure therapy — A timeline. N. Engl. J. Med. *371*, 989–991.

Saeki, K., Yuo, A., Kato, M., Miyazono, K., Yazaki, Y., and Takaku, F. (1997). Cell density-dependent apoptosis in HL-60 cells, which is mediated by an unknown soluble factor, is inhibited by transforming growth factor β1 and overexpression of Bcl-2. J. Biol. Chem. *272*, 20003–20010.

Saelens, X., Festjens, N., Parthoens, E., Vanoverberghe, I., Kalai, M., van Kuppeveld, F., and Vandenabeele, P. (2005). Protein synthesis persists during necrotic cell death. J. Cell Biol. *168*, 545–551.

Sahin, E., Colla, S., Liesa, M., Moslehi, J., Müller, F.L., Guo, M., Cooper, M., Kotton, D., Fabian, A.J., Walkey, C., et al. (2011). Telomere dysfunction induces metabolic and mitochondrial compromise. Nature *470*, 359–365.

Saitoh, M., Nishitoh, H., Fujii, M., Takeda, K., Tobiume, K., Sawada, Y., Kawabata, M., Miyazono, K., and Ichijo, H. (1998). Mammalian thioredoxin is a direct inhibitor of apoptosis signal-regulating kinase (ASK) 1. EMBO J. *17*, 2596–2606.

Sakamoto, H., Parish, L.M., Hamamoto, H., Ryan, L.P., Eperjesi, T.J., Plappert, T.J., Jackson, B.M., St John-Sutton, M.G., Gorman, J.H., and Gorman, R.C. (2007). Effect of reperfusion on left ventricular regional remodeling strains after myocardial infarction. Ann. Thorac. Surg. *84*, 1528–1536.

Sakata, Y., Chancey, A.L., Divakaran, V.G., Sekiguchi, K., Sivasubramanian, N., and Mann, D.L. (2008). Transforming growth factor-β receptor antagonism attenuates myocardial fibrosis in mice with cardiac-restricted overexpression of tumor necrosis factor. Basic Res. Cardiol. *103*, 60–68.

Sala, L., Van Meer, B.J., Tertoolen, L.G.J., Bakkers, J., Bellin, M., Davis, R.P., Denning, C., Dieben, M.A.E., Eschenhagen, T., Giacomelli, E., et al. (2018). Musclemotion: A versatile open software tool to quantify cardiomyocyte and cardiac muscle contraction in vitro and in vivo. Circ. Res. *122*, e5–e16.

Saleh, M., and Ambrose, J.A. (2018). Understanding myocardial infarction. F1000Research *7*.

Salvador, J.M., Brown-Clay, J.D., and Fornace, A.J. (2013). Gadd45 in stress signaling, cell cycle control, and apoptosis. Adv. Exp. Med. Biol. *793*, 1–19.

Sandireddy, R., Cibi, D.M., Gupta, P., Singh, A., Tee, N., Uemura, A., Epstein, J.A., and Singh, M.K. (2019). Semaphorin 3E/PlexinD1 signaling is required for cardiac ventricular compaction. JCI Insight *4*.

Santos, C.X., Hafstad, A.D., Beretta, M., Zhang, M., Molenaar, C., Kopec, J., Fotinou, D., Murray, T. V, Cobb, A.M., Martin, D., et al. (2016). Targeted redox inhibition of protein phosphatase 1 by Nox4 regulates eIF 2α-mediated stress signaling . EMBO J. *35*, 319–334.

Saraste, Pulkki, Kallajoki, Heikkila, Laine, Mattila, Nieminen, Parvinen, and Voipio-Pulkki (1999). Cardiomyocyte apoptosis and progression of heart failure to transplantation. Eur. J. Clin. Invest. *29*, 380–386.

Saunders, J.W., Gasseling, M.T., and Saunders, L.C. (1962). Cellular death in morphogenesis of the avian wing. Dev. Biol. *5*, 147–178.

Saxena, A., Dobaczewski, M., Rai, V., Haque, Z., Chen, W., Li, N., and Frangogiannis, N.G. (2014). Regulatory T cells are recruited in the infarcted mouse myocardium and may modulate fibroblast phenotype and function. Am. J. Physiol. - Hear. Circ. Physiol. *307*, H1233–H1242.

Scarabelli, T., Stephanou, A., Rayment, N., Pasini, E., Comini, L., Curello, S.,

Ferrari, R., Knight, R., and Latchman, D. (2001). Apoptosis of endothelial cells precedes myocyte cell apoptosis in ischemia/reperfusion injury. Circulation *104*, 253–256.

Scatena, M., Almeida, M., Chaisson, M.L., Fausto, N., Nicosia, R.F., and Giachelli, C.M. (1998). NF-κB mediates αvβ3 integrin-induced endothelial cell survival. J. Cell Biol. *141*, 1083–1093.

Schächinger, V., Aicher, A., Döbert, N., Röver, R., Diener, J., Fichtlscherer, S., Assmus, B., Seeger, F.H., Menzel, C., Brenner, W., et al. (2008). Pilot trial on determinants of progenitor cell recruitment to the infarcted human myocardium. Circulation *118*, 1425–1432.

Schmid, K., Schönlebe, J., Drexler, H., and Mueck-Weymann, M. (2010). The effects of cannabis on heart rate variability and well-being in young men. Pharmacopsychiatry *43*, 147–150.

Schmidinger, M., Zielinski, C.C., Vogl, U.M., Bojic, A., Bojic, M., Schukro, C., Ruhsam, M., Hejna, M., and Schmidinger, H. (2008). Cardiac toxicity of sunitinib and sorafenib in patients with metastatic renal cell carcinoma. J. Clin. Oncol. *26*, 5204–5212.

Schröder, D., Heger, J., Piper, H.M., and Euler, G. (2006). Angiotensin II stimulates apoptosis via TGF-β1 signaling in ventricular cardiomyocytes of rat. J. Mol. Med. *84*, 975–983.

Schwartz, R.E., Reyes, M., Koodie, L., Jiang, Y., Blackstad, M., Lund, T., Lenvik, T., Johnson, S., Hu, W.-S., and Verfaillie, C.M. (2002). Multipotent adult progenitor cells from bone marrow differentiate into functional hepatocyte-like cells. J. Clin. Invest. *109*, 1291–1302.

Sdek, P., Zhao, P., Wang, Y., Huang, C.J., Ko, C.Y., Butler, P.C., Weiss, J.N., and MacLellan, W.R. (2011). Rb and p130 control cell cycle gene silencing to maintain the postmitotic phenotype in cardiac myocytes. J. Cell Biol. *194*, 407–423.

Secchiero, P., Zerbinati, C., Rimondi, E., Corallini, F., Milani, D., Grill, V., Forti, G., Capitani, S., and Zauli, G. (2004). TRAIL promotes the survival, migration and proliferation of vascular smooth muscle cells. Cell. Mol. Life Sci. *61*, 1965–1974.

Segraves, J.M., and Frishman, W.H. (2015). Highly sensitive cardiac troponin assays. Cardiol. Rev. *23*, 1.

Seo, Y.W., Shin, J.N., Ko, K.H., Cha, J.H., Park, J.Y., Lee, B.R., Yun, C.W., Kim,

Y.M., Seol, D.W., Kim, D.W., et al. (2003). The molecular mechanism of Noxa-induced mitochondrial dysfunction in p53-mediated cell death. J. Biol. Chem. *278*, 48292–48299.

Serrano-Puebla, A., and Boya, P. (2016). Lysosomal membrane permeabilization in cell death: new evidence and implications for health and disease. Ann. N. Y. Acad. Sci. *1371*, 30–44.

Severino, V., Alessio, N., Farina, A., Sandomenico, A., Cipollaro, M., Peluso, G., Galderisi, U., and Chambery, A. (2013). Insulin-like growth factor binding proteins 4 and 7 released by senescent cells promote premature senescence in mesenchymal stem cells. Cell Death Dis. *4*.

Shan, B., Pan, H., Najafov, A., and Yuan, J. (2018a). Necroptosis in development and diseases. Genes Dev. *32*, 327–340.

Shan, S., Liu, Z., Guo, T., Wang, M., Tian, S., Zhang, Y., Wang, K., Zheng, H., Zhao, X., Zuo, P., et al. (2018b). Growth arrest-specific gene 6 transfer promotes mesenchymal stem cell survival and cardiac repair under hypoxia and ischemia via enhanced autocrine signaling and paracrine action. Arch. Biochem. Biophys. *660*, 108–120.

Sharma, A., Burridge, P.W., McKeithan, W.L., Serrano, R., Shukla, P., Sayed, N., Churko, J.M., Kitani, T., Wu, H., Holmström, A., et al. (2017). High-throughput screening of tyrosine kinase inhibitor cardiotoxicity with human induced pluripotent stem cells. Sci. Transl. Med. *9*, eaaf2584.

Sharma, A., McKeithan, W.L., Serrano, R., Kitani, T., Burridge, P.W., del Álamo, J.C., Mercola, M., and Wu, J.C. (2018). Use of human induced pluripotent stem cell–derived cardiomyocytes to assess drug cardiotoxicity. Nat. Protoc. *13*, 3018–3041.

Sharma, S. V., Haber, D.A., and Settleman, J. (2010). Cell line-based platforms to evaluate the therapeutic efficacy of candidate anticancer agents. Nat. Rev. Cancer *10*, 241–253.

Shelke, G.V., Lässer, C., Gho, Y.S., and Lötvall, J. (2014). Importance of exosome depletion protocols to eliminate functional and RNA-containing extracellular vesicles from fetal bovine serum. J. Extracell. Vesicles *3*, 24783.

Shen, J., O'Brien, D., and Xu, Y. (2006). Matrix metalloproteinase-2 contributes to tumor necrosis factor alpha induced apoptosis in cultured rat cardiac myocytes. Biochem. Biophys. Res. Commun. *347*, 1011–1020.

Shen, J., Zhang, J.H., Xiao, H., Wu, J.M., He, K.M., Lv, Z.Z., Li, Z.J., Xu, M., and Zhang, Y.Y. (2018). Mitochondria are transported along microtubules in membrane nanotubes to rescue distressed cardiomyocytes from apoptosis article. Cell Death Dis. *9*.

Shen, L., Gao, Y., Qian, J., Sun, A., and Ge, J. (2011). A novel mechanism for endothelial progenitor cells homing: The SDF-1/CXCR4-Rac pathway may regulate endothelial progenitor cells homing through cellular polarization. Med. Hypotheses *76*, 256–258.

Sheppard, H.M., Corneillie, S.I., Espiritu, C., Gatti, A., and Liu, X. (1999). New insights into the mechanism of inhibition of p53 by simian virus 40 large T antigen. Mol. Cell. Biol. *19*, 2746–2753.

Shi, M., Zhu, J., Wang, R., Chen, X., Mi, L., Walz, T., and Springer, T.A. (2011). Latent TGF-β structure and activation. Nature *474*, 343–351.

Shiiya, T., Nakazato, M., Mizuta, M., Date, Y., Mondal, M.S., Tanaka, M., Nozoe, S.-I., Hosoda, H., Kangawa, K., and Matsukura, S. (2002). Plasma ghrelin levels in lean and obese humans and the effect of glucose on ghrelin secretion. J. Clin. Endocrinol. Metab. *87*, 240–244.

Shimizu, M., Tropak, M., Diaz, R.J., Suto, F., Surendra, H., Kuzmin, E., Li, J., Gross, G., Wilson, G.J., Callahan, J., et al. (2009). Transient limb ischaemia remotely preconditions through a humoral mechanism acting directly on the myocardium: evidence suggesting cross-species protection. Clin. Sci. (Lond). *117*, 191–200.

Shneyvays, V., Leshem, D., Shmist, Y., Zinman, T., and Shainberg, A. (2005). Effects of menadione and its derivative on cultured cardiomyocytes with mitochondrial disorders. J. Mol. Cell. Cardiol. *39*, 149–158.

Shoemaker, R.H. (2006). The NCI60 human tumour cell line anticancer drug screen. In Nature Reviews Cancer, pp. 813–823.

Silverberg, D.S., Wexler, D., Sheps, D., Blum, M., Keren, G., Baruch, R., Schwartz, D., Yachnin, T., Steinbruch, S., Shapira, I., et al. (2001). The effect of correction of mild anemia in severe, resistant congestive heart failure using subcutaneous erythropoietin and intravenous iron: A randomized controlled study. J. Am. Coll. Cardiol. *37*, 1775–1780.

Simons, M., Annex, B.H., Laham, R.J., Kleiman, N., Henry, T., Dauerman, H., Udelson, J.E., Gervino, E. V, Pike, M., Whitehouse, M.J., et al. (2002). Pharmacological treatment of coronary artery disease with recombinant fibroblast

growth factor-2: double-blind, randomized, controlled clinical trial. Circulation *105*, 788–793.

Singal, P.K., and Iliskovic, N. (1998). Doxorubicin-induced cardiomyopathy. N. Engl. J. Med. *339*, 900–905.

Singh, M., Dalal, S., and Singh, K. (2014). Osteopontin: At the cross-roads of myocyte survival and myocardial function. Life Sci. *118*, 1–6.

Sivasubramanian, N., Coker, M.L., Kurrelmeyer, K.M., MacLellan, W.R., DeMayo, F.J., Spinale, F.G., and Mann, D.L. (2001). Left ventricular remodeling in transgenic mice with cardiac restricted overexpression of tumor necrosis factor. Circulation *104*, 826–831.

Skrzypiec-Spring, M., Grotthus, B., Szelag, A., and Schulz, R. (2007). Isolated heart perfusion according to Langendorff-Still viable in the new millennium. J. Pharmacol. Toxicol. Methods *55*, 113–126.

Sluijter, J.P.G., Verhage, V., Deddens, J.C., van den Akker, F., and Doevendans, P.A. (2014). Microvesicles and exosomes for intracardiac communication. Cardiovasc. Res. *102*, 302–311.

Smart, N., Mojet, M.H., Latchman, D.S., Marber, M.S., Duchen, M.R., and Heads, R.J. (2006). IL-6 induces PI 3-kinase and nitric oxide-dependent protection and preserves mitochondrial function in cardiomyocytes. Cardiovasc. Res. *69*, 164–177.

Smart, N., Risebro, C.A., Melville, A.A.D., Moses, K., Schwartz, R.J., Chien, K.R., and Riley, P.R. (2007). Thymosin β4 induces adult epicardial progenitor mobilization and neovascularization. Nature *445*, 177–182.

Smart, N., Bollini, S., Dubé, K.N., Vieira, J.M., Zhou, B., Riegler, J., Price, A.N., Lythgoe, M.F., Davidson, S., Yellon, D., et al. (2012). Myocardial regeneration: Expanding the repertoire of thymosin β4 in the ischemic heart. Ann. N. Y. Acad. Sci. *1269*, 92–101.

Smilowitz, N.R., and Feit, F. (2016). The history of primary angioplasty and stenting for acute myocardialinfarction. Curr. Cardiol. Rep. *18*, 5.

Smith, C.C.T., Davidson, S.M., Lim, S.Y., Simpkin, J.C., Hothersall, J.S., and Yellon, D.M. (2007). Necrostatin: A potentially novel cardioprotective agent? Cardiovasc. Drugs Ther. *21*, 227–233.

Soldani, C., and Scovassi, A.I. (2002). Poly(ADP-ribose) polymerase-1 cleavage during apoptosis: An update. APOPTOSIS *7*, 321–328.

Song, C.L., Liu, B., Diao, H.Y., Shi, Y.F., Li, Y.X., Zhang, J.C., Lu, Y., Wang, G., Liu, J., Yu, Y.P., et al. (2014). The protective effect of microrna-320 on left ventricular remodeling after myocardial ischemia-reperfusion injury in the rat model. Int. J. Mol. Sci. *15*, 17442–17456.

Songbo, M., Lang, H., Xinyong, C., Bin, X., Ping, Z., and Liang, S. (2019). Oxidative stress injury in doxorubicin-induced cardiotoxicity. Toxicol. Lett. *307*, 41–48.

Soonpaa, M.H., Lafontant, P.J., Reuter, S., Scherschel, J.A., Srour, E.F., Zaruba, M.-M., Rubart-von der Lohe, M., and Field, L.J. (2018). Absence of cardiomyocyte differentiation following transplantation of adult cardiac-resident Sca-1+ cells into infarcted mouse hearts. Circulation *138*, 2963–2966.

Soria, J.C., Smit, E., Khayat, D., Besse, B., Yang, X., Hsu, C.P., Reese, D., Wiezorek, J., and Blackhall, F. (2010). Phase 1b study of dulanermin (recombinant human Apo2L/TRAIL) in combination with paclitaxel, carboplatin, and bevacizumab in patients with advanced non-squamous non-small-cell lung cancer. J. Clin. Oncol. *28*, 1527–1533.

Sosne, G., Qiu, P., Christopherson, P.L., and Wheater, M.K. (2007). Thymosin beta 4 suppression of corneal NFκB: A potential anti-inflammatory pathway. Exp. Eye Res. *84*, 663–669.

Spagnuolo, R., Recalcati, S., Tacchini, L., and Cairo, G. (2011). Role of hypoxia-inducible factors in the dexrazoxane-mediated protection of cardiomyocytes from doxorubicin-induced toxicity. Br. J. Pharmacol. *163*, 299–312.

Squillaro, T., Peluso, G., and Galderisi, U. (2016). Clinical trials with mesenchymal stem cells: An update. Cell Transplant. *25*, 829–848.

Srivastava, R.A., and Srivastava, N. (2000). High density lipoprotein, apolipoprotein A-I, and coronary artery disease. Mol. Cell. Biochem. *209*, 131–144.

Stack, J.P., Moslehi, J., Sayed, N., and Wu, J.C. (2019). Cancer therapy-induced cardiomyopathy: can human induced pluripotent stem cell modelling help prevent it? Eur. Heart J. *40*, 1764–1770.

Steinhelper, M.E., Lanson, N.A., Dresdner, K.P., Delcarpio, J.B., Wit, A.L., Claycomb, W.C., and Field, L.J. (1990). Proliferation in vivo and in culture of differentiated adult atrial cardiomyocytes from transgenic mice. Am. J. Physiol. -

Hear. Circ. Physiol. *259*.

Stewart, D.J., Kutryk, M.J.B., Fitchett, D., Freeman, M., Camack, N., Su, Y., Della Siega, A., Bilodeau, L., Burton, J.R., Proulx, G., et al. (2009). VEGF gene therapy fails to improve perfusion of ischemic myocardium in patients with advanced coronary disease: results of the NORTHERN trial. Mol. Ther. *17*, 1109–1115.

Strauer, B.E., Brehm, M., Zeus, T., Köstering, M., Hernandez, A., Sorg, R. V., Kögler, G., and Wernet, P. (2002). Repair of infarcted myocardium by autologous intracoronary mononuclear bone marrow cell transplantation in humans. Circulation *106*, 1913–1918.

Sugano, Y., Anzai, T., Yoshikawa, T., Maekawa, Y., Kohno, T., Mahara, K., Naito, K., and Ogawa, S. (2005). Granulocyte colony-stimulating factor attenuates early ventricular expansion after experimental myocardial infarction. Cardiovasc. Res. *65*, 446–456.

Sugishita, K., Kinugawa, K. ichiro, Shimizu, T., Harada, K., Matsui, H., Takahashi, T., Serizawa, T., and Kohmoto, O. (1999). Cellular basis for the acute inhibitory effects of IL-6 and TNF-α on excitation-contraction coupling. J. Mol. Cell. Cardiol. *31*, 1457–1467.

Sun, B., Sheng, Y., Huo, R., Hu, C.W., Lu, J., Li, S.L., Liu, X., Wang, Y.C., and Dong, D.L. (2013a). Bone morphogenetic protein-4 contributes to the down-regulation of Kv4.3 K+ channels in pathological cardiac hypertrophy. Biochem. Biophys. Res. Commun. *436*, 591–594.

Sun, B., Huo, R., Sheng, Y., Li, Y., Xie, X., Chen, C., Liu, H.-B., Li, N., Li, C.-B., Guo, W.-T., et al. (2013b). Bone morphogenetic protein-4 mediates cardiac hypertrophy, apoptosis, and fibrosis in experimentally pathological cardiac hypertrophy. Hypertens. (Dallas, Tex. 1979) *61*, 352–360.

Sun, J., Huang, S.H., Zhu, Y.C., Whiteman, M., Wang, M.J., Tan, B.K.-H., and Zhu, Y.Z. (2005). Anti-oxidative stress effects of Herba leonuri on ischemic rat hearts. Life Sci. *76*, 3043–3056.

Sun, X.-M., Butterworth, M., MacFarlane, M., Dubiel, W., Ciechanover, A., and Cohen, G.M. (2004). Caspase activation inhibits proteasome function during apoptosis. Mol. Cell *14*, 81–93.

Sundararaman, S., Miller, T., Pastore, J., Therapy, M.K.-G., and 2011, U. (2011). Plasmid-based transient human stromal cell-derived factor-1 gene transfer improves cardiac function in chronic heart failure. Nature.Com.

Sutherland, F.J., and Hearse, D.J. (2000). The isolated blood and perfusion fluid perfused heart the isolated heart as a model for the study of cardiovascular disease what are the advantages and disadvantages of the isolated perfused heart? Pharmacol. Res. *41*, 613–627.

Suzanne, M., and Steller, H. (2009). Letting go: Modification of cell adhesion during apoptosis. J. Biol. *8*.

Suzuki, Y., Imai, Y., Nakayama, H., Takahashi, K., Takio, K., and Takahashi, R. (2001). A serine protease, HtrA2, is released from the mitochondria and interacts with XIAP, inducing cell death. Mol. Cell *8*, 613–621.

Swain, S.M., Whaley, F.S., Gerber, M.C., Weisberg, S., York, M., Spicer, D., Jones, S.E., Wadler, S., Desai, A., Vogel, C., et al. (1997). Cardioprotection with dexrazoxane for doxorubicin-containing therapy in advanced breast cancer. J. Clin. Oncol. *15*, 1318–1332.

Syed, F.M., Hahn, H.S., Odley, A., Guo, Y., Vallejo, J.G., Lynch, R.A., Mann, D.L., Bolli, R., and Dorn, G.W. (2005). Proapoptotic effects of caspase-1/interleukin-converting enzyme dominate in myocardial ischemia. Circ. Res. *96*, 1103–1109.

Tachibana, A., Santoso, M.R., Mahmoudi, M., Shukla, P., Wang, L., Bennett, M., Goldstone, A.B., Wang, M., Fukushi, M., Ebert, A.D., et al. (2017). Paracrine effects of the pluripotent stem cell-derived cardiac myocytes salvage the injured myocardium. Circ. Res. *121*, e22–e36.

Taimeh, Z., Loughran, J., Birks, E.J., and Bolli, R. (2013). Vascular endothelial growth factor in heart failure. Nat. Rev. Cardiol. *10*, 519–530.

Takahashi, M. (2010). Role of the SDF-1/CXCR4 system in myocardial infarction. Circ. J. *74*, 418–423.

Takemura, G., Ohno, M., Hayakawa, Y., Misao, J., Kanoh, M., Ohno, A., Uno, Y., Minatoguchi, S., Fujiwara, T., and Fujiwara, H. (1998). Role of apoptosis in the disappearance of infiltrated and proliferated interstitial cells after myocardial infarction. Circ. Res. *82*, 1130–1138.

Talan, M.I., and Latini, R. (2013). Myocardial infarction: Cardioprotection by erythropoietin. Methods Mol. Biol. *982*, 265–302.

Tamzalit, F., Barbieux, I., Plet, A., Heim, J., Nedellec, S., Morisseau, S., Jacques, Y., and Mortier, E. (2014). IL-15.IL-15Rα complex shedding following trans-presentation is essential for the survival of IL-15 responding NK and T cells. Proc. Natl. Acad. Sci.

U. S. A. *111*, 8565–8570.

Tang, J., Shen, D., Caranasos, T.G., Wang, Z., Vandergriff, A.C., Allen, T.A., Hensley, M.T., Dinh, P.U., Cores, J., Li, T.S., et al. (2017a). Therapeutic microparticles functionalized with biomimetic cardiac stem cell membranes and secretome. Nat. Commun. *8*.

Tang, J., Li, Y., Huang, X., He, L., Zhang, L., Wang, H., Yu, W., Pu, W., Tian, X., Nie, Y., et al. (2018). Fate mapping of Sca1+ cardiac progenitor cells in the adult mouse heart. Circulation *138*, 2967–2969.

Tang, Y.T., Huang, Y.Y., Zheng, L., Qin, S.H., Xu, X.P., An, T.X., Xu, Y., Wu, Y.S., Hu, X.M., Ping, B.H., et al. (2017b). Comparison of isolation methods of exosomes and exosomal RNA from cell culture medium and serum. Int. J. Mol. Med. *40*, 834–844.

Tani, H., Sadahiro, T., and Ieda, M. (2018). Direct cardiac reprogramming: A novel approach for heart regeneration. Int. J. Mol. Sci. *19*.

Tarzami, S.T., Cheng, R., Miao, W., Kitsis, R.N., and Berman, J.W. (2002). Chemokine expression in myocardial ischemia: MIP-2 dependent MCP-1 expression protects cardiomyocytes from cell death. J. Mol. Cell. Cardiol. *34*, 209–221.

Tarzami, S.T., Calderon, T.M., Deguzman, A., Lopez, L., Kitsis, R.N., and Berman, J.W. (2005). MCP-1/CCL2 protects cardiac myocytes from hypoxia-induced apoptosis by a Gαi-independent pathway. Biochem. Biophys. Res. Commun. *335*, 1008–1016.

Terrovitis, J., Kwok, K.F., Lautamäki, R., Engles, J.M., Barth, A.S., Kizana, E., Miake, J., Leppo, M.K., Fox, J., Seidel, J., et al. (2008). Ectopic expression of the sodium-iodide symporter enables imaging of transplanted cardiac stem cells in vivo by single-photon emission computed tomography or positron emission tomography. J. Am. Coll. Cardiol. *52*, 1652–1660.

Théroux, P., Chaitman, B.R., Danchin, N., Erhardt, L., Meinertz, T., Schroeder, J.S., Tognoni, G., White, H.D., Willerson, J.T., and Jessel, A. (2000). Inhibition of the sodium-hydrogen exchanger with cariporide to prevent myocardial infarction in high-risk ischemic situations. Circulation *102*, 3032–3038.

Thibert, C., Teillet, M.A., Lapointe, F., Mazelin, L., Le Douarin, N.M., and Mehlen, P. (2003). Inhibition of neuroepithelial patched-induced apoptosis by Sonic hedgehog. Science (80-. ). *301*, 843–846.

Thor, H., Smith, M.T., Hartzell, P., Bellomo, G., Jewell, S.A., and Orrenius, S. (1982). The metabolism of menadione (2-methyl-1,4-naphthoquinone) by isolated hepatocytes. A study of the implications of oxidative stress in intact cells. J. Biol. Chem. *257*, 12419–12425.

Tiburcy, M., Hudson, J.E., Balfanz, P., Schlick, S., Meyer, T., Liao, M.L.C., Levent, E., Raad, F., Zeidler, S., Wingender, E., et al. (2017). Defined engineered human myocardium with advanced maturation for applications in heart failure modeling and repair. Circulation *135*, 1832–1847.

Tilokee, E.L., Latham, N., Jackson, R., Mayfield, A.E., Ye, B., Mount, S., Lam, B.-K., Suuronen, E.J., Ruel, M., Stewart, D.J., et al. (2016). Paracrine engineering of human explant-derived cardiac stem cells to over-express stromal-cell derived factor 1α enhances myocardial repair. Stem Cells *34*, 1826–1835.

Tio, R.A., Tkebuchava, T., Scheuermann, T.H., Lebherz, C., Magner, M., Kearny, M., Esakof, D.D., Isner, J.M., and Symes, J.F. (1999). Intramyocardial gene therapy with naked DNA encoding vascular endothelial growth factor improves collateral flow to ischemic myocardium. Hum. Gene Ther. *10*, 2953–2960.

Titmarsh, D.M., Glass, N.R., Mills, R.J., Hidalgo, A., Wolvetang, E.J., Porrello, E.R., Hudson, J.E., and Cooper-White, J.J. (2016). Induction of human iPSC-derived cardiomyocyte proliferation revealed by combinatorial screening in high density microbioreactor arrays. Sci. Rep. *6*.

Todorova, D., Simoncini, S., Lacroix, R., Sabatier, F., and Dignat-George, F. (2017). Extracellular vesicles in angiogenesis. Circ. Res. *120*, 1658–1673.

Toffoli, B., Bernardi, S., Candido, R., Zacchigna, S., Fabris, B., and Secchiero, P. (2012). TRAIL shows potential cardioprotective activity. Invest. New Drugs *30*, 1257–1260.

Toko, H., Takahashi, H., Kayama, Y., Okada, S., Minamino, T., Terasaki, F., Kitaura, Y., and Komuro, I. (2010). ATF6 is important under both pathological and physiological states in the heart. J. Mol. Cell. Cardiol. *49*, 113–120.

Tokudome, T., Otani, K., Miyazato, M., and Kangawa, K. (2019). Ghrelin and the heart. Peptides *111*, 42–46.

Toma, C., Letts, D.P., Tanabe, M., Gorcsan, J., and Counihan, P.J. (2007). Positive effect of darbepoetin on peri-infarction remodeling in a porcine model of myocardial ischemia-reperfusion. J. Mol. Cell. Cardiol. *43*, 130–136.

Torella, D., Rota, M., Nurzynska, D., Musso, E., Monsen, A., Shiraishi, I., Zias, E., Walsh, K., Rosenzweig, A., Sussman, M.A., et al. (2004). Cardiac stem cell and myocyte aging, heart failure, and insulin-like growth factor-1 overexpression. Circ. Res. *94*, 514–524.

Torralba, D., Baixauli, F., and Sánchez-Madrid, F. (2016). Mitochondria know no boundaries: Mechanisms and functions of intercellular mitochondrial transfer. Front. Cell Dev. Biol. *4*.

Toth, A., Kovacs, K., Deres, P., Halmosi, R., Czopf, L., Hanto, K., Kalai, T., Hideg, K., Sumegi, B., and Toth, K. (2003). Impact of a novel cardioprotective agent on the ischaemia-reperfusion- induced Akt kinase activation. Biochem. Pharmacol. *66*, 2263–2272.

Toth, A., Jeffers, J.R., Nickson, P., Min, J.-Y., Morgan, J.P., Zambetti, G.P., and Erhardt, P. (2006). Targeted deletion of Puma attenuates cardiomyocyte death and improves cardiac function during ischemia-reperfusion. Am. J. Physiol. Circ. Physiol. *291*, H52–H60.

Totzeck, M., Hendgen-Cotta, U.B., and Rassaf, T. (2017). Nitrite-nitric oxide signaling and cardioprotection. In Advances in Experimental Medicine and Biology, pp. 335–346.

Tramontano, A.F., Muniyappa, R., Black, A.D., Blendea, M.C., Cohen, I., Deng, L., Sowers, J.R., Cutaia, M. V, and El-Sherif, N. (2003). Erythropoietin protects cardiac myocytes from hypoxia-induced apoptosis through an Akt-dependent pathway. Biochem. Biophys. Res. Commun. *308*, 990–994.

Travis Hinson, J., Chopra, A., Lowe, A., Sheng, C.C., Gupta, R.M., Kuppusamy, R., O'sullivan, J., Rowe, G., Wakimoto, H., Gorham, J., et al. (2016). Integrative analysis of PRKAG2 cardiomyopathy iPS and microtissue models identifies AMPK as a regulator of metabolism, survival, and fibrosis. Cell Rep. *17*, 3292–3304.

Troncoso, R., Ibarra, C., Vicencio, J.M., Jaimovich, E., and Lavandero, S. (2014). New insights into IGF-1 signaling in the heart.

Tsibulnikov, S.Y., Maslov, L.N., Gorbunov, A.S., Voronkov, N.S., Boshchenko, A.A., Popov, S. V., Prokudina, E.S., Singh, N., and Downey, J.M. (2019). A review of humoral factors in remote preconditioning of the heart. J. Cardiovasc. Pharmacol. Ther. *24*, 403–421.

Twomey, J.D., Kim, S.R., Zhao, L., Bozza, W.P., and Zhang, B. (2015). Spatial dynamics of TRAIL death receptors in cancer cells. Drug Resist. Updat. *19*, 13–21.

Tzeng, W.-F., Chiou, T.-J., Wang, C.-P., Lee, J.-L., and Chen, Y.-H. (1994). Cellular thiols as a determinant of responsiveness to menadione in cardiomyocytes. J. Mol. Cell. Cardiol. *26*, 889–897.

Uchida, S., De Gaspari, P., Kostin, S., Jenniches, K., Kilic, A., Izumiya, Y., Shiojima, I., grosse Kreymborg, K., Renz, H., Walsh, K., et al. (2013). Sca1-derived cells are a source of myocardial renewal in the murine adult heart. Stem Cell Reports *1*, 397–410.

Uchinaka, A., Kawaguchi, N., Mori, S., Hamada, Y., Miyagawa, S., Saito, A., Sawa, Y., and Matsuura, N. (2014). Tissue inhibitor of metalloproteinase-1 and-3 improves cardiac function in an ischemic cardiomyopathy model rat. Tissue Eng. - Part A *20*, 3073–3084.

Ulmer, B.M., Stoehr, A., Schulze, M.L., Patel, S., Gucek, M., Mannhardt, I., Funcke, S., Murphy, E., Eschenhagen, T., and Hansen, A. (2018). Contractile work contributes to maturation of energy metabolism in hiPSC-derived cardiomyocytes. Stem Cell Reports *10*, 834–847.

Vadakke-Madathil, S., LaRocca, G., Raedschelders, K., Yoon, J., Parker, S.J., Tripodi, J., Najfeld, V., Van Eyk, J.E., and Chaudhry, H.W. (2019). Multipotent fetal-derived Cdx2 cells from placenta regenerate the heart. Proc. Natl. Acad. Sci. U. S. A. *116*, 11786–11795.

Vagnozzi, R.J., Hoffman, N.E., Elrod, J.W., Madesh, M., and Force, T. (2012). Protein kinase signaling at the crossroads of myocyte life and death in ischemic heart disease. Drug Discov. Today Ther. Strateg. *9*, e173–e182.

Valadi, H., Ekström, K., Bossios, A., Sjöstrand, M., Lee, J.J., and Lötvall, J.O. (2007). Exosome-mediated transfer of mRNAs and microRNAs is a novel mechanism of genetic exchange between cells. Nat. Cell Biol. *9*, 654–659.

Vandenabeele, P., Declercq, W., and Berghe, T. Vanden (2008). Necrotic cell death and ‘necrostatins’: now we can control cellular explosion. Trends Biochem. Sci. *33*, 352–355.

Vandesompele, J., De Preter, K., Pattyn, F., Poppe, B., Van Roy, N., De Paepe, A., and Speleman, F. (2002). Accurate normalization of real-time quantitative RT-PCR data by geometric averaging of multiple internal control genes. Genome Biol. *3*, research0034.1.

Varfolomeev, E.E., Schuchmann, M., Luria, V., Chiannilkulchai, N., Beckmann, J.S., Mett, I.L., Rebrikov, D., Brodianski, V.M., Kemper, O.C., Kollet, O., et al. (1998).

Targeted disruption of the mouse Caspase 8 gene ablates cell death induction by the TNF receptors, Fas/Apo1, and DR3 and is lethal prenatally. Immunity *9*, 267–276.

Vedam, K., Nishijima, Y., Druhan, L.J., Khan, M., Moldovan, N.I., Zweier, J.L., and Ilangovan, G. (2010). Role of heat shock factor-1 activation in the doxorubicin-induced heart failure in mice. Am. J. Physiol. - Hear. Circ. Physiol. *298*.

Velagaleti, R.S., Pencina, M.J., Murabito, J.M., Wang, T.J., Parikh, N.I., D'Agostino, R.B., Levy, D., Kannel, W.B., and Vasan, R.S. (2008). Long-Term Trends in the Incidence of Heart Failure After Myocardial Infarction. Circulation *118*, 2057–2062.

Venturini, M., Michelotti, A., Del Mastro, L., Gallo, L., Carnino, F., Garrone, O., Tibaldi, C., Molea, N., Bellina, R.C., Pronzato, P., et al. (1996). Multicenter randomized controlled clinical trial to evaluate cardioprotection of dexrazoxane versus no cardioprotection in women receiving epirubicin chemotherapy for advanced breast cancer. J. Clin. Oncol. *14*, 3112–3120.

Venugopal, R., and Jaiswal, A.K. (1996). Nrf1 and Nrf2 positively and c-Fos and Fra1 negatively regulate the human antioxidant response element-mediated expression of NAD(P)H:quinone oxidoreductase1 gene. Proc. Natl. Acad. Sci. U. S. A. *93*, 14960–14965.

Vercammen, D., Brouckaert, G., Denecker, G., Van de Craen, M., Declercq, W., Fiers, W., and Vandenabeele, P. (1998). Dual signaling of the Fas receptor: initiation of both apoptotic and necrotic cell death pathways. J. Exp. Med. *188*, 919–930.

Vicinanza, C., Aquila, I., Cianflone, E., Scalise, M., Marino, F., Mancuso, T., Fumagalli, F., Giovannone, E.D., Cristiano, F., Iaccino, E., et al. (2018). Kitcre knock-in mice fail to fate-map cardiac stem cells. Nature *555*, E1–E5.

Volders, P.G.A., Willems, I.E.M.G., Cleutjens, J.P.M., Aren, J.-W., Havenith, M.G., and Daemen, M.J.A.P. (1993). Interstitial collagen is increased in the non-infarcted human myocardium after myocardial infarction. J. Mol. Cell. Cardiol. *25*, 1317–1323.

Volpe, M., Tritto, C., Testa, U., Rao, M.A.E., Martucci, R., Mirante, A., Enea, I., Russo, R., Rubattu, S., Condorelli, G.L., et al. (1994). Blood levels of erythropoietin in congestive heart failure and correlation with clinical, hemodynamic, and hormonal profiles. Am. J. Cardiol. *74*, 468–473.

Vrtovec, B., Poglajen, G., Lezaic, L., Sever, M., Socan, A., Domanovic, D., Cernelc, P., Torre-Amione, G., Haddad, F., and Wu, J.C. (2013a). Comparison of transendocardial and intracoronary CD34+ cell transplantation in patients with nonischemic dilated cardiomyopathy. Circulation *128*, S42–S49.

Vrtovec, B., Poglajen, G., Lezaic, L., Sever, M., Domanovic, D., Cernelc, P., Socan, A., Schrepfer, S., Torre-Amione, G., Haddad, F., et al. (2013b). Effects of intracoronary CD34+ stem cell transplantation in nonischemic dilated cardiomyopathy patients: 5-year follow-up. Circ. Res. *112*, 165–173.

Wai, P.Y., and Kuo, P.C. (2008). Osteopontin: Regulation in tumor metastasis. Cancer Metastasis Rev. *27*, 103–118.

Wang, E.C.Y. (2012). On death receptor 3 and its ligands... Immunology *137*, 114–116.

Wang, G., McCain, M.L., Yang, L., He, A., Pasqualini, F.S., Agarwal, A., Yuan, H., Jiang, D., Zhang, D., Zangi, L., et al. (2014). Modeling the mitochondrial cardiomyopathy of Barth syndrome with induced pluripotent stem cell and heart-on-chip technologies. Nat. Med. *20*, 616–623.

Wang, H., Zhao, Y.T., Zhang, S., Dubielecka, P.M., Du, J., Yano, N., Chin, Y.E., Zhuang, S., Qin, G., and Zhao, T.C. (2017a). Irisin plays a pivotal role to protect the heart against ischemia and reperfusion injury. J. Cell. Physiol. *232*, 3775–3785.

Wang, H., Sheehan, R.P., Palmer, A.C., Everley, R.A., Boswell, S.A., Ron-Harel, N., Ringel, A.E., Holton, K.M., Jacobson, C.A., Erickson, A.R., et al. (2019). Adaptation of human iPSC-derived cardiomyocytes to tyrosine kinase inhibitors reduces acute cardiotoxicity via metabolic reprogramming. Cell Syst. *8*, 412-426.e7.

Wang, J., Wang, F., Zhu, J., Song, M., An, J., and Li, W. (2018a). Transcriptome profiling reveals PHLDA1 as a novel molecular marker for ischemic cardiomyopathy. J. Mol. Neurosci. *65*, 102–109.

Wang, J.X., Zhang, X.J., Li, Q., Wang, K., Wang, Y., Jiao, J.Q., Feng, C., Teng, S., Zhou, L.Y., Gong, Y., et al. (2015). MicroRNA-103/107 regulate programmed necrosis and myocardial ischemia/reperfusion injury through targeting FADD. Circ. Res. *117*, 352–363.

Wang, K., Zhao, X., Kuang, C., Qian, D., Wang, H., Jiang, H., Deng, M., and Huang, L. (2012). Overexpression of SDF-1α enhanced migration and engraftment of cardiac stem cells and reduced infarcted size via CXCR4/PI3K pathway. PLoS One *7*, e43922.

Wang, K., Liu, F., Liu, C.Y., An, T., Zhang, J., Zhou, L.Y., Wang, M., Dong, Y.H., Li, N., Gao, J.N., et al. (2016). The long noncoding RNA NRF regulates programmed necrosis and myocardial injury during ischemia and reperfusion by targeting miR-873. Cell Death Differ. *23*, 1394–1405.

Wang, L., Ma, W., Markovich, R., Chen, J., and Wang, P. (1998). Regulation of cardiomyocyte apoptotic signaling by insulin-like growth factor I. Am Hear. Assoc *83*, 516–522.

Wang, S., Ren, W., Liu, J., Lahat, G., Torres, K., Lopez, G., Lazar, A.J., Hayes-Jordan, A., Liu, K., Bankson, J., et al. (2010). TRAIL and doxorubicin combination induces proapoptotic and antiangiogenic effects in soft tissue sarcoma in vivo. Clin. Cancer Res. *16*, 2591–2604.

Wang, S., Gu, J., Xu, Z., Zhang, Z., Bai, T., Xu, J., Cai, J., Barnes, G., Liu, Q.-J., Freedman, J.H., et al. (2017b). Zinc rescues obesity-induced cardiac hypertrophy *via* stimulating metallothionein to suppress oxidative stress-activated BCL10/CARD9/p38 MAPK pathway. J. Cell. Mol. Med. *21*, 1182–1192.

Wang, Y., Ahmad, N., Wani, M.A., and Ashraf, M. (2004). Hepatocyte growth factor prevents ventricular remodeling and dysfunction in mice via Akt pathway and angiogenesis. J. Mol. Cell. Cardiol. *37*, 1041–1052.

Wang, Y.C., Neckelmann, N., Mayne, A., Herskowitz, A., Srinivasan, A., Sell, K.W., and Ahmed-Ansari, A. (1991). Establishment of a human fetal cardiac myocyte cell line. Vitr. Cell. Dev. Biol. - Anim. *27*, 63–74.

Wang, Z., Chen, K., Han, Y., Zhu, H., Zhou, X., Tan, T., Zeng, J., Zhang, J., Liu, Y., Li, Y., et al. (2018b). Irisin protects heart against ischemia-reperfusion injury through a SOD2-dependent mitochondria mechanism. J. Cardiovasc. Pharmacol. *72*, 259–269.

Ward, C.A., and Giles, W.R. (1997). Ionic mechanism of the effects of hydrogen peroxide in rat ventricular myocytes. J. Physiol. *500*, 631–642.

Wartz, I.E., O'Rourke, K.M., Zhou, H., Eby, M., Aravind, L., Seshagiri, S., Wu, P., Wiesmann, C., Baker, R., Boone, D.L., et al. (2004). De-ubiquitination and ubiquitin ligase domains of A20 downregulate NF-κB signalling. Nature *430*, 694–699.

Watanabe, T., Otsu, K., Takeda, T., Yamaguchi, O., Hikoso, S., Kashiwase, K., Higuchi, Y., Taniike, M., Nakai, A., Matsumura, Y., et al. (2005). Apoptosis signal-regulating kinase 1 is involved not only in apoptosis but also in non-apoptotic cardiomyocyte death. Biochem. Biophys. Res. Commun. *333*, 562–567.

Waters, R., Alam, P., Pacelli, S., Chakravarti, A.R., Ahmed, R.P.H., and Paul, A. (2018). Stem cell-inspired secretome-rich injectable hydrogel to repair injured cardiac tissue. Acta Biomater. *69*, 95–106.

Watkins, S.J., Borthwick, G.M., and Arthur, H.M. (2011). The H9C2 cell line and primary neonatal cardiomyocyte cells show similar hypertrophic responses in vitro. Vitr. Cell. Dev. Biol. - Anim. *47*, 125–131.

Webber, M.J., Han, X., Prasanna Murthy, S.N., Rajangam, K., Stupp, S.I., and Lomasney, J.W. (2010). Capturing the stem cell paracrine effect using heparin-presenting nanofibres to treat cardiovascular diseases. J. Tissue Eng. Regen. Med. *4*, 600–610.

Wei, K., Serpooshan, V., Hurtado, C., Diez-Cuñado, M., Zhao, M., Maruyama, S., Zhu, W., Fajardo, G., Noseda, M., Nakamura, K., et al. (2015). Epicardial FSTL1 reconstitution regenerates the adult mammalian heart. Nature *525*, 479–485.

Wei, X., Song, L., Jiang, L., Wang, G., Luo, X., Zhang, B., and Xiao, X. (2010). Overexpression of MIP2, a novel WD-repeat protein, promotes proliferation of H9c2 cells. Biochem. Biophys. Res. Commun. *393*, 860–863.

Weinlich, R., Oberst, A., Beere, H.M., and Green, D.R. (2017). Necroptosis in development, inflammation and disease. Nat. Rev. Mol. Cell Biol. *18*, 127–136.

Weirather, J., Hofmann, U.D.W., Beyersdorf, N., Ramos, G.C., Vogel, B., Frey, A., Ertl, G., Kerkau, T., and Frantz, S. (2014). Foxp3+ CD4+ T cells improve healing after myocardial infarction by modulating monocyte/macrophage differentiation. Circ. Res. *115*, 55–67.

Wen, J., Shen, J., Zhou, Y., Zhao, X., Dai, Z., and Jin, Y. (2020). Pyrroloquinoline quinone attenuates isoproterenol hydrochloride-induced cardiac hypertrophy in AC16 cells by inhibiting the NF-κB signaling pathway. Int. J. Mol. Med. *45*, 873–885.

Wencker, D., Chandra, M., Nguyen, K., Miao, W., Garantziotis, S., Factor, S.M., Shirani, J., Armstrong, R.C., and Kitsis, R.N. (2003). A mechanistic role for cardiac myocyte apoptosis in heart failure. J. Clin. Invest. *111*, 1497–1504.

Whelan, R.S., Konstantinidis, K., Wei, A.-C.C., Chen, Y., Reyna, D.E., Jha, S., Yang, Y., Calvert, J.W., Lindsten, T., Thompson, C.B., et al. (2012). Bax regulates primary necrosis through mitochondrial dynamics. PNAS *109*, 6566–6571.

White, A.J., Smith, R.R., Matsushita, S., Chakravarty, T., Czer, L.S.C., Burton, K., Schwarz, E.R., Davis, D.R., Wang, Q., Reinsmoen, N.L., et al. (2013). Intrinsic cardiac origin of human cardiosphere-derived cells. Eur. Heart J. *34*, 68–75.

White, S.M., Constantin, P.E., and Claycomb, W.C. (2004). Cardiac physiology at the cellular level: Use of cultured HL-1 cardiomyocytes for studies of cardiac muscle

cell structure and function. Am. J. Physiol. - Hear. Circ. Physiol. *286*.

Wiley, S.R., Cassiano, L., Lofton, T., Davis-Smith, T., Winkles, J.A., Lindner, V., Liu, H., Daniel, T.O., Smith, C.A., and Fanslow, W.C. (2001). A novel TNF receptor family member binds TWEAK and is implicated in angiogenesis. Immunity *15*, 837–846.

Wilkins, E., Wilson, L., Wickramasinghe, K., Bhatnagar, P., Leal, J., Luengo-Fernandez, R., Burns, R., Rayner, M., and Townsend, N. (2017). European Cardiovascular Disease Statistics 2017.

Williams, A.R., and Hare, J.M. (2011). Mesenchymal Stem Cells. Circ. Res. *109*, 923–940.

Winegrad, S., Henrion, D., Rappaport, L., and Samuel, J.L. (1999). Self-protection by cardiac myocytes against hypoxia and hyperoxia. Circ. Res. *85*, 690–698.

Wirbel, J., Cutillas, P., and Saez-Rodriguez, J. (2018). Phosphoproteomics-based profiling of kinase activities in cancer cells. In Methods in Molecular Biology, (Humana Press Inc.), pp. 103–132.

Wollert, K.C., Taga, T., Saito, M., Narazaki, M., Kishimoto, T., Glembotski, C.C., Vernallis, A.B., Heath, J.K., Pennica, D., Wood, W.I., et al. (1996). Cardiotrophin-1 activates a distinct form of cardiac muscle cell hypertrophy: Assembly of sarcomeric units in series via gp130/leukemia inhibitory factor receptor-dependent pathways. J. Biol. Chem. *271*, 9535–9545.

Wu, T.-W., Zeng, L.-H., Wu, J., and Fung, K.-P. (2002). Myocardial protection of MCI-186 in rabbit ischemia-reperfusion. Life Sci. *71*, 2249–2255.

Wu, X.X., Ogawa, O., and Kakehi, Y. (2004). Enhancement of arsenic trioxide-induced apoptosis in renal cell carcinoma cells by L-buthionine sulfoximine. Int. J. Oncol. *24*, 1489–1497.

Wu, Y., Bi, L., Bi, W., Li, Z., Zhao, M., Wang, C., Ju, J., and Peng, S. (2006). Novel 2-substituted nitronyl nitroxides as free radical scavengers: Synthesis, biological evaluation and structure-activity relationship. Bioorganic Med. Chem. *14*, 5711–5720.

Wünsch, M., Sharma, H.S., Markert, T., Bernotat-Danielowski, S., Schott, R.J., Kremer, P., Bleese, N., and Schaper, W. (1991). In situ localization of transforming growth factor β1 in porcine heart: Enhanced expression after chronic coronary artery constriction. J. Mol. Cell. Cardiol. *23*, 1051–1062.

Wysoczynski, M., Guo, Y., Moore, J.B., Muthusamy, S., Li, Q., Nasr, M., Li, H., Nong, Y., Wu, W., Tomlin, A.A., et al. (2017). Myocardial reparative properties of cardiac mesenchymal cells isolated on the basis of adherence. J. Am. Coll. Cardiol. *69*, 1824–1838.

Xiao-Xu, X.X., Liu, Y., Zhang, Y.F., Guan, Y.N., Jia, Q.Q., Wang, C., Liang, H., Li, Y.Q., Yang, H.T., Qin, Y.W., et al. (2017). Rapamycin and CHIR99021 coordinate robust cardiomyocyte differentiation from human pluripotent stem cells via reducing p53-dependent apoptosis. J. Am. Heart Assoc. *6*.

Xiao, J., Li, B., Zheng, Z., Wang, M., Peng, J., Li, Y., and Li, Z. (2012). Therapeutic effects of neuregulin-1 gene transduction in rats with myocardial infarction. Coron. Artery Dis. *23*, 460–468.

Xie, R.-Q., Cui, W., Hao, Y.-M., Liu, F., Li, B.-H., Wu, J.-F., Du, G.-Y., and Zhang, T. (2006). [Effects of remote preconditioning induced by skeletal muscle ischemia on myocardial cells apoptosis and roles of opioid receptors in pigs]. Zhongguo Ying Yong Sheng Li Xue Za Zhi *22*, 474–478.

Xing, Y., Yang, D., Lu, J., and Dong, D.L. (2015). Insulin prevents bone morphogenetic protein-4 induced cardiomyocyte apoptosis through activating Akt. Biochem. Biophys. Res. Commun. *456*, 605–609.

Xu, J., Kimball, T.R., Lorenz, J.N., Brown, D.A., Bauskin, A.R., Klevitsky, R., Hewett, T.E., Breit, S.N., and Molkentin, J.D. (2006). GDF15/MIC-1 functions as a protective and antihypertrophic factor released from the myocardium in association with SMAD protein activation. Circ. Res. *98*, 342–350.

Xu, X.H., Xu, J., Xue, L., Cao, H.L., Liu, X., and Chen, Y.J. (2011). VEGF attenuates development from cardiac hypertrophy to heart failure after aortic stenosis through mitochondrial mediated apoptosis and cardiomyocyte proliferation. J. Cardiothorac. Surg. *6*.

Yacoub, M. (2015). Cardiac donation after circulatory death: a time to reflect. Lancet (London, England) *385*, 2554–2556.

Yagi, H., Horinaka, S., and Matsuoka, H. (2005). Edaravone prevented deteriorated cardiac function after myocardial ischemia-reperfusion via inhibiting lipid peroxidation in rat. J. Cardiovasc. Pharmacol. *46*, 46–51.

Yakimchuk, K. (2015). Exosomes: isolation methods and specific markers. Mater. Methods *5*.

Yamaguchi, O., Higuchi, Y., Hirotani, S., Kashiwase, K., Nakayama, H., Hikoso, S., Takeda, T., Watanabe, T., Asahi, M., Taniike, M., et al. (2003). Targeted deletion of apoptosis signal-regulating kinase 1 attenuates left ventricular remodeling.

Yamaguchi, S., Shibata, R., Yamamoto, N., Nishikawa, M., Hibi, H., Tanigawa, T., Ueda, M., Murohara, T., and Yamamoto, A. (2015). Dental pulp-derived stem cell conditioned medium reduces cardiac injury following ischemia-reperfusion. Sci. Rep. *5*.

Yan, W., Guo, Y., Tao, L., Lau, W.B., Gan, L., Yan, Z., Guo, R., Gao, E., Wong, G.W., Koch, W.L., et al. (2017). C1q/Tumor necrosis factor-related protein-9 regulates the fate of implanted mesenchymal stem cells and mobilizes their protective effects against ischemic heart injury via multiple novel signaling pathways. Circulation *136*, 2162–2177.

Yang, X., Cohen, M. V, and Downey, J.M. (2010). Mechanism of cardioprotection by early ischemic preconditioning. Cardiovasc. Drugs Ther. *24*, 225–234.

Yang, X., Pabon, L., and Murry, C.E. (2014). Engineering adolescence: Maturation of human pluripotent stem cell-derived cardiomyocytes. Circ. Res. *114*, 511–523.

Yang, X., Qin, Y., Shao, S., Yu, Y., Zhang, C., Dong, H., Lv, G., and Dong, S. (2016). MicroRNA-214 inhibits left ventricular remodeling in an acute myocardial infarction rat model by suppressing cellular apoptosis via the phosphatase and tensin homolog (PTEN). Int. Heart J. *57*, 247–250.

Yang, Z., Zingarelli, B., and Szabó, C. (2000a). Effect of genetic disruption of poly (ADP-ribose) synthetase on delayed production of inflammatory mediators and delayed necrosis during myocardial ischemia-reperfusion injury. Shock *13*, 60–66.

Yang, Z., Zingarelli, B., and Szabó, C. (2000b). Effect of genetic disruption of poly(ADP-ribose) synthetase on delayed production of inflammatory mediators and delayed necrosis during mycardial ischemia-reperfusion injury. Shock *13*, 60–66.

Yasukawa, H., Hoshijima, M., Gu, Y., Nakamura, T., Pradervand, S., Hanada, T., Hanakawa, Y., Yoshimura, A., Ross, J., and Chien, K.R. (2001). Suppressor of cytokine signaling-3 is a biomechanical stress-inducible gene that suppresses gp130-mediated cardiac myocyte hypertrophy and survival pathways. J. Clin. Invest. *108*, 1459–1467.

Ye, L., Chang, Y.H., Xiong, Q., Zhang, P., Zhang, L., Somasundaram, P., Lepley, M., Swingen, C., Su, L., Wendel, J.S., et al. (2014). Cardiac repair in a porcine model of acute myocardial infarction with human induced pluripotent stem cell-derived

cardiovascular cells. Cell Stem Cell *15*, 750–761.

Yeghiazarians, Y., Honbo, N., Imhof, I., Woods, B., Aguilera, V., Ye, J., Boyle, A.J., and Karliner, J.S. (2014). IL-15: A novel prosurvival signaling pathway in cardiomyocytes. J. Cardiovasc. Pharmacol. *63*, 406–411.

Yeh, E.T.H., and Chang, H.-M. (2016). Oncocardiology—past, present, and future. JAMA Cardiol. *1*, 1066.

Yeh, W.C., De La Pompa, J.L., McCurrach, M.E., Shu, H.B., Elia, A.J., Shahinian, A., Ng, M., Wakeham, A., Khoo, W., Mitchell, K., et al. (1998). FADD: Essential for embryo development and signaling from some, but not all, inducers of apoptosis. Science (80-. ). *279*, 1954–1958.

Yeh, W.C., Itie, A., Elia, A.J., Ng, M., Shu, H.B., Wakeham, A., Mirtsos, C., Suzuki, N., Bonnard, M., Goeddel, D. V., et al. (2000). Requirement for Casper (c-FLIP) in regulation of death receptor-induced apoptosis and embryonic development. Immunity *12*, 633–642.

Ylä-Herttuala, S., and Baker, A.H. (2017). Cardiovascular Gene Therapy: Past, Present, and Future. Mol. Ther. *25*, 1095–1106.

Yokote, H., Fujita, K., Jing, X., Sawada, T., Liang, S., Yao, L., Yan, X., Zhang, Y., Schlessinger, J., and Sakaguchi, K. (2005). Trans-activation of EphA4 and FGF receptors mediated by direct interactions between their cytoplasmic domains. Proc. Natl. Acad. Sci. U. S. A. *102*, 18866–18871.

Yoon, C.S., Kim, H.K., Mishchenko, N.P., Vasileva, E.A., Fedoreyev, S.A., Stonik, V.A., and Han, J. (2019). Spinochrome D attenuates doxorubicin-induced cardiomyocyte death via improving glutathione metabolism and attenuating oxidative stress. Mar. Drugs *17*.

Yoshida, S., Miyagawa, S., Fukushima, S., Kawamura, T., Kashiyama, N., Ohashi, F., Toyofuku, T., Toda, K., and Sawa, Y. (2018). Maturation of human induced pluripotent stem cell-derived cardiomyocytes by soluble factors from human mesenchymal stem cells. Mol. Ther. *26*, 2681–2695.

Yoshihara, H.A.I., Bastiaansen, J.A.M., Berthonneche, C., Comment, A., and Schwitter, J. (2015). An intact small animal model of myocardial ischemia-reperfusion: Characterization of metabolic changes by hyperpolarized13C MR spectroscopy. Am. J. Physiol. - Hear. Circ. Physiol. *309*, H2058–H2066.

Yousefi, K., Irion, C.I., Takeuchi, L.M., Ding, W., Lambert, G., Eisenberg, T., Sukkar,

S., Granzier, H.L., Methawasin, M., Lee, D.I., et al. (2019). Osteopontin promotes left ventricular diastolic dysfunction through a mitochondrial pathway. J. Am. Coll. Cardiol. *73*, 2705–2718.

Yu, L., and Feng, Z. (2018). The role of toll-like receptor signaling in the progression of heart failure. Mediators Inflamm. *2018*.

Yu, H., Guo, P., Xie, X., Wang, Y., and Chen, G. (2017). Ferroptosis, a new form of cell death, and its relationships with tumourous diseases. J. Cell. Mol. Med. *21*, 648–657.

Yu, J., Vodyanik, M.A., Smuga-Otto, K., Antosiewicz-Bourget, J., Frane, J.L., Tian, S., Nie, J., Jonsdottir, G.A., Ruotti, V., Stewart, R., et al. (2007). Induced pluripotent stem cell lines derived from human somatic cells. Science (80-. ). *318*, 1917–1920.

Yu, J.L., Jin, Y., Cao, X.Y., and Gu, H.H. (2020). Dexmedetomidine alleviates doxorubicin cardiotoxicity by inhibiting mitochondrial reactive oxygen species generation. Hum. Cell *33*, 47–56.

Yu, S.W., Wang, H., Poitras, M.F., Coombs, C., Bowers, W.J., Federoff, H.J., Poirier, G.G., Dawson, T.M., and Dawson, V.L. (2002). Mediation of poty(ADP-ribose) polymerase-1 - Dependent cell death by apoptosis-inducing factor. Science (80-. ). *297*, 259–263.

Yu, X.W., Kennedy, R.H., and Liu, S.J. (2003). JAK2/STAT3, not ERK1/2, mediates interleukin-6-induced activation of inducible nitric-oxide synthase and decrease in contractility of adult ventricular myocytes. J. Biol. Chem. *278*, 16304–16309.

Yu, Y., Xie, Y., Cao, L., Yang, L., Yang, M., Lotze, M.T., Zeh, H.J., Kang, R., and Tang, D. (2015). The ferroptosis inducer erastin enhances sensitivity of acute myeloid leukemia cells to chemotherapeutic agents. Mol. Cell. Oncol. *2*.

Yuan, J., and Horvitz, H.R. (1990). The Caenorhabditis elegans genes ced-3 and ced-4 act cell autonomously to cause programmed cell death. Dev. Biol. *138*, 33–41.

Yuan, J., Shaham, S., Ledoux, S., Ellis, H.M., and Horvitz, H.R. (1993). The C. elegans cell death gene ced-3 encodes a protein similar to mammalian interleukin-1β-converting enzyme. Cell *75*, 641–652.

Yuan, J., Lipinski, M., and Degterev, A. (2003). Diversity in the mechanisms of neuronal cell death. Neuron *40*, 401–413.

Yuan, Y., Tao, Y., Deng, Y., Ye, Q., Lin, B., and Wu, L. (2019). BMP4 Induces Cardiomyocyte Hypertrophy Through the Activation of ERK 1/2 Signaling Pathway in H9c2 Cells. Brazilian Arch. Biol. Technol. *62*.

Yue, Y., Krenz, M., Cohen, M. V., Downey, J.M., and Critz, S.D. (2001). Menadione mimics the infarct-limiting effect of preconditioning in isolated rat hearts. Am. J. Physiol. Circ. Physiol. *281*, H590–H595.

Yumoto, K., Ishijima, M., Rittling, S.R., Tsuji, K., Tsuchiya, Y., Kon, S., Nifuji, A., Uede, T., Denhardt, D.T., and Noda, M. (2002). Osteopontin deficiency protects joints against destruction in anti-type II collagen antibody-induced arthritis in mice. Proc. Natl. Acad. Sci. U. S. A. *99*, 4556–4561.

Yussman, M.G., Toyokawa, T., Odley, A., Lynch, R.A., Wu, G., Colbert, M.C., Aronow, B.J., Lorenz, J.N., and Dorn, G.W. (2002). Mitochondrial death protein Nix is induced in cardiac hypertrophy and triggers apoptotic cardiomyopathy. Nat. Med. *8*, 725–730.

Zafiriou, M.P., Noack, C., Unsöld, B., Didie, M., Pavlova, E., Fischer, H.J., Reichardt, H.M., Bergmann, M.W., El-Armouche, A., Zimmermann, W.-H., et al. (2014). Erythropoietin responsive cardiomyogenic cells contribute to heart repair post myocardial infarction. Stem Cells *32*, 2480–2491.

Zangi, L., Lui, K.O., Von Gise, A., Ma, Q., Ebina, W., Ptaszek, L.M., Später, D., Xu, H., Tabebordbar, M., Gorbatov, R., et al. (2013). Modified mRNA directs the fate of heart progenitor cells and induces vascular regeneration after myocardial infarction. Nat. Biotechnol. *31*, 898–907.

Zaruba, M.M., and Franz, W.M. (2010). Role of the SDF-1-CXCR4 axis in stem cell-based therapies for ischemic cardiomyopathy. Expert Opin. Biol. Ther. *10*, 321–335.

Zhan, Y., Brown, C., Maynard, E., Anshelevich, A., Ni, W., Ho, I.C., and Oettgen, P. (2005). Ets-1 is a critical regulator of Ang II-mediated vascular inflammation and remodeling. J. Clin. Invest. *115*, 2508–2516.

Zhang, K., and Kaufman, R.J. (2006). The unfolded protein response: A stress signaling pathway critical for health and disease. Neurology *66*, S102–S109.

Zhang, J., Wilson, G.F., Soerens, A.G., Koonce, C.H., Yu, J., Palecek, S.P., Thomson, J.A., and Kamp, T.J. (2009). Functional cardiomyocytes derived from human induced pluripotent stem cells. Circ. Res. *104*, e30-41.

Zhang, L., Sultana, N., Yan, J., Yang, F., Chen, F., Chepurko, E., Yang, F.-C., Du,

Q., Zangi, L., Xu, M., et al. (2018). Cardiac Sca-1+ cells are not intrinsic stem cells for myocardial development, renewal, and repair. Circulation *138*, 2919–2930.

Zhang, S., Liu, X., Bawa-Khalfe, T., Lu, L.-S.S., Lyu, Y.L., Liu, L.F., and Yeh, E.T.H.H. (2012). Identification of the molecular basis of doxorubicin-induced cardiotoxicity. Nat. Med. *18*, 1639–1642.

Zhang, T., Zhang, Y., Cui, M., Jin, L., Wang, Y., Lv, F., Liu, Y., Zheng, W., Shang, H., Zhang, J., et al. (2016a). CaMKII is a RIP3 substrate mediating ischemia- and oxidative stress–induced myocardial necroptosis. Nat. Med. *22*, 175–182.

Zhang, T., Zhang, Y., Cui, M., Jin, L., Wang, Y., Lv, F., Liu, Y., Zheng, W., Shang, H., Zhang, J., et al. (2016b). CaMKII is a RIP3 substrate mediating ischemia- and oxidative stress–induced myocardial necroptosis. Nat. Med. *22*, 175–182.

Zhang, Y., Sivakumaran, P., Newcomb, A.E., Hernandez, D., Harris, N., Khanabdali, R., Liu, G.-S., Kelly, D.J., Pébay, A., Hewitt, A.W., et al. (2015a). Cardiac repair with a novel population of mesenchymal stem cells resident in the human heart. Stem Cells *33*, 3100–3113.

Zhang, Y., Liang, X., Liao, S., Wang, W., Wang, J., Li, X., Ding, Y., Liang, Y., Gao, F., Yang, M., et al. (2015b). Potent paracrine effects of human induced pluripotent stem cell-derived mesenchymal stem cells attenuate Doxorubicin-induced cardiomyopathy. Sci. Rep. *5*, 11235.

Zhao, L., and Zhang, B. (2017). Doxorubicin induces cardiotoxicity through upregulation of death receptors mediated apoptosis in cardiomyocytes. Sci. Rep. *7*, 44735.

Zhao, H., Zhang, X., Zheng, Y., Li, Y., Wang, X., Hu, N., Zhou, P., and Wang, K. (2018). Propofol protects rat cardiomyocytes from Anthracycline-Induced apoptosis by regulating MicroRNA-181a in vitro and in vivo. Oxid. Med. Cell. Longev. *2018*.

Zhao, Y., Sun, X., Cao, W., Ma, J., Sun, L., Qian, H., Zhu, W., and Xu, W. (2015). Exosomes derived from human umbilical cord mesenchymal stem cells relieve acute myocardial ischemic injury. Stem Cells Int. *2015*, 761643.

Zhao, Y., Rafatian, N., Feric, N.T., Cox, B.J., Aschar-Sobbi, R., Wang, E.Y., Aggarwal, P., Zhang, B., Conant, G., Ronaldson-Bouchard, K., et al. (2019). A Platform for Generation of Chamber-Specific Cardiac Tissues and Disease Modeling. Cell *176*, 913-927.e18.

Zhao, Y.Y., Sawyer, D.R., Baliga, R.R., Opel, D.J., Han, X., Marchionni, M.A., and

Kelly, R.A. (1998). Neuregulins promote survival and growth of cardiac myocytes: Persistence of ErbB2 and ErbB4 expression in neonatal and adult ventricular myocytes. J. Biol. Chem. *273*, 10261–10269.

Zheng, S.-X., Weng, Y.-L., Zhou, C.-Q., Wen, Z.-Z., Huang, H., Wu, W., Wang, J.-F., and Wang, T. (2013). Comparison of cardiac stem cells and mesenchymal stem cells transplantation on the cardiac electrophysiology in rats with myocardial infarction. Stem Cell Rev. Reports *9*, 339–349.

Zhong, J., and Rajagopalan, S. (2015). Dipeptidyl peptidase-4 regulation of SDF-1/CXCR4 axis: Implications for cardiovascular disease. Front. Immunol. *6*.

Zhou, B., Honor, L.B., He, H., Qing, M., Oh, J.H., Butterfield, C., Lin, R.Z., Melero-Martin, J.M., Dolmatova, E., Duffy, H.S., et al. (2011). Adult mouse epicardium modulates myocardial injury by secreting paracrine factors. J. Clin. Invest. *121*, 1894–1904.

Zhou, H.Z., Swanson, R.A., Simonis, U., Ma, X., Cecchini, G., and Gray, M.O. (2006a). Poly(ADP-ribose) polymerase-1 hyperactivation and impairment of mitochondrial respiratory chain complex I function in reperfused mouse hearts. Am. J. Physiol. - Hear. Circ. Physiol. *291*.

Zhou, L., Azfer, A., Niu, J., Graham, S., Choudhury, M., Adamski, F.M., Younce, C., Binkley, P.F., and Kolattukudy, P.E. (2006b). Monocyte chemoattractant protein-1 induces a novel transcription factor that causes cardiac myocyte apoptosis and ventricular dysfunction. Circ. Res. *98*, 1177–1185.

Zhou, S.S., Jin, J.P., Wang, J.Q., Zhang, Z.G., Freedman, J.H., Zheng, Y., and Cai, L. (2018a). MiRNAS in cardiovascular diseases: Potential biomarkers, therapeutic targets and challenges review-article. Acta Pharmacol. Sin. *39*, 1073–1084.

Zhou, Z., Zhang, Y., Lin, L., and Zhou, J. (2018b). Apigenin suppresses the apoptosis of H9C2 rat cardiomyocytes subjected to myocardial ischemia-reperfusion injury via upregulation of the PI3K/Akt pathway. Mol. Med. Rep. *18*, 1560–1570.

Zhu, D., Wang, H., Zhang, J., Zhang, X., Xin, C., Zhang, F., Lee, Y., Zhang, L., Lian, K., Yan, W., et al. (2015). Irisin improves endothelial function in type 2 diabetes through reducing oxidative/nitrative stresses. J. Mol. Cell. Cardiol. *87*, 138–147.

Zhu, H., Tannous, P., Johnstone, J.L., Kong, Y., Shelton, J.M., Richardson, J.A., Le, V., Levine, B., Rothermel, B.A., and Hill, J.A. (2007). Cardiac autophagy is a maladaptive response to hemodynamic stress. J. Clin. Invest. *117*, 1782–1793.

Zhu, J., Song, J., Yu, L., Zheng, H., Zhou, B., Weng, S., and Fu, G. (2016). Safety and efficacy of autologous thymosin β4 pre-treated endothelial progenitor cell transplantation in patients with acute ST segment elevation myocardial infarction: A pilot study. Cytotherapy *18*, 1037–1042.

Zhu, K., Wu, Q., Ni, C., Zhang, P., Zhong, Z., Wu, Y., Wang, Y., Xu, Y., Kong, M., Cheng, H., et al. (2018). Lack of remuscularization following transplantation of human embryonic stem cell-derived cardiovascular progenitor cells in infarcted nonhuman primates. Circ. Res. *122*, 958–969.

Zielonka, J., Vasquez-Vivar, J., and Kalyanaraman, B. (2008). Detection of 2-hydroxyethidium in cellular systems: a unique marker product of superoxide and hydroethidine. Nat. Protoc. *3*, 8–21.

Zingarelli, B., Cuzzocrea, S., Zsengellér, Z., Salzman, A.L., and Szabó, C. (1997). Protection against myocardial ischemia and reperfusion injury by 3-aminobenzamide, an inhibitor of poly (ADP-ribose) synthetase. Cardiovasc. Res. *36*, 205–215.

Zohar, R., Zhu, B., Liu, P., Sodek, J., and McCulloch, C.A. (2004). Increased cell death in osteopontin-deficient cardiac fibroblasts occurs by a caspase-3-independent pathway. Am. J. Physiol. - Hear. Circ. Physiol. *287*, H1730-9.

Zohlnhöfer, D., Ott, I., Mehilli, J., Schömig, K., Michalk, F., Ibrahim, T., Meisetschläger, G., Von Wedel, J., Bollwein, H., Seyfarth, M., et al. (2006). Stem cell mobilization by granulocyte colony-stimulating factor in patients with acute myocardial infarction: A randomized controlled trial. J. Am. Med. Assoc. *295*, 1003–1010.

Zou, H., Henzel, W.J., Liu, X., Lutschg, A., and Wang, X. (1997). Apaf-1, a human protein homologous to C. elegans CED-4, participates in cytochrome c–dependent activation of Caspase-3. Cell *90*, 405–413.

Zou, Y., Takano, H., Mizukami, M., Akazawa, H., Qin, Y., Toko, H., Sakamoto, M., Minamino, T., Nagai, T., and Komuro, I. (2003). Leukemia inhibitory factor enhances survival of cardiomyocytes and induces regeneration of myocardium after myocardial infarction. Circulation *108*, 748–753.

Zuppinger, C. (2019). 3D cardiac cell culture: A critical review of current technologies and applications. Front. Cardiovasc. Med. *6*.

# Supplementary Material

**Supplement 6.1.** Top 50 Gene Ontologies for Biological Processes associated to each combination of samples as denoted per table, obtained using the ToppFun function in ToppGene Suite. Genes used to generate the GOs were filtered using a threshold of $\log_2$ fold change > 2 and p-value < 0.05.

| Upregulated in IMR90-CMs by menadione treatment<br>TOP 50 GO FOR BIOLOGICAL PROCESSES | | | |
|---|---|---|---|
| **ID** | Name | q-value FDR B&H | Hit Count in Query List |
| **GO:0042127** | regulation of cell population proliferation | 9.91E-20 | 166 |
| **GO:0034097** | response to cytokine | 9.66E-19 | 126 |
| **GO:0051241** | negative regulation of multicellular organismal process | 3.95E-18 | 137 |
| **GO:0071345** | cellular response to cytokine stimulus | 3.95E-18 | 118 |
| **GO:0001775** | cell activation | 3.10E-17 | 138 |
| **GO:0050865** | regulation of cell activation | 6.82E-15 | 79 |
| **GO:0016477** | cell migration | 7.73E-15 | 143 |
| **GO:0001816** | cytokine production | 2.18E-14 | 90 |
| **GO:0010941** | regulation of cell death | 2.25E-14 | 153 |
| **GO:0001817** | regulation of cytokine production | 2.88E-14 | 84 |
| **GO:0043067** | regulation of programmed cell death | 6.74E-14 | 143 |
| **GO:0002694** | regulation of leukocyte activation | 8.30E-14 | 73 |
| **GO:0008284** | positive regulation of cell population proliferation | 8.30E-14 | 102 |
| **GO:0042981** | regulation of apoptotic process | 1.53E-13 | 140 |
| **GO:0051094** | positive regulation of developmental process | 1.53E-13 | 132 |
| **GO:0022610** | biological adhesion | 2.29E-13 | 125 |
| **GO:0019221** | cytokine-mediated signaling pathway | 3.18E-13 | 83 |
| **GO:0051674** | localization of cell | 3.18E-13 | 147 |
| **GO:0048870** | cell motility | 3.18E-13 | 147 |
| **GO:0007155** | cell adhesion | 3.18E-13 | 124 |
| **GO:0001568** | blood vessel development | 3.47E-13 | 85 |
| **GO:0002684** | positive regulation of immune system process | 4.00E-13 | 110 |
| **GO:0033993** | response to lipid | 4.25E-13 | 94 |
| **GO:0030155** | regulation of cell adhesion | 4.82E-13 | 80 |
| **GO:0001525** | angiogenesis | 6.68E-13 | 71 |
| **GO:0045321** | leukocyte activation | 6.68E-13 | 116 |
| **GO:0048514** | blood vessel morphogenesis | 8.28E-13 | 78 |
| **GO:0002682** | regulation of immune system process | 8.90E-13 | 137 |
| **GO:0001944** | vasculature development | 9.08E-13 | 86 |
| **GO:0072358** | cardiovascular system development | 2.05E-12 | 86 |
| **GO:0045597** | positive regulation of cell differentiation | 3.85E-12 | 102 |

| | | | |
|---|---|---|---|
| **GO:0035239** | tube morphogenesis | 4.90E-12 | 94 |
| **GO:1901700** | response to oxygen-containing compound | 5.22E-12 | 138 |
| **GO:0006954** | inflammatory response | 7.63E-12 | 79 |
| **GO:0022407** | regulation of cell-cell adhesion | 1.12E-11 | 55 |
| **GO:0098609** | cell-cell adhesion | 1.16E-11 | 85 |
| **GO:0035295** | tube development | 1.48E-11 | 106 |
| **GO:0046649** | lymphocyte activation | 1.51E-11 | 79 |
| **GO:0030334** | regulation of cell migration | 1.59E-11 | 93 |
| **GO:0051093** | negative regulation of developmental process | 1.88E-11 | 101 |
| **GO:0002683** | negative regulation of immune system process | 1.93E-11 | 59 |
| **GO:1903037** | regulation of leukocyte cell-cell adhesion | 1.93E-11 | 46 |
| **GO:0002521** | leukocyte differentiation | 2.22E-11 | 64 |
| **GO:0051249** | regulation of lymphocyte activation | 3.66E-11 | 60 |
| **GO:0002696** | positive regulation of leukocyte activation | 4.16E-11 | 52 |
| **GO:0009611** | response to wounding | 4.16E-11 | 74 |
| **GO:0007159** | leukocyte cell-cell adhesion | 4.74E-11 | 48 |
| **GO:0050867** | positive regulation of cell activation | 5.65E-11 | 53 |
| **GO:1903039** | positive regulation of leukocyte cell-cell adhesion | 6.10E-11 | 38 |
| **GO:0048646** | anatomical structure formation involved in morphogenesis | 6.10E-11 | 109 |

**Downregulated in IMR90-CMs by menadione treatment**
**TOP 50 GO FOR BIOLOGICAL PROCESSES**

| ID | Name | q-value FDR B&H | Hit Count in Query List |
|---|---|---|---|
| **GO:0060047** | heart contraction | 5.66E-08 | 26 |
| **GO:0003015** | heart process | 5.66E-08 | 26 |
| **GO:0044057** | regulation of system process | 1.47E-07 | 39 |
| **GO:0030001** | metal ion transport | 5.82E-07 | 46 |
| **GO:1903522** | regulation of blood circulation | 5.82E-07 | 25 |
| **GO:0006936** | muscle contraction | 1.24E-06 | 26 |
| **GO:0008015** | blood circulation | 1.90E-06 | 33 |
| **GO:0003012** | muscle system process | 1.97E-06 | 30 |
| **GO:0003013** | circulatory system process | 2.11E-06 | 33 |
| **GO:0070252** | actin-mediated cell contraction | 2.44E-06 | 15 |
| **GO:0035637** | multicellular organismal signaling | 2.45E-06 | 19 |
| **GO:0008016** | regulation of heart contraction | 2.45E-06 | 21 |
| **GO:0043269** | regulation of ion transport | 2.45E-06 | 38 |
| **GO:0030048** | actin filament-based movement | 2.45E-06 | 16 |
| **GO:0034762** | regulation of transmembrane transport | 2.45E-06 | 33 |
| **GO:0098662** | inorganic cation transmembrane transport | 6.00E-06 | 42 |
| **GO:0006941** | striated muscle contraction | 6.00E-06 | 17 |
| **GO:0034765** | regulation of ion transmembrane transport | 6.61E-06 | 29 |
| **GO:0060048** | cardiac muscle contraction | 7.30E-06 | 15 |

| | | | |
|---|---|---|---|
| **GO:0006813** | potassium ion transport | 7.64E-06 | 20 |
| **GO:0098660** | inorganic ion transmembrane transport | 7.74E-06 | 44 |
| **GO:0007267** | cell-cell signaling | 1.18E-05 | 63 |
| **GO:0006812** | cation transport | 2.43E-05 | 51 |
| **GO:0098655** | cation transmembrane transport | 2.43E-05 | 44 |
| **GO:0034220** | ion transmembrane transport | 2.46E-05 | 52 |
| **GO:0071805** | potassium ion transmembrane transport | 2.46E-05 | 18 |
| **GO:0061337** | cardiac conduction | 2.51E-05 | 14 |
| **GO:0006811** | ion transport | 2.70E-05 | 63 |
| **GO:0098916** | anterograde trans-synaptic signaling | 3.80E-05 | 37 |
| **GO:0007268** | chemical synaptic transmission | 3.80E-05 | 37 |
| **GO:0099537** | trans-synaptic signaling | 4.71E-05 | 37 |
| **GO:0002027** | regulation of heart rate | 5.04E-05 | 12 |
| **GO:0055085** | transmembrane transport | 5.92E-05 | 59 |
| **GO:0099536** | synaptic signaling | 6.08E-05 | 37 |
| **GO:0001508** | action potential | 8.66E-05 | 15 |
| **GO:0007610** | behavior | 8.75E-05 | 32 |
| **GO:0086003** | cardiac muscle cell contraction | 9.04E-05 | 10 |
| **GO:1990573** | potassium ion import across plasma membrane | 1.43E-04 | 8 |
| **GO:0086012** | membrane depolarization during cardiac muscle cell action potential | 1.69E-04 | 6 |
| **GO:0051480** | regulation of cytosolic calcium ion concentration | 1.75E-04 | 22 |
| **GO:0042391** | regulation of membrane potential | 1.92E-04 | 25 |
| **GO:0086091** | regulation of heart rate by cardiac conduction | 2.61E-04 | 7 |
| **GO:0015672** | monovalent inorganic cation transport | 3.03E-04 | 30 |
| **GO:0050801** | ion homeostasis | 3.10E-04 | 35 |
| **GO:0086010** | membrane depolarization during action potential | 3.49E-04 | 7 |
| **GO:0086001** | cardiac muscle cell action potential | 3.68E-04 | 9 |
| **GO:0055074** | calcium ion homeostasis | 3.74E-04 | 25 |
| **GO:0043270** | positive regulation of ion transport | 4.62E-04 | 19 |
| **GO:0072507** | divalent inorganic cation homeostasis | 4.62E-04 | 26 |
| **GO:0086018** | SA node cell to atrial cardiac muscle cell signaling | 7.22E-04 | 4 |

**Upregulated by cMSC-conditioned media protected vs menadione-stressed IMR90-CMs**

**TOP 50 GO FOR BIOLOGICAL PROCESSES**

| ID | Name | q-value FDR B&H | Hit Count in Query List |
|---|---|---|---|
| **GO:0006936** | muscle contraction | 4.92E-05 | 20 |
| **GO:0008015** | blood circulation | 4.92E-05 | 25 |
| **GO:0003013** | circulatory system process | 4.92E-05 | 25 |
| **GO:0030001** | metal ion transport | 4.92E-05 | 33 |
| **GO:1903522** | regulation of blood circulation | 5.99E-05 | 18 |

| | | | |
|---|---|---|---|
| **GO:0050801** | ion homeostasis | 8.85E-05 | 30 |
| **GO:0086091** | regulation of heart rate by cardiac conduction | 1.05E-04 | 7 |
| **GO:0003012** | muscle system process | 2.56E-04 | 21 |
| **GO:0002027** | regulation of heart rate | 2.56E-04 | 10 |
| **GO:0044057** | regulation of system process | 3.01E-04 | 25 |
| **GO:0060048** | cardiac muscle contraction | 3.83E-04 | 11 |
| **GO:0006811** | ion transport | 3.83E-04 | 46 |
| **GO:0007267** | cell-cell signaling | 3.86E-04 | 45 |
| **GO:0035637** | multicellular organismal signaling | 4.33E-04 | 13 |
| **GO:0086018** | SA node cell to atrial cardiac muscle cell signaling | 4.33E-04 | 4 |
| **GO:0086015** | SA node cell action potential | 4.33E-04 | 4 |
| **GO:0086001** | cardiac muscle cell action potential | 4.33E-04 | 8 |
| **GO:0006941** | striated muscle contraction | 4.33E-04 | 12 |
| **GO:0048878** | chemical homeostasis | 5.09E-04 | 35 |
| **GO:0060047** | heart contraction | 5.09E-04 | 15 |
| **GO:0086002** | cardiac muscle cell action potential involved in contraction | 5.18E-04 | 7 |
| **GO:0086070** | SA node cell to atrial cardiac muscle cell communication | 5.18E-04 | 4 |
| **GO:0098771** | inorganic ion homeostasis | 5.18E-04 | 26 |
| **GO:0086003** | cardiac muscle cell contraction | 5.18E-04 | 8 |
| **GO:0034220** | ion transmembrane transport | 5.20E-04 | 37 |
| **GO:0003015** | heart process | 5.54E-04 | 15 |
| **GO:0006812** | cation transport | 6.02E-04 | 36 |
| **GO:0086010** | membrane depolarization during action potential | 7.09E-04 | 6 |
| **GO:0007626** | locomotory behavior | 8.30E-04 | 13 |
| **GO:0061337** | cardiac conduction | 8.41E-04 | 10 |
| **GO:0042391** | regulation of membrane potential | 8.52E-04 | 19 |
| **GO:0055080** | cation homeostasis | 8.81E-04 | 25 |
| **GO:0098662** | inorganic cation transmembrane transport | 9.09E-04 | 28 |
| **GO:0001508** | action potential | 1.27E-03 | 11 |
| **GO:0030048** | actin filament-based movement | 1.36E-03 | 10 |
| **GO:0086046** | membrane depolarization during SA node cell action potential | 1.39E-03 | 3 |
| **GO:0098655** | cation transmembrane transport | 1.39E-03 | 30 |
| **GO:0006873** | cellular ion homeostasis | 1.39E-03 | 23 |
| **GO:0098660** | inorganic ion transmembrane transport | 1.51E-03 | 29 |
| **GO:0055085** | transmembrane transport | 1.54E-03 | 41 |
| **GO:0008016** | regulation of heart contraction | 1.54E-03 | 13 |
| **GO:1990573** | potassium ion import across plasma membrane | 1.58E-03 | 6 |
| **GO:0055082** | cellular chemical homeostasis | 1.62E-03 | 26 |
| **GO:0051480** | regulation of cytosolic calcium ion concentration | 1.69E-03 | 16 |
| **GO:0070252** | actin-mediated cell contraction | 1.69E-03 | 9 |

| | | | |
|---|---|---|---|
| **GO:0042310** | vasoconstriction | 2.10E-03 | 8 |
| **GO:0086019** | cell-cell signaling involved in cardiac conduction | 2.10E-03 | 5 |
| **GO:0098916** | anterograde trans-synaptic signaling | 2.10E-03 | 25 |
| **GO:0007268** | chemical synaptic transmission | 2.10E-03 | 25 |
| **GO:0030003** | cellular cation homeostasis | 2.38E-03 | 22 |

**Downregulated by cMSC-conditioned media protected vs menadione-stressed IMR90-CMs**
**TOP 50 GO FOR BIOLOGICAL PROCESSES**

| ID | Name | q-value FDR B&H | Hit Count in Query List |
|---|---|---|---|
| **GO:0042127** | regulation of cell population proliferation | 2.38E-16 | 150 |
| **GO:0016477** | cell migration | 1.29E-15 | 139 |
| **GO:0010941** | regulation of cell death | 8.48E-15 | 147 |
| **GO:0051674** | localization of cell | 8.48E-15 | 145 |
| **GO:0048870** | cell motility | 8.48E-15 | 145 |
| **GO:2000145** | regulation of cell motility | 1.07E-13 | 99 |
| **GO:0030334** | regulation of cell migration | 1.07E-13 | 95 |
| **GO:0001525** | angiogenesis | 1.54E-13 | 70 |
| **GO:0043067** | regulation of programmed cell death | 8.00E-13 | 133 |
| **GO:0001568** | blood vessel development | 8.00E-13 | 81 |
| **GO:0001944** | vasculature development | 8.00E-13 | 83 |
| **GO:0030335** | positive regulation of cell migration | 1.56E-12 | 66 |
| **GO:0072358** | cardiovascular system development | 1.56E-12 | 83 |
| **GO:0035295** | tube development | 1.70E-12 | 104 |
| **GO:0040012** | regulation of locomotion | 1.70E-12 | 100 |
| **GO:0035239** | tube morphogenesis | 2.07E-12 | 91 |
| **GO:0048514** | blood vessel morphogenesis | 2.26E-12 | 74 |
| **GO:2000147** | positive regulation of cell motility | 2.58E-12 | 67 |
| **GO:0048646** | anatomical structure formation involved in morphogenesis | 2.60E-12 | 108 |
| **GO:0051241** | negative regulation of multicellular organismal process | 2.62E-12 | 115 |
| **GO:0051270** | regulation of cellular component movement | 2.83E-12 | 100 |
| **GO:0051272** | positive regulation of cellular component movement | 3.84E-12 | 68 |
| **GO:0042981** | regulation of apoptotic process | 6.33E-12 | 128 |
| **GO:0008284** | positive regulation of cell population proliferation | 8.77E-12 | 92 |
| **GO:0034097** | response to cytokine | 1.13E-11 | 102 |
| **GO:0040017** | positive regulation of locomotion | 2.00E-11 | 67 |
| **GO:0000165** | MAPK cascade | 2.98E-11 | 88 |
| **GO:0023014** | signal transduction by protein phosphorylation | 5.47E-11 | 88 |
| **GO:0001816** | cytokine production | 1.06E-10 | 77 |
| **GO:0051094** | positive regulation of developmental process | 1.08E-10 | 117 |

| | | | |
|---|---|---|---|
| **GO:0071345** | cellular response to cytokine stimulus | 1.16E-10 | 94 |
| **GO:0072359** | circulatory system development | 1.22E-10 | 101 |
| **GO:0001775** | cell activation | 1.25E-10 | 113 |
| **GO:0033993** | response to lipid | 2.25E-10 | 83 |
| **GO:0022610** | biological adhesion | 2.37E-10 | 110 |
| **GO:1902533** | positive regulation of intracellular signal transduction | 3.38E-10 | 89 |
| **GO:0007155** | cell adhesion | 3.84E-10 | 109 |
| **GO:0009611** | response to wounding | 7.84E-10 | 68 |
| **GO:1901700** | response to oxygen-containing compound | 9.77E-10 | 124 |
| **GO:0001817** | regulation of cytokine production | 1.86E-09 | 69 |
| **GO:0009967** | positive regulation of signal transduction | 2.36E-09 | 122 |
| **GO:0042060** | wound healing | 5.22E-09 | 58 |
| **GO:0098609** | cell-cell adhesion | 9.59E-09 | 74 |
| **GO:0048585** | negative regulation of response to stimulus | 9.59E-09 | 125 |
| **GO:0043408** | regulation of MAPK cascade | 9.72E-09 | 71 |
| **GO:0008285** | negative regulation of cell population proliferation | 1.06E-08 | 71 |
| **GO:0001667** | ameboidal-type cell migration | 1.41E-08 | 50 |
| **GO:0070371** | ERK1 and ERK2 cascade | 1.57E-08 | 41 |
| **GO:0050865** | regulation of cell activation | 1.68E-08 | 61 |
| **GO:0007267** | cell-cell signaling | 2.70E-08 | 122 |

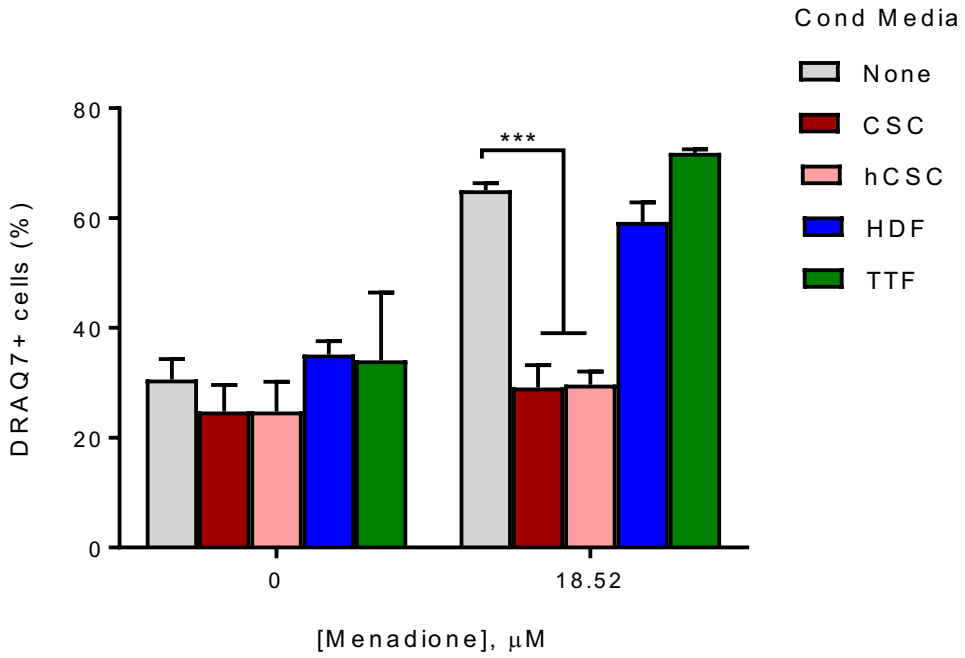
**Upregulated by cMSC-conditioned media protected cells vs untreated IMR90-CMs**
**TOP 50 GO FOR BIOLOGICAL PROCESSES**

| ID | Name | q-value FDR B&H | Hit Count in Query List |
|---|---|---|---|
| **GO:0071395** | cellular response to jasmonic acid stimulus | 2.20E-05 | 1.81E-04 |
| **GO:0009753** | response to jasmonic acid | 2.20E-05 | 1.81E-04 |
| **GO:0044598** | doxorubicin metabolic process | 1.66E-04 | 1.37E-03 |
| **GO:0030638** | polyketide metabolic process | 1.66E-04 | 1.37E-03 |
| **GO:0044597** | daunorubicin metabolic process | 1.66E-04 | 1.37E-03 |
| **GO:0042180** | cellular ketone metabolic process | 1.66E-04 | 1.37E-03 |
| **GO:0030647** | aminoglycoside antibiotic metabolic process | 1.87E-04 | 1.54E-03 |
| **GO:0010876** | lipid localization | 2.58E-04 | 2.12E-03 |
| **GO:0006692** | prostanoid metabolic process | 3.31E-04 | 2.73E-03 |
| **GO:0006693** | prostaglandin metabolic process | 3.31E-04 | 2.73E-03 |
| **GO:0006690** | icosanoid metabolic process | 4.64E-04 | 3.82E-03 |
| **GO:0008202** | steroid metabolic process | 5.72E-04 | 4.70E-03 |
| **GO:0030595** | leukocyte chemotaxis | 6.72E-04 | 5.53E-03 |
| **GO:0042448** | progesterone metabolic process | 6.96E-04 | 5.73E-03 |
| **GO:1902644** | tertiary alcohol metabolic process | 6.96E-04 | 5.73E-03 |
| **GO:0042445** | hormone metabolic process | 7.94E-04 | 6.53E-03 |
| **GO:0006869** | lipid transport | 7.94E-04 | 6.53E-03 |
| **GO:0016137** | glycoside metabolic process | 7.94E-04 | 6.53E-03 |
| **GO:1901568** | fatty acid derivative metabolic process | 1.61E-03 | 1.32E-02 |

| | | | |
|---|---|---|---|
| **GO:0060326** | cell chemotaxis | 2.29E-03 | 1.88E-02 |
| **GO:1901661** | quinone metabolic process | 2.29E-03 | 1.88E-02 |
| **GO:0046457** | prostanoid biosynthetic process | 2.29E-03 | 1.88E-02 |
| **GO:0001516** | prostaglandin biosynthetic process | 2.29E-03 | 1.88E-02 |
| **GO:0010565** | regulation of cellular ketone metabolic process | 2.30E-03 | 1.89E-02 |
| **GO:0097306** | cellular response to alcohol | 2.40E-03 | 1.98E-02 |
| **GO:0071799** | cellular response to prostaglandin D stimulus | 2.40E-03 | 1.98E-02 |
| **GO:0071798** | response to prostaglandin D | 2.40E-03 | 1.98E-02 |
| **GO:0006629** | lipid metabolic process | 2.48E-03 | 2.04E-02 |
| **GO:0050900** | leukocyte migration | 2.74E-03 | 2.25E-02 |
| **GO:0055114** | oxidation-reduction process | 2.88E-03 | 2.37E-02 |
| **GO:0097164** | ammonium ion metabolic process | 2.89E-03 | 2.38E-02 |
| **GO:0015711** | organic anion transport | 2.89E-03 | 2.38E-02 |
| **GO:0046942** | carboxylic acid transport | 2.95E-03 | 2.43E-02 |
| **GO:0015849** | organic acid transport | 2.95E-03 | 2.43E-02 |
| **GO:0030593** | neutrophil chemotaxis | 2.98E-03 | 2.46E-02 |
| **GO:0033559** | unsaturated fatty acid metabolic process | 3.00E-03 | 2.47E-02 |
| **GO:0043068** | positive regulation of programmed cell death | 3.21E-03 | 2.64E-02 |
| **GO:0097529** | myeloid leukocyte migration | 3.21E-03 | 2.64E-02 |
| **GO:0007584** | response to nutrient | 3.45E-03 | 2.84E-02 |
| **GO:1901701** | cellular response to oxygen-containing compound | 3.45E-03 | 2.84E-02 |
| **GO:0008207** | C21-steroid hormone metabolic process | 3.61E-03 | 2.97E-02 |
| **GO:0006631** | fatty acid metabolic process | 3.66E-03 | 3.01E-02 |
| **GO:0042127** | regulation of cell population proliferation | 3.77E-03 | 3.10E-02 |
| **GO:0051674** | localization of cell | 3.81E-03 | 3.13E-02 |
| **GO:0048870** | cell motility | 3.81E-03 | 3.13E-02 |
| **GO:0031394** | positive regulation of prostaglandin biosynthetic process | 3.85E-03 | 3.17E-02 |
| **GO:0031622** | positive regulation of fever generation | 3.85E-03 | 3.17E-02 |
| **GO:0097305** | response to alcohol | 3.94E-03 | 3.24E-02 |
| **GO:0006811** | ion transport | 3.94E-03 | 3.24E-02 |
| **GO:1990266** | neutrophil migration | 3.99E-03 | 3.28E-02 |

**Supplement 6.2. Cytokine array analysis. A,** Protection assay on IMR90-CMs; **B, C,** Java scripts for ImageJ written by Stephen Rothery of Imperial FILM facility and modified by Dr Antonio MA Miranda and myself. **B,** Creates a circular grid on the membrane. **C,** Processes data by inverting the image and subtracting the background and generating integrated density values normalised against the positive controls of the membrane.

**A**




**B**

```
run("Set Measurements...", "area mean min integrated display redirect=None decimal=3");
ColNum=Array.slice(Array.getSequence(31),1,31);
RowNum=Array.slice(Array.getSequence(35),1,31);
//create Grid of rois
roiManager("Reset");
//format
across=30;
down=30;
//size
wd=25; //54 - scale 1 107 - scale 2
ht=25; //54 - scale 1 107 - scale 2
//start position
Xstart=70;//adjust start position
Ystart=60;//adjust start position
roi=0;
for (Row=0;Row<down;Row++){//rows
for (Col=0;Col<across;Col++){//columns
makeOval(Xstart+wd*Col*2.15, Ystart+ht*Row*2.15, wd, ht);
roiManager("Add");
```

```
roiManager("select", roi);
roiManager("rename", "Row "+RowNum[Row]+" Col "+ColNum[Col]);
roi=roi+1;
}
}
roiManager("Show All");
```

**C**

```
run("Set Measurements...", "area mean min integrated display redirect=None decimal=5");
run("Clear Results");
fn=getTitle();
//create copy and invert
run("Select None");
run("Duplicate...", "title=["+fn+" Measurements]");
run("Invert");
//get background wells
//6,7,21,22,36,37,51,52,426,427,441,442,456,457,471,472,846,847,861,862,876,877,891,892
roiManager("select",
newArray(5,6,20,21,35,36,50,51,425,426,440,441,455,456,470,471,845,846,860,861,875,876,890,89
1));
roiManager("Set Color", "red");
roiManager("measure");
//background well values
background_max_values=Table.getColumn("Max");
background_wells=Table.getColumn("Label");
background_IntDen=Table.getColumn("IntDen");
//subtract background
run("Clear Results");
Array.getStatistics(background_max_values, bg_min, bg_max, bg_mean, bg_stdDev);
run("Select None");
run("Subtract...", "value="+round(bg_max));
Max=newArray(1);
Max[0]=round(bg_max);
roiManager("Show All without labels");
//get standardised IntDen
selectWindow(fn+" Measurements");
setTool("rectangle");
```

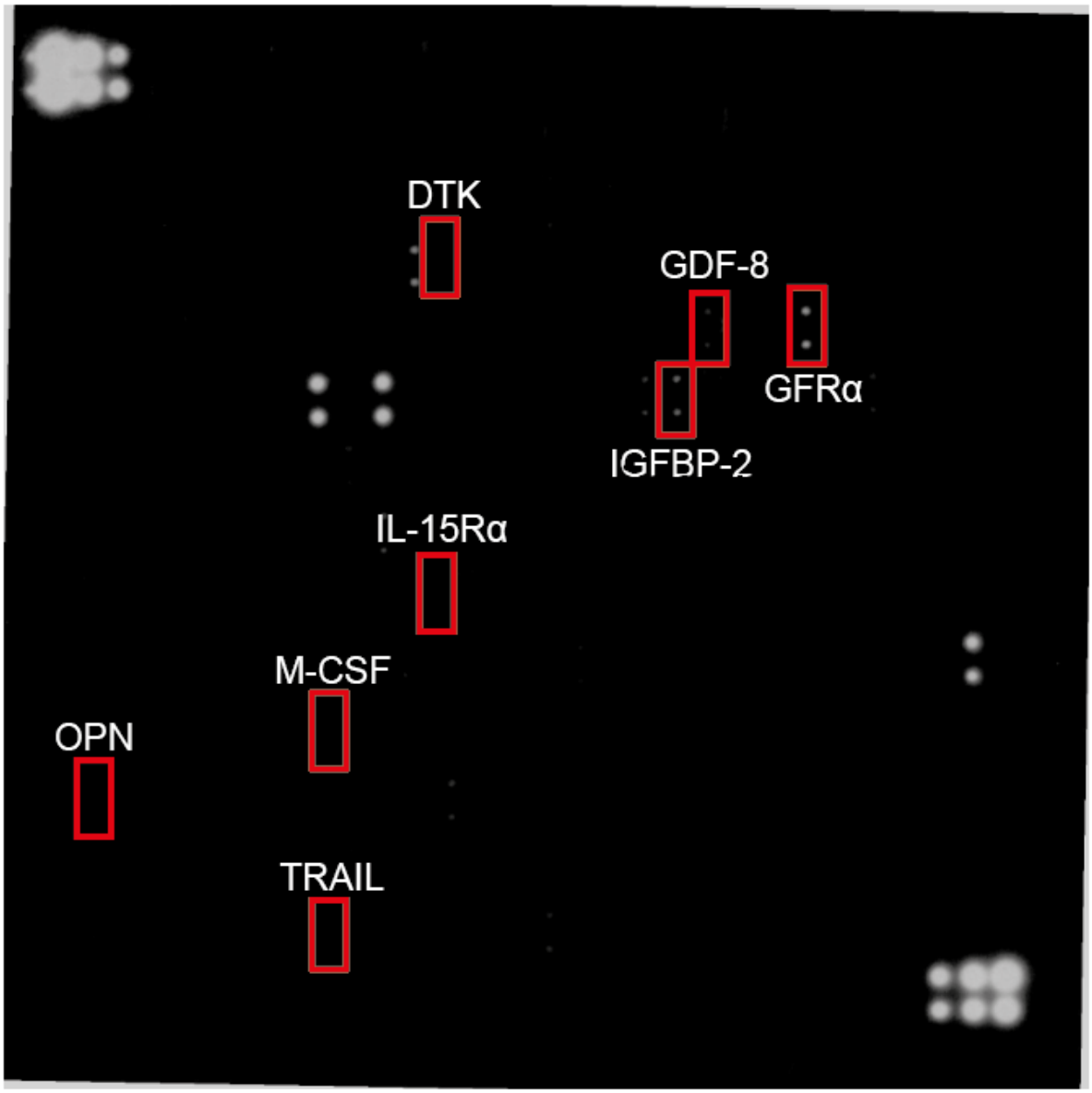
```
roiManager("Show None");
waitForUser("","Draw around top left control set \n then press ok");
tp=getValue("IntDen");
waitForUser("","Draw around bottom right control set \n then press ok");
bt=getValue("IntDen");
standardised_IntDen=newArray(1);
standardised_IntDen[0]=(tp+bt)/12;
//format
across=30;
down=30;
//measure wells
roiManager("deselect");
roiManager("measure");
//select measurement for analysis
//selectWindow("Results");
//DT=split(Table.headings,"\t");
//DT=Array.slice(DT,2,DT.length);
//Dialog.create("Select Data");
//Dialog.addChoice("Select data colums", DT);
//Dialog.addNumber("Number of Colums", across);
//Dialog.addNumber("Number of Rows", down);
//Dialog.show();
//Data_Titles=Dialog.getChoice();
//across=Dialog.getNumber();
//down=Dialog.getNumber();
//
//Data_values=Table.getColumn(Data_Titles);
//get intDen values
Raw_Data_values=Table.getColumn("IntDen");
Corrected_Data_values=newArray(Raw_Data_values.length);
for (res=0;res<Raw_Data_values.length;res++){
Corrected_Data_values[res]=Raw_Data_values[res]/standardised_IntDen[0];
}
//Array.show(Raw_Data_values,Corrected_Data_values);
Calculations=newArray("Max","IntDen Correction value");
Values=newArray(Max[0],standardised_IntDen[0]);
```

```
//Array.getStatistics(Data_values, Data_min, Data_max, Data_mean, Data_stdDev);
//b=lengthOf(toString(Data_max,0))-1;
//Data_max=round(Data_max/pow(10, b))*pow(10, b);
Table.create("background");
Table.setLocationAndSize(300, 300, 800, 400);
Table.setColumn("Well Number", background_wells);
Table.setColumn("Max value", background_max_values);
Table.setColumn("Integrated Density", background_IntDen);
Table.setColumn("Calculations", Calculations);
Table.setColumn("Values", Values);
Table.rename("background", fn+" Background Values");
roi=0;
Table.create("Raw Measurements");
Table.setLocationAndSize(400, 300, 800, 600);
for (Row=0;Row<down;Row++){//rows
        Table.set("Row", Row, "Row "+Row+1);
for (Col=0;Col<across;Col++){//columns
        Table.set("Column "+Col+1, Row, (Raw_Data_values[roi]));
        roi=roi+1;
}
}
Table.rename("Raw Measurements", fn+" Raw IntDen Measurements");
roi=0;
Table.create("Corrected Measurements");
Table.setLocationAndSize(400, 300, 800, 600);
for (Row=0;Row<down;Row++){//rows
        Table.set("Row", Row, "Row "+Row+1);
for (Col=0;Col<across;Col++){//columns
        Table.set("Column "+Col+1, Row, (Corrected_Data_values[roi]));
        roi=roi+1;
}
}
Table.rename("Corrected Measurements", fn+" Corrected IntDen Measurements");
selectWindow("Results");
run("Close");
exit();
```

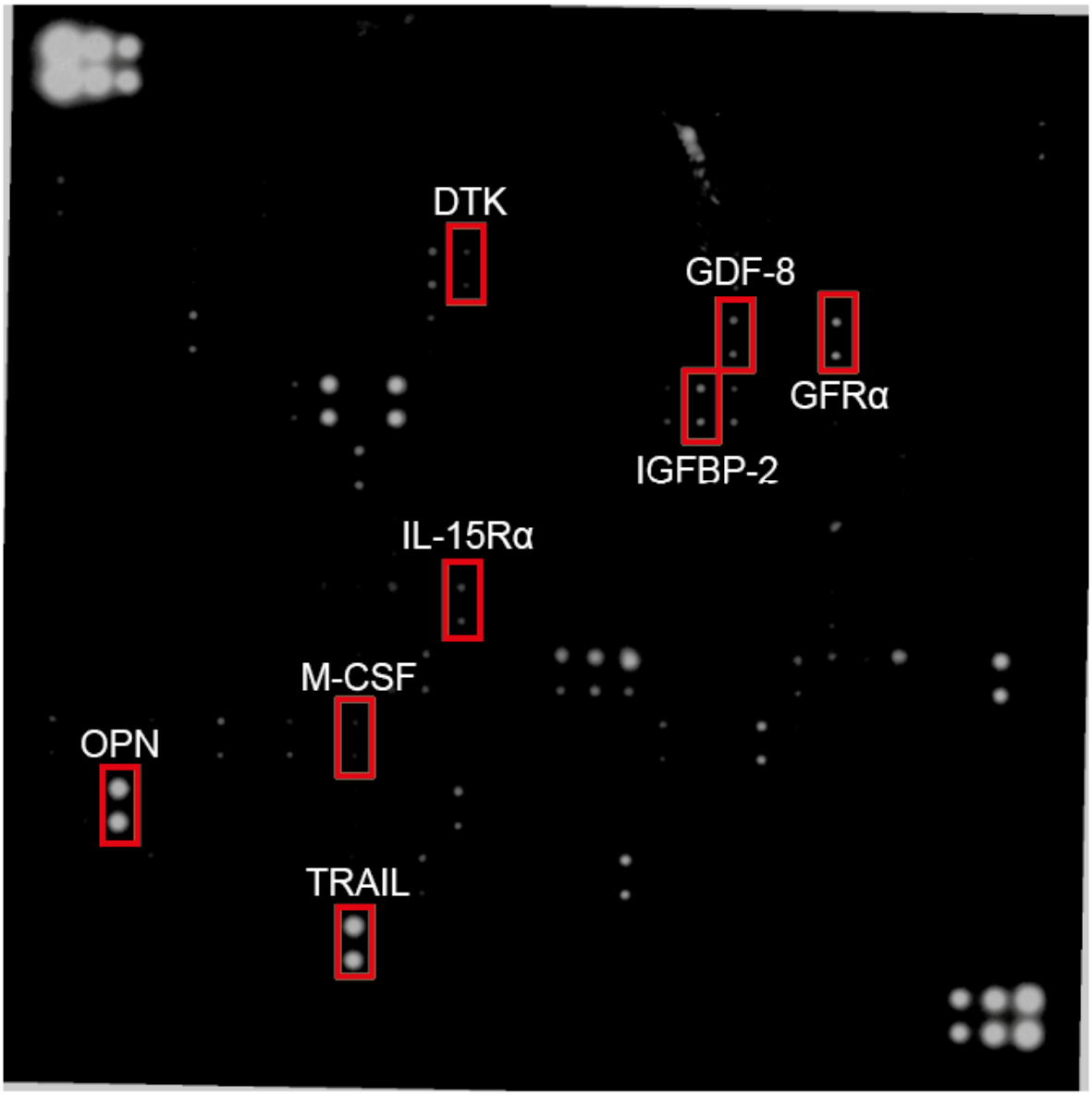
```
sqsz=20;
border=70;
roi=0;
newImage(fn+" "+Data_Titles+" Heat Map", "32-bit black", across*(sqsz+1), down*(sqsz+1), 1);
for (Row=0;Row<down;Row++){//rows
for (Col=0;Col<across;Col++){//columns
makeRectangle((sqsz+1)*Col, (sqsz+1)*Row, sqsz, sqsz);
run("Set...", "value="+Data_values[roi]);
roi=roi+1;
}
}
run("royal");
setMinAndMax(0, Data_max);
//resetMinAndMax();
//waitForUser("","set Brightness and contrast \n then press ok");
run("Canvas Size...", "width="+across*(sqsz+1)+border+" height="+down*(sqsz+1)+border+"
position=Center zero");
run("Canvas Size...", "width="+across*(sqsz+1)+border+100+" height="+down*(sqsz+1)+border+"
position=Bottom-Left zero");
run("Calibration Bar...", "location=[Upper Right] fill=None label=White number=5 decimal=0 font=12
zoom=1 bold overlay");
setColor("white");
drawString("Subtracted background value "+bg, 10, 20);
```

**Supplement 6.3. Cytokine array membranes. (A-C), Mouse array; (D-F) human array. A,** medium; **B, mouse** CSC-conditioned medium; **C,** TTF-conditioned medium; **D,** medium; **E, human** CSC-conditioned medium; **F,** HDF-conditioned medium.

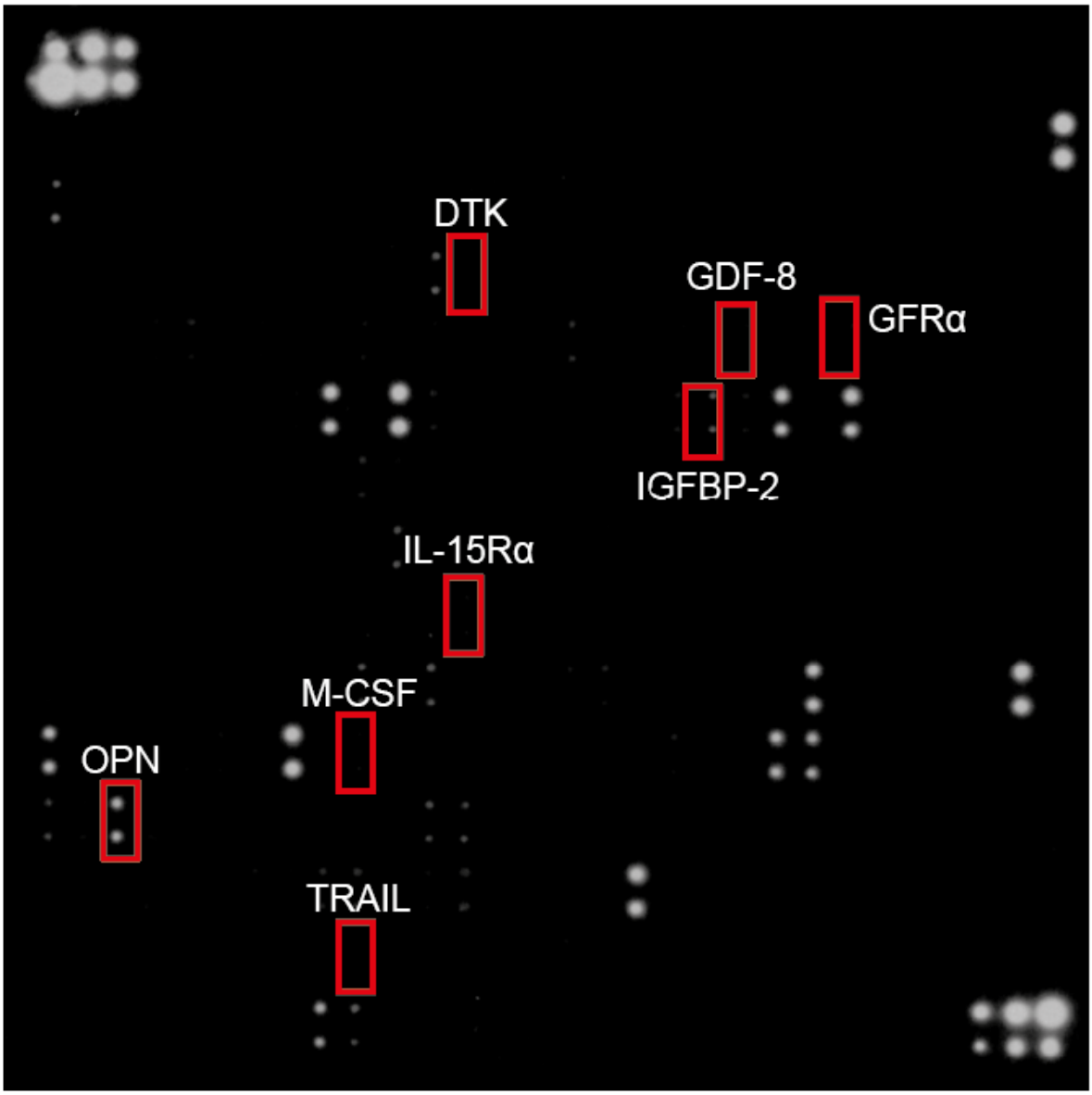
# A. Medium



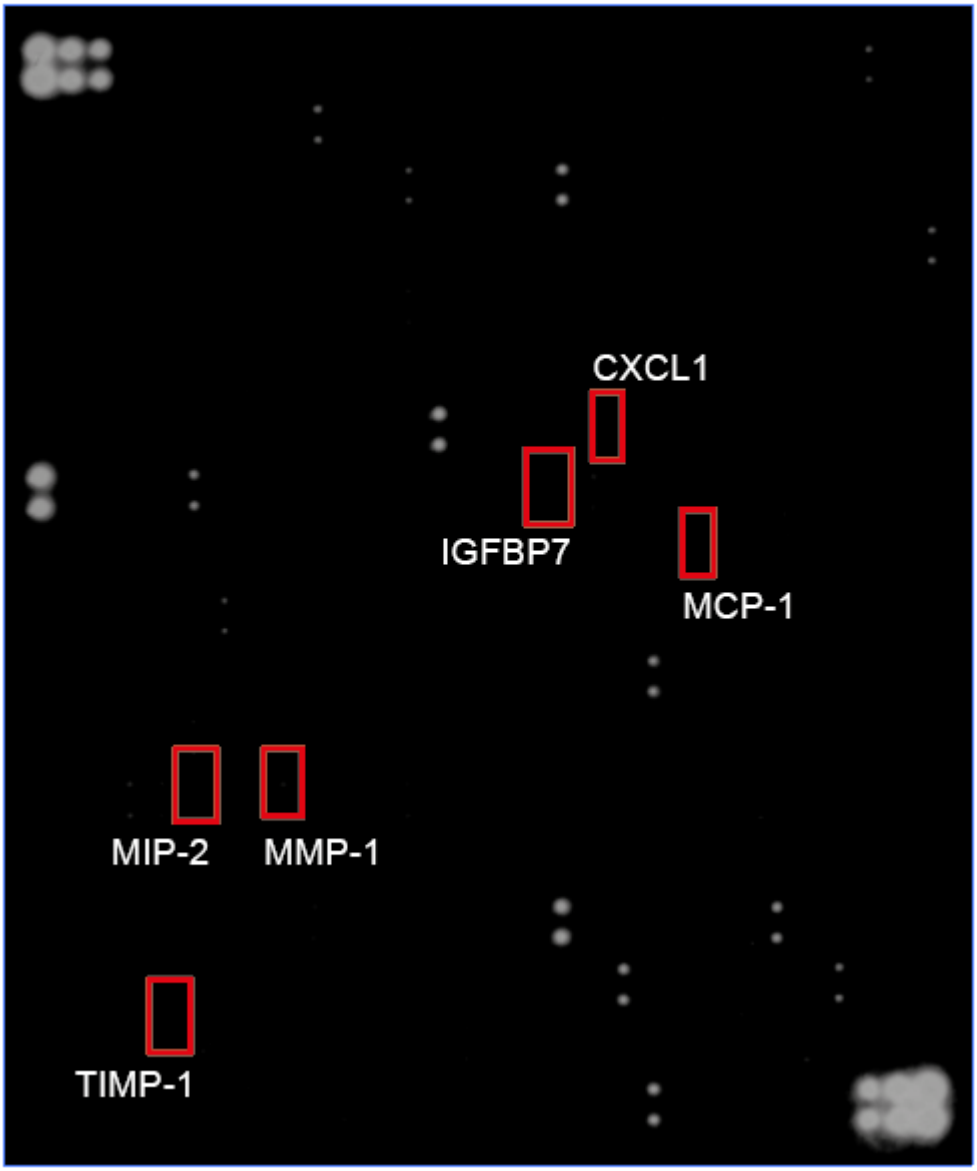
# B. CSC



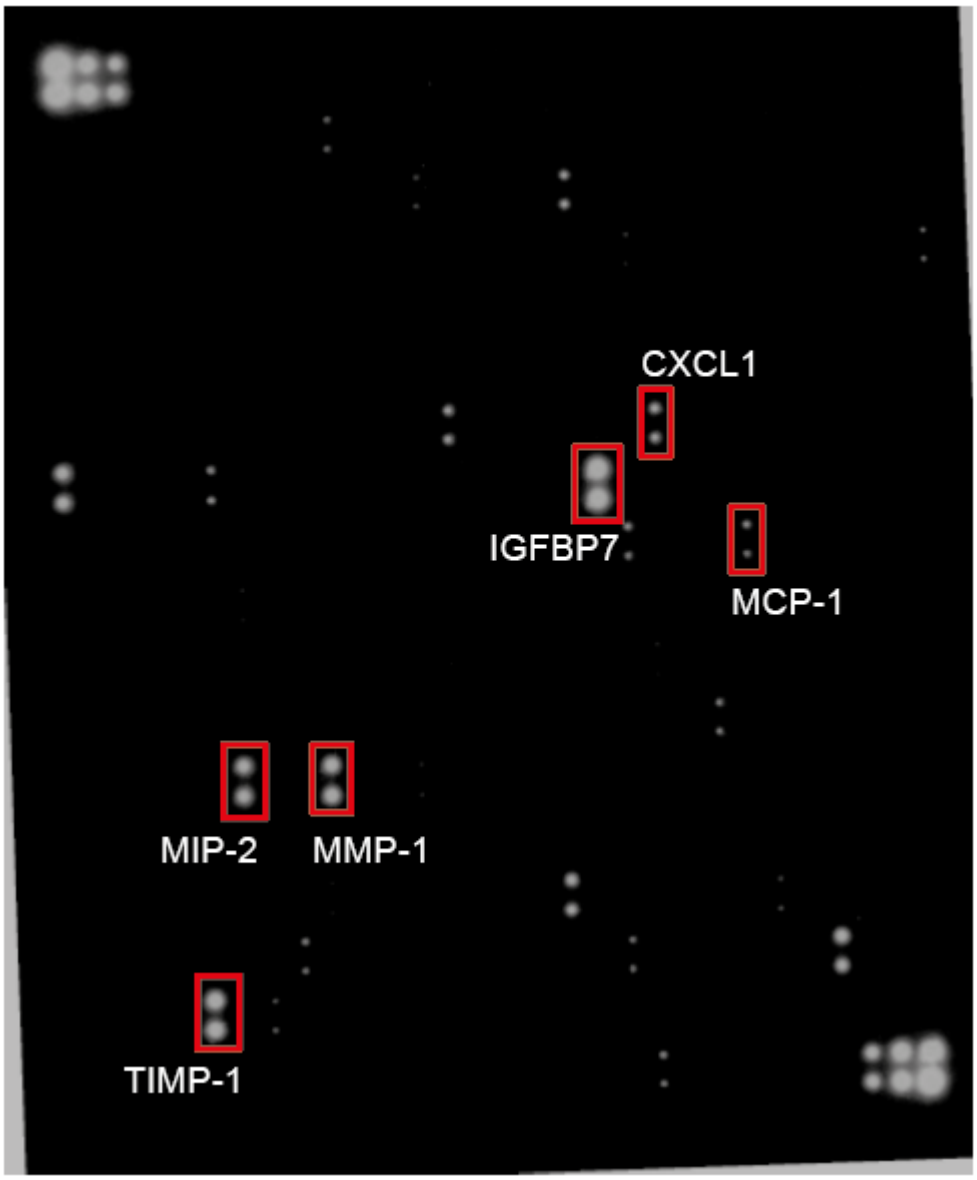
C. TTF



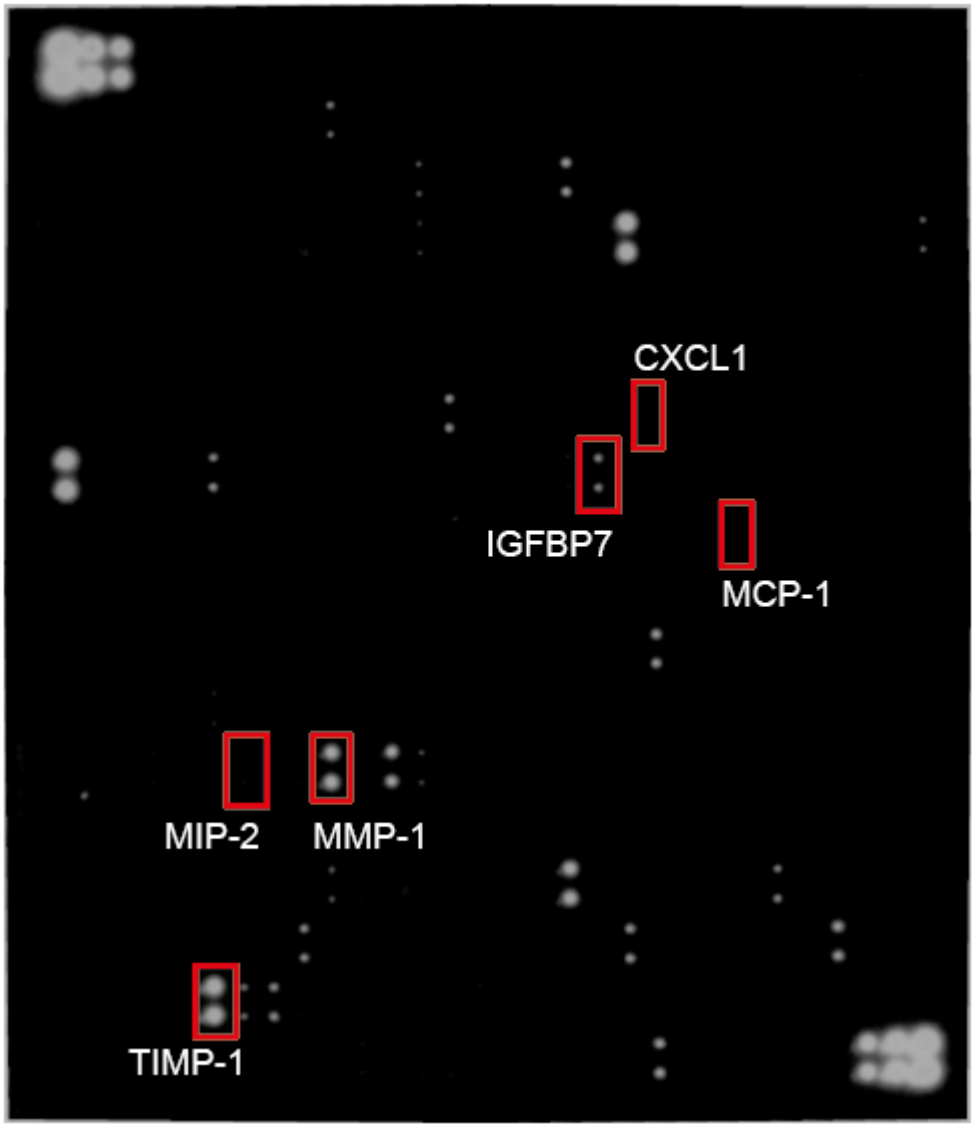
## D. Medium



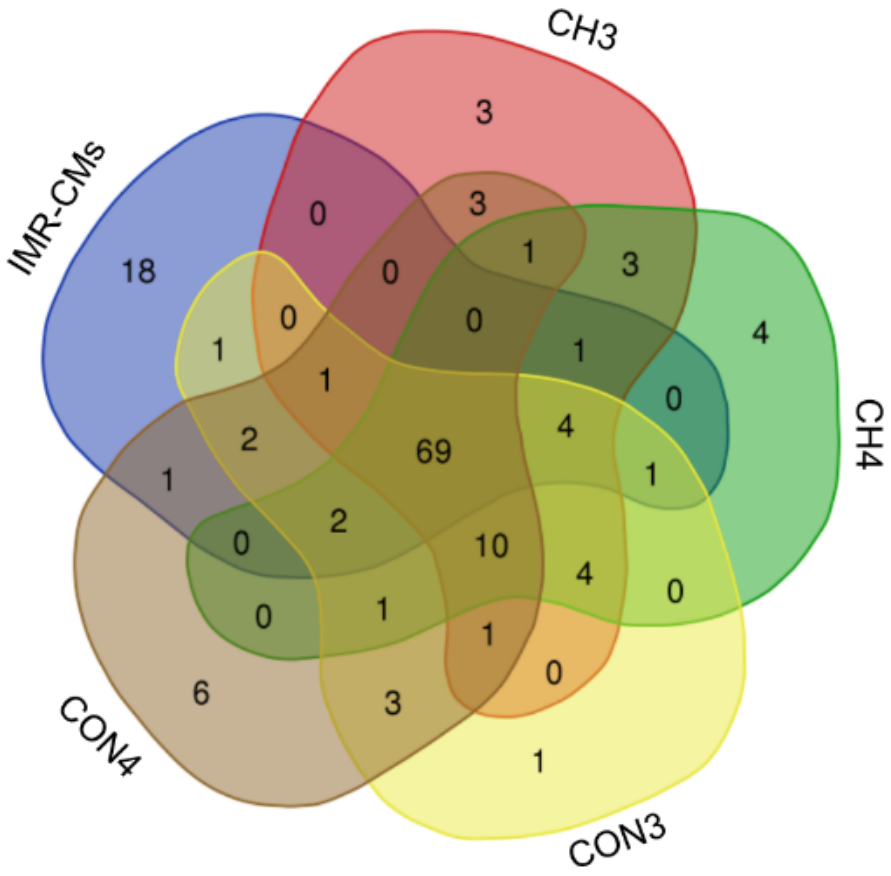
## E. hCSCs



F. HDF



**Supplement 6.4. IMR90-derived CMs have high expression of several cardiomyocyte markers compared to other hPSC-derived CMs**. **A,** Venn diagram intersecting the top 100 expressed genes in IMR90-derived CMs and published hPSC-derived CMs; **B,** List of genes for each intersection on the Venn diagram, with cardiomyocyte specific genes in bold. IMR90-derived CMs have a higher proportion of cardiomyocyte genes (IMR-CMs - 9; CON3 - 7; CON4 - 8; CH3 - 6; CH4 - 6). **C,** Table of top 100 highly expressed genes in IMR90-CMs and control hPSC-CM lines.



**B**

| | |
|---|---|
| Common to all | AC006064.4, AC051649.3, AC093484.3, AC119427.2, **ACTC1**, AL049766.1, AL132855.1, AL138963.4, AL662797.1, ALDOA, ATP5F1B, EEF1A1, EEF2, GAPDH, HSPB1, HSPB7, MIF, MIR1282, MIR198, MIR4709, MT-ATP6, MT-ATP6P1, MT-ATP8, MT-CO1, MT-CO2, MT-CO3, MT-CYB, MT-ND1, MT-ND2, MT-ND3, MT-ND4, MT-ND4L, MT-ND5, MT-ND6, MT-RNR1, MT-RNR2, MT-TC, MT-TE, MT-TG, MT-TH, MT-TL1, MT-TL2, MT-TP, MT-TR, MT-TS2, MT-TY, **MYH6**, **MYH7**, MYL6, MYL7, MYL9, RPL13A, RPL41, RPL7A, RPL8, RPLP0, RPLP1, RPS12, RPS18, RPS2, RPS27, RPS6, RPS8, TMSB10, **TNNC1**, **TNNT2**, TPM1, TPT1, UBB |
| IMR-CMs only | AP000769.5, BEX3, HSPB3, MALAT1, MDK, MIR4721, MT-TA, MT-TF, MT-TS1, MT-TV, MYL4, **NPPA**, RPL29, RPL7, RPS17, RPS3A, SRP14, **TNNI1** |
| IMR-CMs, CH3, CH4, CON3 | FAU, MT-TT, RPL10A, RPS11 |
| IMR-CMs, CH3, CON3, CON4 | AC020909.2 |
| IMR-CMs, CH4, CON3, CON4 | AC023509.4, MT-TW |
| CH3, CH4, CON3, CON4 | AC005944.1, AC053503.4, AC132217.1, AL133415.1, FTL, HSPA8, MIR3606, **MYL2**, TAGLN, TPI1 |
| IMR-CMs, CH3, CH4 | RPL3 |
| IMR-CMs, CH3, CON3 | RPS16 |
| IMR-CMs, CON3, CON4 | **PLN**, MIR3661 |
| CH3, CH4, CON3 | AC092069.1, MIR1244-1, TUBA1B, TUBB |
| CH3, CH4, CON4 | DES |
| CH3, CON3, CON4 | ANKRD1 |
| CH4, CON3, CON4 | H19 |
| IMR-CMs, CON3 | MT-TN |
| IMR-CMs, CON4 | **MYBPC3** |
| CH3, CH4 | CALR, PFN1, TUBA1A |
| CH3,CON4 | AC091564.3, CCN2, TMSB4X |
| CON3, CON4 | COX5B, RTL8C, SLC25A5 |
| CH3 Only | AC145207.3, RPS21, VIM |
| CH4 Only | AC079328.2, COL1A1, MIR3652, RPL19 |
| CON3 Only | IGF2 |
| CON4 Only | AC002398.2, AC004477.2, AC087457.1, ACTA1, MGP, UBC |

**C**

| Rank | IMR-CMs | CH3 | CH4 | CON3 | CON4 |
|---|---|---|---|---|---|
| 1 | MT-RNR2 | MYL7 | MT-CO1 | MT-CO2 | MT-CO2 |
| 2 | MT-ATP8 | MT-CO2 | MT-CO2 | MT-CO1 | MT-ATP6 |
| 3 | MT-CO1 | MT-CO3 | MT-ATP8 | MT-ATP8 | MT-ATP8 |
| 4 | MT-ATP6 | MT-CO1 | MT-CO3 | MT-ATP6 | MT-CO1 |
| 5 | MT-TC | MT-ATP6 | MT-ATP6 | MYL7 | MT-CO3 |
| 6 | MT-TY | MT-RNR2 | MT-ND4 | MT-CO3 | MT-RNR2 |
| 7 | MT-ND4L | MT-ATP8 | MT-RNR2 | MT-RNR2 | MT-ND4 |
| 8 | MT-CO2 | AC006064.4 | MT-ND4L | MT-ND4 | MYL7 |
| 9 | MT-ND4 | MT-ND4 | MT-ND6 | MT-ND4L | MT-ND6 |
| 10 | MT-CO3 | MT-TY | MT-CYB | MT-ND6 | MT-ND4L |
| 11 | MT-ND6 | MT-TC | MYL7 | MT-CYB | MT-CYB |
| 12 | MT-TN | MT-ND6 | MT-ND5 | MT-TE | MT-ND3 |
| 13 | MT-CYB | ACTC1 | MT-TE | MT-ND5 | MT-TE |
| 14 | MYL7 | AL132855.1 | MT-ND2 | MT-ND3 | AL132855.1 |
| 15 | MT-ND5 | MT-TE | MT-ND3 | MT-TY | MT-ND5 |
| 16 | MT-TE | MT-ND3 | AC006064.4 | AC006064.4 | MT-ND2 |
| 17 | MT-ND3 | MT-CYB | MT-ND1 | MT-TC | MT-TY |
| 18 | MT-ND2 | AC051649.3 | MT-TY | AL132855.1 | AC051649.3 |
| 19 | MT-ND1 | MT-ND4L | AC051649.3 | MT-ND2 | AC006064.4 |
| 20 | MT-TS1 | TNNC1 | AL132855.1 | ACTC1 | ACTC1 |
| 21 | MT-TA | GAPDH | ACTC1 | MT-ND1 | MT-TC |
| 22 | MT-RNR1 | MT-ND1 | MT-TC | AC051649.3 | MT-ND1 |
| 23 | AL132855.1 | MIR1282 | GAPDH | GAPDH | MT-RNR1 |
| 24 | ACTC1 | MT-ND5 | MT-TL1 | MTATP6P1 | AC053503.4 |
| 25 | MT-TG | MT-ND2 | MTATP6P1 | MT-TH | MTATP6P1 |
| 26 | AC006064.4 | AL138963.4 | MT-TS2 | AC132217.1 | MIR1282 |
| 27 | MT-TP | AC093484.3 | MT-TH | MT-TL1 | GAPDH |
| 28 | MT-TL1 | TMSB10 | MIR3606 | AL138963.4 | TNNC1 |
| 29 | MIR1282 | MT-TS2 | TNNC1 | TNNC1 | AL138963.4 |
| 30 | TNNC1 | EEF1A1 | MIR1282 | MT-TG | MYH7 |
| 31 | HSPB1 | MT-TH | AL138963.4 | MT-TS2 | MT-TH |
| 32 | MT-TH | HSPB1 | MT-TG | MIR1282 | MT-TL1 |
| 33 | TNNT2 | MYL6 | MT-TL2 | MT-RNR1 | DES |
| 34 | EEF1A1 | MTATP6P1 | EEF1A1 | EEF1A1 | MT-TG |
| 35 | AL138963.4 | MT-TG | AC132217.1 | AC093484.3 | EEF1A1 |
| 36 | MTATP6P1 | MT-TL2 | AL662797.1 | MYH7 | MT-TS2 |
| 37 | GAPDH | AC053503.4 | MT-RNR1 | MT-TL2 | AC093484.3 |
| 38 | MYH7 | AL662797.1 | MIR198 | MT-TP | MYH6 |
| 39 | AC051649.3 | FTL | TMSB10 | AL662797.1 | ACTA1 |
| 40 | AC119427.2 | MT-TL1 | AC093484.3 | RPS2 | MIR3606 |
| 41 | MYH6 | RPS2 | HSPB1 | HSPB1 | HSPB1 |
| 42 | AP000769.5 | UBB | MYL6 | MIR198 | MT-TL2 |
| 43 | MT-TS2 | RPL8 | MYH7 | MYL6 | MT-TP |
| 44 | RPL13A | AC092069.1 | RPS2 | MYH6 | HSPB7 |
| 45 | RPL8 | TPM1 | MT-TR | TMSB10 | MYL2 |
| 46 | MT-TT | MYL2 | AC053503.4 | RPL8 | MYL6 |
| 47 | MT-TL2 | TNNT2 | MYH6 | UBB | MIR198 |
| 48 | NPPA | RPS27 | RPLP0 | RPLP0 | PLN |
| 49 | TPM1 | ANKRD1 | RPL8 | MIR3606 | AC132217.1 |

| | | | | | |
|---|---|---|---|---|---|
| 50 | RPS27 | MIR198 | HSPB7 | MIF | TMSB10 |
| 51 | TMSB10 | MYH6 | TUBB | TPM1 | ANKRD1 |
| 52 | RPS2 | AL133415.1 | RPS27 | MT-TR | RPL8 |
| 53 | RPLP1 | MIF | RPL41 | ATP5F1B | RPS2 |
| 54 | HSPB7 | MYH7 | TPM1 | HSPB7 | ATP5F1B |
| 55 | MT-TW | RPL13A | RPLP1 | RPLP1 | TPM1 |
| 56 | AC093484.3 | TUBA1B | FTL | RPS27 | UBB |
| 57 | RPLP0 | MT-TP | RPL13A | TUBA1B | TNNT2 |
| 58 | RPS16 | RPLP1 | HSPA8 | TUBB | AL662797.1 |
| 59 | RPL7A | RPL7A | TUBA1B | RPL13A | MT-TR |
| 60 | MT-TR | MIR3606 | TAGLN | RPL7A | RPLP0 |
| 61 | BEX3 | MT-RNR1 | TNNT2 | AC053503.4 | H19 |
| 62 | RPS11 | MIR4709 | AL133415.1 | HSPA8 | RPS27 |
| 63 | MYL6 | RPLP0 | UBB | TPT1 | TPT1 |
| 64 | MIR4709 | MT-TR | MT-TP | AC020909.2 | RPL41 |
| 65 | MYL4 | RPL41 | RPL7A | FTL | RPLP1 |
| 66 | MT-TV | TAGLN | AC092069.1 | TNNT2 | TMSB4X |
| 67 | RPS18 | AC020909.2 | ATP5F1B | RPL41 | AC002398.2 |
| 68 | TPT1 | DES | MIF | AC005944.1 | TAGLN |
| 69 | EEF2 | HSPB7 | RPS18 | RPS18 | RPL13A |
| 70 | MIF | AC005944.1 | MT-TW | EEF2 | FTL |
| 71 | AC020909.2 | TUBB | TPT1 | MIR4709 | AC020909.2 |
| 72 | AL662797.1 | MIR1244-1 | AC079328.2 | AL049766.1 | AC005944.1 |
| 73 | MIR198 | AC119427.2 | MYL2 | MT-TW | EEF2 |
| 74 | MYL9 | TPT1 | H19 | PLN | MIF |
| 75 | MYBPC3 | RPS18 | RPS12 | AC023509.4 | MIR4709 |
| 76 | RPS8 | AL049766.1 | RPS6 | ALDOA | RPS18 |
| 77 | RPS12 | MYL9 | DES | RPS8 | MYL9 |
| 78 | PLN | AC132217.1 | MYL9 | MIR3661 | RPL7A |
| 79 | UBB | HSPA8 | ALDOA | IGF2 | ALDOA |
| 80 | RPL10A | RPS8 | COL1A1 | TPI1 | MT-TW |
| 81 | RPL41 | RPL10A | TPI1 | H19 | HSPA8 |
| 82 | ALDOA | ALDOA | MIR4709 | RPS6 | CCN2 |
| 83 | MALAT1 | TPI1 | RPS8 | AL133415.1 | MGP |
| 84 | TNNI1 | TMSB4X | EEF2 | MYL2 | AC119427.2 |
| 85 | ATP5F1B | RPS6 | AC023509.4 | ANKRD1 | AC091564.3 |
| 86 | SRP14 | RPS12 | RPL10A | TAGLN | RTL8C |
| 87 | MIR3661 | CALR | MT-TT | MT-TN | AL133415.1 |
| 88 | RPL29 | ATP5F1B | AC119427.2 | MYL9 | RPS6 |
| 89 | FAU | CCN2 | AC005944.1 | RPL10A | RPS8 |
| 90 | RPL3 | FAU | CALR | RPS12 | RPS12 |
| 91 | MDK | RPS11 | MIR3652 | AC092069.1 | AC023509.4 |
| 92 | HSPB3 | RPS21 | AL049766.1 | AC119427.2 | AC087457.1 |
| 93 | RPL7 | EEF2 | RPS11 | FAU | SLC25A5 |
| 94 | RPS3A | RPL3 | RPL3 | MT-TT | TPI1 |
| 95 | MIR4721 | VIM | TUBA1A | MIR1244-1 | UBC |
| 96 | RPS17 | AC145207.3 | FAU | RPS11 | MYBPC3 |
| 97 | AL049766.1 | TUBA1A | MIR1244-1 | RTL8C | AC004477.2 |
| 98 | MT-TF | AC091564.3 | PFN1 | SLC25A5 | COX5B |
| 99 | RPS6 | PFN1 | RPS16 | COX5B | MIR3661 |
| 100 | AC023509.4 | MT-TT | RPL19 | RPS16 | AL049766.1 |
| | | | | | |

**Supplement 6.5. CellPhone DB predicted interactions.** Significant mean expression values of predicted ligand-receptor interactions between the different cell pairs. The interaction pairs in black font depict the ligand coming from the first cell type and receptor from the second. The interaction pairs in blue font depict the receptors coming from the first cell type and the ligand from the second. A, IMR90-CMs baseline; B, mena-treated IMR-90; D, mena-CondM-treated CMs. Empty cells denote a non-significant mean expression value.

| Interacting Pair | A TTF | B TTF | D TTF | TTF A | TTF B | TTF D | A CSC | B CSC | D CSC | CSC A | CSC B | CSC D |
|---|---|---|---|---|---|---|---|---|---|---|---|---|
| ACKR2_CCL7 | 2.5 | 2.0 | 1.8 | | | | 4.3 | 3.8 | 3.6 | | | |
| AGRP_MC4R | | | | 28 | 28 | 28 | | | | 63.2 | 63.2 | 63.2 |
| AGRP_MC5R | | | | 28 | 28.3 | | | | | 63.2 | 63.3 | |
| AVP_AVPR1A | | | | 33 | 33.8 | 33 | | | | 77.8 | 77.7 | 77.8 |
| AVP_AVPR1B | | | | | 33.7 | | | | | | 77.7 | |
| AVP_OXTR | | | | 38 | 38.9 | 35 | | | | 82.5 | 82.9 | 79.5 |
| CCR2_CCL7 | | | 0.8 | | | | | | 2.6 | | | |
| CCR3_CCL7 | | 0.8 | 0.8 | | | | | 2.6 | 2.6 | | | |
| CCR5_CCL7 | | | 0.8 | | | | | | 2.6 | | | |
| COL14A1_a10b1 complex | 49.5 | 38.8 | 42.8 | | | | | | | 24.1 | | |
| COL16A1_a10b1 complex | 94.0 | | | | | | | | | 94.6 | 87.5 | 88.9 |
| COL16A1_a2b1 complex | | | | | 110 | | | | | 88.1 | 143.8 | 90.1 |
| CORT_SSTR1 | | | | | | | | | | 12.8 | 13.1 | 12.7 |
| CORT_SSTR4 | | | | 1.3 | | | | | | 12.7 | | |
| CXCL10_CXCR3 | | | | | 81 | 81 | | | | | 3585 | 3585 |
| CXCL10_DPP4 | | | | | | | | | | 3585 | 3586 | 3585 |
| EFNA4_EPHA5 | | | | | | | | | | 48.3 | 49.9 | 49.6 |
| EPHA1_EFNA4 | | 24.6 | | | | | 54.3 | 57.5 | 52.9 | | | |
| EPHA3_EFNA4 | | | | | | | 55.6 | 50.8 | 62.2 | | | |
| EPHA8_EFNA4 | | | | | | | 48.0 | 47.8 | 48.1 | | | |
| EPHB6_EFNB1 | | | | | | | 155 | 155 | 155 | | | |
| ERBB4_NRG4 | 127 | | 101 | | | | 147 | 99 | 121 | | | |
| IGF2_IDE | | | | | | | | | | 620 | 600 | 628 |
| IGFL3_IGFLR1 | | | | | | | 3.1 | 3.1 | | 3.3 | 2.9 | 3.1 |
| NODAL receptor_NODAL | 24.8 | | 46.5 | | | | 30.6 | 18.3 | 52.3 | | | |
| OXT_OXTR | | | | | 5.2 | | | | | 4.9 | 5.2 | 1.8 |
| SEMA3E_PLXND1 | | | | | 27.8 | | | | | 58.8 | 60.9 | 56.5 |
| TEK_ANGPT4 | 4.0 | 3.4 | | | | | 5.8 | 5.3 | 4.5 | | | |
| TG_ASGR1 | 28.3 | 28.3 | | | | | | | | 32.8 | 32.0 | 33.9 |
| TGFB1_aVb6 complex | | | | | | | | | | | | 96.3 |
| TGFB1_TGFbeta receptor1 | | | | | | | | | | 146.1 | 120.7 | 138.3 |
| TGFB1_TGFBR3 | | 105 | 99 | | | | | | | 108 | 100 | 106 |
| TNF_TNFRSF1B | | | | | | | | | | 2.3 | | |
| TNFSF12_TNFRSF25 | 20.9 | 21.0 | 22.0 | | | 6.8 | | | | 10.0 | | 8.9 |